An investigation of potential periglacial landforms on the northern plains of Mars: an integrated field, laboratory and remote sensing study

Thesis

An Investigation of Potential Periglacial Landforms on the Northern Plains of Mars: An Integrated Field, Laboratory and Remote Sensing Study

Alexander Matthew Barrett BSc, MRes.

19 December 2014

Revised 11 October 2015

This thesis submitted to the Open University, in the field of Planetary Science for the degree of Doctor of Philosophy.

Abstract

In this investigation the hypothesis that the Northern Plains of Mars have been shaped by periglacial processes is assessed. A periglacial formation mechanism has been proposed for a variety of martian landforms. These were examined with a particular focus on clastic patterned ground.

Periglacial environments occur in cold climate regions of Earth due to the repeated freezing and thawing of water, they require the presence of liquid water to develop. Consequently, if martian landforms are periglacial then they would provide a useful geomorphic marker for locations where water has been liquid in the geologically recent past.

The main strand of this investigation consisted of a survey of high resolution images from the Mars Reconnaissance Orbiter spacecraft. Locations with putative periglacial landforms were examined to test this and other formation hypotheses. This series of surveys was supported by two other research activities; two field campaigns were conducted to examine sorted patterned ground in Iceland. Air photographs, verified by in situ observations, were compared to the martian features studied in the main survey. A laboratory study was also conducted with the aim of testing whether periglacial processes were viable under the low temperature conditions found on the martian surface in the present day. This "proof of concept" study proved inconclusive, but is summarised for completeness.

It was found that the morphology and situation of these martian landforms was a reasonable fit for that which would be expected in a periglacial environment. Two alternative theories to explain the formation of martian clastic networks were rejected, as they did not appear to fit with the observed morphologies. It remains uncertain whether periglacial processes are viable on Mars, but they remain the best theory to explain the occurrence of clastic networks on the Northern Plains.

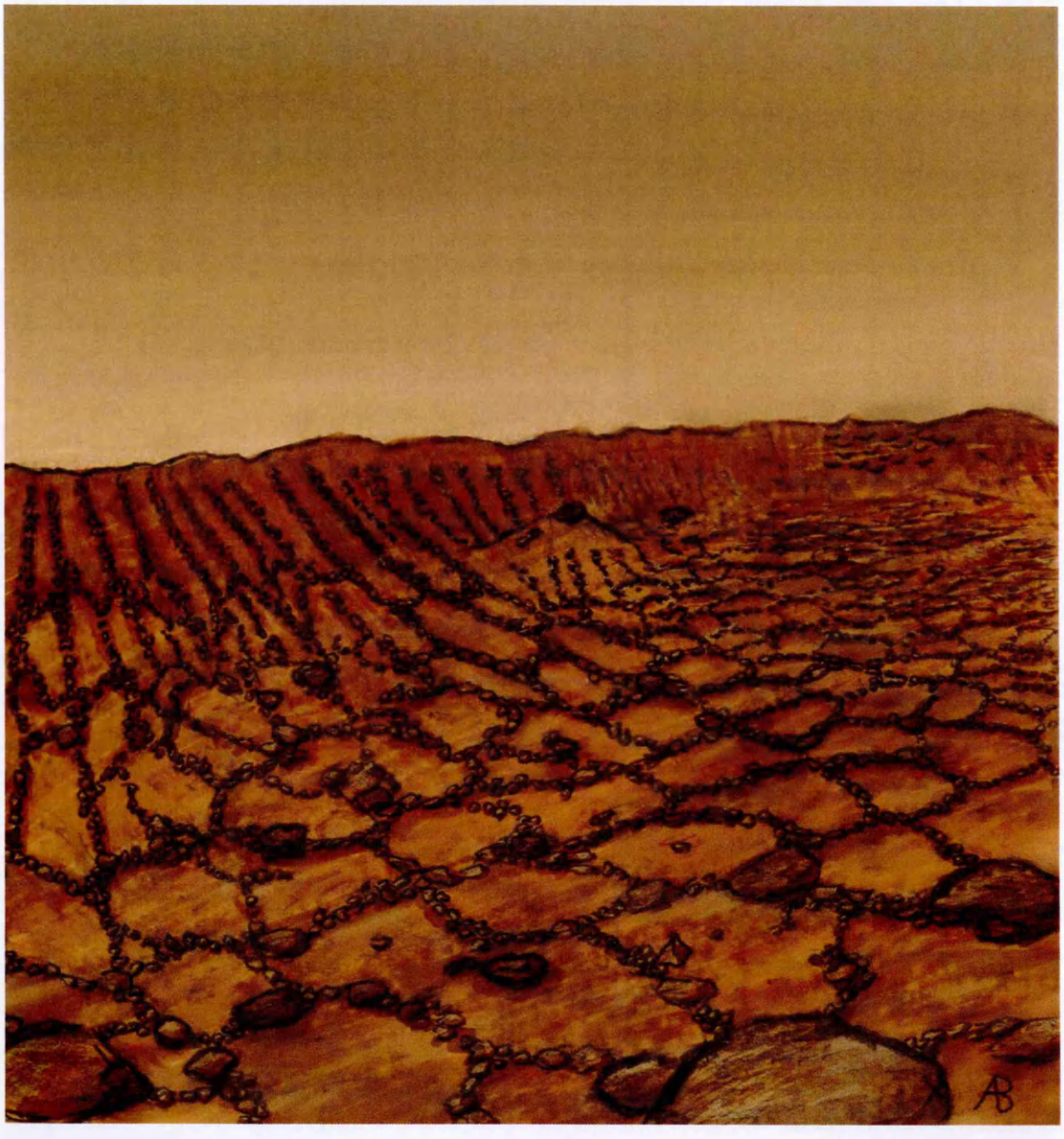

Figure 1.1: Artist's Impression of Sorted Patterned ground in a martian impact crater.

Acknowledgements

This research was funded by the UK Space Agency Aurora program and the Open University's Centre for Earth, Planetary, Space and Astronomical Research (CEPSAR).

The analysis of Icelandic patterned ground detailed in Chapter Four would not have been possible without the support of a number of organisations. Both expeditions used

equipment from the UK's Natural Environment Research Council (NERC) Geophysical Equipment Facility (loan numbers 1006 and minor loan 999). Air photograph data was collected by the NERC Airborne Research and Survey Facility survey EUFAR12-02 funded by the European Facility for Airborne Research (project "ICELAND_DEBRISFLOWS"). Last but by no means least an award of £1000 from the British Society for Geomorphology (BSG) allowed for a second trip to Iceland in 2013.

Many thanks go to my supervisors; Matt Balme, Manish Patel and Axel Hagermann for everything they have done over the course of this project, not least reading a vast number of thesis drafts. I would also like to thank Susan Conway for being an unfailing source of assistance on many occasions.

Both Peter Fawdon and Chris Barrett provided excellent assistance in the field and it was a pleasure to explore northern Iceland in their company. Closer to home Peter Fawdon, Jason Ramsdale, Leanne Gunn, Sion Hughes, Jean-David Bodénan, Mohit Melwani Daswani and Liam Steele have all provided useful thoughts on my research at various points over the last few years. Many thanks to Will Gosling and Encarni Montoya for acquiring mud samples for use in the laboratory study.

Finally none of this would have been possible without the help and support of my family; Chris Barrett, Kim Golding and Lily Golding. They have kept me going at every step of the way and this thesis is dedicated to them.

Table of Contents

List of Illustrations

1 Chapter One: Introduction

This investigation sets out to examine the possibility that liquid water, possibly in the form of highly concentrated brines, has caused the development of periglacial landforms on the surface of Mars. Periglacial processes and landforms will be discussed in detail in Chapter Two. In essence a periglacial landscape is one where the repeated freezing and thawing of the upper layer of ice-rich permafrost shapes the landscape, resulting in a suite of distinctive landforms. These include aggradational features such as frost mounds, and degradational features such as thermokarstic depressions and solifluction lobes. One of the most characteristic periglacial landforms is sorted patterned ground where many freeze thaw cycles set up a positive feedback loop, moving larger stones into circles or stripes around domains of finer grained material.

The formation of all of these features requires the action of liquid water and it is this that makes this suite of landforms significant in a planetary context. Because of the dependence on thawing these landforms should only occur in the presence of ground ice and under conditions where liquid water can occur. Consequently, they offer an important insight into the environmental conditions under which they formed. Periglacial landforms could thus form a useful geomorphic marker for places where repeated thawing of water has been possible in the geologically recent past.

1.1 Water and the Martian Environment

The environment of Mars has fascinated human observers for generations, and for almost all of that time the availability of water has dominated our interest in the planet. The earliest speculation on the martian environment imagined the planet to be much like Earth (e.g. Herschel, 1784). Observers with relatively little information

about the nature of the other planets saw no reason to suppose that they were unlike their own (Kargel, 2004). Even as recently as the start of the 20th century it was speculated, somewhat fancifully, that canals or channels of water might be keeping a dying world alive (Lowell, 1908, 1906, 1895). Water is so intrinsic to the environment of Earth that it is no surprise that its presence or absence on Mars defined our perception of what that planet might be like. The idea that Mars is an Earth-like planet has always caught the public imagination.

Later observations of the Martian surface and climate would prove these assumptions to be false. Modern Mars has no bodies of standing water. Channels that may be ancient river systems are present, but no persistent channelized flows of water, whether natural or artificial, exist in the present day (Bargery et al., 2011). Liquid water at the surface is only metastable and will quickly freeze or sublimate when exposed to Mars' low atmospheric pressure and extremely cold temperatures (Bargery et al., 2010; Carr, 1983; Hecht, 2002). However, despite being extremely cold and dry, Mars does have a large volume of water ice, both as part of the polar ice caps (Plaut et al., 2007; Thomas et al., 1992) and in the subsurface at mid to high latitudes (Boynton et al., 2010; Feldman et al., 2004, 2002).

Although the surface of present day Mars is dominated by aeolian and impact driven processes (Bargery et al., 2011), it remains the most Earth-like of the other terrestrial planets. The range of surface temperatures is not vastly dissimilar: Mars' mean surface temperature is of the order of 210 K, but it can get much warmer, varying between 140 and 300 K (Kieffer et al., 1992). Thus temperatures rise above the freezing point of water in favourable locations on the warmest days of the year (Haberle et al., 2001). There is considerable overlap between the temperatures experienced by Mars' most extreme warm environments and Earth's most extreme cold ones.

While rivers and seas are absent in the present day, there is clear evidence that water has played an active geomorphic role at various points in the planet's history (Baker, 2001; Carr, 2012; Parker et al., 1993). Even metastable water can be an effective erosive agent if it travels far enough before boiling away due to the thin atmosphere, or freezing due to the low temperatures. Large outflow channels were probably carved by water (Baker, 2001; Carr, 2012, 1979; Conway et al., 2011; Sharp and Malin, 1975) and smaller gullies may be evidence of fluvial activity in geologically recent times (Malin and Edgett, 2000). In situ observations of martian sedimentary rocks have provided evidence that many were emplaced under fluvial conditions (e.g. Williams et al., 2013). There has been considerable debate as to whether seas have existed on the northern plains at various points in the past (Baker et al., 1991; M.A. Kreslavsky and Head, 2002; Malin and Edgett, 1999; Parker et al., 1993; Pechmann, 1980).

The presence of liquid water has remained central to many questions of astrobiology. "Follow the Water" is one of the main aims of NASA's Mars exploration program (Johnson, 2010), both due to its importance for resource utilisation on future manned missions and because wet environments are those most likely to harbour life as we know it. Consequently, any means of identifying small scale occurrences of liquid water at the martian surface has value.

Additionally, recent research into "cryobrines" with low eutectic temperatures (e.g. Möhlmann and Thomsen, 2011) has explored the possibility that very saline water could be thawing under a wider range of environmental conditions, and so could be a viable geomorphic agent. The current investigation will further discuss the possibility that brines such as the perchlorate solutions observed at the phoenix landing site (Cull et al., 2010; Hecht et al., 2009) could allow periglacial processes to occur.

1.2 Periglacial Environments?

Large scale fluvial processes are no longer as active on Mars as they once were, and probably never dominated the martian environment to the extent that they do on Earth (Baker, 2001; Carr, 1996; Irwin et al., 2005). Consequently, it is important to consider more extreme environments that are also shaped by the interaction of liquid water with the landscape. Terrestrial cold climate environments are shaped by glacial and periglacial processes and the same may well be true for some parts of Mars.

Discussion of putative periglacial features on the martian surface began during the latter part of the 20th century using images from the Viking orbiters of the mid 1970s (Carr and Schaber, 1977; Costard and Kargel, 1995; Lucchitta, 1981). The start of the 21st century has seen a dramatic increase in the instrumentation both in orbit around Mars and on its surface. Orbiters have been constantly imaging the martian surface since the arrival of Mars Global Surveyor in 1997, and rovers have been operational on the surface since 2004, albeit only at a few isolated locations.

The wealth of data over the last two decades has facilitated the identification of numerous putative periglacial features. These include scalloped depressions in Utopia Planitia (e.g. Soare et al., 2008). These could be the result of processes analogous with terrestrial thermokarst depressions. The clastic stripes and lobate structures observed across the northern high latitudes (Gallagher and Balme, 2011; Johnsson et al., 2012) could be evidence of sorting and solifluction processes. All of these landforms will be discussed in more detail in Chapter Two.

However, while these features appeared to be morphologically similar to terrestrial periglacial landforms the question of how they could have formed remains uncertain. Since periglacial processes require the repeated freezing and thawing of a permafrost active layer they would not be expected to be common on Mars, if they occur at all. It is

also known that landforms resulting from completely different processes can arrive at similar morphologies, a phenomenon termed "*equifinality*". Could seemingly periglacial landforms have evolved through other means?

Equifinality is a major problem when examining the landscape from remotely sensed data, since there is a substantial lack of ground truth observations in martian geomorphology. While it is possible to assess the likelihood that a landform, or preferably a landscape, is the result of periglacial processes it is impossible to be certain of its formation mechanism without in situ observations. Strong evidence is required to prove that landforms resulted from thawing, rather than other processes which would be expected to be more common on Mars.

1.2.1 What makes a compelling case for a periglacial environment?

Firstly the presence of abundant ground ice is required. Without permafrost there cannot be active periglacial processes, only relict landforms from a time when the region was more saturated with ground ice. The focus of this investigation is the Northern Plains of Mars, a large low lying region consisting of Acidalia, Utopia and Arcadia Planitiae. This area is dominated by low lying ground believed to be covered by an extensive ice-dust mantle at mid to high latitudes (Head et al., 2003; Kreslavsky and Head, 2002; Mustard et al., 2001). It is therefore a good candidate for the presence of ice related landforms. If ground ice is stable in this region as suggested by the observations of Boynton et al., (2010) and Feldman et al., (2004, 2002), then this latitude range could provide the substrate needed for periglacial processes.

Secondly, the surface temperature must regularly become high enough to result in the thawing of an active layer. If the ground is perpetually frozen, as may be the case over much of Mars, a periglacial environment cannot occur. This may not necessarily require the temperature to rise above zero °C, as the presence of concentrated salt

solutions within the ground water could potentially depress the freezing point sufficiently to allow thawing to occur at much lower temperatures (e.g. Möhlmann and Thomsen, 2011).

Thirdly, compelling sites should exhibit multiple putative periglacial features in close proximity to one another. These features should exhibit morphological relationships with each other consistent with those seen in assemblages of similar landforms on Earth. Such assemblages would indicate that the constituent landforms probably developed through related processes. Hence, while morphologically similar landforms can form by different processes; those that occur within a coherent assemblage provide a stronger case for a periglacial origin.

Finally, building on the above point, the situation of an assemblage can also be considered. If the morphology of the observed features closely matches that which would be expected as a result of the observed variations in topography, setting or environment then it adds more weight to the analogue. However while many of these factors can rule out a feature as being periglacial they do not provide enough evidence to accept a periglacial hypothesis. A definite answer to the question of how these features formed must await ground truth data from future missions to mars.

1.3 Available Data

The steady increase in the resolution of remotely sensed data allow increasingly more detailed assessments of possible periglacial features to occur and so is invaluable in testing these formation mechanism hypotheses. This investigation makes use of several types of images to survey the Northern Plains of Mars for possible periglacial features. The most important are images from the High Resolution Imaging Science Experiment (HiRISE) camera on the Mars Reconnaissance Orbiter (MRO) spacecraft (Delamere et al., 2010; McEwen et al., 2010).

Images from the HiRISE instrument can have a resolution of 25 cm per pixel. This is sufficient for metre scale boulders to be resolved and detailed examination of the structure of possible areas of sorted patterned ground to be conducted. This makes it possible to assess the likelihood that these very small scale features are periglacial in nature. This study also uses data from the CTX Context camera, also on MRO. This instrument is designed to complement HiRISE and is used to expand the area that can be examined, albeit at a lower resolution of around 6 m per pixel (Malin et al., 2007).

1.4 Aims of the Investigation

This investigation examines the likelihood that a periglacial environment has evolved on the martian surface in the geologically recent past. The aim is to catalogue a variety of putative periglacial landforms across the northern plains and assess the extent to which they fit a periglacial model. The secondary aim is to assess the extent to which a periglacial environment is viable under martian temperature and pressure conditions. The investigation has two main hypotheses:

Hypothesis 1:

The Northern Plains of Mars have been a periglacial environment in the recent past.

Hypothesis 2:

Periglacial processes can occur at temperatures below 0°C as a result of freezing point depression by brines.

In order to test these hypotheses a variety of research activities have been conducted. The main strand of this investigation is an extensive survey of the Martian Northern Plains to examine the distribution of a variety of potential periglacial landforms. This was the main research activity and will be discussed throughout the thesis. Chapter Six sets out the methodology of this project, while the results are presented and analysed in

Chapters Seven through Ten. This remote sensing survey was supported by two smaller projects. A series of laboratory studies were conducted to investigate whether the depression of the freezing point by salt solutions could allow periglacial processes to occur at sub-zero temperatures. Two short field campaigns were also conducted to examine sorted patterned ground in Iceland, and investigate how variations in the morphology of patterned ground with topography compared to the morphology of martian features. The laboratory and field studies are described in Chapters Three and Four respectively, as is all the relevant literature and background to them.

1.4.1 Remote Sensing Surveys

In this project a series of surveys of high resolution remote sensing data have been conducted to locate possible periglacial features and assess whether there is a pattern to the locations in which they occur. This allows the latitudinal, topographic and environmental conditions required for the formation of these landforms to be constrained. This can be used to assess whether they can be explained by a periglacial paradigm or whether another formation mechanism is required. Although a wide range of putative periglacial landforms are examined the focus of much of this study is on clastic networks which could be examples of sorted patterned ground. These are one of the most characteristic periglacial landforms and are also easy to identify as they do not resemble many other landforms.

1.4.2 Laboratory Studies

In this part of the investigation the sorting process was examined using a variety of model experiments. Trays of sand and stones were repeatedly frozen and thawed with the aim of simulating the development of sorted patterned ground in the laboratory. Had this proved successful then the experiment could have been repeated at lower temperatures using possible cryobrines to depress the freezing point. However

problems with the development of a reliable method under terrestrial conditions precluded this line of research. The laboratory work is summarised in appendix one for completeness, but is only referred to briefly in the remainder of the thesis.

1.4.3 Field Studies

In this investigation two field campaigns were conducted in the Skagafjörður region of northern Iceland. A variety of examples of sorted patterned ground were observed and documented. The first expedition was in support of a remote sensing project which generated extensive Aerial photographs and LiDAR of the site. The following year Structure from Motion (SfM) was used to produce Digital Elevation Models of small scale patterned ground to complement the remote sensing data. Numerous examples of sorted patterned ground were characterised and documented on both metre and centimetre scales.

1.5 Thesis structure

This chapter is an introduction to the topic of the thesis, the aims of the research and the reasons for conducting it. The following chapters are described here:

Chapter Two consists of an introduction to the periglacial environment and the processes and landforms found there. The main periglacial landforms are discussed in detail. Terrestrial examples are presented along with the evidence for their presence on Mars within the existing planetary geomorphology literature.

Chapter Three discusses the conditions necessary for the formation of a periglacial environment on Mars and presents a variety of hypotheses as to how such features could form. It examines the role of brines with low eutectic temperatures in facilitating the formation of a periglacial landscape under martian temperature conditions. This chapter also discusses the properties of frost-susceptible soils and the requirements for

freeze thaw sorting. Chapter Three compares and contrasts these requirements with the conditions present on the northern plains of Mars.

Chapter Four examines sorted patterned ground in more detail. This chapter presents the results of the field campaigns examining sorted patterned ground in Northern Iceland. These observations help to set a terrestrial baseline that can be used to categorise martian patterned ground and assess the likelihood that it is periglacial in origin.

Chapter Five builds upon the work in Chapter Four, applying the same methods that were used to characterise Icelandic patterned ground to martian features. The area in and around Lomonosov Crater in the north of Acidalia Planitia is used as a case study to demonstrate that the martian features are comparable to those found on Earth.

Chapter Six discusses the methodology of a series of surveys of Acidalia, Utopia and Arcadia Planitiae using HiRISE and CTX data. The study areas are described and the landforms examined as part of the survey discussed.

Chapter Seven then presents the results of these surveys. The distributions of most of the periglacial features hypothesised to be present on Mars are discussed. This chapter also describes a number of possible periglacial assemblages where multiple putative periglacial landforms could be present.

Chapter Eight examines the parameters that might be controlling the distributions of putative periglacial features discussed in Chapter Seven. Landform distributions are compared to a variety of global environmental and topographic datasets to determine whether any correlations occur.

Chapter Nine focuses on the sites with possible sorted patterned ground. Both Periglacial and non periglacial formation mechanisms are examined. Features around Lomonosov Crater are examined to determine how well these features compare to

terrestrial analogues. The hypothesis that martian patterned ground formed through interaction of boulders with thermal contraction cracks, rather than through periglacial means is tested.

Chapter Ten examines two areas of scalloped depressions around Davies and Lagarto Craters in Acidalia Planitia. These features are categorised using a similar methodology to that applied to scalloped features in Utopia Planitia by Séjourné et al., (2011). The implications for a formation mechanism based on thermokarst processes is discussed.

Chapter Eleven provides a synthesis of the results outlined in the previous three chapters and discusses their implications for the viability of the periglacial environment on the Northern Plains of Mars. Methodological concerns are addressed and the results are put into the context of the wider literature. It finishes by outlining future work which could supplement the studies conducted during the course of this project.

Finally **Chapter Twelve** presents the conclusions of the thesis.

In addition to these chapters the thesis has two appendices. **Appendix one** provides an overview of the laboratory work conducted as part of this investigation. **Appendix two** includes large print versions of key figures from throughout the thesis.

2 Chapter two: The Periglacial Environment

Periglacial landscapes are found in many cold climate environments on Earth where a variety of landforms are generated by the repeated freezing and thawing of a permafrost active layer (e.g. French, 2007). Periglacial processes have been suggested as a formation mechanism for a variety of landforms observed in satellite images of the martian surface, which are morphologically similar to those found in terrestrial periglacial environments (e.g. Gallagher and Balme, 2011).

This chapter provides an overview of the terrestrial periglacial environment and describes in detail the processes which produce solifluction lobes, thermokarst depressions, pingos and patterned ground. It additionally discusses the evidence that these features may be present on Mars.

2.1 Defining the Periglacial Environment

There has been considerable debate on the exact definition of periglacial processes and landforms (Burn, 1998; French, 2007; Slaymaker, 2011). For the purposes of this work they shall be defined as any geomorphic process resulting from the freezing and thawing of ground ice in the permafrost active layer and the landforms resulting from this freezing and thawing (French, 2007).

A permafrost environment is defined as a region of perennially frozen ground; where the majority of the ground remains frozen, or at any rate below 0°C, for more than two consecutive years (Black, 1954; French, 2007). Seasonal thawing still occurs in the upper layer of the ground, this being the active layer, which can be up to a metre thick in warmer periglacial environments (Burn, 1998; Chambers, 1966; French, 2007). The active layer is much shallower in colder, polar climates and can be deeper in some localised circumstances, such as below a large body of water.

Below the active layer the ground remains below 0°C despite seasonal changes in temperature. Unfrozen material can occur in this zone, if for example the presence of salts depresses the freezing point, resulting in pockets of unfrozen brine. The presence of salts can have a significant deleterious effect on the formation of ice lenses and the accumulation of ice within the permafrost. It has been demonstrated that the presence of brines reduces frost heaving and results in the formation of more, smaller ice lenses and spicular ice crystals separated by channels of concentrated unfrozen brine (Arenson and Sego, 2006; Chamberlain, 1983).

2.2 Distribution of Periglacial Features on Earth

Permafrost covers approximately 24% of the Northern Hemisphere of Earth (Zhang et al., 2008). Large swathes of tundra cover the northern high latitudes and permafrost occurs in un-glaciated regions of Antarctica. High altitude regions often exhibit discontinuous permafrost. Periglacial environments have been documented in a variety of cold climate regions particularly Canada, Siberia and Alaska. A variety of studies throughout the 20th century, such as those described by French (2003), detail the distributions of these features. Periglacial landscapes have also been studied at high altitudes in the Tibetan Plateau (e.g. Jin et al., 2000) and relict features can be found in regions that experienced a periglacial climate during previous glaciations (Ballantyne and Harris, 1994). Periglacial features have also been reported in the Antarctic Dry Valleys, an environment which is an excellent analogue for the cold, dry martian climate (Anderson et al., 1972; Marchant and Head, 2007). Many studies have been conducted by terrestrial geomorphologists to catalogue periglacial landforms and determine the processes that lead to their formation (e.g., French, 2003; Humlum and Christiansen, 2008; Washburn, 1956). Figure 2.1 summarises the climatic conditions under which different degrees of permafrost cover occur.

Periglacial processes are found in areas of continuous and discontinuous permafrost, where sufficient thawing occurs to generate an active layer, but ground ice persists for long enough to allow repeated freezing and thawing to occur. Figure 2.2 shows the distribution of terrestrial permafrost in the northern hemisphere of Earth. It can be seen that although it is mainly concentrated at high northern latitudes, areas of permafrost are also present in high elevation regions, such as the Tibetan plateau.

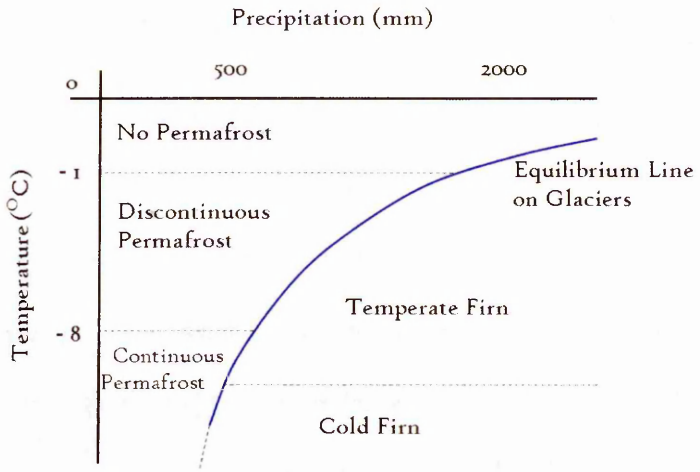

Figure 2.1: Conditions required for permafrost. Periglacial processes occur throughout areas of continuous and discontinues permafrost, at any location where temperatures get sufficiently high to form an active layer at the warmest times of the year (After French, 2007).

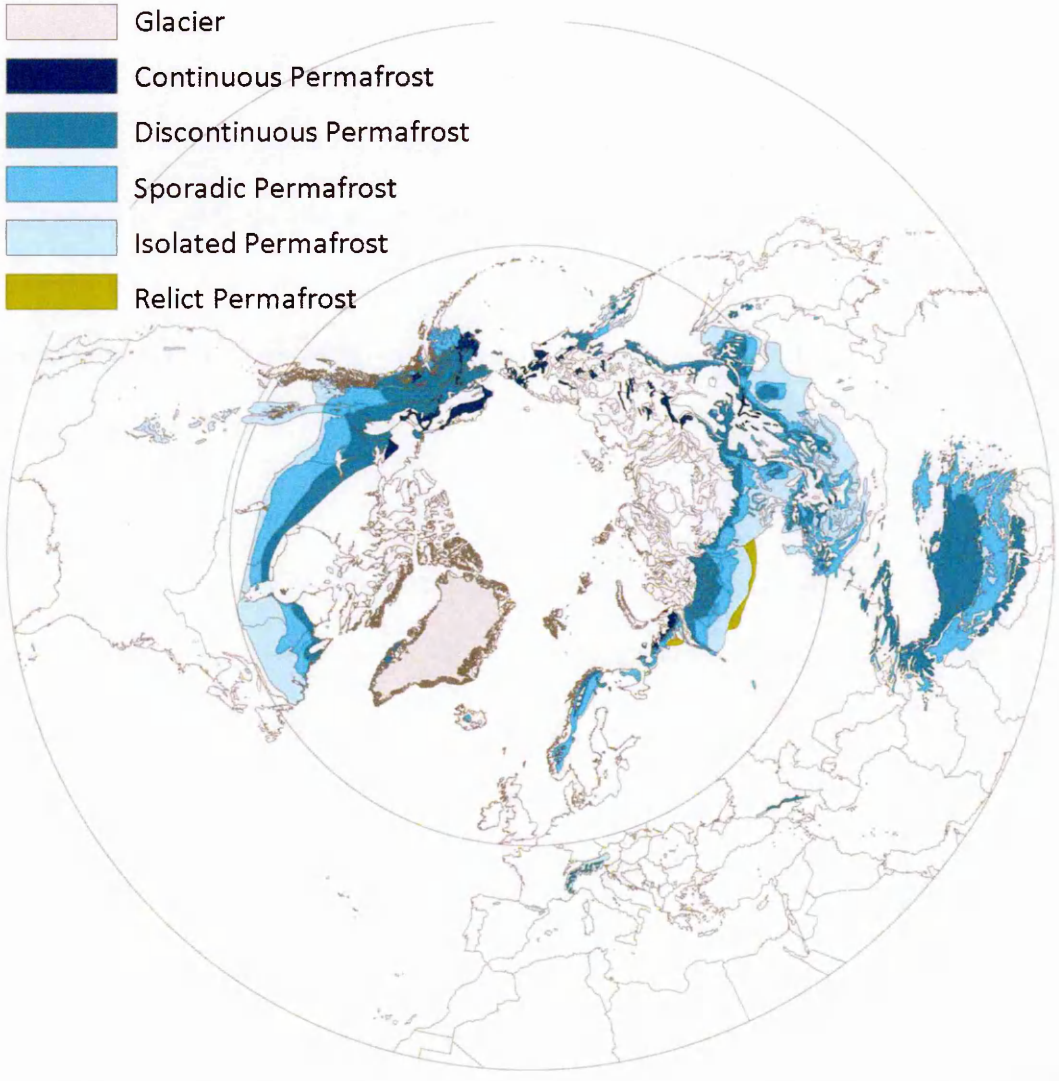

Figure 2.2: The distribution of terrestrial permafrost in the northern hemisphere of Earth. (After Brown et al., 1998).

2.3 Aggradational and degradational landforms

Some landforms are formed as a result of the *aggradation* of permafrost as water-saturated soils freeze, deforming the ground above. This category includes pingos, or frost mounds; conical ice cored hills which result from the formation of a large and coherent mass of ground ice. This ice domes the surface above it creating a mound. Some frost mounds are seasonal features, where others form large hills that persist for many years. Other aggradational landforms include ice wedge polygons, where thermal contraction cracks are widened by a build up of ice, and smaller mounds such as palsas and frost blisters.

Other periglacial features are the result of permafrost *degradation,* when the thawing of excess ground ice causes a loss of volume, or triggers mass movement. For example, thermokarst involves the collapse of the ground due to the thawing of ground ice, forming a lake or depression. Solifluction features result from the thawing of ground ice destabilising a hill slope and triggering the repeated sliding or creeping of surface material.

Regardless of whether a process is aggradational or degradational it will usually require multiple cycles of freezing and thawing for its effects to produce a clear periglacial landform. One of the most distinctive, and indeed diagnostic, periglacial landform types is sorted patterned ground. This forms when the repeated freezing and thawing of the permafrost active layer results in the organisation of soil particles in separate coarse and fine domains, producing stripes, circles or polygons of differently sized particles. Sorted patterned ground will be the focus of this study.

In the next part of this chapter these landforms will be described in more detail. A section for each landform being investigated will outline the mechanism of formation, the history of research surrounding them and the evidence for their presence on Mars.

The second half of the chapter will then discuss the conditions under which martian periglacial features could have evolved.

2.4 Periglacial Processes and Landforms

2.4.1 Solifluction

Solifluction is a slow mass wasting process which occurs due to freeze thaw action on hill slopes in periglacial environments (French, 2007; Matsuoka, 2001). Various processes can cause solifluction, and the exact definition can vary from one study to another. Solifluction was originally proposed by Andersson (1906), based on observations of mass movement features in the Arctic and in the Falkland Islands. Andersson proposed that the saturation of the soil by thaw was responsible for triggering mass movement. This process is now generally referred to as gelifluction. Solifluction is a broader term, which encompasses a range of thaw-related mass movement processes including various types of frost creep as well as gelifluction and plug-like flow (Higashi and Corte, 1971; Matsuoka, 2001). These processes often work in conjunction to produce solifluction. Therefore an individual solifluction lobe will probably be the result of multiple forms of soil creep and gelifluction (Benedict, 1976; Higashi and Corte, 1971). Rates of displacement can be a metre per year or higher in some cases, but are typically lower (Francou and Bertran, 1997). Solifluction typically occurs on relatively shallow slopes between 5-20°, on steeper slopes mass movement would occur much more rapidly, in the form of a landslide or active layer detachment (Beirman and Montgomery, 2014; Benedict, 1976). However these features are not found on slopes with a shallower gradient than 2°, Since they are formed through hill-slope processes (Washburn, 1973).

Figure 2.3: Solifluction lobes on a hillside in Alaska. (US Army Corps of Engineers Cold Regions Research and Engineering Laboratory, CRREL).

2.4.1.1 Frost Creep

Frost creep is a much slower process of mass movement than gelifluction and relies on the heaving of the soil due to either a diurnal or seasonal cycle of freezing and thawing (French, 2007). The formation of subsurface ice lenses as the active layer freezes causes the surface to heave. A particle lifted by frost heave is moved perpendicular to the ground surface. On a hill slope this means that when the ground thaws the raised material will collapse back down in the direction of gravity, being deposited slightly further down the hillside than the location in which it originated. Over a number of cycles this process can result in considerable down slope movement (French, 2007; Matsuoka, 2001). Seasonal freeze thaw cycles penetrate deeper into the ground and so affect a larger volume of material than diurnal cycles. Minor amounts of creep can occur due to the formation of needle ice lifting individual particles because of night time drops in temperature. This does not move large volumes of material but can be significant.

2.4.1.2 Gelifluction

As the active layer thaws liquid water is released into the soil and this can destabilise the upper layer of soil (usually the upper metre or less) resulting in movement. A steep

hillside only remains stable while the shear stress from gravity and other forces acting upon it is less than the soil's shear strength. The pressure of liquid water in a saturated soil forces the soil grains apart, reducing both the internal friction and cohesion of the soil and triggering flow (Harris et al., 1997).

2.4.1.3 Plug-like flow and active layer detachment.

Plug-like flow occurs in a situation where freezing occurs from both above and below resulting in the formation of ice lenses at the base of the active layer. If these lenses thaw before the rest of the active layer then it can create a slippage plane and cause the entire active layer to move down slope as a plug (Matsuoka, 2001).

Active layer detachments occur when the entirety of the active layer thaws from the surface down. The unstable, water rich active layer can become mobilised causing a landslide as it detaches from the still frozen permafrost below. Active layer detachment is not strictly speaking a solifluction process, as it occurs at a much faster rate and the resulting landforms are distinctly different to solifluction features (Lewkowicz and Harris, 2005; Matsuoka, 2001).

2.4.1.4 Solifluction Lobes

The end result of the processes described above is the solifluction lobe. These are lobate structures with a riser of up to 2 metres and widths and lengths which range from a few metres to tens of metres. In some cases they merge into much wider sheets when an entire hill slope is undergoing solifluction (Matsuoka, 2001; Matsuoka et al., 2005).

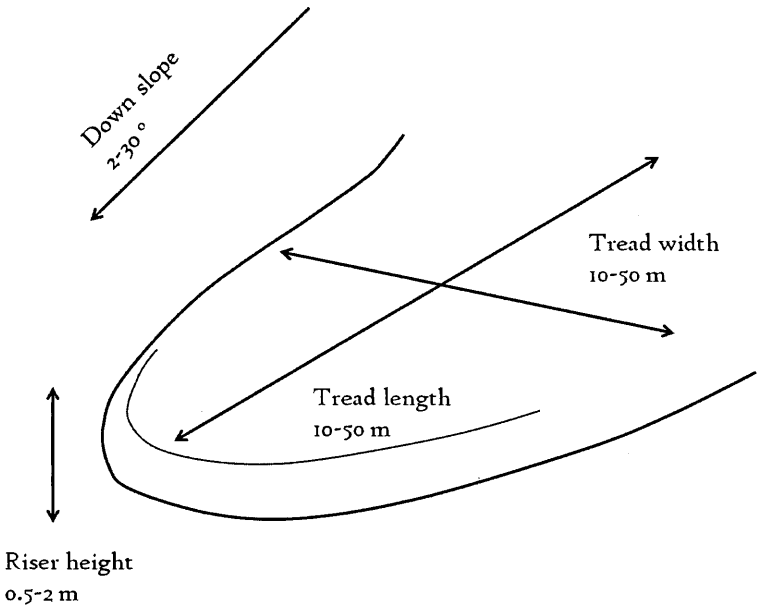

Figure 2.4: Structure of a solifluction lobe.

Lobes generally form where the gradient of the slope decreases, retarding the solifluction process and causing the transported material to bank up, forming a riser (Benedict, 1976). Some solifluction lobes contain clastic material. Stone banked lobes can occur in locations where the material being deformed by the solifluction process is characterised by sorted patterned ground or block fields. If coarse material moves faster than finer grained components then sorting can occur as the solifluction process precedes (Benedict, 1976). Lobes can become demarked by clastic material, with the largest blocks generally angled parallel to the direction of movement. In terrestrial periglacial environments turf banked lobes can be formed due to increased plant growth in the deposited material.

2.4.1.5 Solifluction on Mars?

Lobate, sometimes clastic, features have been observed in a number of locations on Mars. Possible clastic lobes have been observed on the walls of Heimdal crater and in similar environments across the northern high latitudes (Gallagher et al., 2011; Johnsson et al., 2012)

Extensive surveys of both the southern and northern high latitudes have found a variety of lobate structures (Johnsson, 2013; Johnsson et al., 2012; Reiss et al., 2011), some exhibiting clastic lobes, while others appear to be smoother non clastic features. Lobate structures are relatively small, being at most a few tens of metres across. Johnson et al., (2012) report features with sizes between 10 and 30 metres, while some of those observed by Gallagher et al., (2011) are almost 100 metres across. Since these are small scale features they are only clearly visible in the highest resolution images of the martian surface. This means that their presence can only be assessed in locations where high resolution images are available.

However lobate structures do not occur in isolation. A hillside will typically exhibit a large field of lobate structures, all oriented in the same direction, down the slope. In most cases several tiers of lobate steps are observed and the fields are wide enough that their lateral extent can include many tens of lobes. This is consistent with the terrestrial examples shown in Figure 2.3 and in Chapter Four.

Clastic lobate structures on the south eastern wall of Heimdal crater are shown in Figure 2.5. These lobes are slightly less than a hundred metres wide and numerous features are spread over more than a kilometre of hill-slope. At least seven tiers of lobes can be seen with their rounded edges oriented down slope, towards the top left of the image. Faint arcs of clasts, which might be additional tiers of lobes can also be seen further down the hill slope. Unsorted clastic material can be seen at the top of the slope on which these lobes occur.

Figure 2.5: Possible clastic solifluction lobes in Heimdal crater, downhill is towards the upper left corner of the image (After Gallagher et al., 2011).

Examples of non clastic features generally exhibit a similar morphology, but in these cases the edges of the lobes are defined by the shadow of the riser, rather than an arc of clasts. This may make such features harder to distinguish, as they will be most visible under specific illumination conditions, which may not match those at which HiRISE images are usually captured. Where clasts are present they are usually a few metres in diameter. It is likely that smaller material is also making up these structures, but that it is below the resolution of the HiRISE images. Variations in albedo under the clasts shown in Figure 2.5 may be indicative of smaller material which makes up the clastic border of the lobe, but which is not resolvable in these images.

Like their terrestrial analogues these features are typically found on hill slopes, Johnsson et al., (2012) report lobate features on slopes with a gradient of between 10° and 25°, a range which they demonstrate is comparable to that on which similar terrestrial features are observed.

2.4.2 Thermokarst

Thermokarst was first described in Siberia, and was introduced to English language periglacial research by Muller (Czudek and Demek, 1970; Muller, 1944). A large number of studies have been conducted assessing the formation, morphology and climatic sensitivity of thermokarst across the Arctic.

Thermokarst terrain forms in very ice-rich soils when a loss of thermal equilibrium causes the ground ice to melt. As most of the mass of the ground is composed of excess ice, the thawing results in substantial volumetric loss, leaving a depression called an alas, which may fill with melt water to produce a thermokarst lake (Fig. 2.10). These depressions are typically several kilometres in scale (French, 2007; Kääb and Haeberli, 2001; Wallace, 1948). Figure 2.6 illustrates the development of thermokarst lakes and examples of these features are illustrated, along with pingos, in figure 2.10.

Thawing can occur in a variety of circumstances. It could result from a dramatic increase in temperature, or the loss of an overlying layer of soil or rock which was insulating the underlying ice and protecting it from melting. Thermokarst often forms at the intersections of sublimation polygons where the underlying ground ice is exposed to the atmosphere by the contraction cracking (Czudek and Demek, 1970; Washburn, 1973).

Water absorbs more energy from insolation than the surrounding ground. This is partly due to its thermal properties and higher heat capacity, but is also a product of the translucency of the water. Radiation can be absorbed throughout the water column rather than just at the surface. The redistribution of heat throughout a body of water by convection also increases the amount of heat it can absorb.

Consequently, once a pond or lake has formed it will expand rapidly (Harris, 2002). As the ice melts, material will collapse to fill the space previously occupied by the ice. Such

collapses are generally accompanied by an increase in erosion because the ice acted as a cementing agent and so as it melts the strength and cohesion of the material is reduced. As erosion by thaw slumping occurs around the edge of a thermokarst depression its rim will develop a scalloped morphology with the most collapses occurring in the areas which receive the greatest insolation.

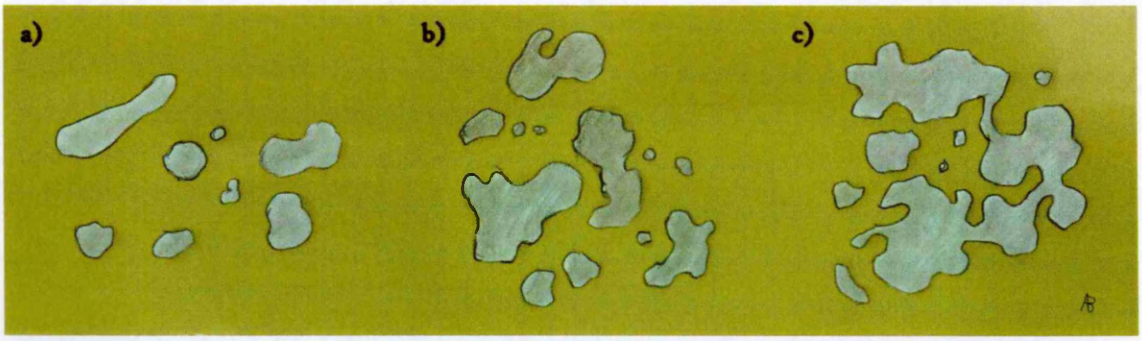

Figure 2.6: Growth and coalescence of thermokarst lakes. a) Young thermokarst features consisting of small near circular lakes. b) More mature landscape with lakes merging into larger basins with scalloped margins, surrounded by small young lakes. c) Very mature landscape where large scalloped basins merge together (after Wallace, 1948).

Young depressions will begin as almost circular features, but over time they will assume a scalloped shape as sections of their rim thaw and collapse. Mature thermokarst features have a highly irregular shape as many small scalloped basins have merged into much larger expanses of depressed ground (Wallace, 1948). As a thermokarst lake expands the collapse of its banks will often allow channels to form and water to drain – a process known as 'tapping'. As thermokarst lakes shrink, steps and terraces can be left within the depression, producing a stepped morphology within the high stand of the lake.

2.4.2.1 Thermokarst on Mars?

Scalloped depressions have been observed across the martian mid latitudes, particularly in central Utopia Planitia (Costard and Kargel, 1995; Séjourné et al., 2011; Soare et al., 2007a; Ulrich et al., 2010). It has been suggested that these features may be the product of a thermokarst process, although it is possible that they have formed through

sublimation, rather than thaw, of ground ice. Liquid water rapidly freezes and sublimates when exposed to the low atmospheric pressure so lakes are unlikely to have occurred on Mars in the geologically recent past. Instead, any thawed water would quickly evaporate or boil. Similarly, ground ice might sublimate directly, causing degradation of the surface without any thaw at all. It is unclear whether such a process should be termed 'thermokarst' as it does not necessarily proceed by thermal degradation. Irrespective of this definition both of these processes would probably leave behind an alas similar to those seen on Earth but lacking interior terraces (Soare et al., 2008). Interestingly, some martian scalloped pits do have internal terraces, but only usually on one side (Figure 2.7). It is possible that these terraces are unrelated to those in terrestrial alases, but are instead a product of the periodic expansion of the depression through retrogressive thaw.

A large number of studies have examined the morphology and distribution of the scalloped depressions in the Utopia Planitia region (Lefort et al., 2010; Morgenstern et al., 2007; Séjourné et al., 2011; Soare et al., 2012, 2008; Ulrich et al., 2010). The majority of scalloped terrains are distinct from pit craters (Mège et al., 2003), as they do not generally form in chains, and have a far less regular morphology. Scalloped pits can be distinguished from the basins created by degraded craters as they lack a rim of the sort usually associated with impact craters. They are also usually more elongate, a morphology which is unusual for cratered terrain (Morgenstern et al., 2007; Soare et al., 2008; Ulrich et al., 2010).

It has been noted that scalloped depressions appear to progress through a similar cycle of development to terrestrial thermokarst (Séjourné et al., 2011). Like terrestrial thermokarst, martian scalloped depressions frequently occur in conjunction with polygonally patterned ground, which occur both outside and inside of the basins.

Pitting, due either to thermokarst or sublimation processes is also quite common in the same region as these features.

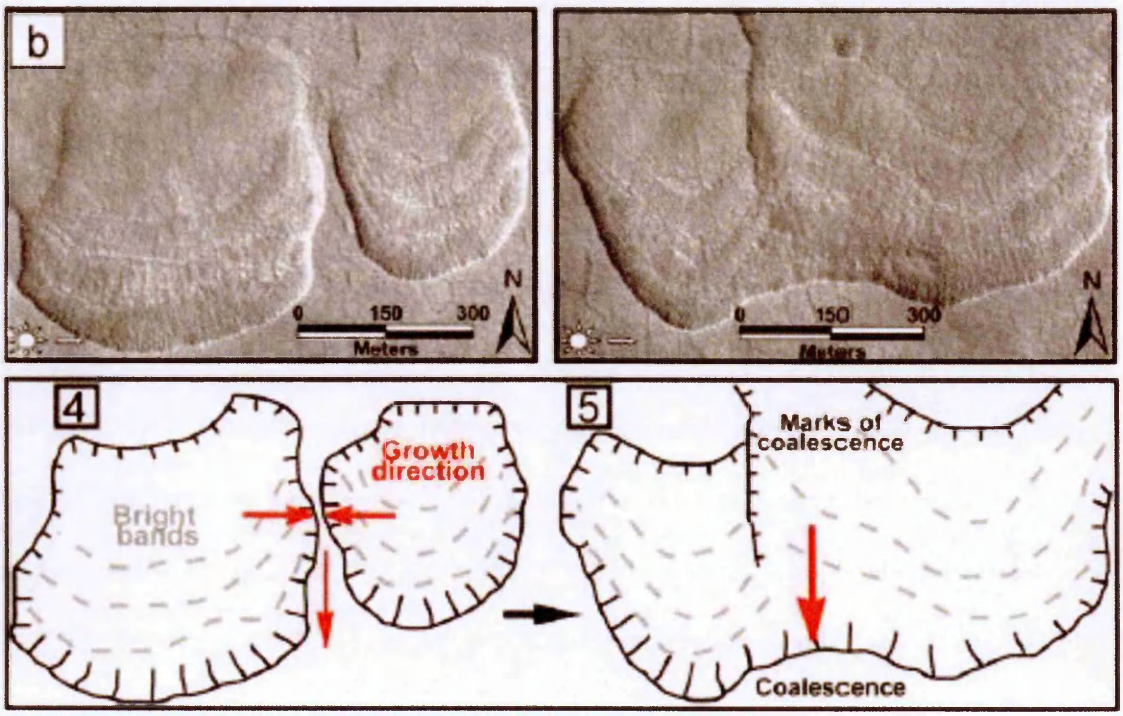

Figure 2.7: Coalescence of mature scalloped depression in Utopia Planitia.

(From Séjourné et al., 2011, fig 8)

Although lakes are improbable in the current martian climate it is possible that they have existed in the past. There is evidence that some martian depressions may have been filled with water for long periods of time resulting in littoral terraces. Cabrol and Grin (2002) describe terraces as being present on many of the large scale lake like features they examined. However they do not discuss scalloped depressions, but are focused on larger putative lacustrine environments such as the interior of Gale Crater.

Other lines of evidence support a mechanism of formation which does not rely upon the ponding of water within a depression. The presence of bright bands in the floors of scalloped depressions, such as that illustrated in Figure 2.7, may suggest multiple phases of development during which scalloped depressions grow. Preferential insolation on a pole or equator facing wall results in growth through retrogressive thawing or

sublimation loss, moving the outer margin of the feature and producing a new band in the depression's interior (Séjourné et al., 2011).

2.4.3 Gullies

Gullies are found in a wide variety of environments on Earth where water erosion leads to the formation of channels on steep hill slopes. They can form through fluvial processes, where erosion by water and water-borne material forms a steep channel, or as the result of debris flows where a mass of water-saturated sediment is the primary erosive agent (e.g. Iverson, 1997). The source region of a gully consists of a large alcove cut into the hillside from which the transported material originates. These source regions can range from a few hundreds of metres to several kilometres in area as illustrated in Figure 2.9.

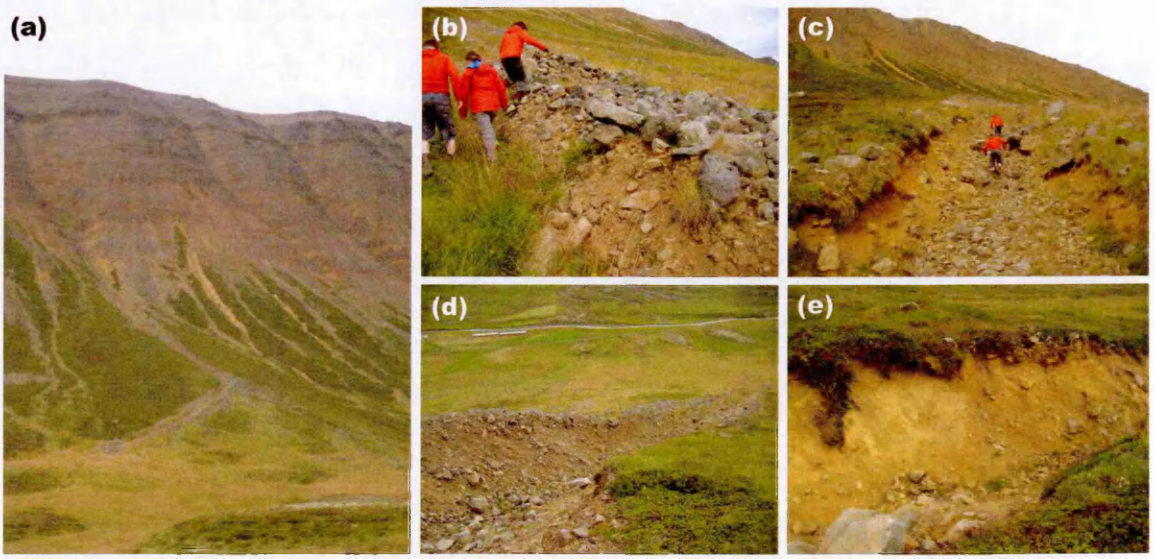

Figure 2.8: Debris flow gullies on the northern fell of Deildardalur, a) Several gullies incising the hillside. b) Levee of well mixed clastic material on edge of channel, c)-e) channel profile at three points along its course. The proportion of loose clastic material decreases towards the upper part of the feature and the channel becomes narrower.

The gully itself typically consists of a narrow channel several metres in width which extends for several hundred metres down the hillside. In the case of gullies carved by debris flows the channel is often flanked by steep levees. The channel of a gully frequently ends in a fan of deposited material where the gradient of the hill slope

decreases. Figure 2.8 shows field observations of gully channel morphology while Figure 2.10 illustrates the appearance of these features in aerial photographs.

Figure 2.9 is mainly occupied by the large alcove of the central gully which covers several square kilometres. Other smaller alcoves can be seen at the heads of the smaller gullies and some of these exhibit debris fans at their distal ends.

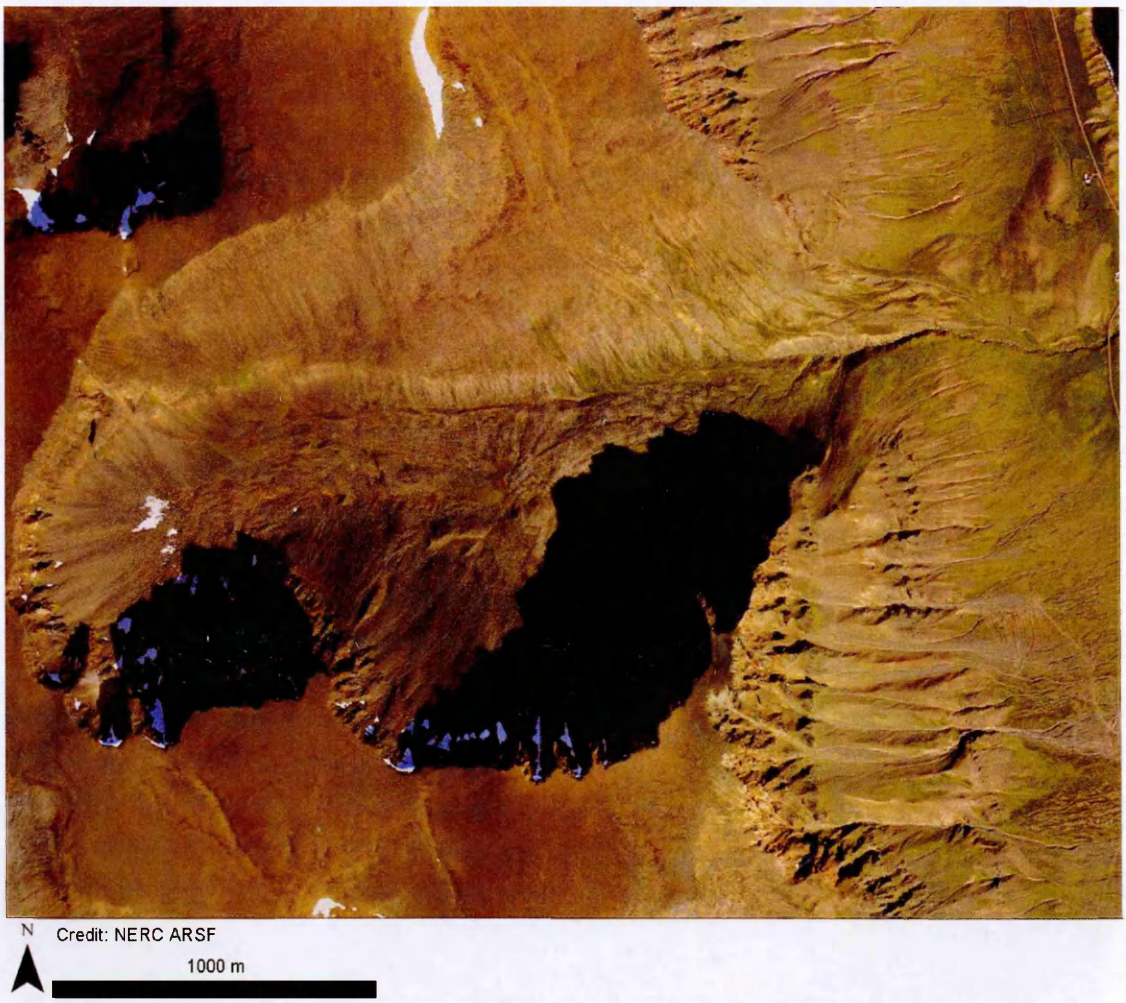

Figure 2.9: Gullies on hillsides in Skagafjörður Northern Iceland, the east side of Tindastóll (Aerial photograph by the NERC Airborne Research and Survey Facility, PI Susan Conway, funded by EUFAR).

Unlike the other features discussed in this chapter gullies are not periglacial in nature. Water is abundant in a terrestrial environment and gullies can be eroded by water from a variety of sources. They are included because in cold climate regions it is possible for similar processes to those associated with the formation of thermokarst pits to result in the formation of gullies. Gullies are thus often found in proximity to periglacial

assemblages. When sapping occurs on a steep, ice-rich hillside the released melt water and debris will flow down the slope eroding a gully into the side of the hill. Some gullies in Greenland and Iceland are believed to have formed in this way, as do small gullies on the sides of collapsing pingos.

2.4.3.1 Gullies on Mars

Gullies have been identified on the Martian surface in Mars Orbiter Camera (MOC) Narrow Angle images from the Mars Global Surveyor spacecraft (Malin and Edgett, 2000). They are found on a large number of crater walls and the sides of canyons. A large number of studies have mapped the distribution of these features (Balme et al., 2006; Dickson et al., 2007; Raack et al., 2012a; Soare et al., 2006). Martian gullies are believed to be among the youngest features on Mars due to their presence on young impact craters and dunes and the general lack of superposing craters (Heldmann et al., 2007). Martian gullies are often found in proximity to scalloped depressions, suggesting that the two features may form part of a periglacial assemblage (Soare et al., 2007). Thawing of near surface ground ice is one of the most common hypotheses to explain these features, in which case they could be closely related to thermokarst (Costard et al., 2002). Most gullies are either pole facing or equator facing and they appear to fall into two separate phases of gully formation. The older more degraded gullies are typically found on equator facing slopes between 40-50°, while younger, fresher features occur on pole facing slopes at lower latitudes, around 30-40 ° (Kneissl et al., 2010; Raack et al., 2012a). During periods of higher obliquity there would have been greater insolation on pole facing slopes. It has been suggested that this would have resulted in increased melting of ground ice, and consequently, enhanced gully formation (Costard et al., 2002), although the presence of brines in the near surface has been put forward as an alternative mechanism which could allow thawing to occur (Knauth et al., 2000).

A wide variety of alternate hypotheses have been suggested for gully formation which would not require the thawing of near surface ground ice. These include; eruptions of water from geothermaly heated aquifers (Gaidos, 2001; Hartmann, 2001; Mellon and Phillips, 2001), erosion by flows of carbon dioxide (Hoffman, 2002; Musselwhite et al., 2001), avalanches of CO_2 frost (Cedillo-Flores et al., 2011; Hoffman, 2002; Ishii and Sasaki, 2004), and dry granular flows (Shinbrot et al., 2004; Treiman, 2003). However thawing remains the dominant hypothesis.

The morphology of these features is most consistent with erosion by liquid water (Johnsson et al., 2014) and with formation as a result of multiple phases of activity (Schon et al., 2009). In addition to being found on crater walls they frequently occur in places where outflow from a subsurface aquifer would not be viable, such as at the crest of a dune (Costard et al., 2002; Mangold et al., 2003). Additionally the difference in volume between a typical gully's source region and the fan in which material is deposited suggests significant volumetric loss, an observation which is most consistent with the loss of water during or subsequent to the feature's formation (Conway and Balme, 2014).

2.4.4 Pingos

Frost mounds form when subsurface water freezes to form a massive ice deposit, deforming the overlying ground into a small hill. Many such mounds are small (a few metres across), transitory features. However, larger perennial frost mounds called pingos can grow to be up to 200 metres in diameter and 60 metres high (French, 2007). The term pingo derives from the local Inuit language of the region of north west Canada in which they were first described (Richardson, 1851) and studied (Mackay, 1988; Porsild, 1938). There are two types of pingos: hydraulic or open system, pingos and hydrostatic or closed system, pingos.

Figure 2.10: Pingos in the Canadian Arctic surrounded by scalloped lakes of probable thermokarst origin (Geological Survey of Canada).

Pingo summits are characterised by degradation and collapse features. Exposure of the ice core results in thawing and loss of material. If the ice lens thaws completely then the pingo will collapse resulting in a depressed feature called a pingo scar (French, 2003; Mackay, 1998).

2.4.4.1 Formation mechanisms

In a hydrostatic or closed system pingo, the formation of an ice cored hill results from the freezing of a layer of water called a talik. These are often found in the beds of drained or frozen lakes and so pingos often form in these environments. Taliks form due to the way in which freezing and thawing fronts propagate through a permafrost active layer. In the spring the active layer thaws from the surface down producing a considerable amount of liquid water. In the autumn and winter the active layer freezes again. The freezing front is also predominantly acting downwards from the surface,

and so a layer of water is trapped between the freezing front and the perennially frozen ground below. It is possible for a second freezing front to propagate upwards from the ice layer, but this process is less common (Corte, 1963). The further the freezing front progresses the greater the hydrostatic pressure on the interstitial water which freezes into lenses of massive ice, forcing the ground upwards (French, 2007; Mackay, 1998).

Open system pingos occur when their structure is maintained by hydraulic pressure. Open system Pingos often form in draining lake basins where the artesian pressure of water in the subsurface is sufficient to deform the ground as the water freezes to form an ice core (French, 2007; Soare et al., 2005).

2.4.4.2 Pingos on Mars?

A number of domes and hills across the martian surface have been identified as being morphologically similar to terrestrial pingos. Features in Utopia Planitia, Cydonia Mensae and Gusev Crater have all been suggested to be putative martian pingos (Burr et al., 2009; Depablo and Komatsu, 2009; Dundas and McEwen, 2010; Dundas et al., 2008). These features are inferred to be young, partly due to the fact that little erosion is apparent, but also due to a lack of superposing small impact craters (Soare et al., 2005). Small mounds are often clustered in depressions as pingos are on Earth and are frequently seen in association with patterned ground (Soare et al., 2005). The tops of some of the features seem to have collapsed to form a crater like structure.

The presence of pingos on Mars would suggest the presence of lakes during the past as terrestrial pingos are generally associated with lakes and alases (Cabrol and Grin, 2002). Alternatively it might suggest the presence of shallow, contained groundwater which would allow open system pingos to form. It has been suggested that pingos could have formed after the evaporation of a northern ocean at a point in the past when Mars's climate was more hospitable (Parker et al., 1993).

However, it should be noted that pingos are equilibrium landforms. They are reliant on the action of liquid water and so can only form in an environment where thawing can occur on a regular basis. The life cycle of the pingo from the initial formation of an ice lens through growth and degradation to collapse can take more than a century. Some structures in excess of a thousand years old have been reported (French, 2007). However on a geological time scale these landforms are transient features dependant on the climate in which they are formed to maintain their structure. This means that their presence on the martian surface would theoretically indicate that water has been active on the surface, or at least in the near subsurface in the relatively recent past.

Current erosion rates on Mars are much lower than those found in wet terrestrial environments (Golombek and Bridges, 2000). This could dramatically increase the lifespan of otherwise transitive features. Even so, features with a lifespan on the order of decades to centuries would still not be expected to remain pristine for millennia.

Another complicating issue is that mounds with dimensions similar to terrestrial pingos can occur through a number of processes. Without ground truth observations can be difficult to tell whether a cratered mound is the result of periglacial processes or whether it has a volcanic origin (Jaeger et al., 2007; Martínez-Alonso et al., 2005) Pingos often exhibit prominent radial cracking, which can distinguish them from rootless cones (Page and Murray, 2006) in other respects their morphologies are similar. Some of the features which have been suggested as putative pingos are also good candidates for mud volcanism (Farrand et al., 2005).

Pingos will not be a major focus of this investigation. Even on Earth they are noted to have a wide variety of morphologies, with many features not appearing much like the type examples described above. Their main distinguishing characteristic; that they have an icy core, is hard to test for martian features. Furthermore the features most likely to

be found on Mars would be pingo remnants, which can be difficult to identify in the field in terrestrial environments, much less using remote sensing data in the absence of ground truth.

2.4.5 Patterned Ground

One of the most distinctive landforms to be found in a periglacial environment is polygonally patterned ground. Various different processes can result in the formation of polygonal networks, some of which are periglacial, while others do not require thawing to occur (Washburn, 1956). Thermal contraction cracking, sublimation polygons and sorted patterned ground will all be discussed. Sorted patterned ground is the most significant for this investigation as it evolves due to the repeated freezing and thawing of the permafrost active layer and is characteristic of a periglacial environment. Its presence indicates the action of liquid water in the geologically recent past.

2.4.6 Thermal Contraction Cracking

Thermal contraction cracking in ice-rich permafrost zones occurs due to repeated temperature changes, but does not require the action of liquid water per-se. Consequently, it can occur in very cold and dry environments where the temperature rarely if ever rises above zero °C.

Changes in temperature result in very small amounts of expansion and contraction of solid materials. As the temperature drops the material will contract slightly and this will induce tensile stress. If the tensile stress due to contraction exceeds the tensile strength of the material then cracking will occur, releasing the tension and deforming the ground surface (French, 2007; Lachenbruch, 1962; Leffingwell, 1915).

In a rocky soil where the tensile strength of the material is very strong this is unlikely to cause significant cracking. However, ice undergoes much more expansion and contraction than rock does and it has a lower tensile strength so fractures form more readily in sediments with very high ice content.

Thermal contraction cracks form on a range of scales; newly formed cracks are typically two cm wide and ten cm deep, extending for many metres laterally. In a heterogeneous soil different regions will contract at different rates and so more stress will occur in some areas than in others. Multiple cracks form perpendicular to a region of high stress and expand, both extensionally and in width, until the ends of the cracks meet and polygonal cells are formed (French, 2007)

Cracks do not remain pristine and clear, but soon fill with 'wedges' of other material such as sand and water (which in turn can freeze into ice). As ice wedges expand and more loose material accumulates in and around the cracks a raised "shoulder" can form at the rim of the polygon giving it a "low-centred" appearance. Expanding wedges open the cracks further and cause them to propagate downwards through the soil, increasing the size of the fracture (Leffingwell, 1915). Polygons frequently form polygonal structures 10-35 m in diameter, their formation requires many cycles both of expansion and contraction and accumulation of material. Consequently, it can take many years for a fully developed ice wedge polygon to form. They remain stable for long periods of time, with many of those seen in Arctic North America and the UK believed to have formed during the Pleistocene.

2.4.6.1 Sublimation Polygons

In environments where sublimation is a dominant process contraction cracks can expose underlying ground ice to degradation. The ice around the cracks sublimatess forming wide troughs several meters wide and deep. The ice in the centre of the

polygons remains protected from sublimation by overlying soil. Consequently, they tend to form high centred polygons in contrast to those with large stable ice or sand wedges (French, 2007; Marchant et al., 2002).

The extent of sublimation is very dependent on the amount of insolation the ground in an area receives. This can lead to asymmetrical features where the equator-facing slope of a trough receives more sunlight, undergoes more sublimation and so is not as steep (Levy et al., 2008). On Earth, thermal contraction cracking occurs in areas where the soil is saturated with ice, but where seasonal thawing cannot take place and sublimation processes predominate.

One of the best examples of this terrain is Beacon Valley, one of the Antarctic Dry Valleys, which is often used as an analogue environment for Mars research (e.g. Levy et al., 2009; Marchant et al., 2002). Many of the polygons in this region show evidence of sublimation processes, being surrounded with deep trenches and having an asymmetrical profile. These landforms are similar in form to many polygonally patterned grounds on Mars. Sublimation can also generate pockmarked terrain covered with small pits where isolated patches of exposed ice have sublimated away (Soare et al., 2008).

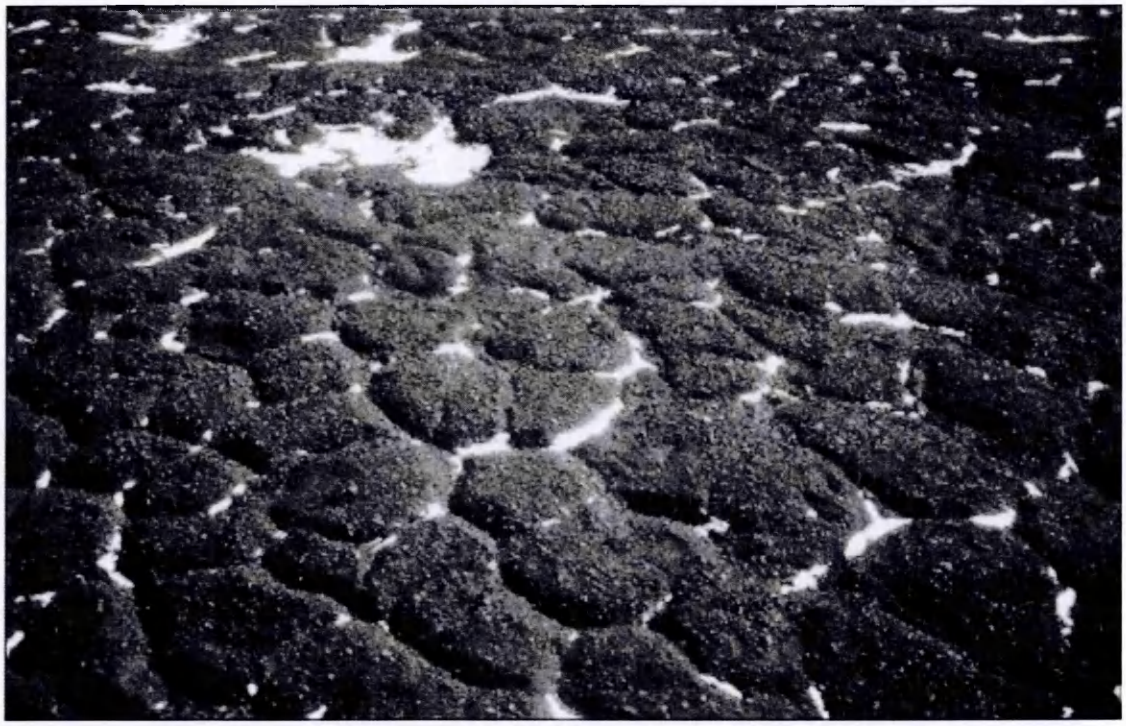

Figure 2.11: Sublimation polygons in Beacon Valley, Antarctica. These polygons are surrounded by deep troughs which have been generated by sublimation of the underlying ground ice as it is exposed by contraction cracking. The polygons are around 20 m in diameter (from Marchant et al., 2002, **fig 4)**

2.4.6.2 Thermal contraction cracking on Mars?

Fracture polygons are very common at high latitudes on Mars (Levy et al., 2010; Mangold, 2005; Mellon, 1997). These structures occur on a variety of scales ranging from small, 10-20 m diameter polygons to larger scale features up to 100 metres across. Many of these features are similar in scale to terrestrial analogues, suggesting that fracturing of ground ice is a likely candidate for their formation. A variety of studies have mapped polygon distribution in both the northern and southern hemispheres (Langsdorf and Britt, 2004; Levy et al., 2010; Mangold, 2005; Mellon, 1997), classified different polygon types (Kuzmin et al., 2002; Langsdorf and Britt, 2005; Joseph S. Levy et al., 2009; Mangold, 2005; Mellon, 1997) and determined automatic systems for polygon recognition. (Pina et al., 2008)

Giant polygons several kilometres across are also observed. These giant polygons are far larger than any features associated with periglacial landscapes on Earth. While it is possible that the environmental conditions on Mars allow for larger polygon growth (Mangold, 2005), many researchers are sceptical that these are periglacial features (Hiesinger and Head, 2000; Mcgill, 1986). The smaller scale features will be the focus of this investigation, with fracture polygons larger than a few hundred metres disregarded as possible periglacial landforms.

Small scale fracture polygons have a variety of different morphologies. The networks themselves are categorised based on their geometry. Some groups of fractures form hexagonal or rectilinear patterns while others exhibit a "random-orthogonal" arrangement where the fractures intersect at a variety of angles (Mangold, 2005). The majority of polygons assume a hexagonal or random-orthogonal pattern, but many regions of rectilinear fractures have been observed (Kuzmin et al., 2002; Langsdorf and Britt, 2005; Mangold, 2005). Smaller polygons, comparable in size to those found on Earth have also been detected and are more likely to be periglacial in origin.

Polygonal structures can be characterised by whether they are high or low centred. High centred polygons consist of a block of un-eroded ground surrounded by deep fractures or troughs. Low centred polygons have the opposite morphology. These occur where the fractures have become in-filled with sand or ice wedges, which are forced up by the repeated opening and closing of the fractures. In these cases the polygonal rim is higher than the polygon interior. Similar structures can be seen in terrestrial periglacial environments, so low centred polygons are a useful marker of possible ice wedge accumulation. These features are believed to be relatively recent, as they occur on all surfaces, have few superposed impact craters, and have been observed to overly gullies in some regions.

Sometimes cracks develop polygon junction pits, where enhanced sublimation occurs at the exposed corners of the polygons (Séjourné et al., 2010). Sublimation pitting has been observed between 40-60°N on Mars where the near surface ground ice is not very stable. It does not require the presence of a fracture pattern, but fracturing exposes subsurface ice to sublimation. Polygon junction pits are found in areas of polygon covered ground across Utopia Planitia (Séjourné et al., 2010). Both high and low centred polygons are found in this area, so it is possible that a suite of processes including thermal contraction cracking, sublimation and sand or ice wedge accumulation are involved in the formation of these features.

There is considerable debate as to whether the polygons observed in Utopia Planitia are periglacial in origin. While they could represent the results of periglacial processes (Levy et al., 2010; Mangold, 2005) it has also been argued that the cracks were formed by the cooling of flood lavas (McGill, 1986) . This explanation is unlikely to explain the small scale features being considered in this investigation and has been discounted by Levy et al., (2010) and Mangold, (2005).

The young age of the smaller polygons also suggests a periglacial origin. Many of the polygons have formed within impact craters and can be seen to be eroding the crater structure. This means that their earliest formation dates can be estimated, since a polygon that superposes an impact crater must be younger than the cratered terrain. Many appear to have formed during the Amazonian (Morgenstern et al., 2007). This makes a volcanic explanation less likely as volcanism would be unlikely to have been occurring this late in martian history, and wouldn't be expected to overlie the most recent craters.

2.4.7 Sorted Patterned Ground

Sorted patterned ground is frequently found in periglacial landscapes on Earth. Fine grained soils are separated from coarser stones and gravels, resulting in patterns such as stripes, circles and polygons where bands of larger stones surround a mass of finer soil. The inverse effect can also occur, resulting in discrete zones of course materials surrounded by finer sediments.

This sorting is the result of cryoturbation, the movement of the soil by the repeated freezing and thawing of interstitial water (Corte, 1963; Kessler and Werner, 2003; Kessler et al., 2001; Krantz, 1990). Since sorted patterned ground results from a freeze thaw cycle it can only occur in an environment where the ground ice regularly undergoes thaw. On Earth sorted patterned ground is reasonably common in permafrost rich areas such as the Canadian Arctic, northern Greenland, Iceland and Spitsbergen (Feuillet et al., 2012a; French, 2007; Washburn, 1956).

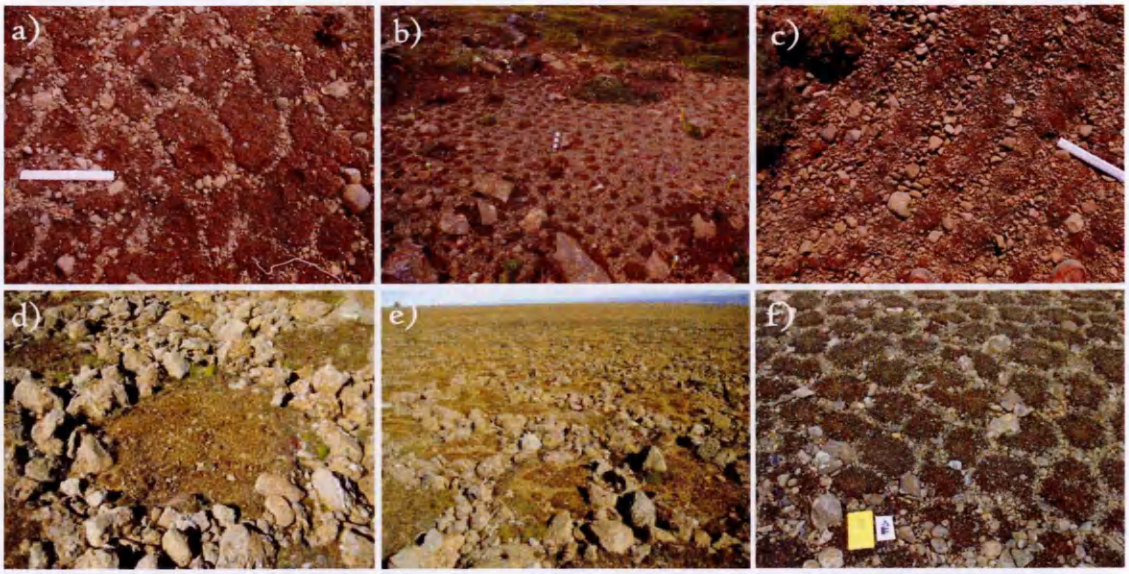

Figure 2.12: Examples of sorted Patterned ground in Iceland. A variety of different pattern morphologies are illustrated; a) Sorted polygons grade into a discontinuous net, b) Small fine domains surrounded by large coarse areas, c) Stripes of large stones are interspersed by bands of smaller material, d) Metre scale sorted polygon comprised of 10 cm scale coarse material, e) Sorting on multiple scales, centimetre scale patterned ground within metre scale polygons. F) Clear cm scale polygonal net (photos a-c by Chris Barrett, d-e Alex Barrett, f Susan Conway and Andrew Wilson).

As cryoturbation occurs larger particles are moved further from their source area than finer particles and so regions of differently sized material are formed, resulting in a positive feedback loop. A range of factors such as the gradient of a hill slope can result in more complicated structures such as stripes, polygons and labyrinths of sorted stones (Kessler et al., 2001; Krantz, 1990; Washburn, 1973, 1956).

In an unconstrained setting material will be displaced uniformly and sorted circles will form. In general this is rarely the case. Sorted structures forming in close proximity will constrain each other's development and so a network of interconnected polygons will form. Sorted stripes occur on shallow hillsides. The gradient of the slope causes changes to the drainage across the feature and the preferential movement of displaced material in one direction. Consequently, sorted polygons elongate, as more material translates down slope these features will develop into true sorted stripes (Krantz, 1990).

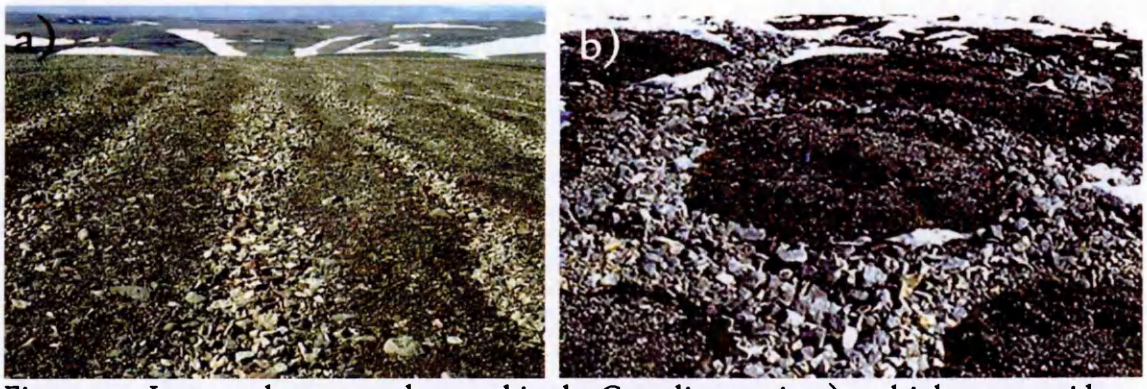

Figure 2.13: Large scale patterned ground in the Canadian arctic; a) multiple metre wide sorted stripes, b) very large scale sorted circles approximately 20m across. (Geological Survey of Canada)

The mechanisms involved in the formation of sorted patterned ground are not well understood. It is believed that they are polygenetic, and that a range of processes including frost heaving and frost creep all have a significant role in the sorting process (Washburn, 1956).

2.4.7.1 Frost Heaving.

Frost heave results from the growth of ice lenses within the soil. Unfrozen ground water is drawn up through the frozen fringe by hydrostatic forces, and forms ice crystals. These grow as more water is drawn up, until a solid lens of ice is formed. The accumulation of subsurface ice lenses can force the entire ground surface to rise, resulting in frost heaving (French, 2007). In a non-homogenous soil, regions of differently sized material are affected differently by the freezing of ground water. A freezing front propagates faster through an area of coarse material such as large stones than it does through a mass of finer soil, as there is less moisture in coarse or stony regions (Corte, 1963; Kessler and Werner, 2003). In a vertical profile larger stones will be brought to the surface, while finer soil particles are transported downwards by the percolation of water through the soil, a process called illuviation (Corte, 1963; Kessler and Werner, 2003).

Over a series of freezing and thawing cycles different grades of particles are gradually separated. A positive feedback then occurs as some regions become dominated by fine grained material while coarser particles accumulate at a different level within the soil profile. This feedback process encourages the preferential accumulation of the same grade of particle in each region of the soil profile.

2.4.7.2 Sorting through differential frost heave.

Frost heaving is central to the formation of sorted patterned ground. When the active layer freezes the formation and growth of coherent lenses of ice within the soil results in the deformation of the surface. On a large scale, expanding ice lenses can force the entire ground surface to rise and lead to the formation of domes (French, 2007). On a smaller scale the difference in heave between the centre of a fine domain and its edge is less pronounced, but is still sufficient to cause sorting to occur.

Since fine grained material is generally more frost-susceptible than coarse grained material it is these regions which undergo the most heaving. Regions of predominantly fine grained soil will expand, pushing stony material to the edges. Were a single fine domain to expand outwards into a stony region it would produce a circular structure, a ring of stones surrounding a fine grained region. In areas where multiple fine domains are heaving they compress the coarse material into increasingly thin bands of stones. A polygonal network develops consisting of thin stony borders surrounding regions of fine grained soil. The gradient between the centre of a region of heaving soil and its edge results in surface creep. Loose stones, whether on the surface or lifted by needle ice will be displaced away from the centre of the region of heaving and towards the stony borders (Kessler et al., 2001). A particle lifted up by frost heave is moved perpendicular to the ground surface. However when thaw occurs a raised particle will fall back down in the direction of gravity. When this process occurs on a slope there is a net movement of particles downhill (French, 2007). Larger particles are subject to a greater displacement by surface creep while finer material will tend to settle into the space left by the larger stones (Kessler and Werner, 2003).

A number of distinctive structures such as stripes, circles, polygons and labyrinths form as a result of these sorting processes; the more complex shapes being the product of the interaction between vertical and lateral sorting (Kessler and Werner, 2003). The complexity of the surface pattern depends upon the gradient of the slope and the distribution of material of different frost susceptibility within the soil.

2.4.7.3 Sorted patterned ground on Mars?

There is evidence that sorting has taken place on Mars in geologically recent times. Putative patterned ground has been identified at low latitudes in Elysium Planitia (Balme and Gallagher, 2009) and at high latitudes in Heimdal Crater (Gallagher et al.,

2011), and across the Vastitas Borealis (Gallagher and Balme, 2011; Orloff et al., 2011). There are some regions where hillside stripes have been interpreted as a possible expression of sorted patterned ground, as they appear to evolve from polygonal networks on flat ground into stripes on the steeper slopes. However the presence of clasts was not positively identified for these sites as the observations predated the arrival of the high resolution HiRISE camera on Mars Reconnaissance Orbiter (Balme et al., 2013; Mangold, 2005).

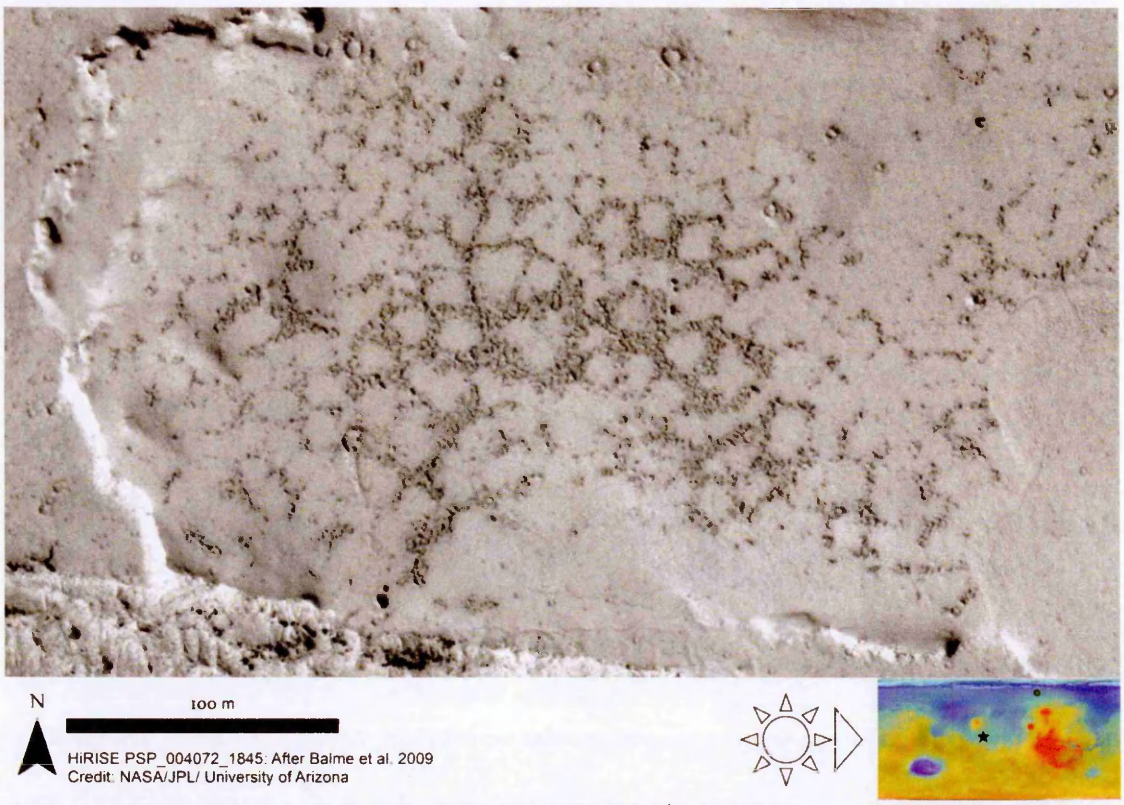

Figure 2.14: Clastic polygons in Elysium Planitia (After Balme and Gallagher 2009, HiRISE image PSP_004072_1854 NASA/JPL/University of Arizona)

There is debate as to how these sorted features were formed. It is possible that they formed during periods of high obliquity, through freezing and thawing, possibly facilitated by cryobrines (Gallagher and Balme, 2011). However it is also possible that a more exotic process is responsible for their formation and that their similarity to terrestrial periglacial structures is misleading.

It has been suggested (Orloff et al., 2011; Orloff et al., 2013) that boulder clustering could result from "ratcheting" without any thaw processes. In this hypothesis, during the winter boulders become trapped in a thick layer of CO_2 frost and are moved along with the contracting ground. During warmer periods the CO_2 frost has sublimated and the boulders are no longer as tightly locked as the frozen ground. The boulders now move freely as the ground beneath them expands and so there is a net displacement over several of these cycles.

There is no terrestrial analogue for this process, and it remains unclear whether it could be responsible for the arrangement of boulders on the northern plains of Mars. Without in situ observations it is impossible to be certain whether such features formed as a result of periglacial processes. However evidence for a periglacial origin can be drawn from sites where these features occur in proximity to other putative periglacial landforms.

2.5 Summary

In summary the terrestrial periglacial landscape may be a useful analogue for a variety of unusual martian features. On Earth periglacial features are found across the cold climate regions where permafrost is present, but surface temperatures are frequently warm enough to melt an active layer. Active layer processes produce a range of distinctive features including thermokarst, solifluction lobes, frost mounds and patterned ground.

3 Chapter Three: A Periglacial Environment on Mars?

As outlined in Chapter Two periglacial features are defined based upon formation mechanisms which require the action of liquid water. Consequently, if the similar features observed on Mars are periglacial in nature then it would provide useful information on the conditions under which they evolved. Determining whether this formation hypothesis holds true requires a detailed comparison of morphologies between the equivalent landforms.

This investigation primarily builds upon the work in the geomorphology studies cited above to assess whether the structure and distribution of certain landforms, particularly scalloped depressions and sorted patterned ground, fit with a periglacial hypothesis. However it is first important to consider the likelihood that a periglacial environment is viable on Mars and under what conditions it is most likely to be found.

The question of whether periglacial conditions are possible on Mars is a matter of some debate. These features could have formed during a past period of higher obliquity or within a specific microclimate where unusual temperature extremes are possible. It has also been theorised that the presence of cryobrines, with low eutectic temperatures, could allow the action of periglacial processes at low temperatures where water would ordinarily be expected to be frozen. These topics will be discussed in more detail throughout this chapter.

A laboratory study was also conducted as part of this project. It was intended to provide an experimental "proof of concept" that the freezing point depression effect associated with the presence of cryobrines could allow periglacial processes to occur. However this strand of the investigation proved inconclusive and so will not be

discussed in great detail here. Full details of the work conducted are presented in Appendix One.

3.1 Identifying Periglacial Landscapes

As discussed throughout the preceding chapter, landforms with a similar morphology to terrestrial periglacial features have been observed in a variety of satellite images of the martian surface. Putative features have been found which match the morphologies of all of the common periglacial landforms described above.

Gullies, which could result from the thawing of near surface ground ice, have been observed at mid to high latitudes across both the northern and southern hemispheres (Balme et al., 2006; Dickson et al., 2007; Malin and Edgett, 2000). Scalloped depressions that have morphologies similar to terrestrial thermokarst basins are found across Utopia Planitia (Costard and Kargel, 1995; Soare et al., 2008). Sorted patterned ground and pingos have been proposed in Elysium Planitia (Balme et al., 2009) and in the Vastitas Borealis (Gallagher and Balme, 2011) and unsorted fracture polygons, which could be the surface expression of buried ice wedge polygons, are reported across the Northern Plains (Levy et al., 2009; Mangold, 2005; Mellon, 1997). Lobate features similar in form to terrestrial solifluction lobes are also observed (Gallagher et al., 2011; Johnsson et al., 2012).

These and other studies provide a variety of evidence for a putative periglacial environment on the Northern Plains of Mars in the geologically recent past, but while the periglacial hypothesis is a plausible explanation for these features it is not the only one.

3.1.1 Equifinality

Even though features may have a similar morphology it does not necessarily follow that they formed as a result of the same process. Numerous hypotheses can explain the morphology of a given landform and in the absence of ground truth such hypotheses can be difficult to test except where morphometric tests can unequivocally distinguish them. It may be impossible to determine with complete certainty whether the observed features are products of a periglacial environment without actually examining them in the field. Alternate formation mechanisms have been discussed in more detail in the sections on each individual landform throughout chapter two.

3.1.2 Landform Assemblages

The most compelling evidence for a periglacial environment comes from places where a suite of potentially periglacial landforms occur in close proximity. An assemblage of landforms is a suite of features which appear to have formed at a similar time, and through related processes. They probably formed under the same climatic conditions and form part of a coherent landscape. For example on Earth the formation of pingos and thermokarst lakes are closely related; they are often, though not exclusively, found together. Consequently, a group of Martian pingo like mounds found in close proximity to scalloped depressions are arguably more likely to be periglacial in nature than if they were found in isolation. Landform assemblages provide a more reliable indicator of periglacial activity than individual landforms.

3.2 Periglacial Processes

As described in Chapter Two a permafrost environment consists of ground which is perpetually frozen, with the exception of a thin active layer up to one metre deep which freezes and thaws on a seasonal cycle. Thawing occurs from the surface down due to

both heating from rising air temperature and due to direct insolation (Washburn, 1973). The frost table descends to the base of the active layer at the warmest part of the year leaving a layer of water-saturated soil. As temperatures begin to cool again the active layer refreezes, both upwards from the frost table and downwards from the ground surface (Mackay, 1984). This process is illustrated in Figure 3.1.

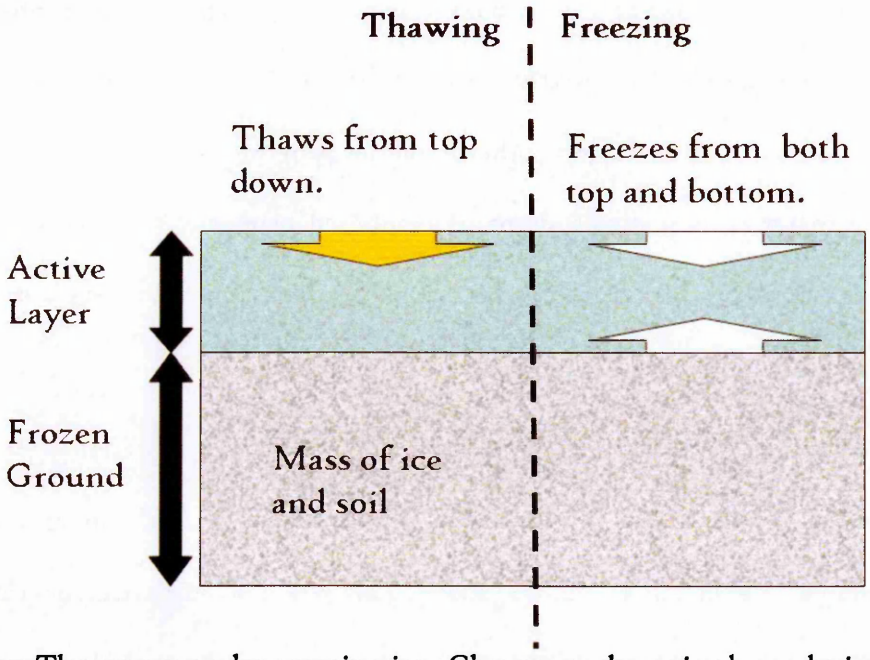

Figure 3.1: The system under examination. Changes to the active layer during thawing and freezing stages of the seasonal cycle.

In a pure water system the downwards freezing front would consist of a zero °C isotherm. In any system where salts are present the temperature of this isotherm will be considerably lower. This freezing front will initially advance through the ground parallel to the surface. However, many factors can result in variations in this front and it will most likely advance at different rates into the soil, depending on local conditions. Factors such as the degree to which the surface is insulated will also have an effect on the morphology of the initial freezing front. The upwards freezing front will likewise be affected by variations in the height of the summer ice table. Once freezing begins the zero degree isotherm will quickly become even more irregular since it will

not travel through the unfrozen ground at a uniform rate, but will move faster through some regions and slower through others.

The rate at which the freezing front penetrates the ground is dependent on a variety of factors. Coarse and fine materials have different physical properties. A coarse grained soil has a lower specific heat capacity than the equivalent volume of fines (e.g. Abu-Hamdeh, 2014), so the freezing front would be expected to propagate faster through this region. This was observed by Matsuoka et al., (2003) in their experimental studies. They reported that the zero degree isotherm did not penetrate as far into regions capped with coarse material as it did in domains composed primarily of finer grained soil. Since the fine domains are the frost-susceptible fraction this results in a differential frost heaving, which may set the sorting process in motion.

The thermal properties of the different materials are not the only factor affecting the propagation of the freezing front. Fine grained regions will retain more water than coarse domains (Kessler and Werner, 2003). This has a strong effect on the rate of freezing, since the energy required to cool the dry regions is substantially less than that required to initiate a phase change in the saturated soil. In a system where this factor dominates, the zero degree isotherm will propagate faster through stony regions than through fine domains.

Consequently, the freezing front is expected to be irregular in the majority of cases, although the precise speed of penetration will likely vary from site to site, depending on the thermal properties of the substrate and the saturation of the soil (Nicholson, 1976). Changes in the angle of the freezing front will result in differential heaving across the feature and be instrumental in setting up lateral sorting within the soil as well as vertical stratification of differently sized particles (Matsuoka et al., 2003). As

ice lenses form the surface heaves and this enhances the perturbations in the freezing front described above, creating a positive feedback loop.

3.2.1 The formation of ice lenses

The frost heave process is the result of the formation of lenses of coherent ice within the soil. As a soil freezes, cracking will occur and a small amount of segregated ice will form within the crack. The freezing front will extend below this, creating a region called the frozen fringe (Millar, 1972). In the frozen fringe, water-filled pores freeze but the presence of air filled pores means that supercooled groundwater, kept liquid by the confining pressure, can still be drawn upwards by capillary action. This water is drawn to the base of the newly forming ice lens, adding to the volume of segregated ice. As the freezing front advances a stack of such lenses will form, with active accumulation occurring at the lowest, warmest lens. The fact that this occurs in a thin active layer surrounded by ice means that the hydraulic conductivity of the frozen fringe is very low. Water cannot easily drain through this region and it remains largely saturated until freezing is complete.

Ice lenses have been produced in the laboratory under conditions typical for the terrestrial arctic (Konrad, 1988; Penner, 1986). Ice lens formation is dependent upon a number of factors, including the frost susceptibility of the soil (dependent on the size of the particles and the size and percentage of void space), the availability of water, and sufficient time for a slow freezing front propagation through the soil column (Bronfenbrener and Bronfenbrener, 2010; Konrad, 1989a; Taber, 1929).

3.3 Periglacial Processes on Mars

For periglacial environments to be reliably identified on Mars, it must be demonstrated that the landforms observed could have formed under periglacial conditions. This

requires the presence of permafrost in these areas, and the conditions necessary for thawing to occur in the upper metre of the soil. Consequently, the stability of liquid water under martian temperature and pressure conditions is of vital importance when considering the viability of a periglacial hypothesis. If water cannot melt from its solid state then a permafrost active layer cannot form and cryoturbation, solifluction and many of the processes associated with periglacial environments also cannot occur.

3.3.1 Presence of Permafrost

On Mars there is evidence for the presence of ground ice near the surface at mid- to high-latitudes, and deeper within the ground at lower latitudes (Boynton et al., 2010; Feldman et al., 2004). The gamma ray and neutron spectrometers on the Mars Odyssey spacecraft have confirmed the presence of high concentrations of hydrogen in areas where ground ice was predicted to be stable at or near the surface by climate modelling (Feldman et al., 2002). The distribution of patterned ground, thought to have formed by thermal contraction processes in ice-rich sediments, also matches the distribution of near-surface hydrogen as measured by Mars Odyssey (Mangold et al., 2004).

The presence of volatiles is also evidenced by the existence of 'softened' terrain, where the ejecta deposits created by large impacts have been deformed by the mobilisation of volatiles (Barlow, 2009; Costard, 1989). Excess ejecta craters, where an ice-rich layer is believed to be covered by crater ejecta and prevented from being lost to the atmosphere as climate change occurs (Black and Stewart, 2008) also provide evidence of ground ice distribution.

Large swathes of the martian northern plains, as well as large areas at high southern latitudes, appear to be covered by an ice-dust mantle known as the Latitude Dependent Mantle (LDM) (Kreslavsky and Head, 2002; Mustard et al., 2001). This may have been emplaced by aeolian processes; the material having been transported from the polar

caps during periods of higher obliquity and deposited across the mid to high latitudes (Black and Stewart, 2008; Head et al., 2003; Kreslavsky and Head, 2002). It is likely that the development of this mantle was strongly obliquity driven; as evidenced by the fact that it is currently undergoing degradation at lower latitudes (Schon et al., 2012).

During the last period of high obliquity (at approximately 2.1 to 0.4 Myr) the martian poles received more insolation than is presently the case. Under these conditions the Polar Regions would have been warmer, leading to increased loss of water to the atmosphere, and its transport to and deposition at lower latitudes. It would have been deposited across the mid to high latitudes creating a regional mantle. (Head et al., 2003; Kreslavsky and Head, 2002).

Geomorphological evidence for large amounts of ground ice has also been observed on regions of the northern plains near the termination of outflow channels. Massive outflow events from the Chryse and Elysium channels could have deposited ground ice in regions which are more southerly than those covered by the LDM (Costard and Kargel, 1995).

These areas of martian ground ice may be similar to the areas of extensive ground ice found in permafrost environments on Earth, and it is possible that under the correct temperature and pressure conditions a dry active layer could have been produced (Kreslavsky et al., 2008). Wet active layer processes would be unlikely even during periods of higher obliquity when the climate is warmer and wetter in the summer, It would also have been colder during winter during such periods.

3.3.2 Thawing of an Active Layer?

The current martian climate is very cold and dry. The mean surface temperature is around 210 K, and ranges from 140-300 K (Kieffer et al., 1992). Thus it can be seen that while the average is far below the freezing point of water, temperatures at which

thawing of ice is possible do occur. Atmospheric pressure at the surface is of the order of 560 Pa (Kieffer et al., 1992). The stability of water under different partial pressure and temperature conditions can be shown using its phase diagram.

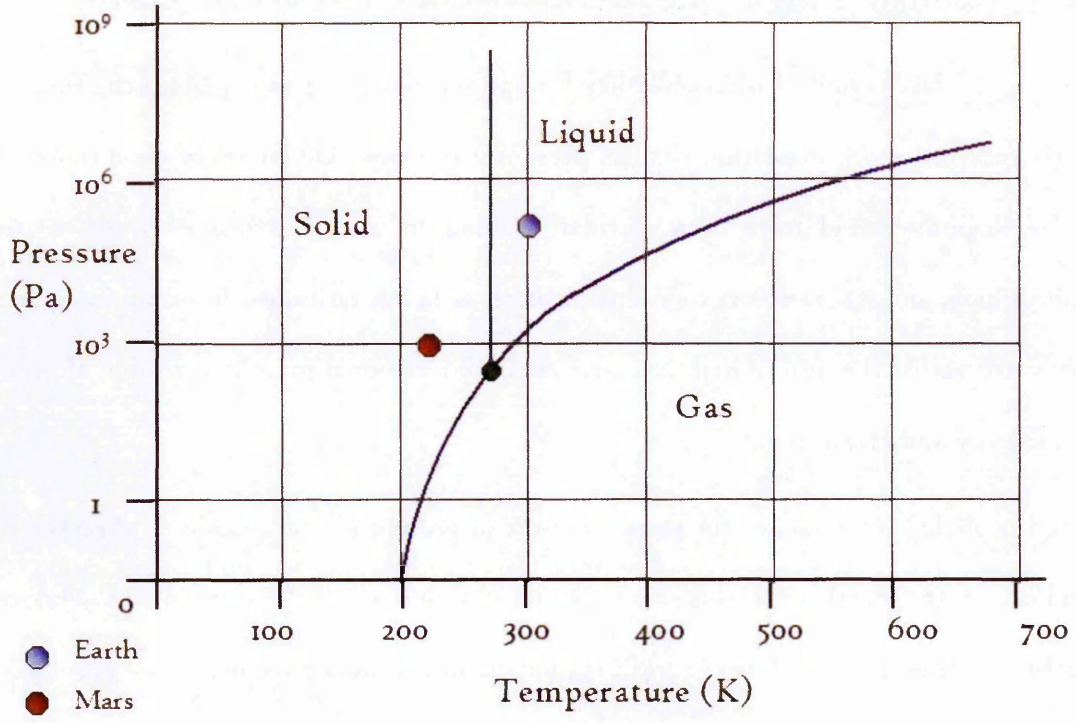

Figure 3.2: Phase diagram for pure water, annotated with the average temperature and pressure conditions for Earth and Mars.

On Earth the mean temperature and pressure conditions are close to the triple point of water. Consequently, water can exist in all three phases on the surface of Earth. On Mars although the temperature and pressure is quite variable the mean conditions plot mostly within the solid and vapour regions of the phase diagram. Any liquid water released onto the surface will quickly freeze, boil or evaporate entering the more stable solid and gaseous phases. Consequently, liquid water can be said to be metastable under martian conditions; it will not remain in its liquid state for very long, but its presence in this state is certainly possible under extreme conditions and for limited periods of time (Bargery et al., 2010; Carr, 1983; Hecht, 2002; Wallace and Sagan, 1979).

The most frequent places where temperatures will rise above the freezing point of water are those that receive a large amount of insolation. It has been suggested that pole facing slopes would have been a good candidate for thaw during periods of higher obliquity. The number of locations where liquid water is expected to be stable is much lower in the modern day. Stable water is more likely at low latitudes than high. It is possible for liquid water to be stable, at least temporarily, during the warmer seasons in the region between 0° and 30° latitude (Haberle et al., 2001). It would not be expected to be stable for very long at latitudes further north or south than 30°. At mid to high latitudes the temperature and pressure conditions are more favourable to the stability of ground ice than liquid water.

The longer liquid water is exposed to the martian environment the more heat it will lose; both due to contact with its cold surroundings and through evaporative cooling. The low atmospheric pressure means that water will readily evaporate and this removes heat from the system. Sufficient energy needs to be present to overcome the evaporative cooling effect keeping the water in a liquid state long enough for it to have a geomorphic effect.

Under these conditions a large body of water will be stable for longer than a small amount. It has been suggested that ice could form on the surface, creating a more stable environment for the water trapped below (Wallace and Sagan, 1979). However, the models of Haberle et al., (2001a) suggest that only thin films of water will be likely to form. This is supported by studies of freezing point depression effects such as those of Sizemore et al., (2014) which suggest that thawing would be limited to thin films even under the most favourable of conditions.

The availability of unfrozen water within the soil column is one of the most critical factors. If the soil freezes too quickly then a frozen fringe will not develop and if there

is insufficient water within the active layer to begin with then ice segregation will be unlikely to produce a large lens. Consequently, one of the most important factors when considering periglacial processes on Mars is the ability for thawing to take place.

3.3.3 Climatic Variations

Although liquid water is only metastable at the martian surface (e.g. Hecht, 2002), this does not rule out a periglacial explanation for the landscape of Mars' northern plains. It is possible that these features could (i) be examples of a relict periglacial environment which formed during a period when the climate was warmer and wetter during the summer, (ii) form only in localised microclimates, (iii) occur only in places where the presence of concentrated salts in the near surface depresses the freezing point of water sufficiently to bring it in line with ambient martian temperatures, or (iv) occur only in places where seasonal warming causes the surface temperature to rise above the freezing point during the warmest parts of the year.

3.3.4 Thaw at Higher Obliquity

It is possible that the landforms being examined are the results of periglacial processes, but that they are relict landforms which formed when different climatic conditions prevailed. It is known that the obliquity of Mars has varied significantly over time (Laskar et al., 2004). The current obliquity is much lower than it was in previous epochs. This results in a lower mean insolation at mid to high latitudes and will have an effect on the planet's mean surface temperature as a function of latitude (Laskar et al., 2004; Mischna et al., 2003). Figure 3.3 shows the variation in obliquity over the last 20 Ma predicted by Laskar et al., (2004)

During periods of higher obliquity the climate would have been warmer, and water would have been less unstable across larger areas of the surface. It has been suggested

that some observed landforms which would require the action of liquid water could have been formed at this time (e.g. Costard et al., 2002). Kreslavsky et al., (2008) suggests that it would have been possible for an active layer to form at high latitudes and on pole facing slopes during approximately 20% of high obliquity excursions between 5 and 10 Ma. However they conclude that such environments have not formed for up to five Ma.

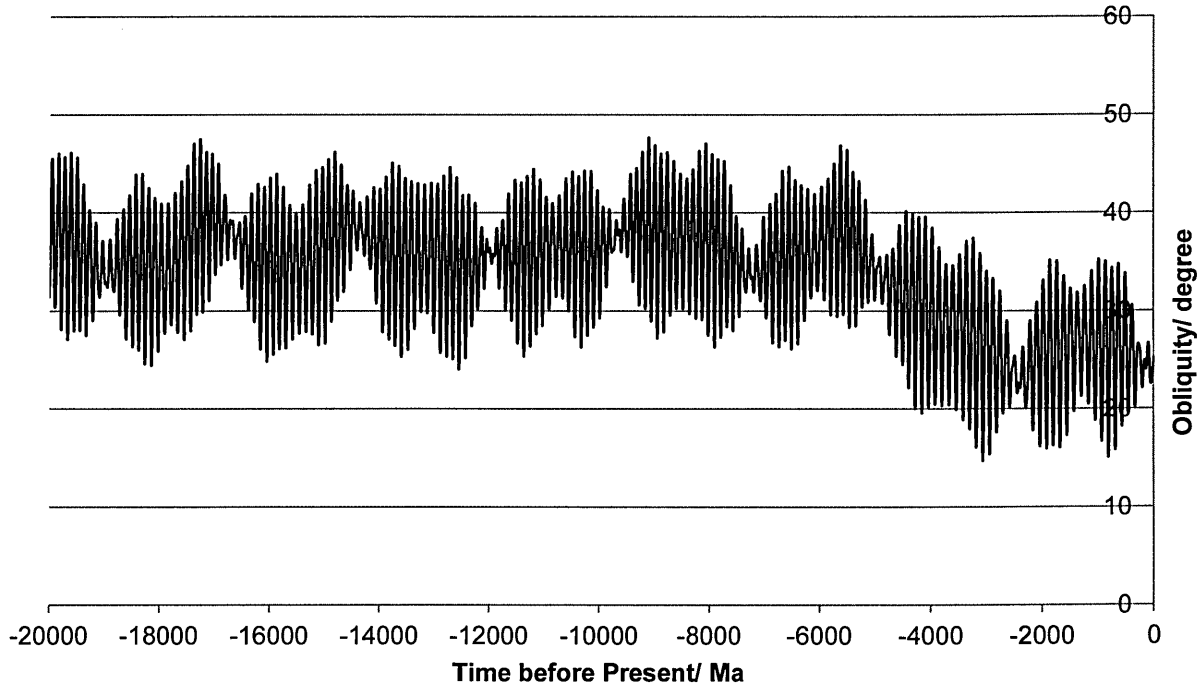

Figure 3.3: Variations in the obliquity of Mars over the last 20 Ma. (From: Laskar *et al.*, 2004).

While formation at higher obliquity could account for the presence of some periglacial features on Mars it is not a perfect solution. Many periglacial features are equilibrium landforms, only remaining stable under specific environmental conditions. Such landforms have relatively short life spans and would be expected to undergo considerable degradation over the course of several million years. Pingos, for example, are dependent on the frozen ice at their core to maintain their shape. Changes in temperature or degradation of the insulating soil cover result in the melting, or sublimation of this ice and the collapse of the frost mound to form a "pingo scar".

Over the course of several million years the ice within a relict pingo would be expected to slowly sublimate where it is not covered by a thick layer of regolith. This will result in the collapse of the frost mound. Consequently, if martian features resembling fresh terrestrial pingos were formed through that mechanism then they are likely to be geologically young. This is true of many other surface expressions of the periglacial environment. Small scale features such as sorted patterned ground and solifluction lobes would be expected to undergo considerable erosion if they are no longer being maintained by periglacial processes. Even with the low erosion rates on Mars (Golombek and Bridges, 2000) there is a limit to how long such features can endure through geological time.

It is difficult to date small scale features such as these, since determining a relative chronology based on the size frequency distributions of impact craters requires an extensive area. However some features, such as many of the contraction crack polygons of the Northern Plains, do appear to be young since they superpose impact craters and in some cases have formed on the surfaces of dunes. Gullies are also believed to be very young (Levy et al., 2011; Levy et al., 2009). This would seem to suggest that thawing can and does occur under the current temperature and pressure regime (Marchant and Head, 2007).

3.3.5 Periglacial Microclimates

Another possibility is that periglacial processes are occurring in the present day, but only in atypical environments. It is possible that variations in climate result in isolated areas where higher pressure and temperature can be found; possibly due to topographic constraints. A site with higher than average insolation, or local volcanism, might receive the additional energy needed to melt ground ice (Cabrol and Grin, 2002). However, even if temperatures can rise above freezing in areas which receive large

amounts of insolation, this will only occur for limited periods of time during the warmest hours of the day (Haberle et al., 2001; Kreslavsky et al., 2008; Richardson and Mischna, 2005).

The main problem with this hypothesis is that a microclimate will need to remain stable for long periods of time in order to produce distinct periglacial landforms; it can take up to fifty years of freeze thaw cycling for sorted patterned ground to emerge (Ballantyne and Matthews, 1982). Their development requires tens to hundreds of freeze thaw cycles and if the conditions for thaw are only occurring as part of a very rare event then it will be difficult for enough freeze thaw cycles to occur to produce a noticeable pattern.

3.3.6 Freezing Point Depression

Another scenario which would allow for the formation of periglacial features in the present day is the depression of the freezing point. Brines freeze at considerably lower temperatures than pure water and various "cryobrines" have been demonstrated to depress the freezing point sufficiently to allow for thaw to occur at ambient martian conditions (Möhlmann and Thomsen, 2011; Möhlmann, 2011).

There is considerable evidence for the presence of concentrated brines on Mars (e.g. Möhlmann and Thomsen, 2011; Tosca et al., 2011). Brines in which salts comprise 30 percent of the solution by weight have been found to be stable between 180 and 210 K (Marchant and Head, 2007). This would potentially allow these solutions to occur in the liquid phase on the surface and in the shallow subsurface of Mars over a much wider latitudinal range than pure water. A variety of brines with sufficiently low eutectic points have been described by Möhlmann and Thomsen (2011). They proposed a variety of salts, including chlorates, chlorides, sulphates and carbonates with eutectic temperatures between 200 and 270 K.

Of particular interest are perchlorates which were detected at the landing site of NASA's Phoenix lander in 2008 (Cull et al., 2010; Gough et al., 2011; Hecht et al., 2009; Navarro-González et al., 2010). Naturally forming perchlorate salts are rare on Earth, but may be more common on Mars than previously thought (Cull et al., 2010; Gough et al., 2011; Hecht et al., 2009; Navarro-González et al., 2010).

This discovery resulted in an increased interest in the possibility of liquid brines in the near subsurface. Even low concentrations of perchlorate can cause considerable freezing point depression as shown in the phase diagram for Magnesium Perchlorate ($Mg(ClO_4)_2$) which has a eutectic temperature close to 200 K.

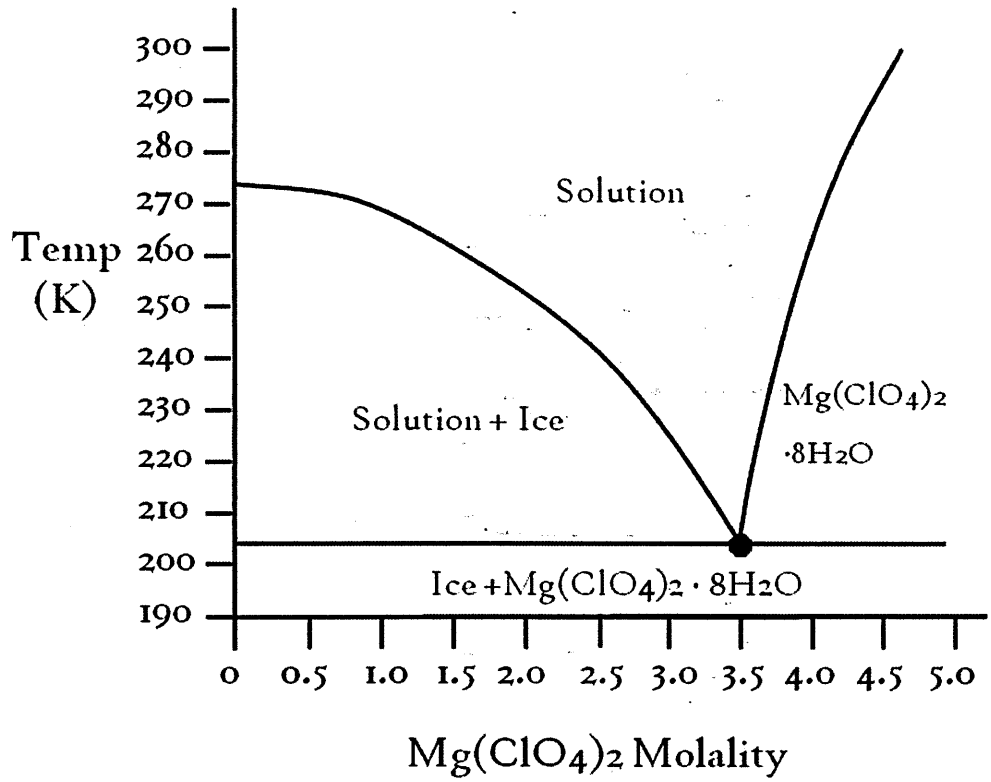

Figure 3.4: Phase diagram for Magnesium Perchlorate.

The freezing point depression due to the presence of even a relatively small amount of magnesium perchlorate could be sufficient to allow the formation of a periglacial environment under Martian temperature conditions (Chevrier et al., 2009; Marion et al., 2010; Robertson and Bish, 2011). A range of cryobrines which could be stable under

martian conditions have since been proposed as illustrated in Table 3.1 (Möhlmann and Thomsen, 2011).

Table 3.1: Eutectic temperatures and compositions of a variety of brines that might be stable under martian temperature and pressure conditions. (from Möhlmann and Thomsen (2011) and references therein).

Brine	Eutectic temperature, (K)	Eutectic composition (%)
Ice + Na_2SO_4 10 H_2O	271	3.8 Na_2SO_4
Ice + K_2SO H_2O	271	7.1 K_2SO_4
Ice + $MgSO_4$ 11 H_2O	269	17 $MgSO_4$
Ice + K_2SO_4 H_2O + KCl	261	0.9 K_2SO_4, 19.5 KCl
Ice + NaCl $2H_2O$	251	23.3 NaCl
Ice + Na_2SO_4 10 H_2O + NaCl $2H_2O$	251	0.12 Na_2SO_4, 22.8 NaCl
Ice + NaCl 2 H_2O + KCl	250	20.2 NaCl, 5.8 KCl
Ice + $Fe_2(SO_4)_3$	247	39 $Fe_2(SO_4)_3$
Ice + $MgCl_2$ 12 H_2O	239.5	21.0 $MgCl_2$
Ice + $MgCl_2$ 12 H_2O + KCl	239	21.0 $MgCl_2$, 1.2 KCl
Ice + $MgCl_2$ 12 H_2O + NaCl $2H_2O$	238	22.7 $MgCl_2$, 1.6 NaCl
Ice + $MgCl_2$ 12 H_2O + KCl	238	22.? $MgCl_2$, 2.? KCl
Ice + $MgCl_2$ 12 H_2O + $MgSO_4$ 7 H_2O	238	20.8 $MgCl_2$, 1.6 $MgSO_4$
Ice + $NaClO_4$ $2H_2O$	236 (±1)	52 $NaClO_4$
Ice + $CaCl_2$ $6H_2O$	223	30.2 $CaCl_2$
Ice + $CaCl_2$ $6H_2O$ + KCl	221	29.3 $CaCl_2$, 1 KCl
Ice + $CaCl_2$ $6H_2O$ + NaCl $2H_2O$	221	29.0 $CaCl_2$, 1.5 NaCl
Ice + $CaCl_2$ $6H_2O$ + $MgCl_2$ $12H_2O$	218	26.0 $CaCl_2$, 5 $MgCl_2$
Ice + $Mg(ClO_4)_2$	212 (±1)	44 $MgClO_4$
Ice + LiCl	207	24.4 LiCl
Ice + $Fe_2(SO_4)_3$	205 (±1)	48 (±2) $Fe_2(SO_4)_3$
Ice + LiI	204	48.2 LiI
Ice + LiBr	201	39.1 LiBr

3.3.7 Formation of Cryobrines

It has been demonstrated that small quantities of brine can form through bulk deliquescence (Fischer et al., 2014; Möhlmann and Thomsen, 2011). When humidity rises salt deposits absorb water vapour from the atmosphere with the result that the salt dissolves, forming liquid brine. This process can only take place when the partial pressure of water in the air is sufficiently high to allow dissolution to occur. Humidity on Mars is generally very low. While super saturation conditions can occur under certain conditions (e.g. Maltagliati et al., 2011) there is usually limited potential for dissolution to occur. In addition to this the surface temperature does not frequently rise above the eutectic temperatures of some cryobrines.

Consequently, it has been thought that deliquescence could only take place under unusual conditions and that it might not occur fast enough to allow large volumes of brine to form. However it has been demonstrated that brines can form much more rapidly in circumstances where ice is present as an additional source of water once deliquescence from the atmosphere triggers brine production (Fischer et al., 2014).

It seems likely that liquid droplets observed by the Phoenix lander were concentrated cryobrines formed in this manner. Also, much of the northern plains of Mars contain ice at shallow depths, so pore-spaces in Mars' near-surface regolith will probably have a much higher humidity than the atmosphere immediately above the surface.

The Phoenix landing site contains numerous contraction crack polygons of the sort described in Section 2.4.6. These features are more likely to have developed through a combination of thermal contraction cracking and sublimation, rather than by thaw, but it should be noted that similar structures are common in terrestrial periglacial environments. Excavations by the Phoenix lander found the ground in that region to largely consist of ice cemented soils where the pores were filled with ice. They also

uncovered some examples of excess ice, which could be evidence of ice lens segregation (Mellon et al., 2009; Sizemore et al., 2014). The formation of brines in this sort of environment could potentially trigger the formation of an active layer if large enough quantities of brine were to form.

3.3.8 Quantity of brines

Frost heaving is most effective when the void space is saturated with water throughout the frozen fringe (Chamberlain, 1981). This is very unlikely to be the case if liquid water exists only in the form of thin films of brine (Mellon et al., 2009; Sizemore et al., 2014). However, ice lens initiation can occur in circumstances where relatively little water is available. Sizemore et al., (2014) have demonstrated that since the processes responsible for ice lens initiation are occurring on a very small scale they can be initiated in the presence of thin films of liquid water.

3.3.9 Reduced frost heaving in saline soils.

The presence of concentrated salts within a soil's pore water does not just affect the freezing point but also the way in which freezing occurs. This may have a detrimental effect on the development of sorted structures. Although regular freezing and thawing may take place under martian conditions, the actual frost heaving and sorting processes do not result from the volumetric increase which water undergoes upon freezing but rather from the physical accumulation of ice crystals into lenses within the upper part of the soil. When saline water freezes the solutes are not incorporated into the ice but rather remain within the unfrozen fraction. As more ice forms the remaining liquid becomes increasingly saline until saturation occurs.

The presence of this unfrozen fraction changes the depth of the unfrozen fringe and impedes the formation of coherent ice structures such as the lenses required for frost

heaving. Rather than freezing into a dense mass, ice crystals are found to form loose structures separated by channels of unfrozen brine (Arenson and Sego, 2006). Chamberlain (1983) found that frost heaving was reduced by as much as 50% in soils saturated with seawater, relative to those containing pure water.

A reduction in the size of the ice lenses was also observed, since many small ice lenses form, each at a different depressed freezing point, rather there being a single freezing site. Many small lenses developed at a variety of accumulation sites throughout an enlarged frozen fringe, but large coherent ice lenses were absent. This reduction in frost heaving could have a significant effect on the development of sorted structures, particularly if the very concentrated brines required to facilitate thaw under martian conditions have a proportionally greater effect on the reduction of heaving.

3.3.10 Frost-susceptibility

The other major factor that must be considered is the degree to which martian soils are suitable for frost heaving in the first place. Some soils are more frost-susceptible than others and undergo more heaving as a result of frost action than non-frost-susceptible materials. Consequently, the proportion of frost-susceptible material at the site will be critical in determining the response of the soil to freezing. The differential heaving between regions of strongly frost-susceptible soil and regions containing more stony material is vital in triggering lateral sorting processes (Matsuoka et al., 2003).

Fine grained soils are more frost-susceptible than coarse grained material because capillary forces are responsible for drawing water through the frozen fringe to an accumulating ice lens (Chamberlain, 1981; Konrad, 1989a). This means that water transfer will occur preferentially in smaller pore spaces, resulting in more water accumulating at the ice lenses and a larger degree of heaving. In soils with large pore spaces the freezing front will propagate much faster preventing the redistribution of

liquid water within the soil. Periglacial processes are frequently found in cold climate regions where silty soils dominate. Silts have frequently been used in studies by various authors to simulate these processes (Konrad and Nixon, 1994; Konrad, 1989a, 1989b; Penner and Goodrich, 1981; Penner, 1986).

Grain size distribution is frequently used to define the limits of a soil's frost susceptibility (Chamberlain, 1981).The distribution of differently sized materials controls the volume of pore space and its interconnectedness, so the percentage of a soil below a specific grain size can be used to determine how likely it is to exhibit heaving. A fine grained soil will contain many very small pore spaces whereas one composed of coarser material will have fewer, larger pores. The former is more conducive to frost heaving.

A soil containing no material smaller than 74 μm will not exhibit frost heaving (Casagrande, 1931; Chamberlain, 1981; Taber, 1929). Casagrande's criteria for frost susceptibility is one of the most commonly used. It requires an assessment of the percentage of grains smaller than 20 μm and the uniformity of the soil. The uniformity coefficient is a parameter defined by the ratio of the diameters of particles comprising the 10% and 60% fractions of the soil. In soils with a low uniformity, in excess of three percent of grains must be smaller than 20 μm in order for ice segregation to occur. In a more uniform soil, 10% of grains smaller than 20 μm are required (Casagrande, 1931; Chamberlain, 1981). Consequently, a soil where a significant fraction consists of fine grained sand and silt will be likely to allow frost heaving.

3.3.11 The frost susceptibility of martian soils

In order to assess whether periglacial processes are likely on Mars it is necessary to determine whether the soils in which they would be forming are frost-susceptible. As discussed in the preceding section, frost susceptibility can be estimated based on the

grain size distribution of the soil. This information is only available for a few sites on Mars where landers and rovers have conducted examinations of the local soil properties.

Each of these missions provides a snapshot view of the conditions at a specific site. Although the Mars Exploration Rovers have traversed a great distance since landing on Mars their observations still only cover an extremely small area of the planet. Similarities in some soil properties between these sample sites suggest that some surficial materials, particularly those composed of windblown dust, are probably global in extent. However it is possible that conditions could differ dramatically in unusual places which have yet to be explored.

Both Viking landers observed patches of fine grained drift material overlying blocky or cloddy material. The blocky material was believed to be similar to dry terrestrial soils, though with lower cohesion, as it quickly disaggregated when sieved (Arvidson et al., 1989; Moore et al., 1987; Stoker et al., 1993). These blocky materials were consequently, interpreted to be formed of clay-sized particles cemented together by salts to form a more cohesive soil. It was concluded that water played an important role in cementing mixtures of aeolian emplaced dust and weathered fragments of the underlying bedrock (Moore et al., 1987). This conclusion is supported by more recent observations of martian brines at the Phoenix landing site (Cull et al., 2010; Hecht et al., 2009).

The majority of the soils sampled by the Viking landers were found to consist of silt to clay-sized particles but much of this fine grained material appears to cohere to form clods a few millimetres in diameter (Moore et al., 1987). Sand-sized grains at these sites may be the result of the presence of this cemented fine grained material (Arvidson et al., 1989). This process could reduce the frost susceptibility of the soil, as the cemented

fine grained material could have a larger effective grain size than would normally be the case.

Fine grained material was interpreted as windblown dust, similar to terrestrial loess (Moore et al., 1987). The fact that similar chemical properties were found at both Viking landing sites suggests that there is a globally uniform soil layer, probably emplaced by aeolian activity (Stoker et al., 1993). This forms a global mantle over whatever underlying soils may be present. The mean particle size for windblown dust on Mars is believed to be less than 2 μm (Allen et al., 1998; Pollack et al., 1995). Consequently, this material could introduce a frost-susceptible component into underlying soils. However, it is uncertain whether it will be present in sufficient quantities to do so at any given site.

The Mars Exploration Rovers also observed bright dust, which was present at both rover landing sites, and so is likely to be part of a global unit (Yen et al., 2005), similar findings from Mars Pathfinder (McSween and Keil, 2000) and global spectroscopic studies support this hypothesis (Ruff, 2002).

Observations by the Spirit rover in the area around Gusev Crater showed a variety of fine to medium grade sands, most likely having been emplaced by aeolian processes. Coarser grained soils were interspersed with very fine grained "flour like" material, forming unstructured soils. Excavation by the rover wheels confirmed that a relatively thin layer of aeolian dust covered weathered bedrock material from which the larger clasts originated (Cabrol et al., 2014). As at the Viking landing sites, aggregates were found consisting of clumps of finer grained material.

Consequently, there is a reasonable probability that a given area on Mars will exhibit frost-susceptible soils, although it would be impossible to be certain without soil

samples which could be assessed using the methods outlined by Casagrande (1931) and Chamberlain (1981).

3.4 Summary

Sorted patterned ground is characteristic of a periglacial environment since it forms as a result of the aggradation of ice lenses within a freezing soil. This can only occur under very specific conditions of frost susceptibility. Evidence from various lander observations suggest that some martian soils could be frost susceptible, if the global dust unit provides sufficient fine grained fraction. In situ observations would be required to confirm that any given site on the martian surface is suitable for periglacial processes.

The availability of liquid water is also critical. Thawing can occur under martian conditions, but is not expected to be common. Unlike some features, patterned ground cannot be explained as the result of an isolated thawing incident. Sorted patterns only occur when an active layer develops and undergoes repeated freezing and thawing over diurnal or seasonal cycles. If the development of an active layer is a rare occurrence it will take proportionally longer for complex structures and large scale features to form.

There are several circumstances under which regular thawing events could occur. The presence of cryobrines in the martian subsurface could allow thawing in the present day. It could also have been viable during the warmer months during past periods of higher obliquity when insolation to pole facing slopes would have been enhanced. It thus seems that conditions exist in the martian environment under which periglacial processes are viable. How common or widespread such conditions are remains to be determined.

4 Chapter Four: Sorted Patterned Ground in Northern Iceland

As previously discussed, sorted patterned ground is one of the most distinctive periglacial landforms. This has important implications for the characterisation of the martian environment. Many of the landforms discussed in Chapter Two are morphologically similar to other, non periglacial features, but this is not the case with sorted patterned ground. While stones can become somewhat organised through other processes, for example due to the removal of finer material by deflation, or the deposition of particles as the result of fluvial processes, these features lack the complexity and striking regularity of periglacial patterned ground.

Only anthropogenic landforms such as the Nazca Lines, a series of geoglyphs created by arranging stones in the desert of southern Peru, come close to the complexity of sorted patterned ground. The Nazca Lines are very distinct in structure, as they do not consist of a grading of material from the most to least fine across the feature, but rather the removal of coarse stones from some patches of ground to form textural differences. Consequently, they can easily be distinguished from periglacial patterned grounds.

Thus presence of sorted patterned ground is characteristic of freeze-thaw-related processes. This is significant for the field of planetary exploration as sorted patterned ground provides a clear geomorphic marker for locations where water has been liquid in the geologically recent past.

Figure 2.12 in Chapter Two illustrates the wide variety of sorted patterns that can be found over a relatively small area in the Skagafjörður region of northern Iceland. This chapter will examine this region in detail. Sorted patterned ground occurs at a range of scales, some of which are likely to be detectable using remote sensing data, and some of

which would require ground based observations to study. The variety of sorted features found across this region and the locations in which they occur will be documented and discussed.

4.1 Aims and objectives

The purpose of this chapter is to determine the extent to which a landscape consisting of sorted patterned ground would be detectable in martian remote sensing data. To this end, aerial photographs of a region of northern Iceland known to exhibit sorted patterned ground were examined. These images have a horizontal resolution of approximately 15 cm per pixel, slightly higher than the 25 cm per pixel resolutions of the best martian images. However martian patterned ground appears to occur on a larger scale than its terrestrial analogues, both in terms of the size of polygons, and of the material making up the coarse domains. Consequently these data sets are comparable.

Fieldwork was conducted to assess the variation in shape and structure which can occur across a terrestrial periglacial environment, both at metre and centimetre scale. The variety of structures present at the site has been documented from the ground. The expression of these features in the air photographs provides an indication of the type of features that would indicate a similar landscape in the martian data. This provides a baseline for the detection of martian patterned ground and the variety of forms and structures that would be anticipated.

A secondary objective was to test the use of *structure from motion* photogrammetry techniques for application to studying this type of environment. The structure from motion process will be detailed in section 4.3.1. It is a relatively new technique which allows digital elevation models to be produced from field photographs and which has applications for a variety of areas of geomorphological research.

In essence this chapter documents a "ground truth" analogue study, performed to explore how effective remote sensing is for identifying and classifying these features, and so that the limitations of applying this method to Mars can be fully understood. Chapter five follows on from this discussion to apply some of the same classification techniques to martian examples.

4.1.1 Background

Sorted patterned ground is well documented in a variety of terrestrial cold climate environments as discussed in chapter two. These features have a range of morphologies including sorted stripes, and polygons. One of the first studies to classify the different types of patterned ground was that of Washburn (1956). This study laid the foundation of the present understanding of sorted patterned ground morphology and was expanded upon by a variety of authors who have studied both the form and formation mechanism of sorted patterned ground (e.g. Goldthwait 1976; Ray et al., 1983; Matsuoka et al., 2003).

The processes behind the formation of sorted patterned ground has long been uncertain, and numerous studies (summarised in the background section to appendix one), have been conducted to simulate the frost heaving process and demonstrate how different sorting patterns develop, these range from the practical experiments (Corte, 1963, 1962; Inglis and Corte, 1965), to the modelling of sorted patterns (Kessler and Werner, 2003; Kessler et al., 2001) and in situ measurements of frost heave in the field (Matsuoka et al., 2003). It seems likely that sorted patterned ground is a polygenetic landform, that results from differential frost heaving (Matsuoka et al., 2003).

The study of Kessler and Werner, (2003) is particularly interesting as it suggests that sorted structures of different morphologies form through self organisation. They were able to model the formation of a variety of complex sorted features resulting from just

two basic mechanisms; frost heaving results in the segregation of fine and coarse material, resulting in coherent coarse and fine domains; while the squeezing of stone domains by the neighbouring regions of finer soil results in the movement of stones along the axis of the domain. The interaction of these two processes with environmental factors such as hill slope result in the variety of sorted structures observed at a periglacial site.

The relevance of this to the current study is that some of the large scale variations in pattern morphology result from environmental conditions which can be independently assessed. Sorted polygons become increasingly elongated as the underlying gradient increases, eventually transitioning into regions of sorted stripes (Krantz, 1990; Washburn, 1956). Other polygonal patterns, such as those resulting from cracking processes do not exhibit this behaviour. It is thus indicative of sorted patterned ground.

In the martian data changes in topography can be measured using digital elevation models, or inferred from the proximity of a region of patterned ground to the wall of an impact crater. Thus a variation in pattern morphology associated with this gradient change would be suggestive of a periglacial origin.

Small scale sorted patterned ground is common in Iceland, but few extensive studies have been made into its distribution and morphology. Sorted patterns were noted by (Hawkes, 1924) who cited them among other indicators of frost action in the Icelandic landscape. The review of Thorarinsson, (1951) describes a variety of types and summarises the literature on the subject at the time. Priesnitz and Schunke, (1983) discuss the distribution of sorted patterned ground in their review of Icelandic periglacial features and conclude that large scale polygons are only found at high elevations, between 350 and 400 metres above sea level. The study of Kruger, (1994) supports this assessment. He examined these features in southern Iceland and noted

that they are common on exposed ground, although the largest features are limited to the central highlands.

The study area chosen for this investigation is the region around the Skagafjörður described in the comprehensive study of Feuillet et al., (2012). They examined the environmental factors controlling the distribution of different patterned ground types at this site. Feuillet et al., (2012) examined a variety of sorted forms in different contexts across the area. They concluded that the diameter of a sorted net was correlated with altitude and the size of coarse clastic material, as well as the proportions of clay and silt within the soil. The second of these observations has application to the present investigation, as a correlation between clast length and polygon diameter should be possible to assess using remotely sensed data.

Several of the sites reported by Feuillet et al., (2012) were visited during the fieldwork section of this project and so their observations proved very useful in efficiently locating areas of sorted patterned ground.

4.2 Study area

The Skagafjörður region of northern Iceland is an easily accessible coastal environment just to the south of the Arctic Circle. The region is shown in Figure 4.1. This area exhibits a variety of landscapes, ranging from steep hillsides to flat moorland. Much of the area is covered in small scale sorted patterned ground. This part of Iceland is dominated by the Skagafjörður itself, a deep glaciated channel approximately 40 km in length and 15 km wide, opening onto the Arctic Ocean. All of the sites examined during this study are in close proximity to the fjord, but none are located on beaches, or in proximity to streams where coastal and fluvial processes would be expected to dominate. Consequently, these processes would not be expected to interfere with the development of periglacial morphologies.

This field site is a wet maritime environment and so is not as similar to the cold, dry martian desert as other candidate sites. It was chosen for its ease of accessibility and because air photographs comparable to the satellite images being used for the martian study were available. Since the purpose of this study was primarily to test the technical limitations of characterising a sorted network from relatively low resolution remote sensing data it was felt that a perfect analogue was not required. This site exhibited extensive sorted networks, including fields of both polygons and stripes. A wide variety of smaller scale features were also available which could be used to test the *structure from motion* procedure.

Features in colder, dryer environments would be likely to bear more similarity to the martian features, since they would be less likely to be influenced by vegetation and water logged soils. The applicability of the Icelandic patterns was assessed during the first field campaign, particularly in regards to disturbance by vegetation. Patterns on the summit of Tindastóll which would appear in the air photo dataset were examined in situ. These structures were found to be largely un-vegetated. The summit of Tindastóll is almost entirely exposed stones and earth. While the smaller scale features at lower elevations do occur in more vegetated regions these structures all appear to be relatively young. It has been suggested by Haugland, (2006), that alteration by vegetation is negligible on features only a few decades in age.

It would be interesting to characterise an Antarctic site from remote sensing data in a similar manner to the analysis performed on martian features. While fracture networks are frequently reported around the Antarctic dry valleys there appears to be less information about sorted features, which are more often reported in wetter, sub-Antarctic regions (e.g. Wilson and Clark, 1994). Sorted patterned ground is unlikely to be found in the coldest, driest environments which are most comparable to Mars. As

with martian examples extraordinary circumstances would be required for these features to evolve. An Antarctic study would also have lacked in situ observations since such sites are less accessible. It was felt that in situ study was essential in order to build familiarity with these landforms and to effectively assess the level of detail that HiRISE images of Mars would provide.

The geology of the Skagafjörður consists of a basaltic bedrock with layers of sedimentary material (Decaulne et al., 2007). Examples of sorted patterned ground can be found in rocky fields near the town of Sauðárkrókur on the south western side of the fjord and on surrounding heath land. The best active examples of patterned ground occur at high elevations to the north-west of the town, with relic features in other parts of the Skagafjörður area (Feuillet et al., 2012b).

Five localities around the fjord were selected where a wide variety of periglacial features occur in close proximity. These were surveyed over the course of two field campaigns in the summers of 2012 and 2013. The surveying techniques applied at each of these sites will be discussed in more detail in the methods section but in brief the objective of the project was to classify the varieties of sorted patterned ground found at each site and determine the extent to which the application of remote sensing techniques could characterise a periglacial environment.

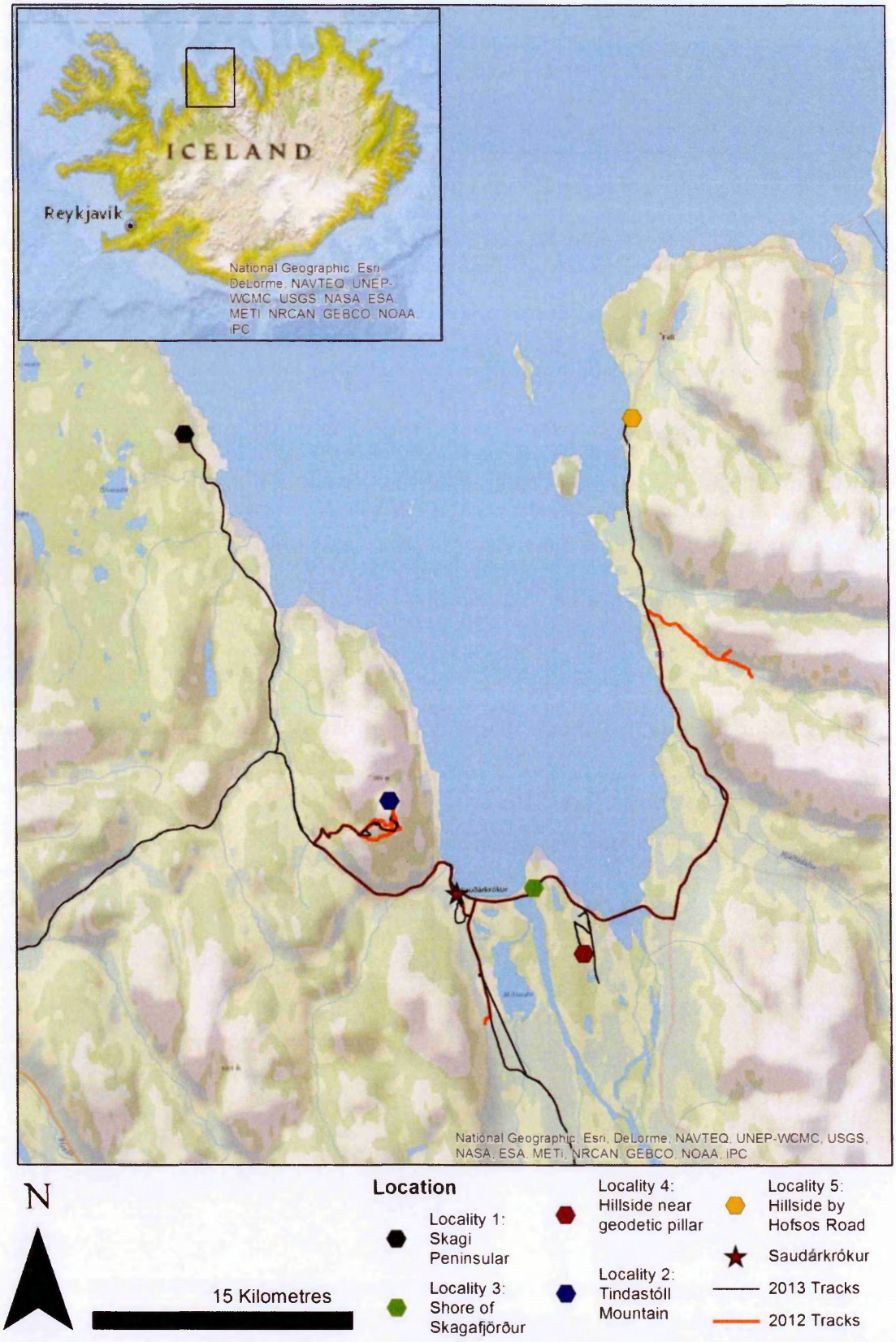

Figure 4.1: Map of the Skagafjörður area showing the locations of the areas surveyed during this project and the GPS tracks of routes used during the two field campaigns. (Frequently red tracks from the 2012 expedition are overlain by blue tracks from 2013).

4.2.1 Locality One: The Skagi Peninsular

To the west of the fjord the Skagi Peninsular consists of open heath land interspersed with numerous lakes and rocky outcrops. Much of the peninsular is vegetated, but many patches of open ground are present and these are almost always covered in centimetre scale patterned ground. This locality was subject to a reconnaissance survey during the 2012 field campaign and a more detailed survey using *Structure from Motion* photogrammetry during 2013. Twenty four sites were examined including sorted stripes, polygons and transitional features. These sites are spread over an open area of heath approximately 50 m above sea level.

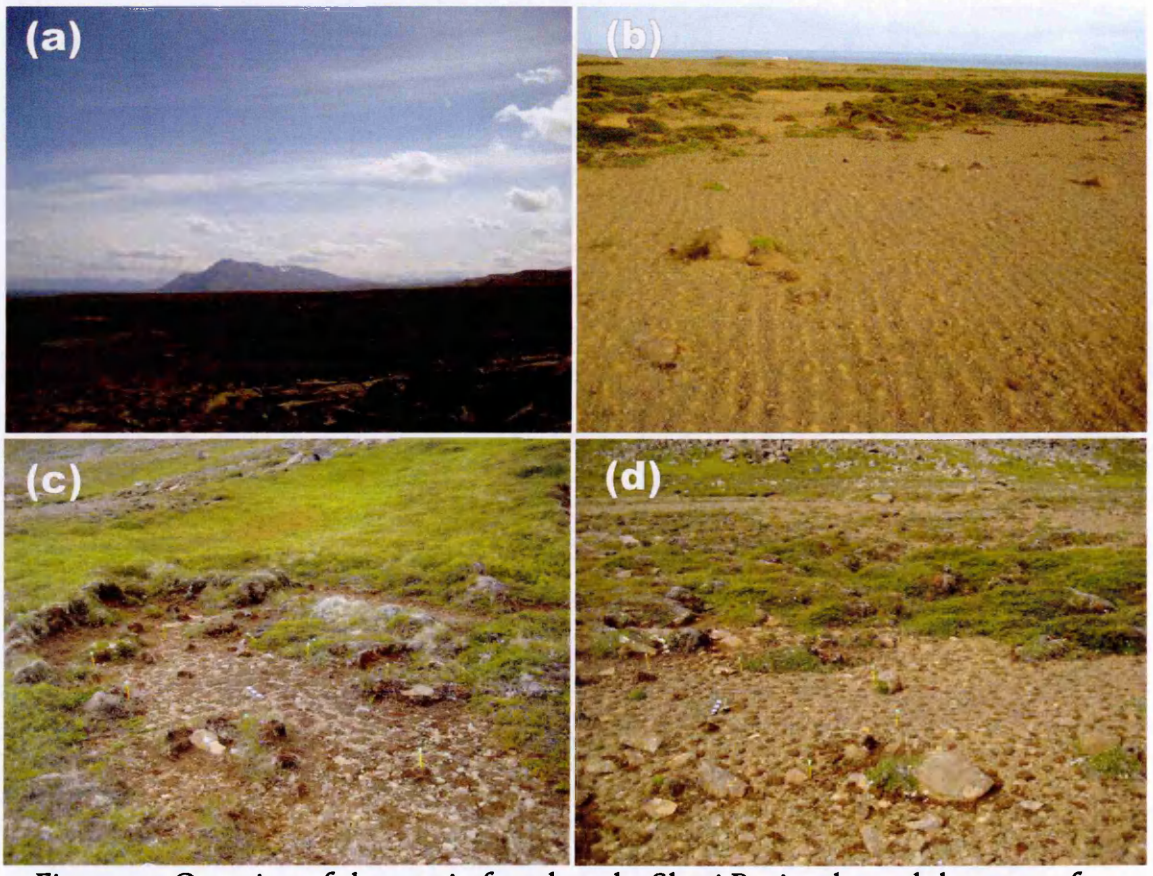

Figure 4.2: Overview of the terrain found on the Skagi Peninsular and the types of sorted features present. The black and white striped rulers present in these and later images are 30 cm in length divided into five cm black and white sections. The sorted stripes shown in inset b have a wavelength of approximately 10 cm. a) Overview of the site, b) 10-20 cm wavelength sorted stripes, c) irregular sorted polygons with 20-30 cm diameter, d) 20-30 cm diameter sorted circles.

A variety of features observed in this locality are illustrated in Figures 4.2 and 4.3. This locality contains mainly small to medium scale features from a few centimetres to a few tens of centimetres across. These generally consist of fine domains of silty soil 10-20 cm across surrounded by irregular polygons of pebble grade material, coarse domains are of varying widths usually 2-10 cm. Most of the features examined were irregular, with very few instances where clear sorted circles occurred. A few larger features were found, consisting of cobble grade material as part of the coarse domains, but no metre scale patterned ground appeared to be present at this site.

Figure 4.3: Small scale sorted circles with large cobbles surrounding fine domains of silty soil. The tent peg is 20 cm in length.

4.2.2 Locality Two: Tindastóll Mountain

The largest topographic feature to the west of the fjord is Tindastóll. This is a wide basaltic hill with a summit approximately 900 m above sea level. The northern face of Tindastóll can be seen in Figure 4.2a. Tindastóll is oriented approximately north-south

and the western and eastern faces are dominated by a number of large gullies. The summit of the hill is approximately 20 km in length and consists of a series of plateaux separated by the alcoves of the gullies. The top of the hill consists largely of weathered basaltic material much of which has been organised into metre scale patterned ground. Smaller sorted features are found on the slopes approaching the hilltop and solifluction lobes appear to be present on the steepest slopes.

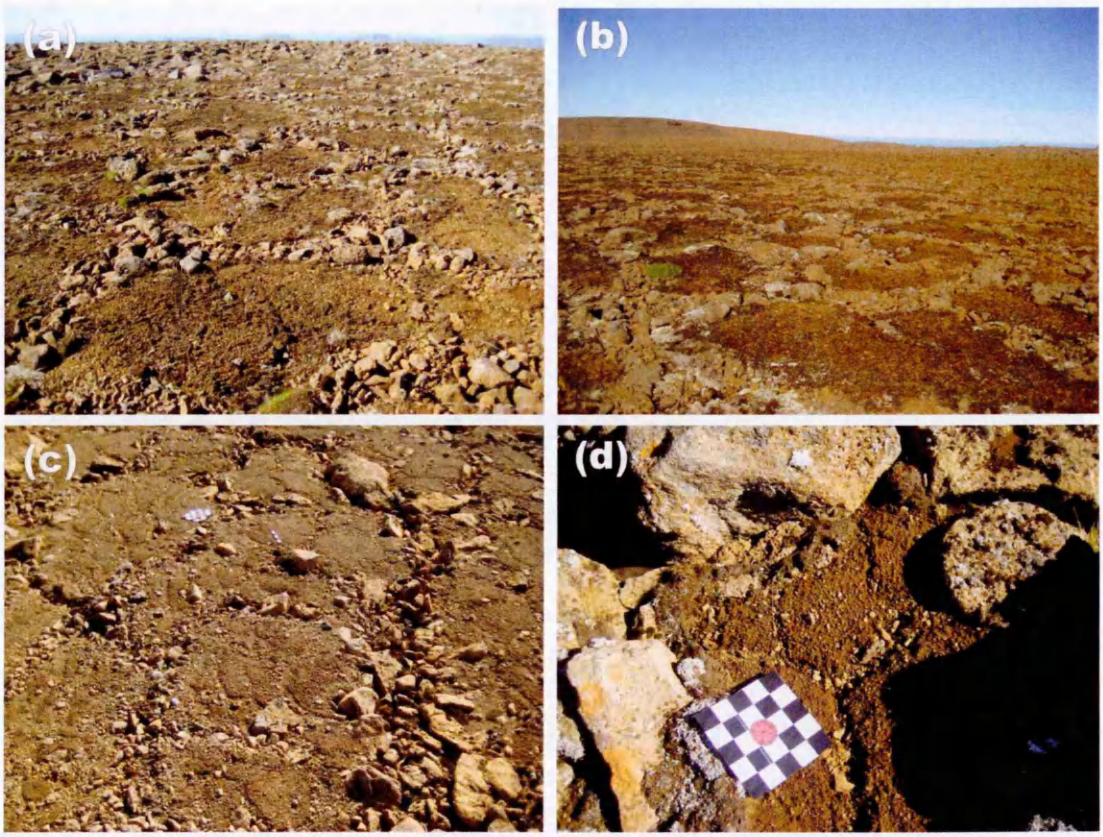

Figure 4.4: Sorted features at a range of scales on the summit of Tindastóll. The scale bar shown in this and future images is a 25 cm square divided into five cm square black and white sections the large circles in frames a and b are 1-2 metres in diameter. c) shows irregular fine material and coarse domains of various sizes, d) shows small coarse domain of granule sized material intersecting a larger fine region surrounded by boulders.

This locality was the site of the most detailed reconnaissance survey of the 2012 expedition and is the site covered by the LIDAR and aerial photography survey. Five examples of 10 cm scale patterned ground at this locality were examined as part of the 2013 *structure from motion* survey. However the large metre scale patterned ground on the hill's summit was inaccessible in 2013 due to heavy snow cover.

The summit of Tindastóll is covered in a network of sorted polygons 1-3 m in diameter which extends across large swathes of the hilltop and transitions to sorted stripes in several places. The fine domains consist of a coarser silt-sand grade soil than at lower elevation sites with numerous small pebbles and granules. The coarse domains are made up of many small boulders with some large cobbles. In many instances smaller features ranging from a few centimetres to several tens of centimetres across are nested within the larger metre scale networks as illustrated in Figure 4.4. Figure 4.4d shows centimetre scale features in the shadow of a large boulder which appeared to be active in 2012.

The soil was partially frozen at this site, suggesting that the small scale features are undergoing freeze thaw processes in the present day. It is impossible to be certain whether any of the other features were active, however the deep snow cover observed at this site in 2013 suggests that the ground here undergoes freezing and thawing on a regular basis so it is likely that all of these features are active in the present day.

4.2.3 Locality Three: Hillside above the shore of the fjord.

A site at the head of the fjord several kilometres to the east of Sauðárkrókur was selected as a study area as it exhibited small scale features of the sort which appeared to be largely ubiquitous across this area. This site consists of a region of bare ground interspersed with rocky outcrops on a small hill approximately 25 m above sea level. Here, as in other locations across the region, most of the exposed ground is a mix of silty soil and stones in the large granule to small pebble range.

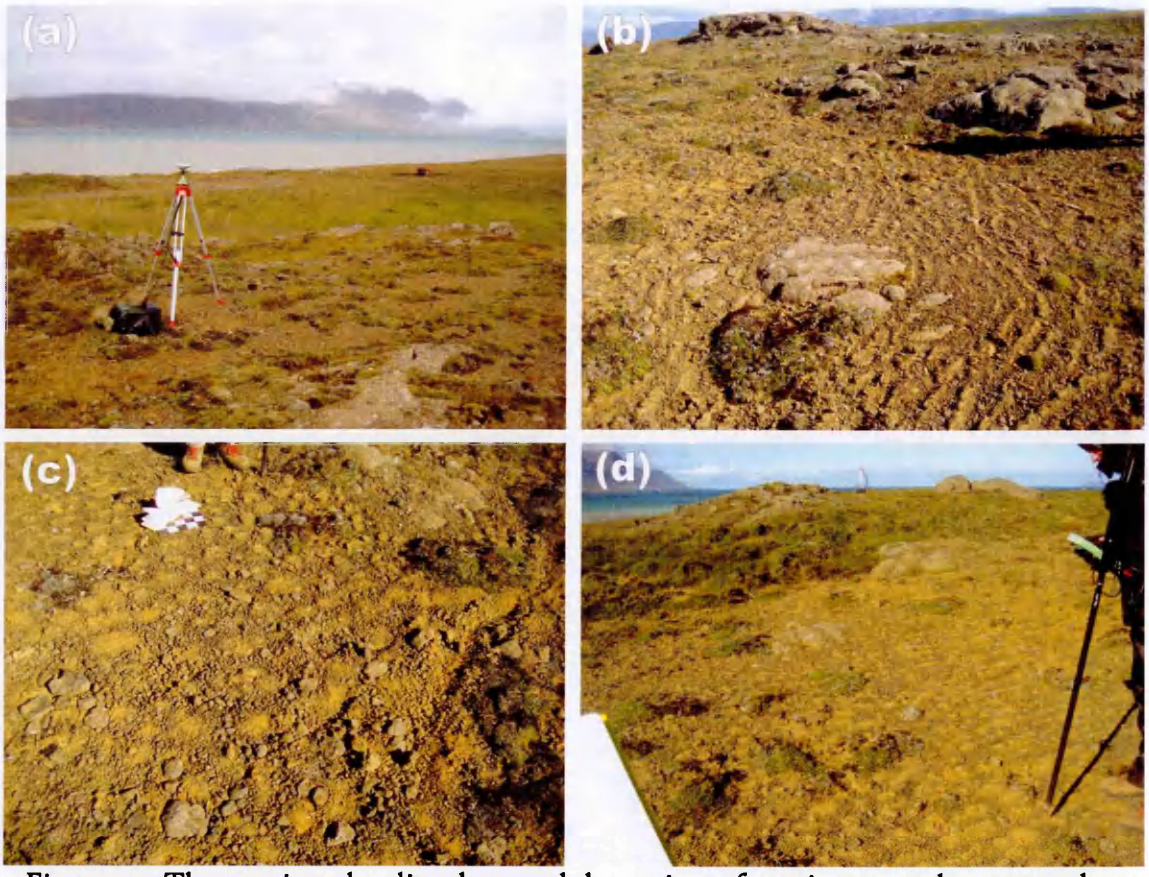

Figure 4.5: The terrain at locality three and the variety of centimetre scale patterned ground observed in this area. a) Overview of the site, b) discontinuous stripes of coarse and fine material. wavelength of 10-20 cm, c) small 10 cm diameter circles, d) a mixture of different feature types of the same scale.

Isolated larger materials, up to small boulders, are common but not ubiquitous. In all locations where the ground was exposed some degree of sorting was observed, with the exception of the gravel roads which are likely to be too frequently disturbed, and may not contain a significant fraction of fine grained material to allow sorting to occur.

This site was surveyed during the 2012 expedition; it was not revisited during 2013. Numerous five to ten centimetre scale features were observed in this region. The majority of these features took the form of elongated polygons, but several areas of stripes and more circular polygonal features were found. Numerous instances of patterns grading from circular features, through elongated fine domains to sorted stripes were observed.

Figure 4.6: Transition from circular polygons at the right hand side of the image to stripes at the left, passing through a transitional region with several types of intermediate features.

4.2.4 Locality Four: Cliff top near to geodetic pillar

This site is located further up the valley from locality three; on a rocky bluff approximately 100 m above sea level. This is in proximity to the location of the geodetic pillar used with the GPS equipment. The sorted features at this site are similar to those observed at locality one and locality three. This site was surveyed in 2012, and revisited in 2013, although no additional measurements were made. It was determined that the general form of the patterned ground at the site had not changed in the intervening time and the decision was made to focus on the areas which had not been examined in as much detail the previous year. There was no need to resurvey the same features to compare morphological changes, as significant variations in pattern morphology would take more than a year to develop and a longer term monitoring program was not viable as part of this investigation.

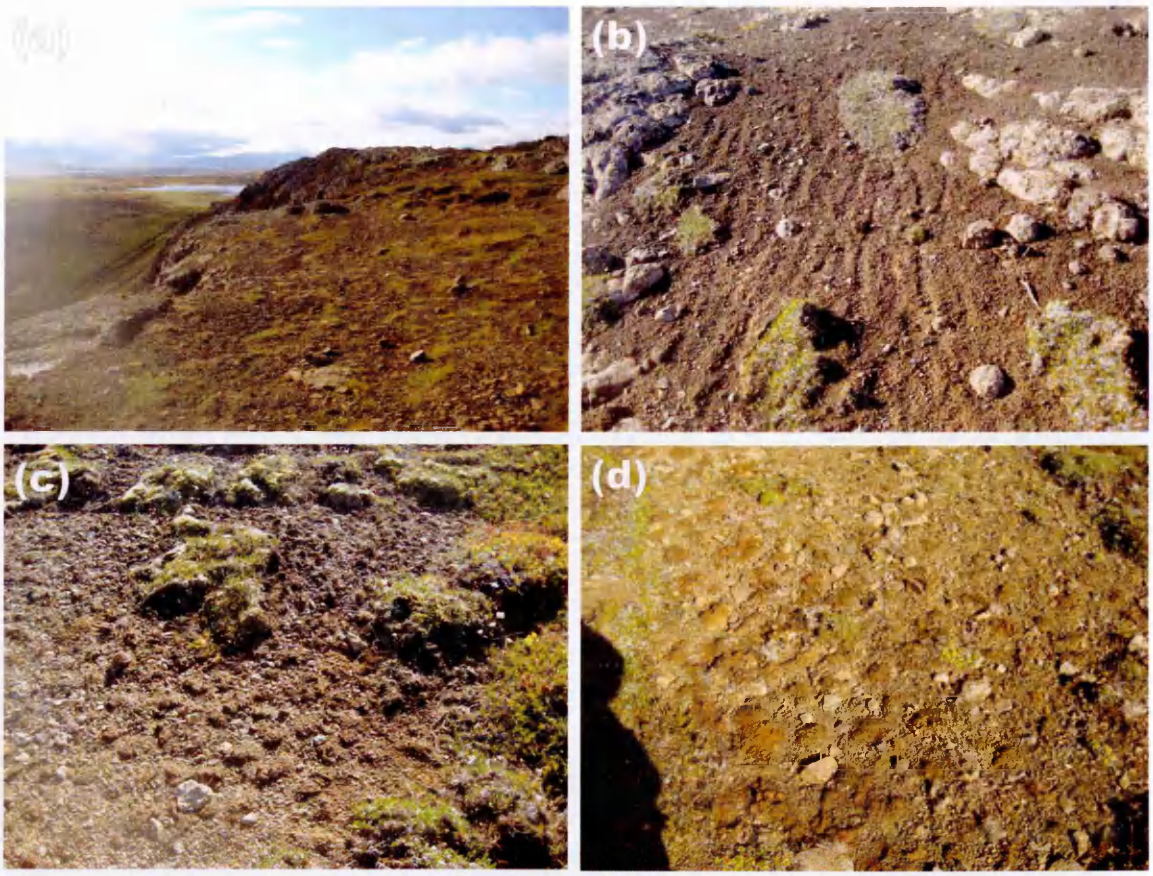

Figure 4.7: The terrain at locality four and the variety of sorted features observed in this area. Sorted features are of the order of ten centimetres across. a) Overview of site, b) 10 cm wavelength sorted stripes, c and d) sorted circles at a similar scale forming in different substrates.

The morphology of these features was compared with those at locality three. The additional elevation seemed to have had minimal effect on the scale of sorted features. These features are at the same scale as those in locality three and in general were found to be smaller than the features observed at locality one. Again a variety of circles, stripes and transitional features were present. The material at this site was similar to that observed at locality three, consisting largely of small domains of fine silt, surrounded by much larger domains of coarse sand and granules, with numerous small pebbles and some isolated patches of coarser material. Numerous rocky outcrops separated the patches of soil on which sorted structures were observed, but relatively few mobile boulders were present so no larger scale sorting had occurred.

4.2.5 Locality Five: Hillside by the Hofsos Road.

The eastern side of the Fjord has less flat heath land. A large number of mountains interspersed with narrow dales are separated from the fjord by a thin band of open ground. A road runs north-south along the edge of the fjord and the ground slopes steeply upwards on the eastern side of the road into overgrown mounds of coarse material which may be spoil heaps from the construction of a road. These were found to be covered in centimetre scale patterned ground. This ground would have been disturbed within the last five decades, probably more recently, making these features relatively young.

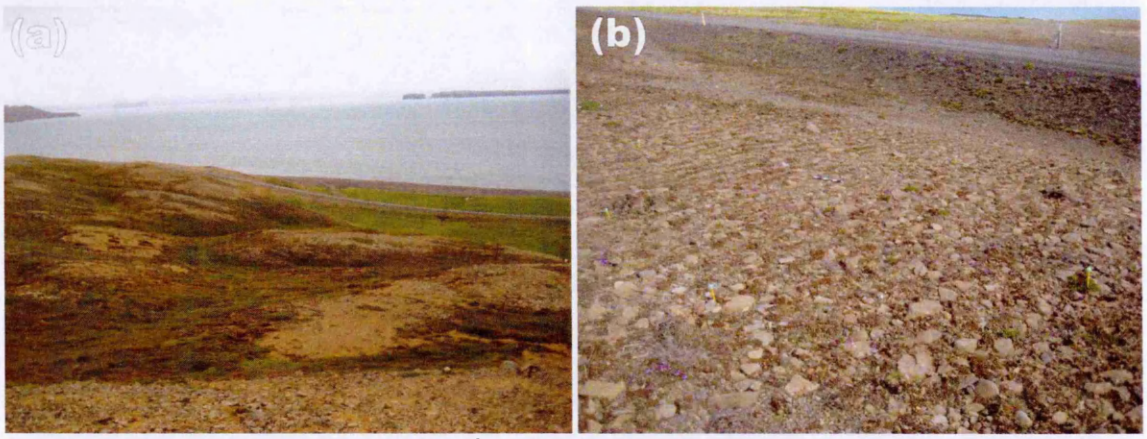

Figure 4.8: The terrain at locality five which is believed to be composed of coarser grained material left over from the construction of the road. a) Overview of site, b) examples of centimetre scale patterns at the site, circles are 20-30 centimetres in diameter.

These features are slightly larger in scale than those found at localities three and four. This is likely due to the generally coarser material in which they are formed. This area was examined during a reconnaissance survey in 2012 and two sites were examined in more detail using *structure from motion* techniques during the 2013 expedition. Relatively little data was collected from this region. It was established that these features were not significantly different to those observed on the western side of the fjord where more numerous features occurred. Numerous examples of sorted stripes were found in this

area. Fewer patches of polygonal terrain were found, possibly due to the greater relief of this region.

4.3 Methodology

Two field campaigns were conducted to survey sorted patterned ground in this region. The first expedition, conducted in the summer of 2012 was as ground support for the acquisition of LIDAR and aerial photographs of Tindastóll using the NERC Airborne Remote Sensing Facility aircraft. While the purpose of this remote sensing survey was unrelated to the current project it produced a large volume of data which could also be used to examine the patterned ground on Tindastóll. While the remote sensing survey was taking place, several reconnaissance surveys were conducted to locate areas with examples of sorted patterned ground. On days when the GPS equipment was not required for the remote sensing campaign more detailed surveys of two of these sites (Localities 3 and 4) were conducted to measure variations in feature type with gradient.

In 2013 a second expedition was conducted to examine the sites which had not been studied in detail in 2012, in particular localities one and two. The 2013 survey included the use of *structure from motion* Photogrammetry (SfM) (Westoby et al., 2012); an efficient technique for building Digital Elevation Models (DEMs) of centimetre to decametre scale landforms in the field using photographs taken from different angles.

The purpose of the study was primarily to produce a set of higher resolution data that would complement the aerial photographs, but also to test the reliability of the *structure from motion* technique as a simple tool for geomorphology research in the field. The original intention was to make high resolution DEMs of features at locality two, which could be directly compared to the aerial photographs from the previous year. Regrettably, heavy snow cover prevented surveying of the summit of Tindastóll. Five

sites lower down the mountain were surveyed, but the metre scale features, which form the focus of the analysis of the aerial photographs were inaccessible.

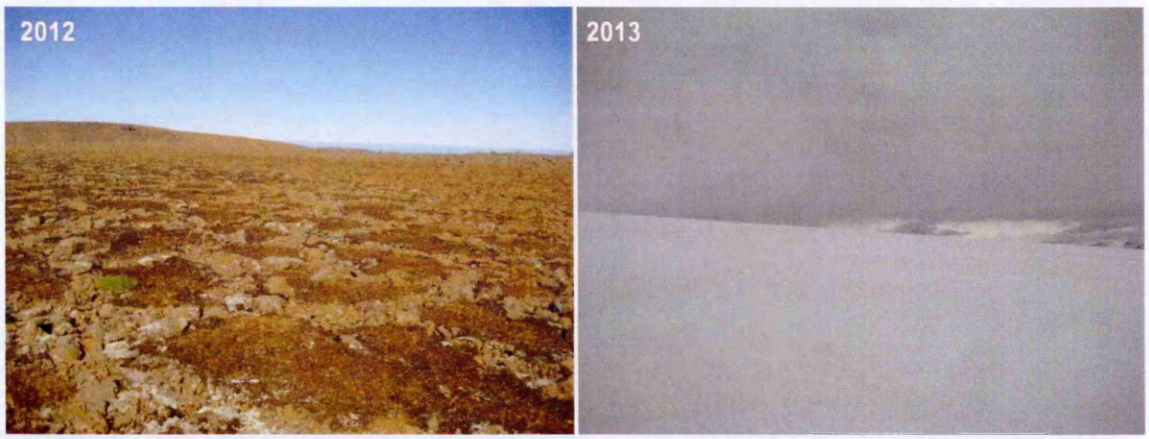

Figure 4.9: Changing conditions on the summit of Tindastóll. The 2012 image shows a net of metre scale sorted patterned ground at the summit; features are 1 to 3 m in diameter. The 2013 image was taken at a lower point on the hill, on the approach to this site, which could not be reached due to deep snow and low visibility.

A number of back up sites had been identified in case of this contingency during the reconnaissance surveys of the previous year. These sites had two disadvantages; firstly they mostly fell outside the area covered by the remote sensing data, and so would not provide higher resolution images of the same features, and secondly the features located below the snowline were predominantly centimetre scale patterned ground. Such features are less directly comparable to the sorts of patterns observed on the martian surface.

Despite these setbacks the data collected provided a wide range of examples of the sorts of structures that would be expected to occur in a martian periglacial environment and can be used to determine what would be expected to be seen in HiRISE images of Mars and what would be below their resolution.

4.3.1 Structure from Motion Survey

Structure from motion is a powerful photogrammetry technique which can be used to construct a three dimensional model using a series of photographs, without needing to

know the exact position from which each photograph was taken. The aim of this section of the field project was to digitise large areas of patterned ground using *Structure from Motion* for analysis in a virtual environment. A variety of analyses were applied to both aerial survey data and martian remote sensing. The *structure from motion* technique can be used to produce comparable datasets covering small scale features at a much higher resolution. This allows a direct comparison to be made.

This technique has applications for both terrestrial fieldwork and planetary science. Ground truth data play an important role in the analysis of remotely sensed images, however they are impossible to acquire for most parts of Mars. The only close observations of the martian surface come from a handful of landers and rovers. Photogrammetry techniques can be used to collect data on Mars which can then be analysed on Earth, which is considerably easier than attempting to make measurements using a rover. Stereo photographs are used by the current generation of Mars exploration rovers. New techniques such as this could be added to the resources available for future missions. However structure from motion is a relatively new technique, it is therefore important to assess whether large patches of small, centimetre scale features can be digitised reliably.

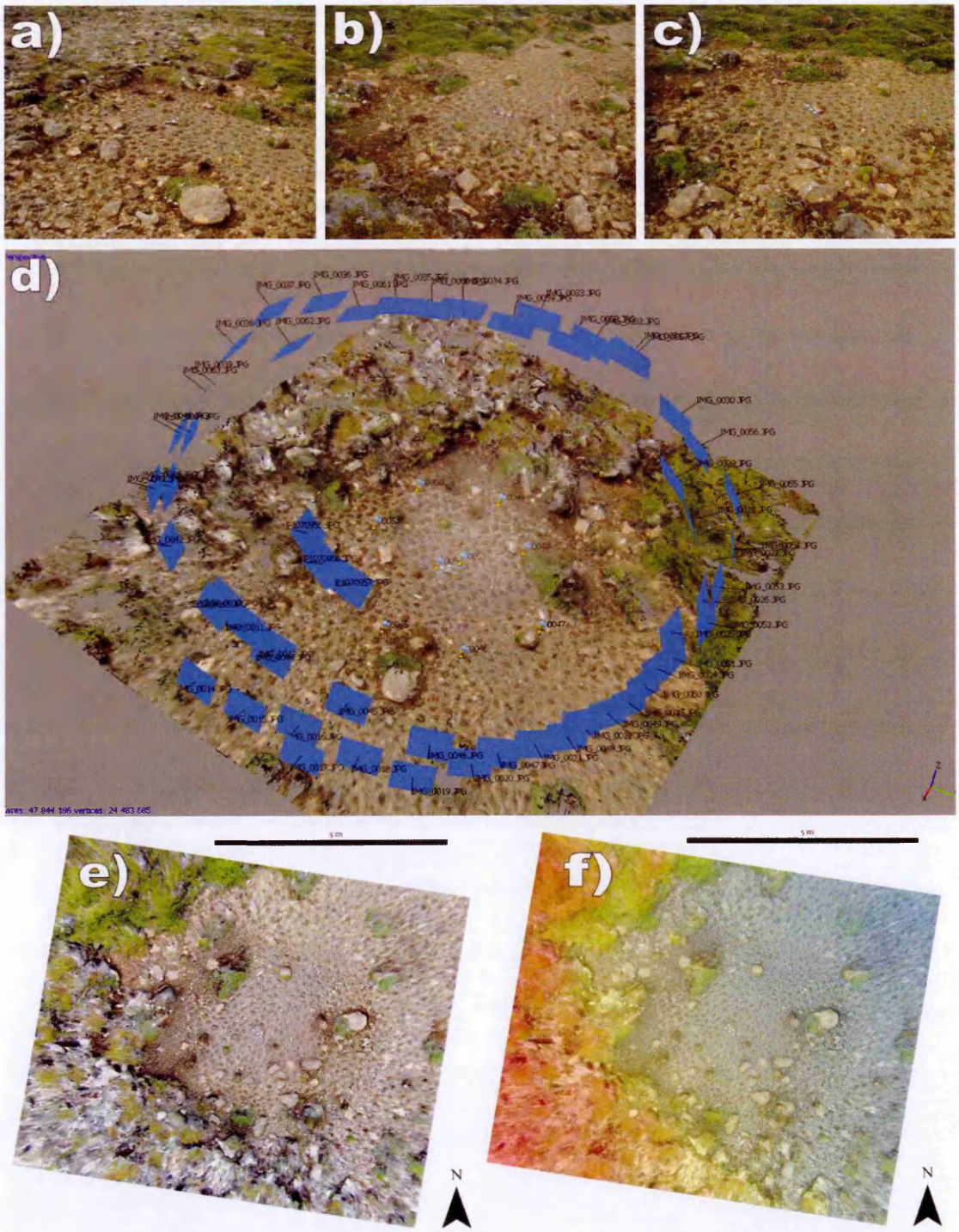

Figure 4.10: Illustration of the digital model and resulting Orthophotos and DEMs produced by the Structure from Motion software for site 11. a-c) Input field photographs, d) 3d model of study site, e) Orthophoto, f) Digital Elevation model.

4.3.2 Structure from Motion Background

The *Structure from motion* (SfM) photogrammetry technique uses a large number of images of the same object or place taken from different positions. By finding matches between the photographs a three dimensional model of the object can be constructed. By using a large number of images this system can reconstruct the object without knowing the positions from which the photographs were taken, as this can be solved as part of the process (Westoby et al., 2012). This makes it a very quick and easy technique for use in the field as walking around an object taking a few tens of photographs from different angles is sufficient to construct a Digital Elevation Model (DEM), the resolution of which is determined by the resolution of the images.

The main advantage of SfM techniques is that expensive specialist equipment is not required. Images can be acquired using any commercially available digital camera and the photographs do not need to be carefully positioned so long as sufficient coverage is acquired. The exact position of the cameras need not be recorded; making the use of images captured by Unmanned Aerial Vehicles (UAVs) more reliable (Fonstad et al., 2013).

Many researchers are applying *Structure from Motion* techniques to geomorphological (Fonstad et al., 2013; Westoby et al., 2012), geological (Tavani et al., 2014) and archaeological research (Hesse, 2014; Koutsoudis et al., 2014). Surveys have been conducted using both ground based images and those acquired from UAVs, with results comparable to those acquired by more traditional LiDAR surveys or laser scanning techniques (Fonstad et al., 2013).

Structure from Motion has been used to augment remotely sensed datasets by incorporating high resolution ground based observations of sites which are only imaged at low resolutions by satellite and aerial images (Hesse, 2014). A similar methodology

will be used in this investigation with *structure from motion* being used to generate high resolution orthophotos that will allow ground based observations to be surveyed and analysed in the same manner as data from the aerial surveys. *Structure from motion* thus has the potential to dramatically speed up surveying.

DEMs and orthophotos of sorted forms can be used to measure a variety of properties of the sorted circle's structure which would normally be measured in the field; clast size, shape and arrangement, the height and width of coarse domains, the surface area of fine domains and the orientation and elongation of sorted forms. All of these measurements can be made in situ in the field, but are time consuming.

Taking photographs of features is fast and inexpensive, and allows all of these measurements to be made at a later date, and in a more efficient virtual environment. Consequently, this technique could be very valuable in allowing far more sites and landforms to be recorded over the course of a day in the field than would otherwise be the case. This could prove useful for long term monitoring campaigns where the same features need to be examined repeatedly over a number of years. DEMs and orthophotos can be produced from field photographs and then compared within a GIS to measure variations in structure and size over that time.

This approach has recently been applied to sorted patterned ground in Svalbard by Kääb et al., (2014). They used existing field photographs taken several years apart to generate two digital terrain models and then analysed the movements of particles at the site over this period of time. They determined that fine domain material was being moved outwards, and coarse domain material being moved inwards, and that the rate of movement was the same for both, approximately 2 cm yr^{-1}. Their methodology did not inform this project, since their research was published after the completion of the field campaigns. However it would be a useful template for future research into this area.

4.3.3 Surveying Procedure

During the 2013 survey 31 sites were examined and photographic datasets for use with the *SfM* technique were collected. On the first day of the survey a number of base stations were set up in proximity to each survey site. The positions of these were precisely measured relative to a base station set up on the triangulation pillar in locality four. Each base station was marked with a peg so that a GPS receiver could be placed at the same site repeatedly throughout the field campaign.

A GPS rover on a surveying staff was then taken to the survey sites and used to make *in-situ* measurements. The most important of these were to establish ground control for the *SfM* data sets. At each site where *SfM* was to be used a set of at least six pegs were placed in the ground at the periphery of the features being imaged. The position of each peg was then recorded with the GPS so that these coordinates could be used to georeference the resulting DEM. These points also allow the gradient of the underlying slope at each site to be calculated using ArcGIS. These data were useful in comparing these sites to those examined in 2012 where similar measurements of gradient were made.

A scale bar was also placed in the approximate centre of the circle and the position of this was also recorded to assist in georeferencing the final DEM. The site was then photographed from all angles with sufficient overlap for the images to be matched.

It was decided that individual photographs should be taken, using a good quality camera. Another alternative would have been to record video in the field which could then be broken down into its constituent frames for use with *SfM*. The latter would have been faster in the field, but taking individual photographs allows for focusing and aligning the images and so produces a better model. Three cameras were taken into the field. A Panasonic G1 micro 4/3, 12 megapixel camera was used for the majority of the

surveying, but both team members also carried canon iXUS 70, 7 megapixel cameras which were used to take context photographs and as a back up on occasions when the primary camera required recharging.

The primary camera had a 14-45mm f/3.5 zoom lens, fitted with a circular polarising filter. Images were taken on the wide angle setting of 14 mm (equivalent to a 28mm lens on a 35mm frame). No filters were used on the Canon cameras, and again these were used on the widest angle setting of 5.8mm (again equivalent to 28mm on a 35mm frame). In both cases an ISO speed of 100ASA was set. For the micro 4/3 images, these were collected as RAW format files, and processed to JPG format using SilkyPix software.

It was found that the more photographs taken the better the resulting model. At least forty photographs were acquired for the majority of sites and many more were taken at some locations. Detailed photographs of the structures being examined were also taken to compare with the results of the SfM and to test the reliability of the method.

The GPS data were processed using Leica Geo Office software. The position of the base station was used to correct the rover position measurements, producing values with centimetre scale precision. Several test models, were produced while in the field to check that the approach was valid, with the rest being processed after the field campaign had finished.

4.3.4 Reliability of the SfM Method

It was found that some datasets produced better results than others. Large scale features were easier to image than smaller scale structures. Although lots of fine detail was preserved in the finished models many exhibited significant distortion at the cm scale. The centre of the site, where the majority of the images overlap, will always have the best result in terms of both resolution and lack of distortion. The further from the

centre, fewer images can be used to reconstruct the model and the greater the distortion of features becomes. Consequently, in order to cover wide areas at high resolution, the site should be broken down into a large number of circular areas, each of which should be imaged and processed separately. Some sites with fairly uniform features were harder to reliably image than those with more varied terrain. Several datasets could not be matched sufficiently to produce a working model.

Some sites produced much better results than others. Several sites had considerable distortion even in the centre of the field and this may be due to inaccuracy in the marking of the ground control points during model construction. On some of the larger sites it was impossible to include all of the markers within each photograph and this may have contributed to the difficulty in precisely georeferencing these sites. In future investigations of this sort it is recommended that a larger number of small sites should be surveyed rather than fewer larger areas. None of the models produced was as good quality as a panorama of images taken from directly above, but the ease of georeferencing the resulting model was of use.

The positions of clasts within a study area could be digitised reliably from structure from motion models. But it was concluded that the possibility of distortion within the model made it impossible for a reliable assessment of clast shape to be made at the centimetre scale. This would probably be less of an issue where larger scale features, with greater topographic relief are imaged. The fact that very small features were examined in this survey probably detracted from the usefulness of the resulting dataset. Small features have insufficient relief to allow easy matching of photographs to be conducted. It would be interesting to attempt a similar survey using a UAV or camera mounted on a long staff in order to produce SfM photo sets containing more down

pointing images in a dome over the features to be surveyed, rather than relying on ground based photographs in a ring.

4.4 Results

In this section the results of several studies into the morphology and distribution of sorted features are presented. Section 4.4 presents a comparison between surveys of the remotely sensed data and ground truth. This includes an analysis of the relationship between the elongation of polygonal structures and the underlying gradient. Sections 4.5-4.6 present the scheme by which these features were classified. Finally Section 4.7 details the application of an *Average Nearest Neighbour* analysis to several sites to determine whether this statistical approach can be used to determine whether the distribution of boulders around sorted patterned ground is significantly different from a random distribution. These approaches demonstrate a variety of criteria which can be used to assess the likelihood that martian features formed as a result of periglacial processes.

4.4.1 Examination of Aerial Photographs and comparison to ground truth

Of the various data collected during this project the aerial photographs of Tindastóll are the most directly comparable with martian remote sensing data. They have a resolution of 15 cm per pixel, slightly better than the 25 cm per pixel resolution of the HiRISE instrument on Mars Reconnaissance Orbiter. However the sizes of the clasts and networks are not the same, the largest boulders on Tindastóll are somewhat smaller than their martian analogues and the networks they form are not as wide. Consequently, a similar amount of detail can be seen in the terrestrial images as in their martian equivalents despite the difference in scale of both the features and the smallest resolvable objects.

The aerial photographs were surveyed using the same protocols that are used when examining martian images (detailed in Chapter Six). The images were loaded into ArcGIS and were inspected manually. Areas where the patterns of boulders, or variations in albedo, suggested the presence of a clastic net were marked. This produced a shape file of sites with putative sorted patterned ground. Lobate structures that could be indicative of solifluction processes were also marked.

The distribution of possible periglacial features in the remote sensing data was then compared to the GPS tracks indicating the route taken through the field during the reconnaissance survey and the approximate locations of the field photographs. This confirmed that the features observed in the remote sensing survey did correspond to the locations of periglacial features observed in the field. Figure 4.11 shows the distribution of sorted patterned ground and solifluction features across the southernmost part of Tindastóll, the area visited during the field campaign.

The area was then expanded, with a range of putative periglacial features being marked on areas of the hillside not visited during the field campaign. The assessment that they are likely to exhibit sorted patterned ground is based entirely on the remote sensing data and the observations of Feuillet et al., (2012). Since these features are morphologically similar to those observed in the southern part of the hillside it can be concluded with some confidence that they are examples of sorted patterned ground. Occurrences of sorted patterned ground and solifluction lobes are discussed in more detail below.

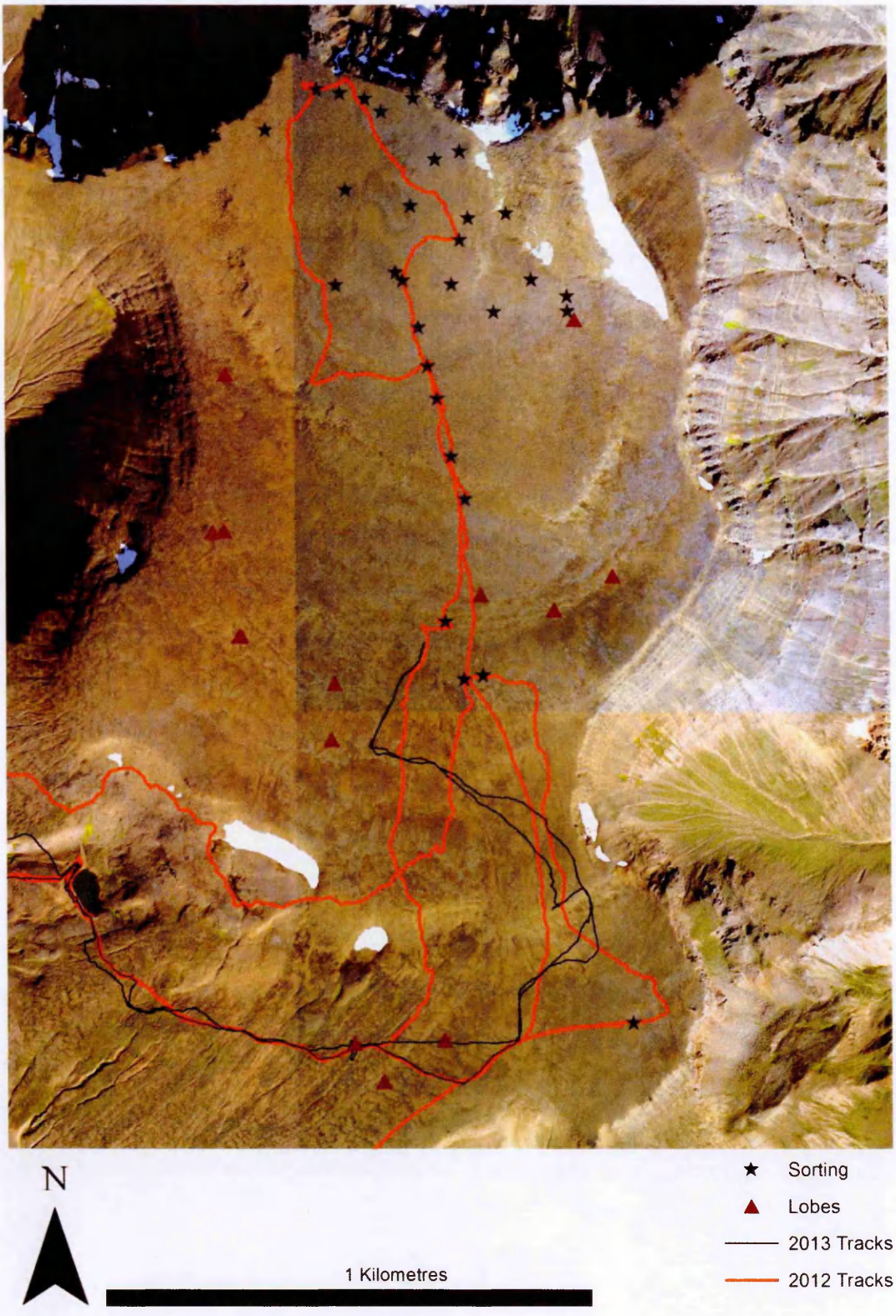

Figure 4.11: The summit of Tindastóll Massif showing the routes taken during the surveys in 2012 and 2013 and the location of various sorted and lobate features.

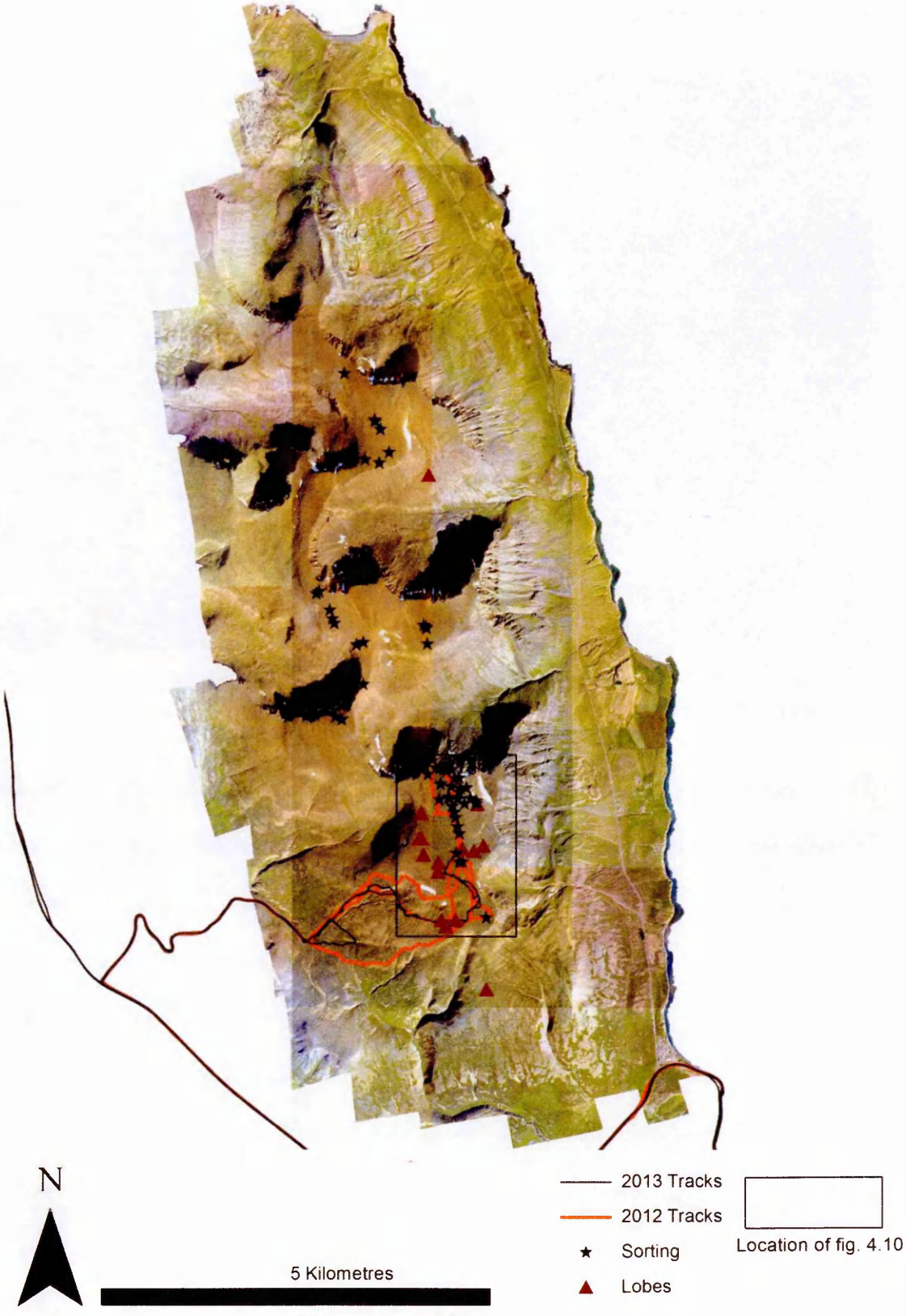

Figure 4.12: Map of the summit of Tindastóll Massif. Black stars indicate locations where sorted patterned ground can be seen in the aerial photographs, while red triangles indicate locations where solifluction lobes are believed to be present.

4.4.2 Sorted Patterned Ground

Figure 4.13: Sorted patterned ground on the summit of Tindastóll

The reconnaissance survey of this site provides ground truth for the variety of features located there through direct observations. Large sorted nets clearly cover much of the hilltop with smaller scale patterned ground being ubiquitous on unvegetated surfaces. High on the hill large nets dominate. Examples of both sorted polygons and stripes were observed. At lower elevations, where large nets are less well-developed, there are frequent instances of better developed centimetre scale features nested within the larger metre scale structures. However these small scale features are well below the resolution of the aerial photographs. From the air, these sites do not resemble a sorted net to the same degree.

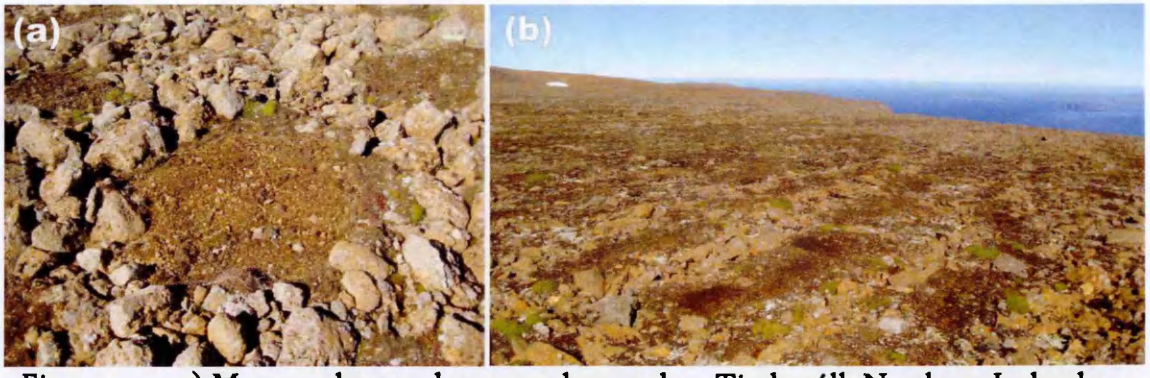

Figure 4.14: a) Metre scale sorted patterned ground on Tindastóll, Northern Iceland. This circle is approximately 1.5 m across and consists of a fine domain made up of silt and gravel sized particles, surrounded by a coarse domain consisting of cobble to boulder sized material. b) Possible sorted stripes at the same site. Stripes of boulders occur 1-3 m apart alternating with bands of finer material. These stripes appear to be orientated orthogonal to the downslope direction.

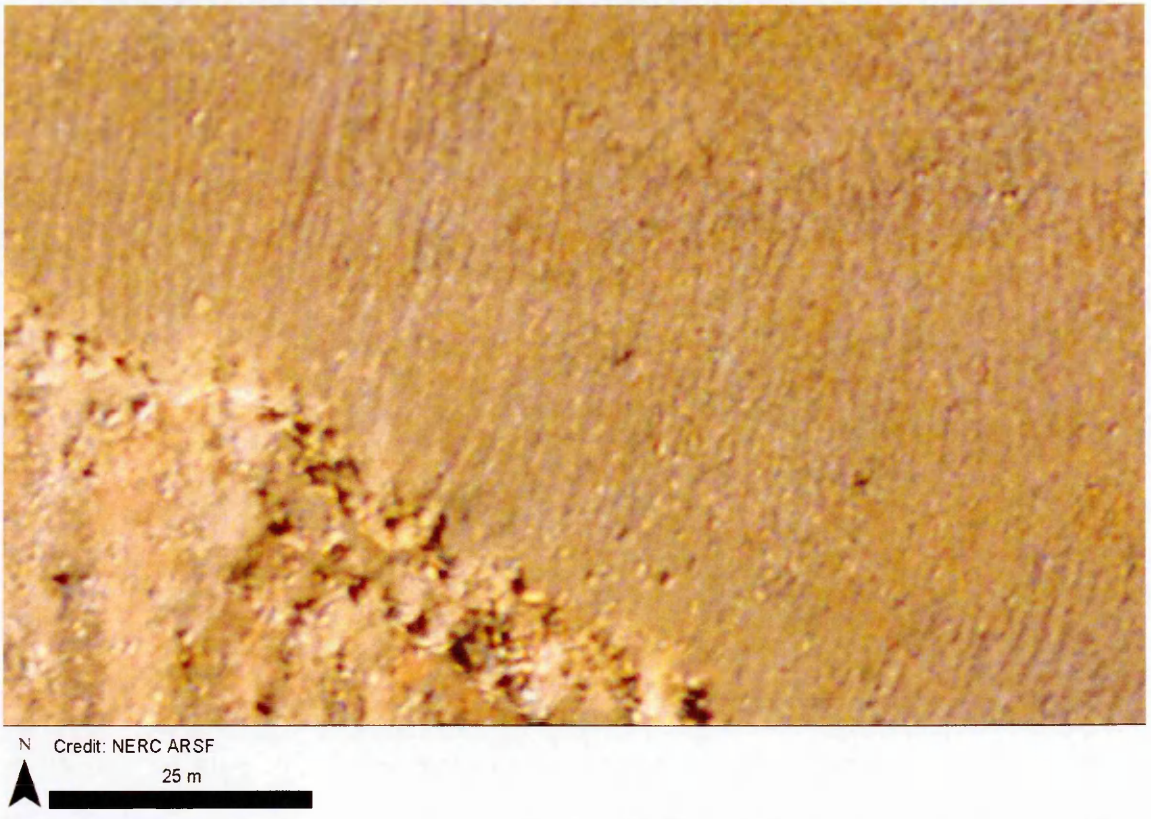

Figure 4.15: Sorted stripes on summit of Tindastóll (downhill is towards the bottom of the image where the top of a gully alcove can be seen).

Figure 4.16: An irregular sorted network consisting of a variety of polygonal structures, and several possible stripes on the right hand side of the image.

Large boulders can clearly be seen in the remote sensing images, and in some cases appear to form a discontinuous net. However in Figure 4.16 the clear polygonal structures shown in figure 4.13 are not as apparent. This site was visited during the 2012 expedition so sorted patterned ground is known to be present there. However, it is not as easy to see in the air photographs. Were it not for the ground truth observations these sites might not be classified as being putative periglacial features at all. A much larger area of the hillside is covered in sorted patterned ground than is apparent from the aerial photographs. Figure 4.12 demonstrates that areas that could be confidently identified as patterned ground were much fewer in areas that lacked in situ observations.

Centimetres scale features are the most common variety of patterned ground across the Skagafjörður region. They are found on most patches of un-vegetated ground. Larger features only appear at a few high elevation sites both on Tindastóll and on the tops of

some of the mountains to the east of the fjord. These are the parts of the fjord that experience the greatest temperature contrast and where the most undisturbed material in the decimetre to metre size range is to be found.

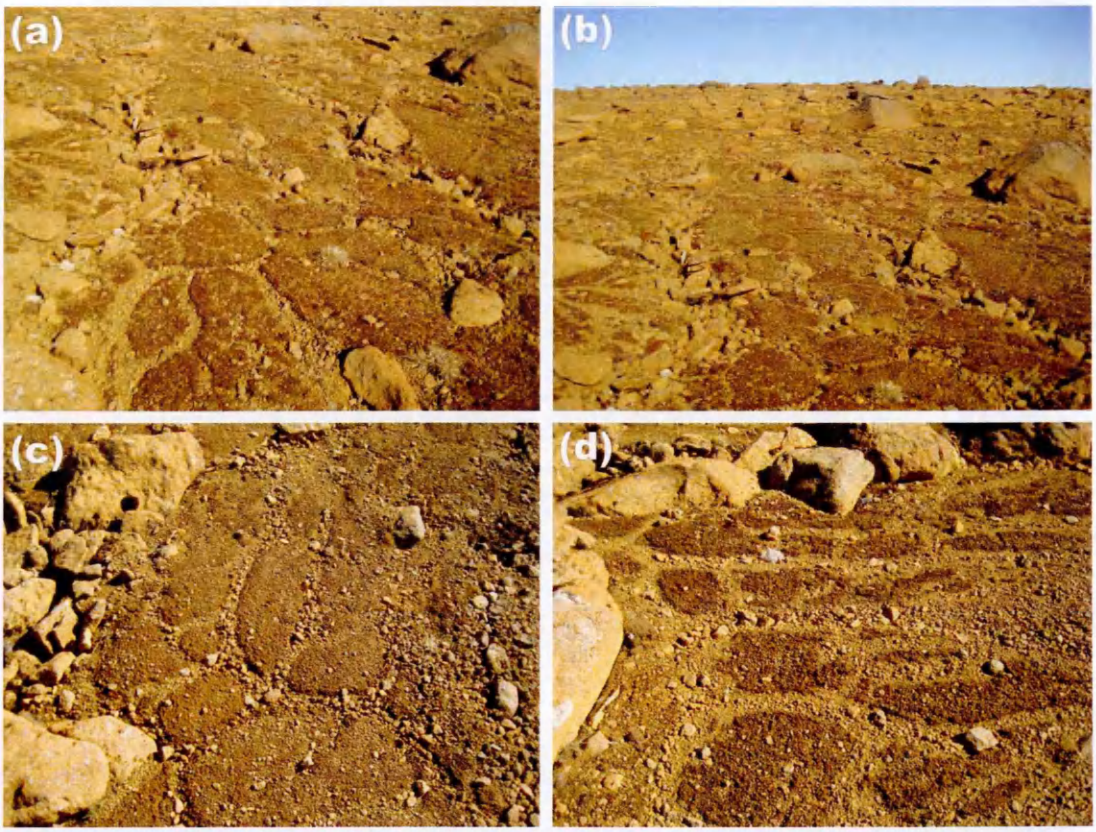

Figure 4.17: Centimetre scale sorted circles. High centred domains of silt and sand (approximately 20 cm across) are surrounded by bands of pebbles and small cobbles. These features are found within larger bands of boulder sized material, indicating that sorting occur at a variety of scales. Panels a) and b) show a mixture of wide and narrow coarse domains, c) narrow coarse domains and d) wide coarse domains.

In summary the survey confirmed that the sorted features visible in the aerial photographs did correspond to locations where extensive and large scale sorted networks were present on the ground, but that a large number of periglacial features went unobserved. Consequently, we can conclude that when looking for a periglacial environment on Mars the majority of the features of interest will be below the resolution of the images. Only the unusually large features, in the locations with the most extreme conditions, will be detectable. These will not be common.

4.4.3 Solifluction Features

A large number of putative solifluction lobes were located in the aerial photographs and LIDAR DTM, mainly on the steeper slopes around the periphery of the summit. Very few of these sites fell near to the tracks from the previous year's expedition, and such features had not been noted at that time. Consequently, it was decided to visit several of these locations during the 2013 survey to confirm that solifluction features were present.

Grass covered lobate features were found to be present at the locations visited; an eight degree slope on the approach to the summit of Tindastóll, approximately 840 m above sea level. In contrast to the examples of sorted patterned ground, these structures were much easier to detect in the remotely sensed data, where the variations in height across the feature mapped in the LIDAR DTM provided a clear image of banks of lobate structures travelling down the slope.

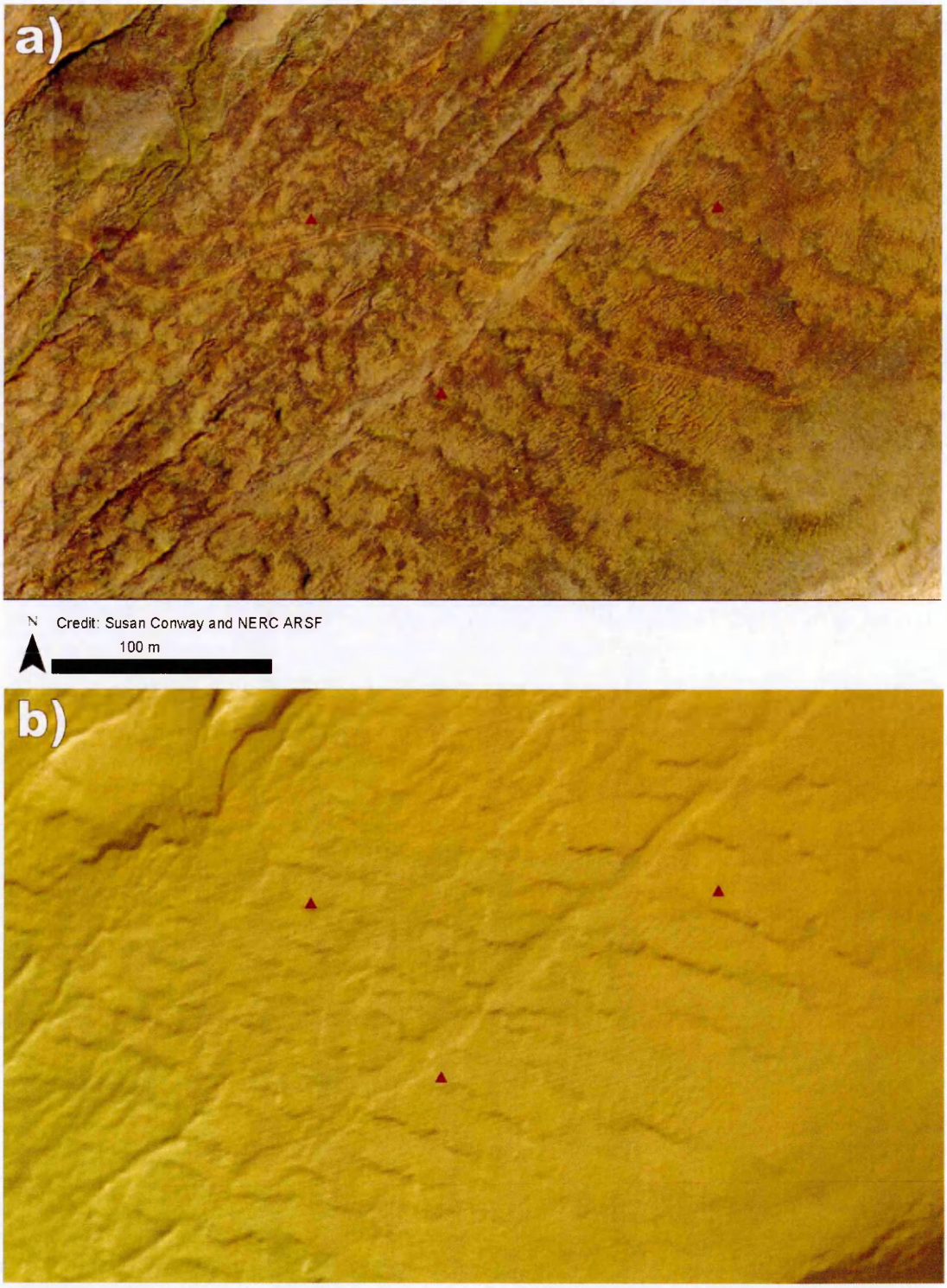

Figure 4.18: Possible solifluction lobes on the hillside of Tindastóll. Down slope is towards the south west. a) In the aerial photographs lobate structures are visible as sheets of light brown material banked with slightly green edges. B) In the lower resolution LiDAR DTM the edges of the lobate structures can be seen.

In the field these grassy banks easily blended into the generally rough topography and were easy to miss when they were not the focus of the investigation. Consequently, it was concluded that the remotely sensed data provided a useful tool for locating this

type of feature and that they could be detected with fairly high confidence on the martian surface, even without ground truth.

Figure 4.19: Solifluction lobes observed in the field, the forward edge of the lobe is marked with a black line; the yellow and green pegs were used in surveying the site and mark the top of the riser.

In addition to these lobate structures at the Tindastóll site, several clastic lobes were identified on a hillside on the Skagi Peninsular (locality 1). These structures occurred on a 30° slope and at an elevation of 95 m above sea level and were morphologically very different to those seen at the Tindastóll site.

The Skagi features consisted only of boulder sized material and were largely overgrown, suggesting that they had formed as clastic solifluction lobes, but were now relict features that had formed sometime in the past. This is supported by the lack of other active periglacial features at this scale in the area. Unfortunately these features are well outside the area covered by the aerial photographs and so cannot be examined in remotely sensed data for comparison to morphologically similar martian features such as the lobate structures illustrated in Figure 2.5.

Figure 4.20: Clastic lobate feature on steep slope at the edge of the Skagi Peninsular field site. The boulders range from several tens of centimetres to more than a metre across.

4.4.4 Classifying polygon elongation

Transitional regions where sorted circles or polygons become elongated and grade into sorted stripes are common across the Skagafjörður region. Figures 4.21 and 4.22 illustrate two such sites, one photographed from the ground and one visible in aerial photographs of the Tindastóll area.

Figure 4.21: Centimetre scale patterned ground on the coast to the east of Sauðárkrókur. Sorted stripes approximately 2-3 cm wide with raised fine domains transition to isolated fine domains surrounded by gravel rings. (Direction of slope is away from the photographer).

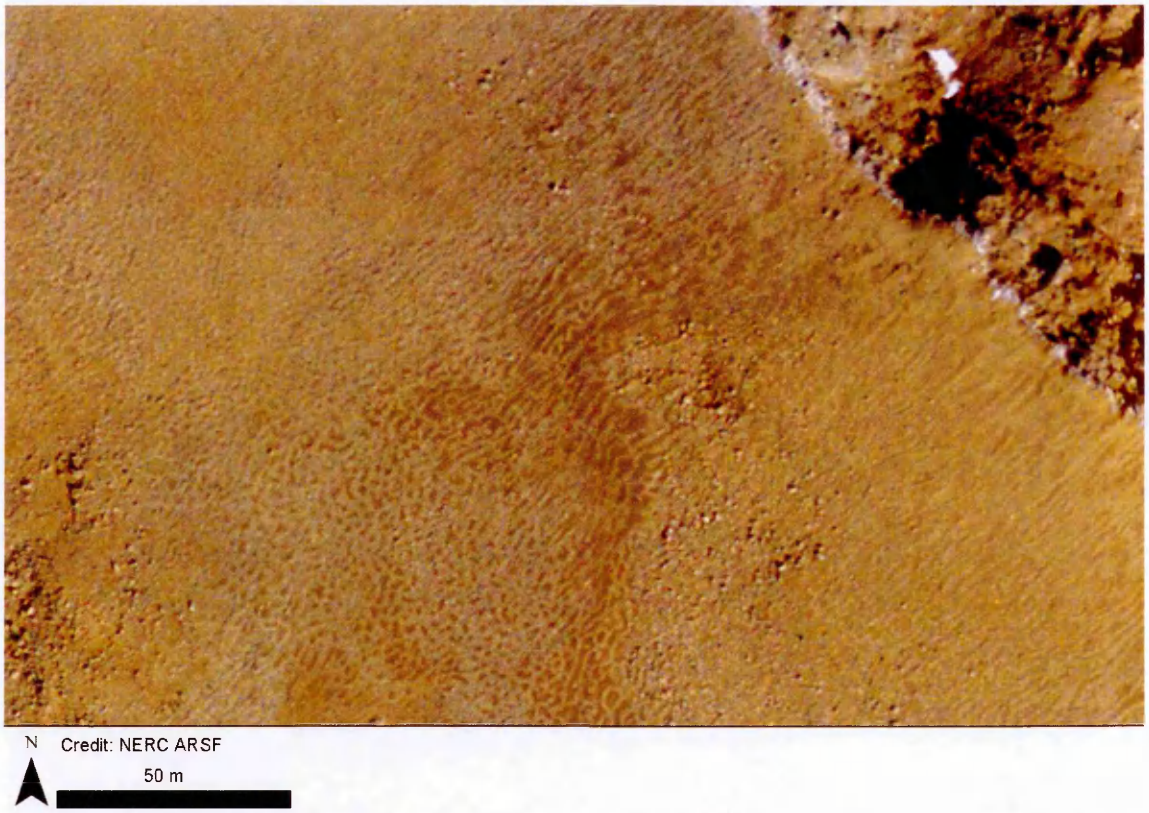

Figure 4.22: Aerial photograph of the summit of Tindastóll. Sorted circles can be seen to become elongated towards the centre of the image and transition to a series of stripes on the right hand side. Circles are 1-3 m in diameter, the direction of slope is towards the upper right hand corner of the image where the alcove of a gully can be seen (Image from the NERC ARSF aerial survey of 2012).

Sorted stripes are known to occur preferentially on steeper slopes whereas polygonal features are found on flatter ground (Washburn, 1956). It is believed that the transition from circular features to elongated patterns is triggered by increases in gradient (Kessler and Werner, 2003; Krantz, 1990). On flat ground horizontal sorting causes patterns to expand in all directions forming circles or polygons. However as the gradient increases there is a larger degree of movement down slope, leading to elongation of polygonal patterns and a transition from polygons to stripes (Kessler and Werner, 2003; Krantz, 1990). The transition between these two feature types usually occurs on slopes of three to seven degrees (Washburn, 1956), although elongated polygons can be found on shallower slopes (Krantz, 1990).

This slope dependence is a characteristic attribute of sorted patterned ground and so could be a useful line of evidence in assessing whether putative martian patterns are periglacial in origin. If circular to stripe-like transitions are observed at locations where martian hillsides become steeper, then they are more likely to be the result of periglacial processes than if they are found on shallower slopes.

Consequently, it was decided to examine the range of gradients on which different types of terrestrial patterned ground were observed. By assessing this parameter in both in situ and air photo datasets it should be possible to determine the extent to which this parameter can be applied to the martian survey. This will indicate whether this can provide an effective test for martian features having formed through periglacial processes.

The elongation of all of the sites examined in detail during both the 2012 and 2013 surveys was graded. All polygonal features were classified using a qualitative scale. Circular and near circular features were classified as type one, with increasingly more elongated structures classified as types two to five. Type three consists of purely transitional features which cannot clearly be said to be polygons or stripes, or which fall between two sets of better defined patterns.

Table 4.1: Definitions of Polygon Elongation ratings.

Type		Description	Example
1	Polygons	Circles	a
2		Elongated circles	b
3	Transitional	Transitional	Type 2 grades to type 4
4	Stripes	Discontinuous stripes	c
5		Stripes	d

Stripes were divided into type four, which consists of discontinuous stripes and type five which includes clear stripes with no or few breaks. Many sites consisted of features in one of the transitional classes, with isolated patches of type one polygons or type five stripes grading into intermediate structures.

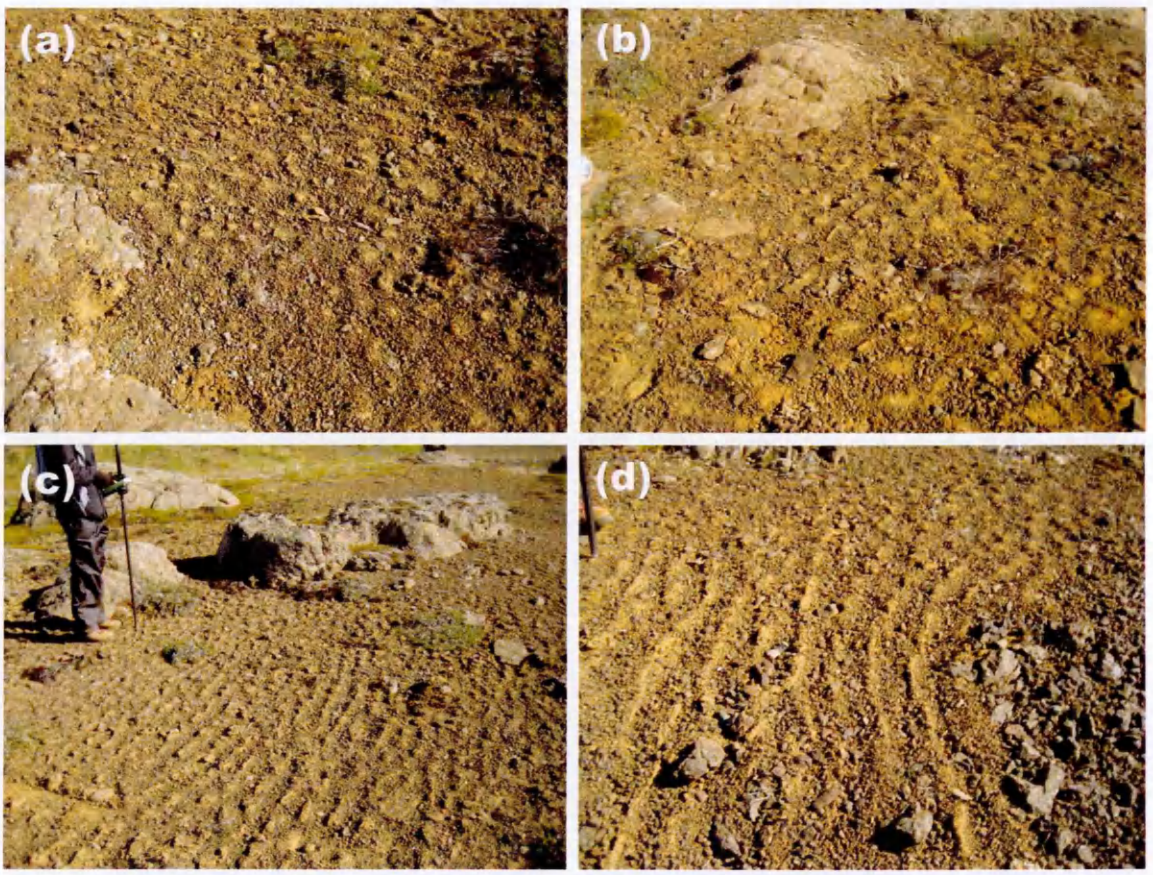

Figure 4.23: Patches of each variety of small scale patterned ground. a) Circular polygons, b) Elongate polygons, c) Discontinuous stripes, d) Continuous stripes

This classification scheme was applied to all of the sites examined during the investigation; however since it was qualitative in nature it was decided to test the reliability of the classification by determining the ratio between the long and short axes of polygons at sites where the structures were digitised. It was found that there was a good agreement between the axis ratio and the qualitative classification for polygonal features. Type one polygons generally have an axis ratio in the range of 1.1-1.5, while type two features were more frequently in the range 1.5-2.5. This pattern held true for type three transitional features, but stripes of types four and five did not exhibit a

direct correlation to axis ratio. This was to be expected, since the distal edges of a set of stripes are less clearly defined than those of polygons, and stripes vary much more in length than in width. Consequently the classification of elongated polygons was concluded to be very reliable, but the classification of stripes was more subjective.

4.4.5 Variety of features at survey sites

Tables 4.2 -4.4 show the variety of features observed at each site. The patterns were classified based on their elongation from stripes to polygons and their general scale. The grain size of the material making up the coarse fraction is also presented. In general the fine fraction was composed of silt grade material with a small amount of coarser sand grade particles.

When the soil was wet the fine domains were generally flat and frequently at the same height or lower than the surrounding coarse domains. However when drying out the finer material puffed up, causing some fine domains to be higher than the surrounding stone banks. As would be expected there is a correlation between larger grain sizes and larger features. Larger polygons incorporate more cobbles and large pebbles, while smaller structures have fewer large clasts.

Irrespective of the size of the largest material to make up a polygon there is a grading from the largest material at the centre of the coarse domain through increasingly finer clasts towards the boundary with the fine domain.

Features of a variety of sizes were examined during this survey. During the 2012 surveys a large number of small 5-10 cm scale features were recorded. These were found at a range of elevations in localities 3 and 4. During the 2013 survey there was a focus on larger structures several tens of centimetres across. This was due to these features being better suited for the application of the *structure from motion* technique.

The metre scale features were only observed at very high elevations; greater than 950 metres above sea level. Smaller features, a few centimetres to several tens of centimetres across, were also found at all elevations but the largest features were only found at the higher elevations, where the temperature variation was likely to be most extreme, and potentially where they were least likely to have been disturbed. This was also the region in which the largest boulders were present overall. Large cobbles and boulders were more prevalent at the highest elevation sites, possibly due to the exposure of the bedrock by deflation of loose drift material, due to the high elevation and lack of vegetation.

On the Tindastóll hillside much larger material is in a loose state and has been reworked into larger features over a much longer period of time. This can be seen in locality five, where the sorted patterns are forming on hillsides covered with coarse granular material which may be the spoil from the construction of the nearby road. Much wider stripes occur and the fine domains have much less of the silt fraction. This is because they are composed of coarse grained sand and granule grade material.

Table 4.2: Survey of patterned ground above the shore of Skagafjörður (Locality 3).

Site	Locality	Primary Grain Size	Secondary Grain Size	Feature Scale /cm	Elongation Rating	Classification	Slope Gradient
Site 1	3	Granules to Pebbles	Small Cobbles	5	4.5	Stripes	4.44
Site 2	3	Granules to Pebbles	Small Cobbles	5	3	Transitional	3.93
Site 3	3	Pebbles	Isolated Cobbles	10	2	Polygons	1.88
Site 4	3	Granules to Pebbles	Small Cobbles	5	4	Stripes	5.83
Site 5	3	Granules to Pebbles	Small Cobbles	10	5	Stripes	12.6
Site 6	3	Granules to Pebbles	Small Cobbles	20	1	Polygons	0.8
Site 7	3	Granules to Pebbles	Small Cobbles	~ 10	2	Polygons	0.89
Site 8	3	Granules to Pebbles	Isolated Cobbles	10	3	Transitional	1.15
Site 9	3	Large Pebbles	Granules	~ 10	4	Stripes	3.35
Site 10	3	Granules to Pebbles		5	1	Polygons	0.85
Site 11	3	Pebbles	Isolated Cobbles	5	3	Transitional	2.1
Site 12	3	Pebbles		5	4	Stripes	5.63
Site 13	3	Granules to Pebbles	Small Cobbles	5	1	Polygons	0.4
Site 14	3	Pebbles		5	3	Transitional	1.07
Site 15	3	Pebbles		~ 10	4	Stripes	4
Site 16	3	Pebbles	Small Cobbles	10	1.5	Polygons	0.17
Site 17	3	Pebbles	Small Cobbles	5	3	Transitional	1.5
Site 18	3	Pebbles	Small Cobbles	10	4	Stripes	4.15
Site 19	3	Pebbles	Small Cobbles	~ 10	2	Polygons	0.83
Site 20	3	Pebbles	Small Cobbles	10	3	Transitional	3.05
Site 21	3	Pebbles	Small Cobbles	5	4.5	Stripes	5.65
Site 22	3	Pebbles		10	2	Polygons	0.87
Site 23	3	Pebbles	Small Cobbles	~ 10	3	Transitional	2.89
Site 24	3	Pebbles	Small Cobbles	~ 10	5	Stripes	4.08
Site 25	3	Pebbles	Cobbles	~ 10	4	Stripes	3.05
Site 26	3	Pebbles		~ 10	3	Transitional	1.46
Site 27	3	Pebbles	Small Cobbles	~ 10	4	Stripes	4.07
Site 28	3	Pebbles		5	5	Stripes	6.18
Site 29	3	Pebbles	Cobbles	~ 10	3	Transitional	2.23
Transect 1	3	Various	Various	~ 10	N/A	Transitional	11.38

Table 4.3 Survey of centimetre scale patterned ground on cliff top around geodetic pillar (Locality 4).

Site	Locality	Primary Grain Size	Feature Scale /cm	Secondary Grain Size	Elongation Rating	Classification	Slope Gradient
Site 1	4	Cobbles	20		3	Transitional	6.02
Site 2	4	Pebbles	~ 10	Small Cobbles	4	Stripes	7.89
Site 3	4	Cobbles	~ 10		1	Polygons	1.92
Site 4	4	Pebbles	~ 10	Small Cobbles	3	Transitional	4.76
Site 5	4	Pebbles	~ 10	Large Granules	2	Polygons	4.11
Site 6	4	Pebbles	~ 10	Small Cobbles	4.5	Stripes	11.52
Site 7	4	Pebbles	~ 10	Small Cobbles	1	Polygons	2.04
Site 8	4	Pebbles	~ 10	Granules and Cobbles	5	Stripes	16.52
Site 9	4	Pebbles	~ 10	Small Cobbles	4	Stripes	8.11
Site 10	4	Pebbles	20	Cobbles	2	Polygons	15.95
Site 11	4	Pebbles	10		5	Stripes	1.49
Site 12	4	Small Pebbles	5		5	Stripes	3.95
Site 13	4	Small Pebbles	5		4	Stripes	10.55
Site 14	4	Small Pebbles	10		3	Transitional	2.94
Site 15	4	Small Pebbles	~ 10		4	Stripes	5.77
Site 16	4	Small Pebbles	5		4	Stripes	6.73
Site 17	4	Pebbles	10	Isolated Cobbles	3	Transitional	3.34
Site 18	4	Pebbles	10	Isolated Cobbles	2	Polygons	3.34
Site 19	4	Pebbles	~ 10		3	Transitional	4.95
Site 20	4	Pebbles	~ 10		3	Transitional	3.23
Site 21	4	Large Pebbles	~ 10		2	Polygons	3.42
Site 22	4	Pebbles	5	Cobbles	4	Stripes	6.05
Site 23	4	Pebbles	10		2	Polygons	2.24
Site 24	4	Pebbles	5		1.5	Polygons	1.92
Site 25	4	Large Pebbles	20	Small Cobbles	1	Polygons	0.5
Site 26	4	Pebbles	20	Small Cobbles	2	Polygons	3.38
Site 27	4	Pebbles	5	Small Cobbles	3	Transitional	4.26
Site 28	4	Large Pebbles	10		3	Transitional	7.26
Site 29	4	Large Pebbles	10		2	Polygons	4.22
Site 30	4	Small Pebbles	10		3	Transitional	2.92
Transect 2	4	Various	~ 10	Various	N/A	Transitional	12.84
Transect 3	4	Various	~ 10	Various	N/A	Transitional	
Transect 4	4	Various	~ 10	Various	N/A	Transitional	10.74

Table 4.4: Survey of sorted patterned ground across the Skagafjörður region.

Site	Locality	Primary Grain Size	Secondary Grain Size	Feature Scale /cm	Elongation Rating	Classification	Slope Gradient
Site 1	2	Pebbles	Cobbles	N/A	N/A	Lobe	8.96
Site 2	2	Pebbles	Cobbles	39	5	Stripes	8.64
Site 3	2	Granules to Pebbles	Cobbles	40	1	Polygons	5.66
Site 4	2	Granules to Pebbles	Cobbles	60	2	Polygons	7.39
Site 5	2	Pebbles to Cobbles	Granules	30	5	Stripes	7.02
Site 6	1	Pebbles to Cobbles	Granules	10	4	Transitional	7.04
Site 7	1	Granules to Pebbles		20	2	Transitional	0.86
Site 8	1	Pebbles to Cobbles	Granules	20	2	Polygons	1.58
Site 9	1	Boulders		N/A	N/A	Lobe	30.58
Site 10	1	Granules to Pebbles		30	1	Polygons	0.15
Site 11	1	Granules to Cobbles		20	1	Polygons	1.98
Site 12	1	Large Pebbles	Cobbles	20	1	Polygons	2.12
Site 13	5	Pebbles	Cobbles	20	4	Stripes	12.78
Site 14	5	Pebbles	Cobbles	20	5	Stripes	11.7
Site 15	1	Pebbles to Cobbles		10	4	Transitional	3.95
Site 16	1	Pebbles to Cobbles		5	2	Polygons	2.26
Site 17	1	Pebbles	Small Cobbles	10	4	Stripes	3.96
Site 18	1	Granules to Pebbles		10	4	Transitional	3.83
Site 19	1	Cobbles		20	N/A	Polygons	3.36
Site 20	1	Pebbles	Cobbles	10	3	Polygons	3.17
Site 21	1	Pebbles	Cobbles	30	1	Polygons	1.38
Site 22	1	Granules to Pebbles	Cobbles	10	5	Stripes	3.14
Site 23	1	Pebbles to Cobbles		5	3	Transitional	1.48
Site 24	1	Pebbles to Cobbles		10	2	Polygons	3.6
Site 25	1	Pebbles	Cobbles	5	4	Stripes	3.67
Site 26	1	Pebbles	Cobbles	10	2	Polygons	3.46
Site 27	1	Pebbles	Cobbles	20	2	Polygons	0.63
Site 28	1	Pebbles	Cobbles	10	2	Polygons	0.84
Site 29	1	Pebbles	Cobbles	5	4	Stripes	6.25
Site 30	1	Pebbles	Cobbles	5	3	Transitional	3.08
Site 31	1	Cobbles	Granules	50	N/A	Polygons	4.05

4.5 Characterising the morphology of sorted patterned ground.

The data produced by the aerial survey in 2012 and the SfM survey in 2013 allow a direct comparison to be made between centimetre scale features on the ground and metre scale features, as seen in remotely sensed images. This is useful for setting a baseline for identification of martian analogues, which are believed to occur on a decametre scale. In order to make this scaling argument a large number of individual polygons were digitised so that their morphology could be characterised using a variety of parameters; the size and elongation of the polygons, the size and number of clasts and the topography of the slopes on which they are found. Similarities in the relationship between structures digitised from in situ observations and those digitised in remotely sensed images would suggest that the air photos provide an effective way to characterising a sorted network. Major differences between the two datasets would indicate that substantial amounts of information about the structure of a sorted net are being lost, due to the low resolution of the images.

4.5.1 Structure from Motion Data

A total of 55 polygons were digitised from the structure from motion data, this included features at sites three and four on the lower slopes of Tindastóll and sites eight, ten and twenty-one on the Skagi peninsula. This provides a data set of centimetre scale polygons at both high and low elevations. These sites were chosen as they had produced the best Digital Elevation Model (DEM) and Orthophoto products from the *structure from motion* surveys and consisted of features which were representative of the area in general.

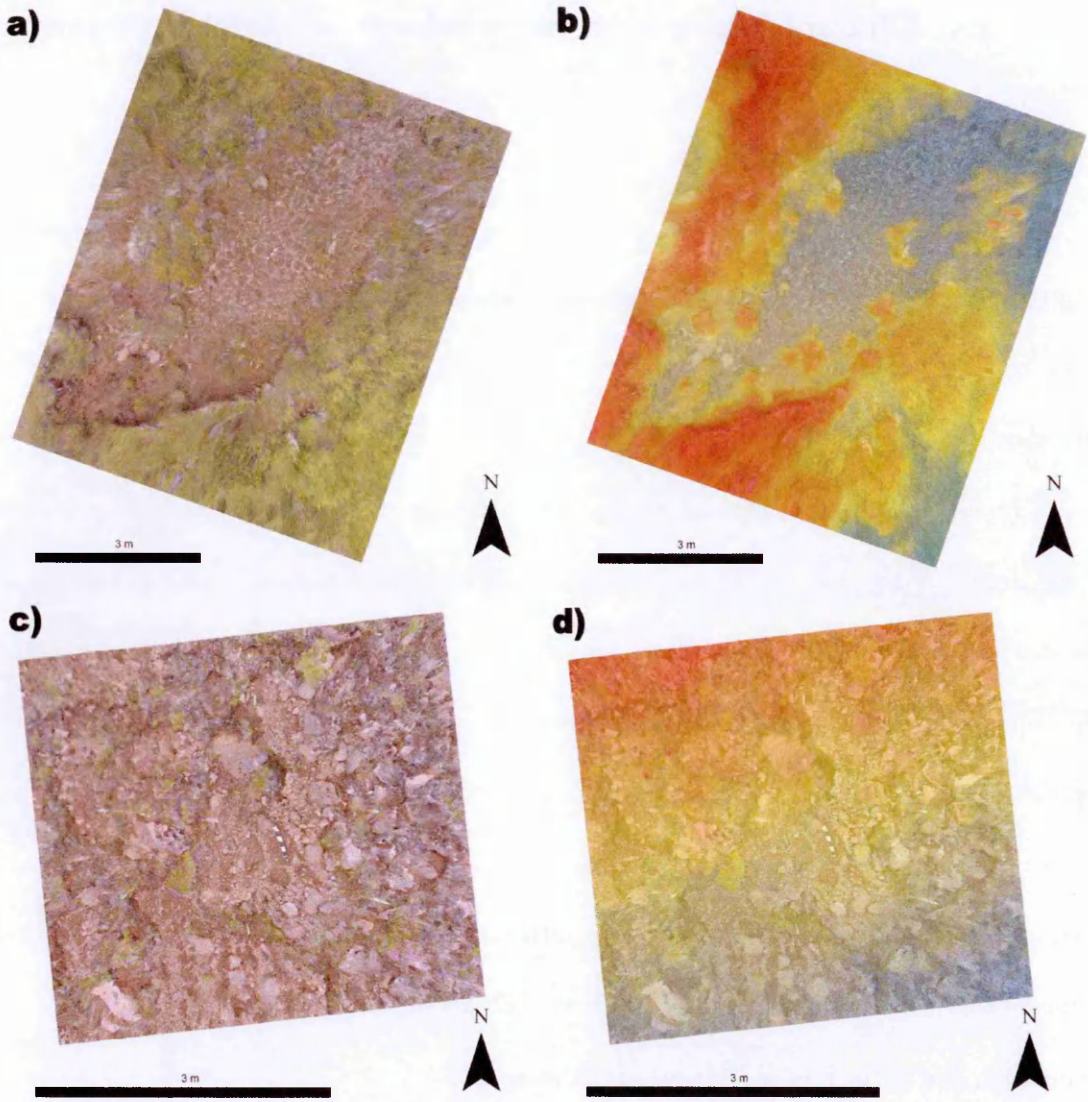

Figure 4.24: examples of the orthophotos and digital elevation models produced by the structure from motion method at two of the field sites. a) Site ten Orthophoto, b) site ten DEM, c) Site three orthophoto, d) site three DEM.

This section of the investigation mainly discusses the differences between circular and elongated polygons, rather than between polygons and stripes. This was partly due to the fact that fewer stripes occurred within these sites and partly because polygonal features could be delineated more easily. Examples of stripes tended to grade into polygonal ground or become less distinct at their distal ends, making categorisation more complex. Stripes were absent from many of the sites with the best SfM results, limiting their usefulness in this comparison.

The features surveyed at the low elevation sites from locality one consist primarily of polygons. There are 21 type one features and an equal number of type two polygons. Two transitional features were also digitised, but stripes were largely lacking from these sites.

At the high elevation sites in locality two a somewhat different suite of features were found. Only one type one polygon was found within these sites, whereas elongated polygons of type two were more common. Eight examples of type two features were recorded as were three examples of discontinuous stripes (type four). No transitional features of type three were found within these areas.

4.5.2 Air Photo Data

A further 41 polygons were digitised from air photographs of the metre scale features on the top of Tindastóll. This data set was based on observations of the features in the air photographs and measurement from the LiDAR DEM. Most of the same parameters can be measured for this data set, but not always to the same degree of precision. The air photo images are much lower resolution than those produced by SfM, having pixels 15 cm across, with a similar vertical resolution. Only the largest clasts could be identified, so an accurate assessment of the number of clasts making up the feature is impossible. However the size of the largest clasts could still be determined. The measurements of clast and circle size are proportionally less precise, but are accurate to within 20-30 centimetres.

Aspect and elevation can be measured from the LiDAR DEM in the same way as for the sites with SfM DEMs, as can gradient. However the larger pixel size of the LiDAR DEM means that gradient measurements are averaged over a far larger area than for the smaller scale survey. Slope measurements derived from the high resolution data

have a mean gradient of 10.66 while those derived from remotely sensed data do not rise above a maximum of 1.79.

This is likely due to the fact that small scale variations in slope have much greater gradient, but are averaged out in the low resolution LiDAR DEM. Consequently, only the larger scale trends are discernible in the remote sensing data, and these are not as extreme. Visual observations of the top of Tindastóll confirm that it has as much small scale variation in slope as the sites on the Skagi peninsula, so a similar range of gradients would be expected were higher resolution topographic data available for these sites. While both types of gradient data are useful on their own they are not comparable with one another.

Table 4.5: Variation in range of gradients at each site.

	All SfM	Tindastóll SfM	Skagi SfM	All RS
Maximum	17.75	17.75	14.52	1.79
Mean	10.66	13.47	9.88	1.14
Range	16.75	8.91	9.49	1.33
Minimum	1	9	5	0

4.5.3 Patterned ground morphology

All of these sites were classified using a variety of parameters, as outlined in the following section. All of these were chosen as they were parameters which could be assessed in both the field observations and the remote sensing data. Consequently they can be applied to similar features in images from Mars.

4.5.3.1 Size and Elongation of Polygons

All of these sites had been characterised with a general rating of polygon elongation. Now the long and short axes of each digitised feature were measured and the ratio of the two calculated. The resulting ratios showed good agreement with the semi-quantitative elongation ratings defined in section 4.4.4, suggesting that these qualitative observations were reliable.

Once a polygonal structure was digitised the circumference and surface area of a digitised polygon were easily calculated using the GIS. The surface area serves as a simple metric for polygon size which can be compared to various other parameters.

4.5.3.2 Size and quantity of coarse domain material

It was decided to test whether clast size scales with polygon size, as appears to be the case on the first order. The number of distinct clasts was recorded including all material in direct contact with the polygon coarse domain and all clasts within the polygon interior. Clasts outside the polygon, but not in contact with other material making up the coarse domain were excluded.

The length of the largest clast in each polygon was measured as was the average size of the five largest clasts. This measurement was made by measuring the long axis of these clasts with a precision of 1-2 centimetres. More precise measurements were difficult because there is some distortion in even the best SfM models. However these clast size data are reliable enough for features a few tens of centimetres across. The orientation of clasts was not measured as this was beyond the scope of this investigation.

In most cases the material making up the coarse domains of these polygons ranged from millimetre scale granules to large cobbles tens of centimetres across. In some cases one or more type predominated, but in most cases a full range was present. A full grain

size distribution would theoretically be possible, but might be limited by the reliability of the data set. Small amounts of distortion will affect measurement of small clasts to a much greater extent than large ones. The precision of measurement will be proportionally much lower.

If a more detailed investigation were to be conducted into grain size distribution in the future then a large number of high resolution photographs would be taken looking down on the polygons, these could then be aligned with the orthophotos produced by SfM, but would not be subject to the same distortion. In essence the SfM base map could be used to georeference the high resolution photographs. Sufficient photos were taken to verify the SfM data in this study, but they were not incorporated into the models.

4.5.3.3 Situation and topography

The gradient of the underlying terrain was determined from the DEM, and averaged over the area of the polygon. This method provides a single mean slope value for each polygon. However the reliability of this method is determined by the resolution of the DEM. In this case it should be precise to within a few tens of centimetres. The aspect of the slope was also obtained in this manner as was the elevation. Again this is reliable to a few tens of centimetres due to the vertical resolution of the Digital Elevation Models.

4.5.3.4 Polygon orientation and alignment to slope

The orientation of the polygon long axis was recorded so that this could be compared with the aspect of the slope on which it occurred. The long axis of an elongated polygon would be expected to align with the hill slope as this is believed to be the factor controlling polygon elongation (Kessler and Werner, 2003). An alignment rating was

derived to determine how well any given polygon fits this pattern. Polygons where the long axis is within 20 degrees of the slope's aspect are well aligned to the slope, those within 45 degrees may be aligned, while those greater than 45 degrees from the aspect of the slope are said to be unaligned.

4.6 Morphological Analysis

4.6.1 Polygon Elongation.

Variations in elongation with gradient can be plotted from both the single polygon dataset and the site based classification shown in Tables 4.2-4.4.

Where in situ measurements were made the gradient of a site can be estimated by fitting a plane through points of known elevation measured using differential GPS and so precise to within a few cm. This is possible for all sites that were surveyed in the field, but not for those digitised from the air photo data. This method does not take into account variations in gradient between the measured points.

When a digital elevation model is available the gradient across an area can be calculated using the slope tool in ArcGIS. The change in elevation across several pixels is used to calculate the slope at any given point within the raster. This is then averaged across the area of the polygon to determine the mean gradient of the underlying ground. This is the only method which is applicable to the martian survey, and only in rare locations where high resolution DEMs are available.

Figure 4.25 shows a plot of gradient underlying patches of similar features identified by in situ observations. Gradient was determined using the first method described above. In contrast figure 4.26 shows gradients beneath individual polygons determined from a DEM, here one data series is derived from the Structure from Motion data, the other from the remote sensing data. There is some overlap between the 2013 measurements in

figure 4.25 and the centimetre scale features in 4.26. This illustrates the dramatic differences between these two approaches of characterising gradient.

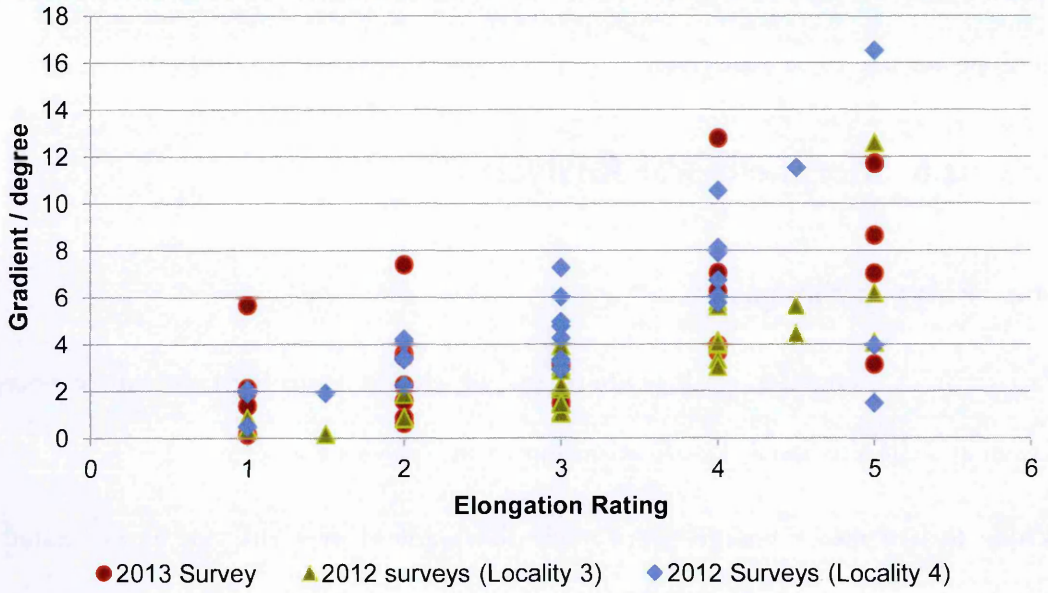

Figure 4.25: Comparison of feature elongation with underlying gradient for patches of polygons. It can be seen that more elongated features are found over a wider range of gradients than less elongated polygons.

Figure 4.25 shows that when considering patches of similar features there is a definite trend. The mean gradient of slopes underlying patches of stripes (elongation of 4 or higher) is consistently greater than those underlying polygons. There is considerable variation within the patches surveyed, but with the exception of a few outliers in each survey area it was found that sorted circles occurred primarily on ground with low gradients and occurred over a much narrower range of gradients. Stripes predominantly occurred on the steeper slopes, although there were some low gradient outliers. This finding is in agreement with the models reported by Washburn, (1973), Kessler et al., (2001) and others.

The result is less clear when the elongation of individual polygons within these patches is considered. An elongation rating was calculated by measuring the ratio between the polygon's long and short axes. An axis ratio of one indicates that both axes are the same length and that the feature is essentially circular. Polygons with axis ratios in

excess of three are equivalent to the transitional features described in Table 4.1. These ratios are equivalent to the feature type classification, a type one polygon will, by definition, have an axis ratio between 1 and 2, while more elongated features have greater disparity between the lengths of their axes.

The precision of the polygon elongation data is determined by the ease with which the edge of the polygon can be determined. For these measurements the error on the data is approximately the width of the coarse domain, around 2-3 cm for centimetre scale features, and 30-50 cm for metre scale features.

The centimetre scale data shown in figure 4.26 are drawn from the areas surveyed in the 2013 SfM survey. Plotting the axis ratio of a feature against underlying gradient does not produce a clear correlation. This may be due to the low data volume for transitional and stripe features.

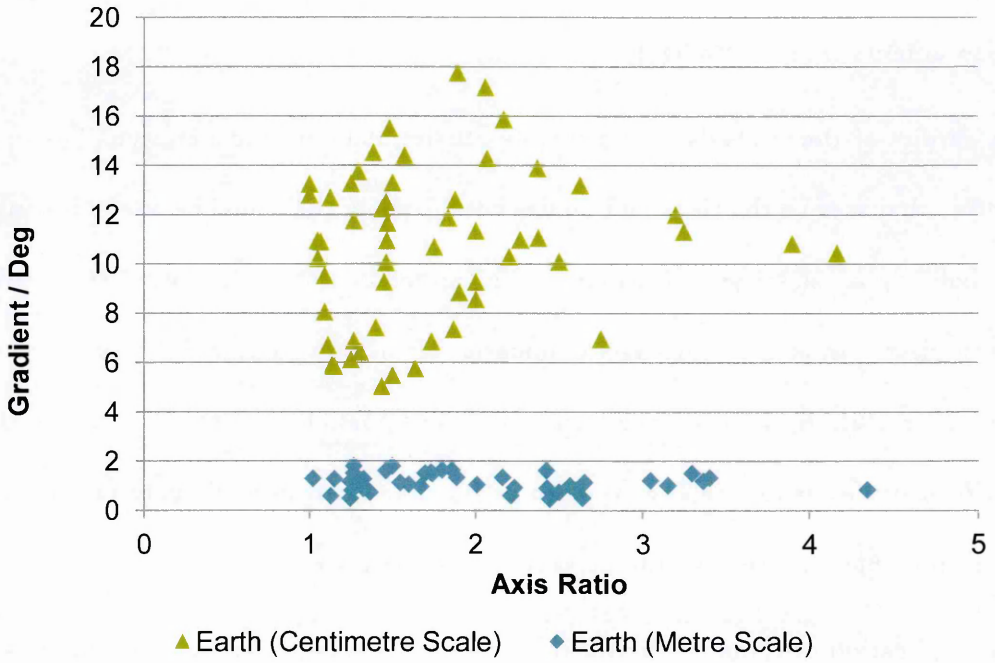

Figure 4.26: Graphs of variation of polygon elongation with gradient.

All transitional features occur within a narrow range of gradients between 10 and 14 degrees. The polygonal features occur over a much wider range of gradients, some lower than those on which elongated structures were observed and some with a much higher gradient. This does not seem to match the general trend seen for these features when the in situ methodology is applied. This suggests that assessing gradient dependency in this manner is much less reliable.

In summary when a patch of polygonal patterned ground is characterised based on the most prevalent feature type a clear trend can be seen, albeit with a large margin of error. This is less clear when the morphology of individual polygons is examined. This is likely due to small scale variations in topography across a polygon, which obscures the general trend of the underlying hill slope. The gradient on which a polygon occurs is averaged from the part of the DEM directly beneath it, but the presence of large clastic material itself has an effect on small scale topography. Consequently, these measurements are not as reliable.

The results of the analysis of the remote sensing data are inconclusive. The opposite trend to that seen in the field data may occur, however this could be due to the inherent unreliability of classifying features in the remotely sensed images. When only the largest clasts can be seen the exact boundaries of the polygons, and the extent to which they are transitioning into stripes, are not always possible to determine. There are also significantly fewer examples of type three features than those of types one and two so it is impossible to be certain how representative these are.

The implication of these results for the martian surveys presented in Chapters six and seven is that significant variations with gradient are most apparent when comparing the broad trend beneath areas characterised by polygons or stripes. The trend seen in figure 4.25 is not as apparent in the remote sensing data as it is in the in situ

measurements. Had the results of the DEM derived results agreed with those from the in situ method then it would have suggested that this could reliably be applied to the martian data. This is not the case. The patch based approach would thus be more useful than assessing the elongation of individual polygonal features.

Both polygon scale and network scale measurements will be made for martian features in Chapter Nine and these results will be compared to those presented here. Other methods, such as examining the change in pattern morphology across the length of a crater wall, will also be used, as these may prove more reliable than attempting to apply this methodology to sites with no in situ data. Caution must be exercised when examining low resolution satellite images. The lack of a trend for elongated polygons to occur on steeper slopes should not be taken to rule out a periglacial hypothesis.

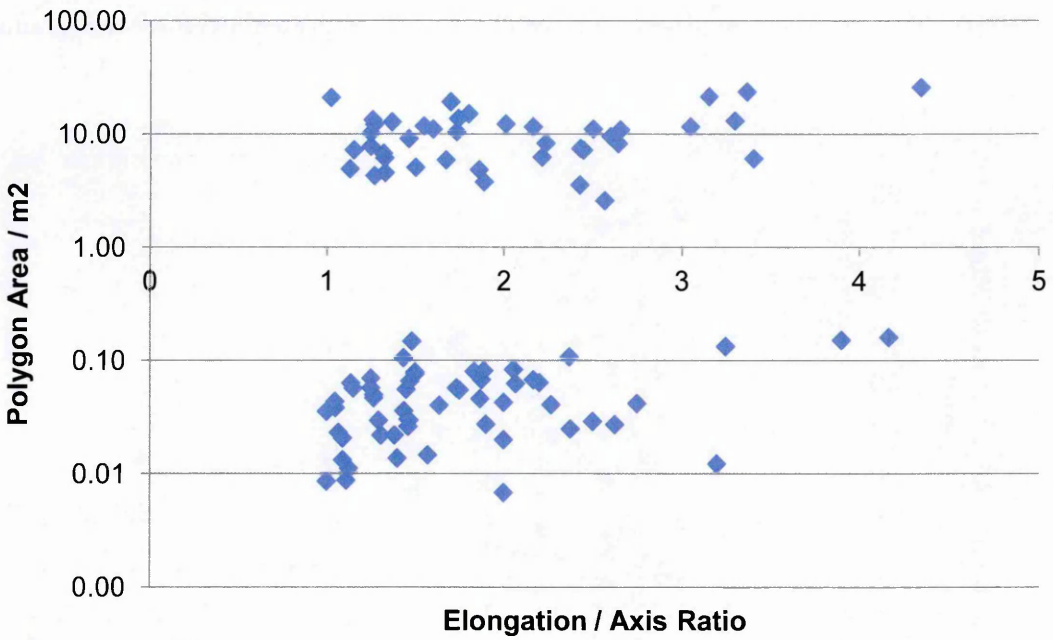

Figure 4.27: Polygon area against elongation. Polygons of all sizes are found to exhibit a range of elongations. No type of polygon appears to be more prevalent at a particular range of sizes.

Figure 4.27 shows that there does not seem to be a correlation between the size of a polygon and its elongation. Circles of various degrees of elongation occurred at all scales, as did stripes, both continuous and discontinuous. Overall the size of feature

seemed most likely to be due to the substrate which it was reworking. The majority of open ground in the Skagafjörður area consists of fine silty soils with many small pebbles and cobbles. In this location centimetre scale structures can easily occur.

4.6.2 Alignment of polygons to underlying slope

If the elongation of a sorted polygon is controlled by the gradient of the underlying slope then it would be expected that the long axis of the polygon would be aligned to the slope. However as stated in the previous section it is possible that the small scale topographic variations in the DEM caused by the presence of large clasts may be obscuring the underlying gradient of the hill slope. If this is the case then alignment to the slope would not be expected, since the predominant factor affecting the underlying gradient would be a product of the polygon's geometry itself, rather than the product of the slope. The apparent gradient thus might not be representative of the gradient controlling polygon elongation.

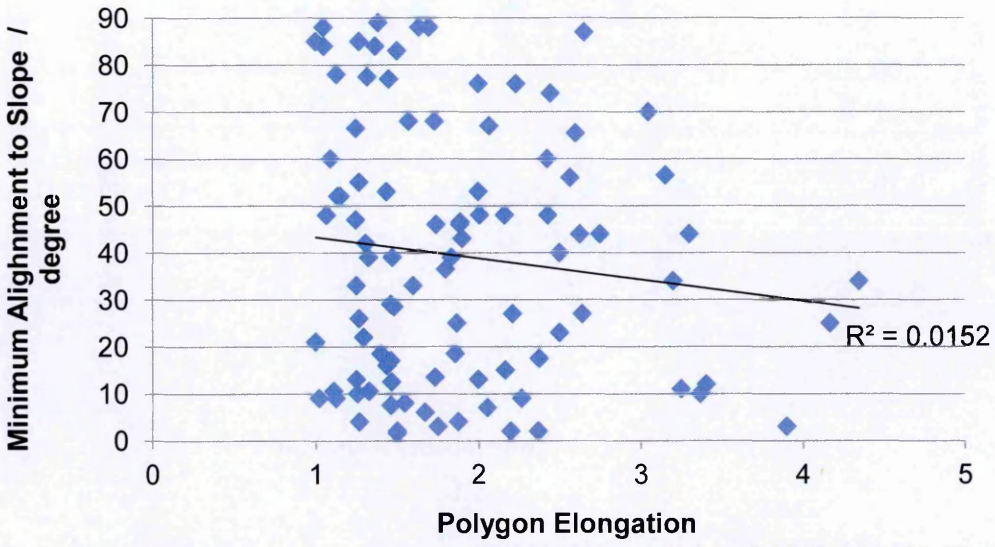

Figure 4.28: Alignment of polygons to slope for all sites. Polygon elongation is determined by taking the ratio of the long and short axes. The minimum alignment to slope is the smallest angle between the direction in which the polygon long axis is aligned and the aspect of the underlying slope, thus an alignment of 0 degrees indicates a polygon that is exactly aligned with the direction of slope while an alignment of 90 degrees indicates a polygon orthogonal to the direction of slope.

These results suggest that the proportion of features aligned to the underlying slope is very low. There is little or no correlation between alignment and elongation and the majority of features have an alignment in excess of 20 degrees. While more type two features are found to be aligned than type one features, these are still a minority compared to those that were found to be more than 22.5 degrees from the direction of slope, which was considered the criteria for good alignment. Roughly equal proportions plot on either side of the 45 degree mark for all elongations below 2.5. Most of those with an elongation between 2.5 and 3.5 are unaligned.

It is interesting to note that all features with an elongation ratio in excess of 3.5 are found to be aligned within 45 degrees of the direction of slope. This may suggest that more elongated features have a slight tendency towards alignment, but few are found to be less than 22.5 degrees from the direction of slope. There are relatively few features with elongations in excess of four, so it is uncertain whether this is a real trend or a coincidence.

All polygons were classified as being aligned (within 22.5 degrees of the direction of slope), uncertain alignment (within 45 degrees) and unaligned (outside of 45 degrees). The results are shown in figure 4.29.

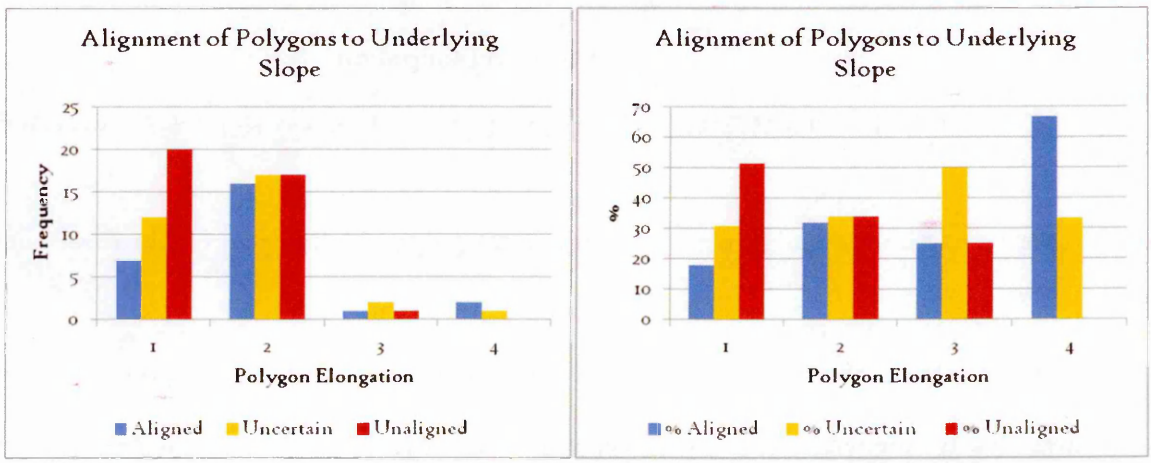

Figure 4.29: Classification of the alignment of polygons to slope data.

Few polygons with an elongation ratio that puts them in the type one category exhibit a strong alignment, while the majority are unaligned. The same is true for elongated polygons, although here the proportion being aligned, uncertain and unaligned are roughly equal. This suggests that the elongated structures are more likely to exhibit alignment to slope, which fits with the assumption that this is the factor controlling their elongation, albeit at this scale slope alignment is not especially pronounced. The fact that grade one features have axes of roughly equal length also means that the uncertainty in determining which is the long axis is slightly greater, although in relatively few cases are they exactly circular.

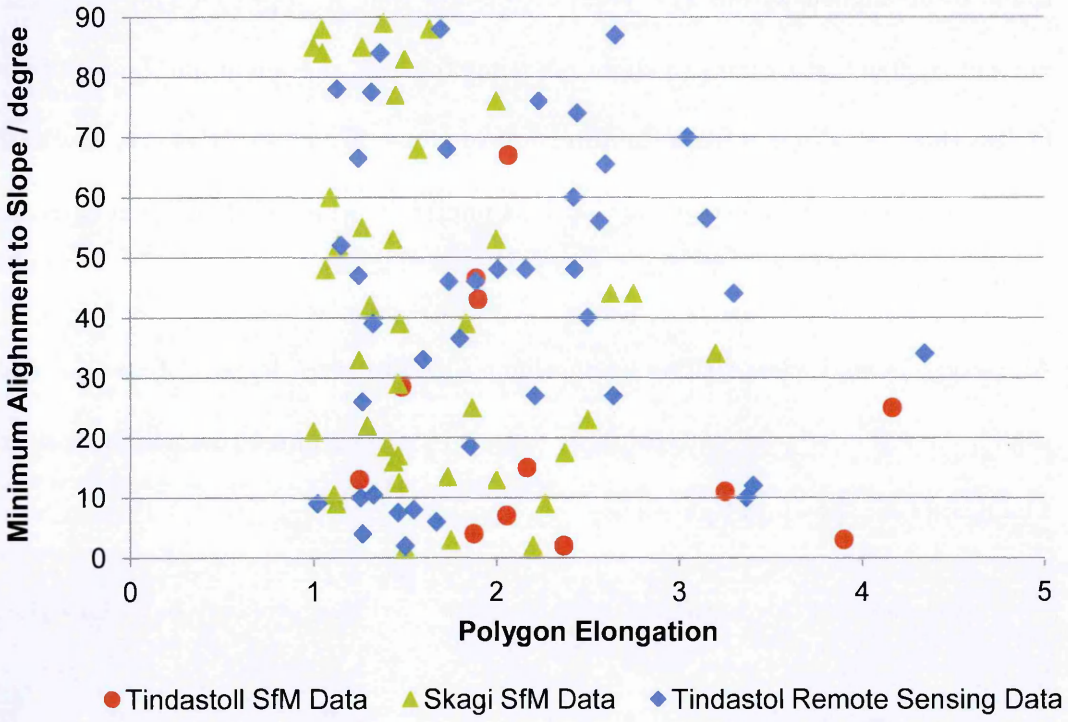

Figure 4.30: Minimum alignment to slope against polygon elongation for the three sites surveyed.

Type three features are primarily of uncertain alignment, with equal proportions of those clearly aligned and not aligned, while the majority of type four features are aligned, with a smaller fraction being uncertain and no unaligned features. This does

seem to support the expected trend; however the low data volumes for features of elongation three and four mean that this analysis should be treated with caution.

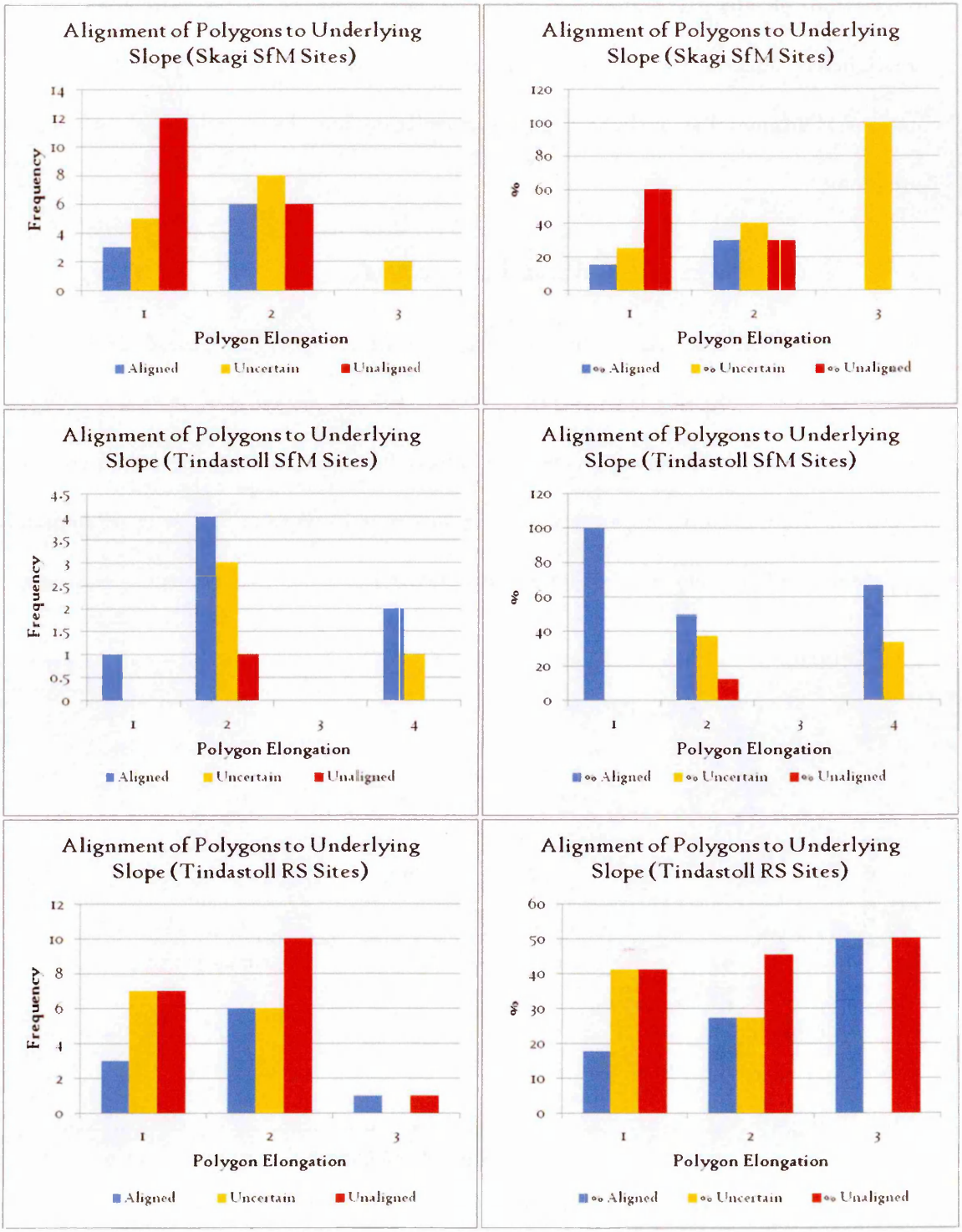

Figure 4.31: Breakdown of alignment results for each study area.

Breaking down the results by site shows that the trends seen in these data are largely tentative. All three areas show similar trends, which are expressed in the grouped data

plot. Significantly the remote sensing dataset shows a similar trend for type one and two polygons to that seen in the ground based data. There is a slight increase in the proportion of aligned features as polygon elongation increases, but the total of unaligned or uncertain polygons does not substantially decrease. The plot of elongation against alignment has a slight negative correlation but the correlation coefficient is only 0.015.

4.6.3 Variations in size and number of clasts.

The number of discernable clasts present within a polygon coarse domain was compared for each of the digitised features. It was accepted that those polygons digitised from low resolution images would have far fewer discernable clasts than those digitised from in situ images. Figure 4.32 shows these results and it is immediately apparent that both data sets exhibit a positive correlation.

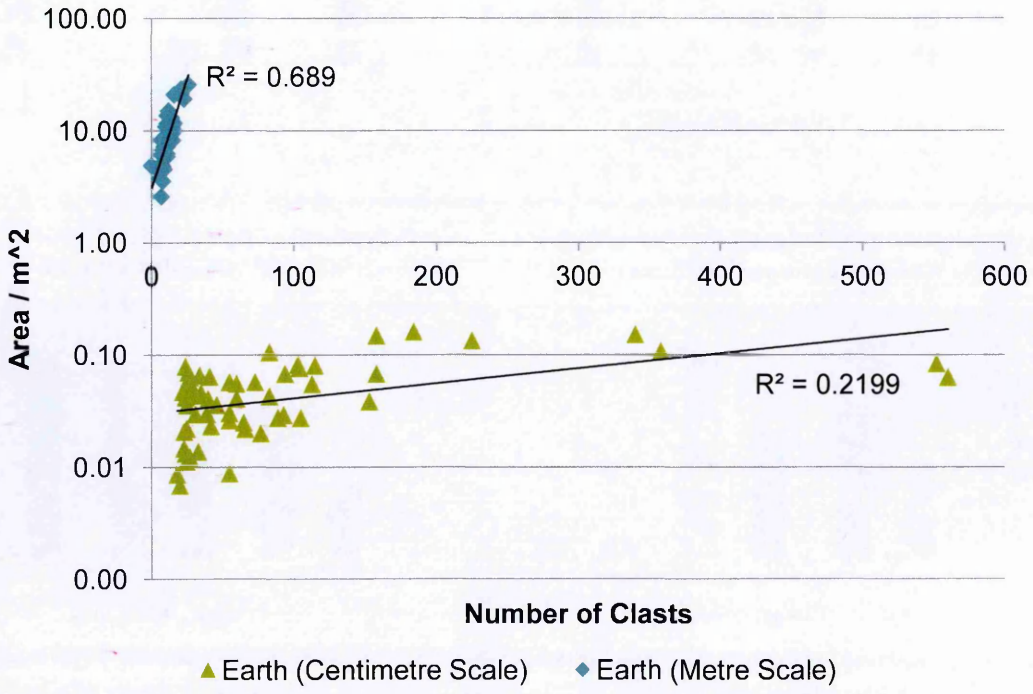

Figure 4.32: Polygon Area against number of clasts

The number of clasts increases with polygon size within both data sets. This is to be expected since a larger polygon has a longer perimeter and so more space for coarse

domain material. However this is where the similarity ends. The correlation is fairly weak when the in situ observations of centimetre scale features are considered (R^2 of 0.22). It is considerably stronger for metre scale features observed in remote sensing data (R^2 of 0.69). This is most likely to be the result of the range of clasts which are resolvable in each case. Since the metre scale features are only represented by the largest material there is a much faster increase in the number of clasts. A small polygon might only have four or five resolvable clasts, while a larger one could have double or triple that number depending on its perimeter. In the case of the centimetre scale features there is a steady increase in the number of clasts, but since total clast numbers are so much higher there is no sudden jump in clast number when comparing smaller and larger circles.

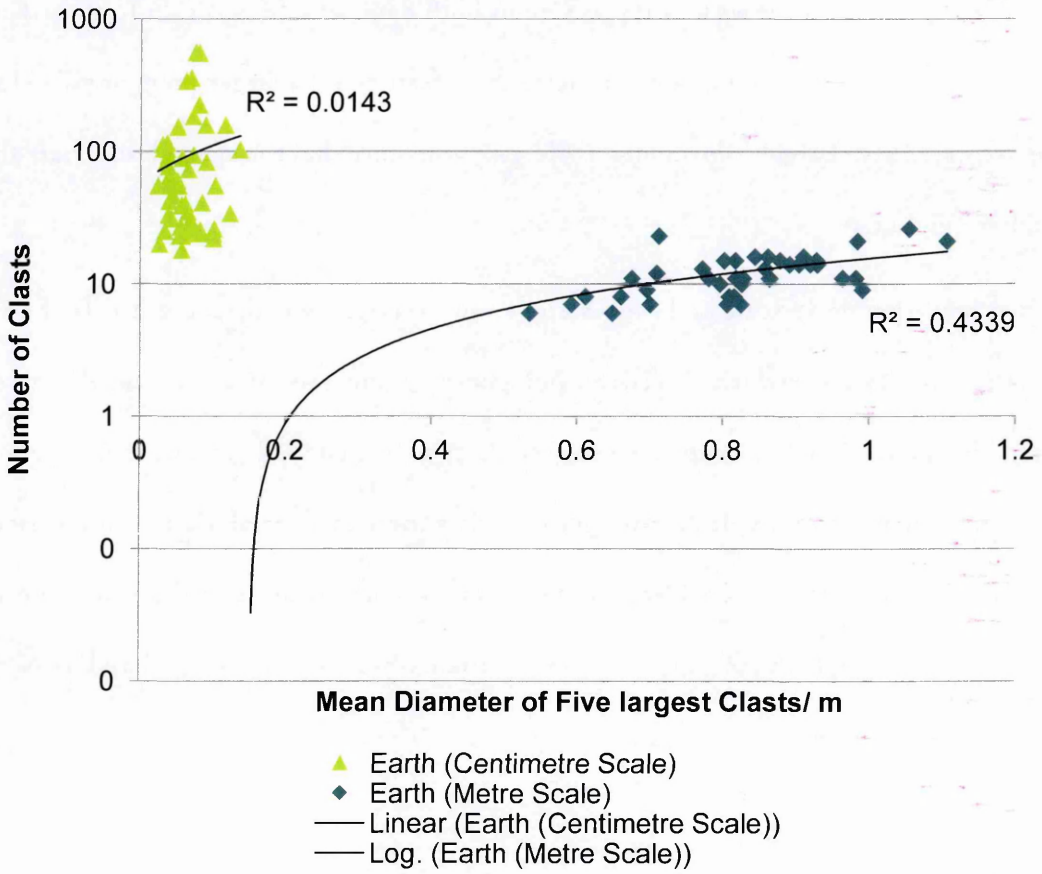

Figure 4.33: plot of number of clasts against mean diameter of five largest clasts.

Comparing size and number of clasts also produces a weak positive correlation. The more clasts occur the larger their mean diameter. Here the trend for the in situ observations is much steeper, while the air photo data exhibit a slightly stronger correlation.

In both cases the controlling variable is likely to be the increase in polygon size. Larger polygons have more clasts, and these are also larger. This is confirmed by the data shown in Figure 4.32 which shows a reasonably strong correlation between polygon area and the size of the largest clasts for both data sets. This is probably the controlling variable for both clast size and number of clasts, explaining their correlation.

Visual observations in the field indicate that the large metre scale features contain more boulder scale clasts. These data support this observation by indicating that clast size does appear to scale with polygon size in both data sets. In addition to there being larger clasts in the coarse domains of metre scale features, the larger polygons also have the larger clasts. Larger centimetre scale polygons also have larger clasts than their smaller neighbours.

When both the metre scale and centimetre scale datasets are considered it is found that there is a positive correlation between polygon area and clast size with an R^2 value of 0.77. The mean diameter of the five largest clasts was used as this value is independent of resolution and so provides a stronger case that there is a correlation than the size of the largest clast. When considered independently both datasets still show a positive correlation although the R^2 values are lower than when both are considered as part of the same population.

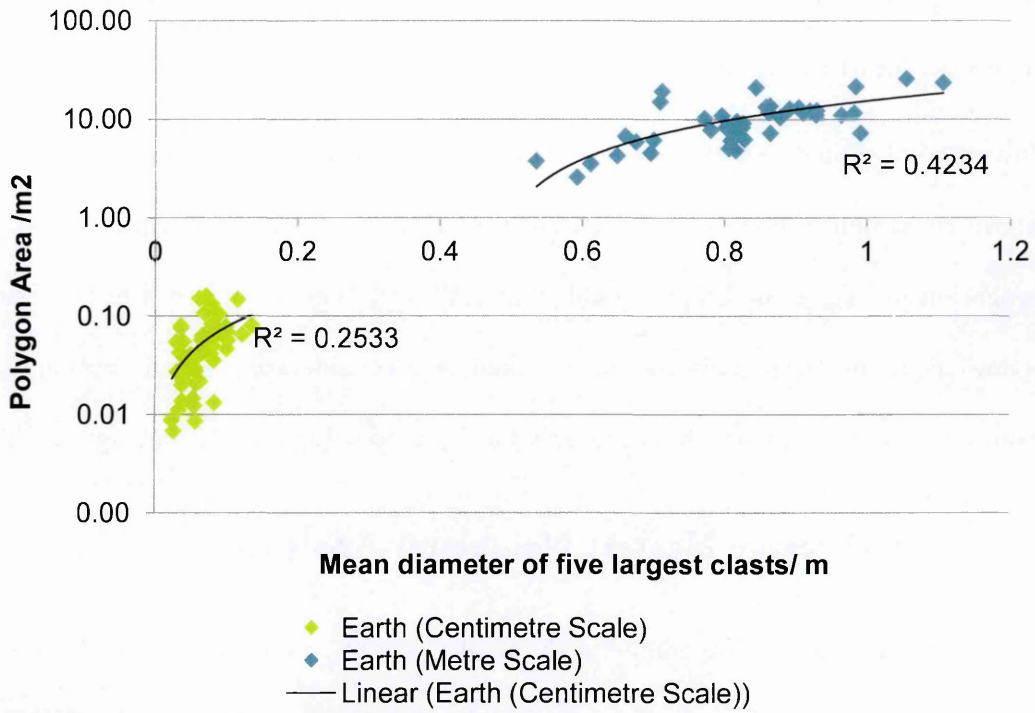

Figure 4.34: plot of the polygon area against the mean diameter of the five largest clasts. Using the mean diameter produces an estimate of maximum clast size which is independent of resolution. Consequently it provides a useful strand of evidence to assessing whether these parameters are related.

This observation is significant for determining whether an array of clasts in a low resolution image is in fact sorted. In some cases a random distribution of points may appear to exhibit some clustering due to the positions of the clasts triggering a human observer's predilection for recognising patterns in collections of points. However in a randomly distributed array the area which appears to be a partial polygon is also random and so would not be expected to be correlated with the size of material within its extent. The size of the largest stones should be independent of the area over which they are sampled.

In summary a variety of parameters including the elongation of polygons, their alignment to slope, and the relationship between clast and polygon size can be used to characterise sorted patterned ground and so might prove useful in determining whether

martian features are in fact periglacial. These metrics are revisited in Chapter Nine when martian data are compared to terrestrial analogues.

However it is noted that the low resolution of martian remote sensing data limits the extent to which some of these parameters can be assessed. Examining polygon elongation in air photographs yielded a very different result to similar features examined in the field. This should be taken into consideration when applying these results to an environment which can only be observed using remote sensing.

4.7 Average Nearest Neighbour Analysis

Comparing the aerial photographs to the field observations illustrates the difficulty in determining whether features are periglacial from remote sensing alone. While the parameters discussed in the preceding section can be useful in determining whether the expected patterns are present they are of limited application for low resolution images.

In the air photo datasets only the largest boulders are visible as distinct objects. The rest of the pattern is only visible as variations in albedo, with the bright coarse stripes standing out against the darker fine domains. In some areas where no large boulders are present, the albedo variation is the only indication that a sorted net is present. The same holds true for the analysis of martian data, but on that planet far fewer examples of albedo variations have been observed. In many cases only the pattern of clasts can be assessed to determine whether an area is sorted.

The distribution of large boulders in the aerial photography is indicative of an underlying pattern. However, were there no ground truth observations it would be difficult to categorically state that a sorted network was present at many of these sites. The human brain is also very good at misidentifying structures in random patterns, and will often observe lines and edges where none in fact exist. Consequently, an

average nearest neighbour analysis was conducted to demonstrate whether or not the arrangement of boulders at these sites was significantly different to a random distribution.

Ten sites across the summit of Tindastóll were digitised by creating a point in an ArcGIS shape file for each resolvable boulder as illustrated in Figure 4.35. These sites were selected because they either had a clear polygonal net visible in the aerial photography, or had been visited during the 2012 survey and a sorted net was visible at the ground.

Figure 4.35: Illustration of digitised boulder pattern.

A further five sites in locality one were also examined, using the orthophoto output from the *structure from motion* survey conducted in 2013. Since these sites were imaged from the ground at far higher resolution, a far greater degree of detail could be seen. All of the clasts greater than 5 millimetres in size were digitised to produce the point distribution necessary for the test. It was anticipated that these data sets would produce

a very different result from those digitised from the aerial photographs since the positions of almost every clast could be included in the analysis. An average nearest neighbour analysis was then conducted on this distribution of points using ArcGIS. The same technique will be used for assessing whether the distribution of martian features is significantly different from a random distribution in the next chapter.

4.7.1 The statistical approach

Average nearest neighbour analysis was developed by Clark and Evans (1954) based on the method of Dice (1952). Although originally devised to facilitate ecological research it has since been applied to a variety of areas of geographical study including the distribution of extraterrestrial geomorphic features in satellite remote sensing data (Bishop, 2008, 2007).

The nearest neighbour analysis is a statistical technique which assesses whether there is a pattern in a population of points by comparing the distances between each point and its nearest neighbours to the expected distance based on the hypothetical random pattern. The resulting ratio (R) indicates whether the features under analysis are randomly distributed, clustered, or dispersed. An R value of zero indicates that all points plot in the same location. R values between zero and one indicate a clustered arrangement while R values greater than one suggest that the arrangement of points is significantly dispersed. The theoretical maximum dispersion is R= 2.149, indicating that the points are arranged in a triangular lattice (Bishop, 2007; Pinder and Witherick, 1972).

The null hypothesis for this test is that the distribution of points is completely spatially random and Consequently, has an R of one. The probability that this is the case is given by the p-value. Low p-values suggest that the distribution is very unlikely to be random, and that the distribution of the points has been influenced by some underlying

process. A z-score gives the standard deviation of the result. A z-score between -1.96 and 1.96 indicates that the pattern is not significantly different from a random distribution at a confidence of 0.05. A z-score less than -1.96 or greater than 1.94 returns a significantly clustered or dispersed result respectively; the null hypothesis can thus be rejected. Significance can be assessed either using the p-value or the z-score.

Table 4.6: Interpretation of R values

R value	Pattern
0	Collocated
< 1	Clustered
1	Random
> 1	Dispersed
2	Square Lattice
2.149	Triangular Lattice

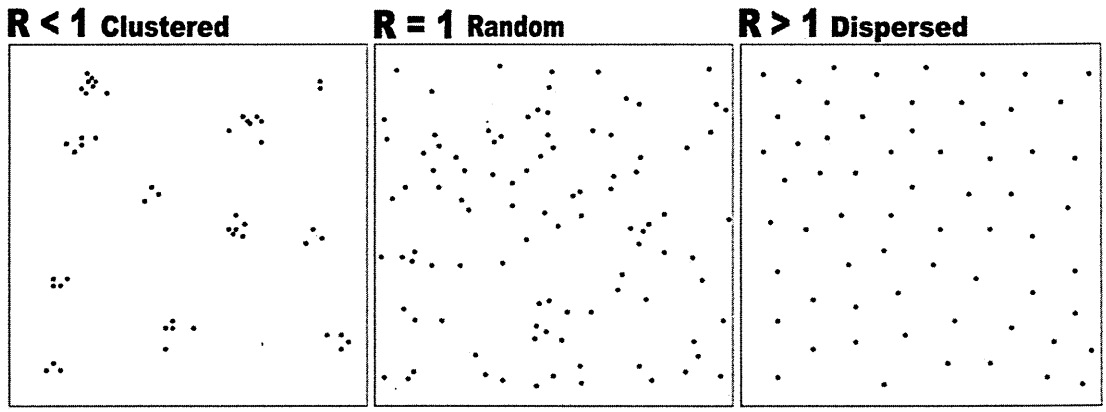

Figure 4.36: Interpretation of average nearest neighbour analysis. Dispersed patterns return R values greater than one while clustered pattens produce lower R values.

4.7.2 Results of the Average Nearest Neighbour Analysis.

The results of the nearest neighbour analysis are presented below. Table 4.7 shows the results of applying the test to the small scale features at locality one digitised using *Structure from Motion*. All of these features returned a strong "clustered" result. The

analysis detected the clustering of clasts into coarse domains in some parts of the image, while many other areas do not have a significantly large clast population.

The analysis of the boulder patterns in the aerial photographs produced a very different result, despite the fact that on the ground these features had very similar morphology. It can be seen that all of the sites with the exception of Site Two produced a strongly "dispersed" result. None of these sites are found to be "clustered".

Table 4.7: Results of the average nearest neighbour analysis of the sorting patterns digitised from small scale patterned ground collected using *structure from motion*.

2013	Mean Distance					
SfM Sites	**Observed**	**Expected**	**R-Value**	**z-score**	**p-value**	**Result**
Site 3	0.02	0.02	0.65	-30.22	0.00	Clustered
Site 4	0.02	0.02	0.85	-9.69	0.00	Clustered
Site 8	0.03	0.04	0.86	-10.88	0.00	Clustered
Site 10	0.02	0.02	0.78	-22.31	0.00	Clustered
Site 21	0.03	0.04	0.81	-14.34	0.00	Clustered

In the high resolution data all of the detail of these sites down to millimetre scale granules can be detected. Consequently, almost every clast is recorded and the clustering within coarse domains registers most strongly in the analysis. When only the very largest boulders can be detected this is not the case. Coarse domains are represented by discontinuous lines of large distinct clasts and albedo differences representing the smaller material which cannot be resolved. It is impossible to see the clustering of clasts within the coarse domains and so only the dispersed pattern of very large clasts can be detected.

The analysis does not return a "randomly distributed" result in most cases, since the boulders are still distributed into a polygonal lattice around open fine domains. Although the occurrence of boulders large enough to be resolved is largely random their

distribution around the feature is not. The large boulders are seen by the algorithm as being spread out around the fine domains and so it returns a dispersed result. Organisation can still be detected in these features despite the fact that most of the detail is below the resolution of the image.

Table 4.8: Results of the Nearest Neighbour analysis of digitised boulder patches within the aerial photographs of the summit of Tindastóll.

2012	Mean Distance					
RS Sites	Observed	Expected	R-Value	z-score	p-value	Result
Site 1	1.12	1.05	1.07	2.91	0.00	Dispersed
Site 2	1.06	1.06	1.01	0.37	0.71	Random
Site 3	2.85	2.44	1.17	7.88	0.00	Dispersed
Site 4	1.16	1.01	1.14	8.60	0.00	Dispersed
Site 5	1.10	0.90	1.22	12.35	0.00	Dispersed
Site 6	0.80	0.66	1.21	14.84	0.00	Dispersed
Site 7	0.87	0.72	1.21	15.02	0.00	Dispersed
Site 8	1.19	1.12	1.06	4.00	0.00	Dispersed
Site 9	1.26	1.14	1.11	7.72	0.00	Dispersed
Site 10	0.91	0.79	1.14	8.46	0.00	Dispersed

Since the nearest neighbour analysis returns a very different result when a sorted pattern is digitised from remote sensing data this must be taken into account when interpreting the results of applying this analysis to martian features. It can be inferred that when testing for the presence of a pattern in martian data a dispersed pattern is most likely to indicate the presence of a clastic network.

4.8 Summary

The results presented in the preceding sections illustrate a range of ways in which the morphology and distribution of sorted patterned ground can be characterised. This defines the attributes that could be used to assess whether an area of boulder strewn

ground on Mars could have resulted from the same processes. However it can be seen that many of these attributes are not found to be consistent when measurements of remote sensing data are compared with more reliable in situ observations.

For example it was found that when patches of coherent features were examined sorted stripes were most common on steeper slopes, while sorted polygons occurred on slopes with lower gradients. Transitional features were found on a range of gradients, with more elongated features occurring on steeper gradients than circular polygons. The elongation of sorted polygons with increasing gradient is well documented (e.g. Kessler and Werner, 2003; Washburn, 1973b). If the elongation of martian features has the same slope dependence then it can be considered to be more likely that they formed through the same processes. If however, stripes and elongated features are found on flatter ground, or polygonal structures on hill slopes then a different explanation is more likely.

However, it was found that this trend was difficult to confirm using the air photograph data. This was partly due to the scarcity of easily digitised stripes in this data set. If the same is true of martian data then elongation against slope might not be the best metric to use to assess martian patterns.

Sorted patterned ground occurs at a wide range of scales, and there does seem to be a correlation between the size of sorted circles and the size of the material that comprises them. Clast size was found to scale with polygon size. This was just as apparent in the air photo data set as in the field observations. Consequently, a similar trend would be expected to occur when martian features are examined.

Finally and most usefully the results of the *average nearest neighbour analysis* indicate that the resolvable clasts in a sorted environment are significantly different from a random distribution. When high resolution data are used to digitise the clast

distribution of small scale patterned ground it is found to be significantly clustered, whereas when larger scale features are digitised from low resolution datasets this is not the case and a dispersed pattern is returned.

This is probably due to the sampling of clasts in these two data sets. In a high resolution image taken from the ground all of the clasts greater than 1 mm in size can be included in the analysis and the clusters of clasts that make up the coarse domains are detected. In the case of a structure digitised from low resolution data this is not the case. Only the largest clasts are included in the analysis and these produce a much stronger dispersed result because the detail within the coarse domains does not obscure the larger scale structure of the polygons themselves.

In Chapter Five the same analysis will be applied to a range of martian features to determine whether they do exhibit the same behaviour and return a significantly dispersed pattern. Since satellite images of Mars are of even lower resolution than the air photos used in this analysis they should exhibit similar trends. A dispersed result would indicate that distribution is similar to terrestrial patterned ground. On the other hand if martian features were found to consist of arrangements of clasts which appear to form a discontinuous net under visual inspection, but which consist of a random pattern, or small clusters of clasts, when analysed, then periglacial sorting is a less likely explanation.

5 Chapter Five: Survey of Possible Sorted Patterned Ground in and Around Lomonosov Crater

5.1 Aims

Chapter Four examined a terrestrial periglacial environment to determine how sorted patterned ground would appear in relatively low resolution remotely sensed images. It was established that an average nearest neighbour analysis could be used to determine whether the large clasts visible in remotely sensed images were distributed randomly or were part of an underlying pattern. Measuring the slopes on which different sorted features occur could provide another strand of evidence for their periglacial origin, but the reliability of this assessment was limited by the low resolution of remote sensing images.

This chapter will build upon the discussion in Chapter Four by applying the average nearest neighbour analysis to a region of the Northern Plains of Mars which could be a periglacial landscape. Since the nearest neighbour analysis involved time consuming digitisation of boulder patterns it could not be applied to the entire survey. Consequently a semi-quantitative ranking was developed that could be easily applied to all sorted features. This is defined in section 5.3.3, and applied to a variety of examples across this case study. The average nearest neighbour analysis is then used to test the reliability of this ranking in section 5.5.1 establishing it as a viable methodology for the main martian survey.

The overall hypothesis of this project is that these martian clastic networks formed through similar processes to their terrestrial counterparts. If this is the case then they would be expected to exhibit the same non-random clast distribution as terrestrial periglacial features. Conversely the presence of a random distribution would indicate

that these boulder patterns probably occurred through chance and are not evidence of a martian periglacial landscape.

Since these features are being examined in relatively low resolution satellite images only the largest clasts can be detected. Consequently, they will be most comparable to the features digitised from air photographs on Earth, rather than the higher resolution sites examined using ground based images. Polygonal structures would thus be expected to have a significantly dispersed arrangement of clasts, whereas rubble piles would be expected to be clustered.

Stripes could exhibit either behaviour depending on the thickness of the coarse domains and the number of clasts within each. If thin stripes, where only a single line of discernible clasts is present, are found, then a dispersed result is most likely. Sites with more clasts in the coarse domains would be expected to return a clustered result, as the groups of clasts within the domains will be more pronounced than the spaces between them. This was the case with the examples of centimetre scale patterned ground analysed in the previous chapter, because every clast was included, clustering was more pronounced.

Unlike the air photographs of Iceland, polygonal variations in albedo are largely absent in images of martian terrains, but there are places where boulders appear to form lines and clusters. These sites are hypothesised to be an expression of sorted patterned ground but since the Northern Plains of Mars are frequently boulder-strewn it is important to determine whether the boulders are the result of a random distribution or not.

The details of the surveys conducted to find putative periglacial sites across the Martian Northern Plains will be discussed in detail in Chapters Six, Seven and Eight.

This section will focus on a single case study where a range of putative periglacial features occur in close proximity.

5.2 Background

Observations of sorted patterned ground on Mars have been described in section 2.4.7. These features occur at a range of locations across the northern plains and different morphologies are found in different places (e.g. Balme et al., 2009; Gallagher et al., 2011; Orloff 2012). The region chosen for this study is characterised by patches of boulder strewn ground many of which contain sorted patterns. These are primarily found at high northern latitudes.

These boulder patches have been documented by Malin and Edgett (2001), who also made the initial observations of the "boulder bounded polygons" in Lyot Crater. Several other boulder patterns are common in this region including the features characterised as "basketball terrain", these were originally observed as regions of stippled terrain in lower resolution images (Head et al., 2003; Kreslavsky and Head, 2002; Malin and Edgett, 2001). This terrain consists of small rubble piles, which can clearly be resolved as such in higher resolution images (Kreslavsky et al., 2011).

Many patches of boulders in this area form "boulder haloes"; rings of rubble which surround small or buried impact craters in this area (Levy et al., 2008a; Orloff et al., 2011). Boulder haloes and boulder patches form the focus of this investigation and are described and illustrated in section 5.2.2. It seems most likely that these clusters of boulders were emplaced through ejection of fragmented material from their associated impact craters (Levy et al., 2008a). The boulders were distributed around the crater, presumably in a random pattern, and later arranged by other processes to form sorted patterns (Levy et al., 2010, 2008a; Mellon et al., 2008; Orloff et al., 2011, 2013; Orloff, 2012).

5.2.1 Study Area

The region of north-eastern Acidalia Planitia in the vicinity of Lomonosov Crater has the densest concentration of putative sorted patterned ground of any region of the Northern Plains surveyed in this investigation. This area was examined as part of the CTX survey of eastern Acidalia Planitia that will be described in Chapter Six. It was found to be characterised by the presence of small buried impact craters surrounded by clusters of boulders as shown in Figure 5.2 in the next section.

Located at 64.9°N, 9.3°W Lomonosov Crater is a 150 km diameter impact structure with a ~ 100 km radius ejecta blanket. The craters ejecta is classified as "diverse" exhibiting some evidence of flow-like emplacement (Barlow et al., 1990; Barlow and Bradley, 1990). Lomonosov Crater lacks a large central uplift feature, although a small ridge can be found near its centre. There is no large icy mound of the sort often observed in craters at high northern latitudes (Conway et al., 2012; Garvin et al., 2000). Lomonosov Crater is surrounded by the generally low lying plains of the Vastitas Borealis. A large number of smaller impact craters can be found in the area around and in some cases within Lomonosov. These provide the majority of the high relief terrain in this part of the northern plains. The only large scale feature of the crater interior is a dune field 20 km long and 12 km wide at its greatest extent. This is located to the east of the crater's centre and may superpose other examples of the boulder patches examined in this study.

Several small conical mounds are located near the centre of the crater which have a similar morphology to those found across the southern part of Acidalia Planitia (Allen, 1979; Farrand et al., 2005). Similar features have been suggested as possible martian pingos (Burr et al., 2009; Dundas and McEwen, 2010) although numerous non-periglacial hypotheses could explain their morphology (Ghent et al., 2012; Oehler and

Allen, 2010). Scott and Underwood (1991) describe a large number of such mounds in the interior of Lomonosov Crater. Their observations were made using low resolution Viking images, and while a few such mounds are present in the centre of Lomonosov in higher resolution CTX data they are not as widespread as suggested by Scott and Underwood. Consequently, it is possible that their "dark-crested hills" may be the first observation of the boulder patches that cover the crater floor.

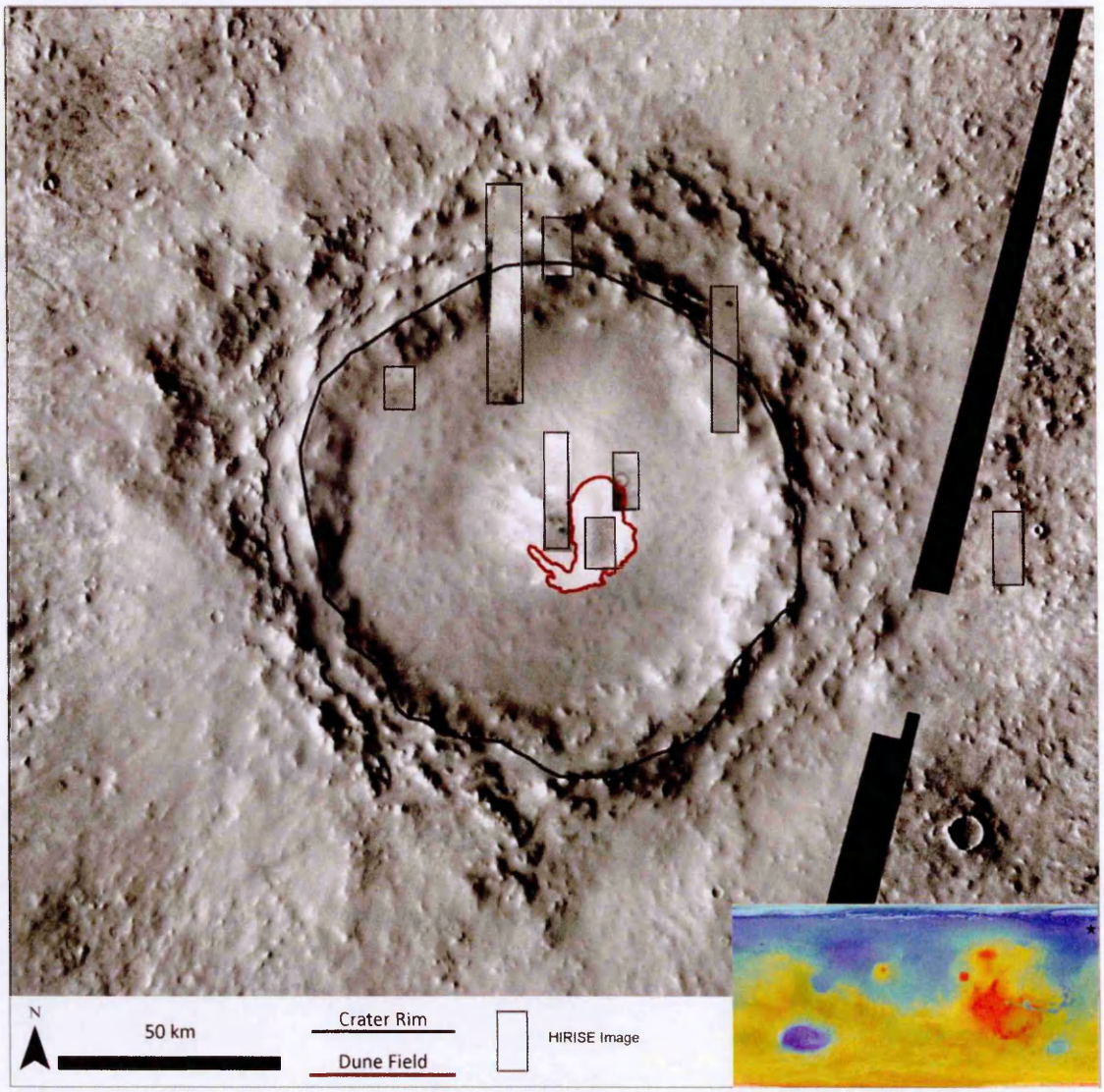

Figure 5.1: Map of Lomonosov Crater showing the location of the crater rim and the extent of the central dune field. The distribution of HiRISE images across the crater interior is shown (THEMIS daytime data).

5.2.2 Boulder Patches

Lomonosov Crater and the surrounding plains (shown in Figure 5.1) are covered with patches of boulder strewn ground which range in size from a few hundred metres to a kilometre across (figure 5.2). These boulder patches generally occur on flat ground and are the densest concentrations of boulders in the area. Some patches appear to form haloes, usually several hundred metres in diameter, around the rims of buried impact craters. Sometimes the crater interiors are free of boulders, while in other cases the boulder patch is almost continuous from one side of the feature to the other. It is possible that completely buried craters are also present beneath those patches which do not appear to form a halo around a pre-existing structure. Some boulder fields are underlain by fracture patterns, while others are on smoother, non-patterned ground.

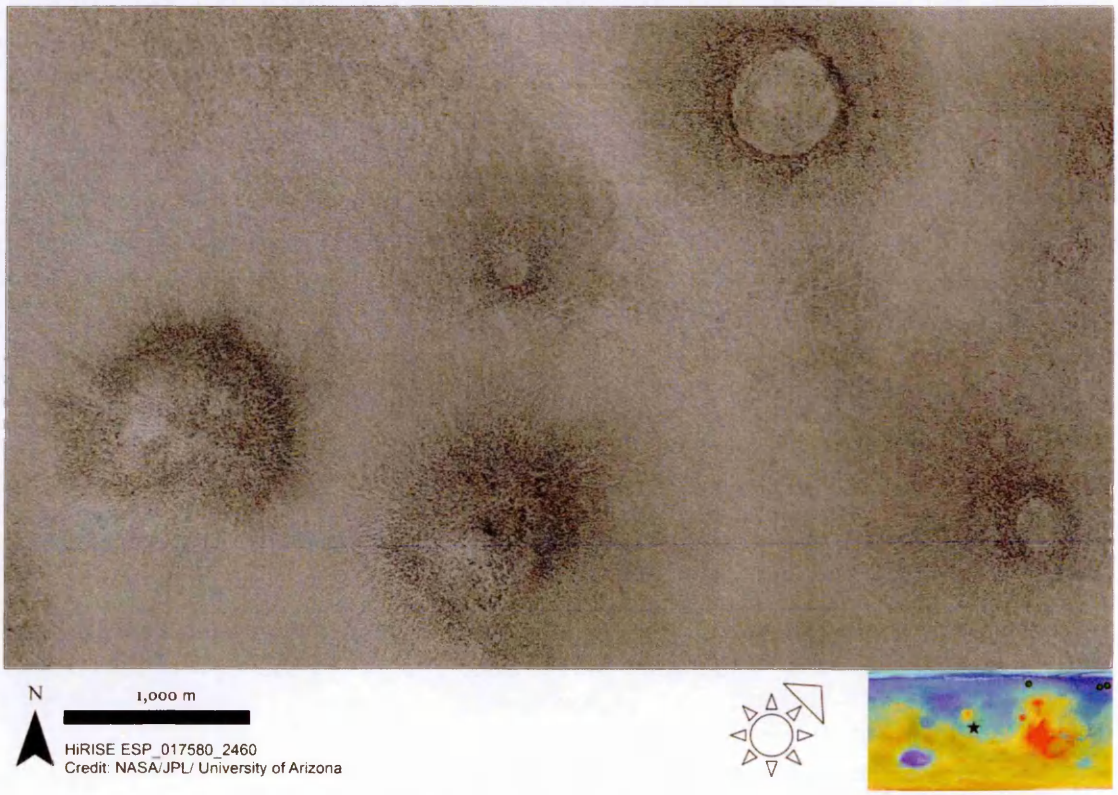

Figure 5.2: Boulder patches in the interior of Lomonosov Crater HiRISE Image ESP_017580_2460.

In some places small patches of boulders radiate from one point on the rims of larger impact craters, rather than forming a coherent ring around the feature. Such a site is

shown in Figure 5.3. This generally seems to be the case for multiple kilometre scale features. In many of these patches there appears to be some degree of organisation. The metre-scale clasts do not appear to be randomly distributed, as is the case over much of the martian surface, instead they form lines and arcs of clasts. In some cases these appear to be part of a discontinuous net. Many of these structures appear to be morphologically similar to the sorted polygons found in terrestrial periglacial environments described in Chapter Four, albeit on a much larger scale.

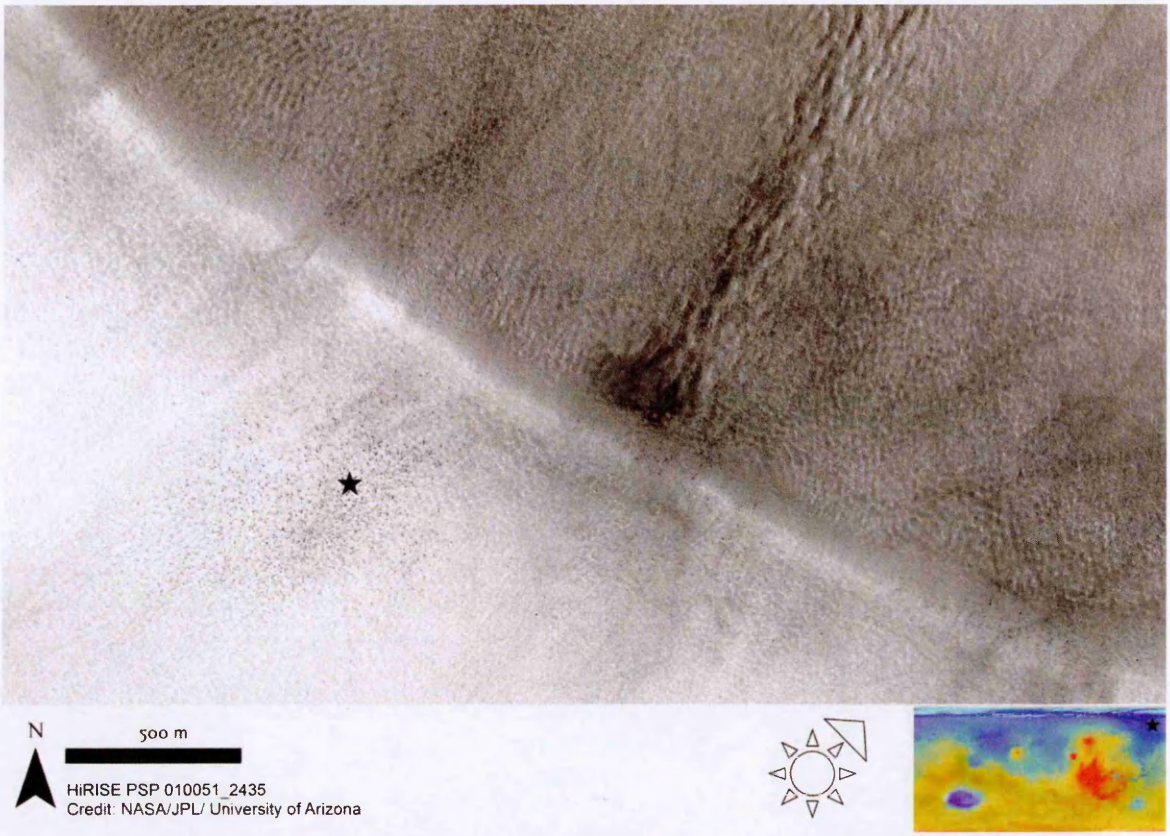

Figure 5.3: Cluster of boulders on the rim of a larger impact crater (marked with a star). A small gully is located on the inner wall of the crater. The boulders are clustered on the outer wall.

5.2.3 Distribution

Boulder patches were found to be common both in the crater interior and across the surrounding plains, but are scarce in the areas covered by the ejecta blanket. Examination of the limited number of HiRISE images in this area confirmed that large

swathes of boulder covered ground appear to exhibit organisation which could be a form of sorted patterned ground. Consequently, this region provides an excellent case study to assess the likelihood that these features are randomly distributed. This site will also be revisited later in this thesis as part of the discussion on the formation mechanism of these features.

Boulder fields are common across the flat plains surrounding the crater, and in the crater interior, but are less common on the steeper slopes around the crater and on the ejecta blanket. The centre-east of Lomonosov crater contains a large dune field and no boulder clusters are present within it. HiRISE images only cover a small area of the interior of the crater, mainly on the northern wall and around the centre; these are the parts of the study site where the most in-depth analysis has taken place. All of the HiRISE images of the area surrounding Lomonosov have also been examined.

5.3 Methods

5.3.1 Resolution of the Data Sets

Figure 5.4 illustrates a boulder patch in the vicinity of Lomonosov crater. The same feature is shown in both HiRISE and CTX images. In the HiRISE image (25 cm/pixel) individual boulders can be distinguished and an assessment can be made of whether organisation is present. In the CTX image (6 m/pixel) the arrangement of the clasts cannot be thoroughly described and it is thus impossible to tell whether organisation is present or not. No examples of sorted patterned ground have been found outside the boulder patches. Clasts are sparsely distributed outside the boulder patches and do not appear to exhibit organisation.

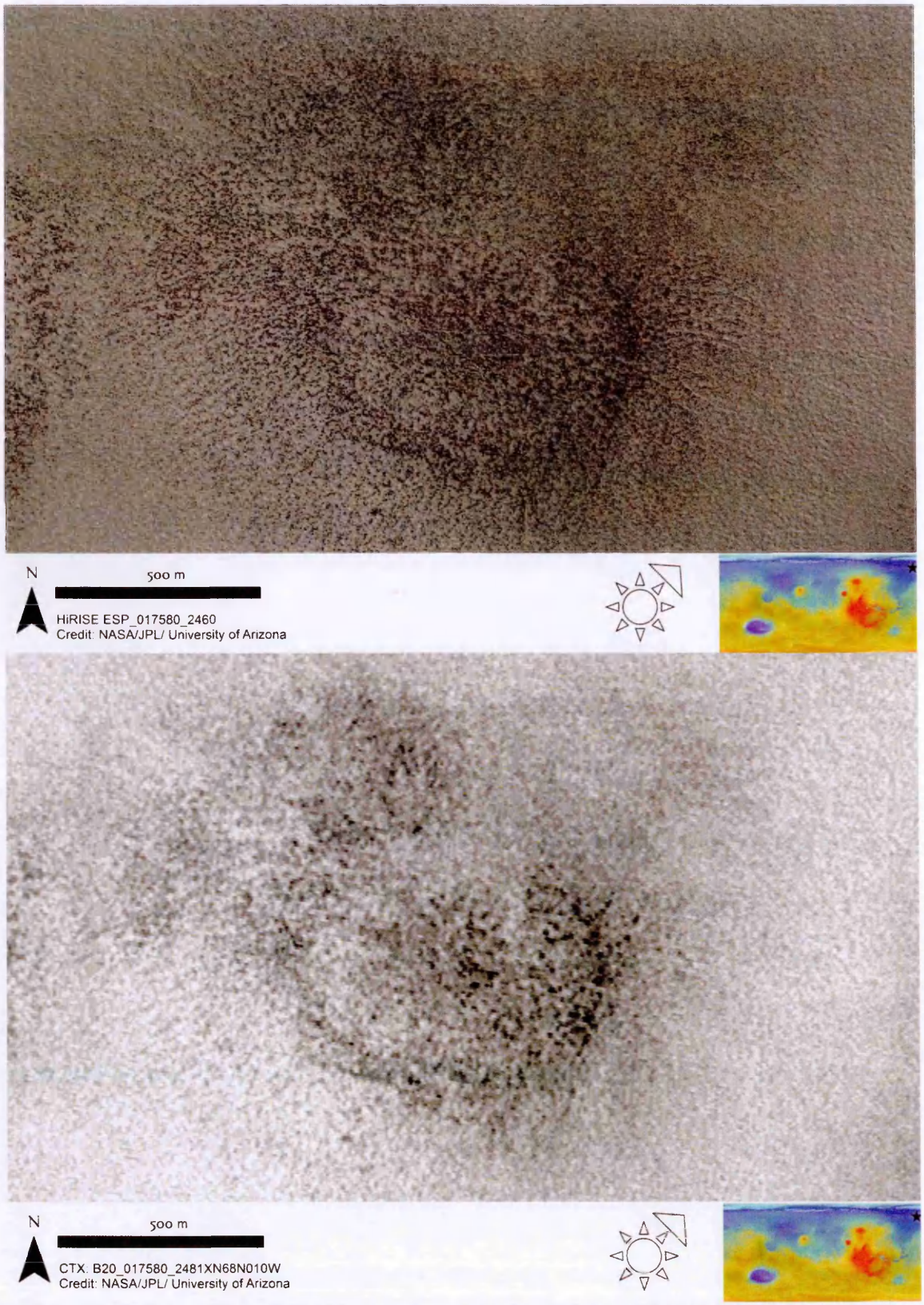

Figure 5.4: Comparison of boulder patches in HiRISE (upper image) and CTX (lower image).

CTX coverage is present across most of the study area, so this can be used to find locations where patches of boulders occur, and thus where sorting is possible. However, it is only possible to locate the sorting patterns themselves in the few locations where HiRISE images are present. This limited HiRISE coverage means that the distribution of the sites examined in this study is uneven. The north western and central portions of Lomonosov Crater have much better coverage than the south eastern region and all HiRISE images are isolated from one another with very little overlap.

On the surrounding plains the HiRISE images are widely distributed and only cover a very limited area. This limits the extent to which regional trends can be assessed as there are not enough points in some parts of the study area to produce a continuous map. However the presence of boulder patches in a relatively large number of randomly sampled locations suggests their presence in areas which have yet to be imaged at HiRISE resolutions. Lower resolution HRSC images have been used to confirm that boulder patches occur in areas which are not covered by the CTX images and are in fact ubiquitous across this region.

5.3.2 Survey Procedure

All boulder clusters within the study area were identified and those covered by HiRISE images were assessed for a number of parameters; the presence and quality of a sorted net, the presence of an underlying fracture pattern and the likelihood that the sorted net was related to the underlying fracture pattern. 147 boulder clusters across the 17 HiRISE images within 500 km of Lomonosov crater were examined. Five of these images cover sections of the crater interior while 12 are located on the surrounding plains. Table 5.1 summarises the HiRISE images examined in this area, and Figures 5.5 and 5.6 show the distribution of HiRISE and CTX images.

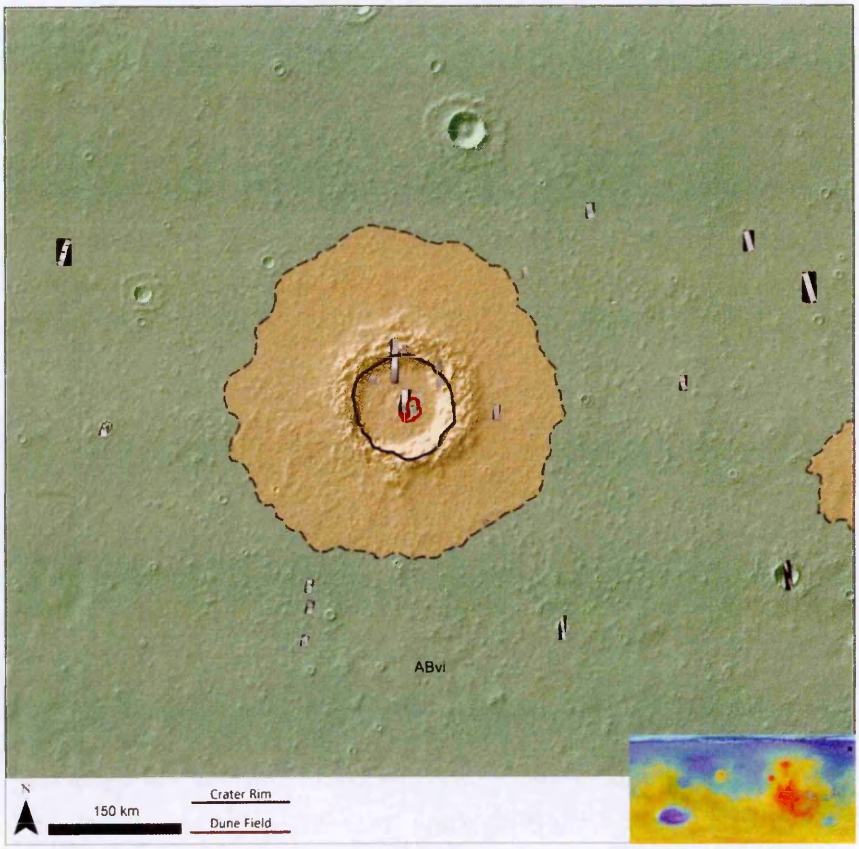

Figure 5.5: Distribution of HiRISE images across the study area.

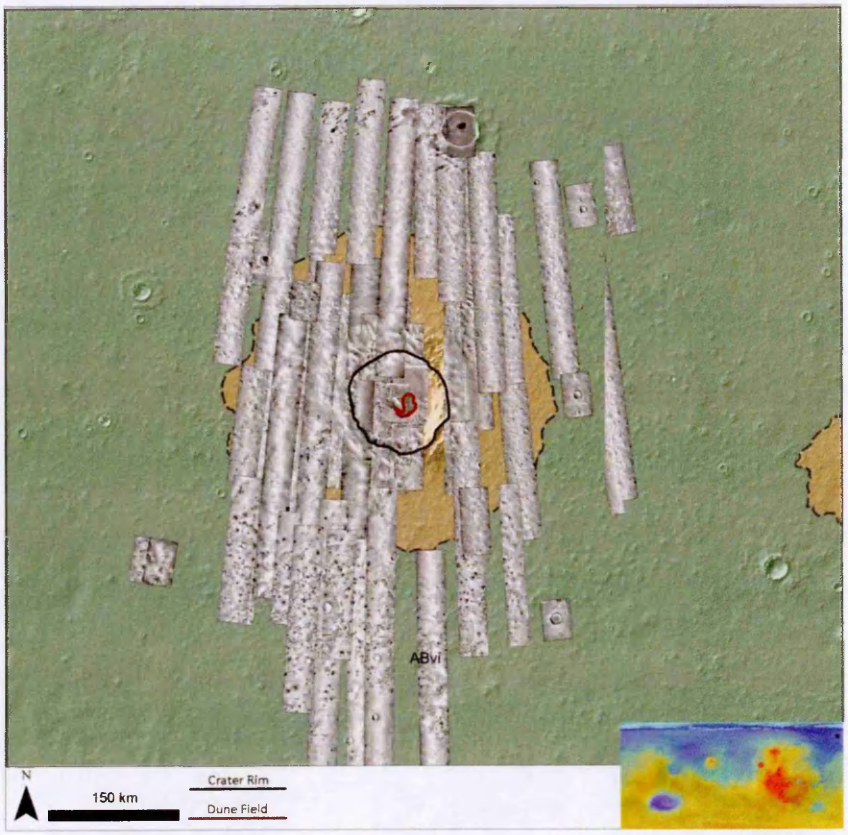

Figure 5.6: Distribution of CTX images across the study area.

Table 5.1: Summary of the HiRISE images examined in this investigation.

Image	Location		Lat	Long	Solar Longitude
PSP_001520_2470	Exterior	West of crater	66.575°	332.881°	139.4°, Summer
PSP_007440_2455	Interior	Crater interior	64.987°	351.008°	37.6°, Spring
PSP_010051_2435	Exterior	West of crater	63.094°	339.264°	128.6°, Summer
PSP_010644_2455	Interior	Crater interior	65.264°	349.498°	151.5°, Summer
TRA_000846_2475	Exterior	East of crater	67.069°	0.012°	114.4°, Summer
ESP_017079_2410	Exterior	South of crater	60.458°	348.761°	66.0°, Spring
ESP_017131_2485	Exterior	East of crater	68.041°	6.672°	67.7°, Spring
ESP_017580_2460	Interior	North wall	65.672°	350.288°	83.0°, Spring
ESP_017632_2475	Exterior	East of crater	67.054°	9.226°	84.8°, Spring
ESP_017685_2490	Exterior	East of crater	68.743°	-1.182°	86.6°, Spring
ESP_019900_2470	Exterior	East of crater	66.925°	9.267°	169.7°, Summer
ESP_023738_2415	Exterior	South of crater	61.061°	348.710°	347.6°, Winter
ESP_025294_2415	Exterior	South of crater	61.426°	348.533°	45.4°, Spring
ESP_025769_2435	Exterior	West of crater	63.168°	339.345°	61.7°, Spring
ESP_026441_2460	Interior	East Wall	65.561°	352.299°	84.6°, Spring
ESP_026850_2475	Exterior	North West	67.343°	345.811°	98.7°, Summer
ESP_027918_2455	Interior	East Wall	65.061°	351.573°	37.6°, Spring

5.3.3 Grading of Sorted Patterns

The degree of sorting at each of these sites was ranked between zero (no evidence of organisation) and five (exhibiting a distinct sorting pattern). The criteria are summarised below (see Table 5.2).

Table 5.2: Classification of sorting grades:

Grade	Description
0	No evidence of organisation
1	Uncertain organisation
2	Clustering of clasts
3	Clear lines and arcs
4	Discontinuous net
5	Continuous pattern

Grade Zero: No Organisation

Boulders are scattered across the image in a seemingly random distribution and no lines or clusters of clasts are apparent.

Grade One: Uncertain Organisation

There may be some clustering or alignment of clasts but whether a pattern is present remains highly uncertain.

Grade Two: Clustering of Clasts

There are some areas where clasts appear to be clustered or coaligned, but they do not form a clear pattern.

Grade Three: Clear Lines and Arcs

Boulders are arranged into lines separated by reasonably clear spaces but do not form coherent polygons.

Grade Four: Discontinuous net

Lines of clasts are common and most clasts appear to fit the edges of a polygonal net, even if that net is not continuous.

Grade Five: Continuous Pattern

Clasts form clear sorted stripes and polygons similar to those seen in terrestrial periglacial environments and examples from the Mars periglacial literature.

In order to perform this classification the observed features were compared to type examples from previous studies on this subject, in particular from (Gallagher et al., 2011b). A grade was chosen based on the arrangement of clasts and the similarity of the features to the type examples. The same procedure was applied to every example of sorted patterned ground examined both in this region and elsewhere on the Northern

Plains and a similar methodology was used to characterise other putative periglacial landforms.

Sites which were classified as falling between grades zero to two are considered to lack patterned ground. There may be a small amount of clustering of clasts, but not sufficient to suggest that the arrangement is indicative of an underlying process. Sites with grade three may suggest that a sorting process is at work but remains uncertain, while those classified as grades four or five are likely to provide strong evidence that these landforms are the result of a specific geomorphic process. Examples of each grade are shown in Figure 5.7.

It is the higher graded features which are of most interest to this study. The region around Lomonosov Crater has the highest concentration of highly graded sites, and the most examples of clastic patterns over all. Consequently, this site is the focus of much of the analysis of sorted patterned ground presented later in this thesis.

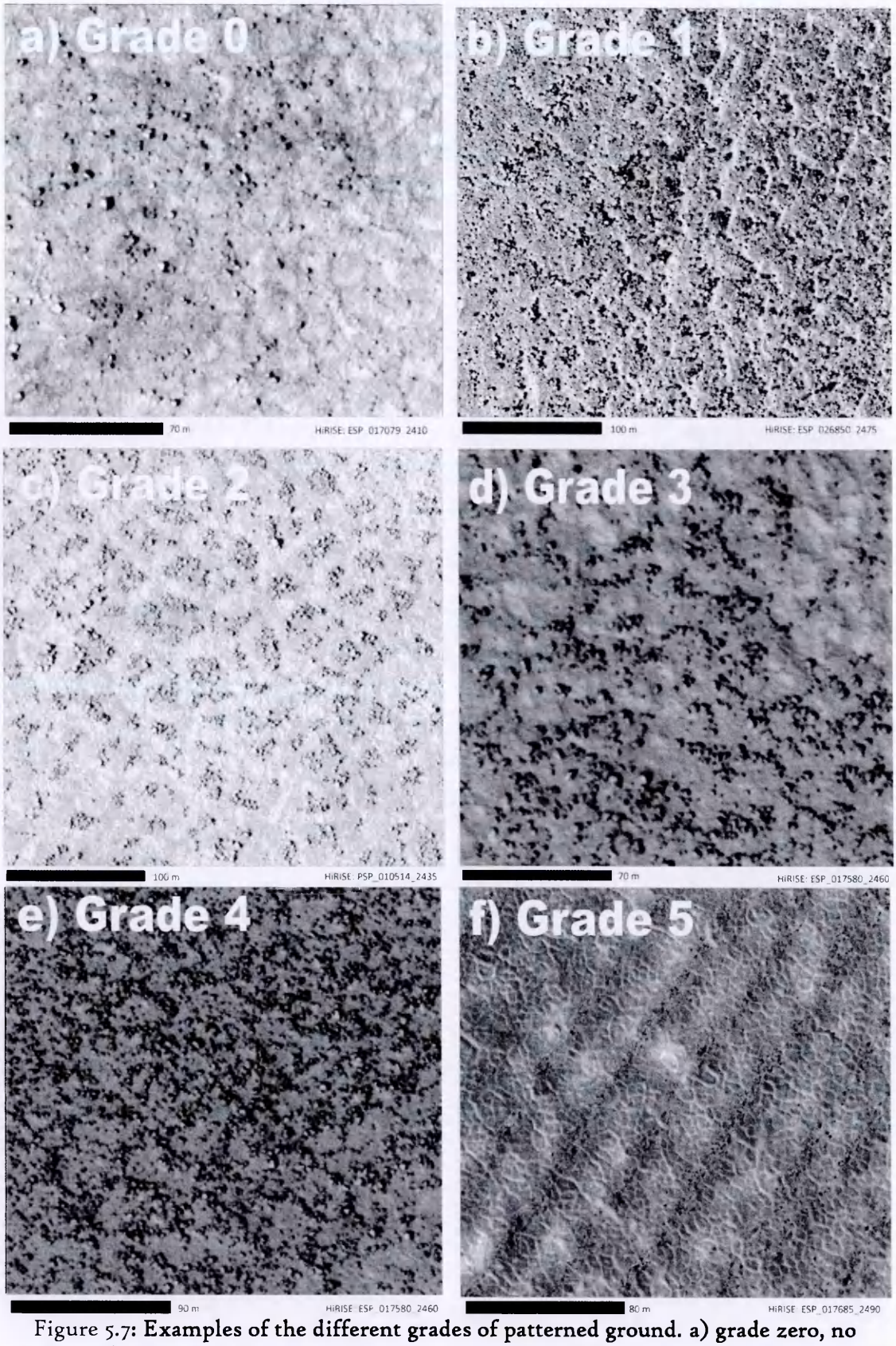

Figure 5.7: Examples of the different grades of patterned ground. a) grade zero, no pattern, b) grade one, c) grade 2, d) grade 3, e) grade four, f) grade five, perfectly clear pattern. An enlarged version of this figure is provided in appendix 2

5.4 Results

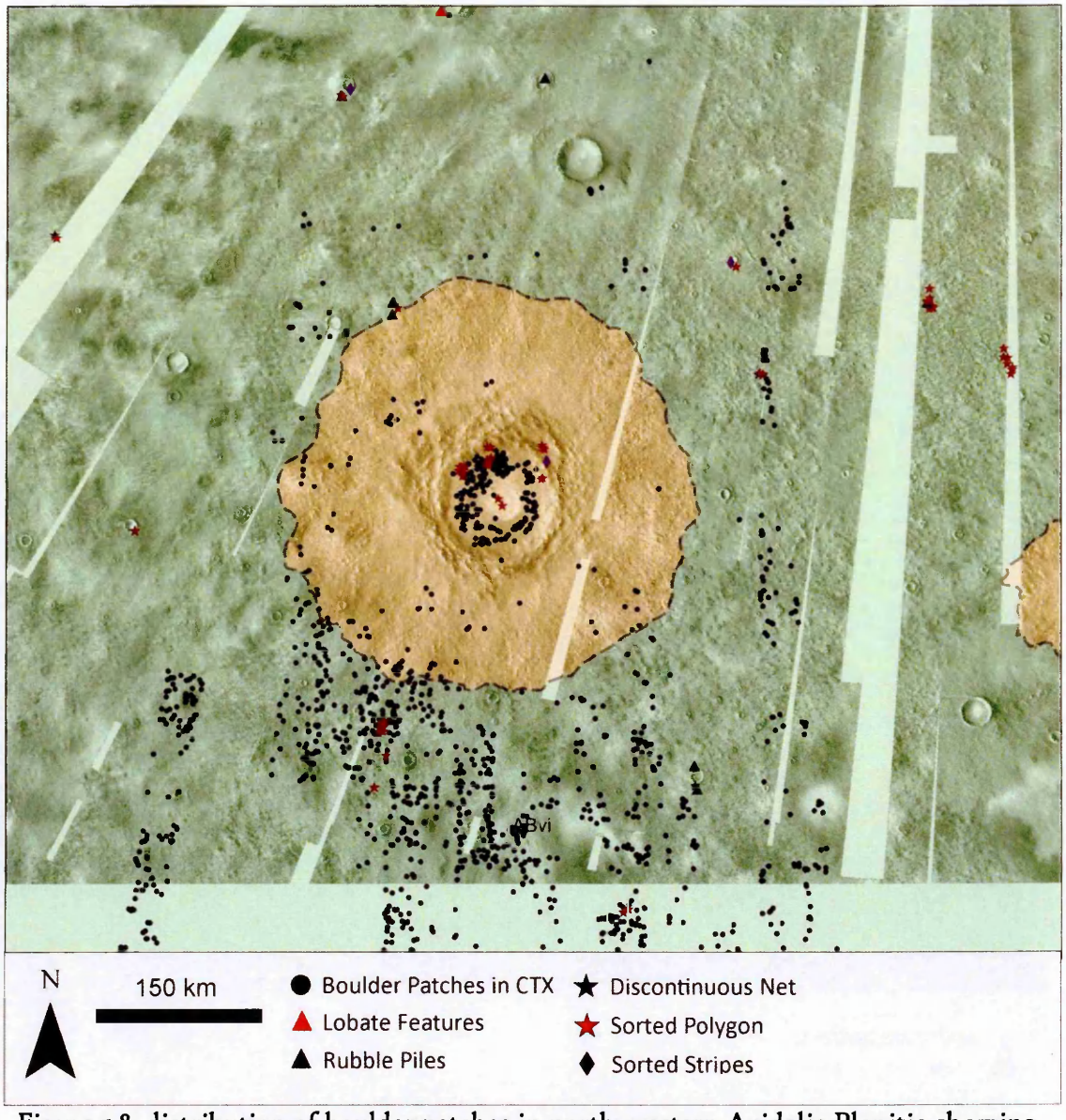

Figure 5.8: distribution of boulder patches in north-western Acidalia Planitia showing the area surrounding Lomonosov Crater. The surrounding plains are uniformly classified as part of the Vastitas Borealis interior unit. An enlarged version of this figure is provided in appendix 2.

Figure 5.8 shows the distribution of boulder patches across the study area. Black circles indicate the presence of boulder fields in CTX images. Red stars indicate sites where these features have been examined using HiRISE images and confirmed to exhibit possible clastic networks. Black triangles indicate rubble piles and purple diamonds possible sorted stripes. Polygonal networks are the most common of these feature types, while clastic stripes are found much less often.

Not all of the rubble piles within the area of HiRISE images exhibited possible sorting, so additional HiRISE images would be needed to confirm whether organisation is present in the boulder patches marked from CTX images. The presence of a boulder cluster does not necessarily indicate sorting, just the environment in which sorting is often found.

5.4.1 Examples of Discontinuous Networks

Figure 5.9: **Possible sorted network on the floor of Lomonosov Crater. Lines of clasts and discontinuous polygons in HiRISE image ESP_017580_2460.**

HiRISE image ESP_017580_2460 overlaps the northern wall of Lomonosov crater. The southern part of the image contains the area illustrated in Figure 5.9; a region of the crater floor where a number of small buried impact craters are surrounded by haloes of boulders. This image contains 21 boulder clusters, all of which show some form of organisation with the highest sorting grade found in the image being three. In several

areas across this image boulders are seen to be grouped into lines and arcs. In a few cases they form regions of clear ground surrounded by discontinuous lines and clusters of metre scale boulders.

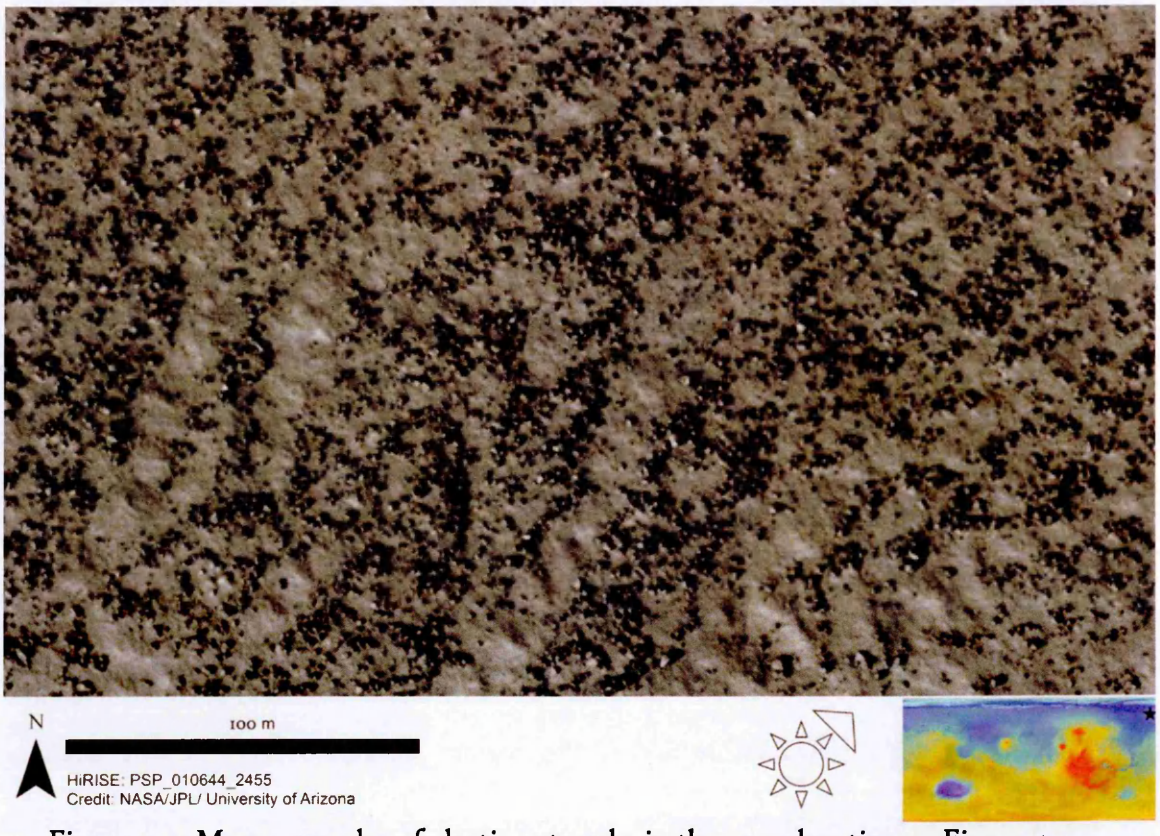

Figure 5.10: More examples of clastic networks in the same location as Figure 5.9 Discontinuous polygons surround clear areas within the rubble field.

Similar structures can be found in HiRISE image PSP_010644_2455, covering the crater interior just to the west of the site detailed in Figure 5.9. Again, clear areas of ground are enclosed by semi-polygons of larger clastic material. Very few areas are completely enclosed, but all 14 boulder patches in this area seem to exhibit some form of organisation (grade 4 in some areas).

A few more discontinuous nets can be found in image PSP_007440_2455 near the centre of Lomonosov Crater. As with the other sites, several fields of boulders can be seen. Here larger, ~4 m diameter, boulders appear to be arranged into a polygonal pattern but the clear areas are much smaller relative to the size of the clasts, making it harder to be certain that this isn't a random arrangement which just appears organised in places.

Figure 5.11: Possible and uncertain polygons in PSP_007440_2455 near the centre of Lomonosov Crater.

Possible sorting is not confined to the interior of Lomonosov crater, similar boulder halos and rubble fields occur across the region. Several images to the south of Lomonosov crater exhibit possible polygons. Image ESP_025294_2415 (Figure 5.12) exhibits some of the clearest discontinuous nets in the area. Here, thin lines of metre-scale boulders enclose open areas and in some cases are accompanied by a slight change in albedo below the clastic lines. Whether this is due to changes in the underlying material or is the result of the boulders shadowing the ground around them is uncertain. All ten boulder patches within this image exhibit possible sorting and the highest grade found in this image is grade four.

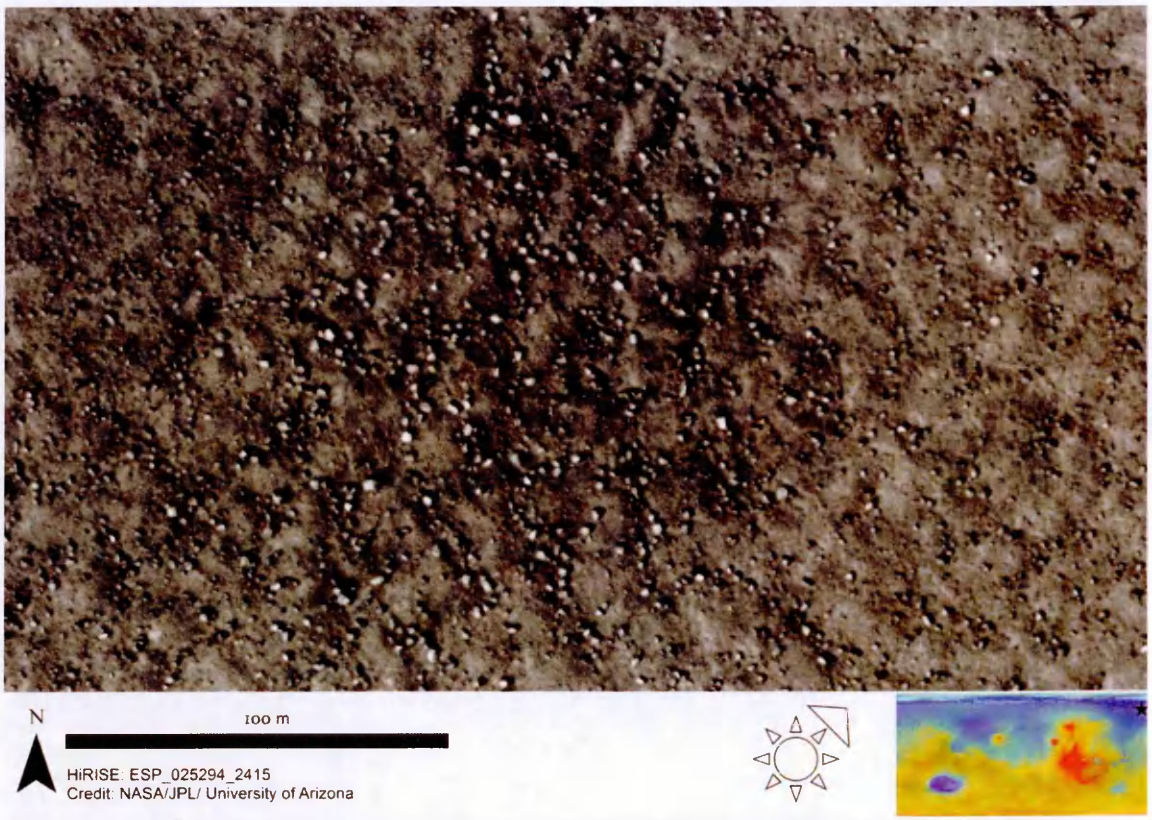

Figure 5.12: Net of discontinuous polygons in HiRISE image ESP_025294_2415, covering flat ground to the south of Lomonosov Crater.

5.4.2 Examples of Clastic Stripes

Two sites exhibiting possible clastic stripes have been found within this area. One, on the eastern wall of Lomonosov Crater (Figure 5.13), is quite uncertain due to low boulder density. The other, on the south western walls of a medium-sized impact crater to the north east of Lomonosov, is far more convincing (Figure 5.14-5.16).

Figure 5.13: Possible discontinuous stripes in ESP_026441_2460 on the east wall of Lomonosov Crater.

Image ESP_026441_2460 exhibits several sites on the floor of Lomonosov Crater where polygons may occur within the boulder patches, but the clast density is lower in this region, so these sites are not as convincing as those to the west. The most interesting feature in this image is an area on the crater rim where there appears to be a faint linear pattern to the arrangement of the metre-scale boulders. The arrangement of smaller clasts (below the resolution of the image) cannot be determined, so it is not possible to be certain whether these are sorted stripes or not.

Image ESP_017685_2490 covers a medium-sized impact crater where clear clastic stripes can be seen across a wide swath of the crater wall. Running from the rim of the crater down into the interior, these features overlay a net of fracture polygons and are also located within a series of light and dark bands: the ground beneath the clasts seems to be darker, while lighter ground is found between the stripes. This could indicate the

presence of smaller stones (below the resolution of the image) in the clastic zones, lending further evidence to these being sorted stripes.

Figure 5.14: Small crater in ESP_017685_2490 to the North East of Lomonosov Crater. The southern wall exhibits alternating bands of dark and bright material.

Figure 5.15: Detailed view of stripes on hillside

Figure 5.16: A closer look at these features reveals distinct clastic stripes over bands of alternating light and dark terrain.

5.5 Assessment of Sorting

It was found that many sites exhibited minor organisation in the range of grades 2-3. Discontinuous nets of grade four and above however were quite uncommon. The results of this classification are shown in Table 5.3 and the locations of the different sites are shown in Figure 5.17.

Table 5.3: Summary of sites and images featuring patterns of each sorting grade.

Grade	Description	Sites	% of Sites	Images	% of Images	
0	No evidence of organisation	26	17.69	6	13.95	Unlikely to be Sorted
1	Uncertain clustering	32	21.77	7	16.28	96 Sites
2	Clustering of clasts	38	25.85	13	30.23	65%
3	Clear lines and arcs	35	23.81	12	27.91	Likely to be Sorted
4	Discontinuous net	15	10.20	4	9.30	51 Sites
5	Continuous net	1	0.68	1	2.33	35%

The only site with grade five sorting occurs in image ESP_017131_2485 where numerous clastic stripes are seen (Figure 5.14-5.16). 15 boulder patches contain features classified as discontinuous nets (grade four sorting.) Several of these are located in the two HiRISE images covering the west of the Lomonosov Crater floor ESP_017580_2460 and PSP_010644_2455. Grade 4 sorting also occurs in ESP_025294_2415, located to the south of Lomonosov Crater, and in PSP_010051_2435, to the far west of Lomonosov.

Figure 5.17: Results of the boulder patch classification

These five images are considered to be most likely to contain evidence of organised, clastic, patterned ground. It is interesting to note that these locations are not restricted to the crater interior, and are in fact scattered quite widely across the study area. They occur within a variety of different terrains ranging from the flat ground of the northern plains to the steeper slopes of crater walls. The presence of the same landforms in widely spaced images would seem to suggest that whatever process is responsible for their formation is occurring across the area, rather than being limited to one or more unusual micro-environments.

Thirty-five sites (23.8% of total) exhibit clear lines of clasts (grade 3) and so may be evidence of a partially developed clastic network. However 26 sites (17.69% of total) show no evidence of organisation and 32 sites (21.77%) have uncertain clustering but no clear pattern, giving a total of 58 sites (39.46%) where sorting is unlikely to be present.

5.5.1 Average Nearest Neighbour analysis

Assessing by eye whether a pattern is present within an arrangement of clasts is inescapably subjective. In Chapter Four it is shown that when the clasts within an area of terrestrial patterned ground are digitised and an *average nearest neighbour analysis* conducted a significantly non random pattern is detected. This approach can be applied to these features to test whether the observed pattern was significantly distinct from a random distribution, and so whether a feature should be considered as a martian analogue for the terrestrial features described in Chapter Four.

5.5.1.1 Approach

The patterns of boulders at twenty-five sites were digitised by placing a point in an ArcGIS shape file over the centre of each of the boulders. A variety of sites that had been classified with different grades of sorting were examined, as well as transitional sites which were less easy to classify. Some locations where no pattern was believed to be present and the boulders appeared randomly distributed were also tested. Several representative sites for each category of the classification system were selected so that this analysis would be applied to all varieties of patterned ground described in the previous section.

Most of the locations that exhibit a high likelihood of sorting are characterised by a polygonal, albeit discontinuous, network. However, a few locations were found with different types of patterned ground: two sites contain possible sorted stripes, and several patches of rubble piles were also studied. These features were all subjected to the nearest neighbour analysis.

5.5.1.2 *Results*

It was found that most of the sites which appeared highly sorted, exhibiting a discontinuous net and scoring four on the classification, yielded results suggesting that they were strongly dispersed. This makes sense as the polygonal patterns are an expression of clasts being spread out, surrounding open spaces. All of the grade four sites returned a dispersed result as did the grade 3 site classified as being transitional with grade four.

One other grade 3 site returned a dispersed result as did several of the higher end grade two sites (although this could be due to the low boulder density at some of these sites rather than the presence of a stronger sorting pattern). Most of the other grade three sites indicated clustering of boulders. Only one low grade 3 site returned a randomly distributed result.

The low grade 2 sites, where very little organisation was observed in the visual survey, generally returned a random classification. Both sites which were selected for their apparent rubble piles returned a "random" result. This is probably because many small clasts surround the denser concentrations of clasts and these randomly distributed clasts are identified as the average structure across these areas rather than the small clusters. If different sizes of boulder could be given a different weighting, then these sites might return a different result.

Both sites with stripes returned clustered results due to the arrangement of clasts within the stripes. This was the expected result for these features. Most of the sites which were selected for their lack of an apparent pattern (grades zero and one) returned a result of clustered with a few detected as being random.

Table 5.4: Results of *Nearest Neighbour Analysis* of sorted patterned ground in and around Lomonosov Crater (note that sites are organised by sorting grade, rather than by Site ID. This is because the Site ID is an artefact of the order in which they were examined and is thus largely arbitrary).

Site	Mean Distance Observed	Expected	R-Value	z-score	p-value	Result	Sorting Grade	Type
Site 4	0.000072	0.000072	1.00	0.14	0.89	Random	0	No Pattern
Site 6	0.000077	0.000082	0.94	-2.89	0.00	Clustered	0	No Pattern
Site 24	0.000107	0.000114	0.95	-3.39	0.00	Clustered	0	No Pattern
Site 5	0.000092	0.000097	0.95	-3.39	0.00	Clustered	1	Net
Site 25	0.000083	0.00008	1.04	2.57	0.01	Dispersed	1	Net
Site 7	0.000064	0.000066	0.98	-1.12	0.26	Random	1-2 transitional	Net
Site 18	0.000067	0.000065	1.03	1.57	0.12	Random	Low 2	Net
Site 17	0.000065	0.000065	1.01	0.66	0.51	Random	2	Rubble Piles
Site 22	0.000068	0.000067	1.02	1.49	0.14	Random	2	Rubble Piles
Site 23	0.00007	0.000067	1.04	2.97	0.00	Dispersed	2	Net
Site 13	0.000118	0.000111	1.07	7.16	0.00	Dispersed	High 2	Net
Site 10	0.000079	0.000068	1.16	8.57	0.00	Dispersed	2-3 transitional	Net
Site 9	0.000098	0.000096	1.02	1.31	0.19	Random	Low 3	Net
Site 14	0.000121	0.000305	0.40	-47.43	0.00	Clustered	Low 3	Net
Site 15	0.00015	0.000205	0.73	-24.73	0.00	Clustered	3	Stripes
Site 16	0.006309	0.053979	0.12	-84.32	0.00	Clustered	3	Net
Site 12	0.000089	0.00009	0.99	-1.67	0.10	Clustered	High 3	Net
Site 20	0.000054	0.000049	1.11	7.72	0.00	Dispersed	High 3	Net
Site 8	0.00007	0.000059	1.19	13.62	0.00	Dispersed	3-4 transitional	Net
Site 1	0.000081	0.000069	1.17	10.67	0.00	Dispersed	4	Net
Site 2	0.000086	0.000076	1.14	11.50	0.00	Dispersed	4	Net
Site 3	0.000067	0.000062	1.08	6.53	0.00	Dispersed	4	Net
Site 19	0.000064	0.000061	1.05	4.22	0.00	Dispersed	4	Net
Site 21	0.000068	0.000066	1.03	1.93	0.05	Dispersed	4	Net
Site 11	0.000036	0.000054	0.66	-24.56	0.00	Clustered	5	Stripes

There does not appear to be a particular pattern in the spatial distribution of clustered, dispersed or random patterns. All types are found both within the crater and without it. Most images have examples of each of the three types.

There is a clear difference between high-graded sites with a consistently dispersed pattern and low-graded sites with a random or clustered result. These results would seem to suggest that the "background" arrangement of clasts is generally either random or clustered depending on the site. Sites with higher sorting grades do display arrangements of clasts which are significantly different to those expected from randomly emplaced clasts. This suggests that an underlying geomorphological process is likely to be responsible for the apparent structure in their emplacement, rather than it being the result of chance. The fact that similar patterns occur across the region, and return similar results in this test, reinforces this conclusion.

5.6 Summary

A visual examination of the boulder patches around Lomonosov crater provided a large suite of possibly periglacial landforms. Of the 147 patches examined all but 26 showed some degree of clustering and 51 sites were found where sorting was believed to be likely. These sites had clear lines and arcs of clasts, and in 15 cases, discontinuous polygons.

Testing whether these apparent patterns were actually significantly different from a random distribution confirmed that these features were genuine non-random arrangements. It was found that the majority of the sites which were believed to exhibit a sorted net as a result of visual inspection and qualitative classification were not random distributions.

Fourteen of the 25 analysed sites were ranked above a grade 3 upon visual inspection. Of these only one returned a "random" result, five were found to be predominantly clustered, while the rest were found to be significantly dispersed. This is the result that would be expected based on the classification of Icelandic patterned ground in Chapter Four where all but one of the ten sites digitised from aerial photographs were found to

be dispersed. The prediction that wide clastic stripes would return a clustered result, due to the proximity of material in the coarse domains being most prevalent, also held true. Both examples of stripes were found to be significantly clustered relative to a random distribution.

The Icelandic air photographs are the most comparable images to martian HiRISE data. It was expected that if the martian results of the *nearest neighbour analysis* were similar to any terrestrial features it would be to the ones digitised from air photographs. This was found to be the case, confirming that the two suites of features are comparable at this range of resolutions.

Since it seems likely that the arrangement of clasts at these sites is non-random it must reflect an underlying geomorphological process. The similarities to Icelandic features illustrates that the movement of large clasts to the periphery of a sorted polygon by periglacial processes is a viable candidate to explain this boulder distribution. However this test is not sufficient to confirm that these structures formed through periglacial processes, further evidence must be assessed before a periglacial hypothesis can be accepted.

6 Chapter Six: Surveying the Martian Northern Plains

In the preceding chapters the suite of landforms that comprise a periglacial environment have been described and the evidence that some of these features could occur under martian conditions has been discussed. A variety of prior studies have identified putative periglacial features on the Northern Plains of Mars. Consequently, a major aim of this investigation is to determine how widespread such features are and to assess the likelihood that they could have formed through periglacial processes. To this end a series of large scale surveys were conducted to identify features with similar morphologies to those described in the studies discussed in the following section. This chapter will outline the surveying procedure and define the study areas surveyed. Chapter Seven will then discuss the results of this investigation, including the distribution of potentially periglacial features at a regional scale in large areas of Acidalia, Arcadia and Utopia Planitiae.

6.1 Background

Various studies have examined the distribution of periglacial features on Mars in the past. The following section summarises the findings of the key studies that informed the present work, and the results presented in chapter seven and analysed in chapter eight. The discussion in chapters nine and ten draws on two of these studies in particular, those of Orloff et al., (2013) and Séjourné et al., (2011) respectively. These are discussed in more detail in the introductory sections of those chapters.

The study from which this investigation follows most directly is that of Gallagher et al., (2011). They used a similar methodology, surveying HiRISE images to locate sites with possible periglacial features. Gallagher et al., present various examples of sorted

stripes and clastic lobate structures across the martian high latitudes, in particular clastic lobes in Heimdal Crater. This study proposes a periglacial explanation for these features. It is noted that gullies pre and post date the putative sorted structures and thus that it is likely that the two landform types form an assemblage indicative of ground ice thaw. The detection of perchlorates at the phoenix landing site (Hecht et al., 2009), in close proximity to Heimdal Crater is postulated to account for high latitude thaw.

The work of Gallagher et al., (2011) helped to define the aims of the present study. Their investigation focuses solely on the high latitudes, with features found between 59-78 °N. Other research by the same group indicates that they could well occur elsewhere on the Northern Plains (e.g. Balme et al., 2009; Balme and Gallagher 2009; Gallagher and Balme 2011). It was decided that this investigation should cover a wider area, and examine a broader suite of landforms, to provide a larger, and hopefully more comprehensive, catalogue of putative periglacial sites. The examples given by these studies formed the first suite of type examples for the identification of other sorted features.

A variety of other studies have also indentified areas of boulder organization on the martian northern plains as described in chapter two. Of particular interest are the studies of Orloff et al., (Orloff et al., 2011, 2013; Orloff, 2012). These investigations catalogue a variety of sites where boulders appear to be clustered. Rather than proposing a periglacial explanation for these features Orloff et al., propose a novel mechanism of boulder ratcheting, whereby a dry sorting process related to the opening and closing of underlying contraction crack polygons results in the movement of boulders. This mechanism, and other hypotheses which could explain the clustering of martian boulders without the need for thaw, are presented in detail in section 9.2. Similar studies include those of Levy et al., (2008a), Levy et al., (2010) and Mellon et

al., (2008) which propose a gravitational sorting mechanism. All of these studies provide useful examples of boulder clustering which have been compared and contrasted with the features found during the present investigation.

These alternate hypotheses require the presence of fracture polygons, which are hypothesised to result from thermal contraction cracking of icy material. if these formation hypotheses were to be tested then an examination of both the distribution of fracture networks, and their relationship to overlying polygonal patterns was neccersary. Fracture polygons are well documented in the martian high latitudes, and their distribution has been mapped by a variety of investigations in particular that of Mangold (2005). Mangold catalogued fracture polygons as far south as 50 °N while other studies by Soare et al., (2012) and levy et al., (Levy et al., 2009; Levy et al., 2010) also provided a useful constraint on the locations where these features were expected to occur. Again the purpose of the present study was to build upon this work, and in particualr to identify examples of these features further south than the boundaries of some of the previous studies. Type examples were drawn from these studies and the range of lattiude across which features occured was compared and contrasted. Sites with fracture polygons in close proximity to sorted polygons were identified and these formed the basis of the analysis of fracture control in chapter nine.

The observations of clastic lobate structures by Gallagher et al., are backed up by very comprehensive surveys of lobate features, both clastic and non clastic by Johnsson et al., They catalogued these features in both the northern (Johnsson et al., 2012) and southern (Johnsson, 2013) hemispheres. Johnsson et al., compared and contrasted the features observed in crater interiors on Mars with terrestrial analogues in Svalbard and concluded that the martian features had likely formed through thaw related processes in the geologically recent past. The examples provided in their northern hemisphere

study provided a good starting point for the examination of lobate structures in the present study and type examples were drawn from this paper. The focus of Johnsson et al.'s surveys was again limited to high northern latitudes, with features found between 60 and 80 °N.

In the case of gullies a very comprehensive catalogue of features exists for both martian hemispheres for example Balme et al., (2006); Levy et al., (2009); Kneissl et al., (2010) and others, with global gully distribution being effectively summarised by (Harrison et al., 2014). Consequently the focus of this investigation was not on expanding the boundaries of the existing observations as in the cases for sorted and lobate features, but rather in examining specific cases where gullies and other putative periglacial features occurred in proximity. Prior studies had indentified gullies as part of possible periglacial assemblages, Gallagher et al., (2011) report gullies with associated clastic features, while Johnsson et al., (2012); and Johnsson, (2013) found lobate structures near and within gully alcoves.

The last landform of interest to this investigation are scalloped depressions which have been proposed to result from thermokarst like processes as discussed in detail in chapter two. A variety of studies informed the analysis of these features including (Morgenstern et al., 2007; Soare et al., 2012; Ulrich et al., 2010). These studies established the extent scalloped terrains around Utopia Planitia and compared and contrasted them with terrestrial thermokarst landscapes, providing a strong case that these degraded areas on the martian northern plains are periglacial in origin. Of particular interest is the analysis of Séjourné et al., (2011), which proposes a scheme for categorizing the maturity of a scalloped landscape in a similar manner to that in which the growth of terrestrial thaw lakes is described by Wallace, (1948) and later terrestrial studies.

Most past studies on scalloped depressions have been focused on the Utopia Planitia region where these features are very numerous. However preliminary investigation made it clear that they were not limited to this basin. Consequently it was decided to map the distribution of these features elsewhere on the planet. In chapter ten the classification scheme proposed by Séjourné et al., (2011) is applied to two sites in Acidalia Planitia.

Since periglacial landforms require ice to form this study also draws extensively upon past studies that have established the distribution of ground ice across the Northern Plains. This includes the geomorphological studies of Costard (1989) and later mapping of near surface ground ice using the Mars Odyssey Neutron and Gamma Ray Spectrometers. (Boynton et al., 2010; Feldman et al., 2004, 2002). Water Equivalent Hydrogen measurements from these investigations are referenced throughout chapter eight. Figure 6.1 shows the global map of WEH measurements from Feldman, (2004).

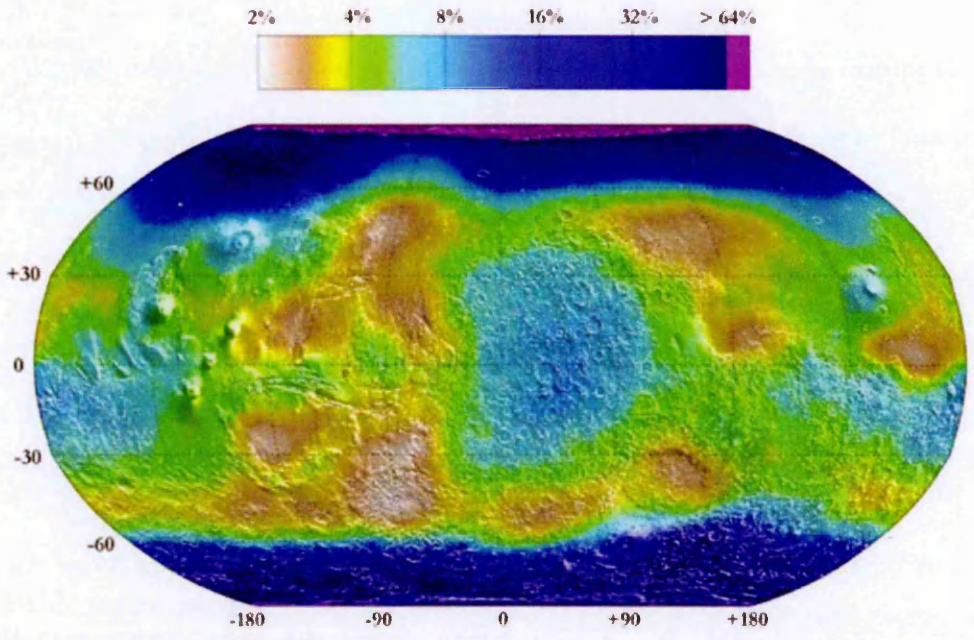

Figure 6.1: Water equivalent hydrogen in the subsurface of Mars, derived from epithermal neutron counting rates. From Feldman, (2004).

It can be seen that the greatest concentrations of water equivalent hydrogen are at high northern latitudes, and that regions of the Northern Plains north of 60 degrees N have the best chance of stable ground ice. However there is considerable regional variation in the rate at which WEH drops off with latitude, and so it is possible that icy terrains occur further to the south as well.

The geological mapping of Tanaka et al., (2005) also proved useful in characterising the terrain types on which features occurred. The maps of the study areas presented in this chapter include Tanaka et al.'s geological map of the Northern Plains. The most prevalent terrain type is the Vastitas Borealis interior unit, which covers large parts of the Northern Plains.

6.2 Aims

The main aim of these surveys was to determine how common possible periglacial features are on the Northern Plains of Mars and to constrain their distribution. The aim was to build on the work of the studies summarised in the preceding section, expanding upon their geographic extents and comparing and contrasting examples from other parts of the planet to the published literature. It is important to consider their distribution in both latitude and longitude so that the prevalence of different types of feature can be compared and contrasted between the different basins that comprise the Northern Plains. Different environmental conditions would be expected at different latitudes; consequently, any trends in latitudinal distribution could be important in constraining formation mechanisms.

The overarching objective of this work remains to test the hypothesis that some martian landforms are periglacial in nature. Chapter Two presents possible martian analogues for each of the key periglacial features it describes, but these analogues are far from certain.

Since thawing would probably be unusual under martian conditions, strong evidence is needed to make the case that these features are its result. Constraining the conditions in which martian features form is a good place to start when testing this hypothesis and this requires a clear picture of their regional distribution. The frequency with which possible periglacial features occur is also important. The presence of landforms which are few and far between carries less weight than those which are ubiquitous and appear in numerous images widely dispersed across the study area.

These surveys were a key component of the wider PhD project as they provided the large scale datasets from which case studies for further analysis were drawn. For example, the areas of sorted patterned ground discussed in Chapter Five were discovered as part of the work outlined in this section.

6.3 Choosing the images.

Various instruments are currently, or have recently been, in operation around Mars, producing a wealth of image data. Each dataset has a different amount of coverage at a different resolution, so deciding which dataset to use for a survey such as this limits not only the area which the survey can cover but also the types of features which are likely to be observed.

Given the small size of most periglacial features (metres to decametres) and the fact that diagnostic features such as clastic patterns are frequently sub-metre in size, it was clear that the majority of the features would only be visible in the highest resolution images. Consequently, it was decided that the surveys should focus on High Resolution Imaging Science Experiment (HiRISE) images from the Mars Reconnaissance Orbiter. Medium-resolution Context Camera (CTX) data could then be used for specific surveys of larger features. As described in Chapter Five, the HiRISE camera provides the highest resolution images of the martian surface, with a resolution of

approximately 25-50 cm per pixel. Larger features, such as scalloped depressions, gullies and large scale fracture polygons, are also visible in the approximately 6m per pixel CTX images.

6.3.1 HiRISE Survey

While the CTX dataset now covers a large proportion of the planet, HiRISE images remain widely spaced with significantly lower overall coverage, 1.6% of the martian surface has so far been imaged by the HiRISE camera. This is not a major disadvantage for a survey of this sort, as the intention is not to map out a coherent area in detail, but rather to produce a catalogue of the features which are found across a given region and to determine their spatial patterns. Enough HiRISE images are available to provide a sufficient spread over the northern plains, each presenting a snapshot of a few tens of square kilometres. Far more HiRISE images are available than could practically have been examined during the course of this project, since surveying even a relatively small area at such high resolution is very time consuming.

It was decided that the available images should be selectively, rather than randomly, sampled so as to focus on the environments that previous studies (e.g. Gallagher et al., 2011) had indicated could be suitable for a periglacial environment. The majority of the northern plains consist of fairly flat, low lying ground with the main source of relief being infrequent impact craters. HiRISE images covering medium to large impact craters typically provide the greatest variety of northern plains terrains. For this reason, it was decided that the focus the survey should be on HiRISE images that covered 2-10 km diameter impact craters in the Northern Plains. Such images usually cover at least some of the crater interior and in some cases also the central peak. Such a peak and the inner and outer crater walls would be expected to provide a good environment for the formation of hill-slope features such as gullies, sorted stripes and solifluction lobes

amidst the otherwise low relief of the northern plains. The edges of such images are generally dominated by the flatter northern plains terrain, which should be representative of the inter-crater area. The crater's ejecta blanket provides a final category of terrain within these images.

6.3.2 CTX Survey

In addition to this sample of HiRISE images, it was decided that one region should also be surveyed using CTX, so that the areas between large craters could be covered, albeit at lower resolution. This survey would ensure that the area around those craters chosen for the HiRISE survey was representative of the surrounding plains, as well as providing a "high coverage/medium resolution" counter point to the "low coverage/high resolution" HiRISE survey. The use of CTX images also made it possible to examine continuous variations in the distribution of those landforms which were discernible in the lower resolution data, such as scalloped depressions and large scale fracture polygons.

The sampling of HiRISE images in the CTX survey region was expanded to include all images, not just those that covered large craters. The decision to extend the survey in this manner was made because many potentially periglacial features were found to be present on the plains surrounding the craters chosen for the initial HiRISE survey, not just within the craters themselves. In an ideal situation a Context survey of this sort would have been conducted for the entire area surveyed in HiRISE, but expanding the entire survey to examine the inter-crater regions using CTX would have been prohibitively time consuming. The time taken to survey a continuous swath of CTX images is far greater than that required for a full examination of isolated HiRISE images.

6.3.3 Constraining the study area

The Northern plains of Mars comprise a series of vast basins which cover much of the northern hemisphere. Their southern extent is bordered by the planetary dichotomy boundary which constrains a roughly triangular region consisting of three large plains, Acidalia, Utopia and Arcadia Planitiae. The northern extents of these plains merge into the Vastitas Borealis, the regions around the northern polar ice cap. Figure 6.2 shows a map of the northern plains in a polar stereographic projection. This will be used for the majority of maps intended to show the entire survey area. Clockwise from the top of the map are the Arcadia, Utopia and Acidalia basins.

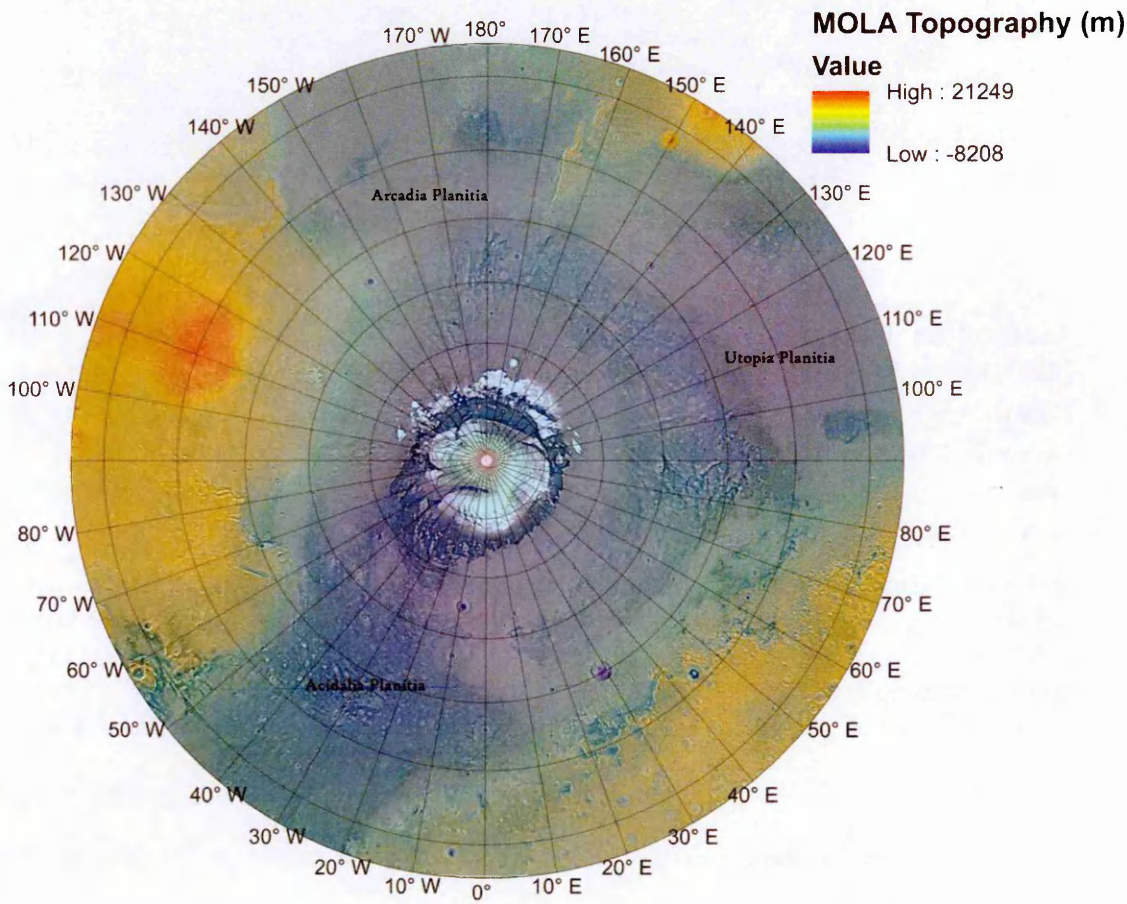

Figure 6.2: Topography of the Northern Plains of Mars.

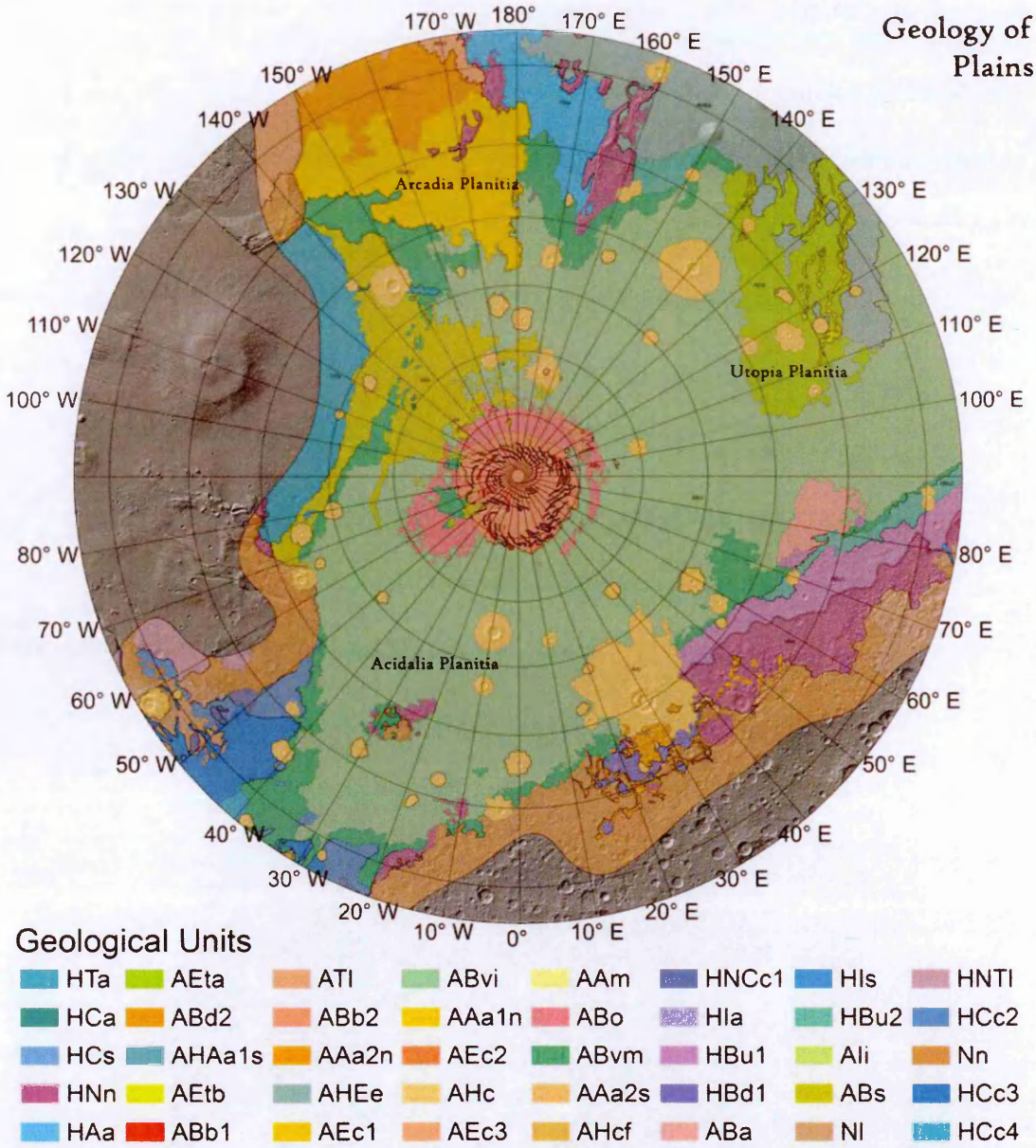

Figure 6.3: Geology of the Northern plains of Mars (Tanaka et al., 2005). The majority of the study areas are located within the pale green Vastitas Borealis Interior Unit (ABvi), interrupted by the pale gold units surrounding large impact craters (AHc). Arcadia Planitia is the exception, since it is instead dominated by the Arcadia Planitia Unit (HAa). Other geological units are defined in the text where they become relevant.

HiRISE coverage in these regions is generally very good. A total of 10,531 Images cover 2.9% of the Northern Plains north of 30°N. There is a good spread of images over most of the different geological units and terrain types. Medium to large impact craters are frequent targets for HiRISE so many have coverage and most of the largest craters such as Lomonosov and Lyot craters have multiple HiRISE images within their extent.

To begin with, the northern hemisphere of Mars was divided into 10° by 10° squares and a Geographic Information System (GIS) with Mars Crater Consortium (e.g. Barlow et al., 1990) data was used to locate craters with diameters of one km or more. All the HiRISE images that intersected these craters were identified. Even by limiting the main survey to those images that overlapped medium-sized impact craters there remained several thousand images available for study. It would have been impossible to survey all of these images within a reasonable time frame.

Consequently, it was decided to define three study areas in each of the large basins of Acidalia, Utopia and Arcadia Planitiae so that comparisons between the three could be made. The qualifying HiRISE images for these regions were downloaded and put into a series of GIS to conduct the surveys. Since the project spanned the duration of the Ph.D. studies these datasets were occasionally expanded to include newly released images which met the selection criteria.

Each of the study areas spans a 50° latitude swath of the mid to high latitudes between 30° and 80° north. In many areas, this meant that the southern extent included or was just to the north of the planetary dichotomy boundary and the edge of the southern highlands. The line of 30° latitude was selected as the southern boundary as this is the southern limit at which stable ground ice is likely to be present (Boynton et al., 2010; Feldman et al., 2004). The northern extent of each study area falls just short of the edge of the polar cap in most places, sometimes including the edge of the circumpolar dune fields which cover the northern part of the Vastitas Borealis. Consequently, the full range of latitudes typically covered by the northern plains was represented within the survey, except for those areas where the planetary dichotomy extended further to the south such as in Utopia Planitia.

The longitudinal constraints of the survey areas were more arbitrarily defined. The Utopia and Arcadia study areas consisted of 60° wide regions selected to be roughly central to the basins, while the Acidalia survey area consisted of a 50° wide block on the eastern rim of the basin. The easternmost 20 degrees of this was selected for the Context Survey since it had very good CTX coverage and contained the area of widespread patterned ground around Lomonosov Crater detailed in Chapter Five. The area between 60° and 130° west is dominated by the Tharsis region. This area has dramatically different terrain to the lower lying Northern Plains; Consequently, no survey was conducted in the narrow band of Vastitas Borealis formation to the north of Olympus Mons. In total 672 CTX images and 468 HiRISE images were selected to be surveyed as shown in Figure 6.4. The HiRISE images cover an area of 69845.2 km^2 or 21.9% of the total area imaged by HiRISE in these regions.

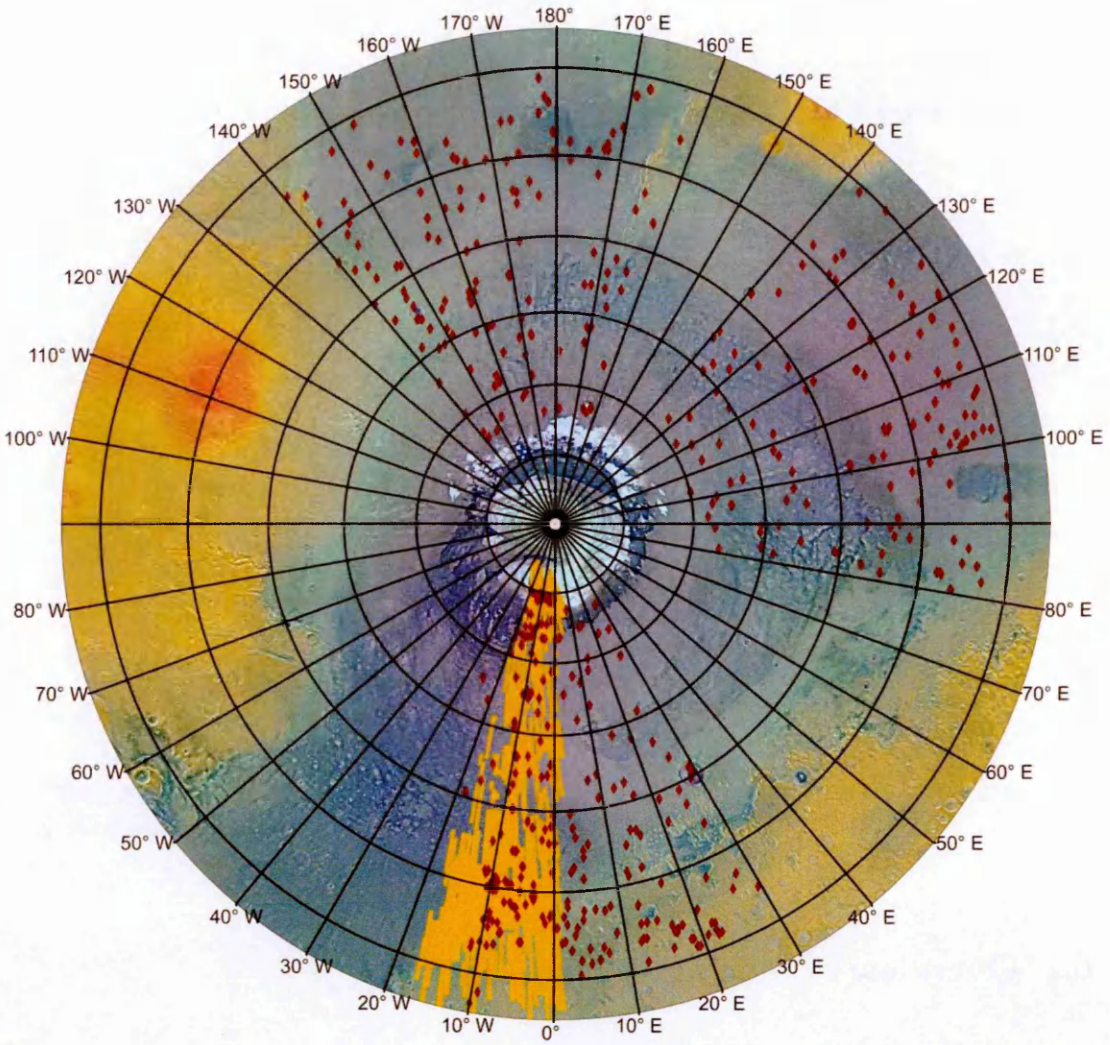

Figure 6.4: The locations of the images used within this survey. Red diamonds indicate HiRISE images, while the gold area is that covered by CTX images. Clockwise from the top the three clusters of images are the Arcadia, Utopia, and Acidalia study areas.

Table 6.1: Area covered by the HiRISE Survey broken down by study area and latitude band.

Area Surveyed km^2	Acidalia	Utopia	Arcadia	Northern Plains >30°N
Total	31548.68	20186.1	18110.4	69845.2
30-40 °N	12186.2	8219.16	5188.19	25593.55
40-50 °N	6557.02	4940.64	3647.79	15145.45
50-60 °N	3159.49	3071.29	4100.88	10331.66
60-70 °N	2779.59	3955	2808.86	9543.45
70-80 °N	6866.38		2364.71	9231.09
% of HiRISE Coverage				
Total	26.75	22.44	16.36	21.92
30-40 °N	31.54	25.45	16.07	24.80
40-50 °N	18.19	16.35	14.60	16.60
50-60 °N	31.02	19.00	19.36	21.74
60-70 °N	48.04	35.07	27.92	35.18
70-80 °N	25.18	0.00	10.65	18.66

6.4 Overview of Study Areas

6.4.1 Eastern Acidalia Planitia

This study area covers a large region of the northern plains between 20° west and 30° east, and 30° and 80° north. It covers a broad swath of Acidalia Planitia, with the southernmost part of the study area located amidst the fretted terrain around the planetary dichotomy in Cydonia and Deuteronilus Mensae. The northern edge extends into the Vastitas Borealis and onto the north polar cap itself.

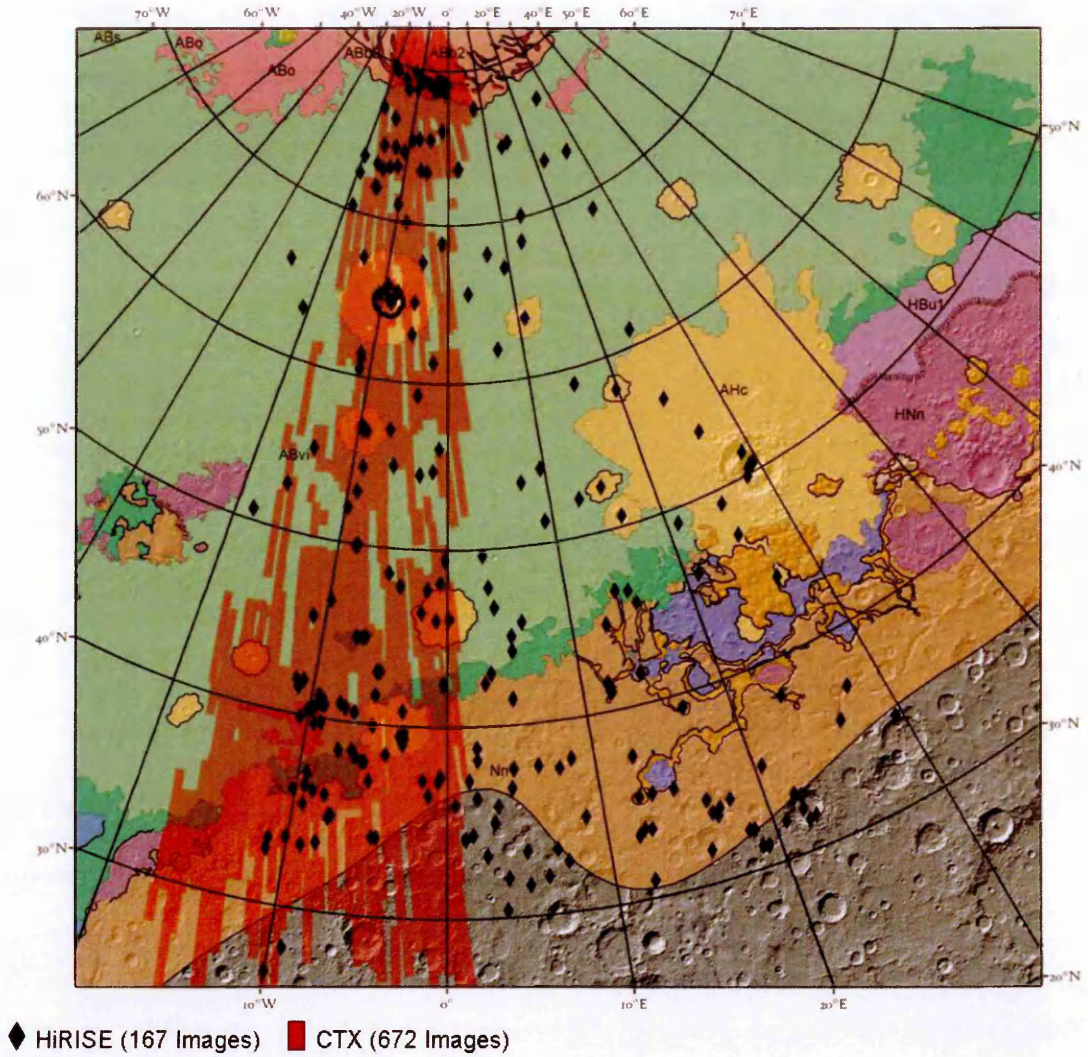

Figure 6.5: Map of the Acidalia Planitia study area showing the distribution of the images used in the surveys of this region. The location of Lomonosov Crater, an important study area, is marked by a dark oval.

The southern part of this study area is dominated by the northern edge of the southern highlands, which occupy much of the 30-40°N latitude band in the west of the study area around Cydonia Mensae and extend into the 40-50°N band in the east in the area of Deuteronilus Mensae. The high latitudes have two large impact craters Lomonosov crater and Kunowsky crater, while the eastern edge of the study area passes through the Lyot impact basin. Other large craters include Davies, Lagarto, Arandas and Bamberg craters, most of which have significantly large ejecta fields to be noted on the geological map.

The majority of the northeast of the survey area consists of the Vastitas Borealis Interior Unit (ABvi) which appears as the light green area on the geological map. The region south of the dichotomy boundary predominantly consists of the Noachis Terra Unit (Nm). The two are separated by a thin band of the Vastitas Borealis marginal unit (ABvm) and Deuteronilus Mensae Units (HBd_1 and ABd_2).

In addition to the dramatic differences between the northern plains and the southern highlands the transitional regions along the dichotomy boundary form an environment that is distinct from both. The area between 30-50° N comprises fretted terrain where numerous flat mesas dominate the landscape, and the canyons between them are frequently filled with lineated valley fill (Sharp, 1973; Squyres, 1978). This is in sharp contrast to the northern part of the study area which largely features smooth northern plains interspersed with patches of fracture polygons and areas where the icy mantle has been degraded to form scalloped depressions. In the north the main topographic features are large impact craters, although smaller hills do occur.

An important factor to consider in analysing the distribution of possible periglacial features is the likelihood that ground ice is present to a significant degree. Consequently, the Water Equivalent Hydrogen (WEH) measurements of Feldman et al., (2004) was also plotted for each study area.

Areas with water equivalent hydrogen abundance of 0.1 or higher are generally found north of 65 °N. WEH abundances in excess of 0.2 are typically found north of 65°N in this region, but occur further north in the western part of the study area. Lomonosov Crater has a slightly lower WEH than expected, and the 0.2 threshold is at around 70°N, to the north of the crater's ejecta.

167 HiRISE images, covering 31,549 km^2 within this region, were examined as part of the main survey. These consisted of all of the images overlapping medium to large

diameter impact craters in the region east of the prime meridian and all of the HiRISE images in the western part of the study area (as of summer 2013). The region west of the meridian was chosen for the context survey and an additional 672 CTX images were surveyed in this area. CTX images cover the majority of this area, although there are several large gaps in the available data, particularly between 50° and 60° north. There is an uninterrupted band of CTX images running from the northern extreme of the survey area to the southern edge of Acidalia Planitia between 350-352°E, Consequently, this was the focus of the context survey with the study area being expanded to the east and west where images were available. Ultimately, sufficient images were examined to produce a good spread of data across the 20° - 50° area despite the gaps in the coverage. It is estimated that approximately 84% of the total area was surveyed.

6.4.2 Central Utopia Planitia

This study area consists of the area between 30-70°N and 80-140°E in the central region of the Utopia basin. This area was chosen as it covers a region where numerous previous studies have proposed periglacial landscapes (e.g. Osinski and Soare, 2007; Séjourné et al., 2012; Soare et al., 2005, 2007, 2012).

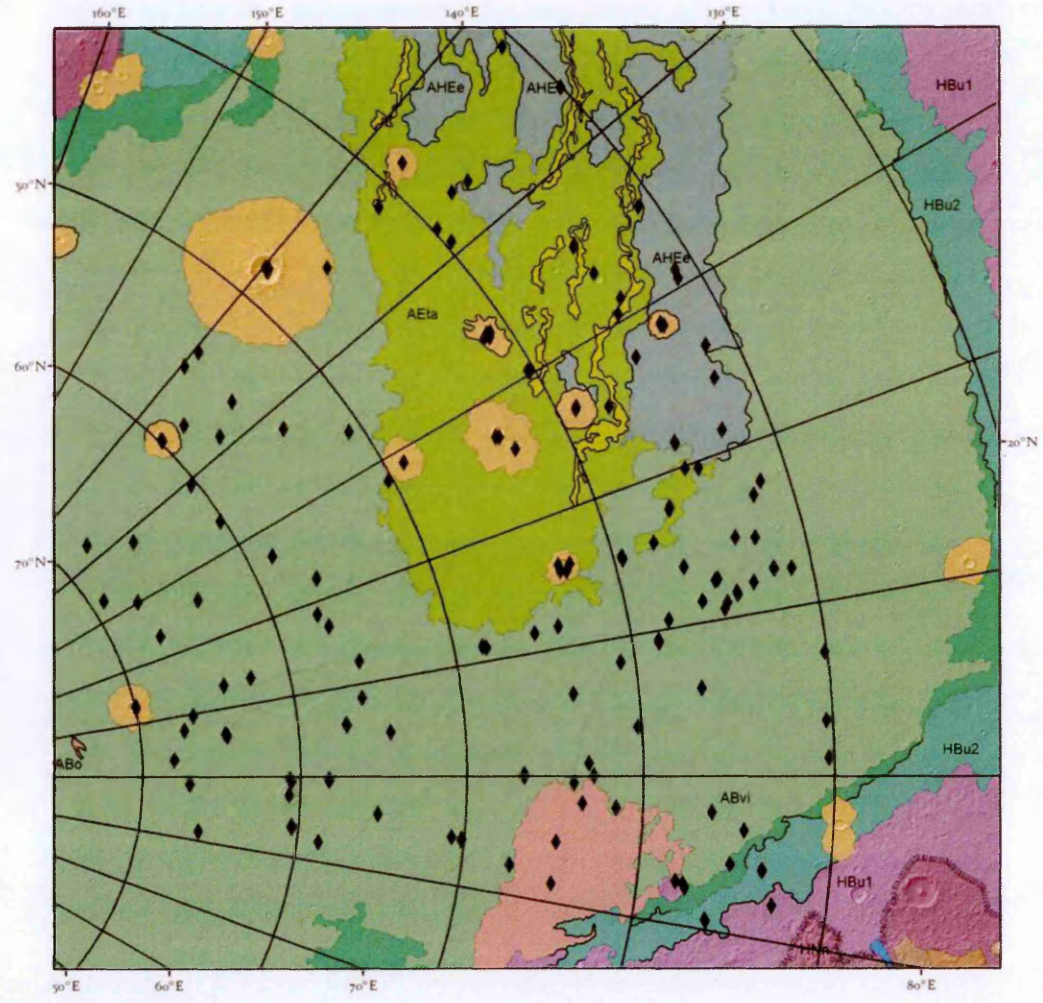

Figure 6.6: Map of the Utopia Planitia study area showing the distribution of the images used in the survey of this region (north is to the bottom left).

The main geological unit present within the Utopia Planitia study area is again the Vastitas Borealis Interior Unit (ABvi), which covers most of the area north of 50°N. This is mainly broken by impact crater units such as Louth Crater in the northern part of the study area, Nier, Vivero and Cebrenia Craters in the southern part of the study area, and Mie Crater, the largest such feature, which is on the easternmost edge of the study area.

The southern part of the study area exhibits more variety. The eastern part is dominated by the Tinjar Valles 'a' Unit (AEta). This area has a slightly lower degree of coverage than most of the rest of Utopia Planitia, as fewer sites meeting the

requirements of HiRISE images of medium-sized impact craters were found on this unit. The Astapus Colles unit (ABa) occupies the western edge of the study area and areas of Elysium Rise Unit (AHEe) encroach on the south eastern edge. This region lacks the fretted terrain which is common in the southern part of the Acidalia study area. Utopia Planitia extends further to the south and so the planetary dichotomy is beyond the southern edge of the study area, which falls near the Adamas Labyrinthus region. Nevertheless, there are few, if any, reports of periglacial terrain in these southernmost regions, so the choice of the southern boundary of the study area was still felt to be appropriate.

As shown in figure 6.1 the regions with water-equivalent hydrogen of above 0.2 are limited to the northernmost parts of this study area. This is generally the area north of 65-70°N. However WEH of 0.1 or greater is generally found north of 60°N across a large part of the study area. It is found as far south as 55°N at the easternmost edge. The south-western region has the lowest WEH while values in the east remain somewhat higher, above 0.05 even as far south as the edge of the study area at 30 degrees

Utopia Planitia has been a focus of martian periglacial research for some time, so it was important to include it in this study. Utopia is believed to have a high concentration of putative periglacial landforms. Therefore comparing results from this area with those from the Acidalia and Arcadia surveys should indicate how common such features are across the martian plains. This will help to determine whether Utopia is a unique case or whether it is representative of the rest of the region, but has simply received more attention than other areas due to the numerous studies that have been conducted there. In total 126 HiRISE images were examined in this study area covering 20,186 km^2 This

survey does not extend to 80° north as the others do due to a lack of HiRISE images in this area that met the criteria for the survey.

6.4.3 Central Arcadia Planitia

This study area consists of a similar area to the Utopia survey covering the region between 30-80 ° N and 160-220°E. Again, all HiRISE images overlapping medium to large impact craters were surveyed.

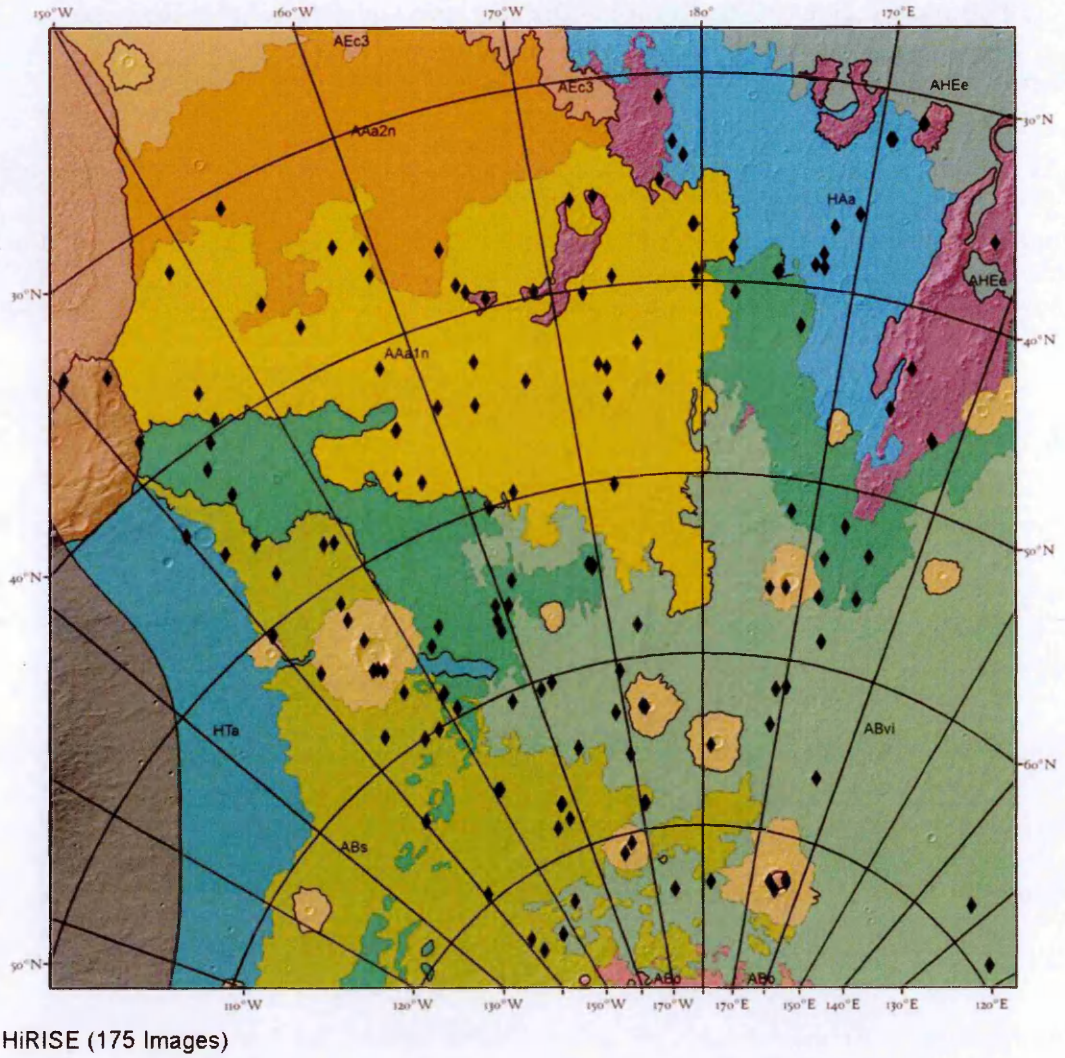

Figure 6.7: Map of the Arcadia Planitia study area showing the distribution of the images used in the survey of this region.

The Vastitas Borealis Interior Unit (ABvi), which was prevalent across the other two study areas, is much scarcer in the Arcadia Planitia study area. It can be found across

some of the north western corner, frequently interrupted by the ejecta of large impact craters, and separated from other terrains by large bands of the Vastitas Borealis Marginal Unit (ABvm).

The centre of the study area is occupied by the Amazonis Planitia North Units (AAa_{1n} and AAa_{2n}) and the Arcadia Planitia Unit (HAa). There are also some patches of Nepenthes Mensae Unit (HNn). The north-east corner of the study area is occupied by the Scandia Region Unit (Abs). This makes Arcadia the most geologically variable of the three study areas examined during this survey. There are several large impact craters, mostly in the northern reaches of the study area. These include the Stokes and Korolev Craters in the west and Milankovic crater in the east. The Erebus and Phlegra Montes can be found in the southern part of this region.

Water-equivalent hydrogen abundances in excess of 0.2 are generally found north of 65°N but extend further to the south, as far as 57°N at the eastern edge of the study area (see figure 6.1). Likewise the boundary of 0.1 WEH varies from as high as 55°N at the western edge of the study area to 47°N at the eastern edge. The regions with lowest WEH are in the south western corner of the study area.

In general most of these geological units have equivalent HiRISE coverage. Most of the large impact craters are included and numerous images are found on each of these terrains. A total of 175 HiRISE images were surveyed in this region covering an area of 18,110 km^2.

6.4.4 Distribution of Images

In general HiRISE images are well spread out over these study areas. There are some large gaps where no HiRISE coverage is present, and some of the 10° by 10° grid squares did not contain any qualifying images, particularly in the northern 10 degrees of the

Utopia Planitia study area. In some cases there is a slight bias to one part of the survey area. For example the southern part of the Acidalia Planitia survey area overlaps the edge of the planetary dichotomy boundary. This part of the study area is located at the edge of the heavily cratered highlands while the northern extent is on the younger northern plains. Consequently, far more craters can be found in the southern region than in the northern part of the survey.

Additionally, the area covered by the surveys is far greater at lower latitudes than at high latitudes, since the survey areas were not defined to have an equal area at all latitudes. There are typically more images in the southern regions but they are more spread out. These variations in the distribution of the source images must be considered when patterns are observed in the resulting data. However it is believed that there is a sufficient spread of images and sufficient representation of all latitudes and terrain types within the survey to produce a representative catalogue of the Northern Plains.

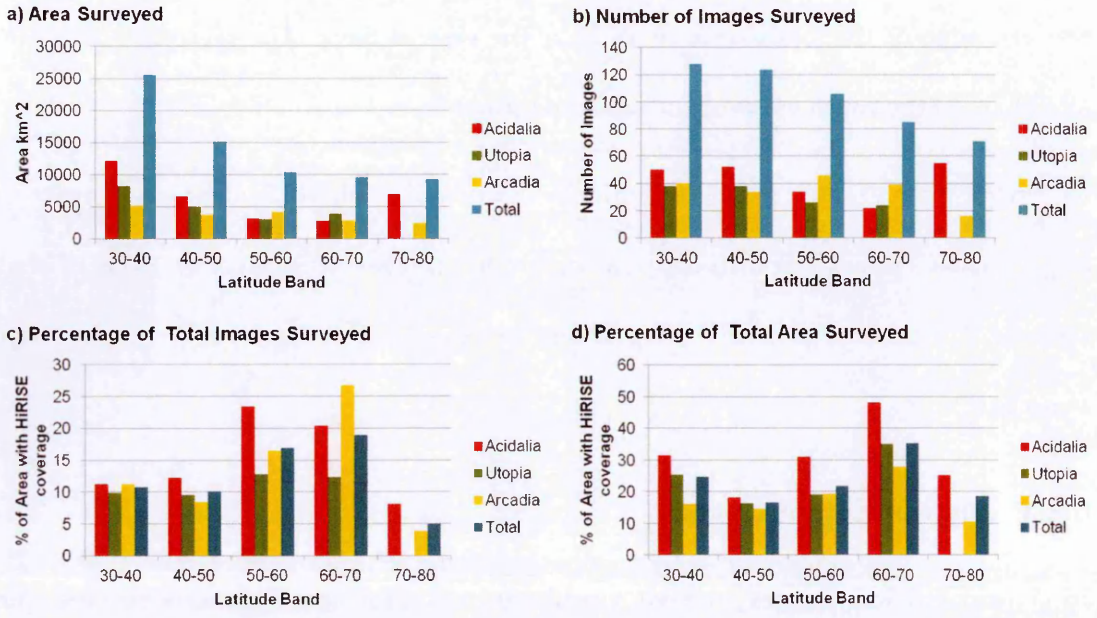

Figure 6.8: The total area surveyed in the HiRISE Survey by latitude; a) number of HiRISE images examined, b) total area covered by those images, c) percentage of the available HiRISE images that were included in the survey and d) the proportion of the total area with HiRISE coverage to have been surveyed.

6.5 Survey Procedure

Once the catalogue of HiRISE and CTX images had been defined they were surveyed. The survey procedure for both HiRISE and CTX surveys, outlined below, was applied consistently across all study areas and was mostly consistent between the HiRISE and CTX surveys. The main differences in approach were due to the different scale of the images and consequently, the variety of features which could be detected. All of these surveys were conducted manually. Automated detection or pattern recognition systems were considered to be too potentially unreliable. While such a system might have been useful in detecting obvious features such as extensive fracture networks, there was concern that more subtle features such as sorted patterned ground might be harder to detect. Developing such a system would be an interesting exercise, but would have entailed a project in and of itself and so was beyond the scope of this investigation (this will be discussed in more detail in the section on future work in Chapter Eleven).

6.5.1 HiRISE Survey

Each HiRISE image was systematically examined on-screen in the GIS, typically at a map scale of 1:10,000 to begin with ('native' HiRISE resolution being approximately 1:1000). This allowed large features to be easily examined. Areas containing possible smaller scale features such as sorted polygons or solifluction features were then examined at or near the full resolution, so that more detailed analysis could be conducted. The slopes in and around the large craters were the main focus of the initial surveys but it quickly became apparent that putative periglacial features could occur in any part of an image. Thus a method for searching images at full resolution was developed in which examination started in one corner of the image and systematically worked across and down from one end to the other.

Whenever features with morphological similarity to periglacial features were found, their positions were marked using GIS shape files, and various parameters relating to the feature's classification were entered into the database. The variety of features likely to be found had been assessed during the course of a small pilot study and a classification scheme for each landform type was developed.

The landform types recorded in the survey are:

- Clastic patterned ground
- Fracture polygons
- Lobate hill slope structures
- Scalloped depressions
- Pitted ground
- Gullies

Type examples for these features are presented in Figures 6.9 through 6.14

Figure 6.9: Fracture Polygons Type example.

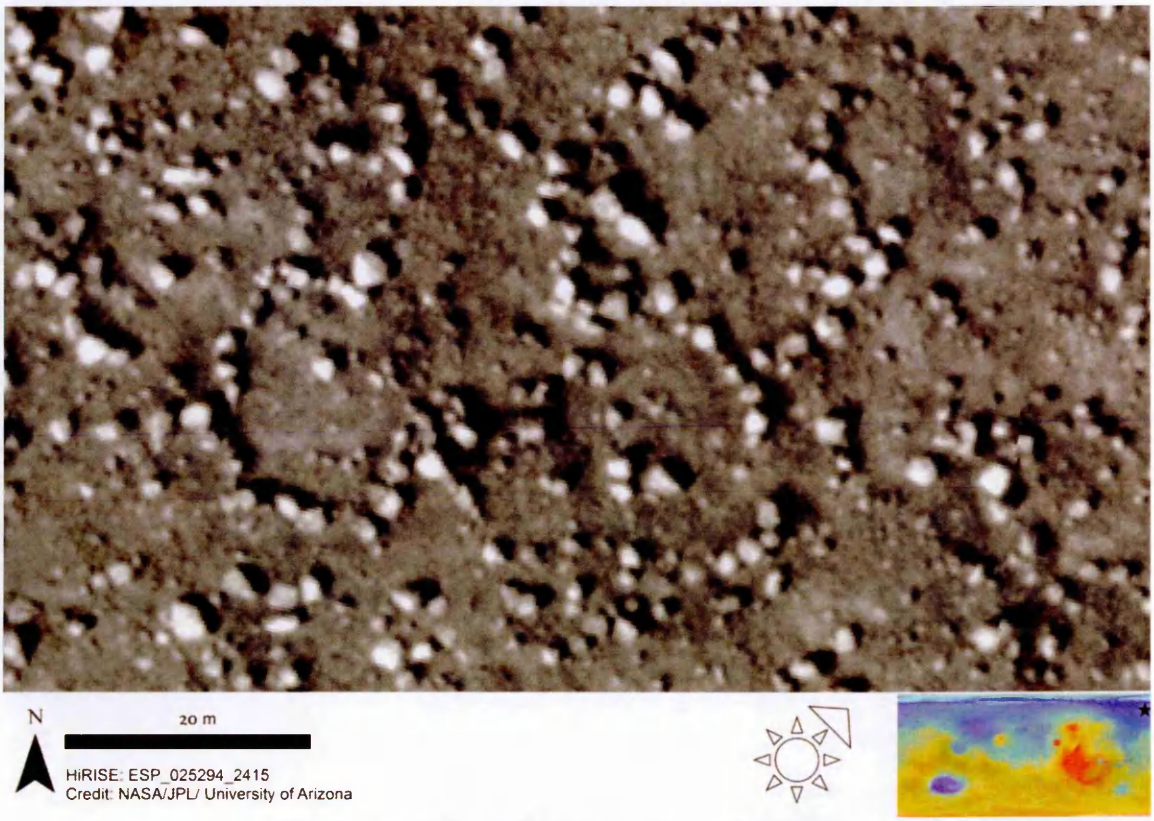

Figure 6.10: Clastic Polygons Type Example

Figure 6.11: Lobate Hill-slope Features Type example.

Figure 6.12: Scalloped Depression Type Example.

Figure 6.13: Pitted Ground Type Example.

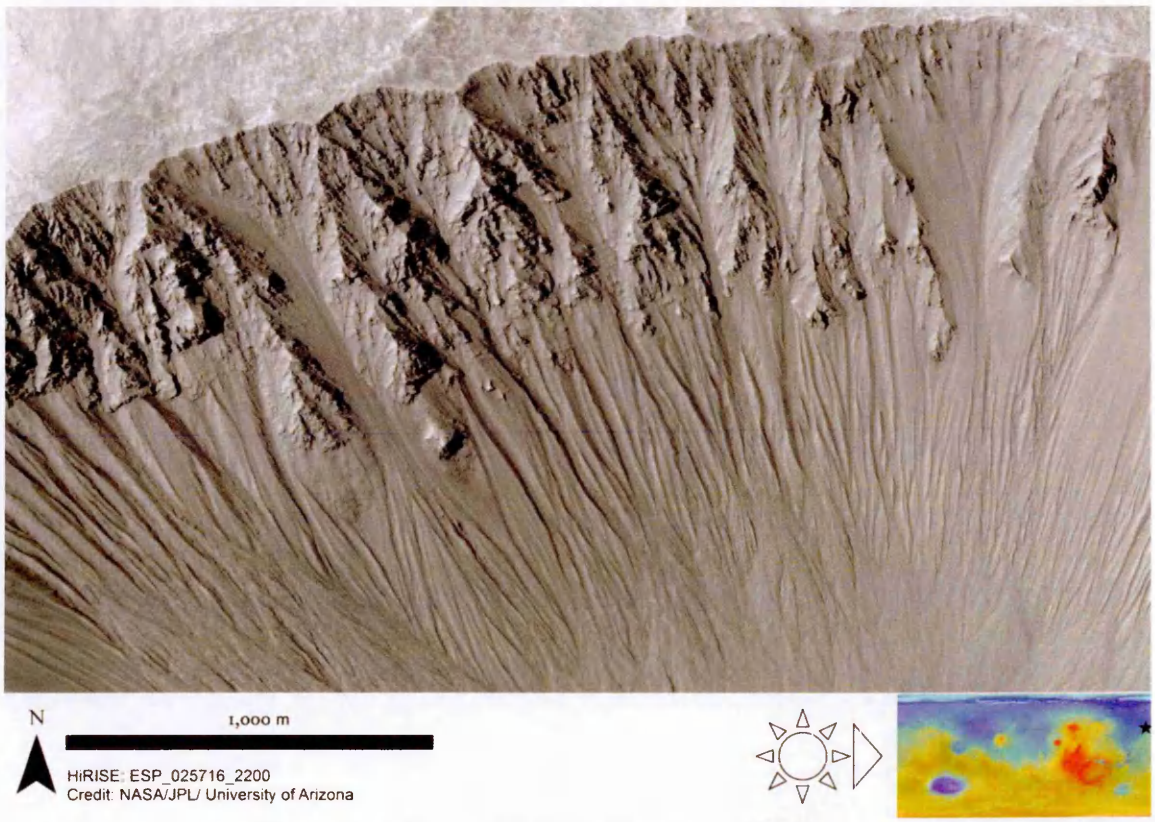

Figure 6.14: Crater Wall Gullies Type Example.

Further classification parameters varied from one landform type to another. For example in the case of fracture patterns it was pertinent to assess whether the polygons were large (~ 100m across) or small (5-20m across), part of a regular pattern, or appearing as isolated features, whether they had a rectilinear or random orthogonal polygonal pattern, and whether they were high or low centred.

In the case of sorted patterned ground, potential features were subdivided into polygonal nets, possible sorted stripes, and rubble piles. Also, the degree to which sorting was present was assessed using the five point scale described in Chapter Five. It was decided to assign a similar grading to other possible periglacial landforms such as lobate structures and scalloped depressions to record the degree to which they resembled the type examples for these features.

In each case a semi quantitative ranking was carried out using five point scale from indicating how representative the feature was for its class. Grade one features were the least representative, while grade five were the most. This methodology was applied to all landforms, although in each case the attributes being assessed were different. The definition of these parameters will be discussed where they are relevant to the classification of these landforms in Chapter Seven. In general they consisted of assessing features such as the scalloped edges of a depression, or the lobate appearance of hill-slope features and assessing the extent to which these features were present in a given example.

Some of these features, such as thermal contraction crack polygons and martian gullies, are not strictly speaking periglacial landforms. However, they are useful to consider as they are landforms which are often found in proximity to periglacial features in terrestrial analogue environments (Hauber et al., 2011). For example, gullies are found in proximity to sorted patterned ground in the Tindastóll study area described in

Chapter Four. The presence of fracture polygons at a site suggests that there is a large amount of ground ice present within the soil, and that it is undergoing (or has recently undergone) thermal cycling, and probably that it is also being degraded through sublimation processes (e.g. Levy et al., 2010).

Other features, such as scalloped depressions and lobate structures, have direct periglacial analogues. However it remains uncertain whether many of these features are periglacial in nature or whether they are more likely to have developed through alternative processes (possibly ice-related, but without thaw). The analysis in Chapter Seven will be used to assess the evidence that these features could have formed as a result of the thawing of ground ice.

6.5.2 Context Survey

The aim of the context survey was primarily to examine the distribution of scalloped depressions and other large scale features such as ~ 100m-scale fracture patterns and gullies. The main survey followed the same procedure as the HiRISE survey, images were examined on a case by case basis and the locations of possible periglacial features were recorded using GIS shape files. Areas where periglacial assemblages occurred, such as the region of extensive patterned ground around Lomonosov Crater, were then examined in more detail using all available CTX and HiRISE images. The original intention was to find regions where gullies and scalloped depressions occurred in close proximity in the CTX data. These could then be examined at HiRISE scale to see whether smaller features such as sorted patterned ground and lobate structures are also found.

In this way the search for possible periglacial assemblages can be focused on areas known to contain some putative periglacial landforms. However, the two most prominent scallop and gully assemblages (detailed in Chapter Ten) both lacked

HiRISE coverage. This methodology proved more successful in the area around Lomonosov Crater, where the boulder patches detected in the CTX data frequently overlapped with HiRISE images.

Another aim of this study was to produce a dataset which can be compared with the distributions of scalloped depressions mapped in Utopia Planitia by Séjourné et al., (2011). Comparing these two regions would allow an assessment of whether scalloped depressions are as numerous outside Utopia Planitia as they are in that area. It would additionally help to determine whether Utopia Planitia is an unusual region of the northern plains, in terms of periglacial and/or ground-ice processes, or just the best studied region to date.

The features examined in this survey include:

- Boulder Patches
- Fracture Networks
- Scalloped depressions
- Pitted ground
- Gullies

Some features that were the focus of the HiRISE survey are excluded. These include sorted patterned ground and lobate structures which are too small to be resolved in CTX images. Boulder patches are included, since many examples of sorted patterned ground occurred within these areas.

6.6 Overview of Following Chapters

The second half of the thesis describes the results of this survey and use the data collected to assess the evidence for a martian periglacial environment.

Chapter Seven focuses on the results of the surveys. The distribution of clastic patterned ground, lobate structures, scalloped depressions, gullies and fracture patterns are all described, and the locations where multiple features occur in close proximity are presented. These potential assemblages provide a strong line of evidence that the constituent features might have formed through related processes.

Chapter Eight compares and contrasts the results presented in Chapter Seven with a variety of parameters which might be expected to control their distribution, the data are plotted against the presence of water equivalent hydrogen to search for correlations, and their topographic and geologic setting is examined.

Chapter Nine then focuses on clastic patterned ground. Martian examples are compared to the terrestrial analogues detailed in chapter four. This section aims to test whether the morphologies of the martian and terrestrial landforms are quantifiably similar, which might indicate that they have formed through similar processes.

It then reviews several alternate hypotheses such as the boulder ratcheting process suggested by Orloff et al., (2011). If the morphology of these features can be shown to be controlled by the morphology of underlying fracture nets, then it would provide strong evidence that they were not formed through the same processes as sorted patterned ground.

Chapter Ten then focuses on scalloped depressions in more detail. It discusses two sites with extensive fields of scalloped depressions, around Davies and Lagarto Craters in Acidalia Planitia. These sites were mapped as part of the Context survey of this region

and are classified using a methodology based upon that of Séjourné et al., (2011) and Wallace (1948).

All of these analyses and case studies, along with the work described in Chapter Five build on the results described in chapter seven, but each examines a subset of the survey data in more detail using a different methodology.

7 Chapter Seven: The Distribution of Possible Periglacial Landforms on the Martian Northern Plains

7.1 Introduction

This chapter discusses the results of the surveys outlined in Chapter Six. Results are broken down by landform. All of the following landforms were examined as part of the HiRISE survey, but only Gullies, Scalloped depressions and fracture patterns were visible in the lower resolution images used for the context survey. Where applicable, context survey results are described directly after those from the HiRISE survey for ease of comparison.

In the following sections the distribution of each of the landforms catalogued in these surveys will be described and examples of such features presented. Finally section 7.7 describes locations where assemblages of possible periglacial landforms occur in close proximity. In Chapter Eight these results will be compared to various parameters which might control their distribution and are discussed within the context of other studies into the distribution of putative periglacial features on Mars.

7.2 Distribution of possible sorted patterned ground

As described in Chapter Five one of the most important strands of this survey was assessing whether organisation occurs in the arrangement of 0.5-2 m scale boulders as has been observed in previous, more regional studies (e.g. Balme et al., 2009; Gallagher et al., 2011; Johnsson et al., 2012). On Earth, sorted patterned ground is one of the most characteristic periglacial landforms. Consequently, the identification of similar features on Mars may provide some of the best candidates for periglacial landscapes.

A variety of sites with possible sorted patterns have been found across all three study areas. These features can be grouped into several different feature types such as stripes, polygons, rubble piles and sorted lobes. Clastic stripes and polygons are described in more detail in Chapter Five. All are described herein except for sorted lobes which are detailed in Section 7.3.

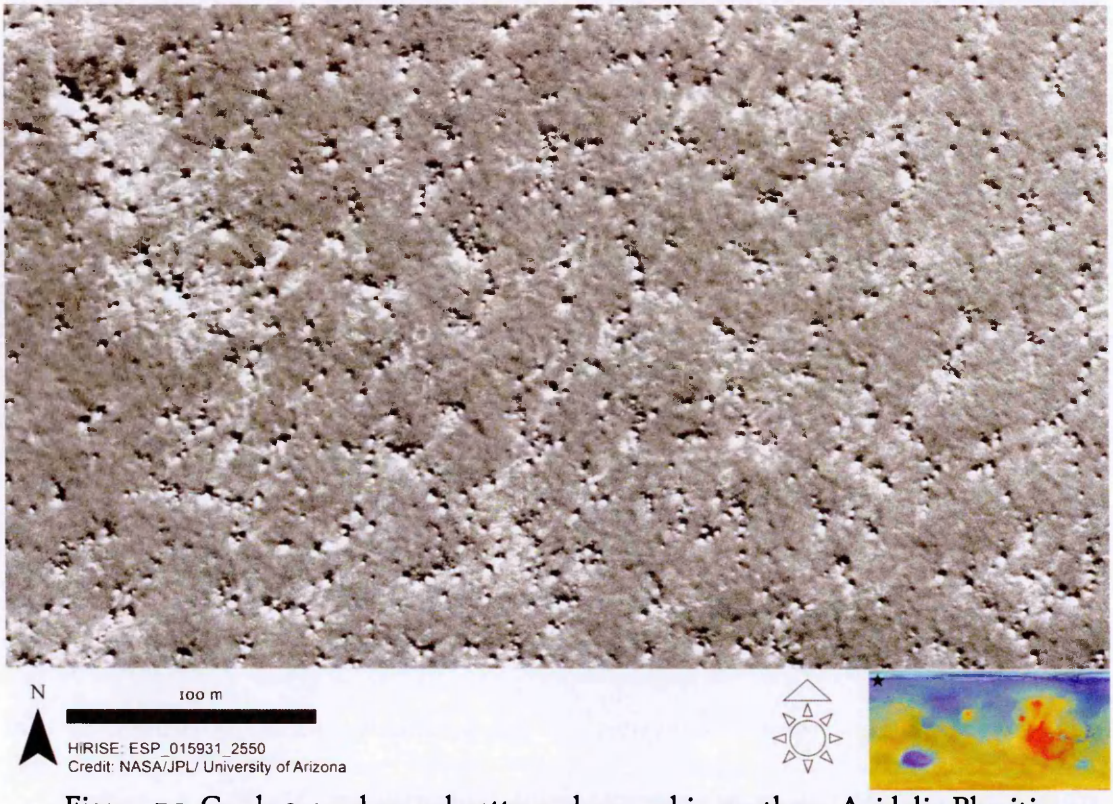

Figure 7.1: Grade 3-4 polygonal patterned ground in northern Acidalia Planitia

The most common variety of clastic patterned ground consists of apparently sorted polygons where clasts are arranged into a network of boulders surrounding patches of non boulder-strewn ground. These networks are frequently discontinuous, consisting of lines or arcs of clasts which appear to be aligned into a polygonal structure. Chapter Five details the classification system used to assess the degree to which a network of aligned clasts conforms to a polygonal pattern. *Average nearest neighbour analysis* is used to confirm that what appears to be a pattern on visual inspection is significantly different from a random arrangement.

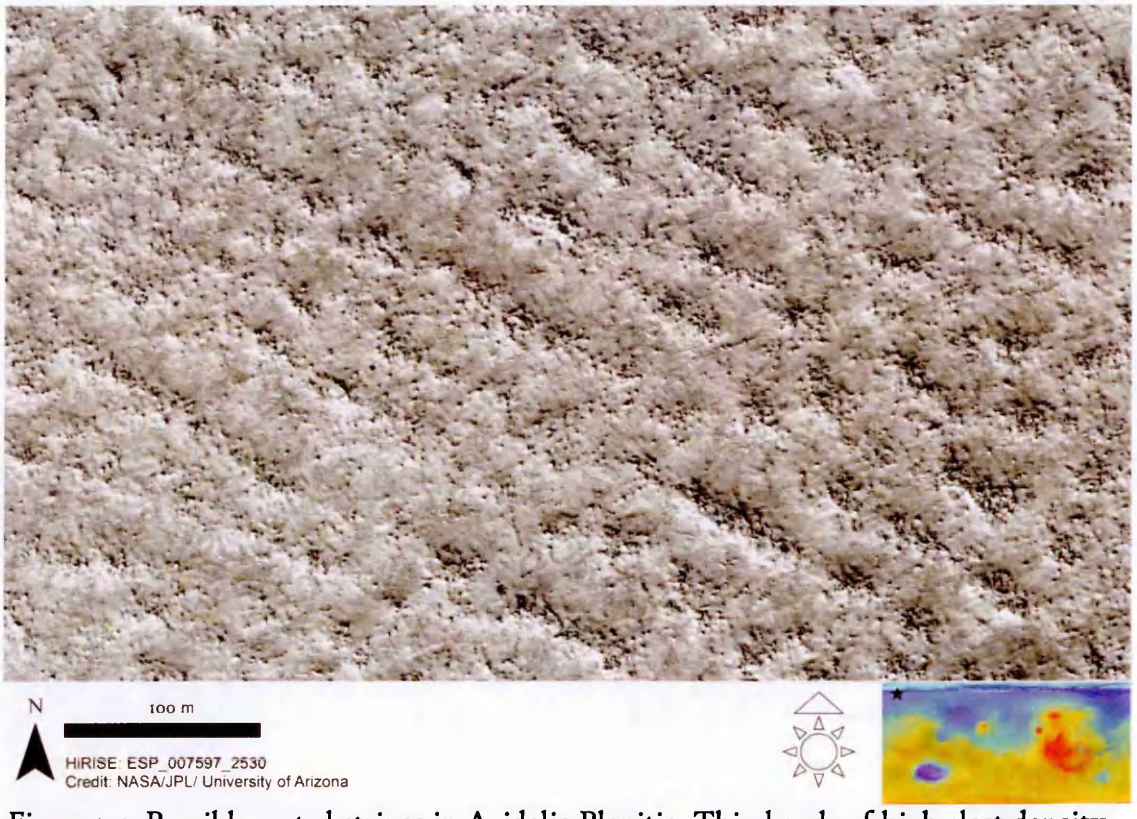

Figure 7.2: Possible sorted stripes in Acidalia Planitia. Thin bands of high clast density are separated by narrow regions with fewer clasts.

Sorted stripes occur where a series of parallel lines of clasts extend for a significant distance in one direction. There were far fewer examples of sorted stripes within the areas surveyed than sorted polygons. Additionally they were not concentrated in any one survey area unlike sorted polygons, which were predominantly found in the Acidalia Planitia study area. Sorted stripes would be expected to occur on hill slopes. Therefore it is probable that the generally flat morphology of the northern plains accounts for their low frequency of occurrence.

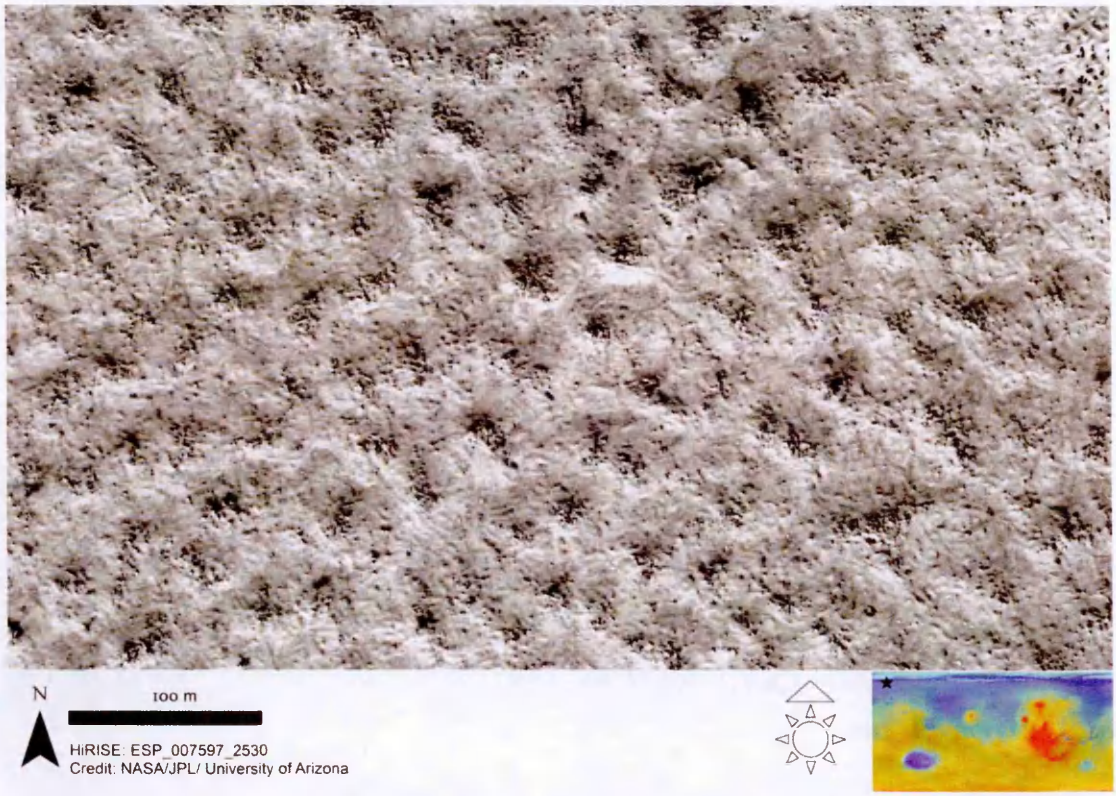

Figure 7.3: Example of Rubble piles on small hummocks which may be a heavily degraded fracture net. Distinct clusters of stones are separated by wide bands of less stony ground.

The final class of clastic features are rubble piles. These consist of small piles of clasts interspersed with large areas of relatively boulder free ground. Rubble piles are reasonably common at high northern latitudes but occur far less frequently further south.

Since only the largest clasts are above the resolution of a HiRISE image (usually 25-50 cm per pixel) evidence of sorting is often ambiguous. Many features exhibit lines of aligned boulders, sometimes converging or intersecting, but with too few clasts to form a coherent polygon. All possible examples were assessed using the same five point scale described in Chapter Five (see Figure 5.7) to determine which were most likely to be evidence of organisation. It has also been shown in Chapter Five that boulder patterns which appear organised upon visual inspection normally do have a non-random arrangement of clasts. The use of the *average nearest neighbour analysis* was restricted to

a small selection of sites, but lends confidence to the observations made in the wider survey.

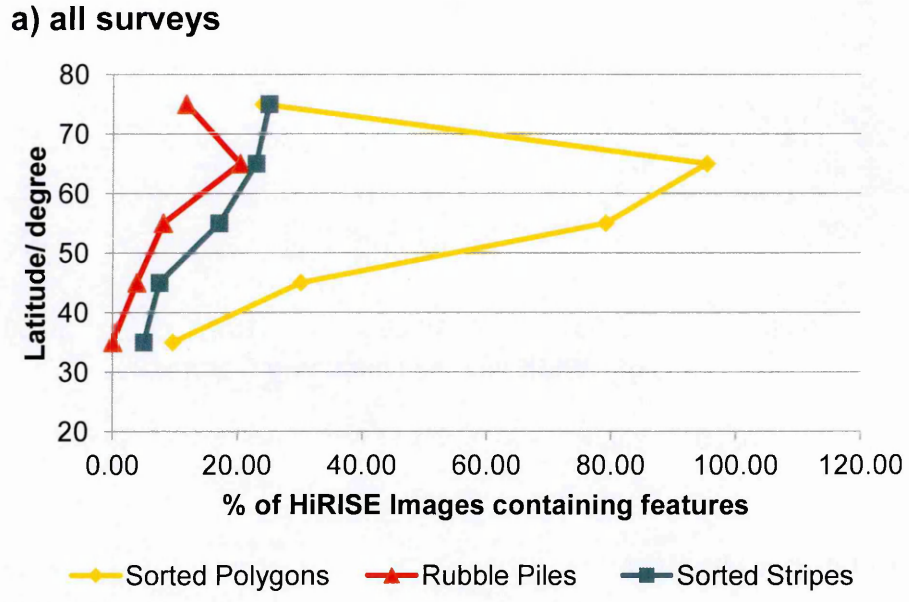

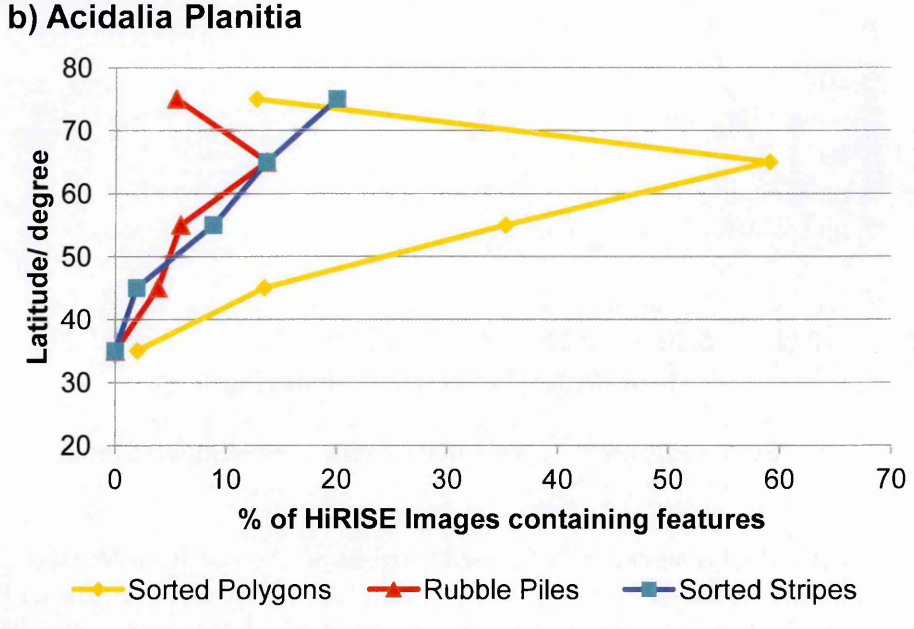

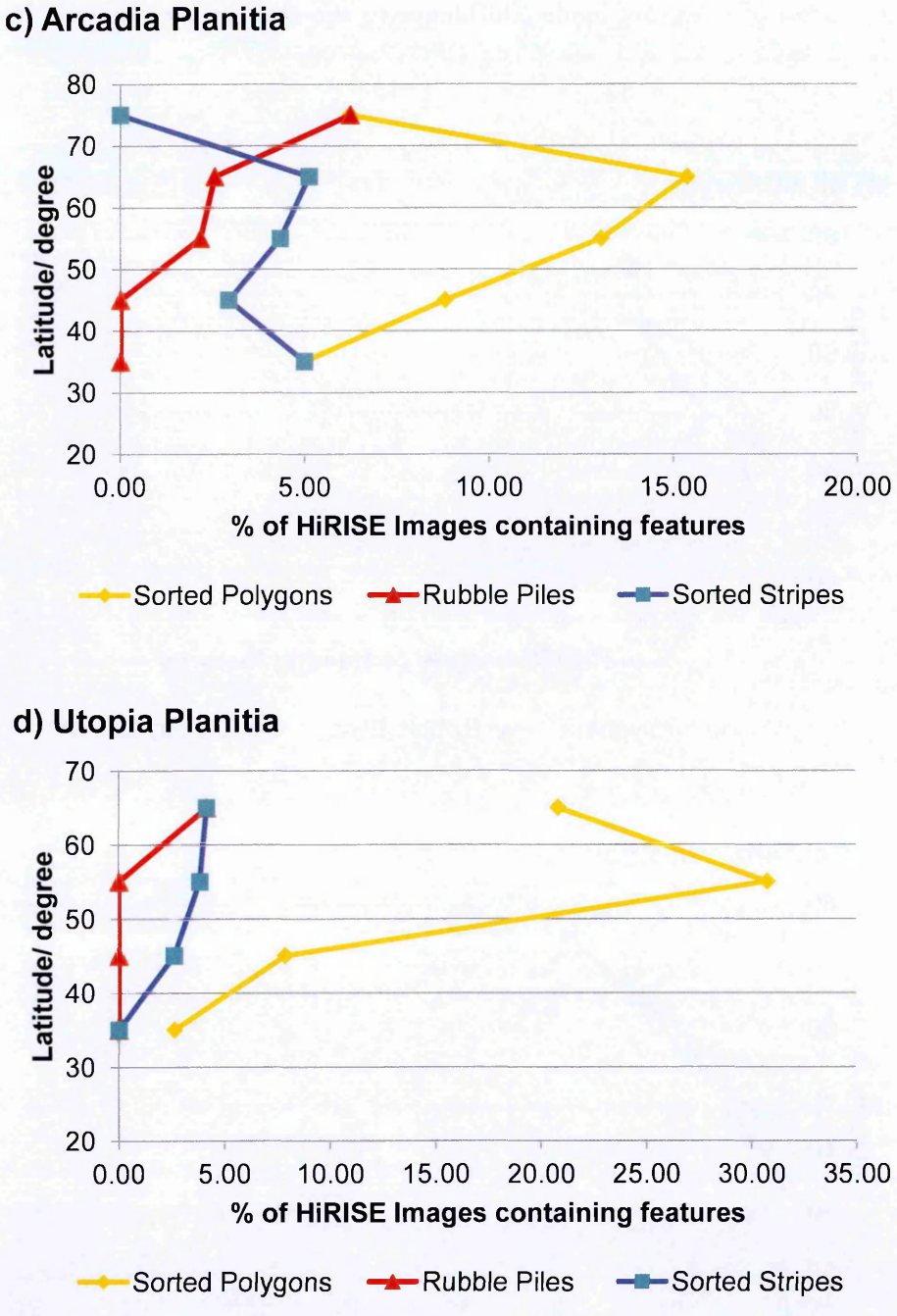

Figure 7.4: Latitudinal distribution of sorted features on the northern Martian plains. a) total of the other three datasets. b) Acidalia Planitia, c) Arcadia Planitia, d) Utopia Planitia These data indicate the number of images in which features occur rather than being normalised by the total area surveyed.

As illustrated in Figure 7.4 occurrences of sorted polygons consistently peak in the 60-70°N range in all of the study areas except Utopia. Here the peak occurrence is in the 50-60°N range. Rubble piles are generally more common in the northern parts of the

study areas, although the latitude at which peak occurrence is found varies. There are too few examples of sorted stripes to draw definite conclusions, but they also appear to be slightly more common at higher latitudes.

Figure 7.5 plots the locations of all features found within the HiRISE survey. It can be seen that sorted features are much more common in the Acidalia study area than in either Arcadia or Utopia. This is largely due to the high concentration of organised boulder patches in the region around Lomonosov Crater, described in Chapter Five. Utopia Planitia has the fewest examples, as very few features are found at lower latitudes in this area.

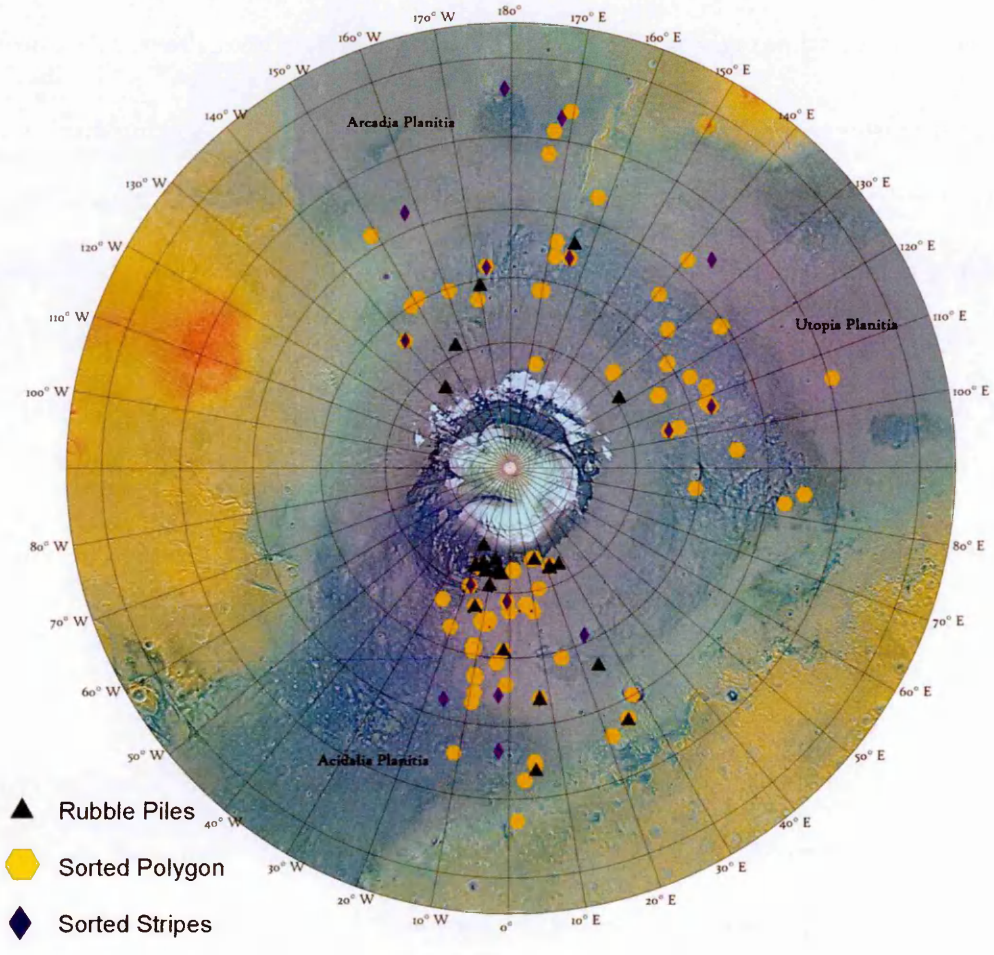

Figure 7.5: Distribution of different types of sorted patterned ground across the northern plains. Polygons are most common, with many rubble piles at high northern latitudes and several examples of possible sorted stripes scattered across the areas surveyed.

The high concentration of possible sorted features in Acidalia Planitia may in part be due to the more extensive survey conducted in this area. Although sorted structures are below the resolution of the CTX images used in the context survey, the boulder patches in which they frequently occur could be detected. Those with HiRISE coverage could then be examined at higher resolution to confirm whether organisation was present, allowing a far larger number of HiRISE images to be surveyed. This methodology should be used in future studies of this sort.

It is possible that sorted features could occur in un-sampled parts of the other study areas, but are not represented in this dataset. More research is required to determine whether the area around Lomonosov Crater is exceptional, or whether it is representative of other regions which fell between the images available for this survey.

The Lomonosov region has the highest concentration of possible sorting sites. 51 sites across 17 HiRISE images exhibit sorting of grade three or above, and most of the best examples from the entire survey can be found in this area of Acidalia Planitia. Elsewhere in Acidalia Planitia 21 possible sorted patterns were found, mostly to the north of 40°N, however only seven of these sites were graded above three. All sites graded four or higher occur north of 50°N and are much more common in the western part of the study area. Rubble piles are predominantly found at high latitudes although one uncertain feature may occur at 43 °N. Possible stripes are found between 35°N and 70 °N.

In Arcadia Planitia possible sorted polygons are found between 36°N and 73°N, with the majority of features, including the higher graded ones, occurring above 55°N. Six possible sorted stripes were observed with large scale stripes located between 64°N and 37°N, and smaller stripes at 34°N. Rubble piles are found between 54°N and 73°N. This

fits with the distribution seen in Acidalia Planitia where rubble piles and higher graded sites occur further north with a few low grade polygons further south.

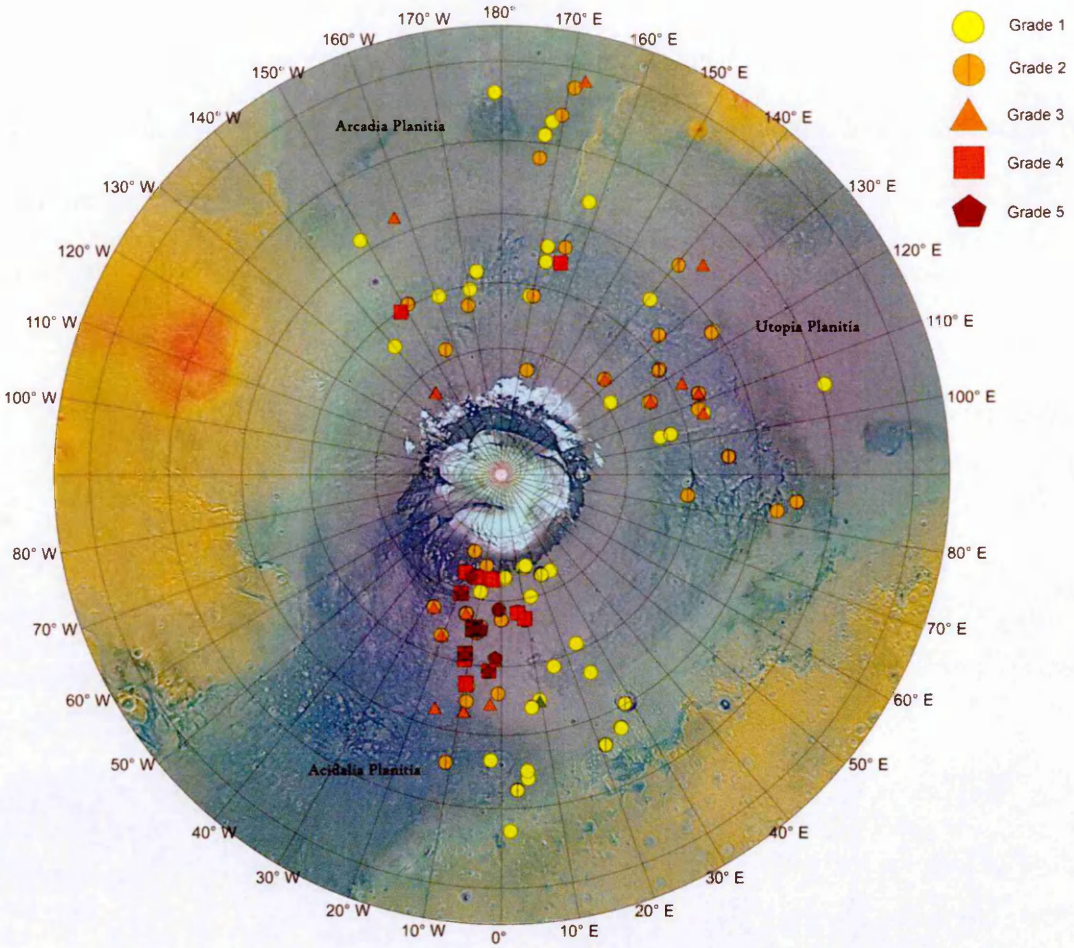

Figure 7.6: Possible sorted features ranked using the five point grading system described in Chapter Five.

This trend is confirmed by the results from the Utopia Planitia study area where areas of possible sorting occur between 40°N and 68°N, but most, including the higher graded sites, occur between 50°N and 65°N. Sorted polygons are always found most frequently, with fewer occurrences of the other types. Three possible examples of sorted stripes were found at 46, 57 and 64°N, but rubble piles were absent from this study area except for one very uncertain example.

Some features were observed which did not exhibit a clastic network but which might nevertheless be evidence of these processes. In these locations a series of polygonal

variations in darkness are observed as illustrated in figure 7.7. These structures lack large clasts, and so may not be related to sorted structures. They do appear similar to the albedo variations that indicate the presence of small scale patterned ground in some terrestrial remote sensing images shown in Chapter Four. For example those illustrated in Figures 4.13 and 4.15. This may suggest that, as with the terrestrial sites, sorting is present below the resolution of the image. Whether this is an example of patterned ground remains highly uncertain, without higher resolution images or ground truth it is impossible to be certain and very few such sites were observed.

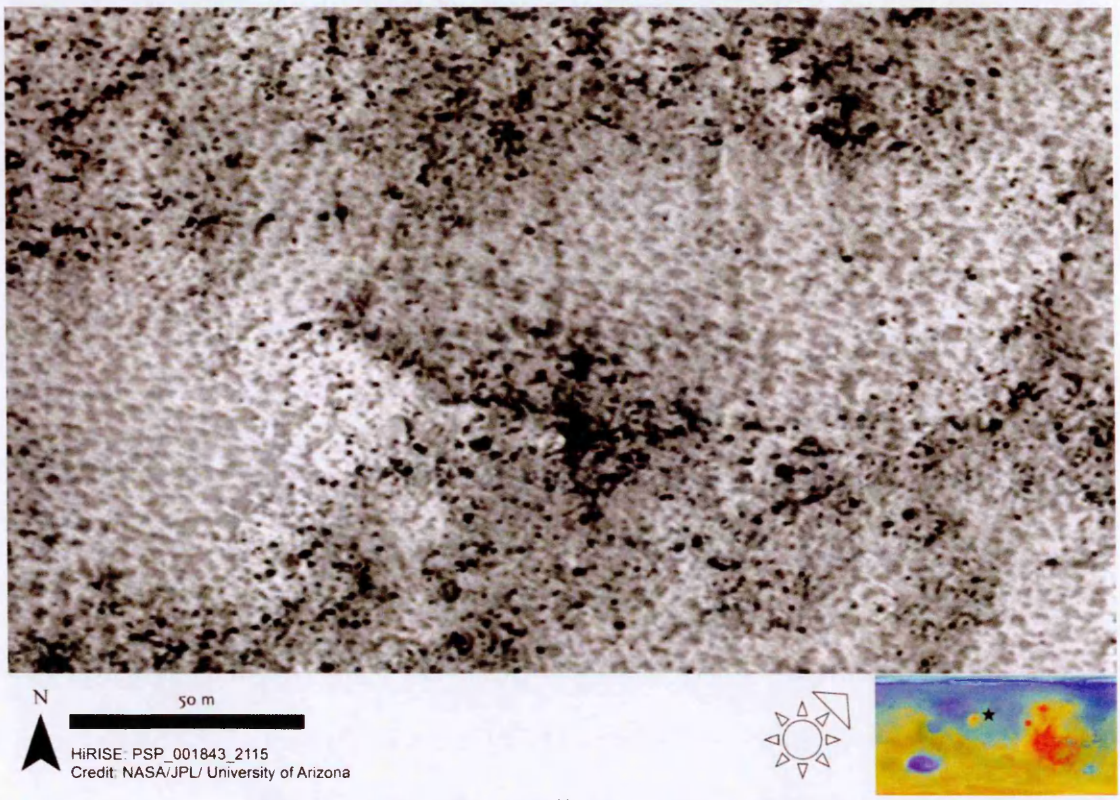

Figure 7.7: Possible small scale patterned ground.

Sorted patterns could not be assessed in the survey of CTX images due to their small size. However it was noted that many of these features occur within the boulder haloes described in Chapter Five. Consequently, it was decided to investigate the distribution of these boulder clusters in CTX images on the assumption that they are an environment in which sorting is often found. It was found that they were largely

ubiquitous in the area north of 50°N. Similar features may occur at more southerly latitudes, although they become harder to distinguish from other dark features in the CTX images, such as dark streaks which become more common to the south of the study area.

Sorted patterns are not common across most the areas surveyed, but they are present over a wider area than previously thought. Most prior surveys were restricted to high northern latitudes. Balme et al., (2009) found sorted patterns at equatorial latitudes but this was an unusual case since it occurred in proximity to the Athabasca Vallis where water has been in abundance in the geologically recent past (Murray et al., 2005). Most southerly regions are expected to have much less ground ice, precluding the easy formation of periglacial features.

The results of this investigation indicate that possible sorted features occur as far south as 35°N, albeit with a lower confidence than many of those sites found further to the north. This is on the edge of the region where ground ice is expected to be stable, so is plausible.

The best and most numerous examples of this terrain are found in the western part of the Acidalia study area, in the vicinity of Lomonosov crater. There is no clear reason why this area should have a higher concentration of possibly sorted sites. In this region sorting is often found within patches of boulders such as those shown in Chapter Five. These features are particularly prevalent in the region around Lomonosov crater, although they are found in other parts of this study area as well. Many such patches are found in and around buried impact craters so could be a result of the burial process.

It is likely that sorting occurs in these areas because the higher concentration of large boulders produces an environment where sorting processes will have more of an effect upon the overall morphology of the region. In locations where large boulders are more

scarce then the sorting process is less likely to generate a distinctive pattern which is visible in HiRISE images.

Boulder patches do not seem to be as common in the other regions examined in this study. Many examples of sorting in Utopia and Arcadia Planitiae do not have an associated patch of boulder strewn ground. However the surveys of these regions were limited to the HiRISE survey, so no continuous CTX survey was conducted. Thus it is possible that sorting within boulder patches does occur in these regions, just not in the parts examined here. Locating boulder patches in lower resolution datasets such as those from the High Resolution Stereo Camera on the Mars Express spacecraft would be a good starting point in identifying other regions where sorted patterned ground might be as prevalent as it is around Lomonosov Crater.

Table 7.1: Distribution of sorted features across the northern plains

Acidalia					
Latitude Band	**30-40**	**40-50**	**50-60**	**60-70**	**70-80**
Area Surveyed (km^2)	12186.2	6557.02	3159.49	2779.59	6866.38
Number of HiRISE Images	50	52	34	22	55
Sorted Polygons	1	7	12	13	7
Rubble Piles	0	2	2	3	3
Sorted Stripes	0	1	3	3	11
% of HiRISE Images					
Sorted Polygons	2	13.46	35.29	59.09	12.73
Rubble Piles	0	3.85	5.88	13.64	5.45
Sorted Stripes	0	1.92	8.82	13.64	20.00
Utopia					
Latitude Band	**30-40**	**40-50**	**50-60**	**60-70**	
Area Surveyed (km^2)	8219.16	4940.64	3071.29	3955	
Number of HiRISE Images	38	38	26	24	
Sorted Polygons	1	3	8	5	
Rubble Piles	0	0	0	1	
Sorted Stripes	0	1	1	1	
% of HiRISE Images					
Sorted Polygons	2.00	5.77	23.53	22.73	
Rubble Piles	0.00	0.00	0.00	4.55	
Sorted Stripes	0.00	1.92	2.94	4.55	
Arcadia					
Latitude Band	**30-40**	**40-50**	**50-60**	**60-70**	**70-80**
Area Surveyed (km^2)	5188.19	3647.79	4100.88	2808.86	2364.71
Number of HiRISE Images	40	34	46	39	16
Sorted Polygons	2	3	6	6	1
Rubble Piles	0	0	1	1	1
Sorted Stripes	2	1	2	2	0
% of HiRISE Images					
Sorted Polygons	4.00	5.77	17.65	27.27	1.82
Rubble Piles	0.00	0.00	2.94	4.55	1.82
Sorted Stripes	4.00	1.92	5.88	9.09	0.00

7.3 Distribution of Lobate Hill slope Features

Lobate structures have previously been observed on crater walls at high latitudes (e.g. Gallagher et al., 2011; Johnsson et al., 2012). These features could be analogous to solifluction lobes which are common in periglacial environments on Earth (Matsuoka, 2001). Several sites with potential lobate structures have been found in this survey, but most are highly uncertain. These features are extremely uncommon and have only been found in a few isolated locations.

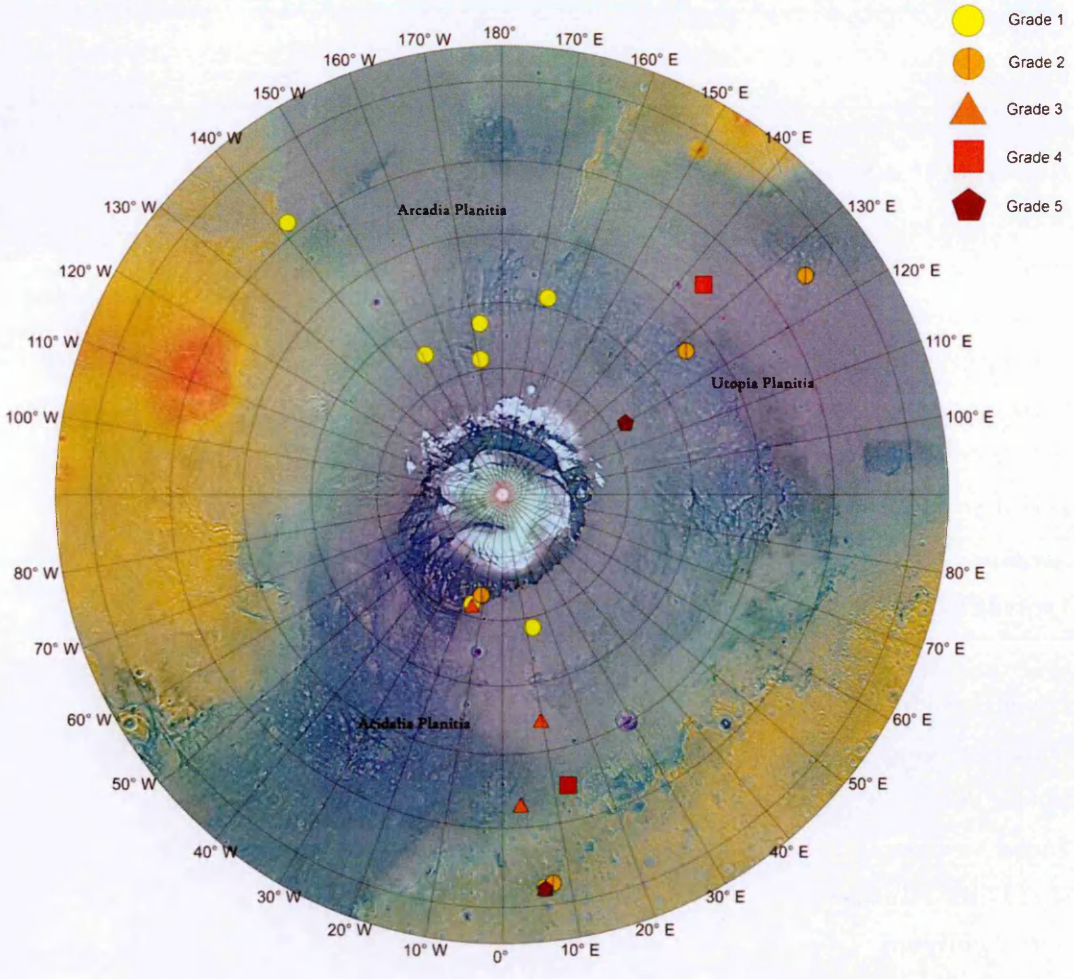

Figure 7.8: Distribution of possible lobate structures in the HiRISE surveys. Grades between 1 and 5 indicate the degree of morphological similarity to solifluction features.

Figure 7.8 summarises the distribution of these features by latitude, showing the location of HiRISE images where lobate structures are to be found. There seems to be a peak in occurrence in the 60-70°N band. This matches the peak occurrence of possible

sorted features as shown in Figure 7.4. However due to the scarcity of these features, and particularly of good examples, this result should be treated with caution.

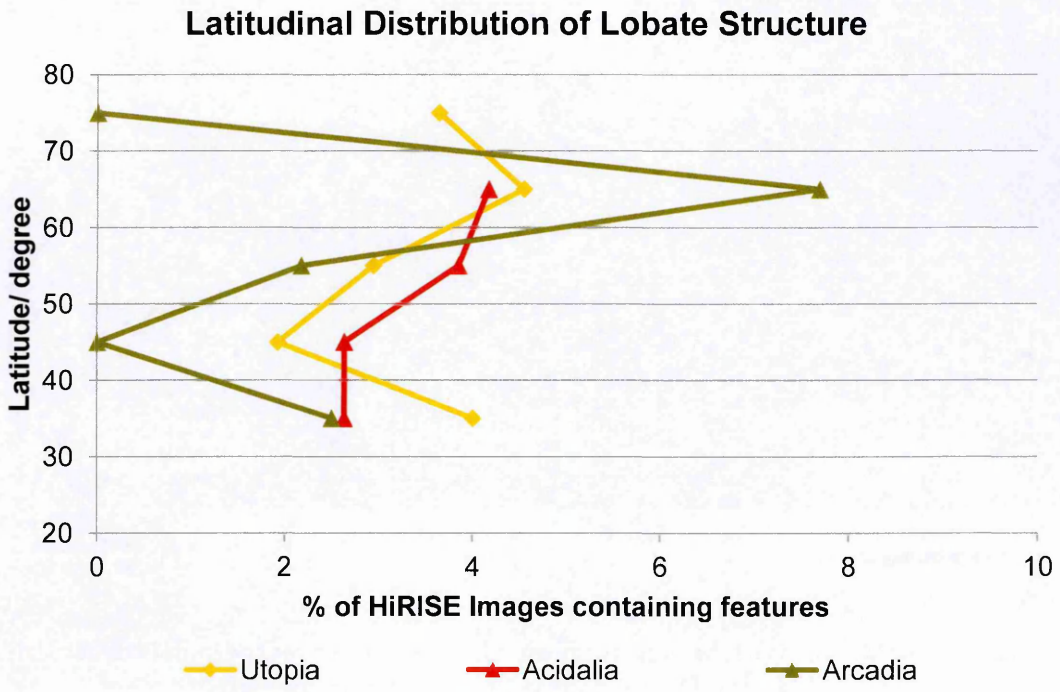

Figure 7.9: Latitudinal distribution of lobate structures on the Martian Northern Plains. These data indicate the number of images in which features occur rather than being normalised by the total area surveyed.

Acidalia Planitia has the most potential lobate structures with nine sites across five HiRISE images. The majority are clustered at low latitudes, below 50°N. Some very unlikely sites are found further north, but these are less likely to be solifluction features. One site at 54°N appears to exhibit curved bands of boulders on a hillside and so could be an example of a clastic solifluction lobe. The most convincing examples come from a rocky crater around 32°N where four areas of possible lobate hillside are found which resemble solifluction lobes. The lobate structures shown in Figure 7.10 are the highest graded of any in these surveys. However these features occur on a shallower slope than would be expected for terrestrial lobate structures.

Figure 7.10: Grade five lobate features on a hillside in the southern part of Acidalia Planitia. Down slope is towards the bottom left.

Figure 7.11: clastic lobes on the wall of a small impact crater in Utopia Planitia. Down slope is towards the bottom left.

Another site also around 32°N contains similar structures although these are not ranked as highly. A crater at 42°N features what could be rounded lobate structures amidst heavily scalloped terrain just outside a large crater. The location of these features is surprising. Previous studies had suggested that lobate structures would be limited to higher latitudes. If these features are evidence of solifluction it would suggest that such processes are viable far further south than previously thought. Utopia Planitia has four sites with possible lobate features. There is no clear trend in latitudinal distribution as possible sites are found at latitudes 35, 46, 54 and 67°N.

The site illustrated in Figure 7.11 is the only one in this survey to exhibit clastic lobes like those described in Heimdal Crater by Gallagher et al., (2011). This location is at a similar latitude to those described by the previous study, as Heimdal Crater is located at 68°N while these features are at 67°N. What might be similar clastic features are found at 54°N in Acidalia but they are not as convincing an example. The other three sites in the Utopia study areas are not stone banked, although one, shown in Figure 7.13, is in proximity to features which could be very thin sorted stripes.

In Arcadia Planitia there are five sites with possible lobes between 59 °N and 68°N and one site at 38°N. Only non-clastic features are observed in this area, and few of the examples are graded particularly highly.

Figure 7.12: Possible lobate structures in Arcadia Planitia.

Figure 7.13: possible solifluction lobes in proximity to thin clastic stripes on the wall of a small impact crater in Utopia Planitia.

In summary, non-clastic lobes are found across a wide range of latitudes, but some of the best examples are found at lower latitudes. This suggests that these features are unlikely to be limited to the high latitudes. Lobes are found in a few isolated locations across the study areas, but are not found frequently enough to infer any patterns from their distribution. Clastic lobes are only found at high latitudes, although very few examples of this type have been found so no real trend can be drawn. Lobate structures are too small to be distinguishable in CTX data, so were not included in the context survey.

Table 7.2: Distribution of lobate structures across the northern plains

Acidalia					
Latitude Band	**30-40**	**40-50**	**50-60**	**60-70**	**70-80**
Area Surveyed (km^2)	12186.2	6557.02	3159.49	2779.59	6866.38
Number of HiRISE Images	50	52	34	22	55
Number with Lobate Structures	2	1	1	1	2
% of HiRISE Images	4	1.92	2.94	4.55	3.64
Utopia					
Latitude Band	**30-40**	**40-50**	**50-60**	**60-70**	
Area Surveyed (km^2)	8219.16	4940.64	3071.29	3955	
Number of HiRISE Images	38	38	26	24	
Number with Lobate Structures	1	1	1	1	
% of HiRISE Images	2.00	1.92	2.94	4.55	
Arcadia					
Latitude Band	**30-40**	**40-50**	**50-60**	**60-70**	**70-80**
Area Surveyed (km^2)	5188.19	3647.79	4100.88	2808.86	2364.71
Number of HiRISE Images	40	34	46	39	16
Number with Lobate Structures	1	0	1	3	0
% of HiRISE Images	2.00	0.00	2.94	13.64	0.00

7.4 Distribution of Scalloped Depressions

Scalloped depressions are common across the northern plains, particularly in Utopia Planitia (e.g. Morgenstern et al., 2007; Séjourné et al., 2011). These features could form through the sublimation of ground ice and may be analogous to the thermokarst depressions found on Earth (e.g. Soare et al., 2008).

Scalloped depressions were frequently found during the HiRISE survey and so were made the focus of the context survey. Since these features are clearly discernible in CTX images it was possible to map their distribution over a far larger area using lower resolution data.

These features have been extensively studied in the Utopia Planitia region (Haltigin et al., 2014; Séjourné et al., 2011; Soare et al., 2008; Ulrich et al., 2010). Consequently, it was decided that the context survey should be used to produce a dataset for Acidalia Planitia which could be compared with the results of the previous investigations. This could be used to determine whether these landforms were more common in Utopia, or whether they were similarly distributed in both regions, but that more studies had meant that more scallops had been identified in the Utopia Basin.

Scalloped depressions range from fairly small structures with reasonably circular morphology to far more complicated terrains comprising multiple phases of scallop formation. Mature structures merge and overlap creating the typical "scalloped morphology". In many places scalloped depressions appear to occur in proximity to patches of heavily pitted or degraded ground. This may represent an early stage of development. As pits are formed, sublimation or melting of the exposed ice is facilitated. This allows an increasing amount of degradation to occur. Pits widen and coalesce forming scalloped depressions.

Figure 7.14: Example of heavily degraded terrain in Acidalia Planitia containing numerous well-developed scalloped depressions.

The scalloped depressions shown in Figure 7.14 show multiple regions of degradation merging to form large basins with extensive scalloped edges. The floors of these depressions are covered with decametre scale fracture networks of the high centred variety described earlier in this chapter. These features are classified as being mature as multiple phases of development and coalescence can be seen. The classification of scalloped depressions will be discussed in more detail in Chapter Ten.

Figure 7.15: Heavily pitted ground which may be an early stage of the development of scalloped depressions.

The majority of features found during the course of these surveys were of the more mature type depicted in Figure 7.14. Far fewer young scallops appeared to be present within the areas surveyed. This suggests that these environments have been developing for a long time and that the formation of scalloped depressions is not a recent development.

Figure 7.16: Example of multiple scalloped depressions in Utopia Planitia developing a nested morphology as smaller depressions erode the floor of a larger basin.

Scalloped depressions are usually found in proximity to contraction crack polygons of the sort described in section 7.5. Fractures typically superpose scalloped depressions and occupy both the interiors of the depressions and the surrounding plains, as can be seen in Figures 7.14 and 7.16.

7.4.1 Distribution of scalloped depressions in the HiRISE Survey

Scalloped depressions were found to be present in all of the study areas. They were most numerous in Utopia Planitia where 132 sites were found across 36 HiRISE images, ranging in latitude between 40°N and 67°N. Such features occur in 24 images in the Acidalia study area ranging in latitude between 30°N and 57°N. Scalloped depressions in this region extend further to the south than in the Utopia study area, but are not found as far north.

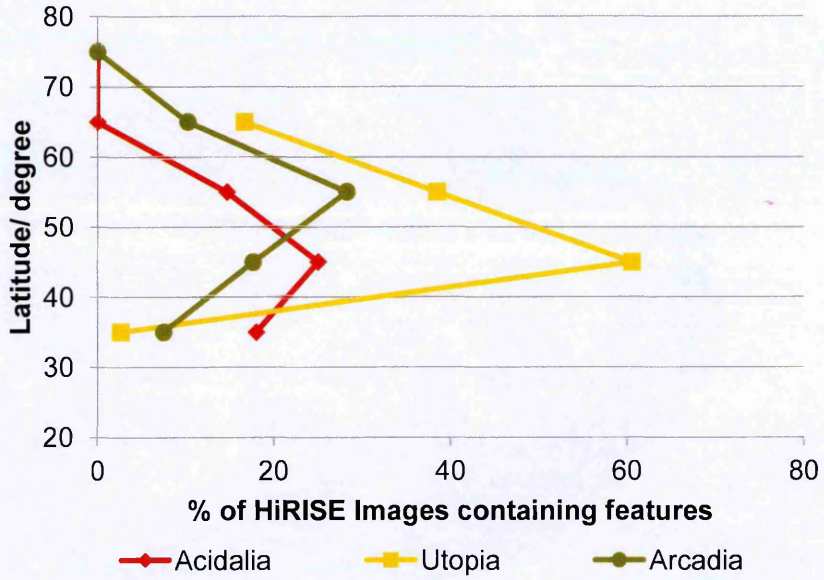

Figure 7.17: Distribution of Scalloped Depressions on the Northern Martian Plains. These data indicate the number of images in which features occur rather than being normalised by the total area surveyed.

Figure 7.17 shows that the peak occurrence of scalloped depressions occurs in the 40-50°N band for both Acidalia and Utopia Planitiae, but is slightly further north in Arcadia Planitia. Occurrences drop off steeply at higher latitudes in all three study areas. The highest concentration of these features is in Utopia Planitia. Although scalloped depressions are found in both Acidalia and Arcadia Planitiae, they are not as numerous. However, more features are found in the most southerly latitude band in these regions, whereas in Utopia Planitia scalloped depressions in the 30-40°N band are scarcer.

Figure 7.18 shows the geographical distribution of these features. In the Arcadia Planitia study area scalloped depressions are primarily found between 37 and 64°N. One feature at 74°N has a similar asymmetric profile and so could be a heavily in-filled depression. There are a total of 37 features, across 27 HiRISE images.

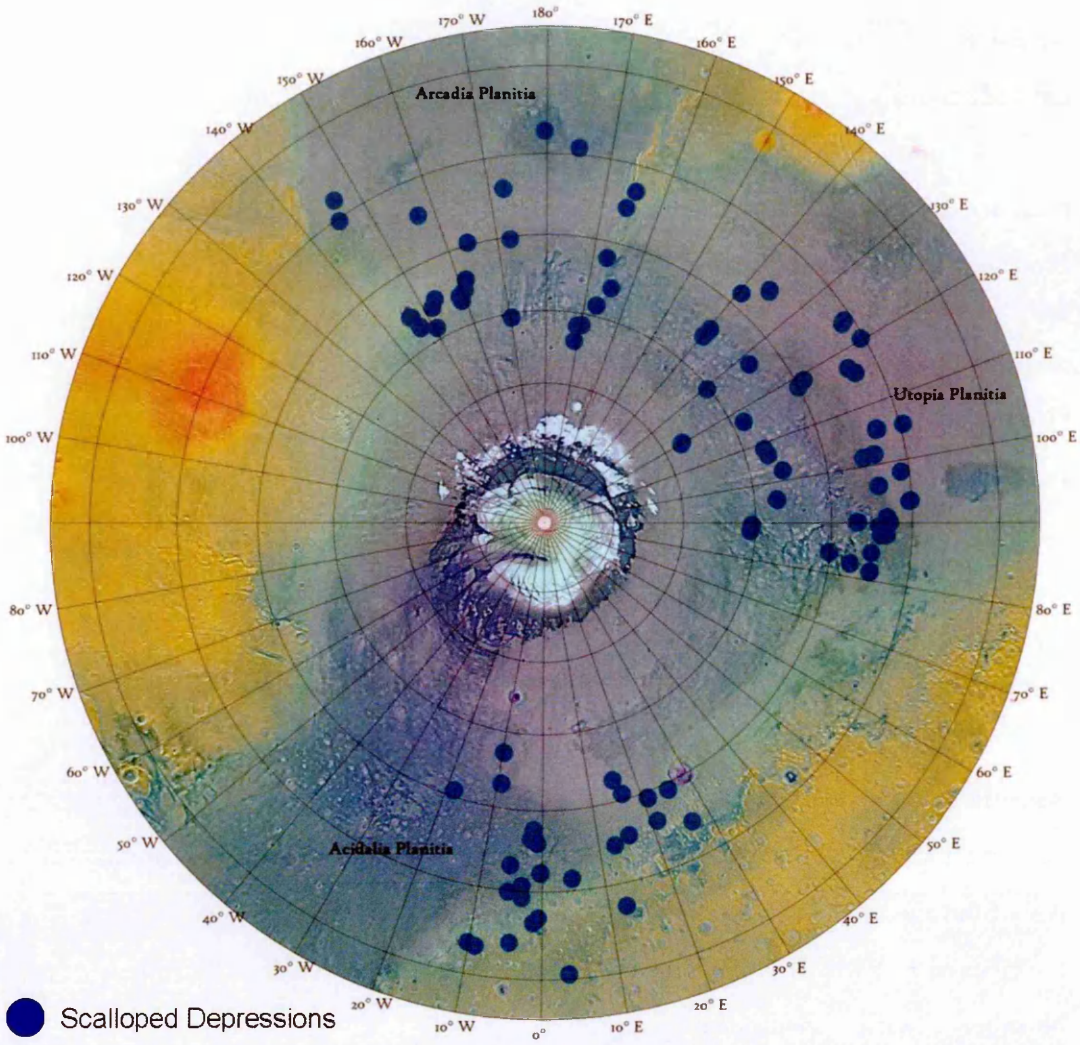

Figure 7.18: Distribution of scalloped depressions on the northern plains of Mars from the HiRISE Surveys.

It initially appears that these features are much less widespread in Acidalia Planitia, where they seem to be confined to the regions south of 55 °N. Examination of CTX images of the northern part of this region confirmed that this was due to a bias in the available HiRISE images. Scalloped depressions in Acidalia Planitia do cover the same latitude range as those in the other two study areas.

Table 7.3: Distribution of scalloped depressions in Acidalia Planitia.

Acidalia					
Latitude Band	**30-40**	**40-50**	**50-60**	**60-70**	**70-80**
Area Surveyed (km^2)	12186.2	6557.02	3159.49	2779.59	6866.38
Number of HiRISE Images	50	52	34	22	55
Number with scalloped depressions	9	13	5	0	0
% of HiRISE Images	18	25.00	14.71	0.00	0.00
Utopia					
Latitude Band	**30-40**	**40-50**	**50-60**	**60-70**	
Area Surveyed (km^2)	8219.16	4940.64	3071.29	3955	
Number of HiRISE Images	38	38	26	24	
Number with scalloped depressions	1	23	10	4	
% of HiRISE Images	2.00	44.23	29.41	18.18	
Arcadia					
Latitude Band	**30-40**	**40-50**	**50-60**	**60-70**	**70-80**
Area Surveyed (km^2)	5188.19	3647.79	4100.88	2808.86	2364.71
Number of HiRISE Images	40	34	46	39	16
Number with scalloped depressions	3	6	13	4	0
% of HiRISE Images	6.00	11.54	38.24	18.18	0.00

7.4.2 Distribution of scalloped depressions in the Context Survey

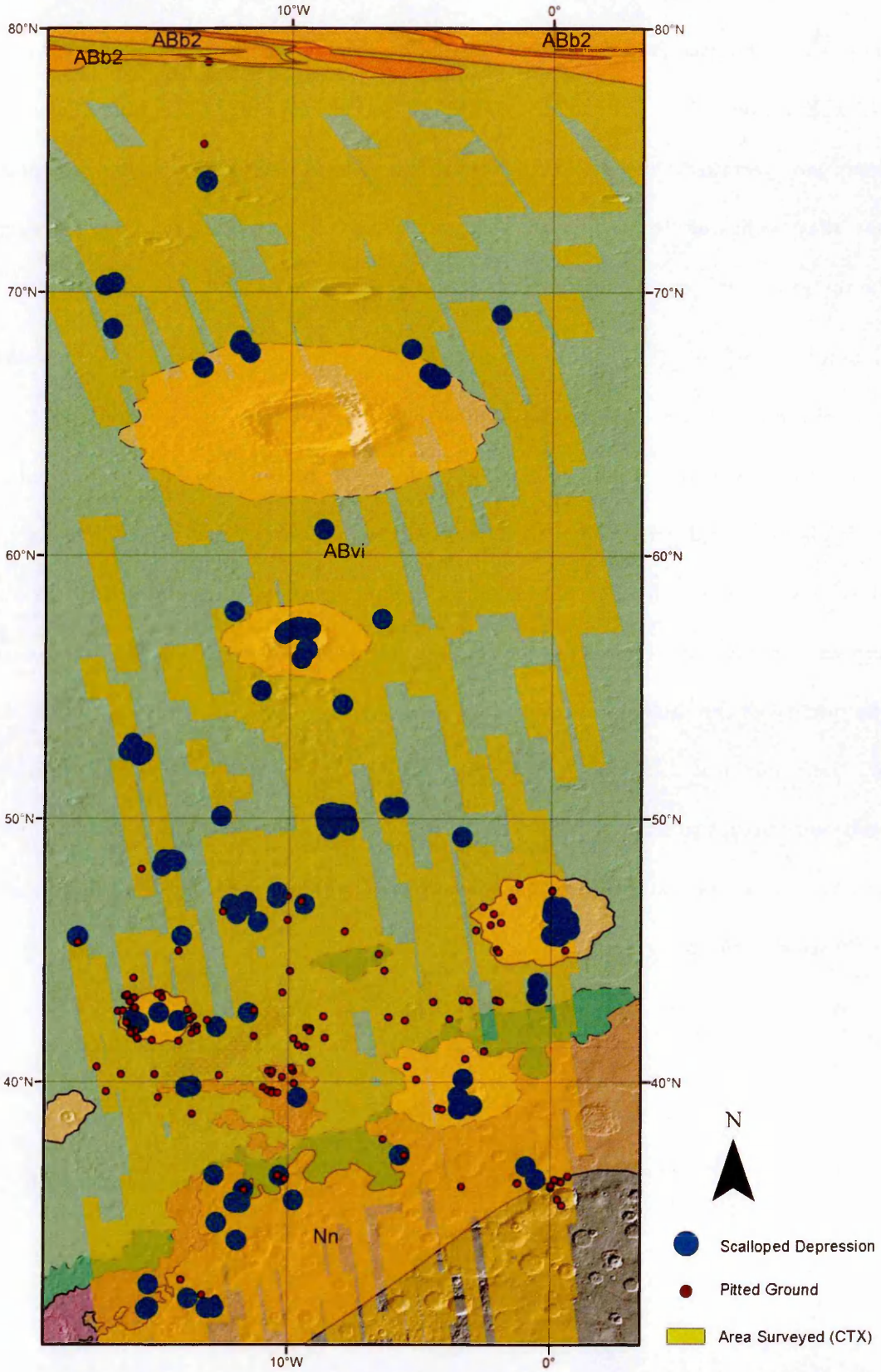

Figure 7.19: Distribution of scalloped depressions and areas of pitted ground that may be forming them in the Context survey.

It is clear that scalloped depressions are much less common in Acidalia Planitia than they are in Utopia Planitia. This was found to be the case for both the CTX and HiRISE surveys. The main difference found was in the northern extent of scalloped depression terrains. Few HiRISE images north of 55°N had exhibited these landforms, but they appeared in several of the northerly CTX images. However, scalloped depressions in the northern part of the study area were not found to be as distinct.

Examples of pitted ground are limited to the area south of 50°N and it is in this region that scalloped depressions are also most common. All of the features marked as scalloped depressions were graded using a similar methodology to that applied to examples of sorted patterned ground and solifluction lobes. Grade five scallops are the clearest examples, with morphologies most similar to type examples such as those shown in Figure 6.11. Those of grade one and two are of uncertain origin. In some cases the quality of the image prevents features from getting a higher grade, in others there are morphological differences that cause it to be graded lower. These features have some similarities to scalloped depressions but many are faint and so hard to distinguish, or have an unclear extent. Many lack some of the characteristic features of a scalloped depression such as asymmetric profiles and bands on the floor of the image. Gradings of all of these features is shown in Figure 7.20.

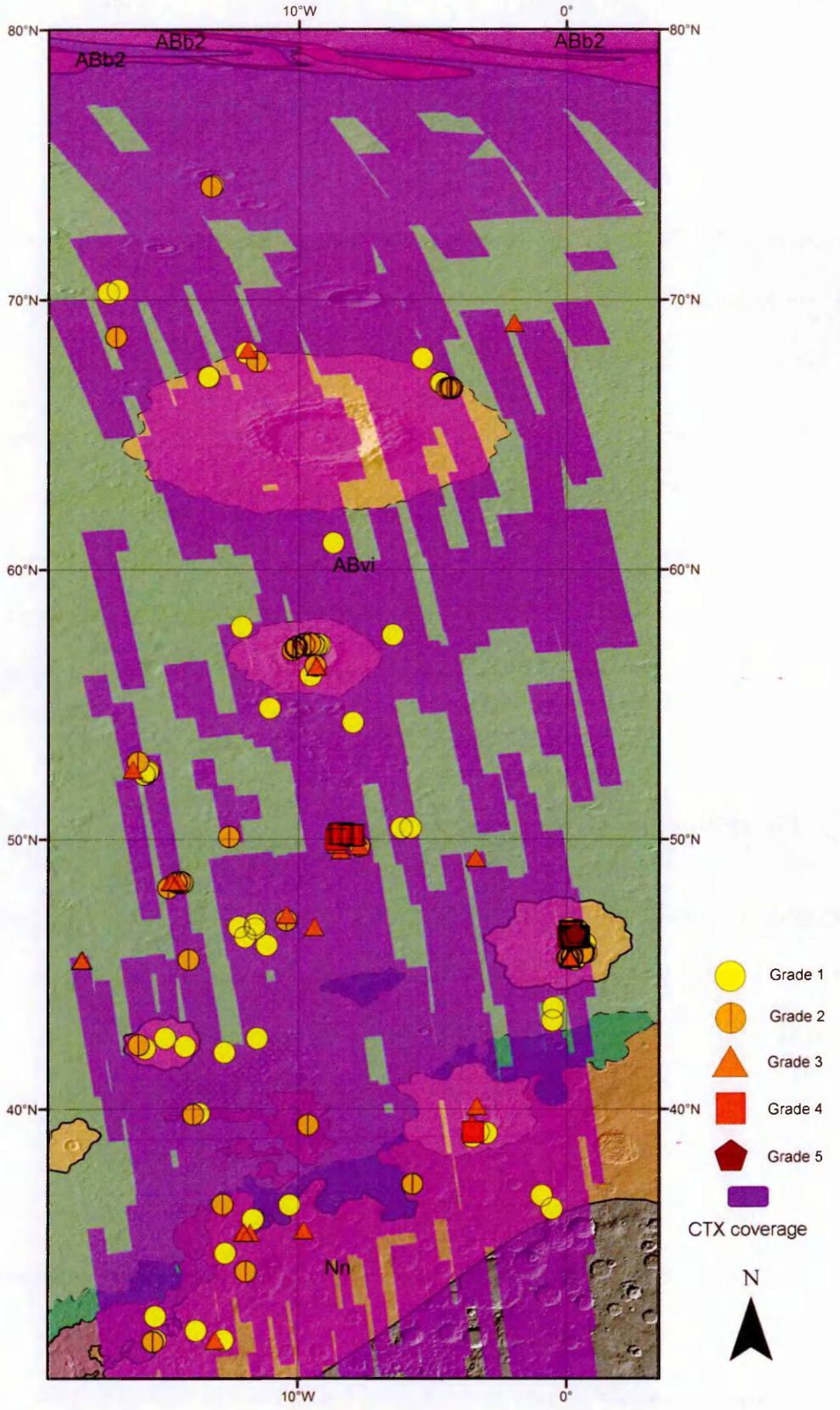

Figure 7.20: Grading of context survey results with 5 being the best examples and 1 the worst.

It can be seen that the majority of highly graded features are found within a few clusters in the 35-50°N band. Most of the widespread features are of low grade, while almost all of those sites with grade four and above scalloped depressions are clustered around two medium-sized impact craters, Lagarto Crater at 49°N 8°W and Davies Crater at 46°N 0°E. These craters are good examples of periglacial assemblages as they contain numerous scalloped depressions in close proximity to crater wall gullies. They will be examined in more detail in Chapter Ten.

The relative scarcity of scalloped depressions in this region sets Acidalia apart from Utopia Planitia. The processes that form scalloped depressions are clearly at work here, but not as extensively or over as wide an area. It is important to note however that only a relatively narrow swath of the area has been examined. Acidalia Planitia covers an area of more than 10,000 square kilometres, much of which could not be examined in this survey.

7.5 Distribution of fracture polygons

Fractures are ubiquitous across all parts of the three study areas, confirming that thermal contraction cracking is an important process in shaping the surface environment of the Northern Plains. These are the most numerous and widespread of the landforms considered here. Many of the surveyed HiRISE images contain at least some fracture patterns. Fractures only become less prevalent below 40°N. This is the region where lineated valley fill (LVF) becomes more common across many of the areas examined. Fracturing does not appear to occur in areas with extensive LVF, possibly suggesting that the materials making up the LVF do not undergo the same fracturing process as the smoother icy ground found further to the north, or that they superpose the fractured ground obscuring the patterns.

7.5.1 Fracture Morphology

Various processes result in the formation of fracture patterns including cooling of lavas or desiccation cracking. Consequently, not all of the fractures on the martian surface are indicative of ground ice. The southern part of these study areas contains many large isolated fractures, usually on a scale of several hundred metres in length. These are unlikely to have formed through modification of ice-rich materials by periglacial processes and so are not as relevant to this investigation as other varieties.

Of more interest are well-defined polygon networks which occur across a range of scales. 'Large scale' polygons can be several hundred metres across and are common across all three study areas. These are frequently found within crater interiors where the morphology of the network appears to be controlled by the constraining crater. In addition, smaller polygon nets, each polygon being several tens of metres across, are also common, sometime occurring alongside the larger fracture polygons and sometimes independently of them.

These structures often appear to be filled with a high albedo material which may be ice or sediment. This possibly suggests that ice and sand wedge polygons are present in some instances; providing another strand of evidence to indicate that they are formed in ice-rich ground. These fracture networks, at both decimetre and hundred metre scales, fall into several of the broad categories of network morphology defined by Mangold (2005).

Some fracture networks exhibit a rectilinear geometry where fractures usually intersect at right angles while others form hexagonal patterns or random orthogonal arrangements which can have a range of corner angles. Hexagonal polygons often occur as part of a larger random orthogonal network. Networks made up entirely of hexagonal fractures were found to be very rare, whereas many of the random

orthogonal networks had at least a small hexagonal component. Since the dominant component of the network is recorded rather than the variations in fracture geometry within the image being mapped the hexagonal class is not used in this discussion.

In many cases sets of nested fractures are found where two or more fracture nets form on more than one scale. For example, a fine mesh of reasonably regular fractures a few metres to ten metres across can be enclosed within a larger net of wider and deeper troughs, some of which will be up to 10 metres wide. These larger scale troughs form polygons on a scale of 100 metres.

Figure 7.21: Random Orthogonal and Rectilinear fracture nets on different scales. Small metre scale fractures with a variety of random orthogonal and rectilinear patterns are nested within much larger predominantly rectilinear fractures.

Fracture polygons can also be categorised as either high or low-centred. High centred polygons consist of a raised centre surrounded by open fractures or troughs of varying width and depth. These seem to be more common than low centred polygons in which a region of flat ground is surrounded by a ridge. Low-centred polygons may be

analogous with the low-centred sand and ice wedge polygons found in terrestrial cold climate environments such as the Antarctic Dry Valleys. Areas of high-centred polygons are sometimes observed to grade into fields of hummocks where fractures are no longer evident.

Fracture patterns frequently occur in proximity to other putative periglacial features. Many gullies are found on or near fractured terrain and in some areas clastic nets which may be examples of sorted patterned ground also superpose fracture nets. It has been proposed (Orloff et al., 2011, 2013) that these clastic nets could be the result of movement of boulders by the opening and closing of fracture polygons. Consequently, the data presented here were used to determine what proportion of possible sorted nets overlie fracture polygons (Figure 7.22). This study will be presented in detail in Chapter Nine.

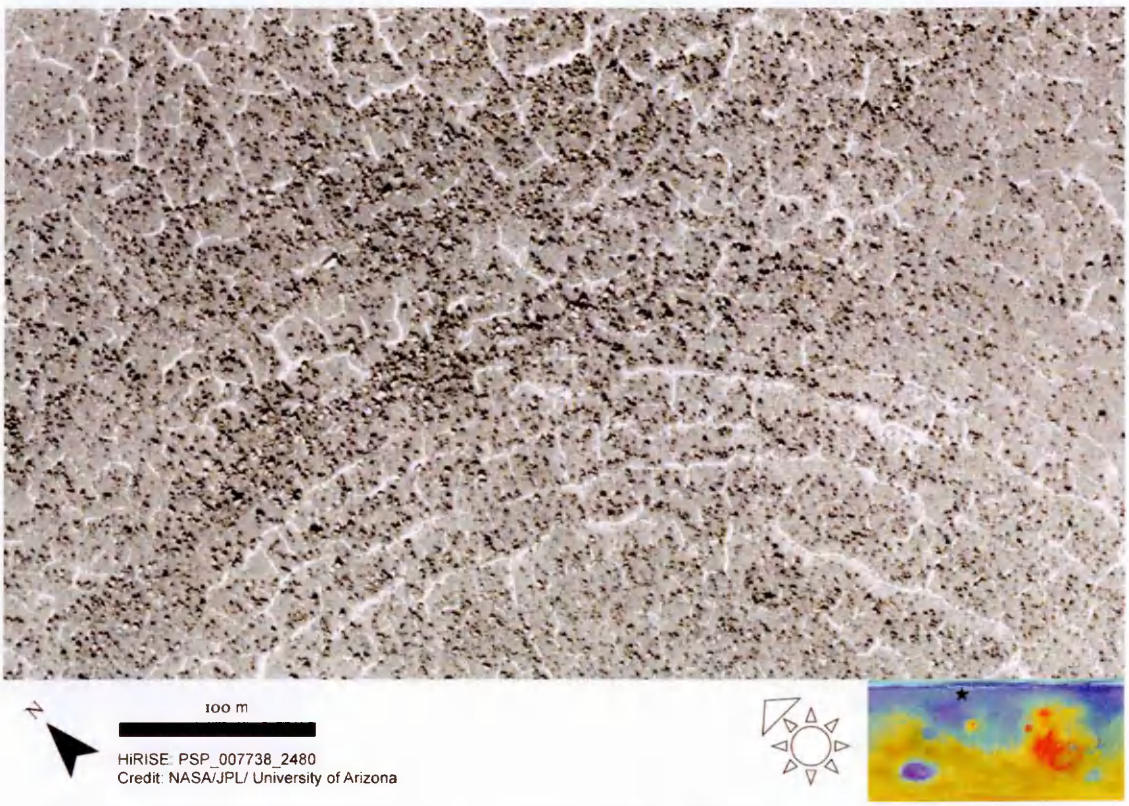

Figure 7.22: Lines of Boulders follow a high albedo fracture net in northern Utopia Planitia

Fracture nets occur both in the regional icy mantle and, more rarely, on top of dunes. These dune-top fractures always have the random orthogonal morphology and only occur at a single scale, being around 10 metres across. This is possibly because the limited size of the area on which they form prevents them from widening over time.

Figure 7.25 shows the distribution of both large and small fracture patterns within the area covered by the context survey. Figures 7.23 and 7.24 show the distribution of fracture patterns observed in the three HiRISE Surveys.

The formation of fracture nets does not necessarily require the thawing of liquid water (although the formation of ice wedges does). If the martian polygonal fracture features do not contain ice wedges then they may well be the result of dry processes rather than being indicative of a periglacial environment. In the terrestrial Antarctic fractures are known to form through a combination of thermal contraction and sublimation processes. This is the most likely process to explain their occurrence on Mars. Without ground truth it is impossible to determine whether ice wedges are forming within a martian fracture net.

The only in situ observations of these features come from the Phoenix Lander, which performed several excavations in a region dominated by degraded fracture polygons. Excess ground ice was found in some of these (Mellon et al., 2009), suggesting that these structures most likely formed through thermal contraction cracking of an ice-rich soil. However, Phoenix's observations do not confirm the presence or absence of ice and sand wedges within developing fracture nets. Since it was a stationary lander, observations were only made of a very small area of the northern plains. The Phoenix landing site is located in a region of the Vastitas Borealis that was not covered by this survey, however the features it examined are representative of their type.

7.5.2 Fracture Polygon Distributions in the HiRISE Surveys

Fracture polygons occur across all areas surveyed in this study, Figure 7.23 summarises their latitudinal distribution. They are generally more common at high latitudes, reaching a peak at 60-70°N. Fewer fractures are found in the 70-80°N band. In the Acidalia and Utopia study areas all fracture morphologies peaked at 60-70 °N. However in Arcadia Planitia rectilinear fracture networks are found to be more common in the northern part of the study area, whereas the random orthogonal polygons are common at a wider range of latitudes. The absence of data in the northern most band of the Utopia survey means that it is impossible to confirm that fracture occurrence peaks at 60-70. However this seems likely give the trend in the other two study areas.

A) All Data

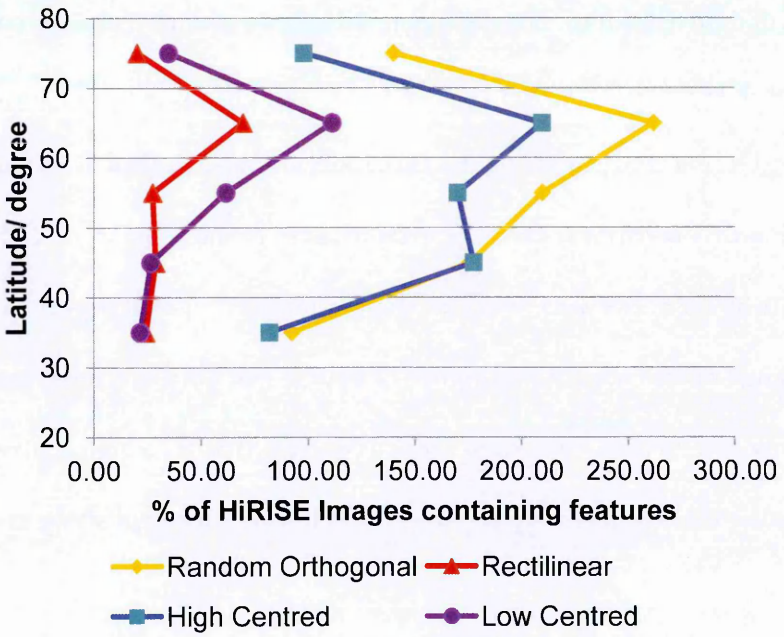

B) Acidalia

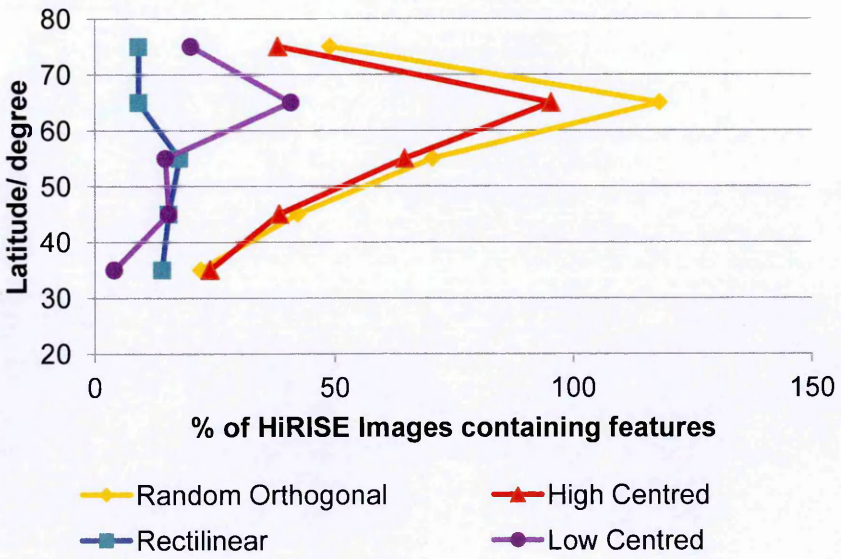

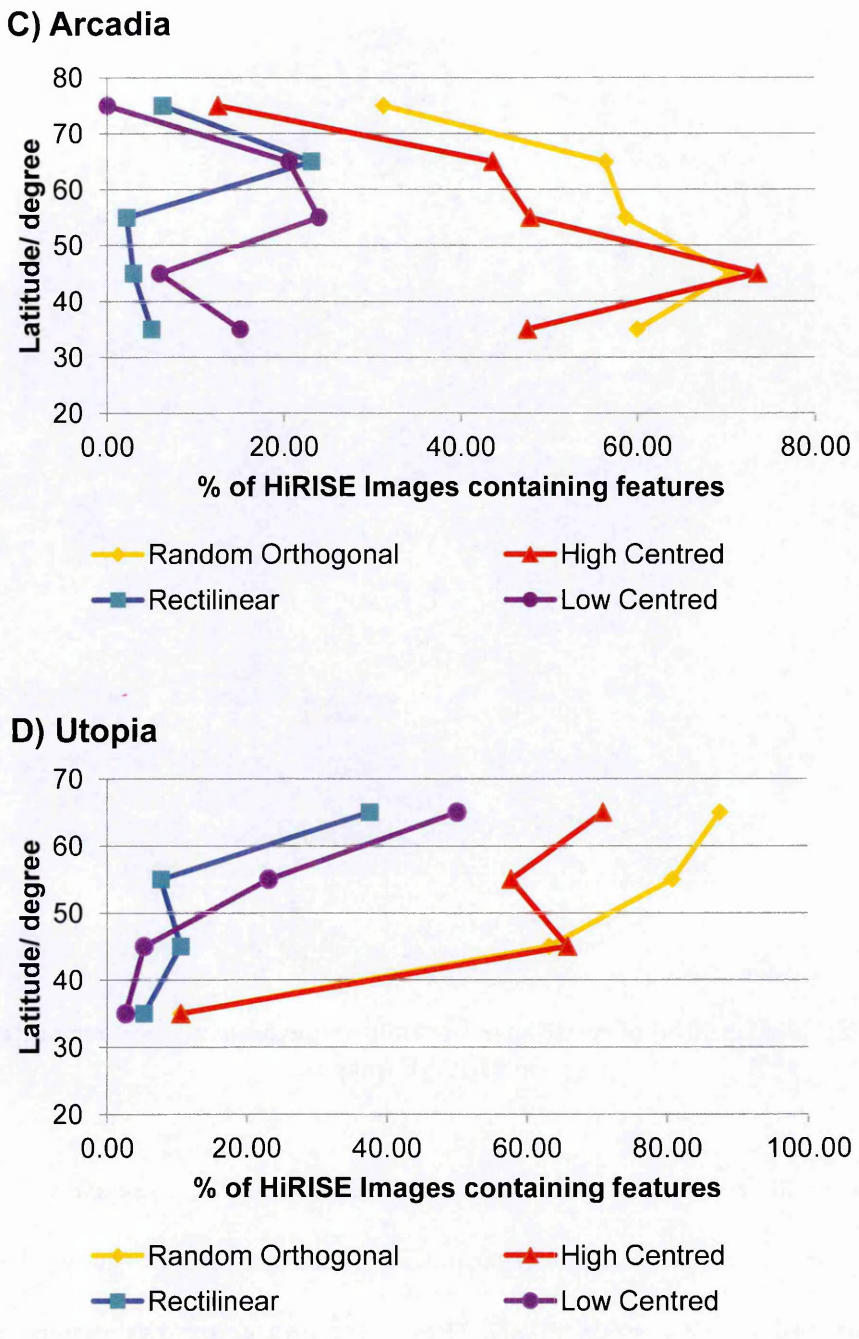

Figure 7.23: Distribution of Fracture Networks on the Martian Northern Plains from HiRISE images. A) Total of the three datasets, B) Acidalia Planitia, C) Arcadia Planitia, D) Utopia Planitia. These data indicate the number of images in which features occur rather than being normalised by the total area surveyed.

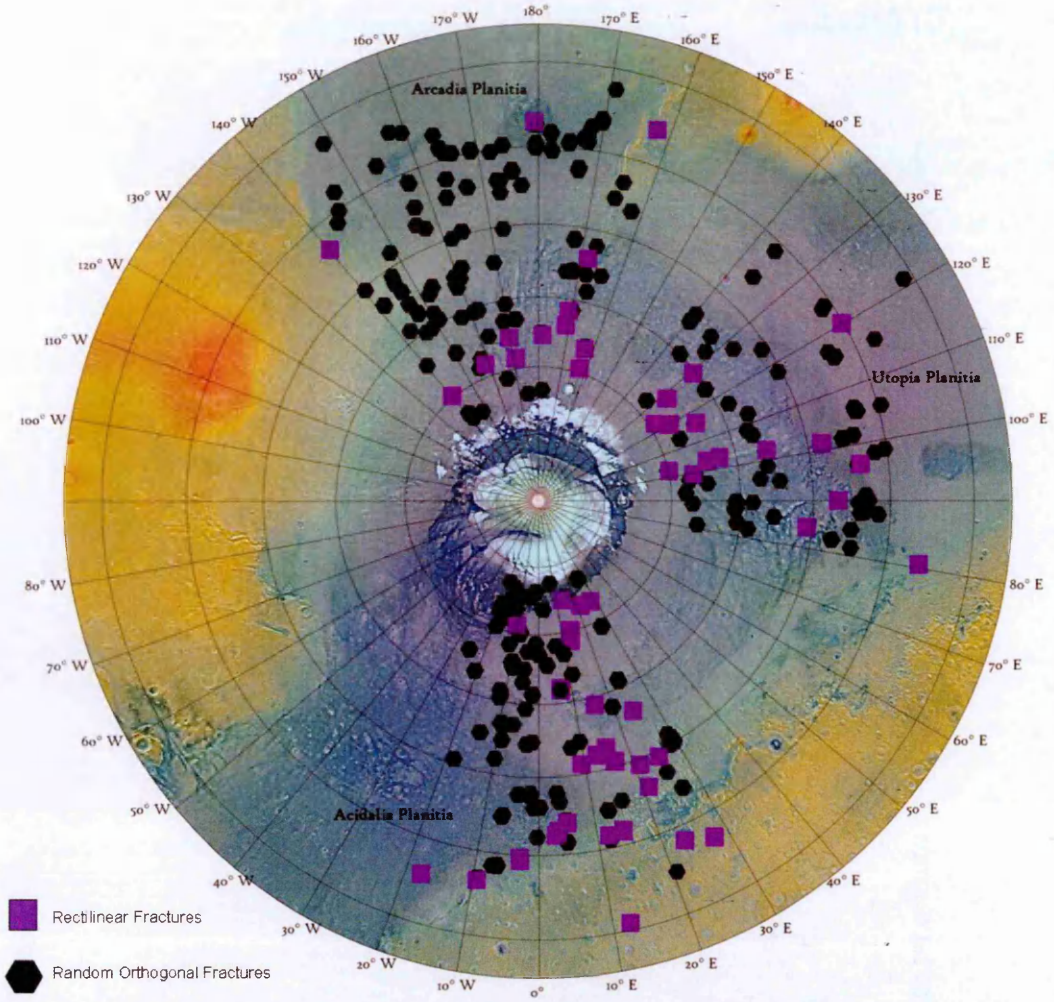

Figure 7.24: Distribution of rectilinear and random orthogonal fracture patterns found in HiRISE images.

As can be seem from Figure 7.24 random orthogonal patterns are far more prevalent than rectilinear ones. Rectilinear structures are most common in the northern parts of the Utopia and Arcadia study areas. They are found across the eastern part of the Acidalia study area but not in the central to western part. Random orthogonal patterns are found in roughly equal numbers in all areas of the HiRISE survey except for those covered by lineated valley fill such as the southern part of Acidalia Planitia.

Table 7.4: Distribution of fracture patterns in Acidalia Planitia.

Acidalia					
Latitude Band	**30-40**	**40-50**	**50-60**	**60-70**	**70-80**
Area Surveyed (km^2)	12186.2	6557.02	3159.49	2779.59	6866.38
Number of HiRISE Images	50	52	34	22	55
Random Orthogonal	11	22	24	26	27
Rectilinear	7	8	6	2	5
High Centred	12	20	22	21	21
Low Centred	2	8	5	9	11
% of HiRISE Images					
Random Orthogonal	22	42.31	70.59	118.18	49.09
Rectilinear	14	15.38	17.65	9.09	9.09
High Centred	24	38.46	64.71	95.45	38.18
Low Centred	4	15.38	14.71	40.91	20.00
Utopia					
Latitude Band	**30-40**	**40-50**	**50-60**	**60-70**	
Area Surveyed (km^2)	8219.16	4940.64	3071.29	3955	
Number of HiRISE Images	38	38	26	24	
Random Orthogonal	4	24	21	21	
Rectilinear	2	4	2	9	
High Centred	4	25	15	17	
Low Centred	1	2	6	12	
% of HiRISE Images					
Random Orthogonal	8.00	46.15	61.76	95.45	
Rectilinear	4.00	7.69	5.88	40.91	
High Centred	8.00	48.08	44.12	77.27	
Low Centred	2.00	3.85	17.65	54.55	
Arcadia					
Latitude Band	**30-40**	**40-50**	**50-60**	**60-70**	**70-80**
Area Surveyed (km^2)	5188.19	3647.79	4100.88	2808.86	2364.71
Number of HiRISE Images	40	34	46	39	16
Random Orthogonal	24	24	27	22	5
Rectilinear	2	1	1	9	1
High Centred	19	25	22	17	2
Low Centred	6	2	11	8	0
% of HiRISE Images					
Random Orthogonal	48.00	46.15	79.41	100.00	9.09
Rectilinear	4.00	1.92	2.94	40.91	1.82
High Centred	38.00	48.08	64.71	77.27	3.64
Low Centred	12.00	3.85	32.35	36.36	0.00

7.5.3 Distribution of fractures in the CTX survey

The large scale polygons with diameters of a hundred metres or more are most common at lower latitudes below 57°N. They are comparable with features in Utopia Planitia which are often found in conjunction with scalloped depressions. Examples in Utopia frequently exhibit polygon junction pits, small but distinct depressions which can form where several fractures meet. These occur due to increased sublimation at the junctions of polygons, since more surface area is exposed at these locations (Séjourné et al., 2010). However polygon junction pits have not been observed in this area. Irregular fractures, large scale features which do not form polygons, are found across the study area, frequently in association with impact craters. These are also unlikely to be related to thermal contraction cracking.

Smaller scale polygons are frequently found north of 35°N. There is a large concentration along the planetary dichotomy boundary, but outside this area they are much less common at lower latitudes. These features become more common to the north of 55°N (at about the same latitude at which larger scale polygons become less common). They are ubiquitous north of 63°N.

The most common morphology is a "random orthogonal" pattern comprising hexagonal, pentagonal and less regular polygons. However, in a few places, rectilinear features are also found. These appear to be most common in places where topographic control constrains the fracture morphology. For example concentric rings of quasi rectilinear fractures are often found to occur within partially buried impact craters. Narrow channels have also been observed to contain a string of rectilinear features. Rectilinear features are most common between 66 and 71°N. This is a region with a large number of impact craters, where rectilinear or radial structures sometimes occur. It is also in the centre of the band in which small scale fractures are most common.

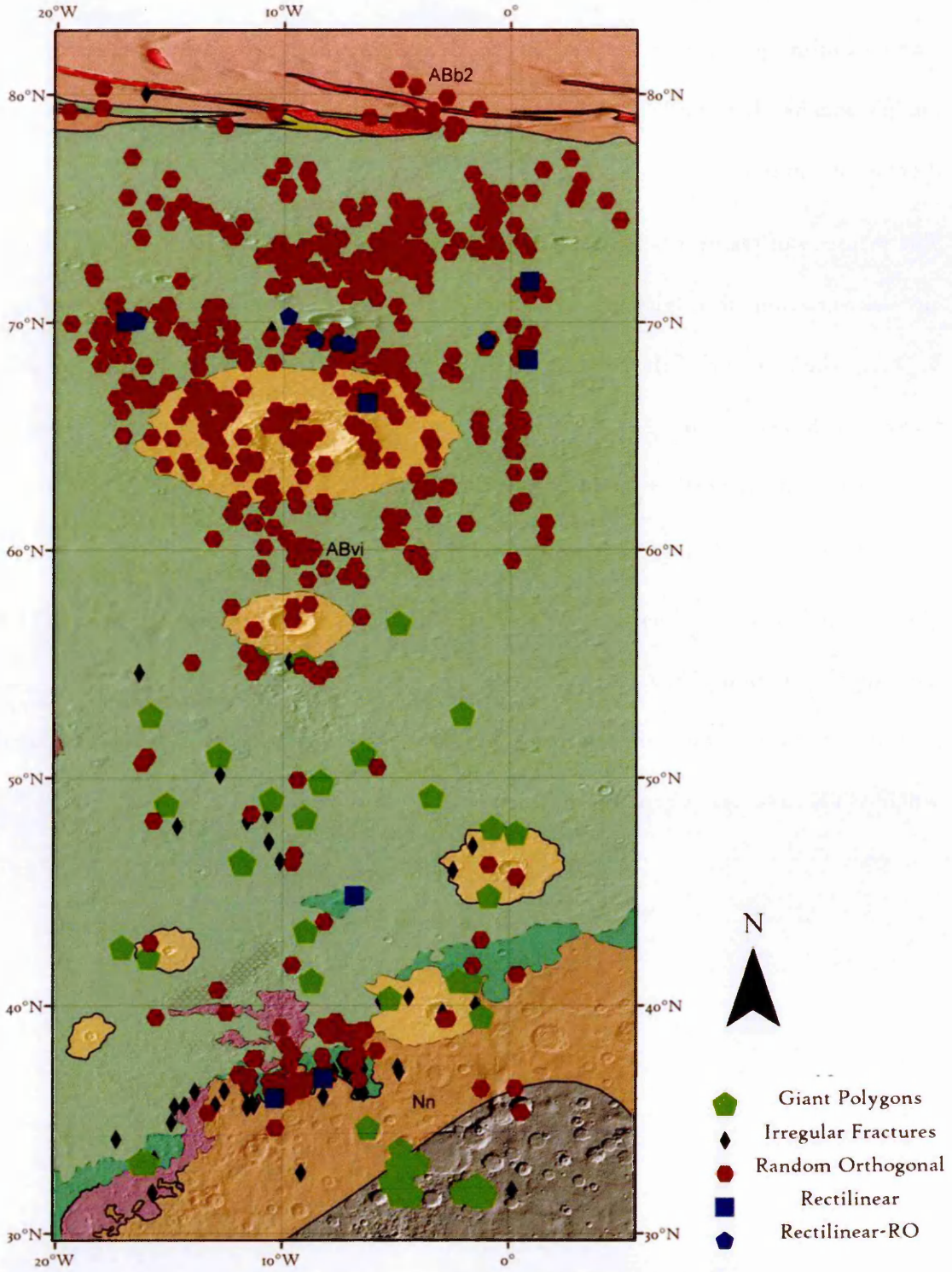

Figure 7.25: Distribution of medium to large scale fracture patterns in the CTX survey of Acidalia Planitia. The large polygons indicated by green pentagons and the irregular or isolated fractures marked with black diamond's are unlikely to be related to ice. The features marked in red and blue are more relevant to the investigation, since these are more likely to have formed as part of a periglacial assemblage.

In general it was impossible to determine whether fractures had low or high centres when examining them in CTX images. This is because the low resolution of the images means that while a network can be distinguished details of the fractures themselves cannot.

The majority of features below approximately 60-70 metres in diameter appear as quasi circular variations in brightness. Where HiRISE images are present these features can be seen to be made up of the same variety of random orthogonal fracture polygons as in areas with larger fracture nets. Albeit on a much smaller scale. Fractures are found in some places on the northern polar cap, and these have a similar morphology to those of the northern plains despite the different substrate.

The scarcity of features between 40-60°N could in part be due to the gaps in the CTX data in this region. This certainly accounts for gaps with no fractures at higher latitudes. However there are far fewer features in this latitude band even in the areas where CTX coverage is good.

7.6 Distribution of Gullies

Gullies have been observed across the surface of Mars (e.g. Balme et al., 2006; Jouannic et al., 2012; Raack et al., 2012), particularly in the southern hemisphere, but also on the walls of northern plains craters (Malin and Edgett, 2000). They are frequently found on crater walls and may suggest the erosive action of liquid water in geologically recent times (Johnsson et al., 2014).

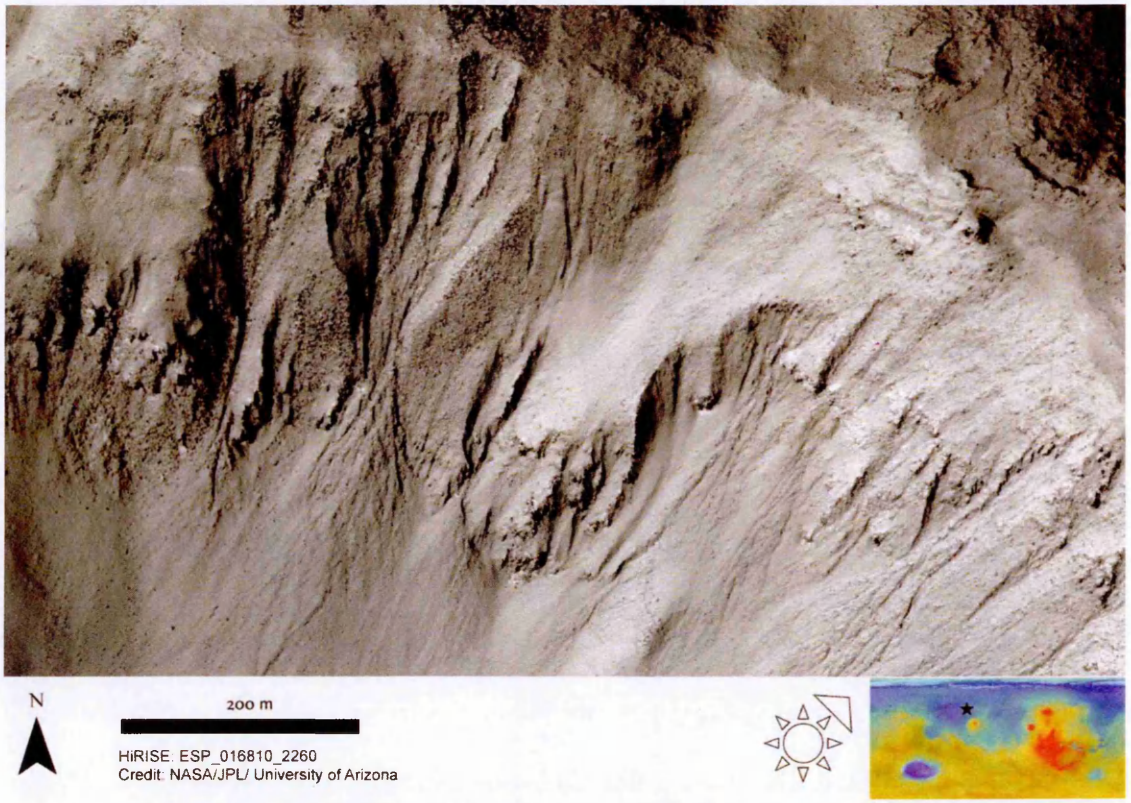

Figure 7.26: Example of Gullies on the rim of a small impact crater in Utopia Planitia.

In this survey gullies were observed across all study areas. Of particular interest were locations where multiple gullies occurred in proximity to other putative periglacial landforms. If gullies are formed through the action of liquid water in geologically recent times, then their presence as part of a periglacial assemblage lends significant weight to the observation. Gullies were frequently found to occur in close proximity to scalloped depressions. The latitudes in which these features are common overlap significantly.

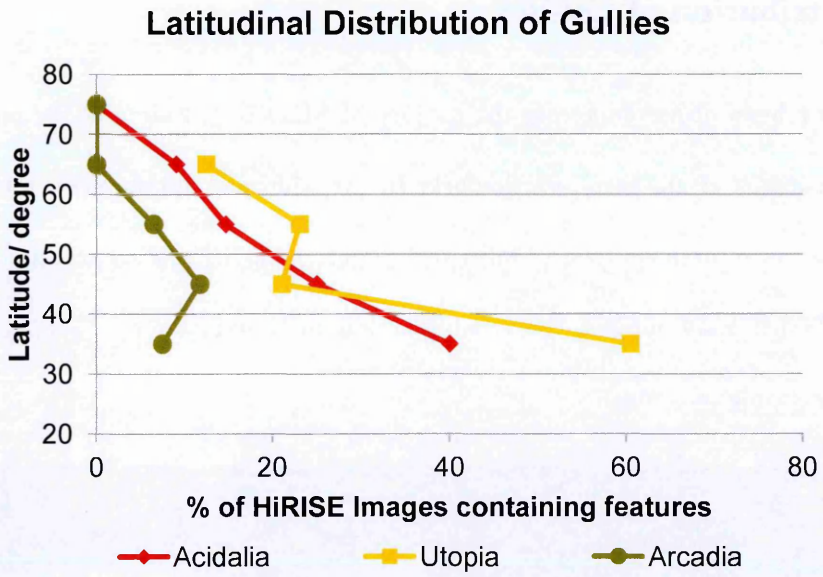

Figure 7.27: Distribution of gullies on the Northern Martian Plains. These data indicate the number of images in which features occur rather than being normalised by the total area surveyed.

As shown in Figure 7.27 gullies are most common at the southern part of all survey areas with the peak occurrence at 30-40°N in Acidalia and Utopia Planitiae and in the 40-50°N band in Arcadia Planitia. The concentration of gullies decreases dramatically further north. The most gullies were found in the Utopia Planitia area. This is the region that also had the highest concentration of scalloped depressions. The Arcadia study area has the fewest gullies, but this does not correlate with depressions as well, since Acidalia and Arcadia have similar scalloped depression distributions.

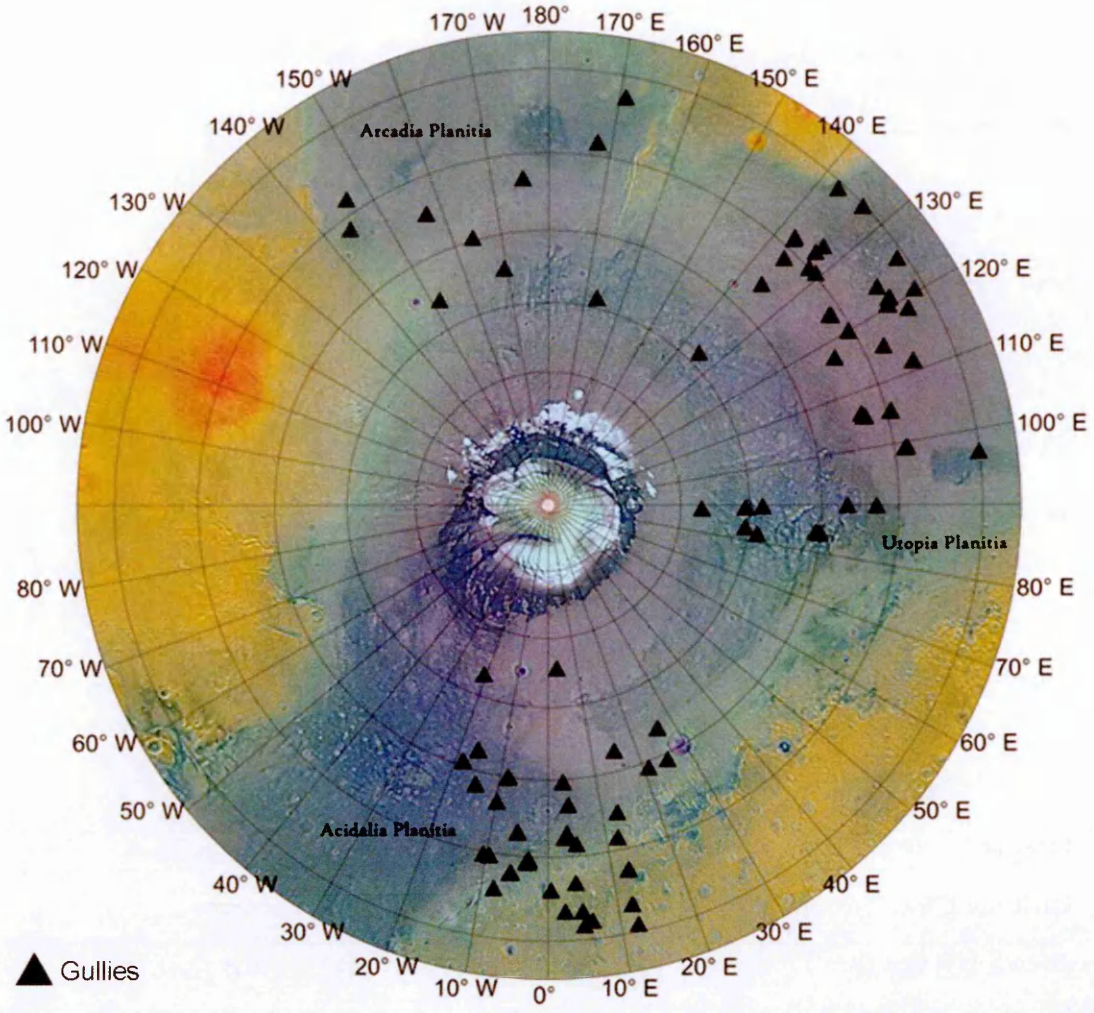

Figure 7.28: Distribution of gullies on the northern plains of Mars.

Figure 7.28 shows the geographic distribution of gullies illustrating that they are common at mid- to low-latitudes in all study areas except Arcadia. Only 10 sites were found in this region, falling between 32°N and 59°N. One possible gully was found which appeared to have been in-filled by later material, while the others were more pristine. 30 sites were found in the Acidalia Planitia area, and these fall between a similar range of latitudes; 31°N to 65°N.

The most examples of gullies are located in the low latitudes of Utopia Planitia where they are found across 40 HiRISE images, although three of these sites appear to contain

gullies that have become in-filled or otherwise degraded. In this study area, they are found between 30°N and 67°N. This is the largest latitudinal range of the three sites, although not dramatically different to the distributions in the other two study areas.

Gullies are far more common at lower latitudes than high. The majority of the features in all three study areas were found at or below 50°N and the same is true of the area surveyed in CTX images.

Table 7.5: Distribution of gullies in Acidalia Planitia.

Acidalia					
Latitude Band	**30-40**	**40-50**	**50-60**	**60-70**	**70-80**
Area Surveyed (km^2)	12186.2	6557.02	3159.49	2779.59	6866.38
Number of HiRISE Images	50	52	34	22	55
Number with Gullies	20	13	5	2	0
% of HiRISE Images	40	25.00	14.71	9.09	0.00
Utopia					
Latitude Band	**30-40**	**40-50**	**50-60**	**60-70**	
Area Surveyed (km^2)	8219.16	4940.64	3071.29	3955	
Number of HiRISE Images	38	38	26	24	
Number with Gullies	23	8	6	3	
% of HiRISE Images	46.00	15.38	17.65	13.64	
Arcadia					
Latitude Band	**30-40**	**40-50**	**50-60**	**60-70**	**70-80**
Area Surveyed (km^2)	5188.19	3647.79	4100.88	2808.86	2364.71
Number of HiRISE Images	40	34	46	39	16
Number with Gullies	3	4	3	0	0
% of HiRISE Images	6.00	7.69	8.82	0.00	0.00

7.7 Possible Periglacial Assemblages

In the preceding sections a variety of examples of features that could be periglacial have been presented. An assemblage is a site where a suite of landforms occurs in a single location with topographic and spatial linkages coherent with a periglacial formation hypothesis. Such sites could provide the strongest evidence that these features are part of a water rich, periglacial landscape, either now or in the geologically recent past. Here several possible examples of consistent periglacial landform assemblages are discussed.

The HiRISE image in Figure 7.29 covers the southern part of a small crater in Arcadia Planitia (at coordinates 58.56°N – 166.87°E.) This crater may show an assemblage of periglacial features. Gullies can clearly be seen on the southern slope of the crater and scalloped depressions occur in the crater interior. The interior also contains a slope covered in angular features which could be solifluction lobes. Fracture polygons indicative of thermal contraction cracking cover much of the interior of the crater. Quasi-rectilinear fractures overly the gully alcoves, while the debris fans from the gullies cover an earlier polygonal terrain which covers most the interior, overlying the scalloped depressions.

These landforms seem to form part of a single landscape. The possible solifluction lobes are forming on the slightly shallower slopes below the mouths of the gullies, while the interior of the crater is dotted with scalloped depressions. All of these features occur within the rim of the crater and so must have formed in the time since the impact occurred.

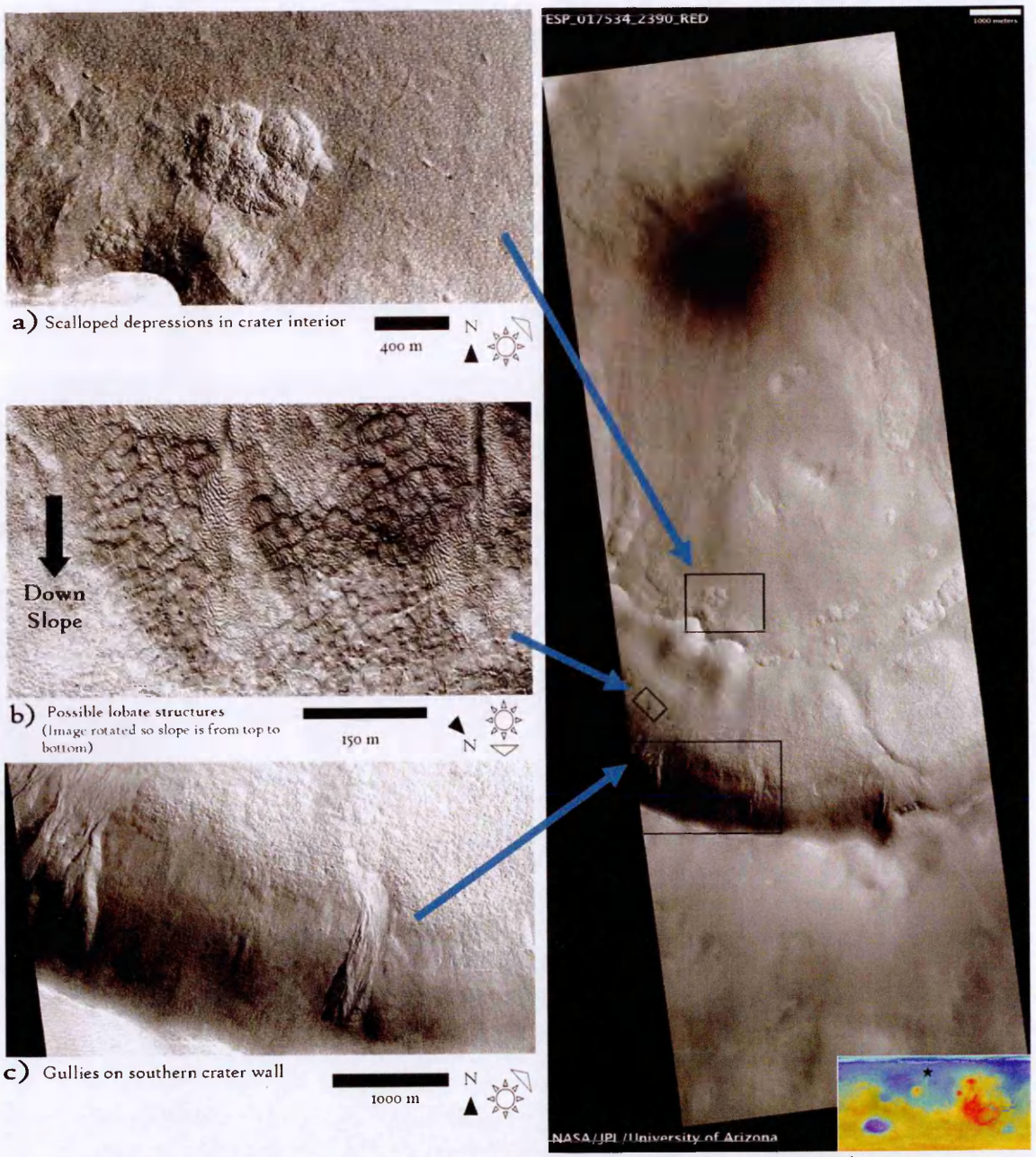

Figure 7.29: Possible Periglacial Assemblage in a crater in Arcadia Planitia.

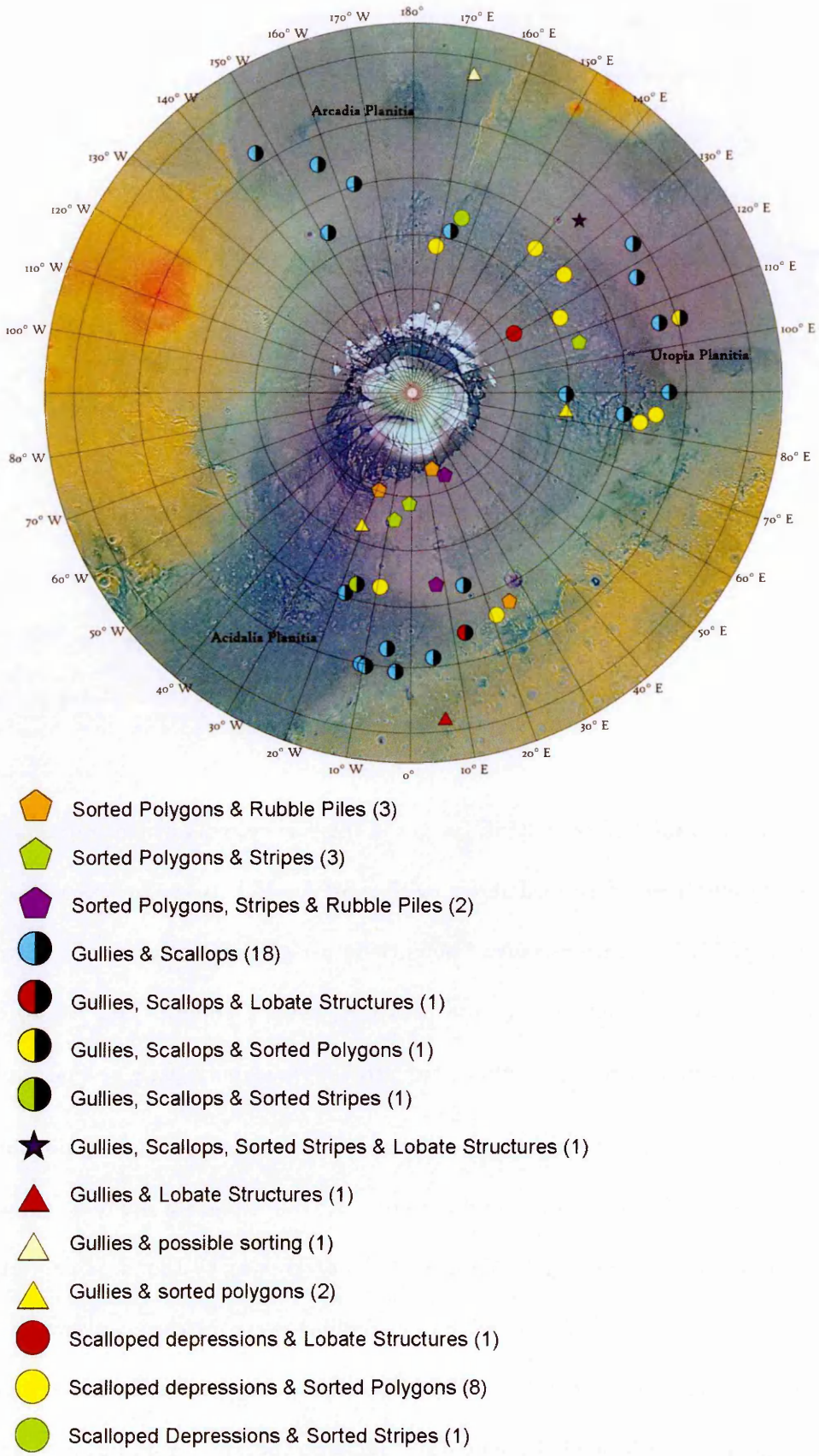

Figure 7.30: Distribution of possible periglacial assemblages on the Northern Martian Plains.

Other assemblages were found across the three study areas. The most common are locations where gullies and scalloped depressions occur in close proximity. Sites where multiple varieties of possible sorted patterned ground occur are also reasonably common within the areas where most sorting is found. Despite the overall scarcity of lobate structures three examples of these features are found as part of a possible assemblage. This adds weight to the hypothesis that they may have formed through periglacial processes.

Figure 7.30 shows the geographic distribution of possible assemblages across the northern plains. These are most common in Acidalia Planitia, where there is a high concentration of possible sorted features, and in Utopia where many examples of scalloped depressions and gullies are found. Arcadia Planitia has fewer of either of these types of feature, and Consequently fewer possible assemblages are found in this region.

There are a total of 44 HiRISE images in the survey areas which contain more than one of the landforms described above, with most found between 40° to 50° north. However in large HiRISE images several potentially periglacial landforms can be present within the same image, but not in close proximity on the ground. This has to be taken into account when deciding whether a site can be considered a periglacial assemblage.

The most common landforms to occur in close proximity are gullies and scalloped depressions. This is primarily due to the fact that these are the most common putative periglacial (or periglacially associated) landforms to be found as part of this survey. Sites where scalloped depressions and gullies occur in close proximity are the most common form of assemblage. This provides an additional strand of evidence that they might both be formed through water related processes. If gullies are carved by water released by melt (as seems most likely (Balme et al., 2006; Conway and Balme, 2014;

Conway et al., 2011; Costard et al., 2002)), then they would be expected to occur in places where conditions for thaw are favourable. Some gully like structures can be explained by other processes which do not require thaw, such as dry granular flows or erosion by CO_2, but erosion by liquid water is a strong possibility to explain their formation (e.g. Conway et al., 2011). The occurrence of gullies in proximity to landforms which resemble terrestrial thermokarst increases the probability that both landforms are forming in locations where thermokarst processes might be viable.

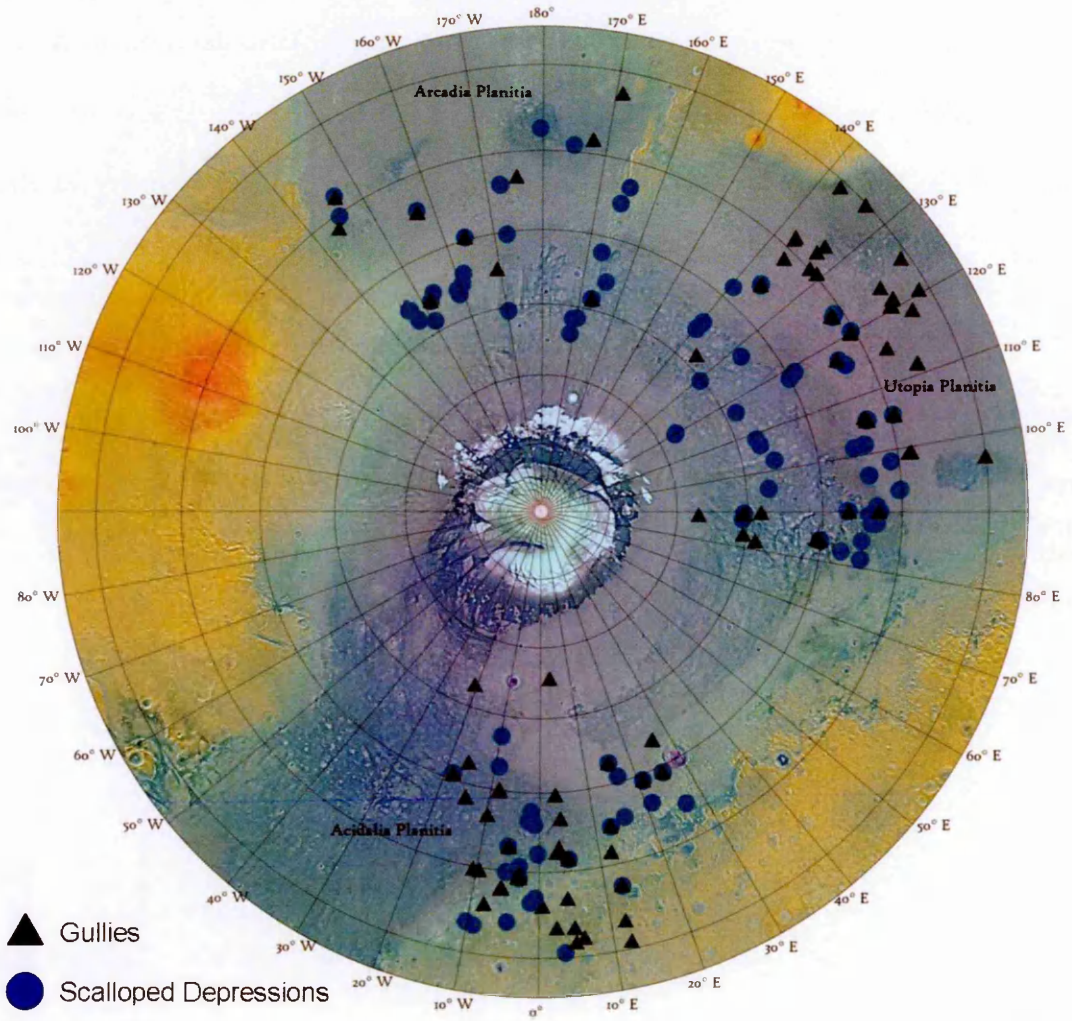

Figure 7.31: Comparison of Scalloped depression and gully distribution on the northern plains of Mars.

Scalloped depressions and gullies occur over much the same range of latitudes in all of the survey areas and there are numerous locations where both types of feature occur in the same HiRISE images. Figure 7.31 shows the distribution of all examples of scalloped depressions and all gullies. It can be seen that there is a considerable overlap between the two datasets in all study areas.

In Acidalia gullies and scalloped depressions occur over the same range of latitudes, approximately 40-67°N. However in Utopia more gullies occur at lower latitudes, while scalloped depressions are not found below 40°N, although other types of pitted ground can be found in this area. This is similar to the range of latitudes seen in Arcadia Planitia. This suggests that Acidalia Planitia may have an anomalously low number of features, although the Arcadia study area also does not contain as many of these features as the Utopia Planitia region.

The tables below list those HiRISE images in which possible assemblages have been found to occur. Possible assemblages are not as common as sites with individual landforms. Examples including the more unusual features, such as sorted patterns and solifluction lobes, are rarer still.

Table 7.6: Images containing multiple periglacial landforms each of the study areas.

HiRISE	Study Area	Degradational Features	Sorting Features
ESP_016828_2120	Acidalia	Gullies	Lobate Structures
ESP_017640_2895	Acidalia		Sorted Polygons & Rubble Piles
ESP_017685_2490	Acidalia		Sorted Polygons & Stripes
ESP_017711_2330	Acidalia	Gullies & Scallops	
ESP_017778_2200	Acidalia	Gullies & Scallops	
PSP_006649_2230	Acidalia	Gullies & Scallops	
PSP_001558_2265	Acidalia	Scalloped Depressions	Sorted Polygons
PSP_001942_2310	Acidalia	Gullies & Scallops	
PSP_007031_2220	Acidalia	Gullies & Scallops	
PSP_007123_2250	Acidalia	Gullies & Scallops	Lobate Structures
PSP_009087_2550	Acidalia		Sorted Polygons & Rubble Piles
PSP_010051_2435	Acidalia	Gullies	Sorted Polygons
ESP_025070_2330	Acidalia	Gullies & Scallops	Sorted Stripes
ESP_026441_2460	Acidalia		Sorted Polygons & Stripes
ESP_025716_2200	Acidalia	Gullies & Scallops	
ESP_027707_2195	Acidalia	Gullies & Scallops	
ESP_027839_2335	Acidalia	Scalloped Depressions	Sorted Polygons
ESP_016841_2340	Acidalia		Sorted Polygons & Stripes & Rubble Piles
PSP_007597_2530	Acidalia		Sorted Polygons & Stripes & Rubble Piles
PSP_006872_2275	Acidalia		Sorted Polygons & Rubble Piles
ESP_016888_2360	Arcadia	Scalloped Depressions	Sorted Stripes
ESP_017534_2390	Arcadia	Gullies & Scallops	
PSP_007472_2250	Arcadia	Gullies & Scallops	
PSP_007539_2420	Arcadia	Scalloped Depressions	Sorted Polygons
ESP_019657_2125	Arcadia	Gullies	Possible Sorting
PSP_010597_2300	Arcadia	Gullies & Scallops	
ESP_026420_2360	Arcadia	Gullies & Scallops	
ESP_027343_2185	Arcadia	Gullies & Scallops	
ESP_016113_2305	Utopia	Gullies & Scallops	
ESP_016573_2475	Utopia	Scalloped Depressions	Lobate Structures
ESP_016600_2370	Utopia		Sorted Polygons & Stripes
ESP_016732_2230	Utopia	Gullies & Scallops	
ESP_016746_2275	Utopia	Scalloped Depressions	Sorted Polygons
ESP_016810_2260	Utopia	Gullies & Scallops	Sorted Stripes & Lobate Structures
ESP_017008_2340	Utopia	Scalloped Depressions	Sorted Polygons
ESP_017181_2405	Utopia	Gullies	Sorted Polygons
ESP_017193_2390	Utopia	Scalloped Depressions	Sorted Polygons
ESP_017247_2250	Utopia	Scalloped Depressions	Sorted Polygons
PSP_002782_2230	Utopia	Gullies & Scallops	
PSP_007001_2200	Utopia	Gullies & Scallops	Sorted Polygons
ESP_018895_2410	Utopia	Gullies & Scallops	
ESP_019658_2345	Utopia	Scalloped Depressions	Sorted Polygons
ESP_020516_2240	Utopia	Gullies & Scallops	
PSP_008846_2220	Utopia	Gullies & Scallops	

7.8 Summary

Figure 7.32 and Table 7.7 summarise the distribution of all of the features discussed in this chapter. Martian analogues can be found for a wide variety of terrestrial periglacial features. Gullies and scalloped depressions are found over a wide range of latitudes in all three of the martian northern plains. Sorted polygons, stripes and solifluction lobes are the most characteristic elements of a terrestrial periglacial environment, but are also the least common landforms found in these surveys. Putative periglacial landforms have been found at lower latitudes than previously thought. Additionally several sites have been found where an assemblage of possible periglacial landforms occur. These are the areas where the evidence for the periglacial environment is strongest. Further evidence will be required to determine whether these features formed by one process rather than another. The next chapter will present the results of several studies to constrain the factors controlling the distribution of these features. This will compare their morphology and situation with analogous features from the terrestrial arctic to constrain whether these features are likely to be periglacial or not.

Table 7.7: Summary of landform distributions across the three study areas.

	Acidalia	31548.68 km²	167 Images	Arcadia	20186.1 km²	175 Images	Utopia	18110.4 km²	126 Images
Landform	Number of occurrences	Min Latitude	Max Latitude	Number of occurrences	Min Latitude	Max Latitude	Number of occurrences	Min Latitude	Max Latitude
Fracture Polygons	95	30	77	90	32	74	69	31	70
Sorted Polygons	38	37	74	17	36	73	17	40	68
Sorted Stripes	9	46	73	6	34	64	3	46	64
Rubble Piles	21	43	77	5	36	73	1	69	69
Lobate Structures	7	32	74	5	38	68	4	53	67
Scalloped Depressions	28	30	57	27	40	64	36	40	67
Gullies	38	31	66	10	32	59	40	30	67

Table 7.8: Number of each landform identified, normalised by the area and number of images surveyed.

	Acidalia	Area 31548.68	Images 167	Arcadia	Area 20186.1	Images 175	Utopia	Area 18110.4	Images 126
Landform	Number	By area	By number of Images	Number	By area	By number of Images	Number	By area	By number of Images
Fracture Polygons	95	3.01×10^{-03}	0.57	90	4.46×10^{-03}	0.51	69	3.81×10^{-03}	0.55
Sorted Polygons	38	1.20×10^{-03}	0.23	17	8.42×10^{-04}	0.10	17	9.39×10^{-04}	0.13
Sorted Stripes	9	2.85×10^{-04}	0.05	6	2.97×10^{-04}	0.03	3	1.66×10^{-04}	0.02
Rubble Piles	21	6.66×10^{-04}	0.13	5	2.48×10^{-04}	0.03	1	5.52×10^{-05}	0.01
Lobate Structures	7	2.22×10^{-04}	0.04	5	2.48×10^{-04}	0.03	4	2.21×10^{-04}	0.03
Scalloped Depressions	28	8.88×10^{-04}	0.17	27	1.34×10^{-03}	0.15	36	1.99×10^{-03}	0.29
Gullies	38	1.20×10^{-03}	0.23	10	4.95×10^{-04}	0.06	40	2.21×10^{-03}	0.32

a) Acidalia Planitia

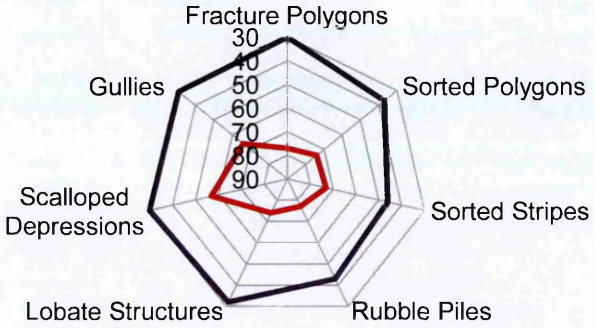

b) Arcadia Planitia

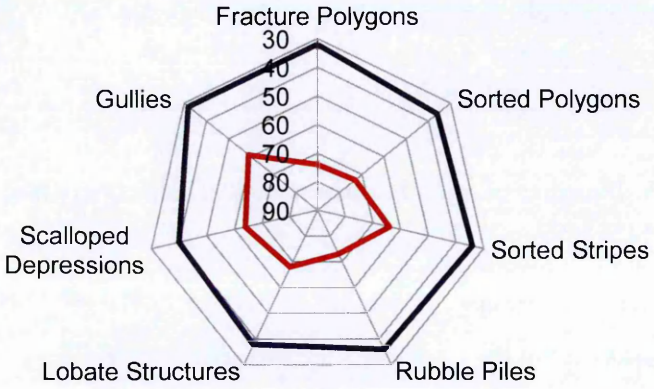

c) Utopia Planitia

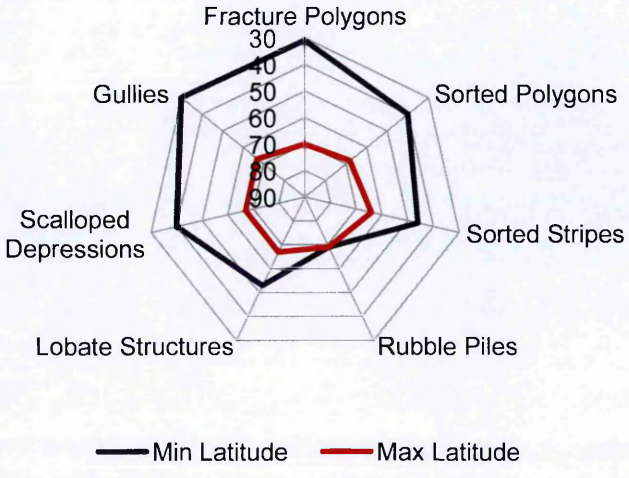

Figure 7.32: Latitudinal extents of the landforms described in this chapter. The red line indicates the northernmost latitude at which a landform is observed, and the blue line the southernmost latitude. a) Acidalia Planitia, b) arcadia Planitia, c) Utopia Planitia.

8 Chapter Eight: Analysis of the distribution of putative periglacial landforms

Chapter Seven has outlined the distribution of a variety of putative periglacial landforms, and possible periglacial assemblages. This chapter will build on those results to determine what factors control the distribution of these features.

The features described in Chapter Seven have morphological similarities to terrestrial periglacial landforms. However the definition of a periglacial landscape is based on process, not morphology. Similarities in morphology are a useful starting point, but further evidence is needed to test whether these landforms fit a periglacial paradigm. Specifically it must be demonstrated that putative periglacial features formed through processes relating to the freezing and thawing of ground ice.

Since in situ observation of these features is not yet an option it may not be possible to definitively conclude which processes led to their formation. However various strands of circumstantial evidence can be assessed to test whether a periglacial explanation for these features is probable. In the sections that follow the distribution of several of these features – clastic patterned ground, lobate structures and scalloped depressions – are compared to various parameters that might be expected to control their distribution if they are periglacial in nature.

8.1 Parameters to consider

For permafrost-related processes to occur, ground ice must be present. Landforms in ice free environments are unlikely to be periglacial, unless they formed during a past period when ground ice was present. Data from the Mars Odyssey Neutron Spectrometer suggest that hydrogen-rich terrain, probably indicative of the presence of water ice in the upper 50-100 cm of the surface, is found to the north of 60°N (Feldman

et al., 2002). The Gamma Ray Spectrometer on the same spacecraft also suggests the presence of ground ice in this latitude band (Boynton et al., 2010). It has been proposed that a layer of buried ice-rich ground, overlain by ice-free material, occurs over much of the mid to high latitudes (Boynton et al., 2010; Feldman et al., 2004, 2002). The insulating layer appears to be thinnest at the poles, and becomes increasingly thicker towards the equator (Boynton et al., 2010;). Ground ice is currently thought to be stable in the near subsurface at mid to high latitudes and a putative ice-dust mantle is observed north of around 40°N (Kreslavsky and Head, 2002; Mellon and Jakosky, 1995; Mustard et al., 2001). Consequently, it can be presumed that the ice-rich environment necessary for periglacial processes is present at mid to high latitudes, being uncommon and unstable to the south of 40°N, and becoming increasingly common and stable at high latitudes.

An ice-dust mix is likely to be a reasonably good medium for periglacial processes provided that the ice can thaw sufficiently to produce an active layer. As discussed in Chapter Three the fine particles believed to make up the global dust layer on Mars could potentially provide the fine grained fraction needed to make martian regolith frost-susceptible. A complete grain size analysis of the soil at these sites would be needed to thoroughly assess frost susceptibility.

Ground ice appears to be most prevalent and closest to the surface at high latitudes, this is thus where periglacial features would be expected to be most common. However this relies upon the occurrence of sites with sufficiently high temperatures to allow thawing to occur. Temperatures high enough to induce thawing are expected to only occur on slopes which receive high insolation and at latitudes above 30°N (e.g. Costard et al., 2002; Kreslavsky et al., 2008). However, even in these locations it would be expected

that thawing would only occur on the hottest days of the year, and may not occur in the current climate.

During periods of higher obliquity pole-facing slopes at mid latitudes will receive the most insolation. Kreslavsky et al., (2008) suggest that thaw could only have occurred on mid latitude, pole-facing slopes during periods of high obliquity. In more recent times, the temperature conditions across much of the northern plains would not be expected to be suitable for periglacial processes.

As described in Section 3.3.6 it is possible that the presence of cryobrines could allow thawing at lower temperatures. This would expand the range of conditions over which periglacial environments could develop, and potentially allow the continued occurrence of a periglacial landscape during periods with less favourable climatic conditions. The presence of cryobrines might allow processes which would otherwise be restricted to pole facing slopes to occur in other locations. More crucially it would allow thawing to occur more frequently, increasing the speed at which a periglacial landscape could develop. Sorted patterned ground requires repeated freezing and thawing, so more frequent thaw events would significantly increase the likelihood of recognisable features developing.

Even if it is possible for periglacial features to occur under a wider range of temperatures they would still be expected to occur preferentially at the sites with the most favourable conditions. Even if periglacial features can occur away from pole facing slopes they should still be looked for there. In summary periglacial features would be most likely to occur:

- At high latitudes,
- In areas with plentiful ground ice
- On slopes with high insolation,

Under present conditions equator facing slopes will receive the most insolation and so be the favoured environment for the formation of periglacial features. Landforms that formed during higher obliquity periods would instead be expected to form on steep pole facing slopes. Consequently, slope aspect can be used to speculate on the period during which these landforms probably developed.

8.2 Latitudinal Control

The latitudinal distributions of these landforms are discussed in detail in Chapter Seven. It is clear that while many features do occur at high northern latitudes they are not limited to them. The majority of clastic polygons and solifluction features are found in the northern part of the survey area, as are many of the best examples. However, other features with similar morphologies are found further to the south as low as 35°N in some cases. These mid-latitude features could have developed in unusual microclimates or in the presence of cryobrines. However, it is also possible that they formed through a process unrelated to the periglacial environment, but which produces a landform with similar morphology.

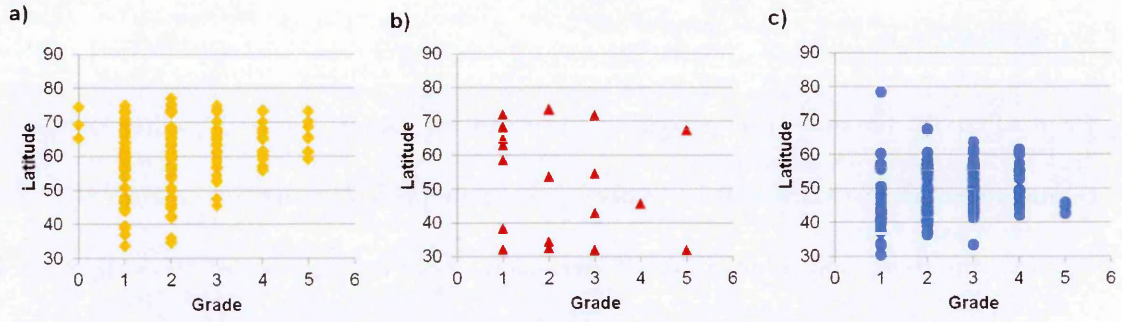

Figure 8.1: Plots of feature grade against latitude. This was assessed using a five point scale with 5 being the most representative features and 1 the least representative. The parameters discussed in chapter five were used for assessing sorted features, while lobes and scallops were graded using a similar methodology and the type examples presented in chapter six. a) Sorted patterned ground, b) lobate structures and c) scalloped depressions.

Figure 8.1 illustrates that while examples of sorted features and scalloped depressions are found across a wide range of latitudes those that were graded as the better examples of the type are predominantly found within much narrower latitudinal ranges. The best examples of sorted features are all found north of 60°N, while the best examples of scalloped depressions fall within the 40-50°N range. The range of latitudes over which a feature is found can be seen to increase with decreasing feature grade.

The preferential occurrence of sorted structures at high northern latitudes fits with prior observations of these features and makes sense in the context of their ideal formation environment. These landforms would be expected to occur in very ice-rich terrain and the northern reaches of the survey area best fit this criterion.

The occurrence of the highest graded scalloped depressions within the mid latitudes fits with the observations of these features in Utopia Planitia by other researchers (e.g. Morgenstern et al., 2007; Séjourné et al., 2011). These landforms may form through the degradation of ice-rich units by sublimation processes, so it is to be expected that they will occur in the region where an icy mantle is less stable as this is where it will most easily be degraded.

Lobate structures would be expected to occur under a similar range of conditions to sorted patterned ground and so should be most prevalent at high northern latitudes. However the best examples of lobate structures do not have a tendency towards a smaller range of latitudes. Features of all grades are found across the entire range of latitudes surveyed. It is interesting to note that two of the three grade 4 and 5 features are found at much lower latitudes than previous studies have detected these features (Gallagher and Balme, 2011; Johnsson et al., 2012).

The highest latitude examples of lobate forms are generally graded much lower. It is possible that the lack of a clear pattern in their distribution is due to the low number of

lobate features found overall. It is likely that if more features were available for analysis a clearer pattern would emerge and it would be possible to determine which, if any, of these examples constitute outliers or occur in specific, favourable microclimates.

8.3 Topographic Control

Since elevation and aspect have a significant effect on the temperature and insolation conditions at the surface, topography is also expected to be an important controlling variable. In the terrestrial case study described in Chapter Four larger sorted polygons occur at higher elevations, while those features at sea level were smaller in scale (see illustrations throughout Chapter Four and in Feuillet et al., 2012). This is likely to be due to the difference in temperature conditions between low and high elevations.

The same pattern of distribution would not be expected on Mars where periglacial features would be limited to the locations where the warmest temperatures occur. The presence of putative features on pole facing slopes at mid latitudes would support the hypothesis that they formed though periglacial processes during periods of high obliquity since such environments would have received increased insolation during the northern summer at high obliquity. A preference for an alternate aspect would favour a different formation mechanism.

The gradient of slopes on which these structures occur could also be significant. Sorted stripes and solifluction features are the result of hill slope processes and so would be expected to occur on steeper slopes than sorted polygons (Francou et al., 2001; Kessler and Werner, 2003). A tendency for these features to be found on slopes with higher gradients would consequently support a periglacial hypothesis, while their occurrence on flat ground would not.

In order to assess topographic control, measurements for aspect and gradient were derived from the global elevation map produced by the Mars Orbiter Laser Altimeter (MOLA). It should be noted that the resolution of this data set is very low relative to the size of the features and so this limits the reliability of these observations. Ideally a similar comparison would be made using gradient and aspect measurements from HiRISE digital elevation models (DEMs). Unfortunately these are only available for a very small fraction of the martian surface and so the majority of sites where putative periglacial features occur lack HiRISE DEMs.

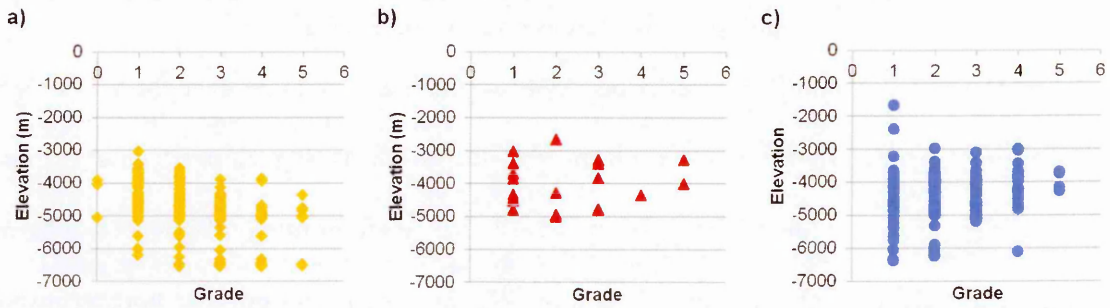

Figure 8.2: feature grade against elevation. a) possible sorting, b) lobate features and c) scalloped depressions.

It can be seen that all of these features occur at a wide range of elevations. Lobate structures tend to not be found at as low elevations as sorted patterned ground with no features occurring below -5000 m elevation. This may be due to their nature as a hill slope feature that is not usually found on low lying, flat ground. The best examples of both scalloped depressions and sorted structures are found at higher elevations than many of the less highly graded features. However numerous low grade features are also found at similarly high or higher elevations.

Since sorted stripes are also hill slope features it would be expected that they would occur at higher elevations than the majority of sorted polygons. This does appear to be the case. Figure 8.3 shows that both possible stripes and rubble piles are generally found at higher elevations than polygons. Possible stripes occur between -5000 and -3500 m

below the datum, while polygonal structures occur over a wider range of elevations, with many examples being found below -5000 metres. Relatively few examples are found above -3500 metres.

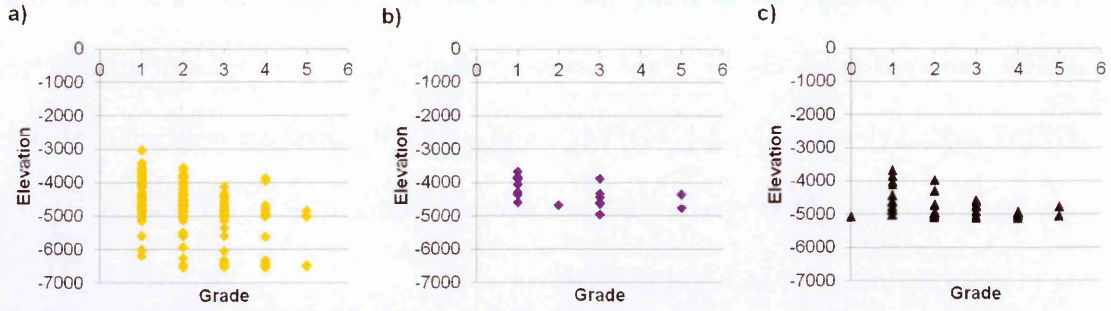

Figure 8.3: Breakdown of elevation data for possible sorted patterned ground into a) polygons, b) stripes and c) rubble piles.

Examples of these landforms occur on slopes with all aspects; however there is a trend for more features to be present on north and south facing slopes. This is most pronounced for the lobate features; however the small number of these landforms limits the reliability of this trend. It is however interesting to note that both examples of grade five lobate structures occur on south-facing slopes, whereas medium graded features are found on both north and south facing aspects.

Substantially more examples of both possible sorting sites and scalloped depressions are found on north or south facing slopes than on those with an easterly or westerly aspect. However in neither case is a northerly or southerly aspect dramatically more common than the other. This bias may suggest that these landforms may be occurring equally on slopes that are high insolation environments both in the present day and during past periods of higher obliquity.

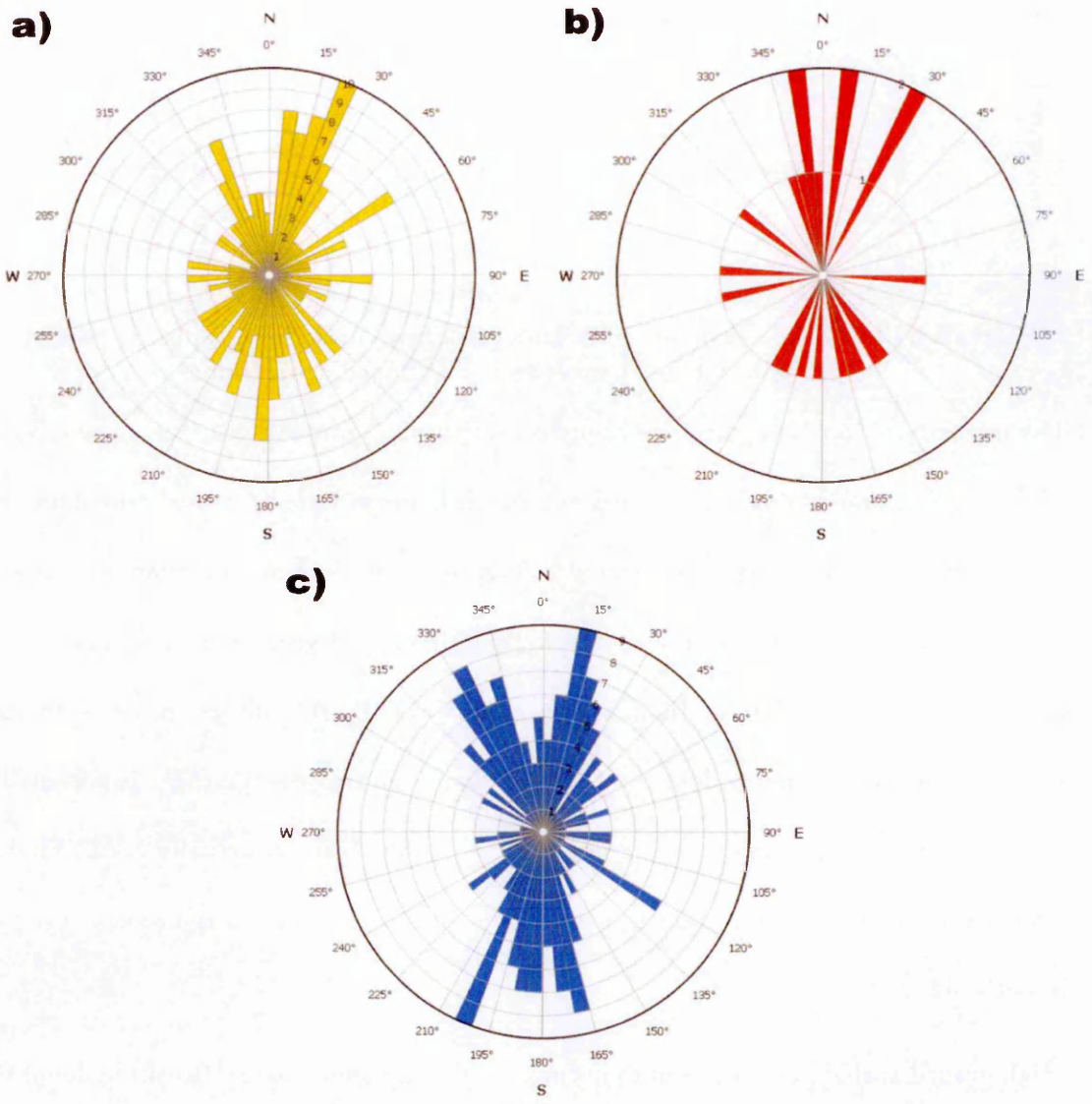

Figure 8.4: distribution of possible periglacial landforms by aspect. a) Sorted features, b) lobate structures, c) scalloped depressions.

The morphology of solifluction lobes is dependent on slope, as they assume a lobate morphology on slopes of greater than five degrees (Ballantyne and Harris, 1994), at which point they transition from a more sheet like structures found on shallower slopes. The plot of gradient for martian lobate structures thus agrees fairly well with them being solifluction features.

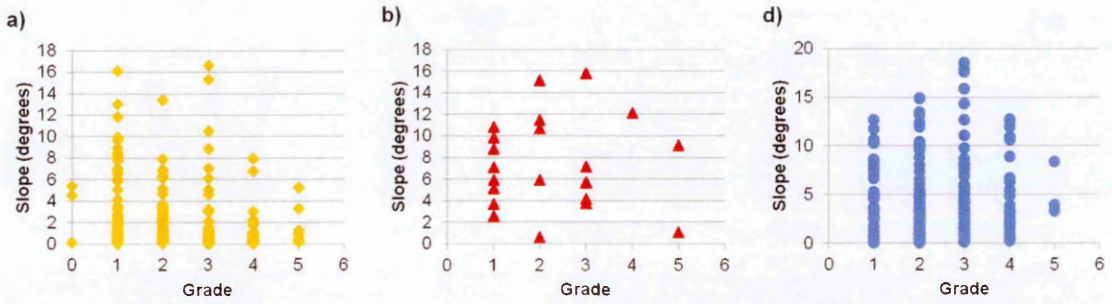

Figure 8.5: Plots of the variation in feature grade with underlying slope. a) possible sorting, b) lobate features and c) scalloped depressions.

The majority of lobate features are found on slopes of 5° gradient or more, although one of the highest graded examples occurs at a much lower gradient casting some doubt on the classification of this site (illustrated in Figure 7.10 in the previous chapter). Several medium graded features occur on slopes as high as 15 degrees which would not be uncommon for terrestrial solifluction lobes. However these numbers must be treated with caution, since the low density of MOLA points means that gradient is potentially averaged over a larger area than the slopes on which the features actually occur. Higher resolution digital elevation models would need to be generated to rigorously test this hypothesis.

High graded sorted patterns tend to occur on lower gradient slopes. Breaking down the possibly sorted features into their individual categories reveals some differences between the three types as shown in Figure 8.5. The majority of polygonal structures are found on slopes with a gradient of less than eight degrees. The majority of sites which occur on steeper slopes are graded much lower. The few examples of grade five polygons are all on very low gradient slopes and the range of gradients can generally be seen in increase as confidence in the features decreases.

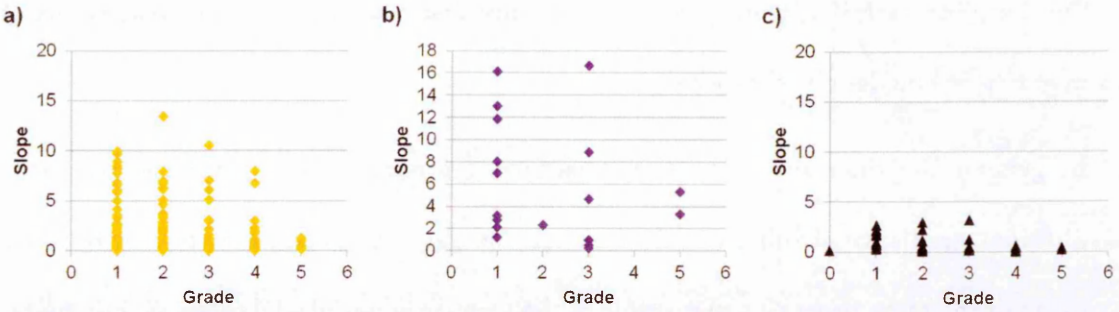

Figure 8.6: Variation in sorting grade with slope gradient. a) Sorted polygons, b) stripes and c) rubble piles.

Fewer examples of stripes occur but they are found over a wider range of gradients than polygonal structures. Once again the high gradient slopes are limited to the lower graded examples. The highly graded instances both occur on lower slopes, although in both cases these are found on crater walls, and so are definitely not flat surfaces, even if they occupy a low gradient pixel in the low resolution MOLA digital elevation model. Neither example of highly graded stripes is as flat as the less than two degree slopes on which the highest graded polygons are found. Rubble piles are all found on relatively low gradient slopes, the majority of features are found on slopes of less than one degree, which is in stark contrast to the examples of sorted stripes.

In the Lomonosov area, where the most numerous examples of patterned ground occur, there are two examples of possible sorted stripes. Both sites with possible stripes occur on steeper slopes, but sites with possible polygons do not seem to be controlled by the gradient. For example, some possible polygons occur on relatively steep slopes near the edge of Lomonosov Crater, although the majority are found either in the crater interior or on the flat surrounding plains. It should be noted that the overall range of gradients found across the study area is very small – as it is over much of the low lying northern plains.

Boulder clusters as a whole are slightly more common on south facing slopes, and least common on East and West facing slopes. However this is likely to be due to a bias in

the sampling as HiRISE images are not evenly distributed across the areas where the majority of boulder clusters occur.

In general the distribution of sorted patterned ground and lobate structures across different gradients of hill slope does match the pattern expected if they were formed through the same processes that result in the terrestrial periglacial features, but analysis of these features using higher resolution DEMs would be required to conclusively demonstrate this.

8.4 Presence of Near-Surface Ground Ice

As previously discussed the existence of a periglacial environment is predicated on the assumption that near-surface ground ice is present. The concentration of water equivalent hydrogen in the near surface is thus a useful indicator of whether ground ice is present at these sites.

Periglacial processes are associated with the presence of excess ice, whether in the form of ice wedges, lenses or needle ice. Excess ice occurs when the volume of ice exceeds the pore volume of the soil. Estimates of soil porosity for the phoenix landing site are in the range of 44%-50.5% by volume, based on a mixture of bulk basalt and hematite which would produce the measured volumetric heat capacity (Zent et al., 2010). Consequently, an excess of 40-50% ice by volume would be expected to equal or exceed the available pore space. Since water ice has approximately one third the density of basalt it can be assumed that Water Equivalent Hydrogen (WEH) in excess of 20-25% (a proportion of 0.2-0.25) by mass is indicative of excess ice in the near subsurface. This value should be treated with caution since it is based on a number of assumptions regarding the composition, density and porosity of martian soils which may not hold true over every site where putative periglacial features are observed. However it provides a rough threshold for the amount of WEH which would be expected at a

periglacial site. Furthermore WEH measurements are limited to the upper part of the soil column; it is possible that a site with a lower WEH could still have excess ice deeper within the subsurface.

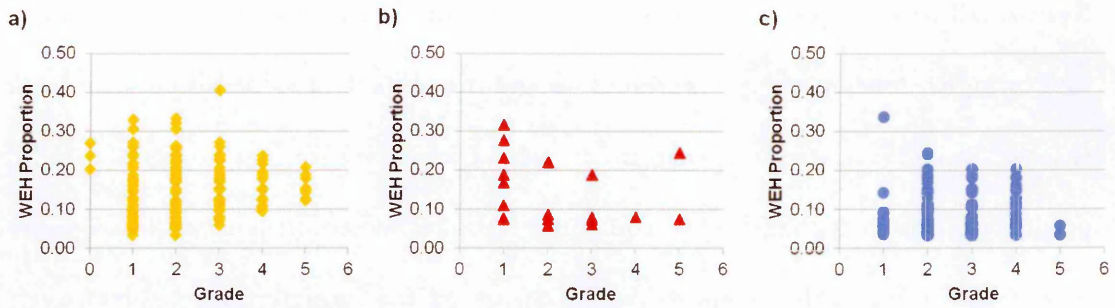

Figure 8.7: Variation in feature grade with proportion of water equivalent hydrogen in the near subsurface (by mass) all values given here and in the text are based on measurements of epithermal neutrons unless stated otherwise. a) Sorted patterned ground, b) lobate features, c) scalloped depressions.

The graphs in Figure 8.7 show the proportion of Water Equivalent Hydrogen (by mass) in the near subsurface at the sites where possible periglacial features occur. The stability of near surface ice is controlled by latitude as discussed earlier in this chapter, so landforms that occur at higher latitudes are also likely to occur where there is a higher proportion of WEH within the upper layer of the ground.

Lobate structures and clastic patterned ground are found in locations with the highest WEH. Some features are found at sites with 30%-40% WEH, indicating a very ice-rich substrate where excess ice is likely to be present. The majority of grade 5 sorting sites have a WEH between 10% and 20%, while some lower graded sites have WEH as high as 40%. The highest graded lobate structures are quite spread out in WEH, one site having a relatively low value of 7.4% while the other is higher, around 24%. The majority of lower graded features are also within this range.

These high WEH sites support a periglacial hypothesis since they confirm that the landforms are present, though not necessarily forming, in an ice-rich environment. However many features are also found at locations with much lower WEH. The

features at these sites could have formed during a period where more water ice was available at these latitudes (it is predicted to have been stable over much of the planet during some periods), or they might not be periglacial in nature.

Even small percentages of ground ice are significant. The lowest WEH at which grade four or higher lobes are found is around 5% and the equivalent value for possible sorting is 10%. While these are lower than the threshold for excess ice they are still fairly high ground ice fractions compared to equatorial latitudes, where little or no ice is present. These results would thus seem to support an ice related formation mechanism, even if there isn't as much ice in the present day as might be expected.

Scalloped depressions are mostly found at sites with lower WEH, with most sites having a lower WEH than the threshold for excess ice. This is probably due to the location of these features at predominantly lower latitudes where there is less stable ice in the near subsurface. Ice probably exists below the depth to which the Neutron Spectrometer can penetrate.

The presence or absence of frost in the vicinity of a feature can serve as an indicator of climate at the time the image was captured, though again not at the time the feature formed. Many fracture polygons exhibit bright material within the troughs which could be water ice. The presence of sharp un-degraded fractures in many locations suggests that they have formed in the recent past.

The WEH at the sites with possible periglacial assemblages were of particular interest. It was found that WEH values in proximity to these sites range from 3.4% to 26%. Only three assemblages have a WEH measurement above 20%. These sites are all at high northern latitudes and feature various permutations of clastic patterned ground. Twelve sites have WEH in excess of 10%. These sites contain a variety of landforms, representing all feature types under examination in various combinations.

Only one site contains all of the landforms: scalloped depressions, gullies, sorted patterned ground (in the form of stripes) and lobate structures. This occurs in HiRISE image ESP_016810_2260 in a cratered terrain region of Utopia Planitia in an unnamed impact crater on the edge of the Mie Crater ejecta blanket. This site has a relatively low WEH of 8.02% for epithermal neutron and 5.86% for fast neutrons, both well below the threshold for excess ice in the near subsurface. This may suggest that these features formed during a period when more ground ice was present, or that they did not require a very large proportion of ice to develop.

8.5 Comparison to Geological Units

It was also decided to test whether there was any correlation between the occurrence of possible periglacial features and any of the geological units mapped for the northern plains by Tanaka et al., (2005). However putative landforms and assemblages were found to occur indiscriminately over most of the geological units within the study areas. Most occur on the Vastitas borealis interior unit, but that is likely because this unit covers the largest area of the survey. All of the represented terrains have at least some examples of possibly periglacial features as shown in Figures 8.8-8.10. It is not thought that these features favour any one unit over another.

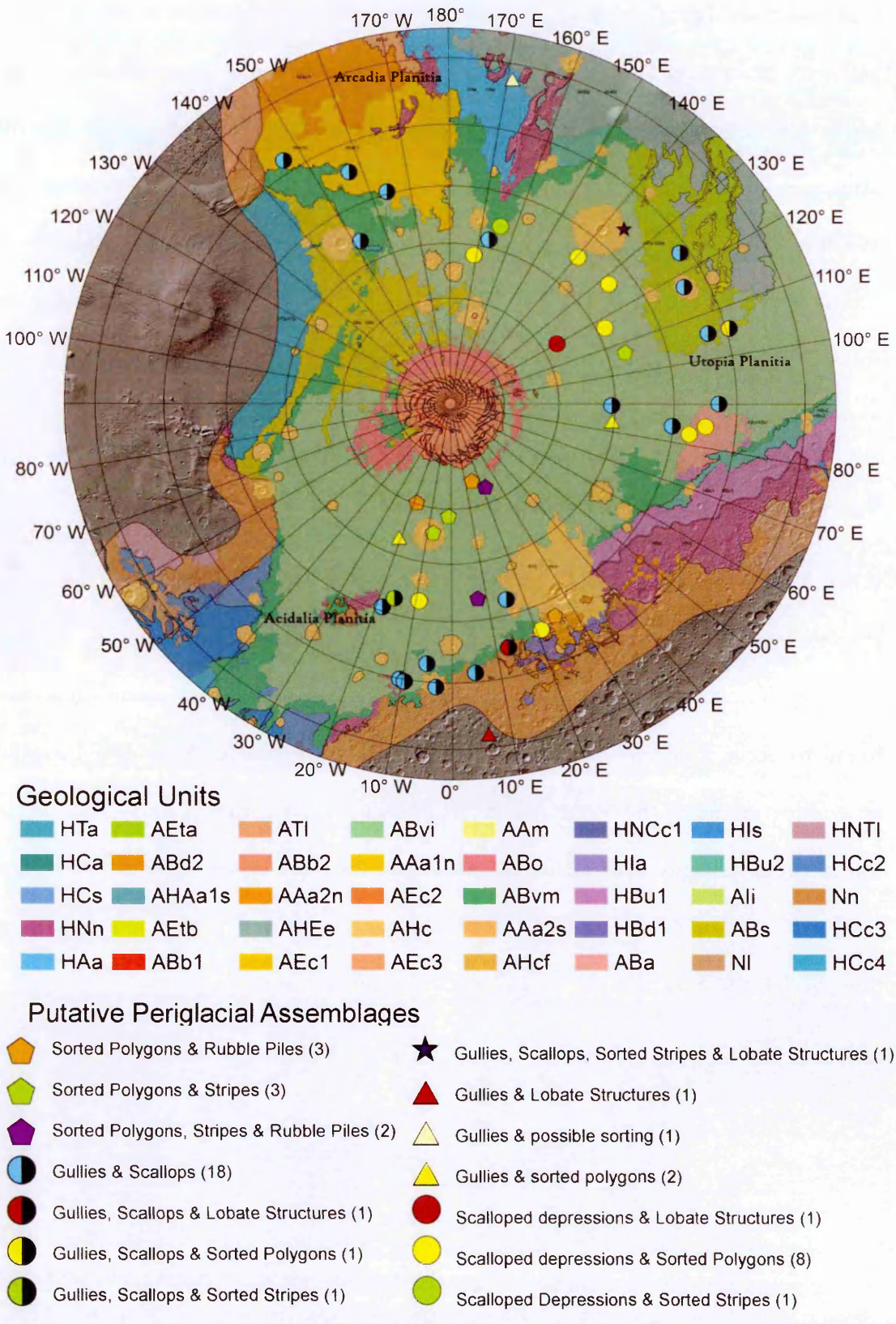

Figure 8.8: Distribution of possible periglacial assemblages plotted over the northern plains geological map of Tanaka et al., (2005). An enlarged version of this figure can be found in appendix 2.

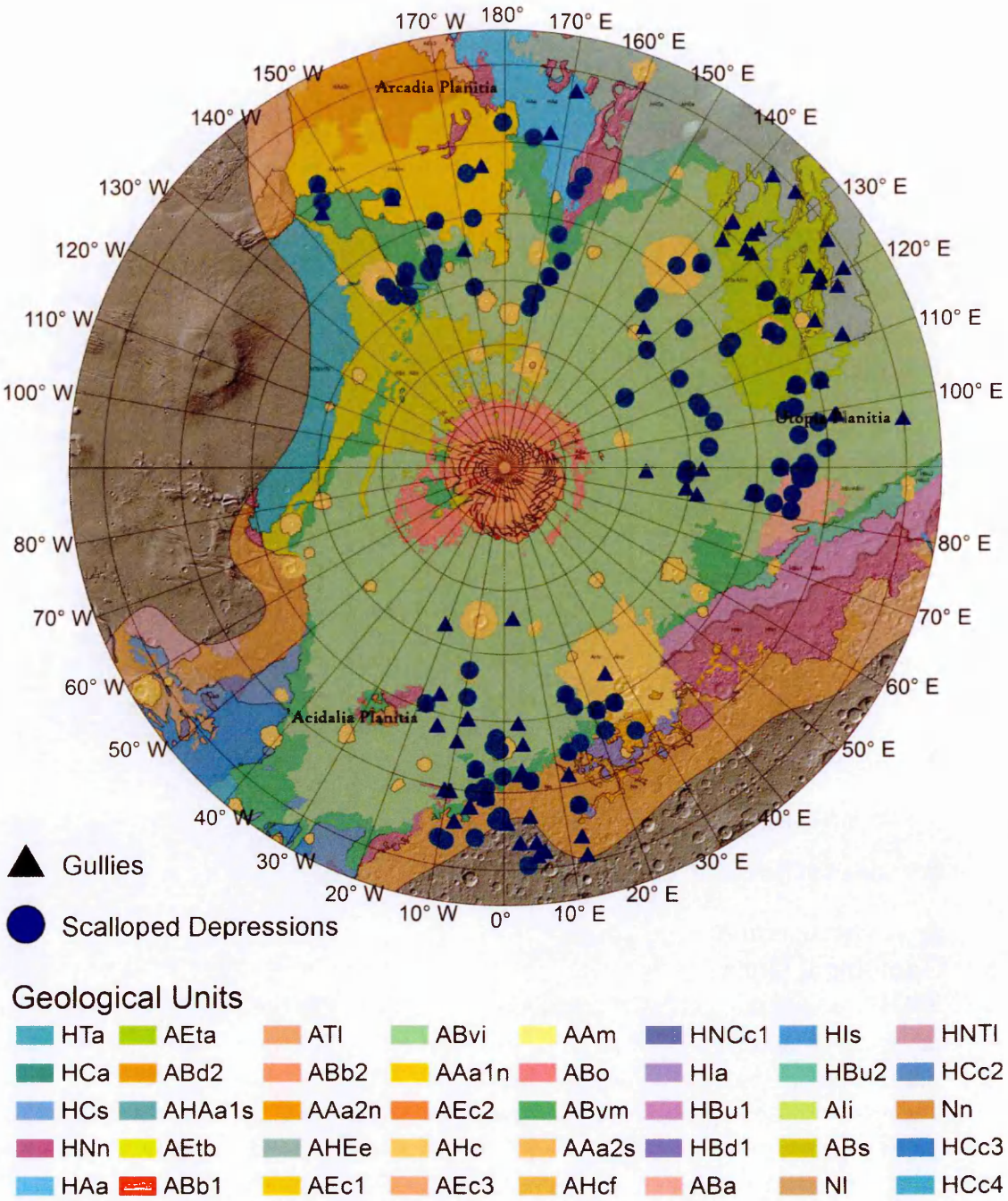

Figure 8.9: Distribution of Scalloped depressions and Gullies plotted over the northern plains geological map. An enlarged version of this figure can be found in appendix 2.

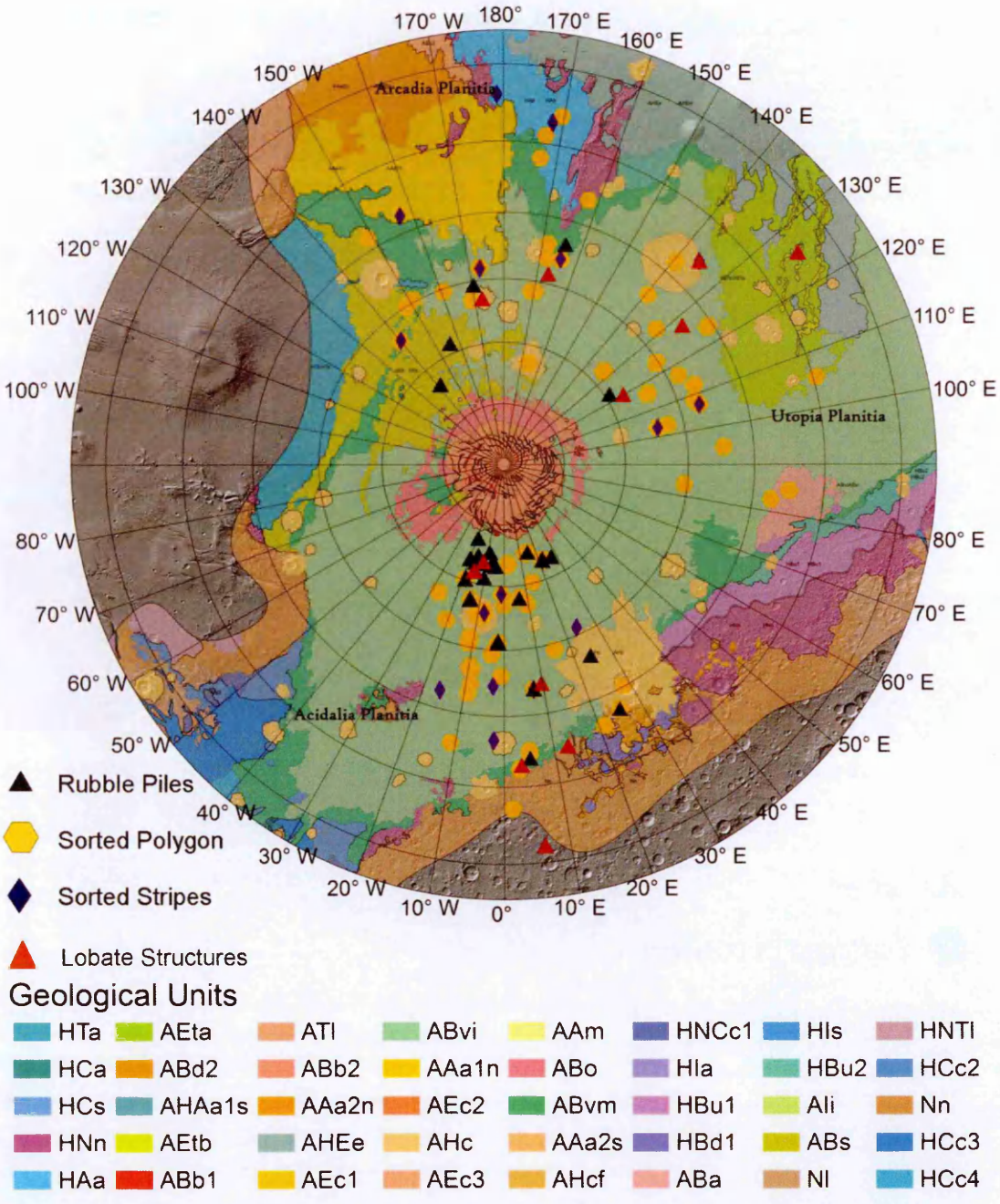

Figure 8.10: Distribution of Sorted Features and Lobate Structures over the geological map of the northern plains. An enlarged version of this figure can be found in appendix 2.

8.6 Summary

In summary the distribution of many of these features provides evidence for a periglacial analogue. Many examples of clastic stripes and lobate structures are found at higher elevations than features which would not be expected to develop on hill slopes and the gradients on which they are found are consistent with the morphologies of terrestrial sorted stripes and solifluction lobes.

Although not all of the examples described in Chapter Seven occur in ice-rich environments, many do. Some of the best examples of sorted patterned ground are found at sites where WEH would indicate the potential for excess ice in the near subsurface.

Scalloped depressions are largely found at low latitudes and this puts them outside the area where excess ground ice is estimated to occur. The lack of ground ice at these latitudes along with the degraded nature of many of these features could support an older formation age and this will be examined in more detail for the case study in Chapter Ten.

No particular link is found between the distribution of these features and the geological units mapped by Tanaka et al., (2005). These features are not thought to develop preferentially in any one geological environment. Their distribution is more likely to be controlled by environmental and situational parameters. When the topography and availability of ground ice are examined some correlations are found between higher graded features and the parameters which would be expected to control them were they periglacial.

9 Chapter Nine: Assessing the hypothesised formation mechanisms for martian clastic patterned ground.

9.1 Introduction

A variety of possible formation mechanisms have been put forward to explain the examples of clastic patterned ground discussed in Chapters Five and Seven. In this chapter several of these hypotheses, periglacial sorting, gravitational sorting and boulder ratcheting by CO_2 frost, will be examined to assess the likelihood that they are responsible for the formation of these landforms.

Since sorted patterned ground is characteristic of a periglacial landscape on Earth, its presence on Mars could provide strong evidence for ground ice thaw in that area. If alternate hypotheses can be demonstrated to explain these landforms without the need for thawing of ground ice then the presence of this landform is less significant.

Martian features around Lomonosov Crater are examined to test the viability of the frost ratcheting and gravitational sorting, collectively referred to as the "fracture controlled" mechanisms. The second part of the chapter then compares the morphology of these features to terrestrial analogues.

9.2 Background

The cold, dry conditions of the martian environment cast some doubt on the veracity of a periglacial explanation for these features. Consequently, some researchers have proposed alternate mechanisms which might allow the development of martian clastic patterned ground without needing to invoke periglacial processes.

Three main hypotheses have been proposed to explain the formation of the boulder patterns observed on the northern plains of Mars. It has been suggested that they could have formed as a result of thaw, either during past periods of high obliquity, or in more recent times due to the influence of perchlorate brines (e.g. Gallagher and Balme, 2011)

Alternately these structures could result from the interaction of boulder strewn ground with fracture polygons. This could occur through gravitational sorting (Levy et al., 2010, 2008a; Mellon et al., 2008) or more exotic processes involving ratcheting of boulders trapped in Carbon Dioxide frost (Orloff et al., 2013). These possibilities, which will collectively be referred to as the Fracture Control hypotheses can be assessed by determining which examples of clastic patterned ground superpose fracture polygons. In locations where both types of network are collocated the patterns can be compared to determine whether boulder distributions match those of the underlying fracture nets, and whether boulders appear to have fallen into contraction cracks through gravitational sorting. Each of these hypotheses is briefly discussed below.

9.2.1 Boulder Ratcheting

In the boulder ratcheting model of Orloff et al., (2013) it has been suggested that apparently sorted, clastic network features could result from the interaction of boulders with a layer of carbon dioxide frost. In the winter, the temperatures drop and CO_2 from the atmosphere condenses to form a slab of frost up to a metre deep, trapping loose boulders. These boulders are locked in place by the CO_2 frost and so are not moved when thermal contraction cracks open in the ground due to the change in temperature. When the temperature rises again it triggers the sublimation of the carbon dioxide frost and the closing of the contraction cracks. The boulders are now free to move and so there will be a net migration towards the contraction cracks. According to Orloff et al.,

(2013), this would result in the formation of a clastic net parallel to the underlying fracture net.

9.2.2 Gravitational Sorting

It has been suggested that boulder patterns in the martian high latitudes could result from the gravitational sorting of large clastic material (Levy et al., 2010, 2008a; Mellon et al., 2008). In this model the presence of degraded fracture patterns can result in the slumping and rolling of clastic material into the topographic lows, producing clastic polygons (Levy et al., 2008a). This hypothesis would neither require the action of freeze thaw nor an interaction of boulders with carbon dioxide frost. Consequently it would provide a simpler mechanism to explain the observed structures at sites where fracture control is apparent.

9.2.3 Periglacial sorting

The formation of sorted patterned ground through freeze-thaw sorting has been discussed in detail in chapter two. Chapter three has presented the mechanisms that could allow thawing to occur in the Martian environment. In summary it seems likely that the presence of brines such as perchlorate in the martian near surface will depress the freezing point and allow thaw to occur (Hecht, 2002; Marion et al., 2010). The recent detection by Ojha et al., (2015) of hydrated salts in the vicinity of recurring slope lineae (RSL) in the equatorial regions of Mars lends considerable weight to this hypothesis.

Periglacial morphology is not as easily identified as fracture controlled arrangements are. The absence of a controlling fracture network at a site does not prove that it formed through this mechanism. However a variety of terrestrial studies have described the form and structure of periglacial features. These characteristics provide a

baseline to assess whether martian patterned ground is morphologically similar to terrestrial analogues, or whether there are key differences which might suggest a different formation mechanism.

Of particular interest to this investigation are studies where the gradient at which sorted polygons transition to a stripe like morphology. Estimates of circle size across a wide range of environments are also important in constraining the range of feature scales extant on Earth.

One of the first studies to systematically classify sorted patterned ground morphologies was that of Washburn, (1956). This study characterised different patterned ground types including sorted polygons, stripes and labyrinths as well as non sorted patterned ground. This study provides a thorough review of the older literature on sorted patterned ground and formed the basis for much of the later work on the subject. Examples are cited across the terrestrial cold climate regions. Washburn reports features at a variety of scales. Polygons of up to 10 m in diameter are described, but larger sorted circles are only said to be up to three metres across. Sorted stripes with widths of 1.5 m are described and the transition from polygons to stripes is noted to occur on slopes of 3 - 7 degrees. Washburn (1979) reports that stripes do not persist on the steepest slopes, in excess of 40 degrees. Goldthwait, (1976) reports that sorted patterns are not usually found on slopes greater than 20 degrees. This review describes larger sorted forms as being in the range of 2 to 20 m.

Later studies support these observations. The studies of Hallet et al., (Hallet, 2013; Prestrud and Hallet, 1986), report circular features in the 3-4 metre range at their study areas in Spitsbergen although they note that elongated features can be larger. Werner and Hallet, (1993) model the development of sorted stripes. They note that stripes are found on gentle hill slopes but do not cite the gradients at which the transition from

polygons to stripes occurs. Similar observations are made by Nicholson, (1976) who notes that elongated forms are generally found as a transitional feature between sets of stripes and more symmetrical polygonal features. Ray et al., (1983) report that the transition to stripes generally occurs on slopes between 3 and 7 degrees, although they are likely reporting the figure given by Washburn, (1956). This study emphasises that predicting the transition with slope is a key feature that models of sorted patterned ground must replicate. This reinforces that this is a diagnostic feature of periglacial patterned ground.

Krantz, (1990) describes sorted polygons grading into stripes on a slope of 2-3 degrees. This would seem to suggest that stripes can occur on shallower slopes. Since a transitional region is characterised by increasingly elongated polygons it is likely that different studies have identified the cut off between polygons and stripes at different points. They suggest that the elongation of polygonal networks is due to the increased drainage of steeper slopes, which elongates the shape of subsurface convection cells from which these patterns originate.

Ballantyne and Matthews, (1982) describe the structure of sorted circles in Norway and note that discontinuous networks are present at their site. This fits with some of the observations of martian features which do not exhibit a coherent coarse domain. They report that the largest circles observed at the site were 3.5 meters in diameter, with most being under a metre. Features larger than 1.5 m in diameter are only found on the crests of moraines which they hypothesise to experience a more extreme temperature regime.

9.2.4 Aims

The aim of this chapter is to test the viability of each of these proposed formation mechanisms. Fracture control is assessed in section 9.3. The relationship between boulder networks and underlying fracture networks is characterised across the

Lomonosov Crater study area. If these features formed as a result of fracture control then boulder networks would be expected to have the same general pattern as the underlying fracture networks. The gravitational sorting mechanism would sort boulders into the fracture troughs, while the boulder ratcheting hypothesis would be more likely to produce lines of clasts parallel to the fractures. Section 9.4 then examines the periglacial hypothesis. This mechanism would not produce a fracture controlled arrangement, but the absence of a fracture relationship is insufficient to accept a periglacial hypothesis. The best indicator of periglacial sorted patterned ground is the elongation of polygons with increasing slope and this is discussed for examples from this study area. The effect of the lower martian gravity on the scale of sorted features is also examined.

9.3 Testing the Fracture Control Hypotheses.

If the hypothesis that the organisation of clasts is controlled by underlying fracture patterns is correct then the observed boulder nets would be expected to occur on terrain containing well-developed fracture networks, and the distribution of clasts should follow the pattern of the fractures. Consequently, it is possible to assess whether the patterns of the boulder nets in a sample region appear to be fracture controlled, or whether the organisation of clasts appears to be independent of any thermal contraction polygons.

The region of extensive patterned ground around Lomonosov Crater in the north of Acidalia Planitia was chosen for this study since it had the largest number of clastic patterns of any site in the survey, and it has already been demonstrated in Chapter Five that these patterns are significantly different from a random distribution.

In this study all of the 147 boulder patches described in Chapter Five were examined. For each, the presence or absence of networks of fractures and clasts were recorded as was the relationship between the networks.

9.3.1 Results

Each site consists of a single boulder patch, which may or may not contain an underlying fracture network or exhibit organisation of clasts. These sites are typically a square kilometre in area. Fractures are found in 13 out of the 16 HiRISE images surveyed, but are much less common in the images covering the crater interior: very faint fractures can be seen at a few sites, but most boulder patches within Lomonosov crater itself do not overlay fracture nets at all. Images covering the plains beyond the ejecta of Lomonosov Crater exhibit more pronounced fracture nets.

Table 9.1: Summary of results of the analysis to determine how many sites exhibited fracture control.

No Fractures	55	/147
Fractures uncertain	7	/147
Fractures present	85	/147
Present, but no relationship to clasts	36	/147
Present, uncertain relationship	35	/147
Present, clear relationship	21	/147
Sites without fracture control	91	/147

Fractures are present in 85 of the 147 boulder patches and are tentatively or uncertainly identified in a further seven. Fifty-five boulder patch sites definitely do not exhibit fractures. Of the sites where fractures can be found only 21 show a clear relationship between the arrangement of clasts and the underlying fracture net. A further 35 sites have an uncertain relationship, in which it is not clear whether the organisation of clasts mirrors that of an underlying fracture net. Even if the presence of a fracture net controls the organisation of boulders at these sites there remain 91 sites where there is

no link between the two, either due to the absence of fractures or the absence of a clear relationship between the patterns.

Table 9.2: Summary of Results

HiRISE Image	Boulder clusters	Showing Organisation	Max Sorting Grade	Description	Fractures Present	Fracture Control Evident
ESP_017580_2460	21	21	3	Clasts by fractures	2	2 possible
ESP_027918_2455	1	1	3	Lines of clasts	0	0
PSP_007440_2455	3	3	4	Discontinuous net	3	1 possible
PSP_010644_2455	14	14	4	Discontinuous net	0	0
ESP_026441_2460	9	8	2	Discontinuous net	1	0
TRA_000846_2475	3	3	3	Lines of clasts	3	3 certain
ESP_017131_2485	27	14	2	Possible clustering	26	9 possible, 1 certain
ESP_017632_2475	28	20	4	Discontinuous net	23	15 possible, 1 certain
ESP_019900_2470	1	1	3	Lines of clasts	1	1 certain
ESP_026850_2475	5	5	5	Clastic stripes	5	5 certain
ESP_025769_2435	1	0	3	Lines of clasts	0	0
PSP_010051_2435	6	6	3	Faint net	5	1 possible, 2 certain
PSP_001520_2470	2	2	4	Discontinuous net	2	2 certain
ESP_023738_2415	6	4	0	No sorting	4	3 possible
ESP_025294_2415	10	10	4	Possible stripes	5	3 possible, 2 certain
ESP_017079_2410	8	7	3	Clasts by fractures	8	1 possible, 4 certain
ESP_026441_2460	2	2	3	No sorting	0	0

The Presence or absence of an underlying fracture net was also filtered against the sorting grade classifications, defined in Figure 5.7, to assess whether the presence of an underlying fracture net appeared to be responsible for the degree of boulder organisation at these sites. Table 9.3 summarises the number of sites of each sorting grade with and without fractures and the number of sites which appear to exhibit fracture control. In cases where the number of sites with or without fractures and with or without fracture control do not add up to the total it is because sites where a fracture net is uncertain have not been counted.

It can be seen that the sites without fractures generally have a higher sorting grade than those with fractures, while the sites where fractures are present, but unrelated, are also correlated with higher sorting grades than sites where there does seem to be a relationship.

Table 9.3: Fracture control assessment.

Grade	Description	All Sites	With Fractures	Without Fractures	Fracture Control	No Relationship	HiRISE Images
0	No evidence of organisation	26	21	4	0	23	6
1	Uncertain clustering	32	27	2	6	9	7
2	Clustering of clasts	38	23	15	9	21	13
3	Clear lines and arcs	35	10	22	5	25	12
4	Discontinuous net	15	3	12	1	12	4
5	Continuous net	1	1	0	0	1	1
	Total:	147	85	55	21	91	16

In many cases sites where the two network types do appear to be related consist of clusters of boulders separated by the fractures, rather than lines of clasts following fracture lines, or discontinuous nets superimposed on the fracture pattern. This morphology is to be expected anywhere a fracture net cross-cuts a boulder field and so is not indicative of the boulder ratcheting processes proposed by Orloff et al., (2013). It is also not consistent with the gravitational sorting mechanism in which clasts are concentrated by slumping into polygon- bounding troughs (Levy et al., 2010; Mellon et al., 2008).

All sites exhibiting probable fracture control on the clastic patterns are located on the plains beyond the ejecta of Lomonosov Crater. This is probably partly due to the lower proportion of fracture patterns within the crater interior.

There are only three images where all of the boulder halos appear to exhibit fracture control: all of the sites within ESP_026850_2475 appear to be fracture controlled. These features consist of clastic networks ranging from grade 1 to grade 3. Some of these features include coherent lines of clasts following the underlying fractures. The same is found in PSP_001520_2470, where both boulder clusters (grade 2 and 3 respectively) exhibit a degree of fracture control. However, in this instance the fractures are much fainter. TRA_000846_2475 is the only other image where all of the sites appear fracture controlled, but here all of the sites within the image are grade 2 and so do not suggest a very strong likelihood that sorting is present in the first place.

Several other images have a few boulder patches which appear to exhibit fracture control, usually corresponding to patches with low sorting grades. The only grade four site to exhibit fracture control is in ESP_025294_2415, to the south of Lomonosov crater. This site overlays faint fractures, which are more pronounced elsewhere in the image. Here the discontinuous net definitely reflects the underlying fracture pattern. One other site in this image contains a grade four net with underlying fractures, but here there is less well-expressed fracture control. PSP_010051_2435 contains a grade four discontinuous clastic net with possible fracture control from the faint underlying polygons, but here it is impossible to be certain that the fractures and the clastic net are consistent in orientation and location.

9.3.2 Boulder ratcheting or gravitational sorting?

The two fracture control hypotheses would produce a different arrangement of clasts. If gravitational sorting predominates then clasts would be expected to be found inside troughs or overlying fractures. If boulder ratcheting is producing the arrangements then boulder patterns would be expected to follow the lines of fractures, but not to overlay them.

In order to determine whether either of these situations predominated within the fracture controlled sites the relationship between clasts and fractures was characterised. Of the sites where fracture control might have been present the likelihood of fracture control was assessed and the type of relationship categorised. The results are summarised in Table 9.4 while table 9.5 lists which sites demonstrated each type of relationship.

Table 9.4: Categorisation of fracture control relationships around Lomonosov crater.

Clast-fracture relationship	Number of sites
Clustering between fractures	41
Clasts in troughs	4
Uncertain	11

It can be seen that the majority of sites where fracture control is possible have a tendency for clasts to be clustered between or around the fractures, rather than overlaying or within them. Sites where clasts can be seen to be in troughs are few and far between, although these are more likely to be definite fracture control sites, due to the clearer relationship making it easier to determine whether they are related. Many of the sites where boulders are clustered between fractures are categorised as possibly exhibiting fracture control, but whether they are or not is often uncertain.

This would seem to suggest that a boulder ratcheting hypothesis is more likely to explain sites where fracture control is evident. However the generally low proportion of sites where fracture control is likely means that these features may simply occur through chance. Many sites have uncertain fracture control; relatively few have a definite relationship between the positions of the clasts and the underlying fracture pattern. Over the entire HiRISE survey only seven sites were found where clastic

patterned ground consisted of clasts clustered within troughs. These sites are found in: ESP_023738_2415, ESP_017079_2410, PSP_008204_2440, ESP_019083_2395, ESP_018990_2395, PSP_006872_2275, and PSP_007738_2480 (Figure 7.22).

9.3.3 Summary

While fracture control may be responsible for some of the lower grade features within the study area, it is clear that the majority of the discontinuous nets across the area are not fracture controlled. In particular while the sorted stripes in ESP_017131_2485, the only feature to score a grade five on the classification scheme within this study area, do overlay a fracture net; they do not exhibit any evidence of fracture control. This is the same relationship observed by Gallagher et al., (2011) in Heimdal crater, and shows that the sorting process and the fracturing process are probably not related. Neither the frost locking nor the gravitational sorting hypotheses therefore seem likely to account for the organisation of clasts apparent in the Lomonosov Crater region.

Table 9.5: List of sites with probable fracture control

Id	Sorting grade	Fracture Control	Description	HiRISE Image
18	1	Possible	Uncertain	ESP_017580_2460
19	2	Possible	Clustering between fractures	ESP_017580_2460
23	3	Possible	Uncertain	PSP_007440_2455
49	2	Yes	Clustering between fractures	TRA_000846_2475
50	2	Yes	Clustering between fractures	TRA_000846_2475
51	2	Yes	Clustering between fractures	TRA_000846_2475
55	2	Possible	Clustering between fractures	ESP_017131_2485
56	2	Possible	Clustering between fractures	ESP_017131_2485
66	1	Possible	Uncertain	ESP_017131_2485
70	2	Possible	Clustering between fractures	ESP_017131_2485
71	2	Possible	Uncertain	ESP_017131_2485
72	2	Possible	Clustering between fractures	ESP_017131_2485
73	2	Possible	Uncertain	ESP_017131_2485
75	0	Possible	Clustering between fractures	ESP_017131_2485
77	1	Yes	Clustering between fractures	ESP_017131_2485

78	1	Possible	Uncertain	ESP_017131_2485
79	1	Possible	Uncertain	ESP_017632_2475
80	2	Possible	Clustering between fractures	ESP_017632_2475
88	1	Possible	Uncertain	ESP_017632_2475
89	1	Possible	Clustering between fractures	ESP_017632_2475
90	1	Possible	Uncertain	ESP_017632_2475
91	1	Possible	Clustering between fractures	ESP_017632_2475
92	1	Possible	Clustering between fractures	ESP_017632_2475
94	1	Possible	Clustering between fractures	ESP_017632_2475
95	1	Possible	Clustering between fractures	ESP_017632_2475
96	1	Possible	Clustering between fractures	ESP_017632_2475
99	1	Possible	Clustering between fractures	ESP_017632_2475
102	1	Possible	Clustering between fractures	ESP_017632_2475
103	0	Possible	Clustering between fractures	ESP_017632_2475
104	1	Possible	Clustering between fractures	ESP_017632_2475
105	1	Possible	Clustering between fractures	ESP_017632_2475
106	1	Yes	Clustering between fractures	ESP_017632_2475
107	3	Yes	Clustering between fractures	ESP_019900_2470
108	1	Yes	Clustering between fractures	ESP_02850_2475
109	3	Yes	Clustering between fractures	ESP_02850_2475
110	1	Yes	Clustering between fractures	ESP_02850_2475
111	1	Yes	Clustering between fractures	ESP_02850_2475
112	2	Yes	Clustering between fractures	ESP_02850_2475
114	2	Yes	Clustering between fractures	PSP_010051_2435
117	2	Yes	Clustering between fractures	PSP_010051_2435
118	4	Possible	Clustering between fractures	PSP_010051_2435
120	3	Yes	Boulders follow Fractures	PSP_001520_2470
121	2	Yes	Clustering between fractures	PSP_001520_2470
122	3	Possible	Uncertain	ESP_023738_2415
126	0	Possible	Possibly clasts in troughs	ESP_023738_2415
127	3	Possible	Clustering between fractures	ESP_023738_2415
128	4	Possible	Clustering between fractures	ESP_025294_2415
129	4	Yes	Clustering between fractures	ESP_025294_2415
134	3	Possible	Clustering between fractures	ESP_025294_2415
135	2	Yes	Clustering between fractures	ESP_025294_2415
136	3	Possible	Uncertain	ESP_025294_2415
140	3	Yes	Clasts in troughs	ESP_017079_2410
141	3	Yes	Clasts in troughs	ESP_017079_2410
143	2	Yes	Clasts in troughs	ESP_017079_2410
144	1	Possible	Clustering between fractures	ESP_017079_2410
145	1	Yes	Clustering Between Fractures	ESP_017079_2410

9.4 Sorted patterns as periglacial features?

The preceding analysis has shown that the fracture control hypotheses for the formation of clastic patterns do not provide a good fit for the landscape around Lomonosov Crater. This might suggest that the remaining periglacial hypothesis is a better fit; however this is far from certain. This section examines the extent to which these features are comparable to terrestrial patterned ground, drawing on earth based examples both from chapter four, and from the studies cited in section 9.2.3.

Upon initial examination martian patterned ground has a substantially different morphology to terrestrial features. The examples in chapters five and seven show discontinuous networks of metre scale boulders, surrounding patches of boulder free ground. This is in sharp contrast to many examples of terrestrial patterned ground which feature a complex coarse domain comprising a range of material from small cobbles up to the larger, boulder scale, clasts. It is interesting to note that discontinuous networks are reported by Ballantyne and Matthews, (1982), although these do not seem to be as common in terrestrial patterned ground.

This can partly be accounted for by the limitations of satellite images. As discussed in chapter four small scale variations in polygon morphology are largely below the resolution of remote sensing datasets. No details of the fine domains can be distinguished and the majority of coarse domain material is below the resolution of the image. Only the largest boulders can be clearly distinguished, and so a coarse domain might be expected to appear as a network of discontinuous clasts.

However in terrestrial images the coarse domain is frequently seen to have a substantially different albedo to the fine domain. In the images presented in chapter four there is a clear network of brighter material which connects larger boulders and

demarks a polygonal network. Similar albedo variations are also apparent in other periglacial sites such as the examples given by Kääb et al., (2014), Hallet (2013) and Kessler and Werner (2003). This would seem to suggest that this is primarily the case in terrestrial examples and the absence of clear changes in texture and albedo in the martian data is surprising.

However it should be noted that none of the examples listed occur on the same scale as the martian features, and none exhibit boulders in the same range of sizes. This discrepancy of form might be the result of the ubiquitous presence of an ice dust mantle in the martian high latitudes. Many of the sites examined in this study are found within haloes of boulders surrounding buried impact craters. It is possible that the same material that has buried the craters also covers the boulder networks, obscuring the textural differences between the coarse and fine domains. In situ examination of the martian sites would be needed to determine whether this is the case.

9.4.1 Morphological parameters

A set of 187 martian clastic polygons were digitised using the same procedure applied to terrestrial patterned ground in chapter four. These were selected from the areas around Lomonosov crater where the nearest neighbour analysis had been conducted. The boulder arrangements at these sites were demonstrated to be significantly different from a random distribution (see Section 5.4.1). Thus these areas had the highest probability of being genuine patterns. High graded areas were chosen and distinct polygons were selected where possible.

A series of parameters were recorded. These were: the area covered by a polygon, its perimeter length, the number of discernible clasts, the diameter of the largest and smallest clast and the mean diameter of the five largest clasts. The ratio of the polygon's long and short axes was used to calculate a dimensionless elongation factor

(long axis/short axis). The orientation of the polygon's long axis was also recorded and this was compared to the aspect of the underlying slope to determine whether the two were aligned.

All of these parameters were measured in the same way as those presented in chapter four. As discussed earlier in the thesis the Icelandic study area is a wet maritime environment and so is not the best analogue for comparison to martian features. The terrestrial survey served as a good test of the reliability of this methodology, but the reliability of direct comparisons between the sites is limited. Icelandic data will be plotted in a few places for comparison with the martian data, and in each case the features digitised from the air photo dataset will be compared. These circles were closest in scale to the martian features and showed the least alteration by terrestrial vegetation. However it is acknowledged that the form and structure of martian features would have evolved in a very different environment and so these datasets are not directly comparable.

Where possible other examples from colder arctic environments will be cited, and the structure of the martian structures will be compared to parameters already established within the terrestrial literature.

The error on these measurements is generally higher for the martian data than the terrestrial data. Measurements of clast size have an error of approximately the length of two pixels. For Earth this is approximately 30 centimetres, while for Mars these measurements are only precise to within 50 centimetres in the highest resolution images, and up to a metre for some of the lower resolution HiRISE areas.

The measurement of a polygon's long and short axes is reliable to within the width of the coarse domain. For martian examples this was generally one to two metres, while for terrestrial examples it was much smaller, within a metre on most of the polygons

digitised. Since estimates of polygon elongation rely on two such measurements they potentially have double the error. The error on the polygon elongation rating is thus in the range of one to two metres for earth based sites, or two to four metres for the martian sites. Estimates of polygon area are based on a digitisation of the polygon's perimeter. These measurements are reliable to within one to two metres on earth, but are somewhat greater on Mars due to the substantially wider coarse domains. The error on the area data is thus on the order of one to two square metres for earth, but four to five square metres for Mars.

9.4.2 Polygon Scale and the effect of gravity.

The main difference between terrestrial and martian features is one of scale. Martian clastic patterns are typically much larger. Martian features can involve boulders several metres in diameter (see Figures 5.9-5.16 and 7.1-7.3). It remains uncertain whether periglacial sorting processes are sufficient to organise clasts of this size, or produce polygons with diameters tens of metres across, even over very long periods of time.

On Earth a few unusual examples from the Canadian arctic are as large as medium-sized martian features, but when typical patterned ground in the range of one to ten metres (Hallet, 2013; Washburn, 1956) is compared between the two planets there is a considerable disparity of scale.

This difference in scale is reflected in the polygons digitised for this study. However the size of the largest clasts relative to the pixel size of the images is equivalent, so a similar amount of detail can be seen in both cases. The diameter of the smallest resolvable clast was measured for all sites in both surveys and the maximum, mean and minimum sizes of smallest resolvable clast are shown in Table 9.6. It can be seen that when the typical number of pixels per clast is calculated the values are similar between the two datasets.

Table 9.6: Comparison of smallest resolvable clast size between Earth and Mars.

	Earth: 15 cm/pixel		Mars: 25 cm/pixel	
	Clast diameter (m)	Pixels/clast	Clast diameter (m)	Pixels/clast
Max	0.69	0.38	3.1	0.5
Mean	0.52	0.29	1.07	0.26
Min	0.4	0.22	0.5	0.08

The dramatically larger size of the martian features may be the result of the lower gravity in which they formed. The weight of a stone will counteract the upwards force of frost heaving, but this will be lower on Mars. In contrast the upwards force of frost heaving is derived from the growth of ice lenses (Matsuoka et al., 2003) and so would not be expected to be altered by the lower gravity.

Consequently, the force of frost heaving would be expected to be proportionally more effective at moving the relatively lighter martian material. The acceleration due to gravity at the martian pole is 3.758 ms^{-2} (Kieffer et al., 1992), approximately one third of that of Earth. Consequently, material three times heavier may be movable.

9.4.2.1 Results and interpretation.

Some of the largest examples of sorted patterned ground known to occur on Earth are those illustrated in Figure 9.1 (Ballantyne, 2013; Gallagher et al., 2011). These circles, on Ellesmere Island in northern Canada, are anomalously large compared to most other features reported in the terrestrial literature. This site provides an upper limit for the size of terrestrial sorted structures.

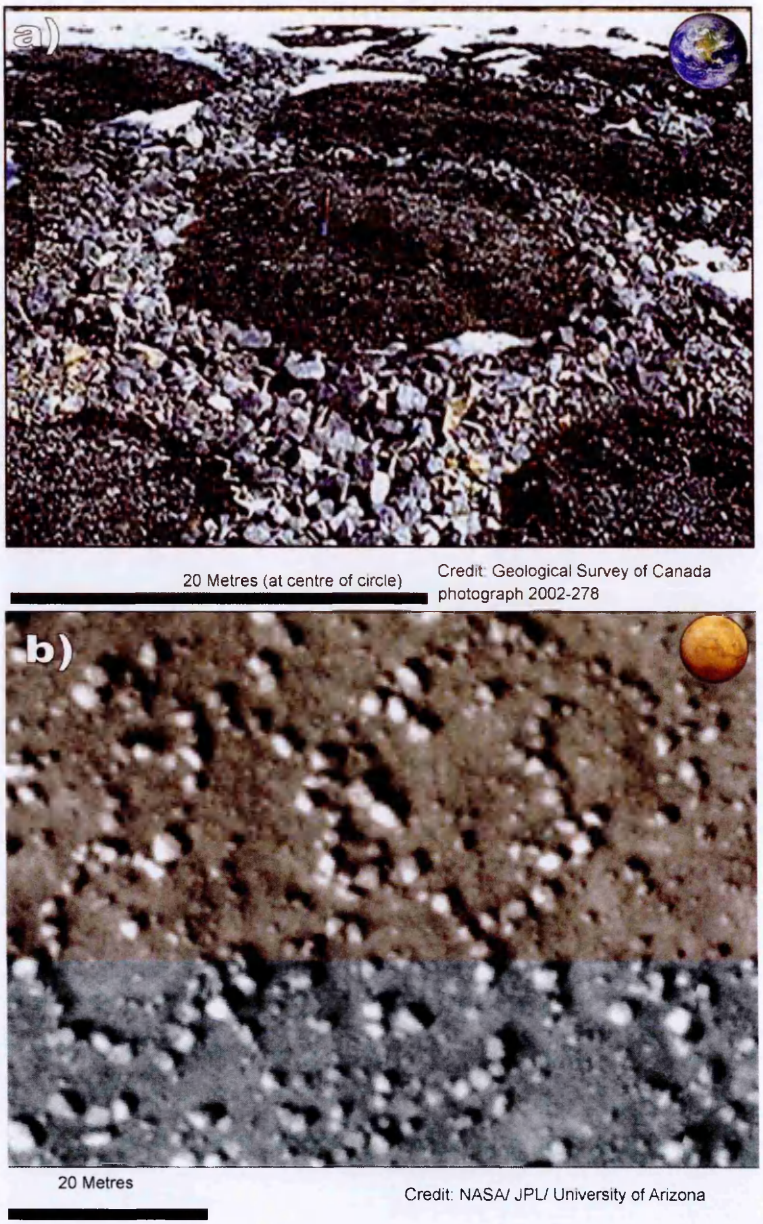

Figure 9.1: Comparison of 20 metre diameter clastic polygons on Ellesmere Island, Earth and Lomonosov Crater, Mars.

Some of the largest blocks making up the coarse domain at this location can be seen to be in excess of a metre in diameter, and several may be up to two metres long. It was not practical to visit this site during the course of this project, so these boulders could not be measured in the field. These numbers are estimates drawn from the photograph from the Geological Survey of Canada, and should thus be treated with caution.

Comparing this site to a typical set of polygons near Lomonosov crater on Mars indicates that although there are similarities in the scale of the polygons themselves the

terrestrial example contains far fewer very large blocks than the martian one. The banks of finer stones that ring the terrestrial polygons would be expected to be visible in a HiRISE scale image, even if the individual clasts were not. It would thus seem that the average size of the smallest resolvable material on Mars is higher.

The size of the largest clasts is also larger in the martian example. It is assumed that so long as the density of the rocks is consistent between the sites then boulders with up to three times the mass of the largest blocks at the terrestrial site should be moved by frost heaving under martian gravity.

This largely fits with the scale of the largest blocks in the martian examples. In the areas of possible sorting around Lomonosov Crater the diameter of the largest clasts were measured and plotted in Figure 9.2. The mean diameter of the largest clasts to form polygons in this region is four metres, while the mean diameter of the five largest clasts in each polygon is approximately three metres. The largest boulder observed to form part of a polygon was 11.6 metres across. Consequently, the size of this material seems to be on the upper limit of that which would be expected to be plausibly moved by equivalent periglacial processes under martian gravity conditions.

While some of this material is far larger than could practically be moved it should be noted that not every boulder within the coarse domain of a sorted circle need be brought there by the sorting process. The centimetre scale features studied in Chapter Four frequently include small boulders which are far larger than all of the other material making up the coarse domain. It seems likely that these anomalously large rocks were not moved by sorting but were part of the existing landscape and the sorted pattern developed around them. If the same is true of some of the larger material in the martian features then it is possible that the majority of the material could have been affected by the sorting process.

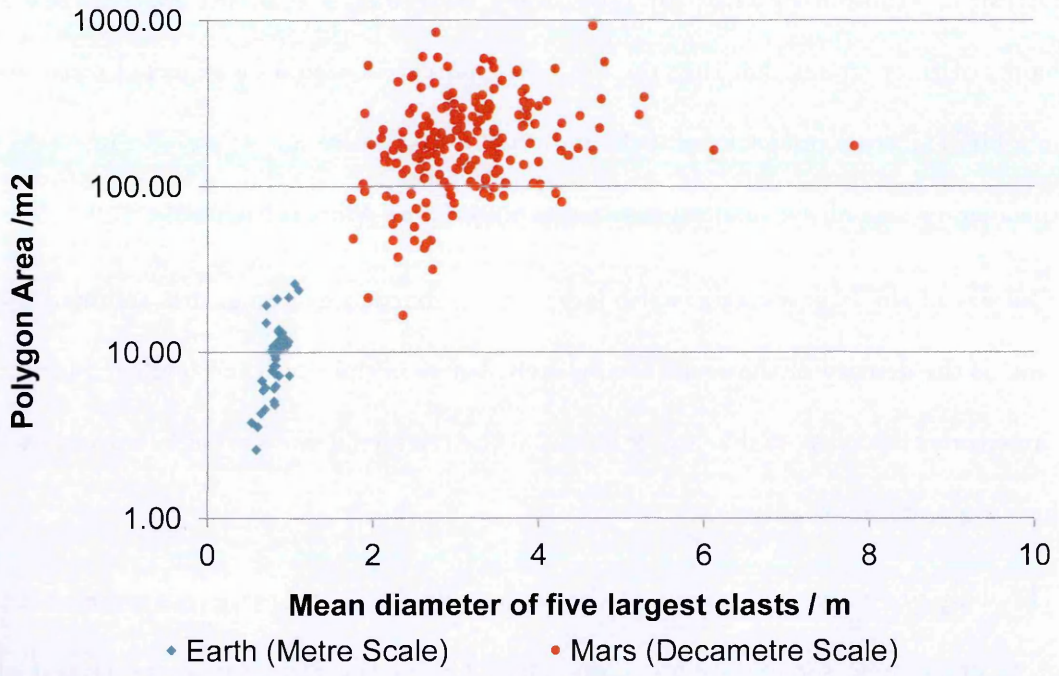

Figure 9.2: Polygon area against the mean diameter of the five largest clasts within a polygon's coarse domains. Data are plotted for Earth (blue) and Mars (red).

Figure 9.2 shows the distribution of clast size against polygon area. It can be seen that the size of the five largest clasts does scale with polygon size in both the terrestrial and martian datasets. However, there is much less scatter for the terrestrial remote sensing data than the equivalent martian features. This may be because on Mars both clasts and polygons have a wider range of diameters. This would lead to a more dispersed set of points than with the equivalent terrestrial features.

The number of clasts is expected to scale with polygon size, since a polygonal structure with a longer perimeter has a proportionally larger coarse domain. However, since only a subset of large clasts are discernible in these images it is useful to plot this relationship to see whether the number of distinct clasts still scales with area.

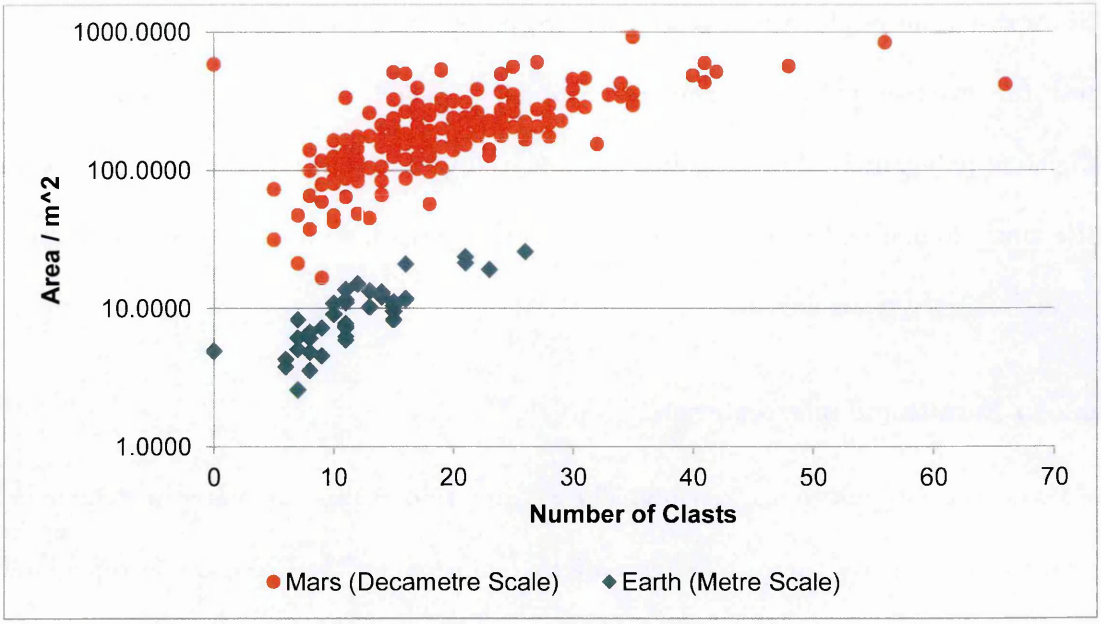

Figure 9.3: Comparison of polygon areas with number of discernible clasts for Earth and Mars.

It is found that there is a strong positive correlation between the polygon size and the number of clasts in both the terrestrial and martian data. Both martian decametre scale features and terrestrial metre scale features show a similar pattern despite the difference in scale. Consequently, making a scaling argument between these features should not be limited by the resolution of the images.

9.4.3 Variation in polygon elongation with slope

It has been established throughout the terrestrial periglacial literature that polygons become more elongated with increasing slope, ultimately transitioning to sorted stripes on slopes of three to seven degrees (e.g. Washburn 1973; Ballantyne 2013). The exact gradient at which the transition occurs might be different due to the effect of martian gravity. It is hypothesised that the transition results from changes to the subsurface convection cells that form from the interface between the horizontal and vertical sorting processes. Whether the rate at which these cells become elongated with slope would change is uncertain, but gravity would likely have an effect.

Since this is an established feature of sorted patterned ground it could serve as a good test for martian features forming through periglacial means. If the axis ratio of digitised polygons is plotted against the underlying gradient it would be expected that the most circular features would be found on flat ground, with more elongated features in increasingly steep slopes.

9.4.3.1 Results and interpretation

This proved difficult to test reliably. The examination of this parameter in chapter four proved inconclusive, despite using a high resolution DEM. Comparable topography data proved impossible to obtain for the martian study area. Stereo pairs were not available to make HiRISE DEMs of the sites with the best examples of sorted patterned ground, so measurements of slope had to be drawn from the global MOLA dataset. Consequently the gradient measurements plotted below should be treated with caution. The scarcity of sorted stripes in the martian surveys also meant that very few features with an elongation rating above 3-4 are present within the dataset.

It can be seen from Figure 9.4 that there is no pattern in the distribution of polygons of different elongation. The martian data plot into two distinct populations corresponding to those features found on flat ground and those found on 4-7 degree slopes; however both clusters have the same range of elongation ratings.

The highest axis ratio is found on relatively flat ground, although the next two highest are on steeper slopes. The cluster of martian data found to occur on flatter ground falls within a similar range to the terrestrial remote sensing data in both gradient and elongation. However, the lack of a trend in either data set means that comparison of these parameters neither confirms nor precludes morphological similarity. Neither dataset matches the transition from circular features to elongated polygons in the two to three degree range reported by Krantz, (1990).

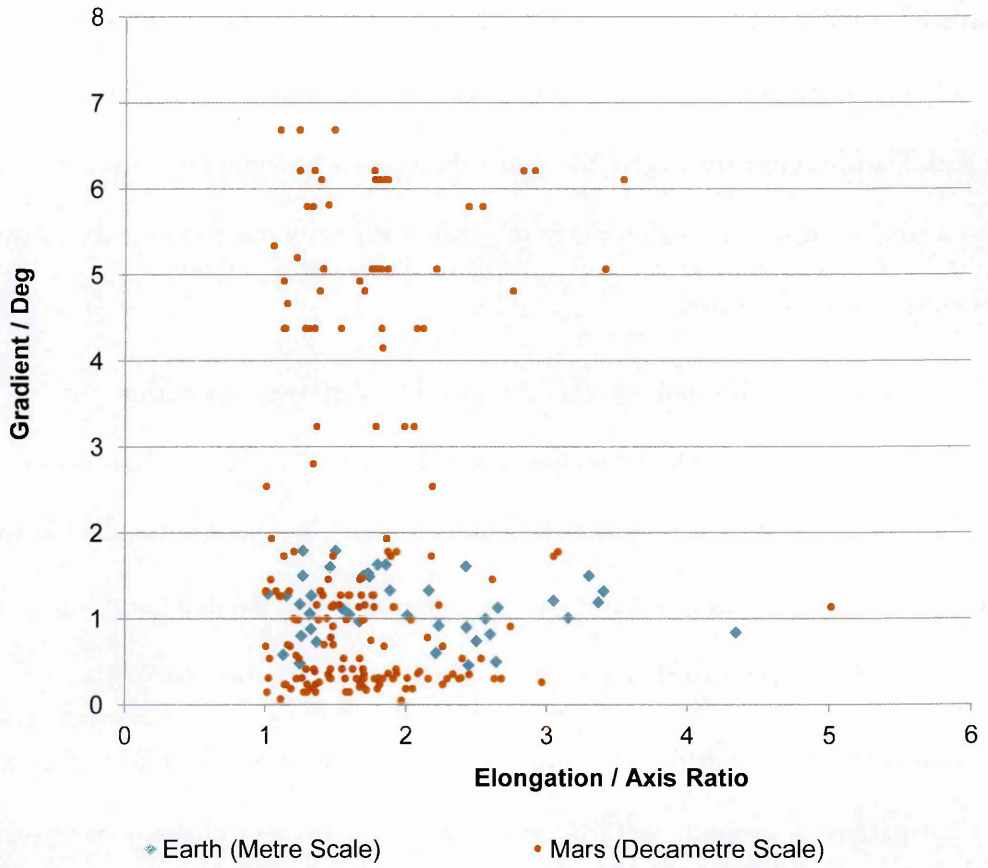

Figure 9.4: Plot of gradient against elongation for all terrestrial and martian data.

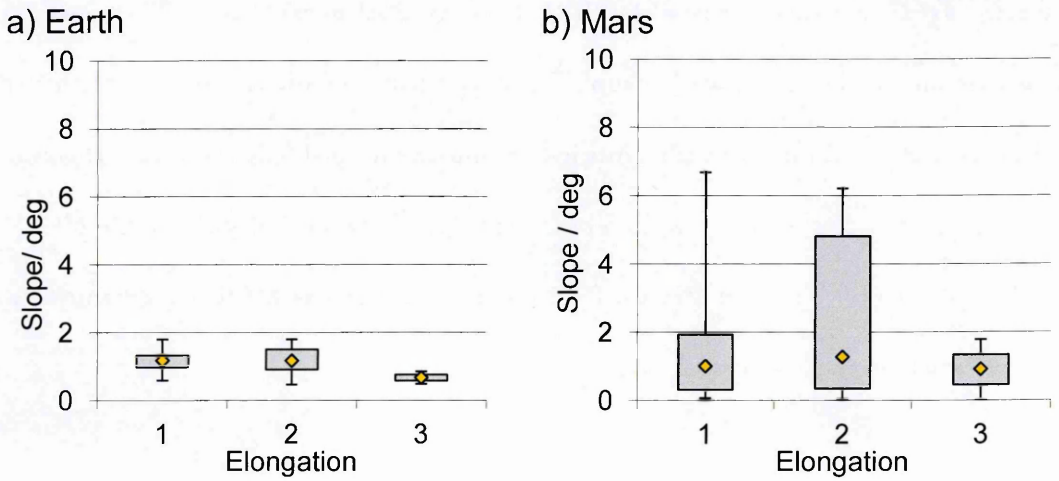

Figure 9.5: Comparison of the ranges of gradients over which polygonal features of different elongations are found on Earth and Mars a) Earth metre scale, b) Mars decimetre scale.

Figure 9.5 shows the range of gradients over which features of each elongation rating are found. Both datasets indicate a slightly wider range of gradients for the majority of elongation two structures, but in both cases this is within the range of the outliers of the polygons with elongation values between 0 and 1.5. However, the median gradients for both feature types are largely the same. Features with elongation values of between 2.5 and 3.5 are found at a smaller range of gradients mainly due to lower data density for these less common features.

This comparison is limited by the dramatically different resolutions of the digital elevation models from which gradients are derived. The aerial photographs have a horizontal resolution of approximately 15 cm per pixel. In the martian dataset the pixel size is far larger than the feature scale, so measurements of slope and aspect may be averaged over a larger area than the slope on which the landform occurs.

To resolve this issue a different approach was taken to assess the effect of gradient on martian patterned ground. MOLA point data were used to plot a series of transects across the small crater to the north east of Lomonosov Crater where the best examples of clastic stripes occurred (located in HiRISE image ESP_017685_2490). The continuous stripes visible on the crater wall occupy the steepest part of the transect, but transition into broken stripes and more labyrinthine arrangements of boulders before the end of the steep section of the crater wall. The crater floor is taken up with rubble piles and labyrinths, with no coherent stripes. Figure 9.6 illustrates the MOLA tracks used, and the profile across the crater wall.

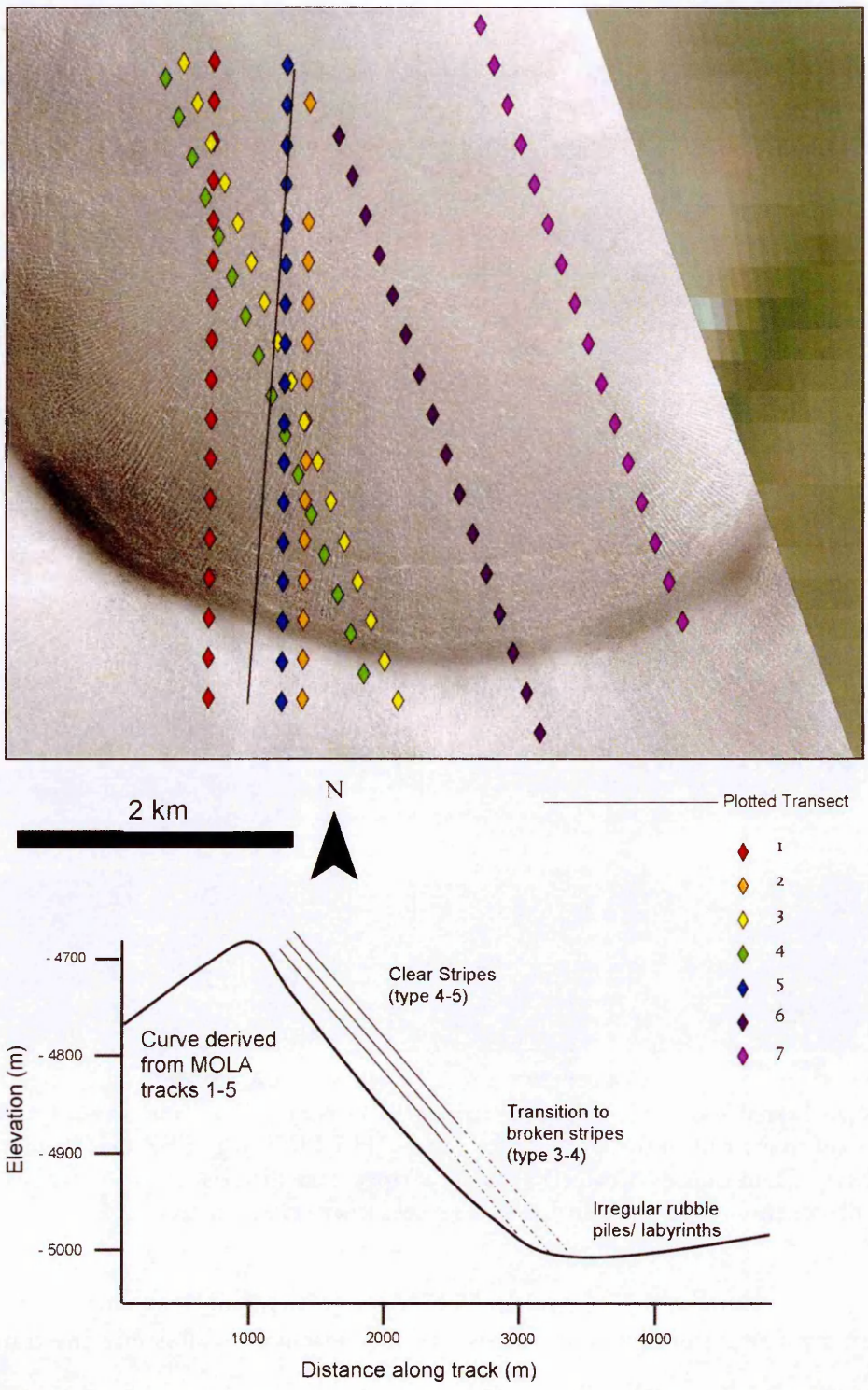

Figure 9.6: Schematic of the elevation transect across the wall of a small crater exhibiting clastic stripes. (ESP_017685_2490 to the North East of Lomonosov Crater) Coloured diamonds mark the position of MOLA elevation measurements. A transect was plotted through the region of densest measurements and the highest points plotted to produce the profile.

In general the expected trend is seen, stripes are found on the slope, whereas less regular structures occupy the flatter ground within the interior. However the topographic data suggest that the transition point from stripes to labyrinths comes before the gradient of the crater wall has substantially changed. The slope beneath the stripe pattern is approximately nine degrees, while transitional features are found on slopes with a gradient of around 7 degrees. This is not as low as the threshold reported in the terrestrial literature.

Although the pattern becomes less regular it maintains its stripe-like morphology down to the centre of the crater where clastic labyrinths replace the stripes. It is uncertain whether this change is due to the shift in gradient or whether it is due to the interference of the stripes where they meet on the crater floor.

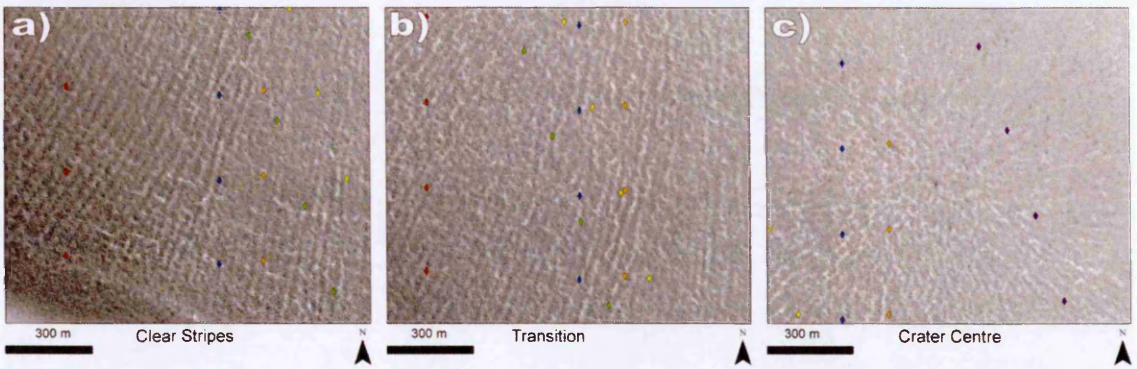

Figure 9.7: Transition from coherent stripes to broken stripes and irregular patterns from the southern rim of the crater to its centre (HiRISE image ESP_017685_2490 to the North East of Lomonosov Crater.) a) Clear stripes near the rim of the crater, b) stripes become discontinuous, c) labyrinthine structures near crater centre.

In Figure 9.7 a series of locations at this site are presented to illustrate the transition. The left most frame shows the area just below the crater rim, where a series of coherent radial stripes can be seen running from the crater rim to its centre (south to north in this frame). The centre frame shows the transition from clear stripes to less regular patches of boulders, between elevations -4888 and -4905.

9.4.4 Alignment of elongated polygons to underlying slope

In a situation where slope controls the polygon elongation then the elongated polygons would be expected to be aligned to the slope. Since the results of the analysis in the previous section showed very little correlation between slope and elongation a large degree of alignment would not be expected. These alignment data were derived from digitised martian polygons using the same methodology by which alignment to slope was determined for terrestrial examples in Chapter Four. However the error on these data is much higher since the only topographic data available for these sites was the global MOLA data set and the resolution of the gradient data is thus larger than the scale of the features.

9.4.4.1 Results and interpretation

Figure 9.8 shows polygon long axis alignment data for all of the martian polygons surveyed and figure 9.9 shows the classification of that data based on the criteria outlined in Chapter Four. Features with an elongation rating of one exhibit no difference between the lengths of their long and short axes. One axis will almost always be longer than another, but not significantly so. It would thus be expected that the direction in which the slightly longer axis is aligned would be random and therefore whether or not the feature is aligned to the slope would also be random. In the case of a feature with an elongation ratio of two or more it is hypothesised that the distinct elongation is a result of the slope. Consequently, a stronger axis alignment would be expected for these features.

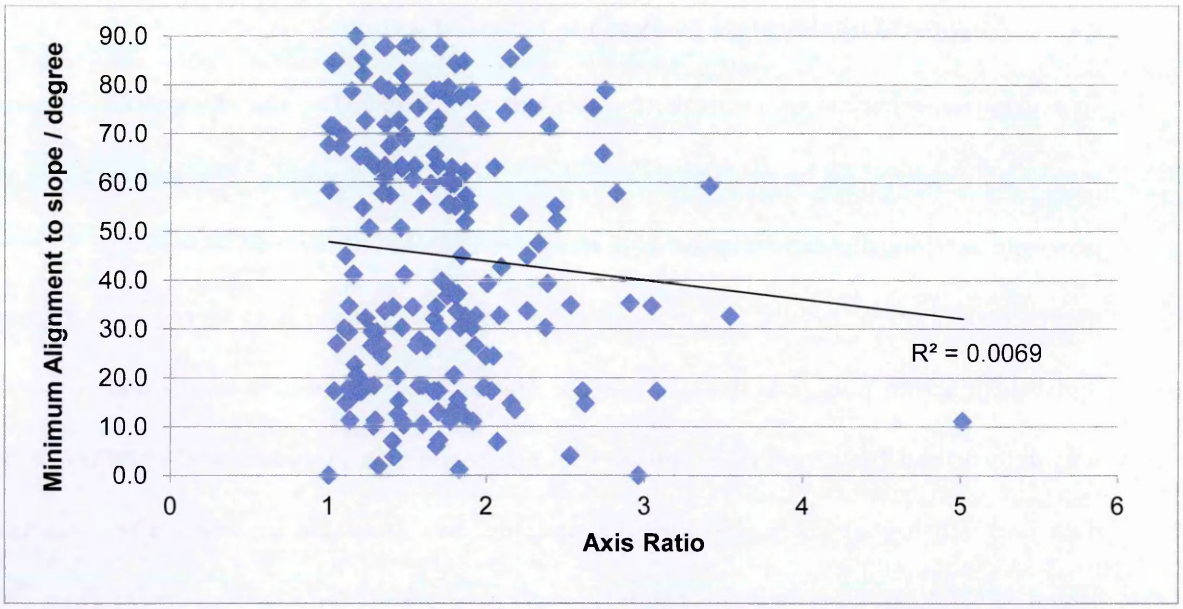

9.8: Alignment to slope against elongation of polygons digitised around Lomonosov crater. Elongation is determined by taking the ratio of the long and short axes. Minimum alignment to slope is the smallest angle between the polygon long axis and the direction of slope.

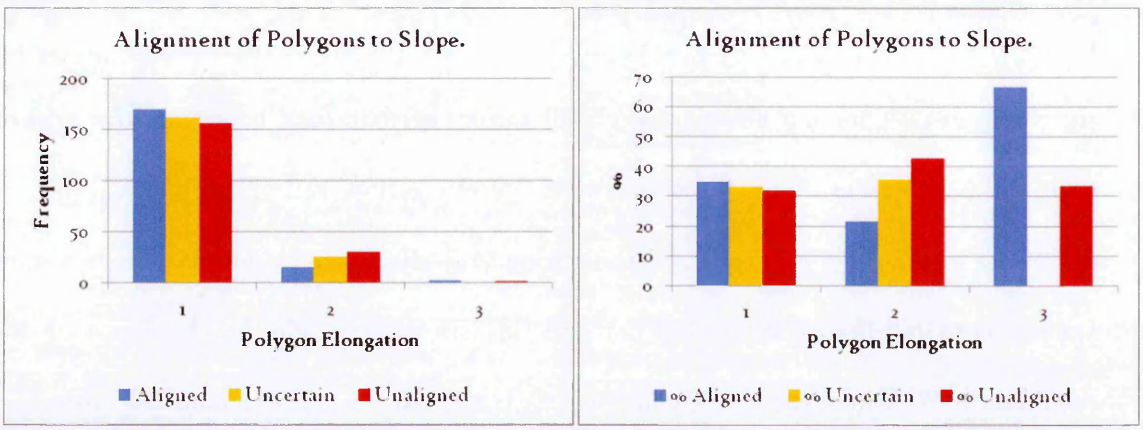

Figure 9.9: Alignment of polygon long axes to underlying slope, both by frequency and as a percentage of sites of each elongation rating to show alignment.

The lack of strongly elongated features is particularly pronounced in this analysis. The majority of features with an elongation ratio of one appear to be aligned to slope, whereas features with elongation ratios of two have a larger proportion of unaligned and uncertain features. This would seem to be contrary to the pattern seen in terrestrial alignment data in Chapter Four where elongation two features were somewhat more likely to be aligned to the slope. Only three examples of type three features were found

within the martian survey, so while two of these were aligned to slope and one was not, it cannot be concluded that this is a general trend of greater alignment for more elongated features.

As with the analysis in the previous section it is possible that the lack of a trend in these data is due to the large scale of the digital elevation model relative to feature size. If a higher resolution digital elevation model were available for this site then more meaningful aspect data could be derived, however HiRISE stereo images are not available for the area around Lomonosov Crater.

9.4.5 Summary

In summary there are some quantifiable similarities between examples of martian clastic patterned ground and their terrestrial analogues. The lower gravity on Mars would account for the larger scale of coarse domain material. Clast size can be seen to scale with polygon size in both the martian and terrestrial cases. Consequently, it seems likely that the large martian polygons are feasible within a periglacial regime.

Analysis of polygon elongation with slope was less conclusive. No clear correlation was found between these parameters. The alignment of polygons to slope also did not support a formation mechanism in which gradient controls polygon morphology. This analysis was undermined by the lack of high resolution topographic data for the study area being examined. While the analysis has been presented here for completeness it should be treated with caution, and not taken to rule out a periglacial explanation for these features.

When a case study was examined in more detail, using higher resolution elevation data, stripes were found to form on the steepest part of the slope, while the flat centre of the crater exhibited labyrinths instead. However the point where the stripes transitioned to discontinuous features does not match the threshold reported in the terrestrial

literature. This procedure would have to be applied to a larger set of examples to conclusively test whether this parameter does support a periglacial case, preferably at sites where polygons are seen to grade into stripes.

9.5 Conclusions

While the more exotic hypothesis for the formation of sorted features seems unlikely it is not possible to unreservedly accept a periglacial explanation. The Martian climate is not conducive to the formation of sorted patterned ground through terrestrial periglacial processes. The surface temperature only gets high enough for water to exist in a liquid state in isolated areas and for short periods of time. Consequently, repeated freezing and thawing would not be expected to be common. It is thus unsurprising that in this study, and others such as Gallagher and Balme, (2011), sites which may exhibit sorting are only found in a few isolated locations.

If these landforms have formed in geologically recent times then their presence could suggest that the local temperature in these areas is regularly rising above zero °C. In which case this sort of environment would be very unusual and these features would be expected to be very rare. While the regions in which possible sorting occurs are very few and far between the abundance of these features in the area around Lomonosov Crater and the fact that sorting appears to be occurring in multiple adjacent images makes this explanation unlikely.

Another possibility is that the freezing point of the local groundwater is being depressed. Magnesium Perchlorate was detected at the phoenix landing site (Hecht et al., 2009). This is one of several cryobrines (Möhlmann, 2011) which could depress the freezing point sufficiently to allow a freeze-thaw cycle to occur (see Chapter Three).

Despite the variety of possible sorted patterned ground in the area, Lomonosov crater has very few examples of other putative periglacial landforms such as solifluction lobes and scalloped depressions. A few possible lobes occur to the north of the area, but these are not in close proximity to the majority of the sorted forms around Lomonosov.

It was found that the majority of sites did not exhibit fracture control. Fractures were present at a large number of sites, but did not appear to be influencing the arrangement of clasts. Furthermore a larger number of boulder patches exhibiting higher grade sorting were found at sites with no evidence of fracture control. While these hypotheses cannot be completely ruled out, it seems less likely that they account for the formation of these features. This may suggest that a periglacial explanation, augmented by the presence of Cryobrines is more likely, but in the absence of ground truth it is impossible to be certain how these structures formed.

10 Chapter Ten: Examination of scalloped depression fields around Davies and Lagarto Craters

10.1 Aims

In this chapter, two assemblages consisting of extensive fields of scalloped depressions around medium-sized impact craters are described. Both sites feature extensive systems of scalloped depressions that overlay the ejecta of the craters. Scalloped depressions are important putative periglacial landforms as they may be evidence of thermokarst-like processes. Characterising depression morphology can reveal how mature these features are, and thus allow some estimation of the time and conditions under which they formed.

Figure 10.1: Scalloped depressions near Davies Crater. Multiple smaller depressions merging into a larger structure.

Scalloped structures at all stages of development are present, but a large number of very degraded features are observed.

This section classifies these features using the systems of Séjourné et al., (2011) and Wallace (1948) to determine which types of feature are most prevalent. As described in Section 7.7, scalloped depressions are often found in an assemblage with gullies. This is the case at both of these sites where gullies are found on the crater walls, and many of the depressions are in close proximity to them.

10.1.1 Background

This analysis builds upon a variety of studies into the structure and distribution of scalloped depressions. Costard and Kargel, (1995) identified regions of kilometre scale depressions across both Utopia and Acidalia Planitia. These frequently occur in proximity to impact craters and they noted the similarity to terrestrial thermokarst lakes and proposed that they might have formed through periglacial means.

Further studies by Soare et al. have provided an extensive analysis of these features. Soare et al., (2007) demonstrates that scallops cross cut some instances of gullies on crater walls. They proposed that this indicates a young age for scalloped terrains. It is possible that at these sites both the scalloped and gullied terrains are the product of the same period of thaw. Soare et al., (2008) lent more evidence to a thaw related formation mechanism. They identified terrace like features within some scalloped depressions which they proposed to be evidence that they formed as a result of the ponding of stable water, rather than through sublimation of ground ice. These observations are largely based on features in Utopia and Elysium Planitiae.

More recent work by Soare et al., (2012) has mapped the distribution of scalloped terrains across a wide swath of Utopia Planitia to compare their distribution with that of the ice dust mantle. They found that putative periglacial terrains often occur in regions where the latitude dependant mantle is absent, perhaps suggesting an earlier period of formation than that proposed by the previous study. The study of

Morgenstern et al., (2007) also mapped the distribution of scalloped depressions across Utopia Planitia and found that the larger and more continuous regions of degradation were more common in the southern part of their study area.

Ulrich et al., (2010) provides an in depth look at the morphology of scalloped depressions in Utopia Planitia, comparing and contrasting the morphology of the martian landforms with terrestrial analogues. They note that the steepness of the slopes of scalloped depressions can be used to determine the preferential direction of development, an observation that has proved useful for determining direction of expansion in this study. This is significant as different expansion directions would have been more likely during different periods of martian history. During high obliquity periods there would have been increased insolation on pole facing slopes during certain times of the years. Whereas if these landforms occurred at a period where obliquity was less pronounced this would not be expected to be the case.

Lefort et al., (2009) report observations of these features in HiRISE imagery, and conclude that there is a co-evolution of scallops and polygons in that area. The study of Haltigin et al., (2014) also supports the co-evolution of scalloped and polygon terrains. Both of these studies were also limited to features in Utopia planitia, although the study of Lefort et al., (2010) expands their observations to features in the southern hemisphere.

The Utopia Planitia examples have also been studied by Séjourné et al., (2011, 2009). who propose a five stage classification of the evolution of depressions, from small isolated features, to large merging basins with extensive scalloped edges. Séjourné et al., (2012) propose that the banding within many scalloped depressions indicates the exposure of sedimentary layers, suggesting that these features are forming within a stratified permafrost soil, likely deposited by aeolian processes. Séjourné et al., (2011)

describe steeper pole facing slopes on many scalloped depression within this area. They propose that these features likely formed during a past period of higher obliquity since pole facing slopes would have received increased insolation during the warmer parts of the year in such a regime.

As can be seen the majority of investigations into these landforms have focused on the Utopia Planitia area. Scalloped depressions are known to occur elsewhere on Mars from observations of these features in Acidalia planitia by Costard and Kargel, (1995), but these sites have not been studied in detail except for the analysis of putative thermokarst in Ares Vallis by Costard and Baker, (2001). One of the objectives of the present study was to locate scalloped terrains in Acidalia and Arcadia Planitiae for comparison with the well documented Utopia Planitia features. It is clear that while there are fewer examples of these features outside of Utopia Planitia they still occur in considerable numbers (see chapter seven). Consequently it was decided to map scallop distribution around two impact craters in the Acidalia study area, and apply the classification scheme of Séjourné et al., (2011) so that features in this region of Mars can be compared and contrasted with the better documented examples cited above.

10.2 Study Areas

The depression assemblages at these sites were located as part of the context survey of eastern Acidalia Planitia. Davies and Lagarto craters were identified as having the highest concentrations of scalloped depressions in the context survey and the highest concentration of highly graded features.

The majority of other sites consist of much smaller fields or isolated depressions showing less evidence of interaction with other possibly periglacial landforms. As previously stated, there are far fewer examples of scalloped features in the Acidalia study area than in the regions of Utopia planitia where these landforms are most

extensively documented (e.g. Costard and Kargel, 1995; Osinski and Soare, 2007; Soare et al., 2008).

10.2.1 Images

In both cases the extents of scalloped terrains were mapped using CTX images. Scalloped depressions were located and their extents mapped using a GIS shape file. Frequently the scalloped depressions appeared slightly different in overlapping CTX images, while this could suggest active features it was concluded that changes in illumination conditions and slight errors in the placement of the images were more likely to be responsible for the differences observed. To ensure that the mapped extents were consistent a single image was used when possible, with the other images only being referred to in places beyond the extent of the main image.

For Davies Crater these features were predominantly mapped from CTX image B21_017949_2263_XN_46N_359W, with a small area from P16_007163_2264_XN_46N359W. In the Lagarto Crater study area two CTX images; B19_016868_2319_XN_51N008W and P15_0067165_2302_XI_50N008W were used. Only a small area of overlap exists between these images; where they did overlap the later image was referred to.

HiRISE coverage was largely unavailable. Several HiRISE images overlap the two craters; however most are centred on the crater interiors. Only one image, ESP_035302_2260, overlaps part of the scalloped depression field of Davies Crater. This image contains a total of 13 scalloped depressions, seven of which are on the southern crater rim, while the remaining six are within the crater itself.

If HiRISE coverage becomes available for this site in the near future then it would be interesting to examine scallop morphology in more detail to determine how well they match the features observed in Utopia planitia. For example bright bands like those

discussed by Séjourné et al (2011) may be present in several of these features, but without higher resolution images it is impossible to be certain. Polygon junction pits, which are a common element of these landforms elsewhere in the northern plains (e.g. Séjourné et al., 2010) were not observed, but once again this might be due to the low resolution of the CTX images.

10.2.2 Crater Morphology

The two impact craters are quite different in morphology: Davies Crater (~ 49 km in diameter) features a prominent central peak and an irregular rim. Several large gullies are found on the northern crater wall, their source regions are in close proximity to some of the scalloped depressions. Lagarto Crater (~ 19.5 km in diameter) is smaller and has a regular, more circular rim and a much smaller central rise. Its floor exhibits a small dune field and a large depressed region to the north west of the centre. Gullies are found across the North West quadrant of the crater wall; these are smaller but more numerous than those found in Davies Crater.

10.2.3 Scalloped depressions around Davies Crater

At this site a large number of scalloped depressions are found above the northern rim of the crater. Other features are found further out on the crater's ejecta to the north. Gullies are found on the northern wall of the crater, some of these have source regions in very close proximity to the edges of the scalloped terrain. To the south of the crater fewer features are found on the ejecta, but a large number of depressions can be seen on the southern crater wall and the southern floor of Davies crater. All of these features are found in the area of the overturned flap of material created by the crater's formation. This ejecta will have an inverted stratigraphy, with ice rich material from as deep as a kilometre within the subsurface exposed by the impact. This thus supports the hypothesis that these features formed by the degradation of an ice rich layer.

10.2.4 Scalloped depressions around Lagarto Crater

The assemblage of scalloped depressions around Lagarto Crater is even larger than that seen at Davies Crater. At this site scalloped depressions extend around the entire crater, at a distance of approximately ten kilometres from the rim. No features are found closer to the crater rim or within its interior, suggesting that they may be limited to the distal parts of the ejecta blanket. These depressions are most concentrated immediately to the north east of the crater. The distribution of these features is similar to that which would be expected for a secondary impact crater population. However this is not believed to be the case in this instance. Lagarto crater is a rampart crater so any secondary impact structures would be expected to have been destroyed by the movements of the crater's fluidised ejecta layer. The structures mapped in this investigation appear to cut into this ejecta layer. It is thus likely that they are formed by degradation of an ice rich material in the near subsurface.

Figure 10.2: Map of scalloped depressions around Davies Crater in eastern Acidalia Planitia. The extents of scalloped depressions are outlined in black.

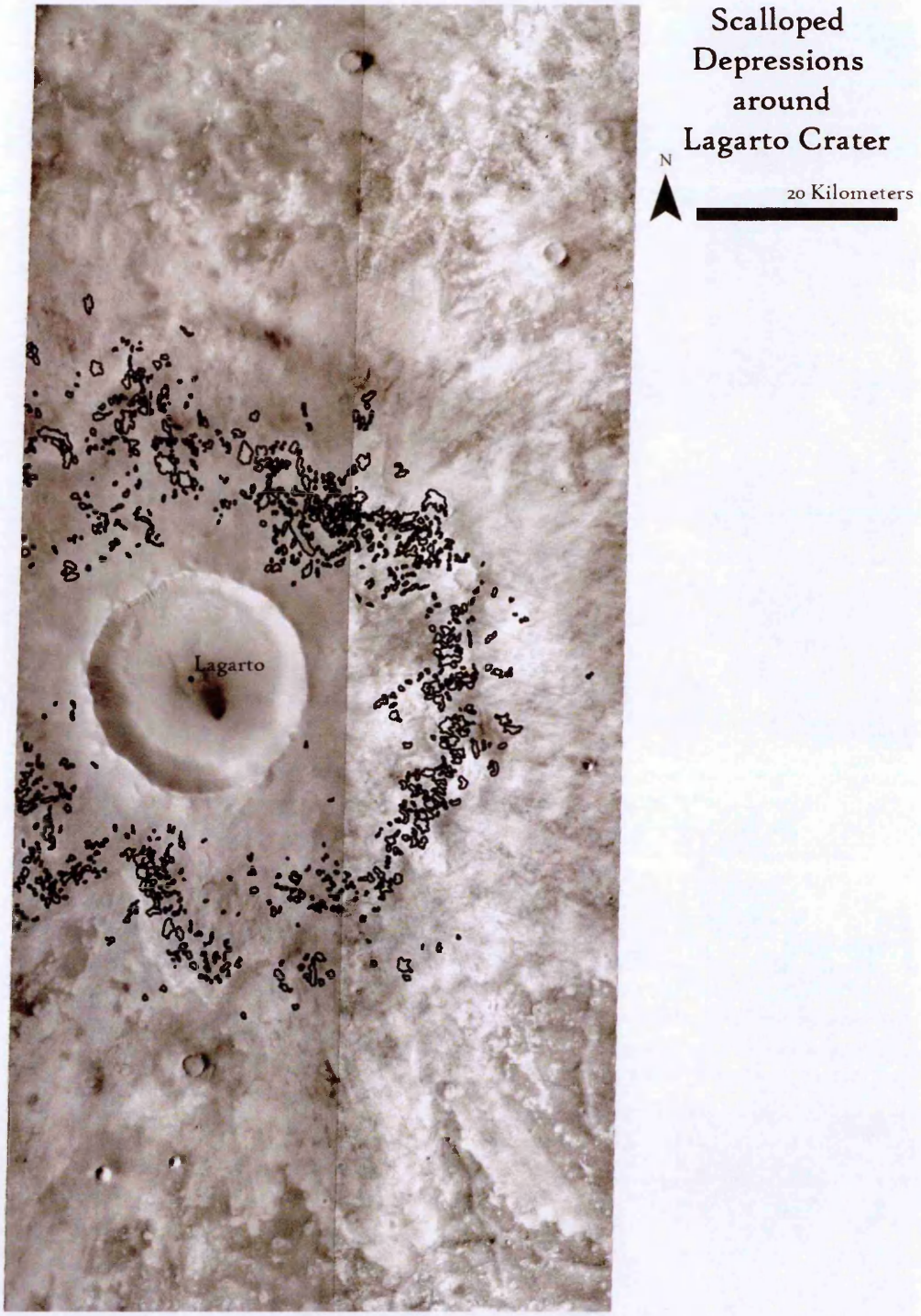

Figure 10.3: Map of Scalloped depressions around Lagarto Crater in eastern Acidalia Planitia. The extents of scalloped depressions are outlined in black.

10.3 Classification of scalloped depressions

A wide range of depression and pit morphologies are found within the two study areas. These structures range from small, near-circular, features through larger depressions with scalloped edges to very large areas where multiple basins merge and many square kilometres of surficial material are degraded.

Although the exact mechanism through which these features form is still a matter of debate there is general agreement that they result from the degradation of ground ice, whether through melting (e.g. Costard and Kargel, 1995; Soare et al., 2007b) or sublimation (e.g. Lefort et al., 2009; Morgenstern et al., 2007). Consequently, they would be expected to occur in areas where ice-rich terrain is present, perhaps as part of the putative ice-dust mantle thought to occur at latitudes north of 40°N, and blankets much of the northern plains (M A Kreslavsky and Head, 2002; Mustard et al., 2001).

Séjourné et al., (2011) define a classification system for scalloped depressions based on the evolution of the features from small sub-circular structures to increasingly complex basins where multiple features merge (shown in Figure 2.7). This classification system is similar to the classification of terrestrial alases by Wallace (1948), summarised in Figure 2.6. These classification schemes were used to assess the development of two areas of scalloped terrain around Davies and Lagarto craters. Séjourné's classification is based on the number of bright bands visible in the floors of depressions in HiRISE images, since HiRISE coverage is absent for this area and bright bands cannot often be distinguished the classification here only approximates Séjourné's scheme.

Séjourné's classification has more detail at the early stages of scalloped depression formation, with the first four categories being equivalent to the young landscapes defined by Wallace, while the fifth and final category, merging features, corresponds to Wallace's mature landscapes. Wallace additionally describes "late mature" and "old

age" thermokarst features where instead of several isolated basins merging together, the landscape is dominated by a large scale assemblage of linked basins. This type of landscape is found in some parts of the survey area, necessitating a sixth type to be added to Séjourné's classification system to describe these "late mature" features. A variety of examples of scalloped depressions of different types are shown in Figures 10.4 and 10.5

Figure 10.4: A variety of Scalloped depressions of types 1-4, as defined by Séjourné et al., (2011).

In addition to classifying each Scalloped depression it was given a grade from 1 to 5 reflecting how well it approximated the type examples for these features (see examples in Chapters Six and Seven), in this case the examples in Séjourné et al., (2011) were referred to extensively. These grades are equivalent to those assigned to the scalloped depressions examined in HiRISE images in Chapter Seven, although the lower resolution of the CTX images will inevitably result in a higher proportion of lower-graded features.

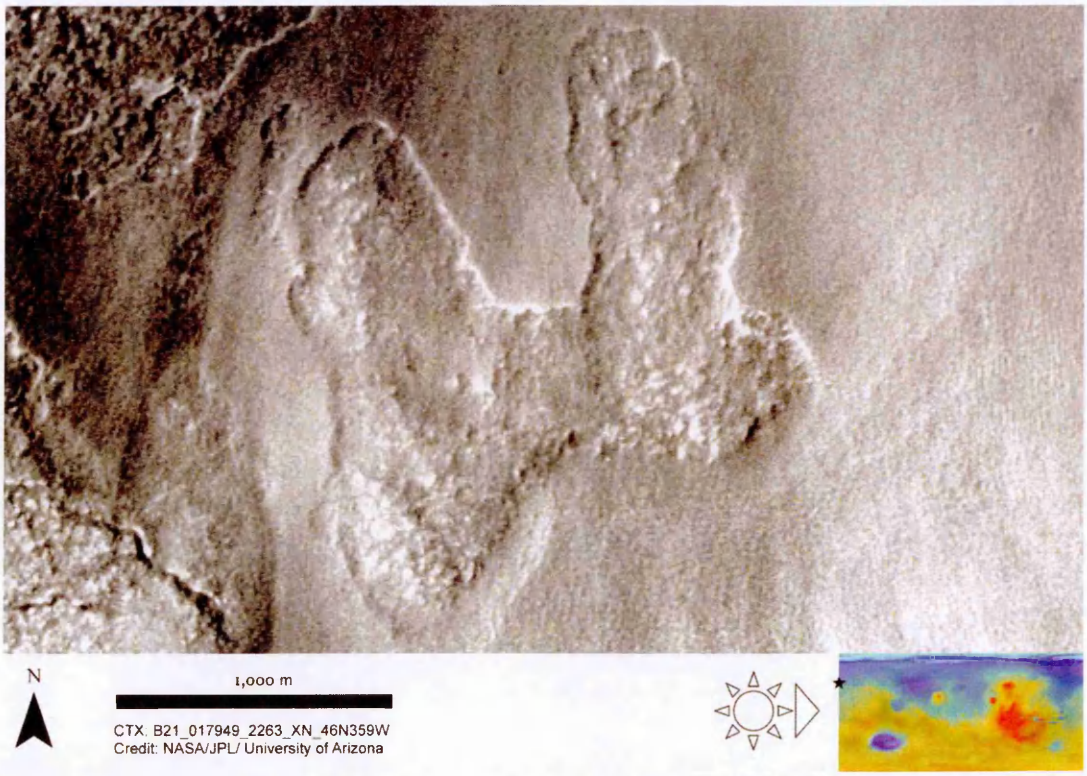

Figure 10.5: A type five scalloped depression where two basins have completely merged into one U shaped feature.

A summary of the results of this classification procedure are plotted in Figure 10.6. While both sites show a similar distribution, with feature frequency peaking in the intermediate types, they are not identical. In the Lagarto Crater area the most common features are those of type three with a steep decrease in frequency for the mature, more degraded types. In Davies crater the most common scalloped depressions are of type four. This suggests that the degraded terrain around Davies crater may be more mature than that around Lagarto Crater. Both sites have large numbers of mature features, suggesting that despite differences in the frequency of features of different types they are both fairly mature landscapes.

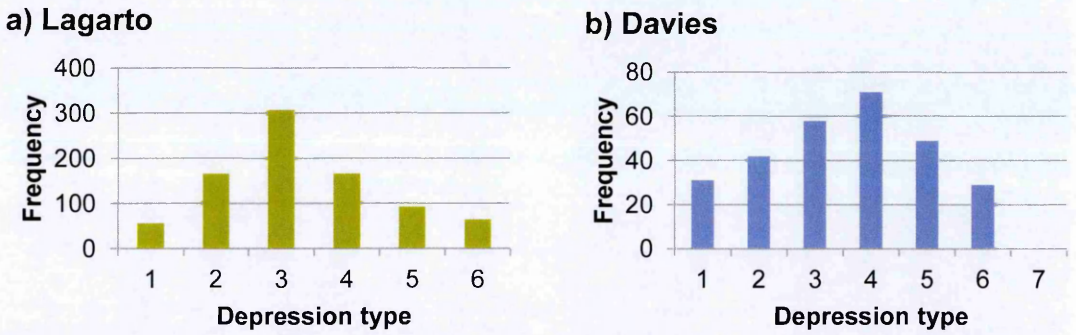

Figure 10.6: Classification of Scalloped depressions at the two study areas into the types defined by Séjourné et al., (2011) and illustrated in figure 10.4. Higher numbered types are believed to be the more mature features while those with lower numbers appear younger. a) Lagarto Crater, b) Davies Crater.

Examining the number of features of each type gives a sense of which are most numerous it does not, however, account for the relative areas of the different features. A type five depression is much larger than a type one feature, and type six regions cover very extensive areas. Since the higher type features form through the coalescence of smaller structures, it would be expected that there would be a drop-off in number of features as the landscape matures, but that the degraded area would continue to increase.

Consequently, it is more useful to consider the total area covered by features of each type and the average area of a feature of any given type. This is plotted in Figure 10.7 while Table 10.1 shows the proportion of the area of each site covered by these features. It can be seen that, although they cover a very large area in terms of square metres, they are only taking up a fraction of the surrounding area.

Table 10.1 Percentage of area degraded by scalloped terrain around each of the two craters.

	Area of CTX Image (m^2)	Degraded Area (m^2)	% of area Degraded
Lagarto Crater	6.24×10^9	1.49×10^8	2.38
Davies Crater	2.79×10^9	1.04×10^8	3.72

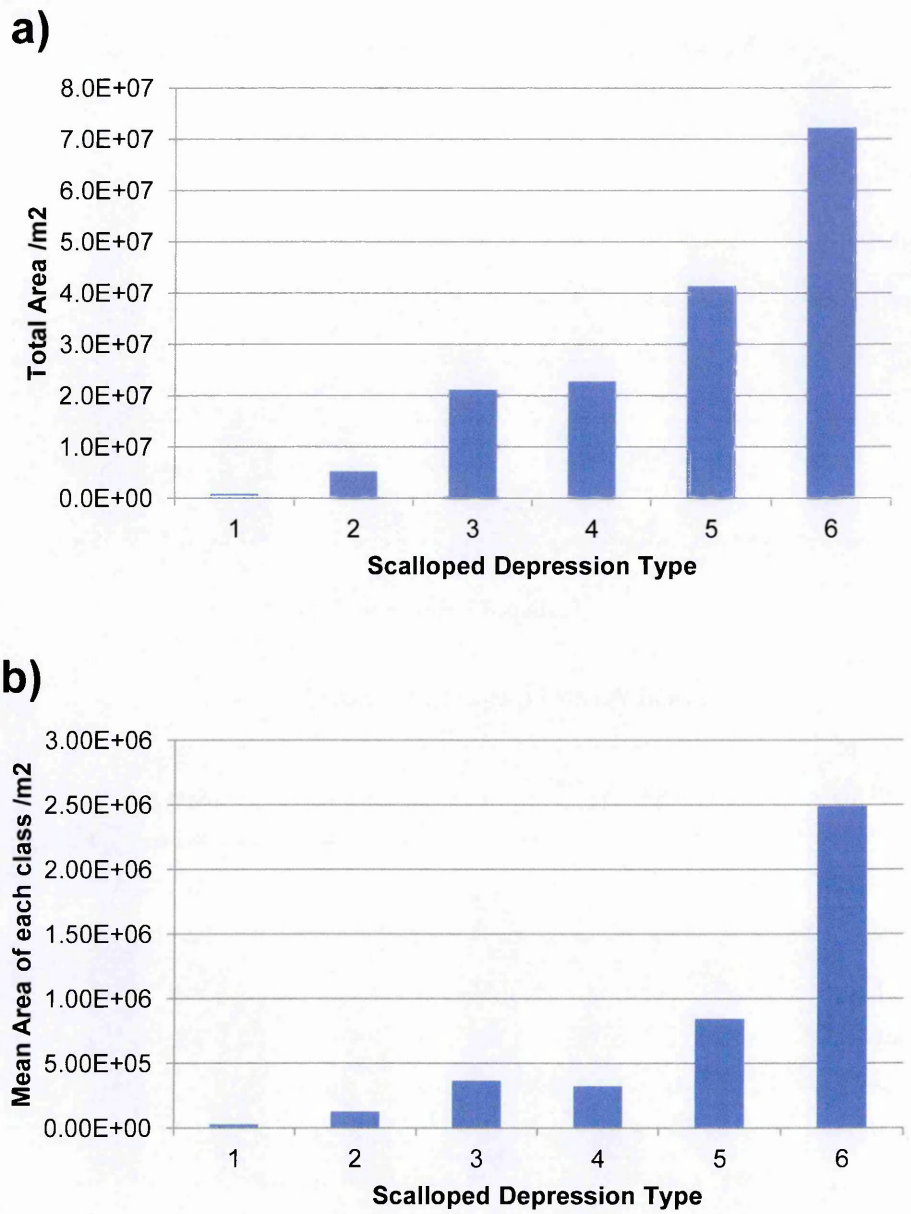

Figure 10.7: Areas covered by scalloped depressions around Davies Crater.

Interestingly, the area covered by scalloped depressions of each type around Davies Crater increases steadily with increasing feature type. Lagarto Crater, on the other hand, has a much larger area covered by grade three features, although grade six features still cover the largest area. This fits with the observation that grade three features were most numerous at this site and confirms that this region has a higher proportion of less mature features.

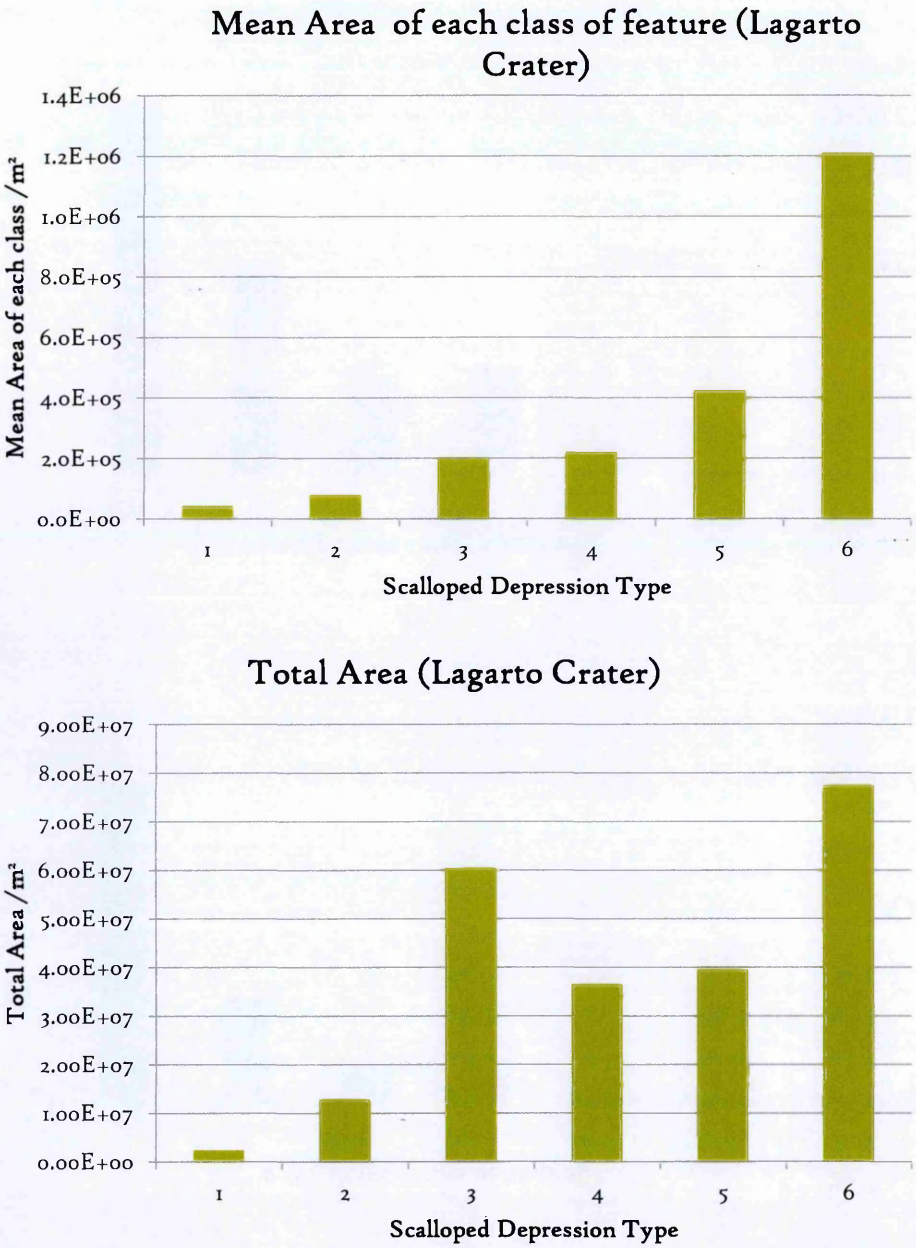

10.8: Area covered by scalloped depressions around Davies Crater.

This may mean that the landscape around Davies crater was active for a longer period of time, allowing more of the very mature features to develop and a larger percentage of the mantled area to become degraded. Although Lagarto crater actually has a slightly larger degraded area it is not as large a proportion of the total area surveyed. However since Lagarto Crater still exhibits numerous large highly degraded areas it is unlikely to

be substantially younger than the Davies area. Both have extensive areas of type six depressions, with a smaller proportion of smaller, less well-developed features.

It is also interesting to note the generally smaller mean areas of all of the Lagarto Crater features. The same trend of increasing mean area is seen in both data sets. But the features around the larger Lagarto Crater are substantially smaller than in the less extensive depression field around Davies crater.

10.4 Presence of Patterned Ground

Fracture polygons have frequently been observed to occur in association with scalloped depressions, as observed by (Haltigin et al., 2014; Levy et al., 2009; Séjourné et al., 2011 and references therin). This is consistent with the substrate being an ice-rich material. Fractures are often found within the scalloped depressions as well as on the surrounding plains, suggesting that they post-date the formation of the depressions (Haltigin et al., 2014; Séjourné et al., 2011). Both study areas contain terrains comprising a regular decametre-scale pattern of dark and light patches as illustrated in Figure (10.8). These patterns give the ground a "stippled" appearance which could be an expression of fracture networks below the resolution of the images. However, the low resolution of CTX images makes it impossible to be certain whether fracture polygons are definitely present at these sites or not.

Figure 10.9: Mature scalloped depressions overlain by stippled terrain, a pattern of dark and light patches which could be evidence of a fracture network below the resolution of the image.

This stippled terrain usually consists of bright patches surrounded by a darker rim, and are generally less than a few tens of metres across, although there are areas where less regular patterns appear. They occur on the expected scale for fracture polygons and their relationship to the scalloped depressions matches the association seen in other parts of the northern plains. It is likely that this stippled terrain is the terrain type described as "basketball terrain" by some studies (Levy et al., 2010; Malin and Edgett, 2001). "Basketball terrain" is known to consists of small rubble piles on the mounds between degraded fracture networks (Kreslavsky and Head, 2000; Levy et al., 2010, 2008c; Malin and Edgett, 2001).

Several patches of stippled terrain are covered by HiRISE images, in these locations the bright centres appear to be the spaces between narrow raised features that could be heavily degraded low centred polygons. It is impossible to be certain that this variety of

patterned ground is indicative of fracture polygons, but this seems to be a reasonable interpretation.

10.4.1 Distribution of Scalloped depressions with associated stippled ground

Figures 10.9 and 10.10 shows the distribution of the scalloped depressions with associated stippled terrain across both study areas. Scalloped depressions around Davies Crater are often, though not universally, found in proximity to this sort of patterned ground. While it is present around all of the features near Lagarto Crater.

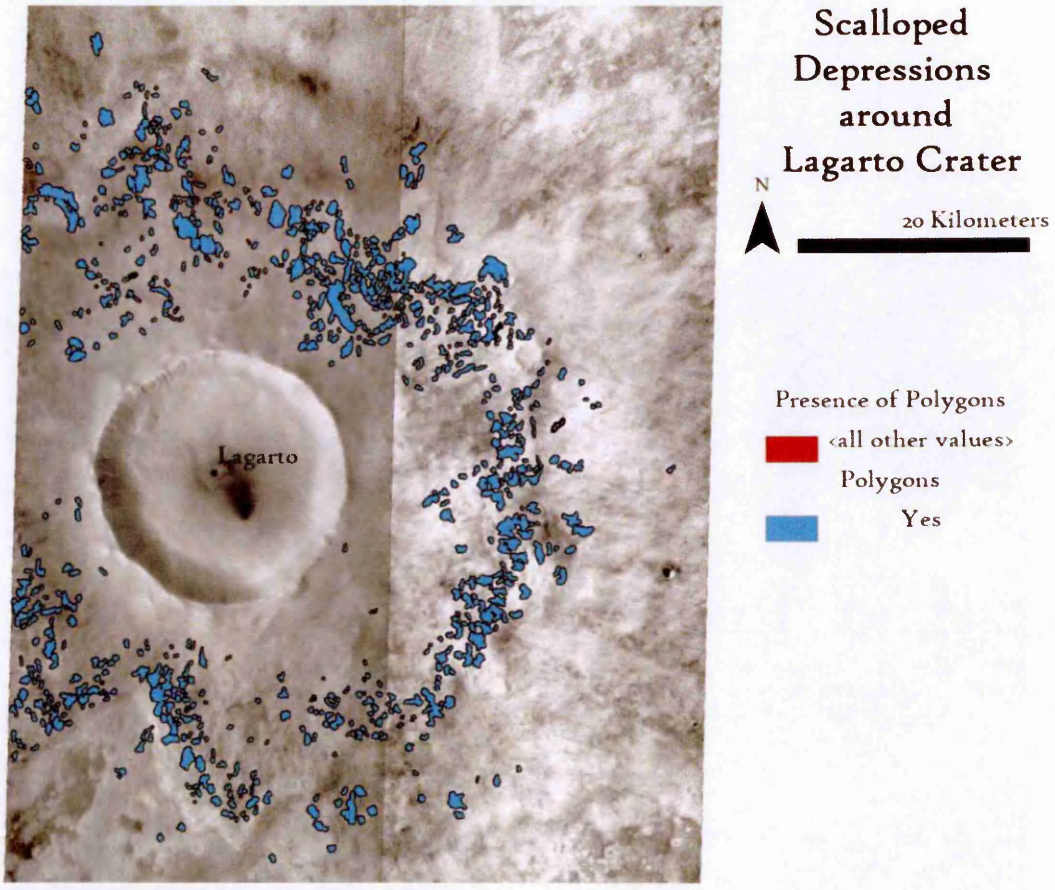

Figure 10.10: Distribution of scalloped depressions with putative fracture polygons around Lagarto Crater. All depressions have at least partial overlap with possibly fractured terrains.

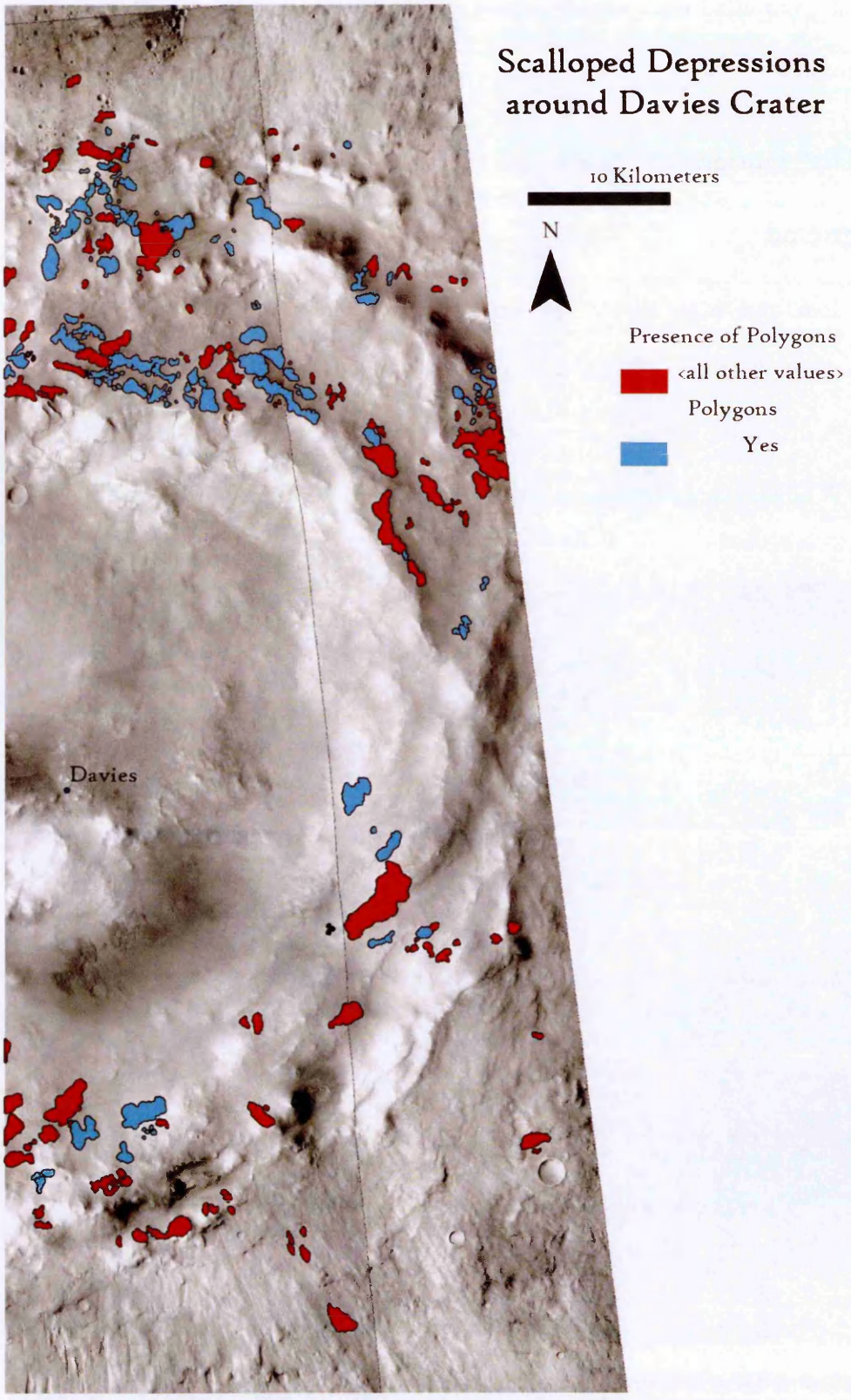

Figure 10.11: Distribution of scalloped depressions with fracture polygons around Davies Crater. Fractured terrain is much less common in this region, and far fewer scallops have formed on them.

The majority of the CTX images covering Lagarto crater are covered by stippled terrain. Consequently, all examples of scalloped depressions in this area were surrounded by stippled ground and many have patterned ground within their interiors.

The same trend was not reflected at Davies crater where only half of the pitted and degraded area exhibits stippled ground. To some extent this may be due to the clarity of the images. Many sites in this area have textures which could be evidence of stippling, However it is impossible to be certain whether these features are present or not. At this site the majority of sites with stippled terrains occur to the north of Davies Crater. Only 16 of the scalloped depressions within the crater rim appear to occur on stippled terrain, the others lacking these textures. None of the relatively sparse features to the south of the crater exhibited stippled ground.

10.4.2 Ground Ice

Assuming that these features do represent fracture polygon networks of the sort discussed in Chapter Seven then their distribution would be expected to be linked to ground ice. These sites are not expected to be particularly ice-rich in the present day. Lagarto Crater is located at 49 °N. Consequently, it could be expected to have more continuous ground ice than Davies crater, located at 45 °N. If the latter crater is far enough south that the ground ice is not continuous then fewer fracture polygons would be expected to form. Alternatively, if the ground ice was thinner here then it is possible that the scalloped terrains have deflated the entire depth of the ice table, leaving only ice-free terrain below, in which this type of patterned ground cannot form.

Values of water equivalent hydrogen (WEH), based on epithermal neutron measurements (Feldman et al., 2004) were compared for the two craters. WEH measurements around Lagarto Crater suggest a proportion of ice in the near subsurface of 5-7% by weight. Measurements around Davies Crater are not as high, ranging from

5-6% by weight. This supports the hypothesis that the ubiquitous stippled terrain around Lagarto Crater could be due to a higher concentration of near surface ground ice.

However both WEH measurements are generally low compared to the high northern latitudes where fracture polygons are more common. It should be noted that such measurements only sample the upper layers of the regolith (the upper 50-100cm; (Boynton et al., 2010; Feldman et al., 2002)) so low WEH measurements do not rule out a larger volume of ice at depth where it would be expected to be more stable at this latitude. It is also possible that these scalloped depressions formed during a period when ice content of the soil in this region was much higher than it presently is.

10.5 Depression asymmetry

While the lack of HiRISE images at these sites limits the extent to which their small scale morphology can be characterised, it is often possible to determine whether the depression is asymmetric or not. Scalloped depressions frequently have one steeper, or better defined, edge, while the other side of the structure is less clear (e.g. Lefort et al., 2009; Morgenstern et al., 2007). The asymmetry of scalloped depression in Utopia Planitia has been used as the basis for several models of formation. The orientation of this steeper wall is significant in determining the origin of these features, as different orientations would be expected under different climatic conditions.

One slope will typically receive more insolation than the other, and ground ice in this slope will experience more thaw or sublimation causing it to erode and the scalloped depression to expand through retrogressive collapse. In the present day it would be expected that the equator facing slope will receive the highest insolation and so this will become the steeper slope (e.g. Lefort et al., 2009; Morgenstern et al., 2007). This is expected to be the dominant model during low obliquity periods.

Conversely a large number of steeper southern, pole facing, slopes would suggest equatorward expansion. This would be more likely to occur under high obliquity conditions. In this case the increased axial tilt means that pole facing slopes receive more insolation (Séjourné et al., 2011, 2009; Ulrich et al., 2010).

In the plots presented below the edge of the structure which is clearer, or appears steeper is displayed, not the aspect of the steepest slope. Thus a depression marked North (N) has a steeper northern, or equator facing, wall, while a depression marked South (S) has a steeper southern, or pole facing, wall.

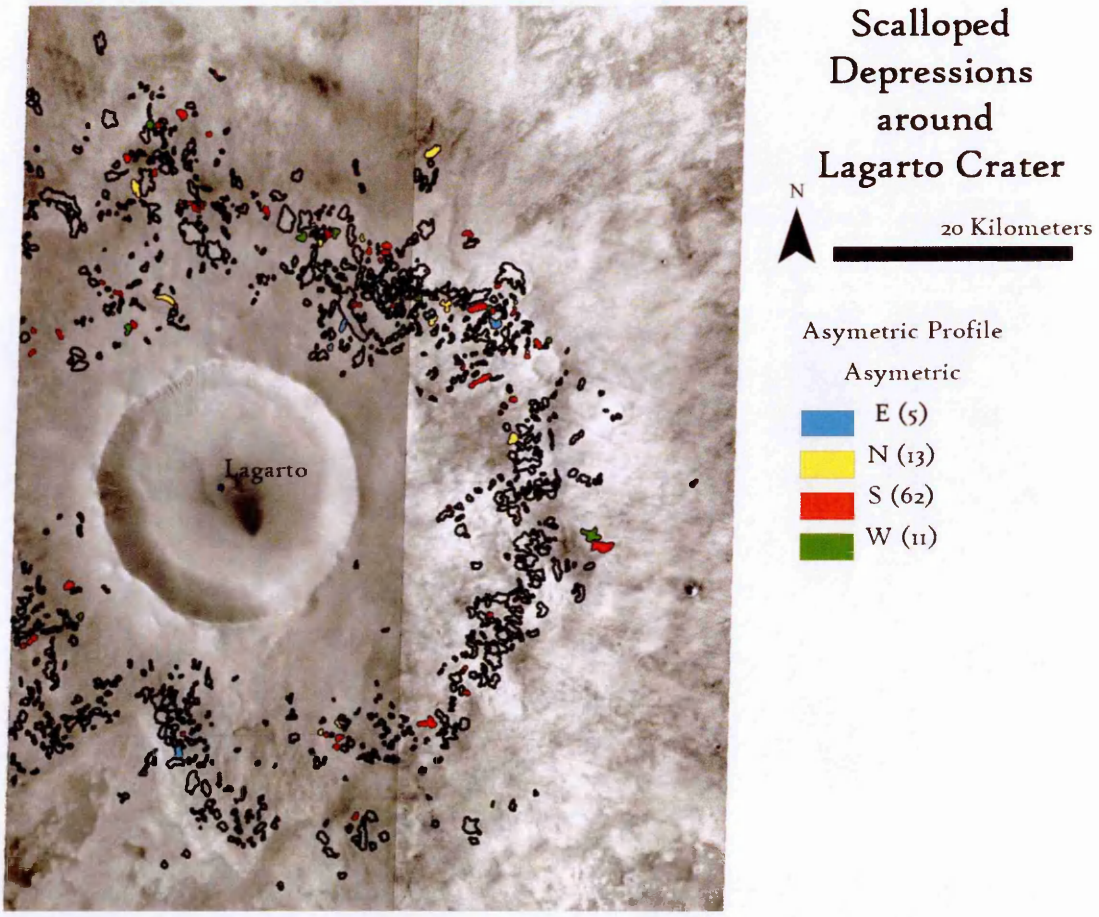

Figure 10.12: Distribution of scalloped depressions with a clear asymmetric profiles around Lagarto Crater. North indicates a steeper northwards, equator facing slope. While South indicates that the southern, pole facing slope is steeper.

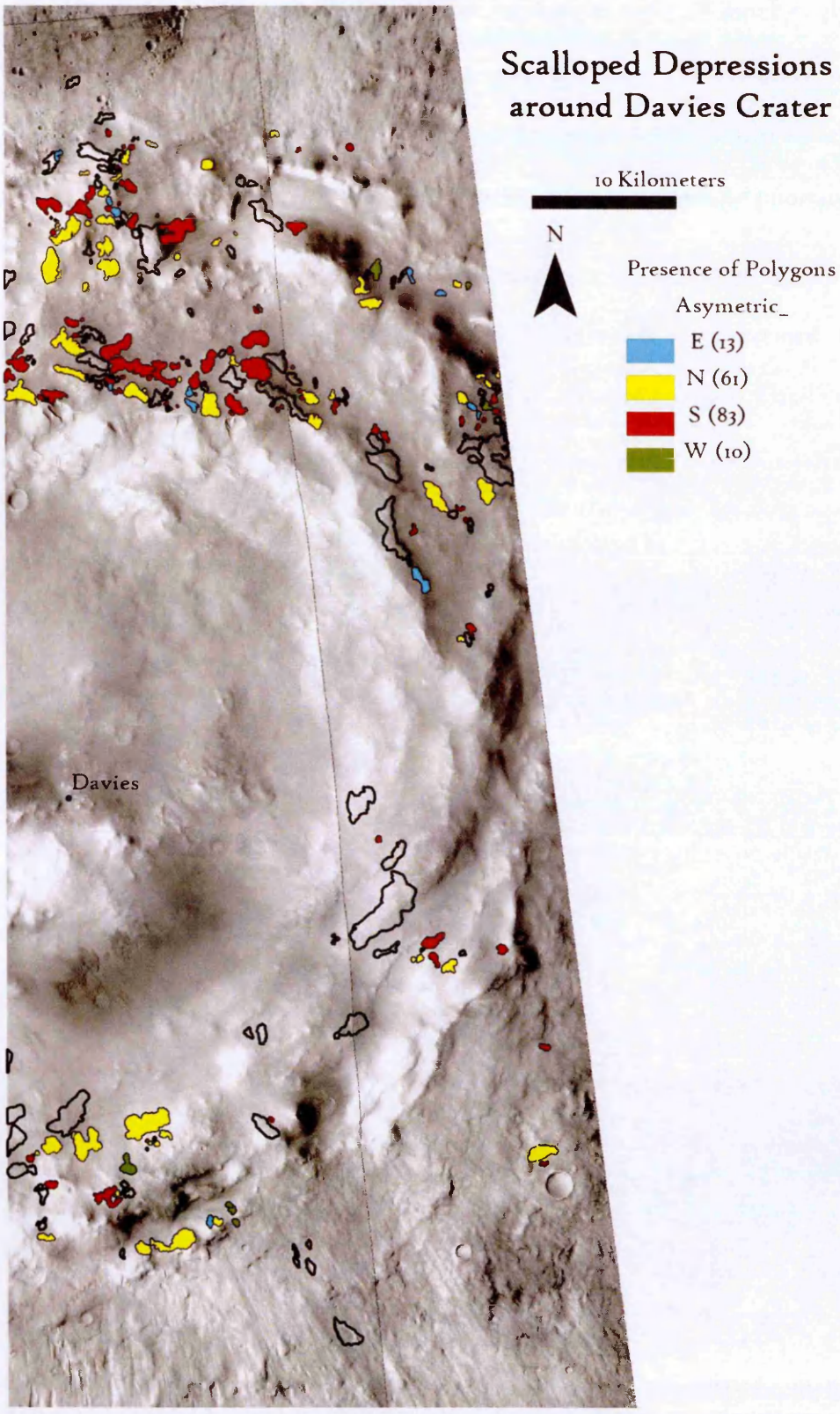

Figure 10.13: Distribution of scalloped depressions with clear asymmetric profiles around Davies Crater.

In Davies Crater it is clear that north and south asymmetry is much more common than east or west asymmetry. This fits with past observations of scalloped depressions where the steeper wall was generally found to be either pole or equator facing. Steep northern walls are more common on the southern side of the crater, where very few scalloped depressions feature a more prominent southern wall. Davies crater has approximately equal proportions of pole and equator facing slopes. Here there are only 22 more south facing features than north facing ones.

This is not the case at Lagarto Crater, where South facing features are much more common. It should be noted that, although this crater has more scalloped depressions overall, fewer of them have a clear asymmetry. Far more features had uncertain asymmetry or no clearly steeper slope. A useful expansion to this investigation would be to construct digital elevation models of these sites so that the profiles of these depressions could be measured directly, alleviating the uncertainties introduced by categorising these features by visual inspection.

10.6 Detailed examination of scalloped depressions in ESP_035302_2260

The 13 scalloped depressions in HiRISE ESP_035302_2260 allow a more detailed examination than is possible using CTX images. Although these depressions have the same scalloped morphology as their cousins in Utopia Planitia, they also have several morphological differences to the features observed by studies in that area.

The depressions are rarely flat floored but frequently have a very rough interior. Often large blocks of material are present within the centre of a depression and numerous pits and hummocks cover them. This could be due to the location of these features on the

ejecta blankets of large impact craters. The degradation of the ice-rich surficial mantle exposes whatever lies beneath, which in this case could be rugged ejecta material.

Alternatively, these features may be relatively old, having been degraded by other erosive processes in the time since they initially formed. This is supported by the rough morphology of many depression rims and the fact that it is the morphologically more mature features which are more likely to have a rough-floored morphology. Many of the smaller structures are smoother, although many are also quite faint, suggesting subsequent degradation or possibly infilling, or that they did not incise very deeply into the mantle material in the first place. These features generally lack the bright bands observed in scalloped depressions in Utopia Planitia.

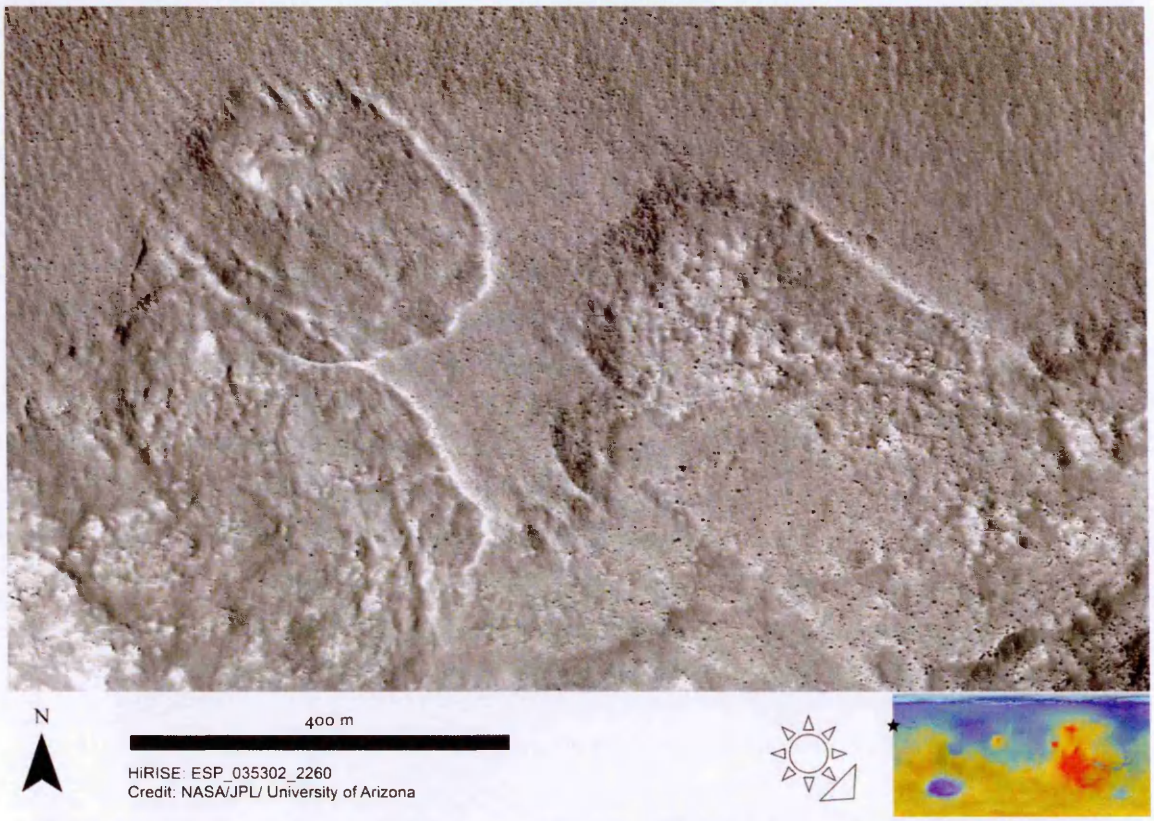

Figure 10.14: Illustration of large grade 3 scalloped depressions. These structures are classified as type 4-5 as several scalloped depressions are merging to form a larger basin. The two southerly features exhibit steeper northern walls while the northern most feature, which is the best defined has a steep south easterly wall.

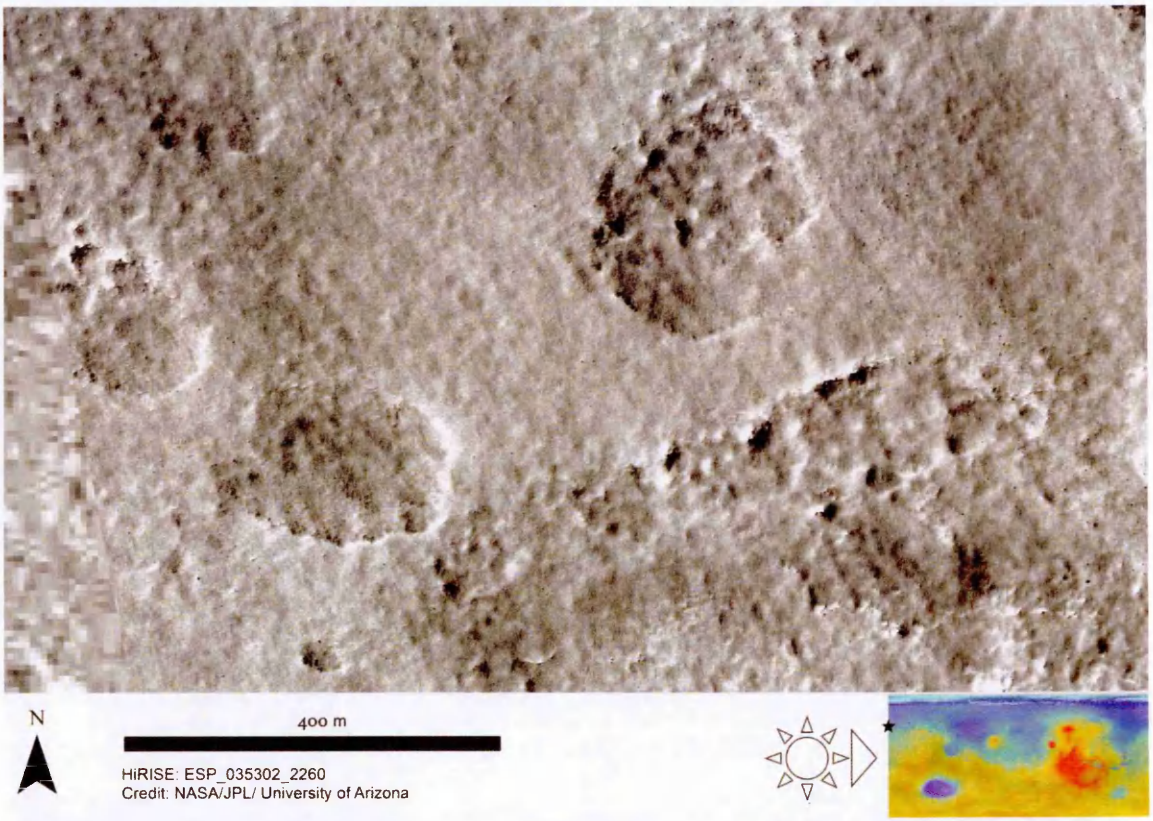

Figure 10.15: Illustration of grade two scalloped depressions with a large number of pits within their interior. These features have sharper southern walls; the westernmost feature is classified as type one while the others are type three features.

10.7 Discussion

In general both sites are fairly similar in morphology. In both cases, the assemblages are clearly well-developed. The largest area is covered by numerous mature depressions which have clearly undergone extensive degradation over long periods of time. Although "old aged" structures are prominent, they have not degraded the entire area, and small features, which have not had time to develop into larger coalesced terrains, are still seen.

This suggests that scalloped depression development may have occurred over a long period of time, rather than in a discrete time period, because there was sufficient time for a large area to evolve from young to mature, but young features were still forming during ongoing degradation.

Both sites exhibit the same variety of depression morphologies, including extensive type six regions which appear to be very mature structures. It is consequently inferred that this is an old landscape that has undergone many phases of degradation. The fact that these depressions appear heavily degraded with rough interior surfaces and irregular rims also supports this possibility.

An asymmetric profile can be observed in many of the scalloped depressions. While the full range of aspects is represented at both sites, it is clear that steep southern walls are more common at both sites. This prevalence for pole facing slopes probably indicates that these structures formed during a period of higher obliquity when the greater axial tilt resulted in increased insolation on pole facing southern slopes. Since the last period during which obliquity exceeded 40 degrees occurred approximately 5 Ma ago, this may constrain the minimum age of the features. This formation period would likely account for the generally degraded look of these depressions, and their classification as a mature landscape.

Despite these similarities it would appear that the two sites do not have an identical evolutionary history. At Davies Crater, the total area covered by each type of depression increases with type, but this is not the case at Lagarto Crater. Here, a far larger area is covered by type three scalloped depressions than by those of type four or five (Figure 10.7). This suggests that these features could have developed over a slightly shorter period of time, so that fewer of these type three features had time to grow and merge into type four and five structures. However the degraded nature of the landscape suggests that it has been a long time since the period when scalloped depression formation was active.

There is also a difference in the prevalence of stippled textured surfaces between the two sites. Almost all of the scalloped depressions around Lagarto crater exhibit this

texture, but many of those in proximity to Davies crater do not. This may suggest that Davies Crater, being the more southerly of the two sites, is not as good an environment for the development of this sort of patterned ground. If the stippled texture reflects ground patterned by thermal contraction polygons then this could be due to climate differences, or the availability of near-surface ground ice.

10.8 Summary

In summary the evidence assessed in this investigations suggests that the scalloped depressions around Davies and Lagarto Craters are relatively old, mature landforms. The dominant aspect of their steeper slopes is consistent with formation during past higher obliquity periods. This is supported by the heavily degraded appearance of these features which appear more eroded than many of the sharp, young looking scalloped depressions of Utopia Planitia. Stippled terrains which may be evidence of the presence of fracture polygons at or below the resolution of the CTX images were found to be more common around the northernmost Lagarto Crater. This could be due to the slightly higher proportions of water equivalent hydrogen at this site, which suggests that more ground ice is present here than at Davies crater. However the differences in WEH are very small and the values for both craters are much lower than those seen at high northern latitudes where fracture polygons are ubiquitous.

11 Chapter Eleven: Discussion

This chapter is divided into three main sections. The first addresses various methodological issues, primarily pertaining to the remote sensing survey, and discusses the ways in which these have been accounted for during the investigation.

The second section provides a synthesis of the results and analysis presented throughout the thesis and discusses their implications for a periglacial hypothesis. This section also compares these results to those of previous studies and discusses the implications of a periglacial environment in the geologically recent past. The chapter concludes by outlining a variety of future projects which could build on the findings of this investigation.

11.1 Methodological Issues

The following sections address several limitations which should be considered when interpreting the results of the investigation. These methodological issues are primarily related to the remote sensing surveys and associated analysis. Issues related to the laboratory and field studies are addressed in their respective chapters.

11.1.1 Image resolution and coverage

The main limitations of this investigation result from the generally low resolution of satellite images from Mars compounded by the generally small scale of characteristic periglacial features. As illustrated in Chapter Four, sorted patterned ground is hard to characterise in satellite or air photographs. Since only isolated large clasts are observed it is difficult to tell whether they form the larger parts of a coherent coarse domain, or whether they are isolated blocks which happen to form a pattern. Morphologic

characterisation of larger scale features, such as scalloped depressions and lobate hill-slope structures, are thus more reliable than those for small scale features.

HiRISE images also cover a relatively small fraction of the martian surface, so any landforms which did not fall within sampled images would have been missed. The survey was thus not a full representation of the entire surface and some "periglacial" sites may exist which were not discovered during this investigation.

Very small features, such as sorted patterns and lobate structures, are only clearly visible at or near an image's native resolution. It was not possible to survey an image solely at the native resolution without losing important context information. Consequently, it is possible that some small scale features might have been missed. Most images were only examined once in their entirety at full resolution. Sites of interest were revisited, but the majority of the image was not examined more than once.

Despite these issues, it is believed that the survey methodology was as comprehensive as possible, and that most of the features which could have been found within the images were recorded. While these limitations must be acknowledged, they have not dramatically impacted the results of the study.

The low resolution of remote sensing data will always be a problem for a study of this type, but the resolution of the HiRISE instrument is unprecedented in the field of Mars remote sensing. It provides an opportunity to examine the surface in far more detail than was previously possible. More detailed examination of these features will have to await future missions with even higher resolution cameras; for the time being the most detailed images available have been used. At the time of writing, the HiRISE instrument is still active, and so the number of images where these small scale features can potentially be detected is increasing all the time.

11.1.2 Sampling

Examining all available HiRISE images within the study areas was beyond the scope of this investigation as it would have taken far longer than the time available. The survey focused on a relatively small fraction of the available images. Consequently, it is possible that biases in sampling could influence the results of the study.

Rather than taking a random sample, it was decided to focus on those images which contained medium-sized impact craters. This sample was selected based on the findings of Gallagher et al., (2011). That study suggested that crater walls were an environment where the formation of visually distinctive stripes and lobate forms were likely to occur. These landforms develop through hill slope processes; crater walls being one of the few sources of steep terrain in the otherwise low-relief northern plains.

A large number of putative periglacial features were found within crater environments, but they were by no means limited to them. Many possible sorted polygons were found on the surrounding plains, rather than in the crater interiors, and so it is possible that many more sites will be present in images which were not sampled.

This was confirmed when additional HiRISE images around Lomonosov Crater were surveyed as part of the context study. It was found that clastic networks were as common on the plains as in the crater interior at this site, so the same will probably hold true in other regions.

Surveying every available image across all three study areas would have been impractical, since thousands of images are available. The sampling procedure was appropriate to the subject of the study, surveying for clastic networks and lobate structures, but it is acknowledged that many sites may be present which were not detected due to the focus on crater interiors. Future studies of this sort could examine all available images, but across a smaller study area.

11.1.3 The lack of ground truth

Ground truth observations are limited to a handful of sites on Mars. Morphological similarities provide a compelling case that some of these features might be periglacial, but without direct observation of their formation environments it is harder to determine their processes of formation. It is however possible to infer information from the few sites visited by landers and rovers, with the assumption that observations at one site are representative of the conditions elsewhere.

One of the most relevant lander observations to this discussion is the observation of contraction crack polygons at the Phoenix landing site. The lander confirmed the presence of excess ground ice in proximity to these features by digging trenches (Mellon et al., 2009). This element of ground truth supports the observations of near surface WEH discussed throughout earlier chapters. It thus provides strong evidence that contraction cracks form through ice related processes, both at the Phoenix landing site and elsewhere on the northern plains.

Similar observations would be useful for areas of possible sorted patterned ground, as direct observation of ground ice at these sites could definitively show that they are likely to be ice related. Unfortunately, the high northern latitudes are not favourable for most landers or rovers relying on solar power, which is reduced at high latitudes. Planetary protection protocols might also rule out the delivery of landers to sites of potential astrobiological interest, which would include putative periglacial environments. Nonetheless, the proximity of some clastic features to contraction cracks provides another piece of consilient evidence for an ice-related formation mechanism.

11.1.4 Subjectivity of Classifications

The classification of landforms is inescapably subjective. Possible landforms were compared to type-examples from the terrestrial literature and to features proposed as periglacial analogues by earlier surveys, in particular Séjourné et al., (2011) for scalloped depressions, Johnsson et al., (2012) for lobate structures and Gallagher and Balme (2011) for sorted patterned ground.

All features were ranked using a five point scale which could be compared to a variety of possible controlling parameters. However, since each type of landform was being assessed based on a different set of morphological criteria, these grades are only comparable within a given landform class. The classification of different landform types, such as varieties of sorted patterned ground in Chapters Five, Seven and Nine, and scalloped depression types in Chapter Ten, are more reliable, since feature type is easier to classify than the likelihood that an example is periglacial. But because no quantitative metric was used to assess feature type, these classifications remain subjective.

Action was taken to limit the effect that subjectivity of classification would have on the results of the study. Randomly selected sites were reassessed to ensure that the grading of features remained consistent between the earlier and later stages of the investigation and every example was examined multiple times. New examples were marked during the initial survey, and given a provisional classification. Each site was then revisited at least once, during which a more detailed classification was conducted. Several sites with especially interesting features were examined multiple times over the course of the project. Using this approach, this system of grading and classification was made as reliable as possible.

11.1.5 Low data volumes

In many cases, small numbers of data have been used during this investigation. Many of the features examined were drawn from a relatively small pool of examples. Instances where low data volumes may influence the results of the investigation have been noted throughout the thesis.

For example, lobate structures are found to be very uncommon despite being quite widely distributed across the study areas. The lack of examples limits the analysis that can be done with these features, and thus their usefulness in assessing the periglacial hypothesis for their formation. Most of the good examples found within the investigation are largely morphologically unique. Only one example of lobes was found to have a clastic morphology, and only one is in proximity to possible sorted stripes. Due to the low data volume, it is impossible to determine whether these assemblages are less common than regular lobate structures, or whether it is a bias in the sampling.

While far more examples of sorted patterned ground were found, there are still issues of data volume. The majority of the analysis conducted on sorted features during the course of this investigation has focused on the region around Lomonosov crater. This is the only area with a large enough population of sorted features for multiple adjacent sites to be examined. Most other possible sorting sites are isolated occurrences. It would be useful to compare and contrast the features in and around Lomonosov Crater with a similar area elsewhere on the planet to determine whether the same patterns hold true at both sites. However, no other area produced the same wealth of examples.

11.2 Synthesis of results

In the preceding chapters a variety of approaches has been applied to testing the hypothesis that periglacial landforms could be present on the Northern Plains of Mars.

The majority of the project consisted of a remote sensing study. Several surveys of HiRISE and CTX images were carried out to determine the distribution of putative periglacial landforms (Chapters Six, Seven and Eight), and to assess the extent to which their morphology matches that of their terrestrial analogues (Chapters Five, Nine and Ten). To support this remote sensing investigation, a field campaign was carried out to examine terrestrial patterned ground, both in situ and from air photographs (Chapter Four). A series of laboratory experiments were also conducted to examine whether periglacial processes are viable under martian conditions (Chapter Three).

These investigations allowed several key research questions to be examined.

- What is the distribution of putative periglacial landforms on the Northern Plains of Mars?
- How frequently do such features form assemblages with similarities to periglacial landscapes?
- To what extent does the morphology and situation of these landforms support a periglacial hypothesis?
- Are the freeze thaw processes that result in periglacial landforms on Earth viable under martian temperature and pressure conditions?

While not all of these questions have been conclusively answered, this project has added a wealth of new evidence to the ongoing debate over martian periglacial landscapes. The following sections will discuss the results in the context of these research questions, drawing evidence from throughout the investigation.

11.2.1 Periglacial Landforms?

In the preceding chapters a variety of distinctive landforms have been examined that might be analogous with terrestrial periglacial structures. Chapter Two provides a detailed overview of the features which are characteristic of a terrestrial periglacial environment.

The main aim of this research was to expand the catalogue of putative periglacial sites beyond the areas examined by previous investigations. This objective was largely successful. Chapter Seven illustrates numerous examples of possible periglacial features, many of which do not appear to have been detected by previous investigations.

The landforms of interest fall into two main categories. The first are the 'diagnostic' landforms; lobate hill slope features and clastic patterned ground. These features are all morphologically similar to features which, on Earth, would form through the freezing and thawing of liquid water. Scalloped depressions are also diagnostic of cryotic processes, although they do not necessarily require thawing since they could have formed through the sublimation of exposed ground ice.

The second class are the auxiliary landforms: gullies and fracture polygons. These features are analogous to landforms which frequently occur in close proximity to periglacial landscapes on Earth, but they are not specifically formed through active layer processes. The distribution of these features is still significant as it can be compared to that of the diagnostic landforms to test whether the same geomorphological relationships that hold true on Earth are repeated in the martian landscape. These features can also be used to test several of the hypotheses surrounding the formation mechanism for the more diagnostic landforms.

11.2.2 The distribution of putative periglacial landforms

Numerous putative periglacial landforms are found across the Northern Plains. Some, such as scalloped depressions and gullies are common while others such as sorted patterned ground are relatively rare. Lobate hill slope features were found to be particularly uncommon, yet examples of these landforms were still observed in multiple HiRISE images. Some examples of all of these landforms were more convincing than others, but multiple examples of each feature type were found to have a convincingly periglacial morphology.

The results presented in Chapter Seven clearly illustrate that, while not common, these features are found across the northern plains of Mars, occurring in all three study areas and over a wide range of latitudes. There are differences in density and distribution of features between Acidalia, Utopia and Arcadia Planitiae, but these are not as dramatic as might be expected considering the scale of these study areas, and the extent to which they are spread across the northern hemisphere. The broad trends that occur are consequently believed to be global, and governed by global processes.

Gullies and scalloped depressions are primarily found at mid latitudes, at the southern edge of the study area. Both landforms occur over a similar latitude range, although there is considerable variation from one study area to the next. This fits with the observations of these features by previous investigations such as those of Morgenstern et al., (2007) and Soare et al., (2012).

Clastic patterned ground and lobate hill slope features were found to be much more common at high northern latitudes. This fits with the observations of these features by previous studies such as Gallagher and Balme, (2010); Johnsson et al., (2012). However, examples of these features were found further south than expected, and beyond the limits of the areas surveyed by previous investigations.

Some landforms are more common in one particular region. The most clearly expressed and most numerous examples of sorted patterned ground are found in the north east of Acidalia Planitia, while the best examples of scalloped depressions are found in Utopia Planitia, where they were first observed. Such features are found over similar latitudinal ranges in the other study areas, but they are less concentrated, and fewer reliably identified examples are found.

It is interesting to note that examples of both lobate structures and clastic patterned ground are found further south than expected. Most prior studies into the distribution of these features had focused on the extreme high latitudes. However, it has been demonstrated in Chapter Seven that, while many of these landforms are most numerous in the northern part of the study area they are not exclusive to high latitudes.

Both lobate structures and clastic polygons are found as far south as 36°N. Johnsson et al., (2012) reports lobes between 60°N and 80°N. Gallagher and Balme (2010) and Gallagher et al., (2011) report clastic lobes between 59°N and 71°N. Clastic polygons are found beyond the southern limits of the studies of Gallagher and Balme (2010) and Levy et al., (2008). The possibility of these landforms occurring at more southerly latitudes is interesting as it suggests that they might have formed in past periods when more ground ice was present at mid latitudes. The observation of clear sorted circles at equatorial latitudes by (Balme et al., 2009) would appear to support this conclusion. These features, which occur at 5°N, show a clear circular pattern and are exhibit denser and more continuous coarse domains than most of the structures observed during the current investigation. However it is important to note that these features have clearly formed as an out of equilibrium event that formed as a result of the presence of ice from catastrophic flood events and thawing during an unusually warm period.

Examples of lobate hill-slope features were scarce, with very few examples scattered widely across the three study areas. However, they are clearly common enough to have been sampled within the relatively small areal proportion of the Northern Plains that was surveyed. There were too few of these features to perform any complex analysis on variations in their morphology. A much larger survey would be required to find more examples.

11.2.3 Periglacial Assemblages

A variety of sites with possible periglacial assemblages are found across the northern plains as shown in Figure 7.30. Forty-four HiRISE images contain multiple putative periglacial landforms. Four of these sites include lobate structures, while 23 sites feature possible sorted features. Some of the most common landforms to occur in close proximity are scalloped depressions and gullies. Since both are hypothesised to form through thermokarst-like processes, this could be an important correlation. Twenty-two sites exhibiting both gullies and scalloped depressions were found, and these landforms, both individually and together, were frequently found in assemblages with sorted and lobate features.

In areas where clastic patterned ground is numerous, it is possible for multiple varieties to occur in close proximity. Most sites with sorted stripes also have either polygonal networks or rubble piles within the same HiRISE image. However, unlike the terrestrial examples described in Chapter Four, there were no sites where sorted polygons are observed to clearly grade into stripes. The site illustrated in Figure 5.14 consists of very clear stripes which grow discontinuous as they transition from the steeper crater wall to the shallower slopes of the interior, the flat ground in the centre of the crater is dominated by sorted labyrinths, similar to the terrestrial features described by Kessler and Werner, (2003). Clear sorted polygons are not observed within

the crater, only on the surrounding plains but the labyrinthine structures likely formed through similar means.

Despite their scarcity, there are several locations where lobate hill slope features are found in the same images as other putative periglacial landforms. One image contains both lobate structures and scalloped depressions. Another site, illustrated in Figure 7.29, features lobes in proximity to gullies, although not within the gully alcove as at the sites reported by Johnsson (2013) and Gallagher et al., (2011). Another image exhibits lobes in proximity to both scalloped depressions and gullies. The most interesting assemblage is one in which lobate structures are found in proximity to possible sorted stripes, shown in Figure 7.13. This HiRISE image also contains gullies and a possible scalloped depression where some degradation of the mantle seems to be taking place. This is the only site where all four varieties of putative periglacial features occur.

The fact that some assemblages in the mid to high latitudes exhibit all varieties of putative periglacial landform could indicate that these landforms can and do form part of a coherent landscape. Some of these landforms may evolve under different conditions, but it is clear that landscapes exist in which the conditions for the development of multiple features occurred, if not concurrently, then at least over short enough time periods that their expressions in the landscape are consistent with terrestrial analogues.

11.2.4 Relationship to ice-rich terrains

Many putative periglacial landforms occur at high northern latitudes where the most water equivalent hydrogen is found in the near subsurface (Boynton et al., 2010; Feldman et al., 2002). Periglacial landforms would be expected to occur in the area where ground ice is plentiful, but where it is also capable of undergoing degradation.

Areas with landforms indicative of sublimation in the geologically recent past are of particular interest.

The latitudinal distribution of scalloped depressions, which appear to cut into the latitude dependant mantle, are thus a good indicator of the latitude band in which periglacial processes would be expected. Gullies and scalloped depressions both occur over much the same latitude range and this suggests that they may result from similar processes. However, clastic patterned ground and lobate features are predominantly found further north. This is the region where ground ice is believed to be most continuous and where water equivalent hydrogen is at its highest. The southerly features may be relict landforms which formed at a time when ground ice was more extensive, or they could have formed through mechanisms which are unrelated to the degradation of ground ice but which nonetheless produced similar features.

11.2.5 Testing formation hypotheses

Gullies are believed to form through the erosive action of liquid water generated by thawing of subsurface ice (Conway and Balme, 2014; Costard et al., 2002). Consequently, the fact that they often form in assemblages with scalloped depressions lends weight to the hypothesis that these depressions also formed through thaw-related processes.

Several hypotheses have been put forward to explain the formation of clastic patterned ground on Mars. Both of the main alternatives to a periglacial paradigm; the boulder ratcheting mechanism of Orloff et al., (2011, 2013) and the gravitational sorting of Levy et al., (2010, 2008) and Mellon et al., (2008) rely on the presence of an underlying fracture network. However, in Chapter Nine it is shown that the majority of clastic patterns do not have associated fractures and that in many of the cases where fractures are present the two networks do not appear to be aligned. This suggests that, in the

areas examined, these fracture control hypotheses do not explain the observed patterns. This might suggest that a periglacial origin is more likely than one related to fracture control, but there is insufficient evidence to unreservedly accept this formation mechanism.

11.3 Comparison to previous studies.

As described in detail in Chapter Two the presence of putative periglacial landforms on Mars is well documented. Extensive catalogues of gully distribution were already in existence when this project began (e.g. Balme et al., 2006; Kneissl et al., 2010; Levy et al., 2009) and fracture polygons have been studied across the martian high latitudes (e.g. Levy et al., 2009; Levy et al., 2010; Mangold, 2005).

Lobate structures have been examined by Johnsson (2013) and Johnsson et al., (2012) in both the northern and southern hemispheres. Clastic lobes were also observed by Gallagher et al., (2011), Clastic patterned ground has been observed by Balme and Gallagher at a number of sites across the northern plains; (Balme et al., 2009; Gallagher and Balme, 2011; Gallagher et al., 2011). As well as in unusual equatorial environments (Balme and Gallagher, 2009) These studies prompted and informed the current investigation.

Scalloped depressions have primarily been studied in the Utopia Planitia region (Costard and Kargel, 1995; Morgenstern et al., 2007; Séjourné et al., 2012, 2011; Soare et al., 2007b, 2012). Their morphology has been classified with the aim of determining their formational history (Séjourné et al., 2011). To what extent do the findings of this investigation confirm the results of previous studies and to what extent does a different pattern emerge? How do the results of the analysis fit into the context of current Mars periglacial research?

Table 11.1 shows the range of latitudes over which each of the features examined in this project were found and compares this to the published ranges of such features in a variety of other studies. In general the latitudinal distributions of landforms found in this survey support those reported by other researchers in different regions of the Northern Plains.

Table 11.1: Comparison of the latitudinal distributions of various putative periglacial landforms to those found by previous studies on the subject.

Feature	This Survey	Example	Published Studies
Sorted Patterned Ground	36-77 °N	59-78 °N	Gallagher *et al.*, 2011
		60-70 °N	Orloff *et al.*, 2011
Lobate Structures	32-74 °N	60-80 °N	Johnsson *et al.*, 2012
		59-75 °N	Gallagher *et al.*, 2011
Gullies	30-67 °N	30-70 °N	Levy *et al.*, 2009
		30-80 °N	Kneissl *et al.*, 2010
Scalloped depressions	30-67 °N	~45 °N	Morgenstern *et al.*, 2007
		40-55 °N	Soare *et al.*, 2012
Fracture Polygons	30-77 °N	50-75 °N	Mangold *et al.*, 2005
		35-75 °N	Levy *et al.*, 2009
		40-55 °N	Soare *et al.*, 2012
Hypothesised ice-rich terrains		47-65 °N	Costard *et al.*, 1989
		>60 °N	Feldman *et al.*, 2002

11.3.1 Scalloped Depressions

The majority of scalloped depressions in these study areas are found to occur within the range 30°N to 55°N. This is comparable with the scalloped depressions mapped in Utopia Planitia by the studies of Soare et al., (2007b, 2012) and Séjourné et al., (2011) which are located around 45°N. Morgenstern et al., (2007) observed greater amounts of degradation and scalloped depression formation at lower latitudes and this is supported by the findings of this study. The majority of scalloped depressions in Acidalia are

concentrated within a similar low- to mid-latitude range with fewer examples at higher latitudes.

One aim of this study was to compare scalloped depressions in other regions of the northern plains with those studied extensively in Utopia Planitia. While fewer scalloped depressions were found in the Acidalia area than in Utopia, they were largely morphologically similar. The large concentrations of scalloped depressions around Davies and Lagarto Craters were found to represent all of the categories of scalloped depression development proposed by Séjourné et al., (2011), although there were some morphological differences which may suggest that these features are an older landscape than some of the fresher looking scalloped depressions in Utopia. The scalloped depressions at these two sites had a generally more degraded appearance than many of those outlined in Séjourné's study. The classification scheme outlined in Séjourné et al., (2011) was expanded with reference to the terrestrial literature (Wallace, 1948) to take into account large areas of degraded ground which were more extensive than the type five features illustrated in (Séjourné et al., 2011).

Heavily degraded areas of this sort have been observed in all three study areas, including in the area surveyed by Séjourné et al., (2011), so it seems likely that similarly degraded features are present in Utopia, but were not the focus of that investigation. Scalloped depressions in general are more common in that region than in Acidalia and Arcadia Planitiae as a whole.

11.3.2 Gullies

Gullies are found to be concentrated at lower latitudes, pre-dominantly between 30-50°N. This is in broad agreement with the observations of previous studies to map these landforms, A variety of studies on the distribution of gullies in the northern hemisphere have found them to occur within the 30°N to 60°N range (Bridges and

Lackner, 2006; Heldmann et al., 2007; Levy et al., 2009; Soare et al., 2007b). Heldmann et al., (2007) report gullies as far north as 70°N. Gullies primarily occur within the same range of latitudes as scalloped depressions, a finding in agreement with the surveys of Kneissl et al., (2010).

11.3.3 Fracture Networks

Fracture polygons were found to be ubiquitous over the area surveyed. This supports the observations of Soare et al., (2012), who observed fractures to be found in high concentrations between 40 and 60°N in Utopia Planitia. Mangold (2005) found polygon morphologies to vary from north to south up to 75°N across the Northern Plains. The upper limit for polygon occurrence in this survey fits with these observations, fracture polygons are found to be ubiquitous within the range described by Mangold. However fractures are also found further south, beyond the extent of Mangold's survey. Fracture polygons were found to be more abundant in images north of 40°N, but seem to be present across the entire range of latitudes surveyed. This fits with the distribution observed by Levy et al., (2009, 2009a, 2011).

11.3.4 Sorting and Lobes

Sorted polygons, stripes and solifluction lobes are the features most characteristic of a periglacial environment, but are also the least common landforms. Both patterned ground and lobate structures are found to occur much further south than established by studies such as Gallagher et al., (2011) and Johnsson et al., (2012 and 2013).

Rubble piles are found in several locations at lower latitudes, however those examples are not as distinct as the rubble piles at higher latitudes, and are harder to distinguish from the more ubiquitous randomly distributed clasts. Orloff et al., (2011, 2013) found

rubble piles to only occur north of 65°N, a distribution which largely fits with that found in this survey.

Orloff et al., (2011, 2013) also found clasts to accumulate in and around the troughs of thermal contraction polygons, forming sorted circles without requiring a freeze-thaw process. This may be the case in some parts of the study area, as several instances of sorted polygons exhibit a tendency to follow the underlying fracture pattern. However, analysis of the extensive fields of clastic patterns around Lomonosov Crater would seem to refute this theory. The majority of cases of boulder organisation in this region are not fracture controlled. The presence of a clastic net in the absence of a controlling fracture pattern would require a different mechanism to that proposed by Levy et al., (2010, 2008), Mellon et al., (2008) and Orloff et al., (2011, 2013), perhaps suggesting that these features are more likely to be periglacial.

There were too few examples of lobate features in the area surveyed for their morphology to be meaningfully characterised. However, comparisons between the relatively distinct features observed in this survey, and those reported elsewhere in the literature reveals some interesting patterns. The example of clastic lobes shown in Figure 7.11 was found on the walls of a crater at 67°N in Utopia Planitia. This is a very similar latitude to that at which the clastic lobate features described by Gallagher et al., (2011) were observed. Johnsson et al., (2012) also reports clastic lobate structures at, and north of, this latitude. These features occur within the latitude range where cryobrines should be stable on warm hill slopes and where the majority of clastic polygons are found. All of the anomalously southerly lobate structures lack a stone banked morphology.

The site with lobate features in proximity to clastic stripes occurs at 45°N. These features strongly resemble many of the examples presented by Johnsson et al., (2012),

although they are much further south than the southern limits of both Johnsson et al., (2012) and Gallagher et al., (2011)'s surveys. This sort of assemblage is nonetheless similar to that which Gallagher et al., (2011) describe further north, indicating that similar associations of possibly periglacial landforms are found to occur in widely separated regions of the northern plains. This might indicate that the processes resulting in these assemblages are not limited to any one part of the planet.

11.4 Viability of periglacial processes

It has been proposed that the depression of the freezing point of water by the presence of salts could facilitate periglacial processes, providing a case for a modern periglacial environment (Möhlmann and Thomsen, 2011). Brines, such as magnesium perchlorate, are believed to be present on the Northern Plains of Mars in proximity to the Phoenix landing site (e.g. Cull et al., 2010; Hecht et al., 2009). This is one of a variety of cryobrines many of which are viable at high northern latitudes and could allow for regular freezing and thawing within the range of temperatures common at the martian surface (e.g. Davila et al., 2010; Möhlmann and Thomsen, 2011).

Möhlmann (2011) has suggested that such cryobrines should be stable between 60°N and 80°N during the late northern spring. This would potentially provide a source of liquid water at the regular intervals required for seasonal periglacial cycles to occur. Möhlmann and Thomsen (2011) suggest that cryobrines are most likely on sun facing slopes, which would be expected to restrict the locations in which periglacial processes regularly occur. They also state that occurrences of cryobrines will be less common at mid to low latitudes.

It has been shown that thin films of water can develop through the interaction of cryobrines with ground ice and that ice lenses should thus be able to evolve (Sizemore et al., 2014). However, it has yet to be demonstrated that periglacial sorting can occur

under such conditions. It is not clear whether the presence of cryobrines would actually disrupt the sorting process. Chamberlain (1983) describes a significant decrease in the effectiveness of frost heaving in soils saturated with seawater, relative to those within a freshwater regime. Compared to most of the cryobrines described by Möhlmann and Thomsen (2011) seawater is not very saline and has a very high eutectic temperature.

The magnesium perchlorate brines hypothesised to account for periglacial processes at the martian high latitudes would be expected to have an even greater effect on the frost heaving system. This might slow down the sorting process, or limit the size and volume of material which can be affected. Conversely the models of Sizemore et al., (2014) suggest that excess ice can develop as efficiently using concentrated cryobrines as with pure water. Consequently, periglacial sorting could result normally despite the saline conditions.

Unfortunately, attempts to test whether sorting would still occur under such conditions proved inconclusive. Because phase one of the laboratory project, simulating sorting or frost heaving under terrestrial conditions, proved unfeasible this strand of the investigation was not continued. Further experiments would be required to determine whether cryobrines are a viable solution for allowing periglacial processes to occur on present day Mars.

Do the results of this survey support the formation of periglacial landforms through the thawing of cryobrines? Möhlmann (2011) suggests that cryobrines should be stable to the north of 60°N. This is further north than many of the features catalogued in this survey. Both gullies and scalloped depressions are typically found at much lower latitudes. However, these landforms are less likely to result from brine facilitated thaw than some of the other putative periglacial features under examination.

Both gullies and thermokarst would require large volumes of thaw which seems unlikely in a scenario where the presence of brines allows thin films of very saline water to develop within the ground. Furthermore there is strong evidence to support the formation of scalloped depressions through sublimation of ground ice (Séjourné et al., 2011; Ulrich et al., 2010) so brine facilitated thaw is not required to explain these features.

The majority of examples of clastic patterned ground are found at latitudes where cryobrines would be expected to form. Almost all of the grade four and five features occur above or around 60°N. However, many lower graded examples occur much further south than the latitude range where cryobrines are predicted to occur. Many of these features also lie beyond the region in which ground ice is currently stable and where the presence of excess ice is estimated from WEH data.

One possibility is that these generally low graded features do not result from periglacial processes. It might be possible for partial patterns to develop within boulder patches either through an alternate processes or random chance. So the presence of grade 1-2 sorted patterns within a non periglacial area would not be surprising.

Another possibility is that low latitude features formed during a period when conditions at those latitudes were more favorable for the development of patterned ground, either facilitated by cryobrines, or due to thawing of purer water. In this case the low graded nature of these structures could be the result of substantially more degradation disrupting older, relict features.

This explanation may account for the presence of highly graded lobate features at low latitudes. Only two examples of lobate structures with a grade of 3 or above are found to the north of 60°N, so it seems likely that these features can develop at a wider range of latitudes than that over which 'freeze-thaw' of cryobrines is expected. If these are

relict landforms this could account for their relative scarcity. Alternatively, the fact that fewer examples of lobes are found might indicate that they are occurring in unusual microclimates where thawing of cryobrines is possible. Möhlmann (2011), does not rule out their presence at lower latitudes completely.

In summary, the thawing of cryobrines remains the preferred option to facilitate the formation of sorted patterned ground, but is perhaps less likely to account for possible solifluction features. In the case of possible sorting, the transition from higher graded to lower graded sites does seem to occur at the latitudinal threshold for cryobrine stability. This would seem to support cryobrine facilitated thaw as a formation mechanism, and rule out the southerly landforms as recent periglacial structures.

11.5 Are these features periglacial?

There is considerable morphological similarity between the features identified in this investigation and those found in terrestrial periglacial environments. Many of these landforms are found in assemblages similar to those that comprise a periglacial landscape on Earth. Do they form through periglacial means? Or are they the result of different processes, which produce a similar end result?

11.5.1 Scalloped depressions as thermokarst

The asymmetry of the scalloped depressions examined in Chapter Ten support formation during a past period of higher obliquity as proposed by Séjourné et al., (2011). This is the period during which periglacial processes would have been most likely to be viable, as the higher obliquity would have resulted in increased temperatures at high latitudes. Consequently, it is possible that these heavily degraded features could be evidence of a past periglacial regime.

However, this tendency for degraded scalloped depressions can only be confirmed to be the case for the two areas of scalloped depressions around Davies and Lagarto Craters. Further examination of scalloped terrains, both in Acidalia Planitia and elsewhere on the Northern Plains would be required to further study this issue. Many examples of scalloped terrains from elsewhere in the HiRISE survey area have a less degraded morphology which might suggest a more recent development. These sites were not examined in the same detail as those discussed in Chapter Ten.

The fresh appearance of many of these features need not rule out formation during past periods of higher obliquity, since many of the examples presented by Séjourné et al., (2011) also have a less degraded morphology than those around Davies and Lagarto Craters. Alternatively, these fresher-looking scalloped depressions could be evidence of more recent degradation as suggested by Lefort et al., (2009) and Morgenstern et al., (2007).

11.5.2 Clastic Patterned Ground through periglacial sorting.

While the clastic polygons discussed in Chapters Five and Nine are similar in form to terrestrial patterned ground, they occur on a far larger scale. The lower gravity on Mars would be expected to result in some difference in scale, which might account for the larger features on the martian surface. Clast size appears to scale with circle size in both the terrestrial and martian data, so it is unsurprising that martian features exhibit both larger boulders and a wider diameter of polygon.

At a first approximation, the mean size of material making up the polygons around Lomonosov crater appears to be slightly higher than three times the size of the largest material making up some of the largest sorted circles reported in the terrestrial literature, for example, the set of very large sorted circles on Ellesmere Island in arctic Canada pictured in Figure 2.13b.

Since the gravity on Mars is approximately one third that of Earth, material of three times greater mass would be expected to be moved by equivalent processes. This would thus put many of the martian features on the upper limit of viability; however, these estimates are tentative. Further research would be needed to compare the size distribution of boulders in the largest terrestrial sorted circles with those of their martian analogues.

It is uncertain whether frost heaving will be as effective under martian temperature conditions. The temperature does not often rise above the melting point of pure water. Consequently, freeze thaw cycles would not be expected to occur very frequently and so it would take a long time for features that require multiple freeze thaw cycles to develop. This might be offset by the much lower erosion rates which would allow substantially more time for these features to develop. Thawing events would of course occur more frequently in systems where cryobrines depress the freezing point, however, this could reduce the efficacy of frost heaving as described by Chamberlain (1983).

It has been demonstrated, in Chapter Nine, that the clastic polygonal networks around Lomonosov crater do not appear to be controlled by the arrangement of underlying fracture networks. Since the fracture control hypotheses of Levy et al., (2010), Mellon et al., (2008) and Orloff et al., (2013) do not fit the observed clast-fracture relationships it seems unlikely that they explain the formation of these features. This could suggest that a periglacial hypothesis is more likely. These features have substantial morphological similarity to terrestrial analogues which adds weight to a periglacial formation mechanism. Some of the best examples of clastic stripes occur on hill slopes of the gradient expected to produce such features.

Many of the higher-graded features are found in regions where sufficient Water Equivalent Hydrogen is detected to suggest excess ice in the near subsurface, however this is not universally the case. The fact that a periglacial explanation would require anomalous conditions means that extraordinary evidence would be required to accept this hypothesis. While some strands of consilient evidence support the mechanism, more research into these features is required to confirm that they formed through periglacial means.

In summary, the periglacial hypothesis is a strong possibility to explain these features. No alternate hypothesis fits the observations better than a periglacial formation mechanism. While there remain some concerns as to the viability of these processes they remain a likely mechanism for the formation of martian clastic patterned ground.

11.5.3 Lobate Structures as solifluction lobes.

There are too few examples of clear lobate structures to allow a full assessment of morphological variations. Each example is slightly different from the others and only one clearly clastic feature was observed. This limits the extent to which their likelihood of being periglacial can be assessed. However, the fact that these features frequently occur in proximity to other putative periglacial features adds some weight to them forming through related processes.

Many examples of these features are also found on steep slopes such as the walls of impact craters. This fits with the topographic constraints under which terrestrial solifluction lobes form and so adds weight to the possibility that they formed through periglacial processes. As with the sorted features described above, lobate structures are not limited to the high northern latitudes. Some possible examples are found further south, beyond the range of latitudes where thaw through cryobrines would be viable. It should be noted that the best low latitude example occurs on a slope with a gradient

well below the five degree slope needed for the formation of a solifluction feature. This casts some doubt on a periglacial explanation for these specific examples.

11.6 Implications

11.6.1 Environmental Implications

The hypothesis that the northern high latitudes are a brine-facilitated periglacial landscape has significant implications for the martian environment both past and present. The presence of periglacial landforms indicates that an active layer can develop in martian ice-rich permafrost. Thawing of ground ice must have occurred both regularly and in sufficient volumes to produce the observed features. The following section assumes a periglacial scenario and summarizes the implications for the martian environment if this is the case.

Regardless of how prevalent cryobrines are in the martian near-surface the conditions for thaw will not be ubiquitous. Thaw is only likely to occur in isolated locations, such as on sun-facing slopes which get sufficient insolation during the mornings and evenings of the northern spring (Möhlmann, 2011). Such environments are likely to be more common in some places than in others. They do not necessarily constitute anomalous microclimates, but nor would they be expected to be ubiquitous.

The results of this survey support this assessment. Across most of the area surveyed examples of patterned ground, and especially lobate structures, are widely dispersed and are not found to be especially common. However, neither are they so rare as to only be found in a handful of images. Numerous examples of most putative periglacial landforms are found, as are assemblages of them.

Gallagher and Balme (2011) proposed that crater interiors might be atypically wet environments, due to a combination of the presence of cryobrines and their abundance

of high insolation slopes. This sort of microclimate would be favorable for periglacial processes, and indeed many expressions of these landforms are found in such places. However, there were also a large number of examples which did not occur in such environments. The results of this survey suggest that periglacial landscapes do not require a specific microclimate, although this doesn't make locations with such microclimates any less suitable for them.

Periglacial landscapes can be sustained in a variety of locations without the large scale topographic control, and stratigraphic inversion, provided by a crater. This is significant as it means that putative periglacial features are potentially more widespread than previously suggested. Future investigations should not focus on crater interiors at the expense of surveying the inter-crater plains. Further research is needed to constrain which more subtle factors, whether chemical, climatic or topographic, control the occurrence of these wet environments.

Since it is not possible to directly measure the presence or absence of cryobrines on the martian surface, putative periglacial features could provide a geomorphic marker for landscapes where thawing may have occurred. This could be very significant for the study of the martian environment, since the regular thawing of water, however brine rich, would provide a useful environment for various forms of extremophilic life.

These observations also have implications for other landforms which are hypothesized to be the result of thaw: for example the Recurring Slope Lineae (RSL) observed in the southern mid latitudes (Ojha et al., 2014). These dark streaks are seen to develop on hillsides and progress further downhill between the acquisition of consecutive HiRISE images, suggesting that whatever process is responsible for their formation is occurring slowly in the present day.

Hence, seasonal flows of brine rich water might be one explanation for these structures. Comparing their distribution to that of putative periglacial features could provide evidence for or against this hypothesis. If they result from thaw-related processes then they would be expected to favour similar environments to those on which sorted stripes and solifluction features would be expected to develop in the present day. If patterned ground could be found in proximity to RSL it would add evidence that those features formed through thaw-related processes rather than through a dry granular flow. RSL are primarily found at low southern latitudes, with only a few examples on the southern edges of the northern lowlands. Consequently, their distribution does not overlap with the study areas examined in this investigation. This limits the extent to which they can be compared with the landforms discussed herein.

11.6.2 Methodological Implications

While HiRISE observations are required to characterise patterned ground, it is possible to map the boulder clusters in which sorted patterns frequently occur using much lower resolution data. Consequently, examination of HRSC and CTX images is sufficient to narrow down locations where sorted patterns are likely to occur. Targeted HiRISE observations could then be used to confirm whether a sorted pattern is in fact present.

It has been shown that an average nearest neighbour analysis can indicate whether a pattern is significantly different from a random arrangement and it is possible that more complex pattern recognition systems could be applied to characterise and perhaps detect polygonal structures automatically. Such a methodology would be far more efficient than the surveying procedure used during this and similar surveys and so could be of use in expanding the field of Mars periglacial research. This was not explored as part of this investigation. Developing and testing an automated system and

ensuring that it was able to detect a large enough proportion of features to be useful would have been beyond the scope of this project.

11.7 Further work

The results of this investigation suggest a variety of additional studies by which the project could be expanded. The following sections will detail several ideas which were beyond the scope of this investigation, but which would provide an interesting expansion of, or addition to, the surveys and experiments conducted herein.

11.7.1 Expansion of the study areas

While several hundred HiRISE images have been examined over the course of this investigation, covering 69845 km^2, this is only 21.9% of the area covered by HiRISE within these study areas. Numerous images were not chosen for this investigation since they did not overlap with medium-sized impact craters. This sampling reduced the available HiRISE images to a number which could reasonably be surveyed as part of a Ph.D. project but inevitably means that some interesting areas will have been missed.

At the time of writing, each study area contains between 1200-1400 HiRISE images. Only 462 of those were surveyed during this investigation. Surveying all available images would thus be impractical. It would also be interesting to expand the extent of the survey. Just under half of the Northern Plains were included in this project's study areas. Examining HiRISE images from other parts of the Northern Plains would provide a useful comparison, as would equivalent latitudes in the southern hemisphere but this would also generate a prohibitively large data volume.

Consequently, it is proposed that future surveys of this sort should focus on a series of smaller study areas a few hundred kilometres in diameter where all available HiRISE images can be easily surveyed. These smaller areas could be spread out across the

northern plains in the gaps not covered by the present investigation, or in regions where a large number of HiRISE images are available, but do not intersect impact craters.

Of particular interest would be HiRISE images in proximity to sites where possible periglacial assemblages were observed. For examples the 100 HiRISE images closest to an assemblage of interest could be surveyed, or all images that fell within 200 kilometres could be selected.

Lower resolution data sets could also be used to target areas of possible interest. Most of the polygonal patterns observed in the Lomonosov area were part of larger boulder clusters. These clusters are visible in CTX images and can also be seen in lower resolution HRSC images. Consequently, their locations could be mapped at low resolution (as was done for the Lomonosov region) and then HiRISE images could be acquired for a sample of these boulder patches to determine whether sorting was present or not. The discovery of the features around Lomonosov came too late in the current investigation for HiRISE image requests to be submitted.

11.7.2 Examination of scalloped depression asymmetry using CTX DEMs

The discussion of scalloped depression asymmetry in Chapter Ten relies upon observations of the steeper slope of a scalloped depression as seen in the CTX image. Often one slope appears clearer than another, despite not being the more shadowed slope determined by the direction of the sun. However, this method of determining which slope is steeper cannot be applied to every depression, as there is often no difference between the boundaries of the feature. Actual measurements of slope are not possible with this method and the results are acknowledged to be somewhat subjective.

In places where multiple CTX images overlap it can be possible to generate a Digital Elevation Model (DEM) using photogrammetry. This would provide elevation data

and make the classification of depression asymmetry more reliable. This method would potentially allow the classification of scalloped depressions where slope asymmetry could not be determined by visual inspection. It would also provide a more quantifiable dataset to test the observations presented in Chapter Ten.

The same approach could be applied to other putative periglacial features, such as the sorted stripes and lobes in the vicinity of Lomonosov Crater. If HiRISE stereo pairs become available for this region, then HiRISE DEMs would allow a far more precise measurement of the underlying slope than is possible using MOLA point data. Currently, these areas only have a small number of overlapping CTX and HRSC images, which do not always coincide with the locations of the most interesting features. Were more time available for the study, additional images could be requested from the HiRISE instrument to allow DEMs of areas of specific interest to be made.

A thorough comparison between the scalloped depressions in these study areas and those described by Séjourné et al., (2011) would require high resolution images. Séjourné et al., (2011)'s classification of these features relies upon the examination of the bright bands frequently found in depression interiors. Since these bands are usually below the resolution of the CTX images in the areas surveyed the classification presented here is somewhat subjective. Acquisition of higher resolution images would allow for a better comparison between the two studies to be made.

11.7.3 Further development of the laboratory study

The investigation into the effect of freezing point depression on sorting that is described in appendix one was eventually discontinued after several experiments that did not produce sorted patterns. Simulating frost heave under terrestrial conditions proved problematic, so the investigation never ran its planned course. Only one trial run was conducted using a salt solution, and true martian conditions were never used.

Considerable further work would be required to refine the method to a point where frost heave can be reliably produced. However, it has been demonstrated in the laboratory by other studies such as Chamberlain (1983), Corte (1963); and Viklander (1998), at least under terrestrial conditions.

The work described in appendix one leaves an essential question unanswered. Can freeze thaw sorting occur under martian conditions? Is it possible to generate ice lenses such as those described by Sizemore et al., (2014) or would the reduction in effectiveness of frost heaving in saline soils (Chamberlain, 1983) prevent the significant deformation of the ground?

Details on how this experimental work could be continued are presented in more detail in Section 14.5. In summary, a series of experiments would be run using a range of identical soil columns which were known to heave under terrestrial conditions. Each would be saturated with a different brine solution, some with eutectic temperatures within the range required for frost heaving under martian conditions. Such an experiment would provide a proof of concept for freezing and thawing under martian temperature conditions and so demonstrate whether periglacial processes should be theoretically possible. Once a low temperature system had been successfully tested, further experiments could examine the role of pressure using a large vacuum chamber.

While a proof of concept study of this sort would be useful there is a limit to the information about a putative martian periglacial regime that it could provide. To assess the properties of a martian sorted net and how they differed from terrestrial patterned ground a range of factors such as the gravity of Mars and the scale of martian features would need to be properly constrained. This adds a level of complexity to the study which was beyond the scope of this investigation, as it would have required a

considerable investment of time and resources to assess, neither of which were available during the current project.

11.7.4 Pattern recognition

It has been shown in Chapters Four and Five that an average nearest neighbour analysis can be used to determine whether an area of seemingly sorted boulders is in fact significantly different from a random distribution. This is a useful tool in assessing whether these sites are evidence of sorting. However, a more sophisticated pattern recognition system could potentially go much further. It would be interesting to develop a system to automatically detect and classify polygons based on factors such as the scale and elongation of the features. This would require being able to identify which elements of a digitised boulder pattern comprised the exterior of a polygonal pattern, and which did not.

This is not possible using the nearest neighbour analysis, which can only indicate whether an area of patterned ground is significantly clustered relative to a random distribution, or whether it is significantly dispersed. While it provides evidence for organisation, this is not the most useful means of classifying areas of sorted patterned ground. An approach which looked at the relative sizes of fine and coarse domains, the elongation of polygons and the dispersion of clasts within coarse domains would be more useful. The latter could be used to assess how likely a line of aligned clasts was to be part of an actual linear feature.

In this study, polygons were manually digitised; however this was extremely time consuming and so limited the number of areas that could be examined. A method capable of distinguishing between different polygons would enable automatic classification of areas of boulder strewn ground as well as classification of the scale and elongation of these features. It is possible to automatically identify boulders and their

shadows in HiRISE images (Golombek et al., 2012, 2008). This technique has been used to assess the safety of potential landing sites to avoid damage to landers during descent onto large rocks.

This suggests that it should be possible to program an automated system to identify rocks and to look for patterns in boulder distribution such as stripes and polygons. A future study to investigate the arrangement of polygonal patterns on Earth and Mars using pattern recognition could prove very valuable in testing the hypothesis that these features formed through similar processes on both planets.

11.7.5 *Structure from Motion* for long term monitoring campaigns

The field campaign described in Chapter Four tested the use of *structure from motion*, a relatively new photogrammetry technique which has the potential to provide a valuable resource for future field campaigns (Westoby et al., 2012). The technique enables researchers to produce high resolution digital elevation models from field photographs and this has applications for many areas of geomorphology.

One potential use for this technology would be as part of a long term monitoring campaign to study the evolution of sorted patterned ground in the field. Such a project has only limited applications to assessing whether martian features are analogous to terrestrial patterned ground, but would be very useful for terrestrial periglacial research. One study by Kääb et al., (2014) has used photograph sets taken several years apart to assess the development of sorted patterned ground in an area of Spitsbergen and a similar methodology could be applied to other, more accessible sites.

A program could be instigated to record *structure from motion* data sets on an annual basis at several sites where sorted patterned ground is prevalent. Since Unmanned Aerial Vehicles (UAVs) are becoming increasingly inexpensive it would be possible to record a *structure from motion* dataset which included low elevation air photographs.

This would provide a higher resolution intermediate step between ground-based observations, and those from aerial photographs.

Two field campaigns were conducted as part of this investigation, but *structure from motion* only formed a significant part of the second expedition. Consequently, determining whether change was taking place within specific features was beyond the scope of this project. It is likely that a single year is too short a time for significant changes in the morphology of a patch of sorted patterned ground to occur. The Iceland site is easily accessible and contains features on a variety of scales. It would thus be reasonably simple to obtain several years of data intended specifically for structure from motion processing. The longer the time series, and the greater the frequency with which the site is visited, the more information about the changes taking place at the site can be gleaned.

12 Chapter Twelve: Conclusions

In this investigation, a variety of sites where putative periglacial features occur on the Northern Plains of Mars have been described. Many features with similar morphologies to terrestrial periglacial landforms are found in areas where ground ice is believed to be present (Boynton et al., 2010; Feldman et al., 2004). There are also a large number of sites where multiple periglacial features are present. While by no means common, these potential periglacial assemblages are found in all three study areas, across a fairly wide range of latitudes, and on all terrain types surveyed. These sites provide the best evidence for a periglacial origin.

Different types of landform are more common across different regions of the study areas. Sorted features are most common at high northern latitudes, while assemblages featuring scalloped depressions and gullies are found throughout the mid latitudes. Sites where lobate structures occur in proximity to other putative periglacial landforms are surprisingly common considering the very low number of lobate features found overall. It seems unlikely that these assemblages are the result of chance, since sites with lobate features are so scarce.

It is interesting to note that both clastic patterned ground and lobate features occur further south than previously thought within these study areas. Some sites have been observed much further south, but not within the area surveyed in this investigation where most observations had been limited to high northern latitudes. Examples of both are found as far south as 35°N. However, the more southerly clastic networks are generally graded lower than their northern counterparts, and so are less likely to be periglacial. Some examples occur in regions where ground ice is not currently predicted to be stable. This might mean that these features are relict landforms, remaining from a

past period when ground ice was stable at these latitudes; alternatively they could have formed through unrelated processes. This finding certainly suggests that future surveys should not be limited to the high latitudes.

Landforms which are predicted to be topographically controlled are frequently found to be consistent with terrestrial analogues. For example, lobate structures are not found at as low elevations as many examples of clastic networks and scalloped depressions. This makes sense if they are predominantly forming on hill slopes through solifluction processes. The same is found to be true for sorted stripes and rubble piles. Stripes are also predicted to be hill slope features.

Many examples of stripes and lobes occur on steeper slopes than most of the higher graded polygonal patterns. The majority of these features are found on slopes of the gradients which are in agreement with terrestrial observations of sorted stripes and solifluction lobes. While some examples of lobes and stripes are found on too shallow a slope and some polygonal networks occur on steeper slopes than would be expected, most are consistent with a periglacial explanation, based on terrestrial experience.

Numerous scalloped depressions were found across the study areas. The concentration of such depressions was highest in Utopia Planitia, but they were still common in all regions surveyed. Scalloped depressions are often found in assemblages with gullies and this could indicate that their formation mechanisms are related. Thermokarst-like processes are one possibility, as it has been suggested that gullies could be the result of thawing (Costard et al., 2002).

There is debate as to whether scalloped depressions form through thawing of ground ice (e.g. Costard and Kargel, 1995) or retrogressive sublimation of ice-rich material (e.g. Lefort et al., 2010). The observations made during this study cannot rule out either of these hypotheses. Sublimation would seem to be the most likely formation mechanism,

given the cold, dry environment of present day Mars. However, there is evidence that the scalloped depression fields around Davies and Lagarto Craters could have formed during a past period of higher obliquity when thaw might have been viable.

The scalloped depressions identified around these craters have a heavily degraded morphology and seem to have steeper pole facing slopes. These features are predominantly of type three features on the classification system of Séjourné et al., (2011), indicating that they are expanding and exhibit scalloped edges. However, many type four and five features, where multiple scalloped depressions merge into larger structures, are also present.

Many areas which are even more degraded than type five depressions are observed. This suggests a mature, well-developed landscape. The steeper slope of a scalloped depression is believed to indicate the part of the feature which received the most insolation, and thus where the majority of thaw or sublimation occurred (Séjourné et al., 2011). Pole-facing slopes would be expected to receive higher insolation during high obliquity excursions. In the present day the equator facing slopes would be expected to have greater insolation. Both Davies and Lagarto Craters show steeper pole facing slopes and thus support formation in the past.

The highest concentration of possible sorted patterned ground was found in the region around Lomonosov Crater. It has been demonstrated using an *average nearest neighbour analysis* that clastic networks were found to be significantly dispersed relative to a random distribution. This is consistent with the data gathered when the same analysis technique was applied to terrestrial features, in which organisation was confirmed by in situ observations. This confirms that a clastic pattern is present at these and other sites within this region.

The martian clastic patterns studied here are morphologically similar to those found at the terrestrial field sites, but are much larger in scale. Sorting through frost heave would be expected to be more efficient under lower gravity, as the upwards force of frost heaving would be expected to remain the same. Since martian gravity is a third that of Earth it should be possible for material of three times greater mass to become organised. This broadly fits with the larger size of the boulders observed at the martian sites compared to those on Earth.

Analysis to determine whether elongated polygons were aligned downslope was inconclusive, largely due to the lack of higher resolution digital elevation models from which slope aspect could be derived. The scaling of clast size with polygon size was shown to be similar to that seen in terrestrial sorted patterned ground. Clast size does scale with polygon area, but the terrestrial examples show a much stronger correlation than equivalent martian landforms.

While these structures have several morphological similarities to terrestrial analogues, it is uncertain whether periglacial sorting can occur under martian conditions. The laboratory experiments to determine whether freeze thaw sorting could be facilitated by cryobrines proved to be inconclusive. It is possible that the presence of brines could depress the freezing point sufficiently to allow these processes to occur, but this has yet to be demonstrated. It is uncertain whether the effect of dissolved salt on the frost heaving process would reduce its efficacy (e.g. Chamberlain, 1983) and what the result would be for a martian periglacial environment. While some martian soils should be frost-susceptible, this casts some doubt over the viability of a periglacial hypothesis.

Consequently, the alternate hypotheses which suggest that these features formed through interaction of clasts with underlying fracture networks were also assessed. These include gravitational sorting (Levy et al., 2010, 2008a; Mellon et al., 2008) and

boulder ratcheting (Orloff et al., 2011, 2013). However, these hypotheses do not seem to fit with the observed network morphologies around Lomonosov crater. For example clastic patterns frequently occur in the absence of a discernible network of underlying fractures. Where both clastic and fracture networks are superposed they do not always appear to be related. Consequently, it seems unlikely that these structures formed through fracture control and thus by either of the mechanisms cited above.

Chapter Eleven presents a variety of projects which could expand upon the work presented here. More complex pattern analysis techniques could be used to further characterise clastic networks. The Construction of HiRISE DEMs could allow more precise measurements of gradient and topographic control. Some of the techniques used in this project could be applied to the study of terrestrial patterned ground in the field, and the lessons learnt from the surveys could be used to conduct more targeted studies in the future. Finally the aborted laboratory study could be revisited, using the findings of this investigation to develop a working methodology.

In summary; numerous sites containing putative periglacial landforms have been catalogued and characterised. The following conclusions have been drawn;

- Examples of clastic networks and lobate hill-slope features are found further south than previously thought, beyond the extents of previous studies of these features.
- Scalloped depressions around Davies and Lagarto Craters have a degraded and mature appearance. The presence of steep pole facing slopes on these features also supports formation during a past period of higher obliquity.
- The arrangements of clastic patterns around Lomonosov crater return a dispersed result when an average nearest neighbour analysis is conducted,

suggesting that patterns are significantly different from a random boulder distribution

- The clastic networks at this site are morphologically similar to examples of sorted patterned ground examined in northern Iceland, which produce the same result when a nearest neighbour analysis is applied.
- These clastic networks do not appear to be controlled by underlying fracture networks, making formation by gravitational sorting or boulder ratcheting unlikely.

In conclusion, a periglacial hypothesis remains the best explanation for areas of clastic patterned ground on Mars. These features have been shown to occur in non-random arrangements and neither of the two competing theories to explain their formation through fracture control fit the clast-fracture relationships seen in the area around Lomonosov Crater. The periglacial explanation is not yet fully demonstrated, as the viability of cryobrine facilitated thaw has yet to be confirmed. However, until another explanation for these features can be advanced it remains the formation mechanism most likely to explain the observed morphologies.

13 References

Abu-Hamdeh, N., 2014. Specific Heat and Volumetric Heat Capacity of Granular Materials as Affected by Moisture and Density. Appl. Mech. Mater. 575, 103–107.

Allen, C.C., 1979. Volcano-ice interactions on Mars. J. Geophys. Res. 84, 8048–8059.

Allen, C.C., Jager, K.M., Morris, R. V, Lindstrom, D.J., Lindstrom, M.M., Lockwood, J.P., 1998. Martian Soil Simulant Available for Scientific , Educational Study. EOS, Trans. Am. Geophys. Union 79, 405–412.

Anderson, D.M., Gatto, L.W., Ungolini, F.C., 1972. An antarctic analog of Martian permafrost terrain. Antarct. J. 7, 114–116.

Andersson, J.. G.., 1906. Solifluction , a Component of Subaërial Denudation. J. Geol. 14, 91–112.

Arenson, L., 2004. The effect of saline pore water on the freezing of loose Devon Silt, in: Canadian Young Geotechnical Engineers and Geoscientists Conference Manoir St-Castin, October 27-30.

Arenson, L.U., Sego, D.C., 2006. The effect of salinity on the freezing of coarse-grained sands. Can. Geotech. J. 337, 325–337. doi:10.1139/T06-006

Arvidson, R.E., Gooding, J.L., Moore, H.J., 1989. The martian surface as imaged, sampled, and analyzed by the viking landers. Rev. Geophys. 27, 39–60.

Baker, V.R., 2001. Water and the martian landscape. Nature 412, 228–36. doi:10.1038/35084172

Baker, V.R., Strom, R.G., Gulick, V., Kargel, J., Komatsu, G., Kale, V.S., 1991. Ancient oceans, ice sheets and the hydrological cycle on Mars. Nature 532, 589–594.

Ballantyne, C.K., 2013. Encyclopedia of Quaternary Science, Encyclopedia of Quaternary Science. Elsevier. doi:10.1016/B978-0-444-53643-3.00098-4

Ballantyne, C.K., Harris, C., 1994. The Periglaciation of Great Britain. Cambridge Univ. Press, Cambridge.

Ballantyne, C.K., Matthews, J.A., 1982. The Development of Sorted Circles on Recently Deglaciated Terrain , Jotunheimen , Norway. Arct. Alp. Res. 14, 341–354.

Balme, M., Mangold, N., Baratoux, D., Costard, F., Gosselin, M., Masson, P., Pinet, P., Neukum, G., 2006. Orientation and distribution of recent gullies in the southern hemisphere of Mars: Observations from High Resolution Stereo Camera/Mars Express (HRSC/MEX) and Mars Orbiter Camera/Mars Global Surveyor (MOC/MGS) data. J. Geophys. Res. 111, E05001. doi:10.1029/2005JE002607

Balme, M.R., Gallagher, C., 2009. An equatorial periglacial landscape on Mars. Earth Planet. Sci. Lett. 285, 1–15. doi:10.1016/j.epsl.2009.05.031

Balme, M.R., Gallagher, C.J., Hauber, E., 2013. Morphological evidence for geologically young thaw of ice on Mars: A review of recent studies using high-resolution imaging data. Prog. Phys. Geogr. 37, 289–324. doi:10.1177/0309133313477123

Balme, M.R., Gallagher, C.J., Page, D.P., Murray, J.B., Muller, J.-P., 2009. Sorted stone circles in Elysium Planitia, Mars: Implications for recent martian climate. Icarus 200, 30–38. doi:10.1016/j.icarus.2008.11.010

Bargery, A., Balme, M.R., Warner, N., 2011. A background to Mars exploration and research, in: Balme, M.R., Bargery, A.S., Gallagher, C. (Eds.), Martian Geomorphology. Geological Society, London, Special Publications, pp. 5–20.

Bargery, A.S., Balme, M.R., Warner, N., Gallagher, C.J., Gupta, S., 2011. A background to Mars exploration and research. Geol. Soc. London, Spec. Publ. 356, 5–20. doi:10.1144/SP356.2

Bargery, A.S., Lane, S.J., Barrett, A., Wilson, L., Gilbert, J.S., 2010. The initial responses of hot liquid water released under low atmospheric pressures: Experimental insights. Icarus 210, 488–506. doi:10.1016/j.icarus.2010.06.019

Barlow, G., Boyce, M., Costard, M., Craddock, A., Garvin, B., Sakimoto, E.H., Kuzmin, O., Roddy, J., Soderblom, L.A., 1990. Standardizing the nomenclature of Martian impact crater ejecta morphologies. J. Geophys. Res. Planets 105, 26,733–26,738.

Barlow, N.G., 2009. What we know about Mars from its impact craters. Geol. Soc. Am. Bull. 122, 644–657. doi:10.1130/B30182.1

Barlow, N.G., Bradley, T.L., 1990. Martian Impact Craters : Correlations of Ejecta and Interior Morphologies with Diameter , Latitude , and Terrain. Icarus 87, 156–179.

Beirman, P.R., Montgomery, D.R., 2014. Key Concepts in Geomorphology. WH Freeman and Company, New York.

Benedict, J.B., 1976. Frost creep and gelifluction features: A review. Quat. Res. 6, 55–76. doi:10.1016/0033-5894(76)90040-5

Bishop, M., 2007. Point pattern analysis of north polar crescentic dunes, Mars: A geography of dune self-organization. Icarus 191, 151–157. doi:10.1016/j.icarus.2007.04.027

Bishop, M., 2008. Higher-order neighbor analysis of the Tartarus Colles cone groups, Mars: The application of geographical indices to the understanding of cone pattern evolution. Icarus 197, 73–83. doi:10.1016/j.icarus.2008.04.003

Black, B.A., Stewart, S.T., 2008. Excess ejecta craters record episodic ice-rich layers at middle latitudes on Mars. J. Geophys. Res. 113. doi:10.1029/2007JE002888

Black, R., 1954. Permafrost- a review. Bull. Geol. Soc. Am. 85, 839–856.

Boynton, W.V., Feldman, W.C., Squyres, S.W., Prettyman, T.H., Brukner, J., L.G., E., Reedy, R.C., Starr, R., Arnold, J.R., Drake, D.M., Englert, P.A.J., Metzger, A.E., Mitrofanov, I., Trombka, J.I., D'Uston, C., Wänke, H., Gasnault, O., Hamara, D.K., Janes, D.M., Marcialis, L., Maurice, S., Mikheeva, I., Taylor, G.J., Tokar, R., Shinohara, C., 2010. Distribution of Hydrogen in the near Surface of Mars: Evidence for Subsurface Ice Deposits. Science (80-.). 297, 81–85.

Bridges, N.T., Lackner, C.N., 2006. Northern hemisphere Martian gullies and mantled terrain: Implications for near-surface water migration in Mars' recent past. J. Geophys. Res. 111, E09014. doi:10.1029/2006JE002702

Bronfenbrener, L., Bronfenbrener, R., 2010. Modeling frost heave in freezing soils. Cold Reg. Sci. Technol. 61, 43–64. doi:10.1016/j.coldregions.2009.12.007

Brown, J., Ferrians, O.J., Heginbottom, J.A., Melnikov, E.S., 1998. Circum-arctic map of permafrost and ground ice conditions.

Burn, C.R., 1998. Short Communication: The Active Layer : Two Contrasting Definitions. Permafr. Periglac. Process. 9, 411–416.

Burr, D.M., Tanaka, K.L., Yoshikawa, K., 2009. Pingos on Earth and Mars. Planet. Space Sci. 57, 541–555. doi:10.1016/j.pss.2008.11.003

Cabrol, N. a., Herkenhoff, K., Knoll, A.H., Farmer, J., Arvidson, R., Grin, E., Li, R., Fenton, L., Cohen, B., Bell, J.F., Aileen Yingst, R., 2014. Sands at Gusev Crater, Mars. J. Geophys. Res. Planets 119, 941–967. doi:10.1002/2013JE004535

Cabrol, N.A., Grin, E.A., 2002. Overview on the formation of paleolakes and ponds on Mars. Glob. Planet. Change 35, 199–219.

Carr, M.H., 1979. Formation of Martian flood features by release of water from confined aquifers. J. Geophys. Res. 84, 2995. doi:10.1029/JB084iB06p02995

Carr, M.H., 1983. Stability of Streams and Lakes on Mars. Icarus 56, 476–495.

Carr, M.H., 1996. Water on Mars. Oxford University Press, New York.

Carr, M.H., 2012. The fluvial history of Mars. Philos. Trans. A. Math. Phys. Eng. Sci. 370, 213–215. doi:10.1098/rsta.2011.0500

Carr, M.H., Schaber, G.G., 1977. Martian Permafrost Features. J. Geophys. Res. 82, 4039–4054.

Casagrande, A., 1931. Discussion of frost heaving. Highw. Res. Board, Proc. vol. 11, p. 168–172.

Cedillo-Flores, Y., Treiman, A.H., Lasue, J., Clifford, S.M., 2011. CO_2 gas fluidization in the initiation and formation of Martian polar gullies. Geophys. Res. Lett. 38, 1–5. doi:10.1029/2011GL049403

Chamberlain, E.J., 1981. CREEL Monograph 84-2: Frost Susceptibility of Soil, Review of Index Tests. Hanover, NH.

Chamberlain, E.J., 1983. Frost Heave of Saline Soils, in: Permafrost, 4th International Conference. Fairbanks, AK. p. 6.

Chambers, M., 1966. Investigations of patterned grround at signy island south orkeny islands: II Temperature regimes in the active layer. Br. Antarct. Surv. Bull. 10, 71–83.

Chevrier, V.F., Hanley, J., Altheide, T.S., 2009. Stability of perchlorate hydrates and their liquid solutions at the Phoenix landing site, Mars. Geophys. Res. Lett. 36, 1–6. doi:10.1029/2009GL037497

Clark, P.J., Evans, F.C., 1954. Distance to Nearest Neighbor as a Measure of Spatial Relationships in Populations. Ecology 35, 445–453.

Conway, S.J., Balme, M.R., 2014. Decameter thick remnant glacial ice deposits on Mars. Geophys. Res. Lett. 41, 5402–5409. doi:10.1002/2014GL060314

Conway, S.J., Hovius, N., Barnie, T., Besserer, J., Le Mouélic, S., Orosei, R., Read, N.A., 2012. Climate-driven deposition of water ice and the formation of mounds in craters in Mars' north polar region. Icarus 220, 174–193. doi:10.1016/j.icarus.2012.04.021

Conway, S.J., Lamb, M.P., Balme, M.R., Towner, M.C., Murray, J.B., 2011. Enhanced runout and erosion by overland flow at low pressure and sub-freezing conditions: Experiments and application to Mars. Icarus 211, 443–457. doi:10.1016/j.icarus.2010.08.026

Corte, A.E., 1962. Vertical Migration of Particles in Front of a Moving Freezing Plane. J. Geophys. Res. 67, 1085–1090.

Corte, A.E., 1963. Particle Sorting by Repeated Freezing and Thawing. Science 142, 499–501. doi:10.1126/science.142.3591.499

Costard, F., 1989. The spatial distribution of volatiles in the Martian hydrolithosphere. Earth, Moon Planets 45, 265–290.

Costard, F., Baker, V.R., 2001. Thermokarst landforms and processes in Ares Vallis, Mars. Geomorphology 37, 289–301. doi:10.1016/S0169-555X(00)00088-X

Costard, F., Forget, F., Mangold, N., Peulvast, J., 2002. Formation of Recent Martian debris flows by melting of near surface ground ice at high obliquity. Science (80-.). 295, 110–113.

Costard, F., Kargel, J.S., 1995. Outwash plains and thermokarst on Mars. Icarus 114, 93–112.

Cull, S., Arvidson, R.E., Mellon, M.T., Skemer, P., Shaw, A., Morris, R. V., 2010. Compositions of subsurface ices at the Mars Phoenix landing site. Geophys. Res. Lett. 37, 2–5. doi:10.1029/2010GL045372

Cull, S.C., Arvidson, R.E., Catalano, J.G., Ming, D.W., Morris, V., Mellon, M.T., Lemmon, M., 2010. Concentrated perchlorate at the Mars Phoenix landing site : Evidence for thin film liquid water on Mars. Geophys. Res. Lett. 37, 6. doi:10.1029/2010GL045269

Czudek, T., Demek, J., 1970. Thermokarst in Siberia and Its Influence on the Development of Lowland Relief. Quarternary Res. 1, 103–120.

Davila, A.F., Duport, L.G., Melchiorri, R., Jänchen, J., Valea, S., de Los Rios, A., Fairén, A.G., Möhlmann, D., McKay, C.P., Ascaso, C., Wierzchos, J., 2010. Hygroscopic salts and the potential for life on Mars. Astrobiology 10, 617–28. doi:10.1089/ast.2009.0421

Decaulne, A., Sæmundsson, Þ., Jónsson, H.P., Sandburg, O., 2007. Changes in deposition on a colluvial fan during the upper holocene in the Tindastoll Mountain, Skagafjördur region North Iceland: Preliminary Results. Geogr. Ann. Ser. A, Phys. Geogr. 89, 51–63.

Delamere, W.A., Tornabene, L.L., McEwen, A.S., Becker, K., Bergstrom, J.W., Bridges, N.T., Eliason, E.M., Gallagher, D., Herkenhoff, K.E., Keszthelyi, L., Mattson, S., McArthur, G.K., Mellon, M.T., Milazzo, M., Russell, P.S., Thomas, N., 2010. Color imaging of Mars by the High Resolution Imaging Science Experiment (HiRISE). Icarus 205, 38–52. doi:10.1016/j.icarus.2009.03.012

Depablo, M., Komatsu, G., 2009. Possible pingo fields in the Utopia basin, Mars: Geological and climatical implications. Icarus 199, 49–74. doi:10.1016/j.icarus.2008.09.007

Dice, L.R., 1952. Measure of the spacing between individuals of a population. Contrib. from Lab. Vertebr. Biol. Univ. Michigan 55, 1–23.

Dickson, J.L., Head, J.W., Kreslavsky, M., 2007. Martian gullies in the southern mid-latitudes of Mars: Evidence for climate-controlled formation of young fluvial features based upon local and global topography. Icarus 188, 315–323. doi:10.1016/j.icarus.2006.11.020

Dundas, C.M., McEwen, A.S., 2010. An assessment of evidence for pingos on Mars using HiRISE. Icarus 205, 244–258. doi:10.1016/j.icarus.2009.02.020

Dundas, C.M., Mellon, M.T., McEwen, A.S., Lefort, A., Keszthelyi, L.P., Thomas, N., 2008. HiRISE observations of fractured mounds: Possible Martian pingos. Geophys. Res. Lett. 35, L04201. doi:10.1029/2007GL031798

Farrand, W.H., Gaddis, L.R., Keszthelyi, L., 2005. Pitted cones and domes on Mars: Observations in Acidalia Planitia and Cydonia Mensae using MOC, THEMIS, and TES data. J. Geophys. Res. 110, E05005. doi:10.1029/2004JE002297

Feldman, W.C., Boynton, W.V., Tokar, R.L., Prettyman, T.H., Gasnault, O., Squyres, S.W., Elphic, R.C., Lawrence, D.J., Lawson, S.L., Maurice, S., Mckinney, G.. W., Moore, K.R., Reedy, R.C., 2002. Global Distribution of Neutrons from Mars: Results from Mars Odyssey. Science 297, 75–78.

Feldman, W.C., Prettyman, T.H., Maurice, S., Plaut, J.J., Bish, D.L., Vaniman, D.T., Mellon, M.T., Metzger, A.E., Squyres, S.W., Karunatillake, S., Boynton, W. V., Elphic, R.C., Funsten, H.O., Lawrence, D.J., Tokar, R.L., 2004. Global distribution of near-surface hydrogen on Mars. J. Geophys. Res. 109, E09006. doi:10.1029/2003JE002160

Feuillet, T., Mercier, D., Decaulne, A., Cossart, E., 2012a. Classification of sorted patterned ground areas based on their environmental characteristics (Skagafjörður, Northern Iceland). Geomorphology 139-140, 577–587. doi:10.1016/j.geomorph.2011.12.022

Feuillet, T., Mercier, D., Decaulne, A., Cossart, E., 2012b. Classification of sorted patterned ground areas based on their environmental characteristics (Skagafjörður, Northern Iceland). Geomorphology 139-140, 577–587. doi:10.1016/j.geomorph.2011.12.022

Fischer, E., Martínez, G.M., Elliott, H.M., Rennó, N.O., 2014. Experimental evidence for the formation of liquid saline water on Mars. Geophys. Res. Lett. doi:10.1002/2014GL060302

Fonstad, M. a., Dietrich, J.T., Courville, B.C., Jensen, J.L., Carbonneau, P.E., 2013. Topographic structure from motion: a new development in photogrammetric measurement. Earth Surf. Process. Landforms 38, 421–430. doi:10.1002/esp.3366

Francou, B., Bertran, P., 1997. A Multivariate Analysis of Clast Displacement Rates on Stone-banked sheets, Cordillera Real, Bolivia. Permafr. Periglac. Process. 8, 371–382.

Francou, B., Le Méhauté, N., Jomelli, V., 2001. Factors controlling spacing distances of sorted stripes in a low-latitude, alpine environment (Cordillera Real, 16 degrees S, Bolivia). Permafr. Periglac. Process. 12, 367–377. doi:10.1002/ppp.398

French, H., 2003. The development of periglacial geomorphology: 1- up to 1965. Permafr. Periglac. Process. 14, 29–60. doi:10.1002/ppp.438

French, H., 2007. The Periglacial Environment, 3rd editio. ed. Wiley, Chichester.

Gaidos, E., 2001. Cryovolcanism and the Recent Flow of Liquid Water on Mars. Icarus 153, 218–223. doi:10.1006/icar.2001.6649

Gallagher, C., Balme, M.R., 2010. Landfom assemblages indicative of northern High lattitude thaw on mars, in: 41st Lunar and Planetary Science Conference (2010). p. 2.

Gallagher, C., Balme, M.R., 2011. Landforms indicative of ground-ice thaw in the northern high latitudes of Mars. Geol. Soc. London, Spec. Publ. 356, 87–110. doi:10.1144/SP356.6

Gallagher, C., Balme, M.R., Conway, S.J., Grindrod, P.M., 2011. Sorted clastic stripes, lobes and associated gullies in high-latitude craters on Mars: Landforms indicative of very recent, polycyclic ground-ice thaw and liquid flows. Icarus 211, 458–471. doi:10.1016/j.icarus.2010.09.010

Garvin, J., Sakimoto, S.E.H., Frawley, J.J., Schnetzler, C., 2000. North Polar Region Craterforms on Mars: Geometric Characteristics from the Mars Orbiter Laser Altimeter. Icarus 144, 329–352. doi:10.1006/icar.1999.6298

Ghent, R.R., Anderson, S.W., Pithawala, T.M., 2012. The formation of small cones in Isidis Planitia, Mars through mobilization of pyroclastic surge deposits. Icarus 217, 169–183. doi:10.1016/j.icarus.2011.10.018

Goldthwait, R.P., 1976. Frost sorted patterned ground: A review. Quat. Res. 6, 27–35. doi:10.1016/0033-5894(76)90038-7

Golombek, M., Huertas, A., Kipp, D., Calef, F., 2012. Detection and Characterization of Rocks and Rock Size-Frequency Distributions at the Final Four Mars Science Laboratory Landing Sites. Mars 7, 1–22. doi:10.1555/mars.2012.0001

Golombek, M.P., Bridges, N.T., 2000. Erosion rates on Mars and implications for climate change: Constraints from the Pathfinder landing site. J. Geophys. Res. 105, 1841–1853.

Golombek, M.P., Huertas, a., Marlow, J., McGrane, B., Klein, C., Martinez, M., Arvidson, R.E., Heet, T., Barry, L., Seelos, K., Adams, D., Li, W., Matijevic, J.R., Parker, T., Sizemore, H.G., Mellon, M., McEwen, a. S., Tamppari, L.K., Cheng, Y., 2008. Size-frequency distributions of rocks on the northern plains of Mars with special reference to Phoenix landing surfaces. J. Geophys. Res. 113, E00A09. doi:10.1029/2007JE003065

Gough, R.V., Chevrier, V.F., Baustian, K.J., Wise, M.E., Tolbert, M.A., 2011. Laboratory studies of perchlorate phase transitions: Support for metastable aqueous perchlorate solutions on Mars. Earth Planet. Sci. Lett. 312, 371–377. doi:10.1016/j.epsl.2011.10.026

Haberle, R.M., Mckay, C.P., Schaeffer, J., Cabrol, N.A., Grin, E.A., Zent, A.P., Quinn, R., 2001. On the possibility of liquid water on present day Mars. J. Geophys. Res. 106, 317–326.

Hallet, B., 2013. Stone circles : form and soil kinematics. Philos. Trans. R. Soc. 371, 17.

Haltigin, T.W., Pollard, W.H., Dutilleul, P., Osinski, G.R., Koponen, L., 2014. Co-evolution of polygonal and scalloped terrains, southwestern Utopia Planitia, Mars. Earth Planet. Sci. Lett. 387, 44–54. doi:10.1016/j.epsl.2013.11.005

Harris, C., Davies, M.C.R., Coutard, J.-P., 1997. Rates and processes of periglacial solifluction: an experimental approach. Earth Surf. Process. Landforms 22, 849–868. doi:10.1002/(SICI)1096-9837(199709)22:9<849::AID-ESP784>3.0.CO;2-U

Harris, S.A., 2002. Causes and consequences of rapid thermokarst development in permafrost or glacial terrain. Permafr. Periglac. Process. 13, 237–242. doi:10.1002/ppp.419

Harrison, T.N., Osinski, G.R., Tornabene, L.L., 2014. Global documentation of gullies with the Mars Reconnaissance Orbiter context camera (CTX) and implications for their formation., in: LPSC XXXXV. p. 2.

Hartmann, W.K., 2001. Martian seeps and their relation to youthful geothermal activity. Space Sci. Rev. 96, 405–410.

Hauber, E., Reiss, D., Ulrich, M., Preusker, F., Trauthan, F., Zanetti, M., Hiesinger, H., Jaumann, R., Johansson, L., Johnsson, a., Van Gasselt, S., Olvmo, M., 2011. Landscape evolution in Martian mid-latitude regions: insights from analogous periglacial landforms in Svalbard. Geol. Soc. London, Spec. Publ. 356, 111–131. doi:10.1144/SP356.7

Haugland, J.E., 2006. Short-term Periglacial Processes , Vegetation Succession , and Soil Development within Sorted Patterned Ground : Jotunheimen , Norway Short-term Periglacial Processes , Vegetation Succession , and Soil Development within Sorted Patterned Ground : Jotunhei. Arctic, Antarct. Alp. Res. 38, 82–89.

Hawkes, L., 1924. Frost action in superficial deposits, Iceland. Geol. Magzine 61, 509–513.

Head, J.W., Mustard, J.F., Kreslavsky, M.A., Milliken, R.E., Marchant, D.R., 2003. Recent ice ages on Mars. Nature 426, 18–25.

Hecht, M., 2002. Metastability of Liquid Water on Mars. Icarus 156, 373–386. doi:10.1006/icar.2001.6794

Hecht, M.H., Kounaves, S.P., Quinn, R.C., West, S.J., Young, S.M.M., Ming, D.W., Catling, D.C., Clark, B.C., Boynton, W. V, Hoffman, J., Deflores, L.P., Gospodinova, K., Kapit, J., Smith, P.H., 2009. Detection of perchlorate and the soluble chemistry of martian soil at the Phoenix lander site. Science 325, 64–7. doi:10.1126/science.1172466

Heldmann, J.L., Carlsson, E., Johansson, H., Mellon, M.T., Toon, O.B., 2007. Observations of martian gullies and constraints on potential formation mechanisms II. The northern hemisphere. Icarus 188, 324–344. doi:10.1016/j.icarus.2006.12.010

Herschel, W., 1784. On the remarkable appearances at the polar regions on the planet Mars, the inclination of its axis, the position of its poles, and its spheroidal figure; with a few hints relating to its real diameter and atmosphere. Philosphical Trans. R. Soc. London 74, 233–273.

Hesse, R., 2014. Combining Structure-from-Motion with high and intermediate resolution satellite images to document threats to archaeological heritage in arid environments. J. Cult. Herit. doi:10.1016/j.culher.2014.04.003

Hiesinger, H., Head, J.W., 2000. Characteristics and origin of polygonal terrain in southern Utopia Planitia , Mars : Results from Mars Orbiter Laser Altimiter and Mars Orbiter Camera data. J. Geophys. Res. 105, 11999–12022.

Higashi, A., Corte, A.E., 1971. Solifluction: a model experiment. Science 171, 480–2. doi:10.1126/science.171.3970.480

Hoffman, N., 2002. Active polar gullies on Mars and the role of carbon dioxide. Astrobiology 2, 313–23. doi:10.1089/153110702762027899

Humlum, O., Christiansen, H.H., 2008. Lowland Periglacial Research : A Review of Published Advances 2003 - 2007. Permafr. Periglac. Process. 19, 211–235. doi:10.1002/ppp

Inglis, D.R., Corte, A.E., 1965. Particle Sorting and Stone Migration by Freezing and Thawing Particle Sorting and Stone Migration by Freezing and Thawing. Science 148, 1616–1617.

Irwin, R.P., Craddock, R. a., Howard, A.D., 2005. Interior channels in Martian valley networks: Discharge and runoff production. Geology 33, 489. doi:10.1130/G21333.1

Ishii, T., Sasaki, S., 2004. Formation of recent martian gullies by avalanches of CO_2 frost, in: Lunar and Planetary Science XXXV (2004). pp. 7–8. doi:10.1029/2002JE001900.Figure

Iverson, R.M., 1997. The physics of debris flows. Rev. Geophys. 35, 245–296.

Jaeger, W.L., Keszthelyi, L.P., McEwen, A.S., Dundas, C.M., Russell, P.S., 2007. Athabasca Valles, Mars: a lava-draped channel system. Science 317, 1709–1711. doi:10.1126/science.1143315

Jin, H., Li, S., Cheng, G., Shaoling, W., Li, X., 2000. Permafrost and climatic change in China. Glob. Planet. Change 26, 387–404.

Johnson, J.R., 2010. Mars Science Goals , Objectives , Investigations , and Priorities : 2010.

Johnsson, A., 2013. Small-scale lobes in the Southern Hemisphere, Mars: Suggestive of transient liquid water in the recent past., in: EPSC 2013. pp. 3–4.

Johnsson, A., Reiss, D., Hauber, E., Hiesinger, H., Zanetti, M., 2014. Evidence for very recent melt-water and debris flow activity in gullies in a young mid-latitude crater on Mars. Icarus 235, 37–54. doi:10.1016/j.icarus.2014.03.005

Johnsson, A., Reiss, D., Hauber, E., Zanetti, M., Hiesinger, H., Johansson, L., Olvmo, M., 2012. Periglacial mass-wasting landforms on Mars suggestive of transient

liquid water in the recent past: Insights from solifluction lobes on Svalbard. Icarus 218, 489–505. doi:10.1016/j.icarus.2011.12.021

Johnsson, A., Reiss, D., Hauber, E., Zanetti, M., Hiesinger, H., Johansson, L., Olvmo, M., 2012. Periglacial mass-wasting landforms on Mars suggestive of transient liquid water in the recent past : Insights from solifluction lobes on Svalbard. Icarus 218, 489–505. doi:10.1016/j.icarus.2011.12.021

Jouannic, G., Gargani, J., Costard, F., Ori, G.G., Marmo, C., Schmidt, F., Lucas, A., 2012. Morphological and mechanical characterization of gullies in a periglacial environment: The case of the Russell crater dune (Mars). Planet. Space Sci. 71, 38–54. doi:10.1016/j.pss.2012.07.005

Kääb, A., Girod, L., Berthling, I., 2014. Surface kinematics of periglacial sorted circles using structure-from-motion technology. Cryosph. 8, 1041–1056. doi:10.5194/tc-8-1041-2014

Kääb, A., Haeberli, W., 2001. Evolution of a High-mountain Thermokarst Lake in the Swiss Alps. Antarct. Alp. Res. 33, 385–390.

Kargel, J.S., 2004. Mars a Warmer Wetter Planet. Springer- Praxis, Chichester.

Kessler, M.A., Murray, A.B., Werner, B.T., Hallet, B., 2001. A model for sorted circles as self-organized patterns. J. Geophys. Res. 106, 13287. doi:10.1029/2001JB000279

Kessler, M.A., Werner, B.T., 2003. Self-organization of sorted patterned ground. Science 299, 380–3. doi:10.1126/science.1077309

Kieffer, H.H., Jakosky, B.M., Snyder, C.W., Matthews, M.S., 1992. Mars. University of Arizona Press, Tucson.

Knauth, L.P., Klonowski, S., Burt, D., 2000. Ideas about the surface runoff features on Mars. Science (80-.). 290, 711–712.

Kneissl, T., Reiss, D., van Gasselt, S., Neukum, G., 2010. Distribution and orientation of northern-hemisphere gullies on Mars from the evaluation of HRSC and MOC-NA data. Earth Planet. Sci. Lett. 294, 357–367. doi:10.1016/j.epsl.2009.05.018

Konrad, J.M., 1988. Influence of freezing mode on frost heave characteristics. Cold Reg. Sci. Technol. 15, 161–175.

Konrad, J.M., 1989a. Pore water pressure at an ice lens: Its measurement and interpretation. Cold Reg. Sci. Technol. 16, 63–74.

Konrad, J.M., 1989b. Influence of cooling rate on the temperature of ice lens formation in clayey silts. Cold Reg. Sci. Technol. 16, 25–36. doi:10.1016/0165-232X(89)90004-9

Konrad, J.M., Nixon, J.F., 1994. Frost heave characteristics of a clayey silt subjected to small temperature gradients. Cold Reg. Sci. Technol. 22, 299–310. doi:10.1016/0165-232X(94)90007-8

Koutsoudis, A., Vidmar, B., Ioannakis, G., Arnaoutoglou, F., Pavlidis, G., Chamzas, C., 2014. Multi-image 3D reconstruction data evaluation. J. Cult. Herit. 15, 73–79. doi:10.1016/j.culher.2012.12.003

Krantz, W.B., 1990. Self-organization manifest as patterned ground in recurrently frozen soils. Earth-Science Rev. 29, 117–130. doi:10.1016/0012-8252(90)90031-P

Kreslavsky, M.A., Head, J.W., 2000. Kilometer-scale roughness of Mars: Results from MOLA data analysis. J. Geophys. Res. 105, 26,695–26,711.

Kreslavsky, M.A., Head, J.W., 2002. Fate of outflow channel effluents in the northern lowlands of Mars: The Vastitas Borealis Formation as a sublimation residue from frozen ponded bodies of water. J. Geophys. Res. 107, 5121. doi:10.1029/2001JE001831

Kreslavsky, M.A., Head, J.W., 2002. Mars: Nature and evolution of young latitude-dependent water-ice-rich mantle. Geophys. Res. Lett. 29, 9–12.

Kreslavsky, M.A., Head, J.W., Marchant, D.R., 2008. Periods of active permafrost layer formation during the geological history of Mars: Implications for circum-polar and mid-latitude surface processes. Planet. Space Sci. 56, 289–302. doi:10.1016/j.pss.2006.02.010

Kreslavsky, M.A., Korteniemi, J., Head, J.W., 2011. Recent processes and timing of events in high latitude patterned ground on Mars, in: Fifth Mars Polar Science Conference. pp. 1–2.

Kruger, J., 1994. SORTED POLYGONS ON RECENTLY DEGLACIATED TERRAIN IN THE HIGHLAND OF. Geograpfiska Ann. 76, 49–55.

Kuzmin, R.O., Ershow, E.D., Komarow, I.A., Kozlov, A.H., Isaev, V.S., 2002. The comparative morphometric analysis of polygonal terrain on Mars and the Earth high latitude areas., in: LPSC XXXIII. pp. 19–20.

Lachenbruch, A.H., 1962. Mechanics of thermal contraction cracks and ice-wedge polygons in permafrost. Geol. Soc. Am. Spec. Pap. 70, 69.

Langsdorf, E.L., Britt, D.T., 2004. Periglacial processes in the southern hemisphere of Mars., in: Lunar and Planetary Science XXXV. p. 2.

Langsdorf, E.L., Britt, D.T., 2005. Classification and distribution of patterned ground in the southern hemisphere of Mars., in: Lunar and Planetary Science XXXVI. p. 2.

Laskar, J., Correia, a. C.M., Gastineau, M., Joutel, F., Levrard, B., Robutel, P., 2004. Long term evolution and chaotic diffusion of the insolation quantities of Mars. Icarus 170, 343–364. doi:10.1016/j.icarus.2004.04.005

Leffingwell, E.K., 1915. Ground-Ice Wedges: The Dominant Form of Ground-Ice on the North Coast of Alaska. J. Geol. 23, 635–654.

Lefort, A., Russell, P.S., Thomas, N., 2010. Scalloped terrains in the Peneus and Amphitrites Paterae region of Mars as observed by HiRISE. Icarus 205, 259–268. doi:10.1016/j.icarus.2009.06.005

Lefort, A., Russell, P.S., Thomas, N., McEwen, a. S., Dundas, C.M., Kirk, R.L., 2009a. Observations of periglacial landforms in Utopia Planitia with the High Resolution Imaging Science Experiment (HiRISE). J. Geophys. Res. 114, E04005. doi:10.1029/2008JE003264

Lefort, A., Russell, P.S., Thomas, N., McEwen, A.S., Dundas, C.M., Kirk, R.L., 2009b. Observations of periglacial landforms in Utopia Planitia with the High Resolution Imaging Science Experiment (HiRISE). J. Geophys. Res. 114, 1–18. doi:10.1029/2008JE003264

Levy, J.S., Head, J., Marchant, D., 2009. Thermal contraction crack polygons on Mars: Classification, distribution, and climate implications from HiRISE observations. J. Geophys. Res. 114, 1–19. doi:10.1029/2008JE003273

Levy, J.S., Head, J.W., Marchant, D.R., 2008a. Origin and arrangement of boulders on the martian Northern Plains: Assessment of emplacement and modification environments, in: Lunar and Planetary Science XXXIX (2008). pp. 1–2. doi:10.1029/2005GL024360.

Levy, J.S., Head, J.W., Marchant, D.R., 2011. Gullies, polygons and mantles in Martian permafrost environments: cold desert landforms and sedimentary processes during recent Martian geological history. Geol. Soc. London, Spec. Publ. 354, 167–182. doi:10.1144/SP354.10

Levy, J.S., Head, J.W., Marchant, D.R., Dickson, J.L., Morgan, G.A., 2009. Geologically recent gully–polygon relationships on Mars: Insights from the Antarctic Dry Valleys on the roles of permafrost, microclimates, and water sources for surface flow. Icarus 201, 113–126. doi:10.1016/j.icarus.2008.12.043

Levy, J.S., Head, J.W., Marchant, D.R., Kowalewski, D.E., 2008b. Identification of sublimation-type thermal contraction crack polygons at the proposed NASA Phoenix landing site: Implications for substrate properties and climate-driven morphological evolution. Geophys. Res. Lett. 35, 1–4. doi:10.1029/2007GL032813

Levy, J.S., Head, J.W., Marchant, D.R., Kowalewski, D.E., 2008c. Identification of sublimation-type thermal contraction crack polygons at the proposed NASA Phoenix landing site: Implications for substrate properties and climate-driven morphological evolution. Geophys. Res. Lett. 35, L04202. doi:10.1029/2007GL032813

Levy, J.S., Marchant, D.R., Head, J.W., 2010. Thermal contraction crack polygons on Mars: A synthesis from HiRISE, Phoenix, and terrestrial analog studies. Icarus 206, 229–252. doi:10.1016/j.icarus.2009.09.005

Lewkowicz, A.G., Harris, C., 2005. Morphology and geotechnique of active-layer detachment failures in discontinuous and continuous permafrost, northern Canada. Geomorphology 69, 275–297. doi:10.1016/j.geomorph.2005.01.011

Lowell, P., 1895. Mars. Houghton, Mifflin, Boston, New York.

Lowell, P., 1906. Mars and its canals. Macmillan, New York, London.

Lowell, P., 1908. Mars as the abode of life. The Macmillan Company, New York.

Lucchitta, B.K., 1981. Mars and Earth: Comparison of cold-climate features. Icarus 45, 264 - 303.

Mackay, J.R., 1984. The frost heave of stones in the active layer above permafrost with downward and upward freezing. Arct. Alp. Res. 16, 439–446.

Mackay, J.R., 1988. The Birth and Growth of Porsild Pingo , Tuktoyaktuk Peninsula, District of Mackenzie. Arctic 41, 267–274.

Mackay, J.R., 1998. Pingo Growth and collapse, Tuktoyaktuk Peninsula Area, Western Arctic Coast, Canada: a long-term field study. Géographie Phys. Quat. 52, 271. doi:10.7202/004847ar

Malin, M.C., Bell, J.F., Cantor, B. a., Caplinger, M. a., Calvin, W.M., Clancy, R.T., Edgett, K.S., Edwards, L., Haberle, R.M., James, P.B., Lee, S.W., Ravine, M. a., Thomas, P.C., Wolff, M.J., 2007. Context Camera Investigation on board the Mars Reconnaissance Orbiter. J. Geophys. Res. 112, E05S04. doi:10.1029/2006JE002808

Malin, M.C., Edgett, K.S., 1999. Oceans or seas in the Martian northern lowlands: High resolution imaging tests of proposed coastlines. Geophys. Res. Lett. 26, 3049–3052. doi:10.1029/1999GL002342

Malin, M.C., Edgett, K.S., 2000. Evidence for Recent Groundwater seepage and Surface Runoff on Mars. Science 288, 2330–2335.

Malin, M.C., Edgett, K.S., 2001. Mars Global Surveyor Mars Orbiter Camera: Interplanetary cruise through primary mission. J. Geophys. Res. 106, 23429. doi:10.1029/2000JE001455

Maltagliati, L., Montmessin, F., Fedorova, A., Korablev, O., Forget, F., Bertaux, J.-L., 2011. Evidence of water vapor in excess of saturation in the atmosphere of Mars. Science 333, 1868–1871. doi:10.1126/science.1207957

Mangold, N., 2005. High latitude patterned grounds on Mars: Classification, distribution and climatic control. Icarus 174, 336–359. doi:10.1016/j.icarus.2004.07.030

Mangold, N., Costard, F., Forget, F., 2003. Debris flows over sand dunes on Mars: Evidence for liquid water. J. Geophys. Res. 108, 5027. doi:10.1029/2002JE001958

Mangold, N., Maurice, S., Feldman, W.C., Costard, F., Forget, F., 2004. Spatial relationships between patterned ground and ground ice detected by the Neutron Spectrometer on Mars. J. Geophys. Res. 109, E08001. doi:10.1029/2004JE002235

Marchant, D.R., Head, J.W., 2007. Antarctic dry valleys: Microclimate zonation, variable geomorphic processes, and implications for assessing climate change on Mars. Icarus 192, 187–222. doi:10.1016/j.icarus.2007.06.018

Marchant, D.R., Lewis, A.R., Phillips, W.M., Moore, E.J., Souchez, R.A., Denton, G., Sugden, D.E., Potter Jr, N., Landis, G., 2002. Formation of patterned ground and sublimation till over Miocene glacier ice in Beacon Valley , southern Victoria Land , Antarctica. GSA Bull. 114, 718–730.

Marion, G.M., Catling, D.C., Zahnle, K.J., Claire, M.W., 2010. Modeling aqueous perchlorate chemistries with applications to Mars. Icarus 207, 675–685. doi:10.1016/j.icarus.2009.12.003

Martínez-Alonso, S., Jakosky, B.M., Mellon, M.T., Putzig, N.E., 2005. A volcanic interpretation of Gusev Crater surface materials from thermophysical, spectral, and morphological evidence. J. Geophys. Res. 110, E01003. doi:10.1029/2004JE002327

Matsuoka, N., 2001. Solifluction rates, processes and landforms: a global review. Earth-Science Rev. 55, 107–134. doi:10.1016/S0012-8252(01)00057-5

Matsuoka, N., Abe, M., Ijiri, M., 2003. Differential frost heave and sorted patterned ground: field measurements and a laboratory experiment. Geomorphology 52, 73–85. doi:10.1016/S0169-555X(02)00249-0

Matsuoka, N., Ikeda, A., Date, T., 2005. Morphometric analysis of solifluction lobes and rock glaciers in the Swiss Alps. Permafr. Periglac. Process. 16, 99–113. doi:10.1002/ppp.517

McEwen, A.S., Banks, M.E., Baugh, N., Becker, K., Boyd, A., Bergstrom, J.W., Beyer, R. a., Bortolini, E., Bridges, N.T., Byrne, S., Castalia, B., Chuang, F.C., Crumpler, L.S., Daubar, I., Davatzes, A.K., Deardorff, D.G., DeJong, A., Alan Delamere, W., Dobrea, E.N., Dundas, C.M., Eliason, E.M., Espinoza, Y., Fennema, A., Fishbaugh, K.E., Forrester, T., Geissler, P.E., Grant, J. a., Griffes, J.L., Grotzinger, J.P., Gulick, V.C., Hansen, C.J., Herkenhoff, K.E., Heyd, R., Jaeger, W.L., Jones, D., Kanefsky, B., Keszthelyi, L., King, R., Kirk, R.L., Kolb, K.J., Lasco, J., Lefort, A., Leis, R., Lewis, K.W., Martinez-Alonso, S., Mattson, S., McArthur, G., Mellon, M.T., Metz, J.M., Milazzo, M.P., Milliken, R.E., Motazedian, T., Okubo, C.H., Ortiz, A., Philippoff, A.J., Plassmann, J., Polit, A., Russell, P.S., Schaller, C., Searls, M.L., Spriggs, T., Squyres, S.W., Tarr, S., Thomas, N., Thomson, B.J., Tornabene, L.L., Van Houten, C., Verba, C., Weitz, C.M., Wray, J.J., 2010. The High Resolution Imaging Science Experiment (HiRISE) during MRO's Primary Science Phase (PSP). Icarus 205, 2–37. doi:10.1016/j.icarus.2009.04.023

McGill, G.E., 1986. The Giant Polygons of Utopia, Northern Martian Plains . Geophys. Res. Lett. 13, 705–708.

McSween, H.Y., Keil, K., 2000. Mixing relationships in the Martian regolith and the composition of globally homogeneous dust. Geochim. Cosmochim. Acta 64, 2155–2166.

Mège, D., Cook, A.C., Garel, E., Lagabrielle, Y., Cormier, M., 2003. Volcanic rifting at Martian grabens. J. Geophys. Res. 108, 5044. doi:10.1029/2002JE001852

Mellon, M.T., 1997. Small-scale polygonal features on Mars: Seasonal thermal contraction cracks in permafrost. J. Geophys. Res. 102, 25617. doi:10.1029/97JE02582

Mellon, M.T., Arvidson, R.E., Marlow, J.J., Phillips, R.J., Asphaug, E., 2008. Periglacial landforms at the Phoenix landing site and the northern plains of Mars. J. Geophys. Res. 113, 1–15. doi:10.1029/2007JE003039

Mellon, M.T., Arvidson, R.E., Sizemore, H.G., Searls, M.L., Blaney, D.L., Cull, S., Hecht, M.H., Heet, T.L., Keller, H.U., Lemmon, M.T., Markiewicz, W.J., Ming, D.W., Morris, R. V., Pike, W.T., Zent, A.P., 2009. Ground ice at the Phoenix Landing Site: Stability state and origin. J. Geophys. Res. 114, E00E07. doi:10.1029/2009JE003417

Mellon, M.T., Jakosky, B.M., 1995. Distribution and behavior of martian ground ice during past and present epochs. J. Geophys. Res. 100, 11,781–11,799.

Mellon, M.T., Phillips, R.J., 2001. Recent gullies on Mars and the source of liquid water. J. Geophys. Res. 106, 23165–23179.

Millar, 1972. Freezing and heaving of saturated and unsaturated soils. Highw. Res. Rec. 393, 1–11.

Mischna, M.A., Richardson, M.I., Wilson, R.J., McCleese, D.J., 2003. On the orbital forcing of Martian water and CO 2 cycles: A general circulation model study with simplified volatile schemes. J. Geophys. Res. 108, 5062. doi:10.1029/2003JE002051

Möhlmann, D., Thomsen, K., 2011. Properties of cryobrines on Mars. Icarus 212, 123–130. doi:10.1016/j.icarus.2010.11.025

Möhlmann, D.T.F., 2011. Latitudinal distribution of temporary liquid cryobrines on Mars. Icarus 214, 236–239. doi:10.1016/j.icarus.2011.05.006

Moore, H.J., Hutton, R.E., Clow, G.D., Spitzer, C.R., 1987. Physical Properties of the Surface Materials at the Viking Landing Sites on Mars. U.S. Geol. Surv. Prof. Pap. 1389, 222.

Morgenstern, A., Hauber, E., Reiss, D., van Gasselt, S., Grosse, G., Schirrmeister, L., 2007. Deposition and degradation of a volatile-rich layer in Utopia Planitia and implications for climate history on Mars. J. Geophys. Res. 112, 1–11. doi:10.1029/2006JE002869

Muller, S.W., 1944. Common frontiers in geology and related science in the U.S.S.R. and the U.S.A., in: Science in Soviet Russia. Jacques Cattell Press, Lancaster, Penn, pp. 11–17.

Murray, J.B., Muller, J.-P., Neukum, G., Werner, S.C., van Gasselt, S., Hauber, E., Markiewicz, W.J., Head, J.W., Foing, B.H., Page, D., Mitchell, K.L., Portyankina,

G., 2005. Evidence from the Mars Express High Resolution Stereo Camera for a frozen sea close to Mars' equator. Nature 434, 352–356. doi:10.1038/nature03379

Musselwhite, D.S., Swindle, T.D., Lunine, J.I., 2001. Liquid CO_2 breakout and the formation of recent small gullies on Mars. Geophys. Res. Lett. 28, 1283–1285.

Mustard, J.F., Cooper, C.D., Rifkin, M.K., 2001. Evidence for recent climate change on Mars from the identification of youthful near-surface ground ice. Nature 412, 411–414.

Navarro-González, R., Vargas, E., de la Rosa, J., Raga, A.C., McKay, C.P., 2010. Reanalysis of the Viking results suggests perchlorate and organics at midlatitudes on Mars. J. Geophys. Res. 115, 1–11. doi:10.1029/2010JE003599

Nicholson, F.H., 1976. Patterned Ground Formation and Description as Suggested by Low Arctic and Subarctic Examples. Arct. Alp. Res. 8, 329–342.

Oehler, D.Z., Allen, C.C., 2010. Evidence for pervasive mud volcanism in Acidalia Planitia, Mars. Icarus 208, 636–657. doi:10.1016/j.icarus.2010.03.031

Ojha, L., McEwen, A., Dundas, C., Byrne, S., Mattson, S., Wray, J., Masse, M., Schaefer, E., 2014. HiRISE Observations of Recurring Slope Lineae (RSL) during Southern Summer on Mars. Icarus. doi:10.1016/j.icarus.2013.12.021

Ojha, L., Wilhelm, M.B., Murchie, S.L., McEwen, A.S., Wray, J.J., Hanley, J., Massé, M., Chojnacki, M., 2015. Spectral evidence for hydrated salts in recurring slope lineae on Mars. Nat. Geosci. doi:10.1038/ngeo2546

Orloff, T., Kreslavsky, M., Asphaug, E., Korteniemi, J., 2011. Boulder movement at high northern latitudes of Mars. J. Geophys. Res. 116, 1–12. doi:10.1029/2011JE003811

Orloff, T.C., 2012. Geomorphological analysis of boulders and polygons on martian periglacial patterned ground terrains. University of California Santa Cruz.

Orloff, T.C., Kreslavsky, M.A., Asphaug, E.I., 2013. Possible Mechanism of Boulder Clustering on Mars. Icarus 225, 992–999. doi:10.1016/j.icarus.2013.01.002

Osinski, G.R., Soare, R.J., 2007. Circular structures in Utopia Planitia, Mars: impact v. periglacial origin and Implications for assessing ground ice content., in: Lunar and Planetary Science XXXVIII (2007). pp. 10–11. doi:5110.1029/2001JE001831.

Page, D.P., Murray, J.B., 2006. Stratigraphical and morphological evidence for pingo genesis in the Cerberus plains. Icarus 183, 46–54. doi:10.1016/j.icarus.2006.01.017

Parker, T., Gorsline, D., Saunders, R., Pieri, D., Schneeberger, D., 1993. Coastal geomorphology of the Martian northern plains. J. Geophys. ... 98, 11061–11078.

Pechmann, J.C., 1980. The Origin of Polygonal Troughs on the Northern Plains of Mars. Icarus 210, 183–210.

Penner, E., 1986. Aspects of ice lens growth in soils. Cold Reg. Sci. Technol. 13, 91–100.

Penner, E., Goodrich, L.E., 1981. Location of segregated ice in frost susceptible soil. Eng. Geol. 18, 231–244.

Pina, P., Saraiva, J., Antunes, J., Bandeira, L., 2008. Automatic recognition of diverse types of polygons on Mars, in: Lunar and Planetary Science XXXIX. p. 2.

Pinder, D.A., Witherick, M.E., 1972. The Principles, Practice and Pitfalls of Nearest-Neighbour Analysis. Geography 57, 277–288.

Plaut, J.J., Picardi, G., Safaeinili, A., Ivanov, A.B., Milkovich, S.M., Cicchetti, A., Kofman, W., Mouginot, J., Farrell, W.M., Phillips, R.J., Clifford, S.M., Frigeri, A., Orosei, R., Federico, C., Williams, I.P., Gurnett, D. a, Nielsen, E., Hagfors, T., Heggy, E., Stofan, E.R., Plettemeier, D., Watters, T.R., Leuschen, C.J., Edenhofer, P., 2007. Subsurface radar sounding of the south polar layered deposits of Mars. Science 316, 92–5. doi:10.1126/science.1139672

Pollack, J.B., Ockert-Bell, M., Shepard, M.K., 1995. Viking Lander image analysis of Martian atmospheric dust. J. Geophys. Res. 100, 5235–5250.

Porsild, A.E., 1938. Earth mounds in unglaciated arctic northwestern America. Geogr. Rev. 28, 46–58.

Prestrud, S., Hallet, B., 1986. Dynamics of Periglacial Sorted Circles in Western Spitsbergen. Quarternary Res. 26, 81–99.

Priesnitz, K., Schunke, E., 1983. The Significance of Periglacial Phenomena in Iceland. Polarforschung 53, 9–19.

Raack, J., Reiss, D., Hiesinger, H., 2012a. Gullies and their relationships to the dust-ice mantle in the northwestern Argyre Basin, Mars. Icarus 219, 129–141. doi:10.1016/j.icarus.2012.02.025

Raack, J., Reiss, D., Hiesinger, H., 2012b. Gullies and their relationships to the dust-ice mantle in the northwestern Argyre Basin, Mars. Icarus 219, 129–141. doi:10.1016/j.icarus.2012.02.025

Ray, R.J., Krantz, W.B., Caine, T.N., Gunn, R.D., 1983. A model for sorted patterned - ground regularity. J. Glaciol. 29, 317–337.

Reiss, D., Hauber, E., Zanetti, M., Hiesinger, H., Ulrich, M.R., Olvmo, M., Carlsson, E., Jaumann, R., Trauthan, F., 2011. Possible freeze and thaw landforms on high latitude slopes on Mars, Insights from terrestrial analogs in Spitsbergen Svalbard., in: 42nd Lunar and Planetary Science Conference (2011). p. 2. doi:10.1016/j.icarus.2010.09.010.

Richardson, J., 1851. Arctic searching expedition, vol. 1. Longman, Brown, Green and Longmans, London.

Richardson, M.I., Mischna, M.A., 2005. Long-term evolution of transient liquid water on Mars. J. Geophys. Res. 110, E03003. doi:10.1029/2004JE002367

Robertson, K., Bish, D., 2011. Stability of phases in the Mg(ClO 4) 2 · n H 2 O system and implications for perchlorate occurrences on Mars. J. Geophys. Res. 116, 1–7. doi:10.1029/2010JE003754

Ruff, S.W., 2002. Bright and dark regions on Mars: Particle size and mineralogical characteristics based on Thermal Emission Spectrometer data. J. Geophys. Res. 107, 5127. doi:10.1029/2001JE001580

Schon, S.C., Head, J.W., Fassett, C.I., 2009. Unique chronostratigraphic marker in depositional fan stratigraphy on Mars: Evidence for ~1.25 MA old gully activity and surficial meltwater origin., in: 40th Lunar and Planetary Science Conference (2009). p. 2. doi:10.1029/2002JE001900.

Schon, S.C., Head, J.W., Fassett, C.I., 2012. Recent high-latitude resurfacing by a climate-related latitude-dependent mantle: Constraining age of emplacement from counts of small craters. Planet. Space Sci. 69, 49–61. doi:10.1016/j.pss.2012.03.015

Scott, D.H., Underwood, J.., 1991. Mottled Terrain: A Continuing Martian Enigma. Proc. Lunar Planet. Sci. 21, 627–634.

Séjourné, A., Costard, F., Gargani, J., Marmo, C., Forget, F., Madeleine, J.-B., Soare, R.J., 2009. Periglacial Processes in Utopia Planitia, Evolution of Scalloped Terrains: New Insights from HiRISE Observations, in: 40th Lunar and Planetary Science Conference (2009). p. 2.

Séjourné, A., Costard, F., Gargani, J., Soare, R.J., Fedorov, A., Marmo, C., 2011. Scalloped depressions and small-sized polygons in western Utopia Planitia, Mars: A new formation hypothesis. Planet. Space Sci. 59, 412–422. doi:10.1016/j.pss.2011.01.007

Séjourné, A., Costard, F., Gargani, J., Soare, R.J., Marmo, C., 2010. The Polygon Junction Pits as an evidence of a particularly ice rich area in Utopia Planitia. 41st Lunar Planet. Sci. Conf. 11–12.

Séjourné, A., Costard, F., Gargani, J., Soare, R.J., Marmo, C., 2012. Evidence of an eolian ice-rich and stratified permafrost in Utopia Planitia, Mars. Planet. Space Sci. 60, 248–254. doi:10.1016/j.pss.2011.09.004

Sharp, R.P., 1973. Mars: Fretted and Chaotic Terrains. J. Geophys. Res. 78, 4073–4083.

Sharp, R.P., Malin, M.C., 1975. Channels on Mars. Geol. Soc. Am. Bull. 86, 593–609.

Shinbrot, T., Duong, N.-H., Kwan, L., Alvarez, M.M., 2004. Dry granular flows can generate surface features resembling those seen in Martian gullies. Proc. Natl. Acad. Sci. U. S. A. 101, 8542–8546. doi:10.1073/pnas.0308251101

Sizemore, H.G., Zent, A.P., Rempel, A.W., 2014. Initiation and growth of martian ice lenses. Icarus. doi:10.1016/j.icarus.2014.04.013

Slaymaker, O., 2011. Criteria to distinguish between periglacial, proglacial and paraglacial environments. Quaest. Geogr. 30, 85–94. doi:10.2478/v10117-011-0008-y.a

Soare, R., Kargel, J., Osinski, G., Costard, F., 2007a. Thermokarst processes and the origin of crater-rim gullies in Utopia and western Elysium Planitia. Icarus 191, 95–112. doi:10.1016/j.icarus.2007.04.018

Soare, R., Kargel, J., Osinski, G., Costard, F., 2007b. Thermokarst processes and the origin of crater-rim gullies in Utopia and western Elysium Planitia. Icarus 191, 95–112. doi:10.1016/j.icarus.2007.04.018

Soare, R.J., Burr, D.M., Wan Bun Tseung, J.M., 2005. Possible pingos and a periglacial landscape in northwest Utopia Planitia. Icarus 174, 373–382. doi:10.1016/j.icarus.2004.11.013

Soare, R.J., Costard, F., Pearce, G.D., Séjourné, a., 2012. A re-interpretation of the recent stratigraphical history of Utopia Planitia, Mars: Implications for late-Amazonian periglacial and ice-rich terrain. Planet. Space Sci. 60, 131–139. doi:10.1016/j.pss.2011.07.007

Soare, R.J., Osinski, G.R., Roehm, C.L., 2008. Thermokarst lakes and ponds on Mars in the very recent (late Amazonian) past. Earth Planet. Sci. Lett. 272, 382–393. doi:10.1016/j.epsl.2008.05.010

Soare, R.J., Wan Bun Tseung, J.M., Osinski, G.R., 2006. Gully formation, periglacial processes and possible near surface ground ice in Utopia Planitia., in: Lunar and Planetary Science XXXVII (2006). p. 2.

Squyres, S.W., 1978. Martian Fretted Terrain: Flow of Erosional Debris. Icarus 34, 600–613.

Stoker, C.R., Gooding, J.L., Roush, T., Banin, A., Burt, D., Clark, B.C., Flynn, G., Gwynne, O., 1993. The Physical and Chemical properties and resource potential of martian surface soils., in: Lewis, J.S., Shapley Matthews, M., Guerrieri, M.L. (Eds.), Resources of near-Earth Space. UNiversity of Arizona Press, pp. 659–707.

Taber, S., 1929. Frost Heaving. Geology 37, 428–461.

Tanaka, K.L., Skinner, J.A., Hare, T.M., 2005. Geologic Map of the Northern Plains of Mars. 1:15, 000, 000, US Geological Survey Scientific Investigations Map 2888.

Tavani, S., Granado, P., Corradetti, a., Girundo, M., Iannace, a., Arbués, P., Muñoz, J. a., Mazzoli, S., 2014. Building a virtual outcrop, extracting geological information from it, and sharing the results in Google Earth via OpenPlot and Photoscan: An example from the Khaviz Anticline (Iran). Comput. Geosci. 63, 44–53. doi:10.1016/j.cageo.2013.10.013

Thomas, P., Squyres, S., Herkenhoff, K.E., Howard, A., Murray, B., 1992. Polar Deposits of Mars, in: Kieffer, H.H., Jakosky, B.M., Snyder, C.W., Matthews, M.S. (Eds.), Mars. University of Arizona Press, Tucson, pp. 767–798.

Thorarinsson, S., 1951. Notes on Patterned ground in Iceland , with particular reference to the Icelandic "flas." Geogr. Ann. 33, 144–156.

Tosca, N.J., McLennan, S.M., Lamb, M.P., Grotzinger, J.P., 2011. Physicochemical properties of concentrated Martian surface waters. J. Geophys. Res. 116, 1–16. doi:10.1029/2010JE003700

Treiman, A.H., 2003. Geologic settings of Martian gullies: Implications for their origins. J. Geophys. Res. 108, 8031. doi:10.1029/2002JE001900

Ulrich, M., Morgenstern, A., Gunther, F., Reiss, D., Bauch, E., Hauber, S., Rossler, S., Schirrmeister, L., 2010. Thermokarst in Siberian ice-rich permafrost: Comparison to Asymetric Scalloped depressions on Mars. J. Geophys. Res. 115.

Viklander, P., 1998. Laboratory study of stone heave in till exposed to freezing and thawing. Cold Reg. Sci. Technol. 27, 141–152. doi:10.1016/S0165-232X(98)00004-4

Wallace, D., Sagan, C., 1979. Evaporation of Ice in Planetary Atmospheres: Ice-Covered Rivers on Mars. Icarus 39, 385–400.

Wallace, R.F., 1948. Cave-in lakes in the Nabesna, Chisana and Tanana River valleys, eastern Alaska. J. Geol. 56, 171–181.

Washburn, A.L., 1956. Classification of Patterned Ground and Review of Suggested Origins. Geol. Soc. Am. Bull. 67, 823–866. doi:10.1130/0016-7606(1956)67

Washburn, A.L., 1973. Periglacial Processes and Environments. Edward Arnold.

Washburn, A.L., 1979. Geocryology. Wiley, New York, N.Y.

Werner, B.T., Hallet, B., 1993. Numerical simulation of self-organized stone stripes. Nature 361, 142 - 145. doi:doi:10.1038/361142a0

Westoby, M.J., Brasington, J., Glasser, N.F., Hambrey, M.J., Reynolds, J.M., 2012. "Structure-from-Motion" photogrammetry: A low-cost, effective tool for geoscience applications. Geomorphology 179, 300–314. doi:10.1016/j.geomorph.2012.08.021

Williams, R.M.E., Grotzinger, J.P., Dietrich, W.E., Gupta, S., Sumner, D.Y., Wiens, R.C., Mangold, N., Malin, M.C., Edgett, K.S., Maurice, S., Forni, O., Gasnault, O., Ollila, A., Newsom, H.E., Dromart, G., Palucis, M.C., Yingst, R. a, Anderson, R.B., Herkenhoff, K.E., Le Mouélic, S., Goetz, W., Madsen, M.B., Koefoed, A., Jensen, J.K., Bridges, J.C., Schwenzer, S.P., Lewis, K.W., Stack, K.M., Rubin, D., Kah, L.C., Bell, J.F., Farmer, J.D., Sullivan, R., Van Beek, T., Blaney, D.L., Pariser, O., Deen, R.G., 2013. Martian fluvial conglomerates at Gale crater. Science 340, 1068–1072. doi:10.1126/science.1237317

Wilson, P., Clark, R., 1994. Development of miniature sorted patterned ground following soil erosion in East Falkland, South Atlantic. Earth Surf. Process. Landforms 16, 369–376.

Yen, A.S., Gellert, R., Schröder, C., Morris, R. V, Bell, J.F., Knudson, A.T., Clark, B.C., Ming, D.W., Crisp, J.A., Arvidson, R.E., Blaney, D., Brückner, J., Christensen, P.R., DesMarais, D.J., de Souza, P.A., Economou, T.E., Ghosh, A.,

Hahn, B.C., Herkenhoff, K.E., Haskin, L.A., Hurowitz, J.A., Joliff, B.L., Johnson, J.R., Klingelhöfer, G., Madsen, M.B., McLennan, S.M., McSween, H.Y., Richter, L., Rieder, R., Rodionov, D., Soderblom, L., Squyres, S.W., Tosca, N.J., Wang, A., Wyatt, M., Zipfel, J., 2005. An integrated view of the chemistry and mineralogy of martian soils. Nature 436, 49–54. doi:10.1038/nature03637

Zent, A.P., Hecht, M.H., Cobos, D.R., Wood, S.E., Hudson, T.L., Milkovich, S.M., DeFlores, L.P., Mellon, M.T., 2010. Initial results from the thermal and electrical conductivity probe (TECP) on Phoenix. J. Geophys. Res. 115, E00E14. doi:10.1029/2009JE003420

Zhang, T., Barry, R.G., Knowles, K., Heginbottom, J.A., Brown, J., 2008. Statistics and characteristics of permafrost and ground-ice distribution in the Northern Hemisphere. Polar Geogr. 31, 47–68. doi:10.1080/10889370802175895

14 Appendix One: Periglacial processes under martian conditions: A laboratory study

Chapter Three discusses the possibility that the presence of salts in the subsurface could depress the freezing point of interstitial brines sufficiently to allow more frequent thawing events to occur. This could potentially allow sorted patterned ground to develop over a wider range of conditions than would otherwise be the case. However it is uncertain whether sorted patterns can develop in highly saline environments or whether the presence of brines will disrupt the formation of the coherent ice lenses required to heave the soil.

This appendix presents the results of a series of experiments aimed at simulating these processes in the laboratory. However after significant work and multiple changes in approach, these experiments did not produce satisfactory results, either negative or positive. Therefore, after several attempts and nearly two years of work, the focus of the PhD was shifted to the remote sensing side of the study. Nevertheless, the experimental background and literature, and the descriptions of the experiments themselves, are included here, both for sake of completeness and also to provide important context for some of the topics discussed throughout the thesis.

14.1 Aims

This stage of the investigation was a "proof of concept" study to determine whether the conditions in the martian subsurface in the present day would be suitable for the development of ice lenses and the formation of sorted patterned ground. Although the presence of concentrated brines provides an interesting avenue to allow these processes to occur it is possible that the sensitivity of the system to factors other than temperature could hinder the development of sorted patterned ground. For example

patterned ground will only form in locations with frost-susceptible soil and where sufficient water is present to allow the development of a frozen fringe.

To determine whether this is the case a series of laboratory studies were conducted attempting to simulate freeze thaw sorting in the lab and determine which parameters are most significant in controlling the sorting process. If heaving of large particles can be triggered in a brine saturated soil, without the temperature rising above zero °C, it would provide a proof of concept for sorting with even more exotic brines. It would indicate that periglacial processes could occur at much lower temperatures than those simulated in the lab, in the presence of more exotic brines. The magnesium perchlorates believed to occur at the Phoenix landing site being one such example (Cull et al., 2010; Hecht et al., 2009).

14.2 Methodology

A variety of different methodologies were used during this investigation as the experiment was redesigned several times over the course of the project. A variety of experimental setups were tested as unforeseen confounding variables came to light. The basic intention throughout this iterative procedure was to develop a simple method which would, over a number of freeze thaw cycles, result in clear evidence of frost heaving.

The objective was not to produce a sorting pattern, or to assess the distribution of particles of different sizes within the soil column before and after sorting. The desired result was a procedure which could be replicated at a range of low temperatures, to investigate whether the use of brines would allow the sorting or heaving process to occur. The ideal test would be an experimental set up where, over a relatively short period of time, stones within the subsurface could be seen to rise towards the surface, or the height of the surface to rise due to frost heaving.

14.2.1 Prior Investigations

Over the course of the 20th century a variety of studies have been conducted into the sorting and frost heaving processes; all used a slightly different procedure, but some methodological elements remain constant and can inform the current study. This section provides a brief overview of the literature and how these studies influenced the current experimental design.

Taber (1929) was the first study on the subject. Taber found that frost heave was the result of the formation of ice lenses within the soil, rather than the expansion of ice upon freezing. He concluded that ice lenses are more likely to form as a result of a slow freezing process rather than a sudden temperature drop. Particles are moved in the direction of ice growth and this is away from the direction of cooling. Therefore if a sample is cooled from below then ice will grow in an upwards direction, moving particles with it.

Taber concluded that ice lens segregation occurs preferentially within a matrix of very fine grained particles (<1 μm), when the rate of cooling is slow, and when the percentage of void space is high, and water is available to replenish that frozen into the ice lenses.

Corte (1962, 1963) investigated the factors that affected frost heave when a sample was subjected to a series of ~ 20 temperature cycles. Corte used a cold plate to simulate cooling from below and a heating tape to provide heating from above. He found that sorting occurred when the freezing front advance rate was between 30-44 mm h^{-1}. Fine particles of diameters less than 0.1-0.5 mm migrated when the rate of freezing was high or low, while coarser particles only migrated when subjected to low rates of freezing. Corte concluded that the area of contact between the particle and the freezing front was critical in allowing thawing to take place, and found that water content was important.

A layer of water may well be required between the freezing front and the particles in order for movement to occur.

Mackay (1984) discussed two different processes that could contribute to frost heave; a "frost pull theory" where a stone becomes trapped within a downwards freezing front and lifted and a "frost push theory" where the growth of ice beneath a stone causes it to be lifted. He simulated both upwards and downwards freezing, but used a large stone on a block of ice, rather than a stone suspended within a soil matrix. Mackay found that ice lenses grow on the cold side of a stone, presumably that closest to the nearest freezing front, and that this would push it into the unfrozen soil on the far side, thus away from the freezing front. However he concluded that the process is very complicated and that more research into it is required.

In the study of Viklander (1998), a single (25 mm) stone was placed within a matrix of finer material and its position monitored by repeated X-ray imaging. The sample was frozen from the top down in this study. But frost heaving was still observed, suggesting that frost pull processes were taking place. They observed upwards movements of the large clast in samples with small amounts of void space, while downwards movement, probably due to settling, was seen when large void spaces were present.

This procedure would work well for this investigation as the movement of a large stone within a simple soil matrix would provide a good indicator that heaving is occurring. However the equipment necessary to monitor the position of a stone by X-ray imaging was not available for use in the current investigation, so a different approach was used.

Matsuoka et al., (2003) conducted an experiment to measure the difference in heave between a fine domain and one consisting of fines overlain by several centimetres of coarse gravel. They insulated all sides of the container except for the top, from which the sample was both cooled and heated. They found that the heaving of the soil was

suppressed by the presence of coarse material, and that it heaved later than the finer domain, and subsided earlier. This is in keeping with the observations of Corte (1962, 1963) that the fine domain is likely to be more susceptible to frost heaving.

These studies show that frost heaving has been demonstrated in the laboratory under a range of conditions; critically, with the dominant freezing direction being both upwards, and downwards. Sorting usually occurred within 10-20 cycles of the start of the experiment. The importance of cooling from the bottom up should be tested to determine to what extent the direction of cooling is significant.

All of these researchers appear to have placed their samples within a cold room, maintaining a specific low air temperature, usually ranging between 0°C and -20°C, for the duration of the experiment. All heating and cooling was independent of the overall environmental control. In the current investigation a cold room was not available, but a freezer could be used to maintain a stable low temperature while a separate heating system was used to cycle the temperature.

14.2.2 Materials

A range of materials were used over the course of this investigation. A variety of fractions of different sized particles were required (as illustrated in Figure 14.1). The most important of these was a substrate that would serve as the soil column for the experiments. This material needed to be sufficiently frost-susceptible to allow heaving to occur, while also being available in large quantities. Several different options were considered and tested as the experimental work progressed.

Initially the JSC Mars-1 simulant (Allen et al., 1998) was considered for use. This material consists of weathered volcanic ash selected to be a good analogue for the materials observed by landers on the martian surface. The majority of this material has a grain size in the 10 to 100 μm range; consequently, it should prove frost-susceptible.

Ultimately it was decided that this simulant should not be used for this investigation as the large quantities that would be required would prove prohibitive to acquire. However it provided a useful starting point for assessing the type of material that was likely to be present on the martian surface.

Instead the initial set of experiments was conducted using medium grained sand with a mean grain size of approximately 250 microns. This was somewhat coarser than the Mars analogue would have been, but was available in much larger quantities, allowing experiments with far larger soil columns to be conducted. The properties of this material were well within the constraints expected for a martian surface material, and similar material had been used to simulate the martian surface by other studies (e.g. Conway et al., 2011).

The mean grain size of this material is on the upper limit of frost susceptibility, but it was used mainly for pilot studies, to begin to understand how the experimental system behaved. This medium grained sand was later mixed with fine grained clay particles to produce a new substrate with a slightly different grain size distribution. It was hoped that this would increase its frost susceptibility. During the experiments, however, it was found that the clay particles aggregated into small clusters that actually had a larger grain size than that of the sand. It was decided to use this material as an alternate substrate since it did have some similarity to the cohesive clay component which has been described as being present in martian soils.

Finally, a series of experiments were conducted using a sample of fine grained mud, extracted from the bed of Walton Lake, a water body adjacent to the Open University's Milton Keynes Campus. This material was sieved until only the fraction that passed the 500 micron sieve remained. This material did not pass the 90 micron sieve without forcing. However it was believed that this was due to the high clay concentration

which caused the particles to cohere. Finer particles were present, but may not have been an active component of the material due to their clumping into clusters with a larger effective grain size. Several samples of this fine grained mud were mixed with sand and the clay-sand mixtures to provide a variety of different materials.

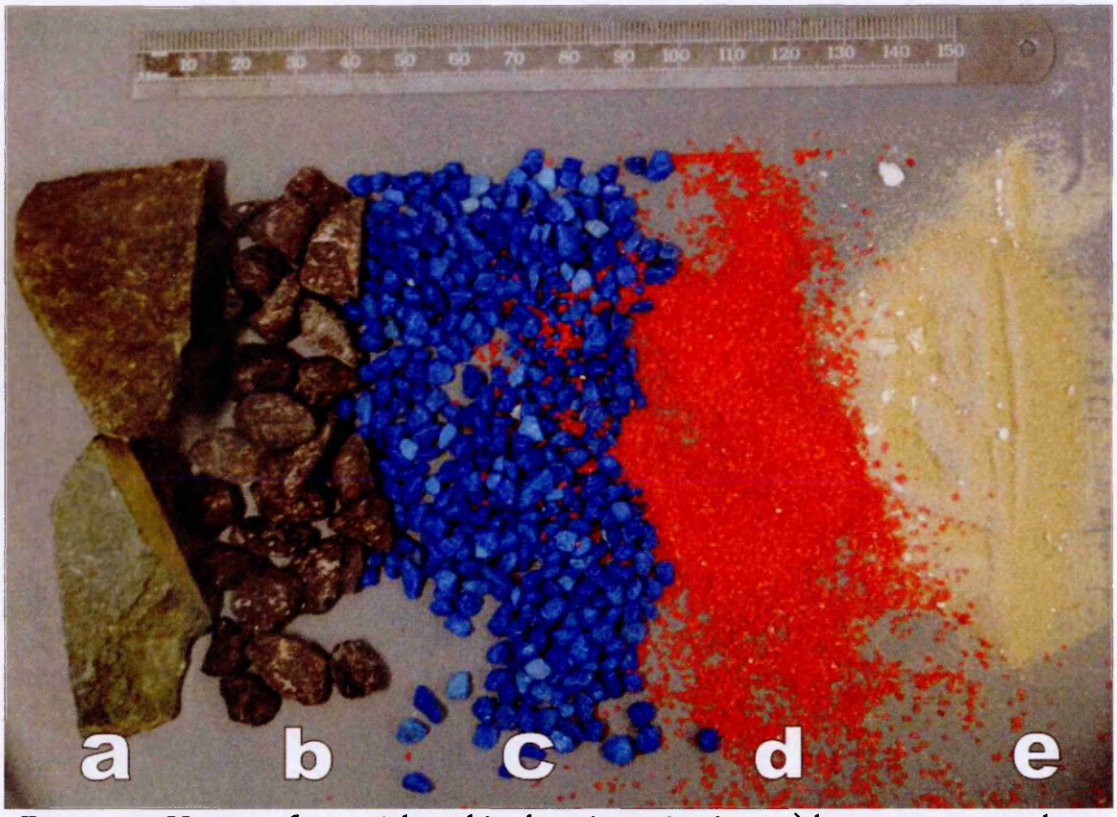

Figure 14.1: Variety of material used in these investigations: a) large stones: 5 cm long pebbles, b) black fraction: 1-2 cm small pebbles, c) blue fraction: 3-4 mm granules, d) red fraction: 0.5-1 mm coarse sand, e) yellow fraction: 25 μm fine sand mixed with 1-5 mm clusters of cohered clay (white fraction).

The coarse fraction consisted of several different grades of stones. These were bought from an aquarium supplier, so that each fraction was dyed a different colour. This made the different fractions easier to distinguish when mixed with the yellow sand and made it easier to assess whether any movement was occurring within the soil column. The range of materials used is illustrated in Figure 14.1

14.2.3 Sodium Chloride Brines

A set of sodium chloride solutions were prepared so that brines with a variety of freezing point depressions could be tested. A saturated solution was prepared and this was then diluted to produce solutions of 0, 10%, 20% 23.3%, 25% and 30% saturations.

The eutectic solution of 23.3% produces the greatest freezing point depression, reducing the freezing point to -21.1°C. This is far higher than the temperatures that would be required for freeze thaw sorting to occur on Mars. In that situation a more exotic brine with a lower eutectic temperature would be required. However it was decided that, to begin with, an easily accessible and handled salt with a moderate freezing point depression should be used, rather than a more difficult to use salt such as magnesium perchlorate, which would have required more complex procedures to store and handle safely. By using sodium chloride it was also not necessary to cool the chambers to the very low temperatures characteristic of the martian environment, merely to temperatures below the eutectic temperature of the salt.

This arrangement provides a warmer analogue: if sorting could occur with sodium chloride brines at temperatures of -30°C then it provides a proof of concept that sorting could occur with magnesium perchlorate brines at temperatures as low as -70°C. If sorting were observed at a moderately reduced temperature, then it would be likely that the presence of the brine did not impede the sorting process sufficiently, and this mechanism would be viable at lower temperatures. If however this relatively low freezing point depression was sufficient to prevent significant frost heaving then it might rule out more exotic brines from facilitating the development of periglacial features on Mars.

It is possible that the presence of very concentrated brines could adversely affect the sorting process. A reduction in frost heaving has been observed in soils saturated with

brines relative to those containing pure water (Chamberlain, 1983). Studies into the formation of ice lenses suggest that the presence of a concentrated brine can result in a less coherent structure, where channels of unfrozen brine are interspersed with regions of pure ice (Arenson, 2004; Arenson and Sego, 2006). This would be expected to affect the sorting process. The effect of the expansion and contraction of water upon a phase change has a negligible effect on frost heaving, which is mainly the result of the accumulation of coherent lenses of ice within the soil. Consequently any adverse effect upon volumetric change due to salt concentration would be unlikely to have as significant an impact as the disruption to ice lens development.

Martian temperatures are difficult to maintain in a laboratory for extended periods of time, but had the initial run of experiments proved successful at moderately low temperatures then a small series of Mars condition runs could have been attempted to test the scaling argument.

14.3 Overview of Experimental work

This section will discuss the series of experiments conducted over the course of the project. Several of the experiments described herein did not produce useful results. Consequently, the method was repeatedly redesigned to take additional factors into consideration so in some cases the changes made to the experimental procedure are the focus of a section rather than the elements that remained constant from previous tests. It was initially hoped that this experimental design process would be completed fairly rapidly, however this ultimately did not prove to be the case.

The basic methodology of Corte (1963) was chosen as a simple case where demonstrable sorting occurred. However, that study demonstrated the sorting process takes a long time to produce measurable changes in the soil column, in excess of 20 cycles in the

case of Corte (1963). Consequently, each experiment had to be continued for many weeks to determine whether or not it was producing results.

This meant that the overall development process took far longer than would have been ideal. Ultimately a working system, producing validated results, was not achieved and so the effect of freezing point depression was not explored further. Since the findings of the previous studies could not be replicated it was not possible to proceed with further testing.

After two years of redesigns it was decided that this aspect of the thesis should be halted to free up more time for other, more reliable strands of the investigation. The results of the laboratory work are presented in overview, as they provide a useful illustration of the sensitivity of this system to various conditions such as soil type, availability of water and rate of cooling.

14.3.1 Sorting experiment one: Pilot Study.

The first experiment in this series was intended as a pilot study to see how susceptible the materials were to freezing and thawing. A random mixture of several particle sizes was repeatedly frozen and thawed to determine whether movement of the particles would occur. It was hypothesised that frost heaving would occur and that this would be visible in several ways: firstly, because the vessel used was transparent, the formation of segregated ice would be visible within the soil column and so this was monitored by a web-camera for the duration of the experiment. Secondly, frost heaving would be apparent as an increase in the height of the surface, and thirdly, the movement of specific large stones (whether due to frost pull or frost pushing) would be apparent, as their final positions would differ from their initial ones.

14.3.1.1 Setup.

A 1000 mL beaker was filled with four of the different particle sizes shown in Figure 14.1. 500 g of black stones with a mean diameter of 9-13 mm, 300 g of blue with 2-3 mm diameters, 200 g of red sand of 0.1-0.5 mm and 200 g of finer grained yellow sand which was expected to be the most frost-susceptible component. The four sizes of material were manually mixed and blue and black stones were scattered throughout the column, with a thicker layer at the top and at the bottom. The column was then saturated with 100 mL of deionised water, leaving a head of approximately 1 cm to ensure that it infiltrated all of the way into the soil column. The arrangement of clasts at the start of the run is shown in Figure 14.2.

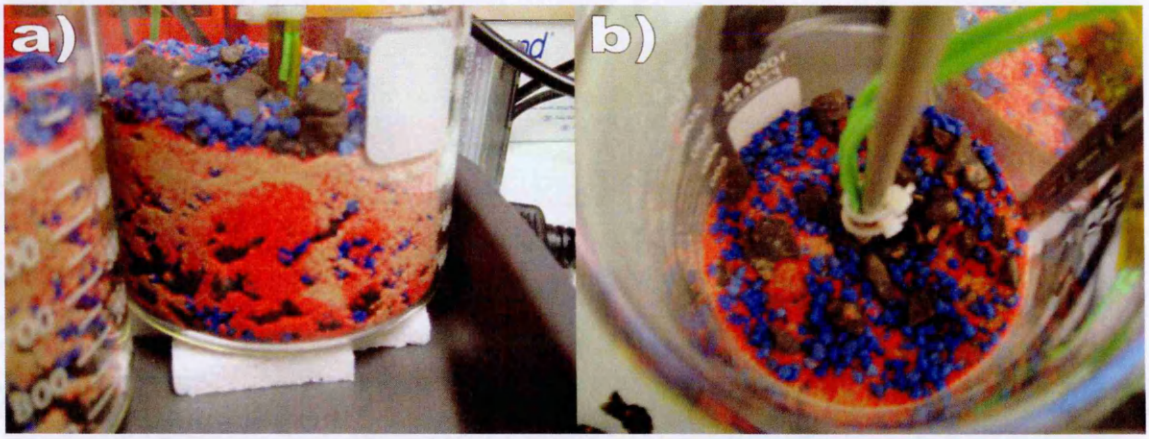

Figure 14.2: beakers of mixed material before freeze-thaw cycling began. Granule sized material is randomly distributed within a column of coarse and fine grained sand. The central column is the mounting for thermocouples and the beakers are raised on foam blocks to prevent preferential cooling of the bottom due to contact with the chamber floor. a) Side view, b) view of the surface.

Two beakers were prepared, containing the same proportions of the differently sized materials. One was instrumented with a central plastic rod, on which three thermocouples were mounted, spaced 2.5 cm apart with the bottom most sensor being one cm from the base of the sample and the topmost falling just below the surface when the beaker was filled with approximately 500 mL of material. Hermetically sealed K type thermocouples were chosen (HSTC-TT-KI-24S-1M). This would allow the

temperature within the column to be monitored and the rate at which the freezing front penetrated into the soil to be determined. In this instance, both beakers contained deionised water.

Both cylinders were then placed within a thermal cycling chamber. This device could be programmed to vary the air temperature within the chamber over a specified period of time. An initial value was set, and the value to which the temperature should rise or fall over a designated period of time. The chamber then changed the temperature at a constant rate over that period. The temperature was set to cycle between 10°C and -10°C twice per day, thus cooling and heating at a rate of 1.67°C per hour. A low rate of cooling was required to ensure the low freezing front progressions described by Corte (1963) as being a key parameter in producing the requisite sorting effect. 80 freeze thaw cycles were conducted over a period of 40 days. This was chosen to be well in excess of the number of cycles required to generate frost heaving by the previous studies from which this method was derived.

The cylinder was placed on foam blocks to insulate it from the chamber floor as illustrated in Figure 14.2. Consequently, the upper surface of the column should cool fastest, as the sides would be insulated by the glass. Adding further insulation to the sides was considered, but it was decided that this would interfere with the ability to monitor movement within the soil column while the experiment progressed. Data from the thermocouples confirmed that the surface cooled faster than the interior, however, in retrospect a better temperature gradient within the sample would have been produced if more insulation had been used.

14.3.1.2 Results

After eighty cycles no evidence of sorting or frost heave could be seen. Before and after images from the webcam are shown in Figure 14.3 and show no appreciable difference.

The surface had not exhibited vertical displacement at any point during the experiment and no segregated ice was observed forming during this time. Ice froze within the pores, but the volumetric increase resultant from freezing was insufficient to have a significant effect on the position of any of the surrounding clasts.

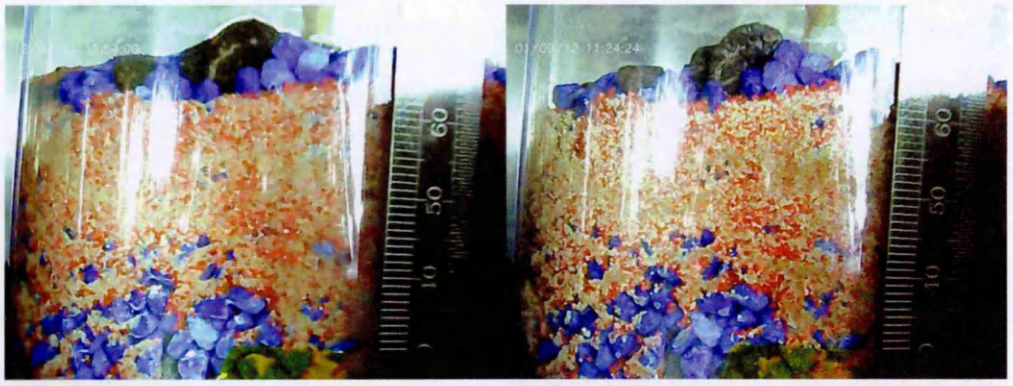

Figure 14.3: Images of the soil column captured by the web-camera in the chamber before and after the freeze thaw cycling. No significant change in the position of the soil particles has occurred.

Several factors could have resulted in the lack of a response from this set up. Firstly, the mixture of coarse grained materials could have resulted in the pore spaces between the particles being too large to allow the development of a frozen fringe (i.e. the soil was not sufficiently frost-susceptible). Secondly, it is possible that the sample froze too rapidly for an unfrozen component to develop. Slower rates of freezing might have exhibited more of a result. Finally, the vessel used for this experiment was reasonably small and it was hypothesised that edge effects could be preventing bulk movement from occurring, as the soil column was constrained on all sides by the walls of the beaker.

It was decided that the next set of experiments would use a larger tray, to reduce the possibility of edge effects and that a more limited set of materials would be used, with a much larger fraction of the fine grained components. Most importantly it would be set up so that cooling was from below the soil column rather than from above.

14.3.2 Sorting experiment two: Directional Cooling.

Since there were several parameters which could have resulted in the lack of change in the first experiment it was decided to try a radically different set up for the second so that more factors could be controlled. This experiment deliberately used a much simpler system, consisting of larger stones suspended within a matrix of fine sand. The smaller granules were removed, as it was feared that they might have adversely affected the flow of water through the sample during experiment one.

14.3.2.1 Setup

In this test a metal tray was used to hold the soil column rather than a glass beaker. An RS ltd. die cast aluminium circuit box 20 cm on a side was selected for this purpose. This provided a larger sample size and ensured that the primary direction of cooling was from below, due to the good thermal contact between the metal tray and the base of the chamber. Since the larger sample size made it too large for the thermal cycling chamber a different system was set up. A large chest freezer was modified to hold a liquid nitrogen cold plate as shown in Figure 14.4. The temperature at the base of the soil column could thus be controlled by the flow of liquid nitrogen through the system. One advantage of this set up was that much lower temperatures, potentially comparable with those on Mars, could be reached. However this came with the disadvantage that the exact rate of cooling was harder to control.

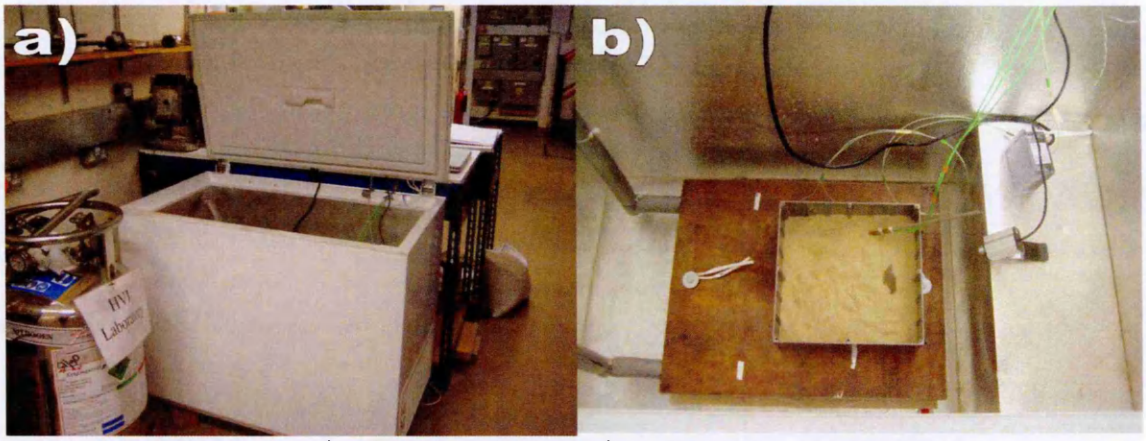

Figure 14.4: a) Chest freezer with b) liquid nitrogen cold plate.

Three thermocouples were placed at the bottom, middle and surface of the soil column. Two were attached to the cold plate and another measured the air temperature of the chamber. A web camera was pointed down at the surface of the soil column to observe any changes in the position of the large stones, only one of which was initially visible.

The soil column was composed of sand of the same type as the fine fraction used in the previous run. Rather than mixing gravel with the sand it was decided to place three 4 cm long stones at different depths within the sand column and see whether they showed any movement after repeated freeze thaw cycles. This would make it easier to quantify movement, rather than trying to track the positions of a large number of smaller stones. One stone was placed at the bottom of the soil column, with its upper surface 2 cm above the base of the column, one was placed in the middle of the column, with its base at a height of one cm from the bottom and its top at a height of two cm; one cm below the top of the sand. The third stone was placed at the surface of the column, with its base at a height of two cm, just below the surface, and its upper extent at three cm height; approximately one cm above the surface of the sand. The soil column was saturated with a eutectic sodium chloride solution. This should have a freezing point of -21.2 °C. This setup is illustrated in Figure 14.5 and a schematic diagram is shown in figure 14.6.

Figure 14.5: The soil column is saturated with brine prior to being placed within the chamber.

Due to the use of a metal tray it was impossible to see what was going on at depth within the soil column, but thermocouples were placed at the bottom, middle and top of the soil column so that the rate of temperature change could be monitored. This would be very important with this set up since the variation in temperature had to be manually controlled using the liquid nitrogen. The liquid nitrogen cold plate was used to oscillate the temperature between -10 °C and -30°C nine times.

Initially thawing was achieved by opening the freezer and switching it off. Later a lamp was introduced, a control system was then set up to allow the lamp to be shut off automatically when the temperature in the chamber approached zero, ensuring that any thawing had to be the result of the depression of the freezing point. The initial run with no lamp consisted of 4 cycles, then a further three cycles were conducted with the lamp and then two more with a lamp and control system.

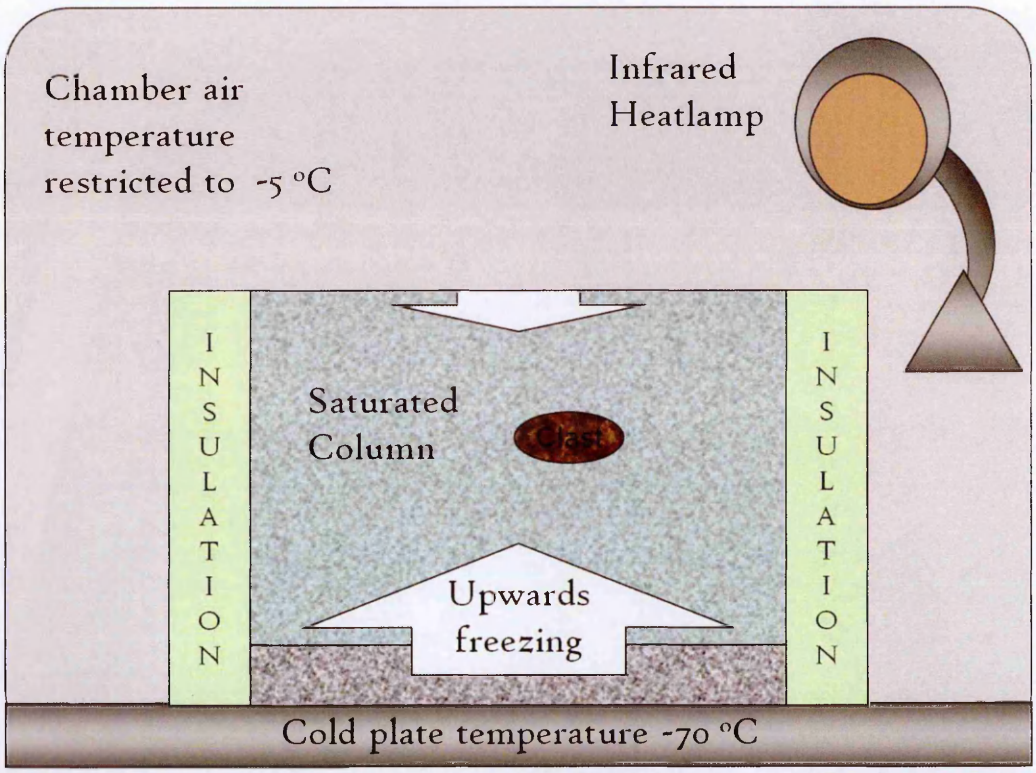

Figure 14.6: Apparatus for the second set of sorting experiments. The temperature gradient within the soil is controlled by the difference between the air temperature, maintained by the freezer and the cold plate temperature when liquid nitrogen is introduced into the system. Consequently, cooling should occur from the bottom up.

14.3.2.2 Results

No change in the positions of the stones was noted and the surface was not observed to heave over the course of the experiment. However disks of white ice spread out to cover the surface each time the sample froze. These are believed to be a product of the crystallisation of the concentrated salt solution being used, as they were not observed in similar conditions where pure water was used.

The sample was excavated after nine cycles and it was found that the sample was no longer saturated with water near the surface. This was due to evaporation of the water while the sample was standing between freezing cycles, gradually drying out the soil column. Drying out was most pronounced at the top of the column, but given sufficient time the entire soil column would lose its interstitial water. Consequently, it was

decided that the water level should be topped up in future runs, although this might have an effect on the concentration of the salt solution.

Overall no change in the positions of the stones was observed. It is suspected that there was insufficient water within the system to allow ice lenses to accumulate, certainly not enough to exert significant pressure on the stones. It is possible that using large stones prevented significant heaving, as the pressure required to lift a larger stone would be proportionally greater. Consequently, it was decided that two changes should be made for the next experiment: firstly, smaller material should be used, and secondly, the system would be resupplied with water to more accurately simulate the availability of water in a thawing active layer.

14.3.3 Sorting experiment three: Smaller stones

14.3.3.1 Setup

A modified version of the previous experiment was set up using the same apparatus. In this run the water was replenished from the top down, by pouring additional water onto the corner of the sample when the surface appeared to have dried out. Polystyrene blocks were also placed around the metal tray to try to insulate the sides, so as to ensure that cooling would only occur from the bottom up and to a lesser extent from the top down, however it was recognised that without building a custom vessel, full insulation would be impossible due to conduction from the walls of the tray to its base, since the aluminium box used had a high thermal conductivity.

The soil column consisted of a mass of sand 4 cm deep with the small granules of the black grade placed in two layers at one cm above the bottom and one cm below the surface. A schematic of this setup is shown in Figure 14.7. Pure water was used so that

replenishing it would not affect the salt concentration. If the setup had worked then salt solutions would have been introduced in a later experiment.

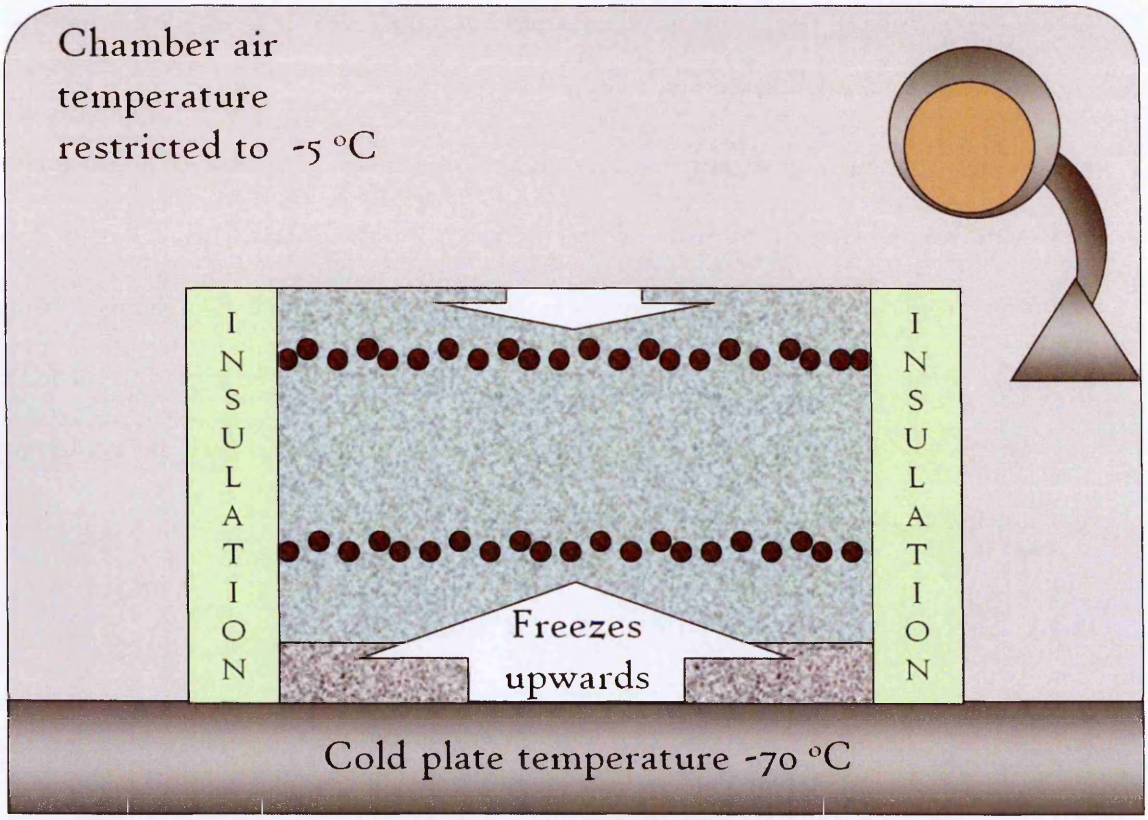

Figure 14.7: thin layers of black stones used rather than several larger clasts.

14.3.3.2 Results

Replenishing the water level from above presented a significant problem, as it eroded the finer material, exposing the stone layer buried just beneath the surface. This had the result that it was impossible to tell whether there had been an upward movement of the stones due to heaving or not.

After 6 cycles, using a mixture of the liquid nitrogen cold plate and the freezers own cooling system, the column was dissected. The clear test for stone movement would have been the presence of stones in contact with the bottom of the tray for downwards movement, or at the surface for upwards movement. However replenishing the water from above disrupted the level of the surface making it hard to determine whether there had been a change in the position of the stones. None were found in contact with

the base of the tray, suggesting that no significant downward movement had occurred. It was concluded that there might have been movement out of the stone layers, but this was highly uncertain and this setup was concluded to be ineffective.

14.3.4 Sorting experiment four: Improving the water supply.

14.3.4.1 Setup

The setup was revised to correct for the problems encountered in the previous run. A perforated pipe was buried in the bottom of the tray so that water could be replenished from the top up, without risking disrupting the surface. It was found that it took more than 2 days for the column to completely dry out even with the heat lamp on. Consequently, topping it up regularly (once per day) should suffice to keep the column replenished. Additional water was added until no more percolated into the soil column and a head of excess water remained at the surface.

A layer of stones was buried 2 cm below the surface of the 4 cm deep sand column. It was hoped that using a single stone layer would reduce the uncertainty involved in determining whether there had been movement upwards or downwards within the column. As with the previous run the presence of stones at the surface would be a definite indication that heaving had occurred.

Liquid nitrogen was not used during this run, since pure water was being used no freezing point depression was expected and thus the freezer's cooling system would be sufficient to cool the sample to freezing. There was also some concern that the rate of freezing in the previous run had been too high for ice lenses to form within the soil, as the entire sample appeared to have frozen very rapidly, rather than the cold plate generating a freezing front which slowly propagated through the sample.

14.3.4.2 Results

It was found that using the freezer's cooling system did not significantly reduce the rate of freezing, and in fact the sand around the lower end of the perforated pipe froze, preventing water from being effectively fed into the sample.

No significant movement of the stone layer was observed when the column was excavated after 12 cycles. A section through the excavated column is shown in Figure 14.8. Dipping a ruler into the sand until it encountered the tops of the stones produced a range of depths for the top of the stone layer between 1.3 and 2 cm below the surface. This fits with the original burial depth, as the stones were buried at 2 cm depth and are up to 0.5 cm high. A few stones appeared to be higher up, but they were located above the water pipe and so were likely to have been displaced when the pipe was being lifted to feed more water into the system.

Most stones were found to be 1.5 cm above the bottom of the column, or 1.4 cm near the centre of the sample. A few stones might have been as low as 1 cm above the bottom of the tray, but as it was harder to make measurements down from the stone layer than up these observations are not conclusive. It is impossible to conclude that sorting had occurred in this run.

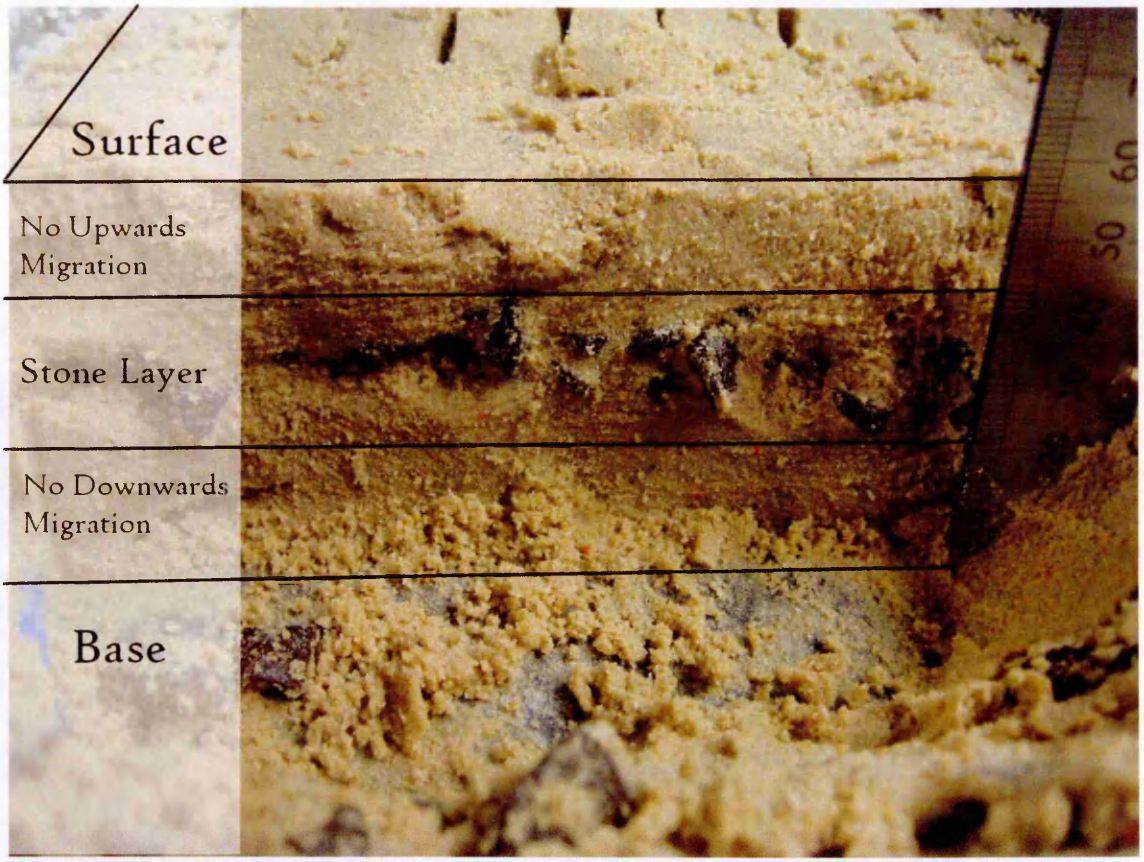

Figure 14.8: cross section through the soil column showing that there had been no significant displacement of stones from their original burial depth.

14.3.5 Sorting experiment 6

Since it seemed likely that past experiments have frozen too rapidly, preventing the development of a frozen fringe and thus ice lens segregation, it was decided to abandon the use of the cold plate altogether. An experiment was conducted with a very slow rate of cooling to test this hypothesis.

14.3.5.1 Setup

An experimental setup similar to that used for experiment one was created; a transparent box, slightly larger than the original glass beakers was filled with a column of sand/clay mixture 8 cm high. Equal parts of sand and clay had been mixed in an attempt to generate a finer fraction; however it formed clumps which were no finer than the sand grains themselves. A layer of gravel was placed at a height of between 3

and 5 cm, along with a band of red coloured sand, which was slightly coarser than the main substrate. The column was saturated with pure water by adding water to the top of the column and allowing it to drain into the soil over a period of a day, until a head of water remained above the top of the soil column. The setup for this experiment is shown in Figure 14.9.

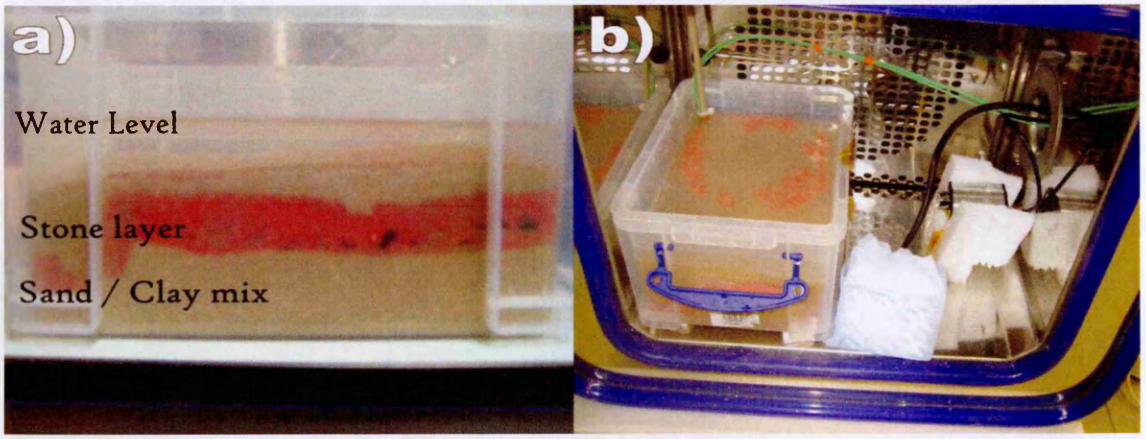

Figure 14.9: Apparatus for the final sorting experiment. Red sand was used to demark the boundary of the layer in which the stones were expected to be found. a) Side view of the sand column, b) experimental setup.

The layers of sand and stones were originally flat; however the addition of the water disrupted the levels of the different layers. Consequently, all measurements were made with reference to the surfaces shown in Figure 14.9. The column was saturated by emplacing a head of water above the surface and allowing it to drain through the matrix over the course of a day.

The thermal cycling chamber used in experiment one was programmed to cool the air from 5°C to -10°C at a rate of 0.2°C per hour and heat at 0.4°C per hour. A webcam was set up to record a frame every minute so that any movement of stones would be recorded. Four cycles were conducted over the period of a month. After which the sample was removed from the oven and examined. As with the previous experiments in this series no significant movement of the stones could be seen. A further four cycles were conducted, the cooling rate remained unchanged at 0.2°C h^{-1} but the rate of heating

was increased to 2.5°C h^{-1} to speed up the process, since it was believed that the rate of cooling was more significant to the ice lens formation process.

14.3.5.2 *Results*

After a total of eight cycles it was concluded that there was no significant change in the position of the stones between the start of the experiment and its conclusion. Figure 14.9 shows before and after images from the webcam and indicates a lack of movement in the clasts, but that the fine red sand has been displaced. The camera position shifted during the course of the second stage of the experiment, but this had a minimal effect on determining the lack of displacement as the relative position of the clasts was clearly unchanged.

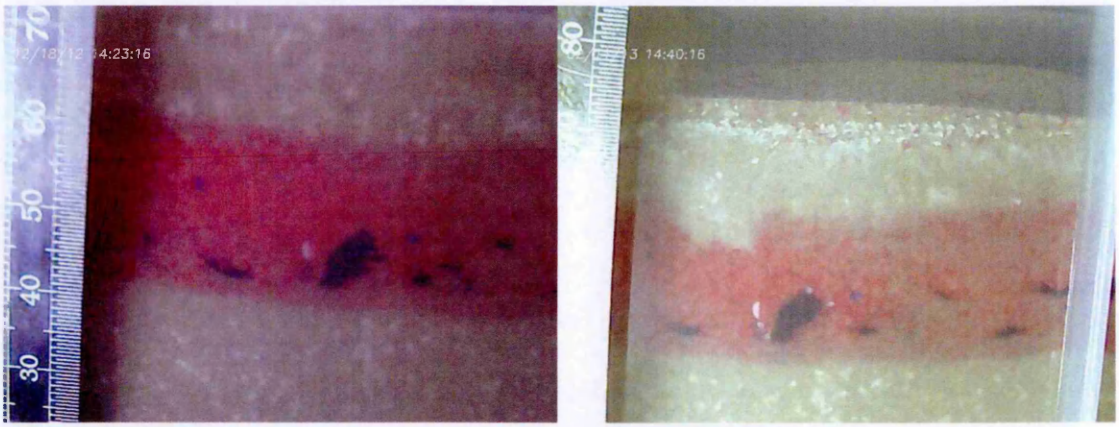

Figure 14.10: Before and after photos of the soil column, showing no movement in the large black clasts as a result of the freeze thaw cycling.

There was a slight displacement of the red sand grains, the layer had been distorted at the edges and corners, but whether this was due to the disturbance caused by pouring water into the sample is unknown. Little change was observed during the second stage of the experiment when water was already in place. It is possible that the column was too saturated, as the head of water that was emplaced above the top of the surface did not entirely disappear, however this was in line with the methodology of several of the previous studies discussed in Section 14.2.1, in particular that of Corte (1963). There

appears to be a migration of the small clusters of clay particles down through the sand column to below the level of the red layer. This may indicate illuviation of this material by the water saturating the column.

No evidence of ice lens growth can be seen in the photographs. A freezing front cannot be seen to propagate down through the sand column. The surface was not observed to heave during the course of the freezing cycles so it would appear that the reduced freezing rate was not sufficient to allow ice segregation to occur under these conditions. Whether the material being used was insufficiently frost-susceptible, or whether the saturation conditions were incorrect remains uncertain.

14.4 Further work

Despite the various revisions to the experimental methodology it proved impossible to initiate sorting using the laboratory set up available for this study. Consequently, it was not possible to confirm whether the sorting process is viable at the low temperatures found at the martian surface.

It seems likely that the lack of sorting in these experiments was largely due to one of two factors. Firstly the materials available were not sufficiently frost-susceptible. In retrospect the medium-grained sand that was used for most of the experiments almost certainly didn't have a sufficiently large proportion of the fine grained component for ice lens formation to easily initiate. However the fact that finer grained material also did not produce acceptable results suggests that this was not the only factor preventing the success of the experiment.

Ice lens formation requires a very low rate of cooling. It seems likely that in many of these experiments the soil column was cooled too fast and so froze completely, a frozen fringe did not have time to develop and so ice lens formation could not be initiated. Producing a frozen fringe under laboratory conditions would probably require a very

different set up where the soil column was frozen slowly from the top down, while liquid water was constantly resupplied from below. The Study of Corte (1963) used a freezing rate of 30-42 mm h^{-1}. A reservoir of water could be located outside the cold chamber, separated from the soil column by a membrane. The sides of the cylinder could be better insulated, so that cooling only occurred from the top, as the air temperature within the chamber was lowered slowly, using a computer controlled system. Unfortunately there was insufficient time at the end of this investigation for a complete redesign of the system to take place. It would be very interesting to conduct another series of experiments, perhaps using exactly the same system as one of the studies described in Section 14.2.1. That way the experiment could more quickly advance to studying the effect of freezing point depression.

Once a functional methodology was developed, then the original plan to test the efficacy of the frost heaving effect at lower temperatures could be conducted as outlined in the methodology section. In would also be useful to investigate the effect of brines on the sorting effect to determine whether the reduction in frost heaving observed by Chamberlain (1983) becomes worse when more exotic and concentrated brines, with proportionally lower eutectic temperatures, are used.

14.5 Summary

The main conclusion which can be drawn from this work is that the system is sensitive to a wide variety of conditions. The rate of cooling, and thus the temperature gradient through the soil column, must be very low for sorting to occur. This is not necessarily the case under martian conditions where extremes of temperature may be more prevalent. Water must be readily available to form an extensive frozen fringe and the substrate must be sufficiently frost-susceptible to allow frost heaving to occur.

The lack of water availability under martian conditions would be a major limiting factor in determining whether such soils are frost-susceptible or not. Thin films of water have been shown to form under martian conditions (Sizemore et al., 2014) but only in unusual circumstances. Consequently, it can be concluded that these processes should not be expected to be common under martian conditions. Periglacial environments should only be found in isolated locations where the properties of the soil are conducive to the formation of ice lenses, and sufficiently concentrated brines are present in the subsurface to allow thawing to occur.

Although the effect of brines on ice lens formation could not be assessed in this study it seems likely that the decreased frost heaving of saline systems described by Chamberlain (1983) would mean that it would take far longer for a significant degree of sorting to develop if cryobrines are being relied upon to depress the freezing point. It is impossible to conclude whether sorted patterned ground could occur under martian conditions without considerable further work to develop a working method.

15 Appendix Two: Large print reproductions of Important Maps.

Several of the larger maps presented in this thesis contain fine detail and small print and symbols. This section contains copies of these figures at twice the size presented in the text for ease of legibility. They are otherwise identical.

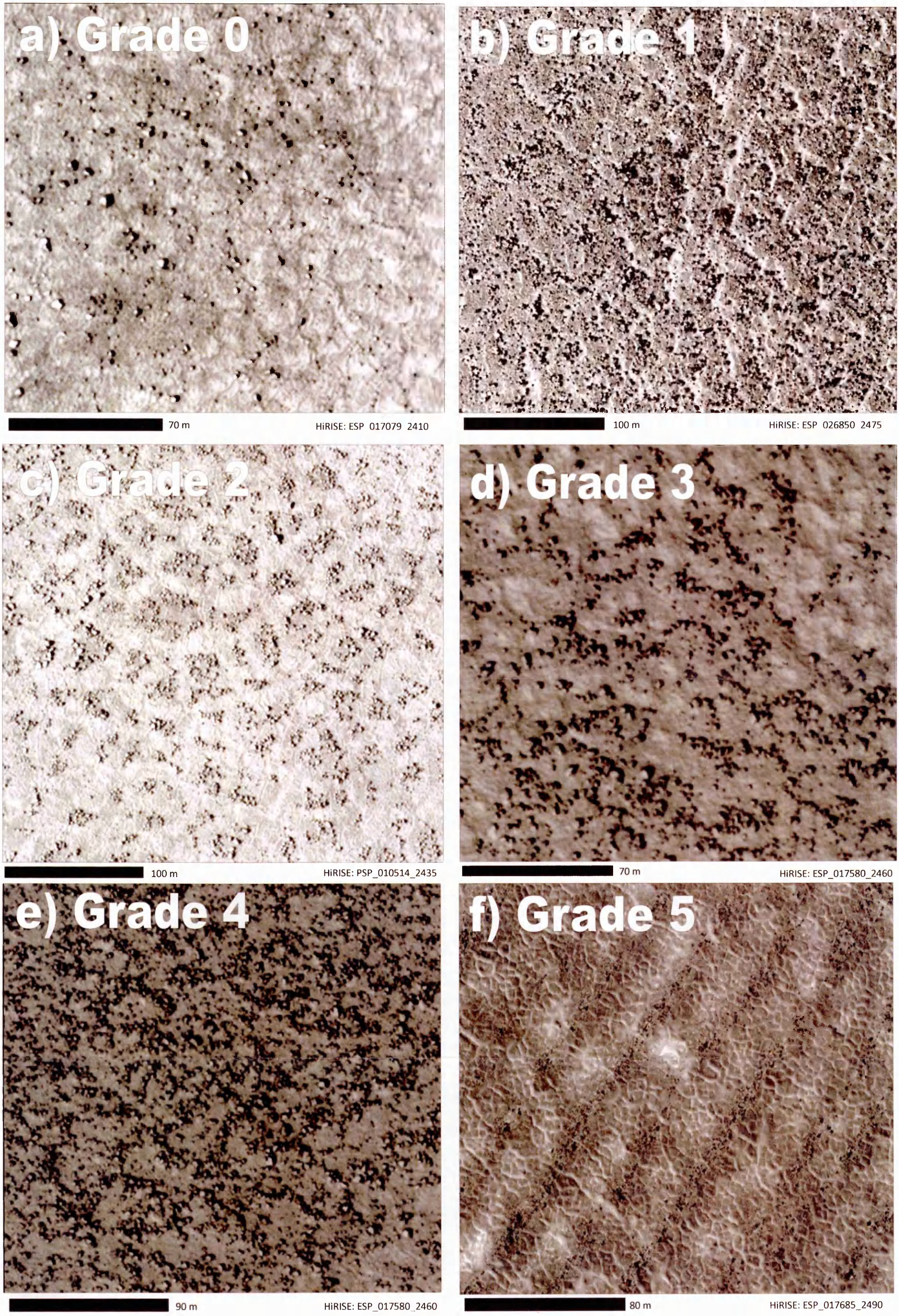

Figure 5.7: **Examples of the different grades of patterned ground. a) grade zero, no pattern, b) grade one, c) grade 2, d) grade 3, e) grade four, f) grade five, perfectly clear pattern.**

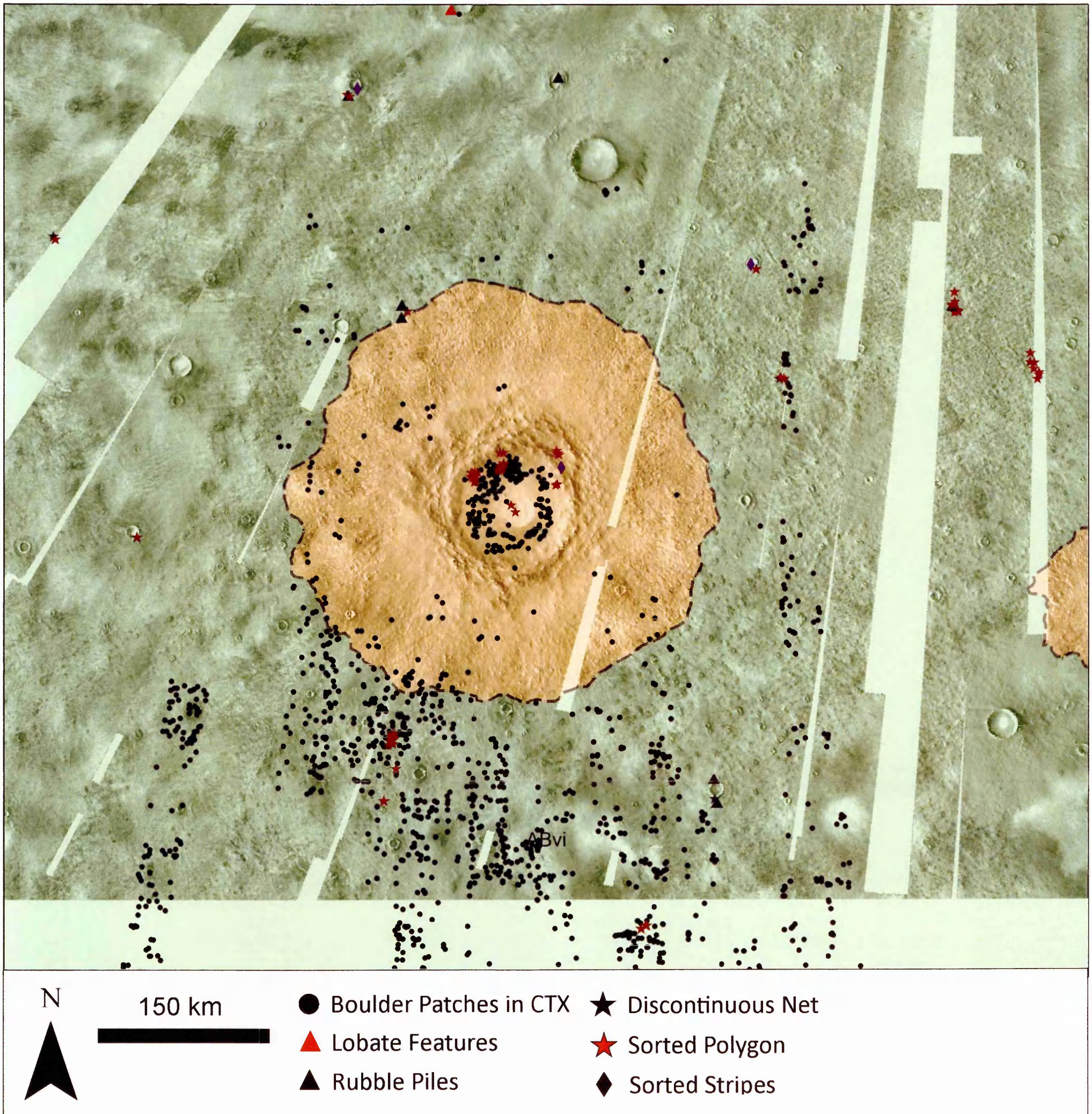

Figure 5.8: distribution of boulder patches in north-western Acidalia Planitia showing the area surrounding Lomonosov Crater. The surrounding plains are uniformly classified as part of the Vastitas Borealis interior unit.

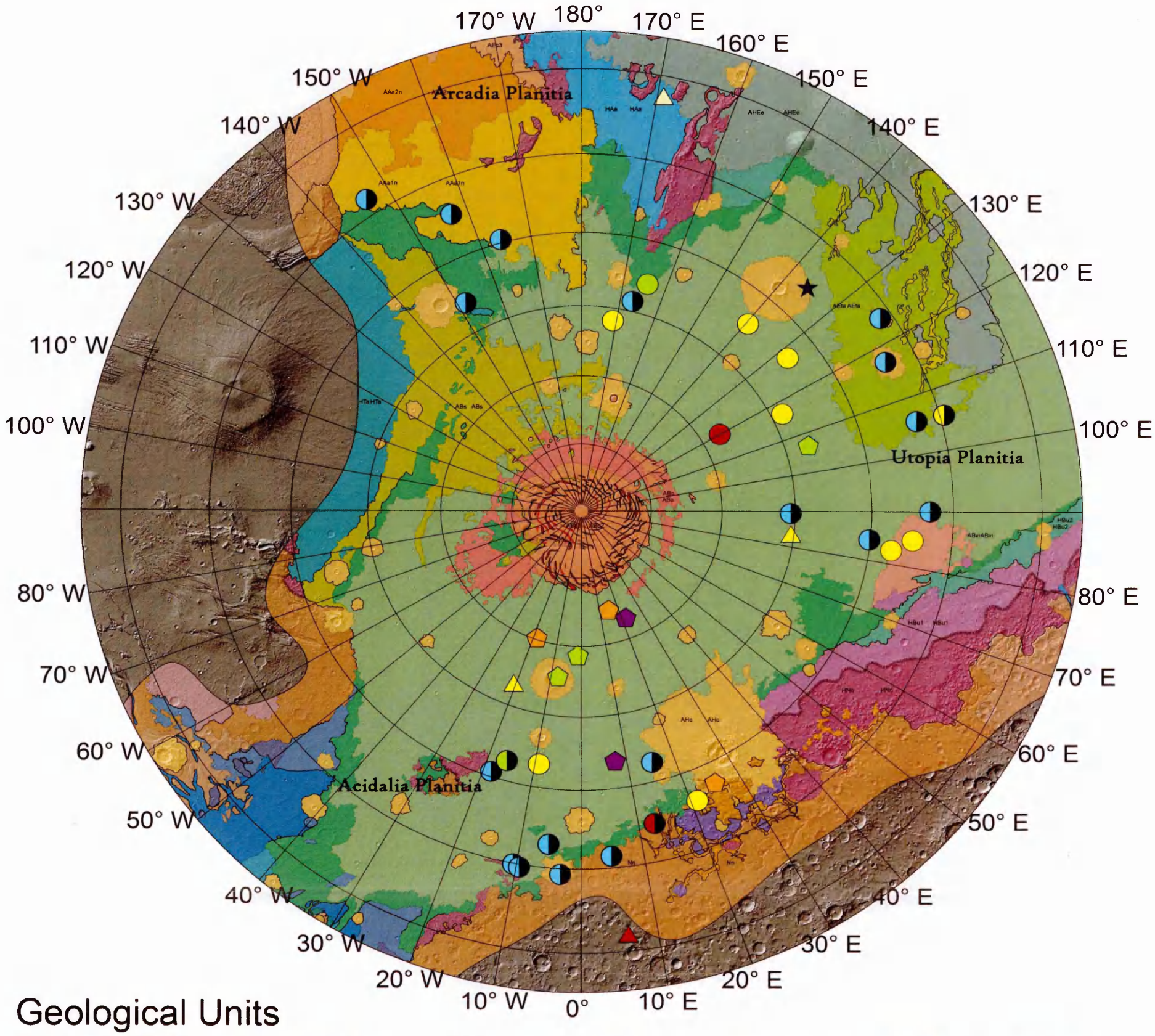

Geological Units

HTa	AEta	ATl	ABvi	AAm	HNCc1	HIs	HNTl
HCa	ABd2	ABb2	AAa1n	ABo	HIa	HBu2	HCc2
HCs	AHAa1s	AAa2n	AEc2	ABvm	HBu1	AIi	Nn
HNn	AEtb	AHEe	AHc	AAa2s	HBd1	ABs	HCc3
HAa	ABb1	AEc1	AEc3	AHcf	ABa	Nl	HCc4

Putative Periglacial Assemblages

- Sorted Polygons & Rubble Piles (3)
- Sorted Polygons & Stripes (3)
- Sorted Polygons, Stripes & Rubble Piles (2)
- Gullies & Scallops (18)
- Gullies, Scallops & Lobate Structures (1)
- Gullies, Scallops & Sorted Polygons (1)
- Gullies, Scallops & Sorted Stripes (1)
- Gullies, Scallops, Sorted Stripes & Lobate Structures (1)
- Gullies & Lobate Structures (1)
- Gullies & possible sorting (1)
- Gullies & sorted polygons (2)
- Scalloped depressions & Lobate Structures (1)
- Scalloped depressions & Sorted Polygons (8)
- Scalloped Depressions & Sorted Stripes (1)

Figure 5.8: distribution of boulder patches in north-western Acidalia Planitia showing the area surrounding Lomonosov Crater. The surrounding plains are uniformly classified as part of the Vastitas Borealis interior unit.

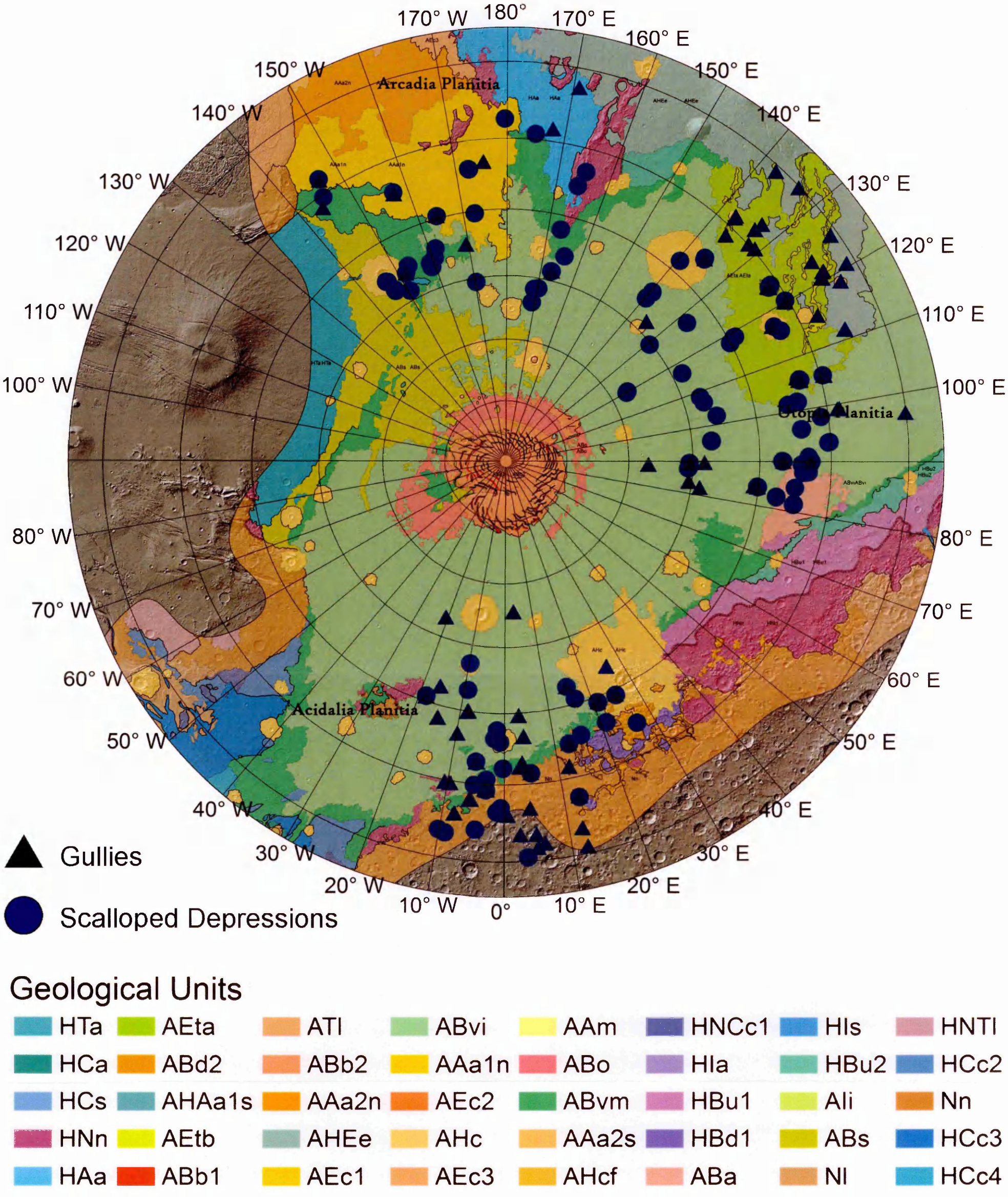

Figure 8.9: Distribution of Scalloped depressions and Gullies plotted over the northern plains geological map.

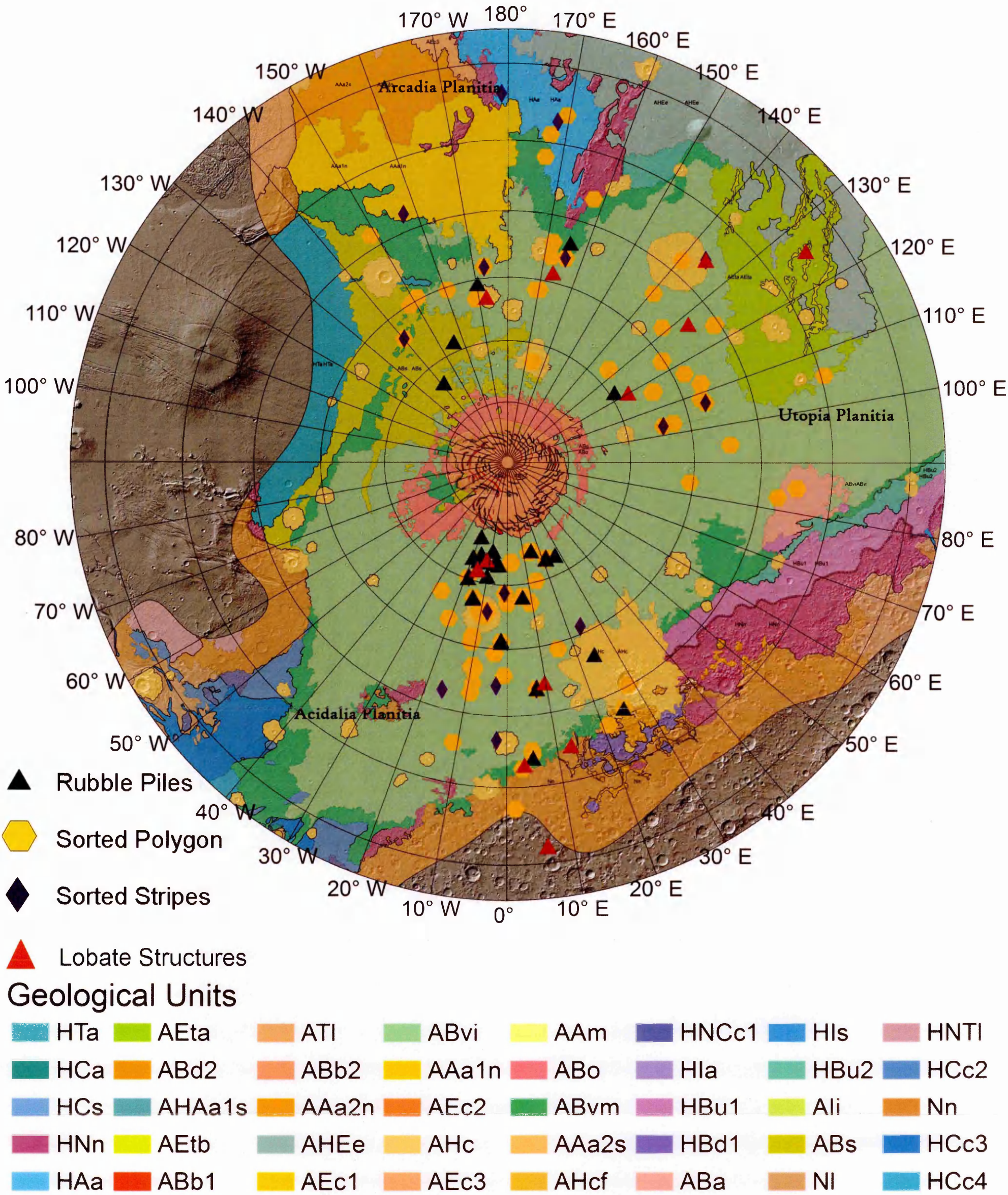

Figure 8.10: Distribution of Sorted Features and Lobate Structures over the geological map of the northern plains.